An investigation into how the cell cycle and the Notch signalling pathway regulate pronephrogenesis in *Xenopus laevis*

Richard William Naylor, B.Sc. (Hons.).

A thesis submitted to the University of Warwick for the degree of Doctor of Philosophy.

Genes and Development Research Interest Group,

Department of Biological Sciences,

University of Warwick,

Coventry,

CV4 7AL.

February 2009.

Contents

Chapter 2. Materials and Methods

Chapter 4. $p27^{Xic1}$ interaction with Gadd45γ and a speculative analysis of its role in primary neurogenesis

Chapter 5. A role for the "Wntch" signalling pathway in development of the proximal region of the *Xenopus laevis* pronephros

Table of Figures

Figure number **Page number**

Table of tables

Acknowledgements

During my time in the lab over the past three years, two people have stood out as being essential for my initiation into working in a research environment. Professor Liz Oliver-Jones has supported me exactly the way I perceive a great supervisor should; helping me when I needed it, but also permitting me enough independence for the creative thought processes, essential in more senior scientists, to develop. I can't ever remember Liz saying "no" to having a meeting or to any experiment I believed would be beneficial to this thesis. The second person I owe much gratitude to is Dr. Karine Massé. As well as being a great personality, Karine taught me all the molecular biology techniques I know (and detest!). So thank you very much Liz and Karine for all your help over the past three and a bit years. I also promise to Karine that I will become a more organized researcher in the future!

I also must thank Surinder, for his unique comedy and ability to raise points of discussion in the lab so the day is more interesting than just poking tadpoles! Also, thanks to Stéph and Jun-ichi for their help in the lab and chats in the office and Paul Jarrett for all the frogs and oocytes I have asked for!

As I have been inundated with friends and family who wish to have some sort of complimentary immortality by being mentioned in this thesis, I must thank veryfatpat, Matt "it's awwll Dudley" McD and Dave "Wya" for being housemates throughout my PhD, in particular Pat for the cheap rent (but not for making me watch Corrie and Star trek!). Also thanks to my Mum and sisters Pants, Lu, and Claire for at least pretending they were interested in my PhD. Finally, thanks to all my mates who can't understand why I work on frogs (read my discussion!) and haven't got a proper job now I'm 25 (Bordy, Angus, Dives, Kieran and Radford Albion FC).

This research was funded by the BBSRC

Declaration

All results presented in this thesis are the work of the author unless specified.

Dissections were performed by Professor Elizabeth Oliver-Jones. Wax-embedding and sectioning was undertaken by Mr Surinder Bhamra. Hormone injections to *Xenopus laevis* females were given by Mr Paul Jarrett. The anti-phosphohistone H3 staining (and the accompanying statistical analysis) described and discussed in Chapter 4 was carried out by Dr. Karine Massé.

Sources of information have been acknowledged by reference.

None of the work interpreted in this thesis has previously been used to apply for degree.

Summary

The connections between cell cycle exit and terminal differentiation remain poorly understood. Cyclin dependent Kinase Inhibitors (CKIs) provide a possible link between entry into the quiescent state and differentiation. The initial aim of this project was to further investigate if the CKI $p27^{Xic1}$ could promote differentiation in addition to, and independently of, its well characterised cell cycle exit function. $p27^{Xic1}$ has been shown to be involved in cell fate determination during gliogenesis, neurogenesis, myogenesis and cardiogenesis and many mammalian Cip/ Kip CKI homologues of $p27^{Xic1}$ have been described as important regulators of cellular processes beyond control of cell division. We aimed to investigate these roles during development of the embryonic kidney, the pronephros. We discovered that $p27^{Xic1}$ does not affect differentiation during pronephrogenesis, but instead controls pronephric organ size through its cell cycle exit function. In addition we identified a previously unrecognised role for the cell cycle exit function of $p27^{Xic1}$ in allocation of the somites during paraxial mesoderm segmentation.

Preliminary results had suggested *$p27^{Xic1}$* expression in the pronephros was under the control of the Notch signalling pathway. Over-expressing a constitutively active form of Notch, *Notch-ICD*, and a dominant negative form of the Delta ligand, *$Delta^{STU}$*, showed that both mis-activation and suppression of Notch signalling inhibited *$p27^{Xic1}$* expression. However, when investigating the effects these over-expressions had on pronephros development, we identified novel results indicating the Notch signalling pathway, which has previously been implicated in pronephros development, is essential for the separation of the proximal lateral and medial

pronephric mesoderms. This process we propose is mediated by the Notch signalling pathway through the establishment of a boundary between these two distinct populations of cells, permitting both compartments to develop in isolation.

The results in this thesis suggest novel mechanisms by which cell division controls *X. laevis* segmentation and organ size and how the Notch signalling pathway is able to pattern the pronephros anlagen such that the different compartments of the mature pronephros are able to develop, and thus function.

Abbreviations

AP	alkaline phosphatase
APS	ammonium persulphate
ATP	adenosine triphosphate
bHLH	basic Helix-loop-helix
bp	base pairs
BSA	bovine serum albumin
cDNA	complementary deoxyribonucleic acid
Cdk	Cyclin dependent kinase
Ci	Curie
Cip	Cdk-interacting protein
CKI	Cdk inhibitor
CSL	CBF1/ RBP-Jκ/ Suppressor of Hairless/ LAG-1 transcription complex
C-terminal	carboxyl-terminal
DAB	3.3'-diaminobenzidine
dATP	deoxyadenosine triphosphate
dCTP	deoxycytidine triphosphate
dGTP	deoxyguanosine triphosphate
dH_2O	distilled water
DIG	digoxygenin
DNA	deoxyribonucleic acid
DNase	deoxyribonuclease
dNTPs	deoxyribonucleoside triphosphates
dpc	days postcoitum
DSL	Delta/ Serrate/ Lag-2 Notch ligands
E	embryonic day
E.coli	*Escherichia coli*
EDTA	ethylene diamine tetra acid
EST	expressed sequence tag
FGF	fibroblast growth factor

g	gram
GFP	green fluorescent protein
HCl	hydrochloric acid
H_2O	water
H_2O_2	hydrogen peroxide
hpf	hours post-fertilisation
HRP	horseradish peroxidase
ICD	intracellular domain
Ink	Inhibitor of kinase
l	litre
LBroth	Luria Broth
kb	kilobases
kDa	kilo Dalton
Kip	Kinase inhibitor protein
Kix	Kinase inhibitor of *Xenopus*
M	molar
MBT	mid-blastula transition
mg	milligram
ml	millilitre
mM	millimolar
MMLV	moloney murine leukaemia virus
MOPS	3-[N-morpholino] propane sulphonic acid
MO	morpholino oligonucleotide
mRNA	messenger ribonucleic acid
NaCl	sodium chloride
ng	nanogram
nl	nanolitre
nM	nanomolar
NP40	nonidet P40
nt	nucleotides
N-terminal	amino-terminal
PAGE	polyacrylamide gel electrophoresis
PBS	phosphate buffered saline

PBT	phosphate buffered tris
PBST	phosphate buffered tris
PCD	programmed cell death
PCNA	Proliferating Cell Nuclear Antigen
PCR	polymerase chain reaction
pH3	phosphohistone H3
pM	picomolar
pmol	picomoles
PMSF	phenylmethylsulphonyl fluoride
RA	retinoic acid
RGC	retinal ganglion cells
RNA	ribonucleic acid
RNase	ribonuclease
rpm	revolutions per minute
RT-PCR	reverse transcription PCR
SDS	sodium dodecylsulphate
SOP`	Sensory organ precursor
ssDNA	single stranded DNA
TACE	Tumour necrosis factor-Alpha Converting Enzyme
TBE	tris buffered EDTA
TBS	tris buffered saline
TdT	Terminal deoxynucleotidyl transferase
TEMED	N, N, N'-Tetramethylethylenediamine
TGFβ	transforming growth factor β
Tris	tris (hydroxymethyl) aminomethane
Tris-Cl	tris (hydroxymethyl) aminomethane, pH adjusted with HCl
TUNEL	Tdt mediated dUTP Nick-End labelling
UTR	untranslated region
V	volts
Xic	*Xenopus* inhibitor of Cdk
u	units
μg	microgram
μl	microlitre

μM	micromolar

Chapter 1

Introduction

The kidney has many biological functions, its role in blood filtration and whole body homeostasis makes it a vital organ both during embryonic development and in adult organisms. Kidney malfunction as a consequence of disease or damage presents a major problem for the body. In the UK chronic kidney disease (CKD), the collective term for a wide range of renal diseases, is a huge burden to the National Health Service. To highlight this burden, the age-standardised prevalence of CKD was 8.5% in a 162,113 sample of the UK population (Crowe et al., 2008). Understanding how the kidney forms and functions through research may yield information on how better to treat renal diseases, and would have a profound impact on the nation's health.

Originally, the study of nephrogenesis aimed to elucidate the interactions that promote mesenchyme to epithelial transitions. Reversal of this process has relevance to tumour metastasis (Wu and Zhou, 2008) and occurs in many progressive kidney diseases, such as renal fibrosis (Burns et al., 2007). Further study of nephrogenesis has improved our understanding of epithelial cell polarization (Hartwig et al., 1990; Horster et al., 1999), regulation of apoptosis (Smith and Mackay, 1991), cell migration (Hara-Chikuma and Verkman, 2006; Wada et al., 2008), branching morphogenesis (Costantini, 2006), organ repair (Ishibe and Cantley, 2008), and how

major signalling pathways act to induce and pattern discrete cell populations (Kopp, 2002; Dressler, 2008). Despite knowledge of the spatial and temporal arrangement of cells within the developing nephric system being relatively advanced, the complexity of the signals directing these arrangements are not so well understood and present the next step in kidney research.

1.1 The vertebrate kidney

The vertebrate adult kidney arises from a succession of nephric forms that differ in complexity and size, but which have similar functions (Saxén, 1987) (Fig 1.1). The first to form is the pronephros, the simplest renal structure (Vize et al., 1997; Brändli, 1999; Drummond, 2005; Jones, 2005; Dressler, 2006). The pronephros is similar to a single nephron found in the adult kidney. Anamniotic vertebrates, such as *Xenopus laevis* and zebrafish, require a pronephros for osmo-regulation and waste excretion during early development. In amniotes the pronephros is rudimentary, but nevertheless necessary for the induction of the second kidney form, the mesonephros. The mesonephros acts as the functional excretory organ in adult amphibians and teleost fish, but is a transitory organ in mammals. It also has additional developmental roles, such as promoting limb formation (Smith et al., 1996) and induction of the gonads in amniotes (Yoshioka et al., 2005). The mesonephros contains 10-50 nephron-like tubule structures, depending on the species. In anamniotic vertebrates, all these tubules are functional and develop from the pronephric duct. However in mammals there are two sets of tubules that are either connected or not connected to the Wolffian duct, with

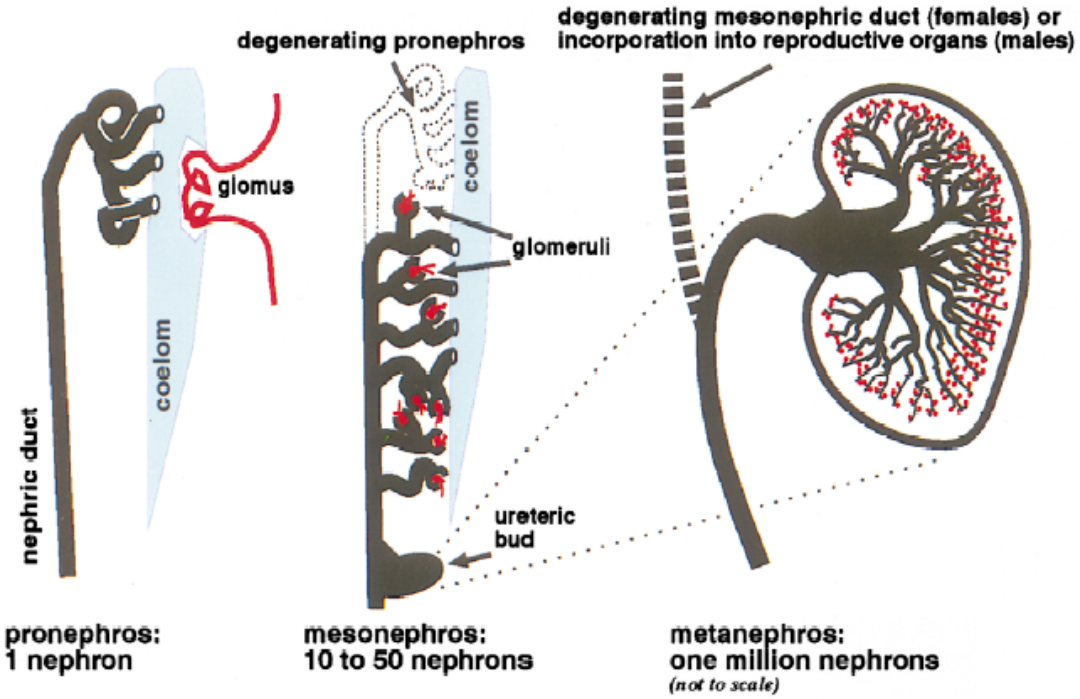

Figure 1.1 Organisation of the triad of kidney forms that occur during vertebrate development. The pronephros develops as a single nephron, whereas the mesonephros, the permanent functional kidney form in anamniotic vertebrates, is more complex, incorporating multiple tubular structures to aid blood filtration and maintain osmotic balance in the body. The metanephros is the functional kidney of reptiles, birds and mammals. Consisting of 1 million nephrons, it is the most complex kidney form. (Reproduced from Vize et al., 1997)

the former being functional and the latter vestigial (Croisille, 1976). In mammals all mesonephric tubules are transient and degenerate through apoptosis during the regression phase. However mesonephros development is essential for formation of the final and most complex kidney, the metanephros, which contains over 1 million nephrons and is the permanent kidney in amniotes. Outgrowth from the ureteric bud into the metanephric mesenchyme initiates branching morphogenesis and mesenchyme-epithelial interactions, initiating development of the metanephros (Dressler, 2006). Whilst the mesonephros and metanephros have additional roles, the triad of kidney forms that appear during development are primarily functional units in the body controlling waste disposal and water balance.

1.2 The *Xenopus laevis* pronephros

This thesis investigates how the cell cycle and the Notch signalling pathway regulate development of the pronephros in *Xenopus laevis*. The availability of a wide range of pronephric markers and the ease with which this model organism can be manipulated, have made *X. laevis* pronephros development an attractive model for kidney development and organogenesis in general.

1.2.1 The structure and function of the pronephros in *Xenopus laevis*

The pronephros is a paired organ that develops in the intermediate mesoderm either side of the midline, immediately ventral to anterior somites 3-5 (Fig 1.2). Developmental cues direct the pronephros anlagen to form a non-integrated nephron consisting of four distinct regions; the glomus, coelomic cavity (nephrocoel),

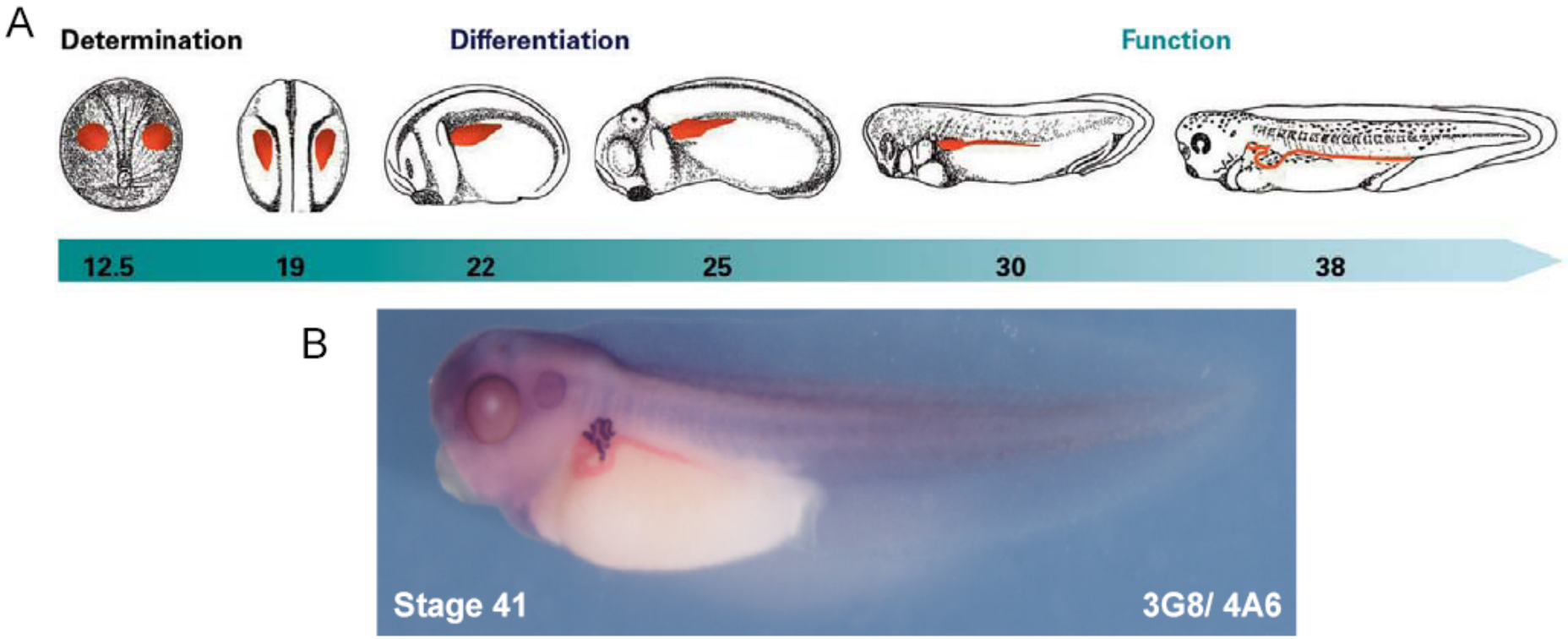

Figure 1.2 Spatial development of the pronephros in *Xenopus laevis*. (A) The pronephros develops from the intermediate mesoderm immediately ventral to the anterior somites. Specification occurs at stage 12.5, from which stage the mass of un-patterned and un-differentiated pronephric cells, termed the pronephros anlagen, commences differentiation and morphogenesis to form a functional pronephros by stage 38 (Reproduced from Chan et al., 2006). (B) A mature pronephros can be immunostained with 3G8, which detects an epitope in the nephrostomes and proximal tubules, and 4A6, which detects an epitope in the intermediate and distal tubules, to clearly identify the tubular structure of the functional pronephros at stage 41.

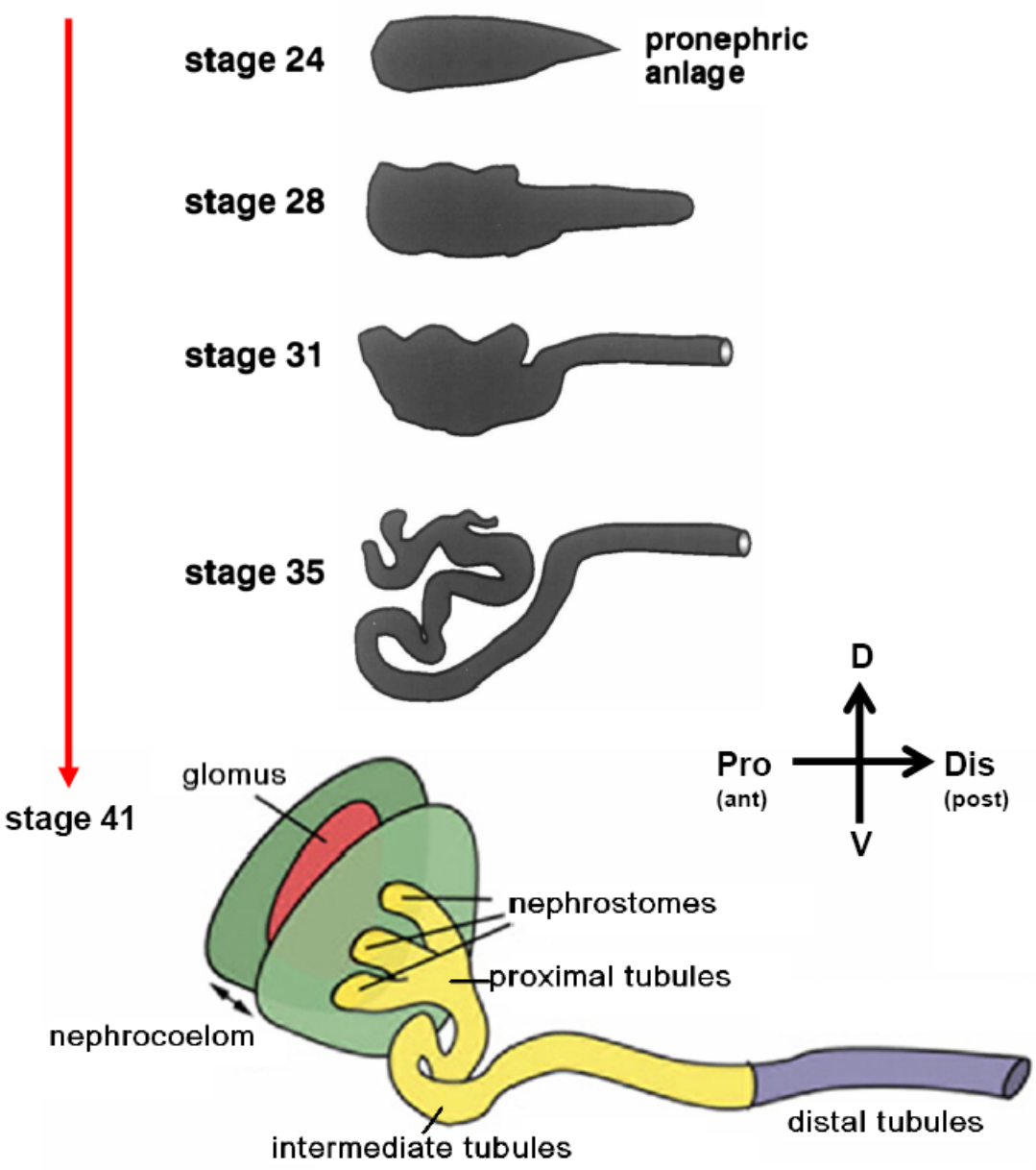

Figure 1.3 Schematic of the compartmentalization of the mature pronephros. The *X. laevis* pronephros develops from an anlagen to a functional pronephros between stages 12.5 and 38. A functional pronephros is compartmentalized into 4 distinct regions, the glomus, nephrocoel, nephrostomes and tubules (which are further characterized into the proximal, intermediate and distal tubules). The glomus is composed of the blood vasculature that expels fluid into the coelomic cavity (nephrocoel). Multi-ciliated funnel-like tubes called nephrostomes generate a flow of fluid from the coelom into the lumen of the tubules, where re-absorption of electrolytes and water occurs. All waste fluid is then passed to the exterior via the cloaca. (Schematic modified from Tran et al., 2007 and Vize et al., 1997)

nephrostomes, and tubules (which are further characterized as proximal, intermediate, distal and connecting tubules) (Fig 1.3).

The glomus is the pronephric filtration unit, also called the pronephric corpuscle (a collective term for the glomus and nephrocoel). Its vasculature, which originates from the dorsal aorta, selectively expels fluid into the coelomic cavity. The medial side of the nephrocoel consists of a visceral epithelia cell layer with which the glomus is believed to be in contact and, together with podocytes and endothelial cells, form a basement membrane that regulates blood filtration (Brändli, 1999). A parietal epithelia cell layer resides on the opposite (lateral) side of the coelom. Three tubes extend out of this epithelial layer, connecting the coelom with the tubules. These three tubes are the nephrostomes, which are completely ciliated to enable their function in generating a flow of fluid through the pronephric tubules. Once fluid is passed through the nephrostomes, essential electrolytes and water still required by the body are re-absorbed in the tubules, before waste fluid is passed to the exterior via the cloaca.

1.2.2 The cellular and molecular basis of pronephrogenesis

Dissected presumptive pronephric mesoderm isolated from intermediate mesoderm at gastrula stages of development, does not form pronephros in saline solution (Brennan et al., 1998). Furthermore, transplantation of pronephric mesoderm to a heterologous site, away from the normal position of pronephros development, does not form pronephros in the transplanted region (Fales, 1935). Thus a signal, originating from tissues surrounding the presumptive pronephric intermediate mesoderm, is required for pronephric induction (Fig 1.4B and 1.5).

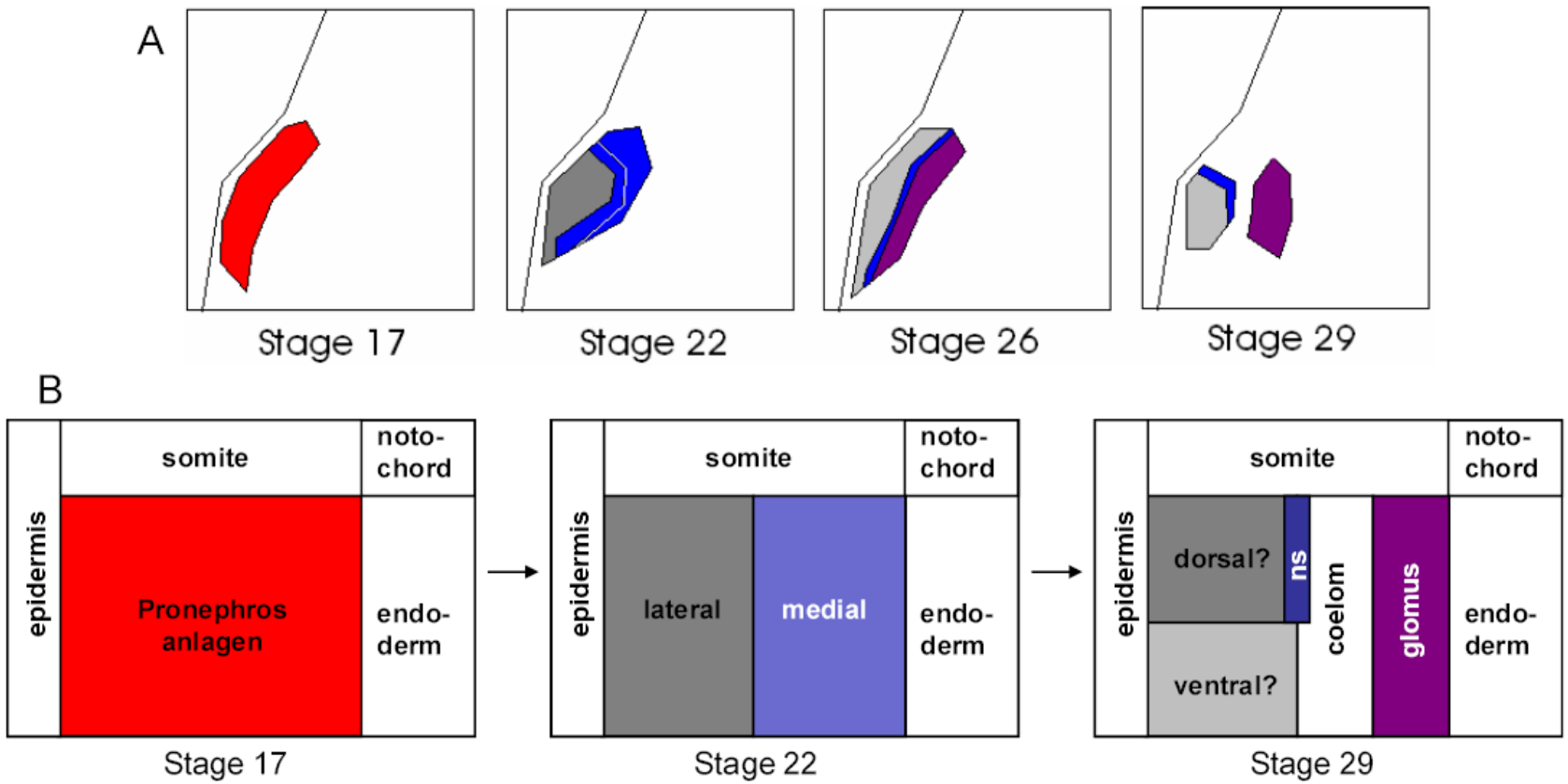

Figure 1.4 The distribution of cells in a transverse section across the proximal region of the pronephros. (A) The pronephros anlagen is a mass of un-differentiated and un-patterned cells at stage 17. By stage 22 the pronephric mesoderm has split down the midline into the lateral (grey) and medial (blue) pronephric mesoderms. The medial pronephric mesoderm at the boundary of the lateral and medial pronephric mesoderms is fated to form the nephrostomes (dark blue), which are induced to form in this position by a signal originating from the medial pronephric mesoderm. By late tail bud stages of development the medial pronephric mesoderm splits from the lateral pronephric mesoderm and nephrostomal mesoderm to produce the coelomic cavity. Consequently the tubules and nephrostomes develop on the lateral side of the coelom and the glomus on the medial side of the coelom. (B) Schematic representation of the pronephric and surrounding tissue distribution from late neurula to late tail bud stages of development. (Both illustrations adapted from Vize et al., 1997) (ns = nephrostomes)

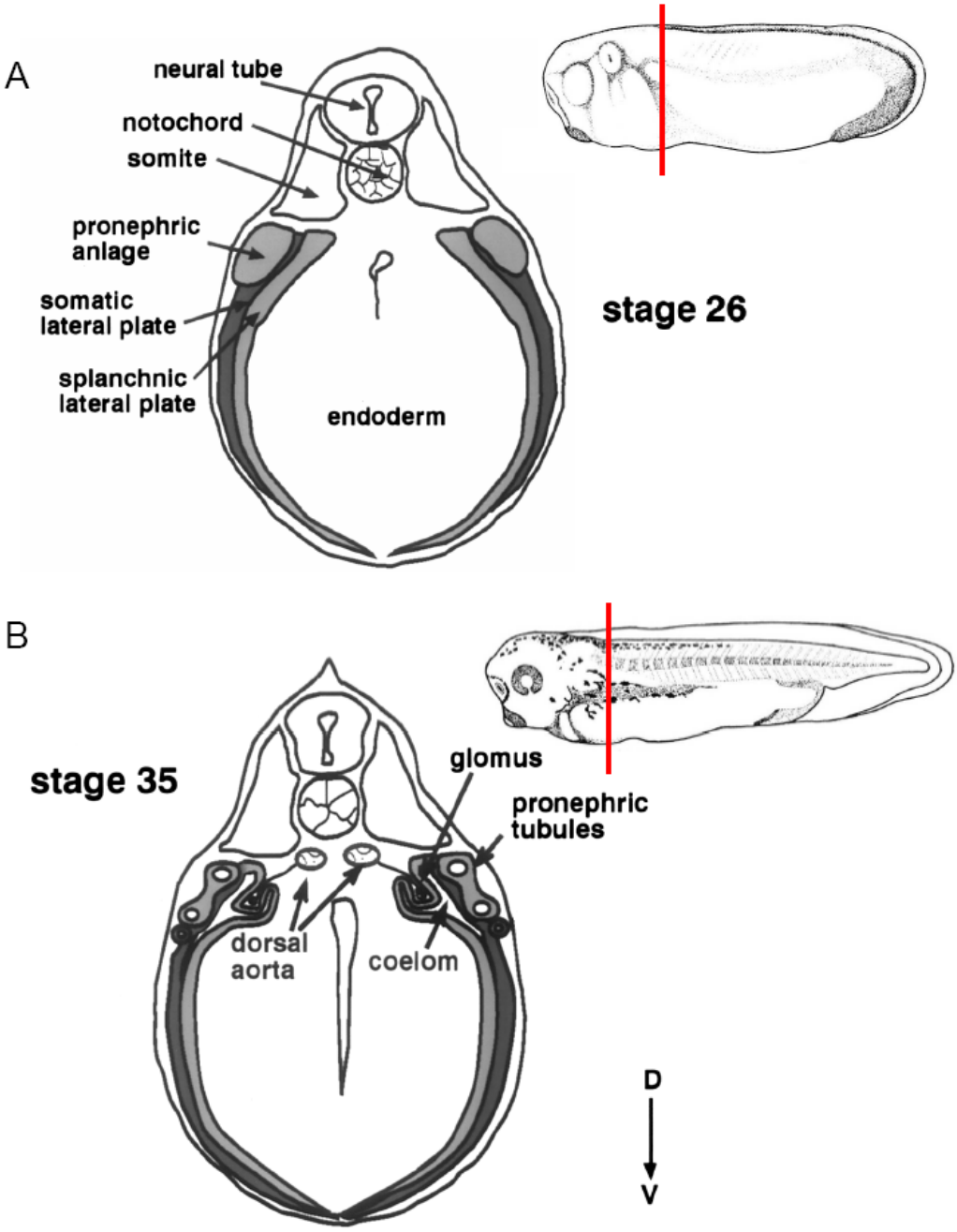

Figure 1.5 Transverse section of embryos at stage 26 and 35 highlights the cross-section arrangement of the pronephros. (A) At stage 26 the pronephros anlagen is not morphologically distinct or compartmentalized. (B) By stage 35 the pronephros has formed and the glomus, coelom, and tubules can all be observed by section. It is important to note that the glomus is medial to the tubules, not dorsal as many schematics (including Fig 1.3) illustrate. (Reproduced from Vize et al., 1997)

The most important inductive signal to the intermediate mesoderm comes from the anterior somites (Seufert et al., 1999; Mauch et al., 2000; Mitchell et al., 2007). The nature and timing of this signal have not been elucidated, but the anterior somites are both necessary and sufficient to impart pronephric cell fates in dissected presumptive pronephric mesoderm (Holtfreter, 1933; Tételin, Thesis 2008). Whilst the transcriptional targets of this signal are unknown, it is likely to induce, either directly or indirectly, expression of genes encoding early markers of the pronephros anlagen, namely the paired box gene *Pax-8* and the homeobox transcription factor *Lim-1*, which act synergistically to establish the early pronephric primordium (Carroll and Vize, 1999).

By mid-neurula stages of development the pronephros anlagen has been induced, but remains a mass of cells requiring patterning to allocate the different regions of the mature pronephros (Fig 1.4). Developmental cues pattern the pronephros anlagen and establish two molecularly defined axes, the medio-lateral axis across the proximal pronephros anlagen, and the proximal-distal axis across the entire lateral pronephros anlagen. The first genes that begin to pattern the pronephros are Wilms' tumour gene-1 orthologue, *WT-1*, and the LIM homeodomain protein, *Lmx1b* (Carroll and Vize, 1996; Wallingford et al., 1998; Haldin et al., 2008). Lmx1b is believed to act upstream of *WT-1*, which is expressed from stage 18, but only in the medial region of the pronephros anlagen. Lmx1b and WT-1 initiate medio-lateral patterning and separation of the glomus (medial pronephric mesoderm) from the tubules (lateral pronephric mesoderm) (Figure 1.4A). *WT-1* expression restricts expression of *Pax-8, Lim-1* and other markers of the pronephros anlagen, such as *Pax-2*, to the lateral pronephric mesoderm, by inhibiting their expression in the

medial pronephric mesoderm (Vize et al., 1997). Some researchers do not include the medial pronephric mesoderm a part of the pronephros as it will form the vasculature that makes up the glomus, and is physically removed from the tubules by the coelomic cavity later in development. However, the medial pronephric mesoderm gives rise to a number of pronephric tissues, as shown by a series of experiments performed by Ruth Howland (1916) in the spotted salamander, *Amblystoma punctatum*. She showed that removal of the entire embryonic pronephros minus the medial pronephric mesoderm (the aorta anlagen), permitted the glomus to form and the nephrostomes to regenerate, but not the tubules. In conclusion the medial pronephric mesoderm in *A. punctatum* is necessary for formation of the nephrostomes, despite their final location on the lateral side of the coelomic cavity at the tips of the proximal tubules. Therefore the medial pronephric mesoderm is required for formation of the glomus, coelom and nephrostomes. Additionally, some authors contest what stage the pronephric corpuscle is specified. The proximal pronephros has been shown to be specified around stage 12.5, with the distal pronephros anlagen specified later, around stage 14 (Brennan et al., 1998). The glomus and tubules develop separately as a consequence of the proximal pronephros anlagen splitting down its midline, producing the lateral and medial pronephric mesoderms. The pronephric corpuscle is most likely specified at the same time (stage 12.5) as the rest of the proximal pronephros anlagen (Brennan et al., 1999a). Furthermore, despite surrounding tissues contributing signals to induce pronephros formation in the intermediate mesoderm, none have been shown to contribute cells to the pronephros anlagen that could potentially form the pronephric corpuscle. This supports the view that the pronephric corpuscle is derived from pronephric intermediate mesoderm.

In the literature, patterning of the lateral pronephric mesoderm is perceived to occur in both dorso-ventral and proximo-distal directions to form the proximal and distal tubules. Previous publications have concluded that the gene expression patterns of *Wnt-4*, *Notch-1* and *Serrate-1* suggest they have a role in regulation of this dorso-ventral patterning of the lateral pronephros mesoderm (Vize et al., 1997). However, results in this thesis show *Wnt-4* and Notch signalling are not involved in dorsal-ventral patterning of the lateral pronephric mesoderm. Furthermore, our results suggest that this region undergoes anterior-posterior patterning rather than a dorsal-ventral patterning event. The lateral pronephric mesoderm forms one continuous tubule that extends from the base of the three nephrostomes to the cloaca and is subdivided functionally along its length; this subdivision being exemplified by specific gene expression patterns which define different functional domains (Raciti et al., 2008). In theory, there is no requirement for a dorsal-ventral signal. Examples of dorsal-ventral patterning during development include establishment of the dorso-ventral body plan of *Drosophila* (Roth, 2003) and vertebrates (Holley et al., 1995), the dorsal-ventral axis of the limb bud (Capdevila and Izpisua Belmonte, 2001; Robert, 2007), and dorsal-ventral boundary formation in the *Drosophila* imaginal wing disc (Irvine, 1999). All these examples require dorsal-ventral patterning as the dorsal side of the axis is morphologically and/ or molecularly distinct from the ventral side. The pronephric tubules do not differ across their dorsal-ventral axis; hence there is seemingly no requirement for molecular control of this axis during pronephros development.

Whilst the lateral pronephros mesoderm is not molecularly divergent across its dorsal-ventral axis, it is across its proximal-distal axis. Evidence for this is

provided from the differing developmental stages for the specification of the proximal (stage 12.5) and distal (stage 14) pronephros (Brennan et al., 1998). Furthermore, the molecular expression patterns of genes expressed in the tubules display distinct proximal-distal patterns (Reggiani et al., 2007), and the Notch signalling pathway has been proposed to regulate proximal-distal patterning across the whole pronephros (McLaughlin et al., 2000).

In conclusion, this interpretation of the literature combined with our new experimental data, leads us to conclude that the two axes important in patterning the pronephros at the molecular level are the medio-lateral axis across the proximal pronephros anlagen, and the proximal-distal axis across the lateral pronephric mesoderm. These two axes are fundamental to patterning of the pronephros, with the medio-lateral signal allocating the glomus, coelom and nephrostomes and the proximo-distal signal patterning the tubules.

1.3 Cell cycle and organ size

The cell cycle is a fundamental process in biology. Regulation of the amount of cell division, the plane of cell division and when that division occurs is a significant part of appropriate development. Understanding regulation of the cell cycle during organogenesis will enable us to improve our knowledge of the ways in which organ cell number and size is determined (or pre-determined), as cell proliferation is a major factor regulating organ size.

1.3.1 The cell cycle and its regulation

As illustrated in Figure 1.6, the cell cycle consists of four major phases. After division the cell enters the first gap phase (G1), where transcription permits cellular function and prepares the cell for the next stage in the cell cycle, the S (DNA synthesis) phase. After duplication of the genome there is a second gap phase (G2), before entry into the M (mitosis) phase, where cytokinesis produces two daughter cells, each containing a single copy of each parental genome. In *X. laevis*, the initial cell divisions require no gap phases as stores of maternally stockpiled protein and other molecules ensure they are not needed, thus only S and M phases occur. Cell cycles with absent gap phases ensure rapid cell divisions (roughly 30 minutes at room temperature), which is necessary so the embryo can quickly produce enough cells to permit the next stage in development; re-organisation of cells into the three germ layers during gastrulation. The point in development when growth phases appear and zygotic transcription is initiated is called the mid-blastula transition (MBT), which in *X. laevis* occurs around stage 8.5 after 12 cell divisions (Newport and Kirschner, 1982; Philpott and Yew, 2008).

The master regulators of the cell cycle are the cyclins and cyclin-dependent kinases (cdks), which complex together to promote cell cycle progression. Studies in yeast, mice and frogs have determined that different cyclins and cdks regulate various stages of the cell cycle (Doree and Hunt, 2002). Cyclin D is the first cyclin produced in the cell cycle in response to extra-cellular signals such as growth factors. Cyclin D interacts with cdk4 or cdk6 to form an active serine/ threonine kinase that partially phosphorylates the retinoblastoma protein (RB) (Weinberg, 1995). Hypo-

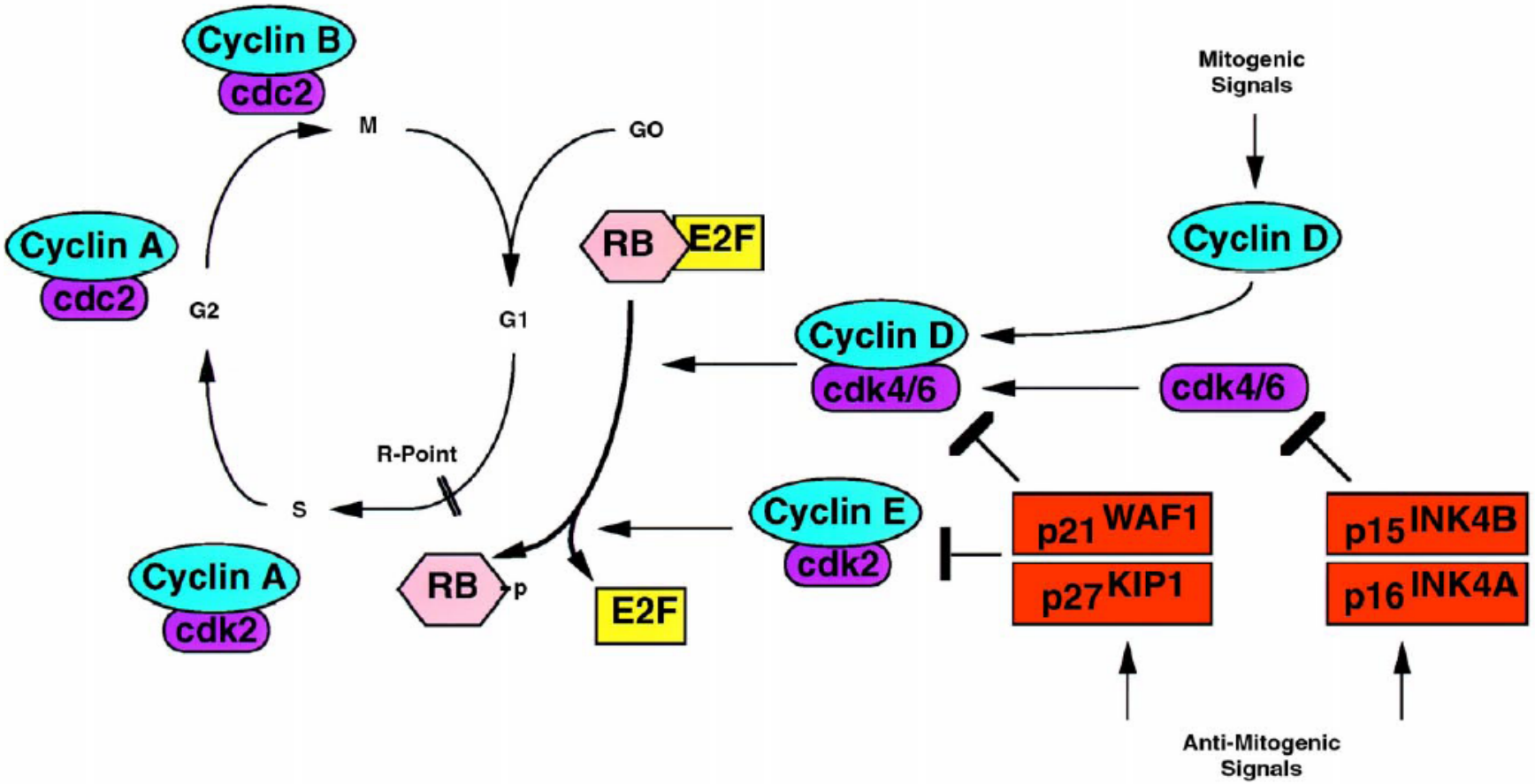

Figure 1.6 The cell cycle. A schematic illustrating the basic cell cycle and the proteins that are expressed to control the various checkpoints. If a proliferating cell decides to enter the cell cycle, the first cyclin it will express is *Cyclin D*. Cyclin D binds cdk4/6 and acts as a kinase, phosphorylating the Retinoblastoma (RB) transcription factor. This phosphorylation releases E2F from RB, switching it from a transcriptional repressor to a transcriptional activator. Phosphorylated RB will induce expression of genes whose products promote cell cycle progression. One such gene product is Cyclin E, which binds cdk2, and further phosphorylates RB to enhance cell cycle progression. Cyclin A/ cdk2 regulates S phase progression, and during the G2 phase Cyclin B interaction with cdc2 regulates entry into mitosis. Cyclin dependent Kinase inhibitors (CKIs) are able to regulate the cell cycle. Most notably, this regulation occurs during the G1 phase where Cip/ Kip (such as $p21^{WAF1}$ (also known as $p21^{Cip1}$) and $p27^{Kip1}$ shown in the diagram) and Ink4 (such as $p15^{ink4B}$ and $p16^{ink4A}$ shown in the diagram) inactivate Cyclin/ cdk complexes by phosphorylation. (image taken from Lundberg et al., 1999)

phosphorylated RB is bound to the transcription factor complex E2F/ DP1, ensuring this complex acts as a transcriptional repressor (Nevins, 1998). The action of cyclin D/ cdk4/ 6 hyper-phosphorylates RB, causing it to dissociate from E2F/ DP1. E2F, when not bound to RB, becomes a transcriptional activator, inducing expression of genes such as *cyclin A*, *cyclin E*, *cdk2*, *PCNA*, *DNA polymerase α* and *Histone H2A*, which promote S phase entry (Lundberg and Weinberg, 1999). Cyclin E and cyclin A, produced from E2F transcriptional activation, bind to cdk2, promoting entry into the S phase by further phosphorylating RB, and increasing the amount of free E2F in the nucleus. Upon completion of the S phase, cyclin B interactions with cdc2 regulates transition into the M phase through activation phosphorylation of multiple substrates, including proteins involved in nuclear breakdown, chromosome condensation and spindle assembly (Nigg, 1991; Nigg et al., 1996).

Activity of the cyclin/ cdk complexes is tightly regulated at multiple levels within the cell. The assembly of cyclin/ cdk subunits, inhibitory phosphorylation of either subunit, and the activity of cyclin-dependent kinase inhibitors (CKIs) are mechanisms by which cyclin/ cdk activity is regulated (Obaya and Sedivy, 2002). In this study we observe the regulation of pronephrogenesis by the CKI $p27^{Xic1}$. In mammals there are two families of CKIs, Ink4 and Cip/ Kip (Sherr and Roberts, 1999). The Ink4 family consist of $p16^{Ink4A}$, $p15^{Ink4B}$, $p18^{Ink4C}$, and $p19^{Ink4D}$ proteins that selectively inhibit the action of cdk4 and cdk6. Consequently the Ink4 family of CKIs are involved in preventing entry of the cell into the G1 phase of the cell cycle, promoting the G0 latent state. In mammals the Cip/ Kip family of CKIs consists of three proteins; $p21^{Cip1}$, $p27^{Kip1}$ and $p57^{Kip2}$. These CKIs are capable of inhibition of all cdks involved in the G1/ S transition, although their activity may be more

complex than originally thought as $p27^{Kip1}$ has been shown to be involved transiently in the assembly of cyclin D/ cdk4 (Blain, 2008). There are also many examples of these CKIs acting beyond cell cycle regulation (Besson et al., 2008, and see below). The role of CKIs in regulation of the G2/ M transition also remains unclear, however a cell that has undergone DNA replication will need to divide to avoid polyploidy, thus it is likely the role of CKIs in the G2 phase of the cell cycle is to control the timing of entry into the M phase, rather than inhibit it entirely, as can be the case with the G1/ S transition.

1.3.2 The multi-faceted roles of Cyclin Dependent Kinase inhibitors

The Cip/ Kip family of CKIs share amino acid sequence homology in their N-terminus cyclin/ cdk binding regions. However the rest of their sequence has diverged (Fig 1.7), suggesting each protein has distinct functions beyond cyclin/ cdk mediation. The importance of the cyclin/ cdk independent functions in CKIs has only begun to be understood recently. CKIs are now known as key regulators of cell survival, transcription, differentiation, migration and cytoskeletal dynamics, in addition to cell cycle (as reviewed in Besson et al., 2008).

Perhaps the most well established role of CKIs, in addition to their control of cyclin-cdk interactions, is regulation of differentiation, which has been shown to occur both indirectly and directly in many organisms. $p21^{-/-}$ mutant mice have hypomyelinated cerebella due to failure of oligodendrocyte formation. Importantly, these mice had no aberrant cell cycle exit phenotypes, therefore loss of $p21^{Cip1}$ during development directly inhibits oligodendrocyte differentiation (Zezula et al., 2001). $p27^{Kip1}$ has been shown to be involved in neuronal differentiation and migration

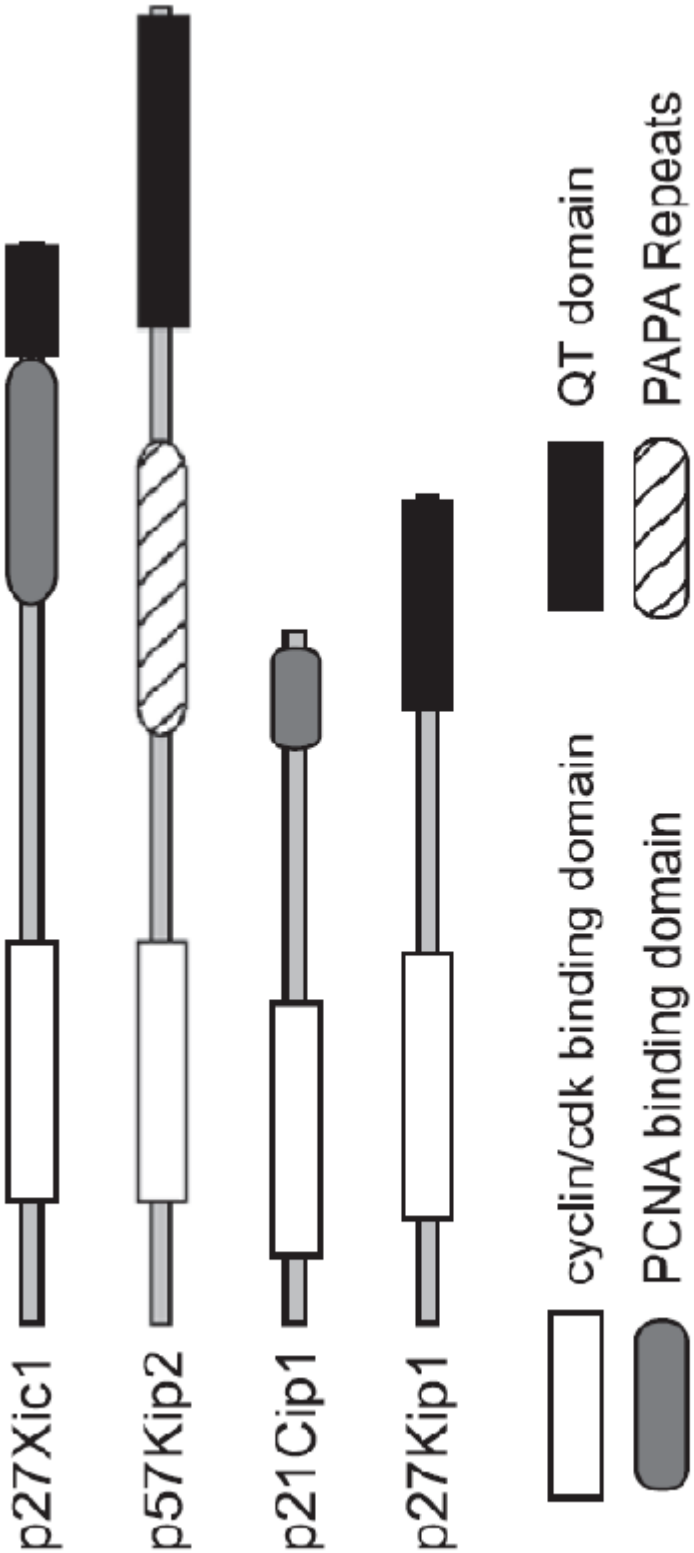

Figure 1.7 Illustration representing the different protein domains present in mammalian Cip/ Kip proteins and *Xenopus* p27^{Xic1}.

(Nguyen et al., 2006). The N-terminus of $p27^{Kip1}$ contains both the conserved cell cycle exit function and an uncharacterised differentiation function with the ability to stabilise Neurogenin-2 and promote formation of neuronal progenitors in the cortex. Nguyen et al (2006) used a mouse homozygous for a cell cycle mutant allele of $p27^{Kip1}$, *p27*$^{CK-}$, to show the increase they observed in neuronal markers was independent of cell cycle exit. Similarly, an N-terminal α-helix, spanning the conserved cyclin and cdk binding regions of $p57^{Kip2}$, has been shown to directly interact with MyoD and prevent its degradation, thus promoting expression of muscle-specific genes and directly stimulating myogenesis (Reynaud et al., 1999; Reynaud et al., 2000).

In *Xenopus*, three Cip/ Kip family members have been described; $p27^{Xic1}$, $p16^{Xic2}$ and $p17^{Xic3}$, the latter two are orthologues of $p21^{Cip1}$ and $p27^{Kip1}$ respectively (Su et al., 1995; Vernon et al., 2003; Vernon and Philpott, 2003; Daniels et al., 2004). The expression of $p16^{Xic2}$ and $p17^{Xic3}$ is highly developmentally regulated, suggesting they might be involved in cell cycle exit and cell fate determination in a tissue-specific manner (Daniels et al., 2004). The other homologue is $p27^{Xic1}$, which shows structural and functional similarities to $p21^{Cip1}$, $p27^{Kip1}$ and $p57^{Kip2}$ (Su et al., 1995; Shou and Dunphy, 1996) (Fig 1.7). The expression of *p27*^{Xic1} in early and tail bud embryos has been described and shown to play a role in neurogenesis, myogenesis, gliogenesis, and cardiogenesis where it regulates cell fate and determination, in addition to the cell cycle (Ohnuma et al., 1999; Ohnuma et al., 2002; Vernon et al., 2003; Vernon and Philpott, 2003; Movassagh and Philpott, 2008). Analysis of $p27^{Xic1}$ domains revealed the region responsible for this regulatory effect overlaps with, but is distinct from the cyclin/ cdk binding domain

located in the N-terminus (Ohnuma et al., 2002). In the nervous system $p27^{Xic1}$ has been shown to specifically stabilise X-NGNR-1, a homologue of mammalian Neurogenin-2, and in the muscle $p27^{Xic1}$ regulates myogenesis by synergizing with MyoD (Vernon et al., 2003; Vernon and Philpott, 2003). In *X. laevis*, neurogenesis and myogenesis are inhibited by $p27^{Xic1}$ depletion using morpholino oligonucleotides (MOs). These effects can be rescued by co-injecting the human homologue $p21^{Cip1}$ (Vernon et al., 2003; Vernon and Philpott, 2003), illustrating the similarity in function between $p27^{Xic1}$ and mammalian Cip/ Kip family members.

1.3.3 The role of the cell cycle in regulating organ size

Organogenesis requires directed cell cycle exit and differentiation to form organs of desired size and structure. Little is known about the molecular controls of growth that control organ size, it is likely these signals act to modulate the cell cycle and thus define organ growth and structure (Leevers and McNeill, 2005; Crickmore and Mann, 2008). Knowledge of the signalling pathways involved in regulating organ size has progressed mainly through research in plant organogenesis as the ability to produce larger crops has economical advantages to the agriculture industry. The *Arabidopsis thaliana* regulatory gene *AINTEGUMENATA* (*ANT*) is a transcription factor that regulates cell division and is required for floral organ growth as loss-of-function *ant-1* allele reduced the size of mature leaves through reduced cell number (Mizukami and Fischer, 2000). Jasinski et al over-expressed a tobacco CKI, *NtKIS1a*, in transgenic *A. thaliana* and found it reduced organ growth, producing plants with a reduced cell number (Jasinski et al., 2002). In metazoans organ size is also tightly regulated. Surgically reduced human livers are able to regenerate, growing back to pre-surgery size, then ceasing growth (Michalopoulos

and DeFrances, 2005). Dissected larval imaginal wing discs, transplanted into adult flies are able to regenerate and then develop into fully functional wings of appropriate size (Bryant and Schmidt, 1990). The authors of this paper described how neighbouring cells signal to each other through gap junctions, regulating cell proliferation and differentiation. Thus organ size is regulated in an organ-autonomous manner, though it is not clear if this mechanism is conserved.

Despite these conclusions, experiments in some model systems have shown the number of cell cycles does not regulate the size of an organ, but cell size is the important factor. Increased expression of *cyclin E* in the *Drosophila* imaginal wing disc enhanced cell proliferation, increasing the number of cells in the wing disc by 4-5 fold, but this did not alter the size of the mature wing (Neufeld et al., 1998). Tetraploid mice, prepared by electro-fusion and allowed to develop for 14 days were 85% the size of normal diploid mice, yet consisted of about half the number of cells (Henery et al., 1992). Organ size must therefore be regulated by more than just cell division, indeed cell growth, apoptosis, migration, and adhesion are all additive factors controlling organ size. CKIs are multi-functional proteins, thus it is highly likely they are involved in regulation of organ size through their dynamic array of functions.

1.4 Developmental control by the Notch signalling pathway

The animal kingdom utilises a strikingly small number of signalling pathways to ensure appropriate development. These signalling pathways are conserved between and utilised by all species to differing degrees of complexity. One such

example is the Notch signalling pathway, which is used during development to control cell fates, cell proliferation and cell death (for reviews see Lewis, 1998; Kadesch, 2004; Bray, 2006; Fiuza and Arias, 2007; Hayward et al., 2008).

The Notch signalling pathway involves extra-cellular interactions between large trans-membrane proteins that mediate binary cell signalling events. These interactions occur between the single trans-membrane Notch receptor and its ligands, Delta and Serrate/ Jagged, which are also trans-membrane proteins, on neighbouring cells (Fig 1.8). In mammals there are four *Notch* genes, three *Delta-like* genes and two *Jagged* genes. *Drosophila* has only one *Notch*-encoding gene, and one *Serrate* and one *Delta* homologue. *C. elegans* has two genes encoding Notch (*glp-1* and *lin-12*) and several Delta/ Serrate/ Lag-2 (DSL) homologues. In *X. laevis*, only one *Notch* gene, two *Serrate* genes and two *Delta* genes have been identified. Understanding the interactions between these gene products in *C. elegans* and *Drosophila* has paved the way for understanding mechanisms for how Notch signalling regulates development in vertebrates (Heitzler and Simpson, 1993; de Celis and Bray, 1997). This knowledge has aided our work in observing the regulation of pronephrogenesis by the Notch signalling pathway.

1.4.1 The core pathway

Figure 1.9 illustrates the core Notch signalling pathway that was deciphered during the 1990s. Notch receptors are constitutively cleaved in the Golgi apparatus by a furin-like convertase prior to transport to the plasma membrane. This post-translational modification is essential for formation of hetero-dimeric active Notch receptors in mammals (Logeat et al., 1998), although this modification is not

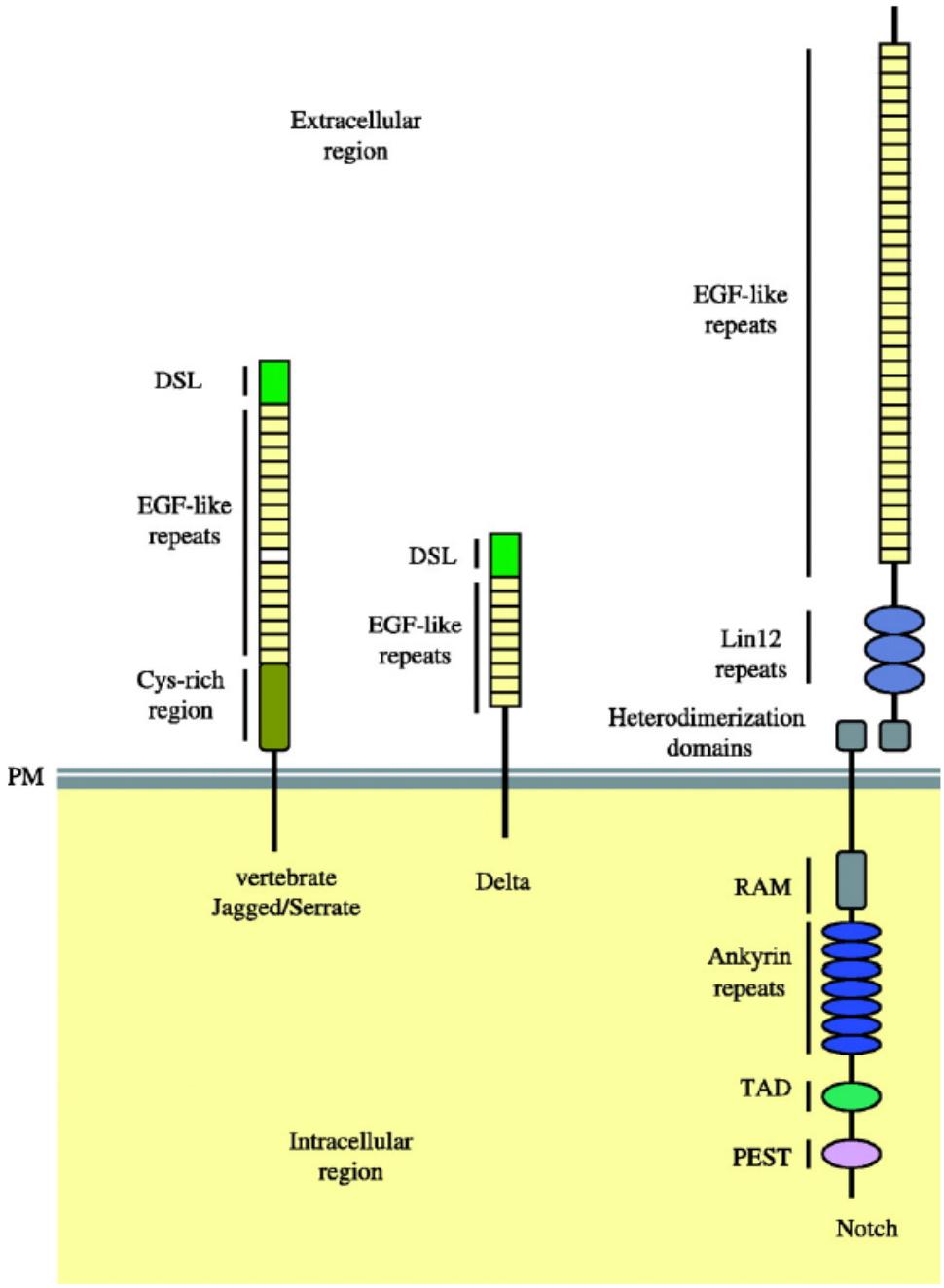

Figure 1.8 The structure of Notch and its ligands, Delta and Serrate (Jagged). A prototypical Notch gene encodes a single trans-membrane receptor whose extra-cellular domain consists of an array of conserved epidermal growth factor (EGF) repeats. Up to 36 EGF repeats can be present, of which EGF repeat 11 and 12 are sufficient for ligand interaction. Three juxta-membrane cysteine-rich Lin-12-Notch (LN) repeats modulate interactions between the extra-cellular and intra-cellular domains of the receptor. A hetero-dimerization domain non-covalently binds the membrane-tethered and extra-cellular regions of the receptor. The intra-cellular domain consists of seven ankyrin repeats (acting as structural motifs) flanked by two nuclear localisation signals, a transactivation domain (TAD) and a proline, glutamine, serine, threonine-rich (PEST) region. Delta and Serrate are each composed of a DSL region that interacts with the Notch receptor, and several EGF repeats, with Serrate/ Jagged also containing a juxta-membrane cysteine-rich region. (PM= Plasma membrane) (Schematic taken from Fiuza et al., 2007)

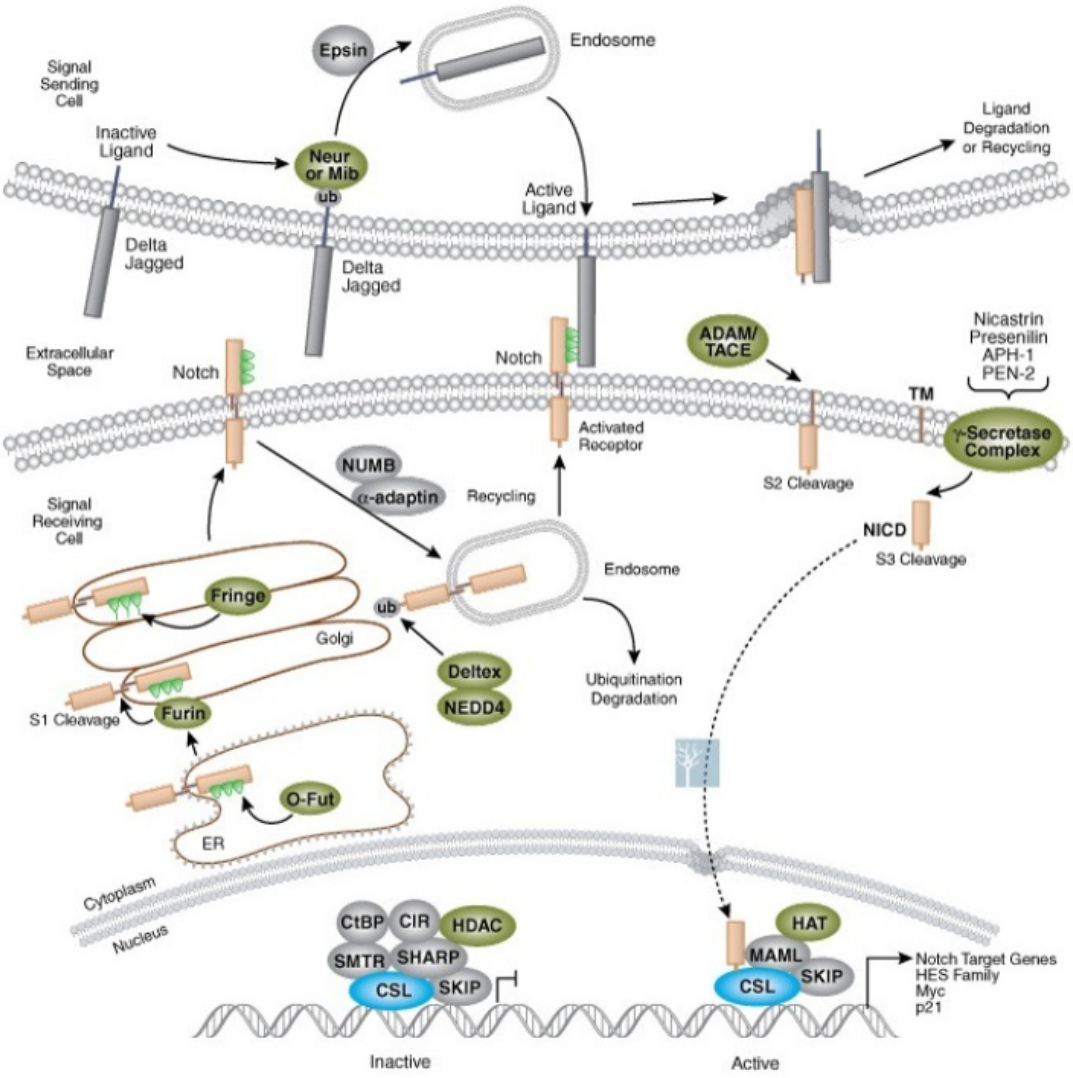

Figure 1.9 Schematic representation of the Notch signalling pathway. A representation of the post-translation modifications, the protein-protein interactions, protein degradation and the transcriptional activation events that occur during Notch signalling and which serve to control cell division, differentiation and death. See section 1.4.1 of the text for description (Schematic taken from Cell Signaling®)

necessary in flies (Kidd and Lieber, 2002). Notch receptors can be modified further by the Fringe class of proteins (Johnston et al., 1997; Irvine, 1999; Bruckner et al., 2000; Visan et al., 2006). Fringe proteins are glycosyl transferases that add sugar residues to sites on the extracellular EGF repeats of the Notch receptor that have been fucosylated by *O*-Fucosyl transferase (Okajima and Irvine, 2002). This modification increases affinity of Notch receptors for Delta ligands, but reduces Notch-Serrate interactions (Haines and Irvine, 2003). Once at the plasma membrane, mature Notch receptors can bind Delta and Serrate (DSL) ligands on opposing cells, this interaction results in two cleavage events on the Notch receptor (Kopan and Goate, 2000). Firstly a S2 cleavage, mediated by the metalloprotease TACE, releases the extra-cellular domain of the Notch receptor (Brou et al., 2000). This proteolysis enables the γ-secretase enzyme complex to perform a presenillin mediated S3 cleavage, liberating the intracellular domain of the Notch receptor (Notch-ICD) (Schroeter et al., 1998; Taniguchi et al., 2002). Notch-ICD then translocates to the nucleus where it binds to the CSL transcription factor switching it from a transcriptional repressor to a transcriptional activator (Jarriault et al., 1995). This altered gene expression directs the cell towards a specified cell fate.

The simplicity of the canonical Notch signalling pathway described above does not accurately reflect the actual processes that occur in the cells relaying the signal. Notch signalling is much more complex and regulation occurs at many levels (Kadesch, 2004; Bray, 2006). In recent years this complexity has been exposed and novel mechanisms have been discovered that further our understanding of how the Notch signalling pathway works. For example, recent research has shown Notch interaction with its DSL ligand switches the Notch receptor from an auto-inhibited

conformation, to a state that permits metalloprotease mediated S2 cleavage (Gordon et al., 2007). Despite such advances, many questions remain unanswered as to how the Notch signalling pathway elicits a cell response, and how signal transduction is regulated. A significant gap in our knowledge of how the Notch signalling pathway works is in the activity and regulation of the DSL ligands. Endocytosis of the extracellular remains of the Notch receptor, bound to its DSL ligand, is mediated by Neuralized (Neur) and Mind bomb (Mib) (Le Borgne et al., 2005a; Chitnis, 2006). Both are E3 ubiquitin ligases that share few structural similarities, yet can perform the same function (Le Borgne et al., 2005b). A mechanism for how these two proteins promote Notch signalling has yet to be defined. One suggestion is that Neur and Mib activate DSL ligands through partial degradation (Bray, 2006). Neur- and Mib-mediated ubiquitination of DSL ligands makes them targets for adaptor proteins such as Epsin (Wang and Struhl, 2004; Wang and Struhl, 2005). Such adaptor proteins promote endocytosis, which may be necessary for activation of DSL ligands or may occur after binding of the Notch receptor to its ligand, thus promoting Notch signalling as endocytosis permits S2 cleavage of the Notch receptor. The exact mechanism is yet to be defined, but ubiquitination of DSL ligands is necessary for Notch-ICD generation (Koo et al., 2005). Additionally, modulation of the Notch signalling pathway also occurs through ligand and Notch trafficking, ligand processing, CSL regulation, epigenetic regulators, ligand localisation, and Wnt signalling (see reviews Bray, 2006; Fiuza and Arias, 2007), with more levels of regulation likely to be discovered in the future. Notch signalling can also be activated and its signal processed independently of the core pathway illustrated in Figure 1.9. Calcium ions bind to EGF repeats on the Notch receptor, inhibiting its activity. In tissue-culture cells where calcium ions are depleted from the extra-cellular space,

there is potent ligand-independent activation of Notch receptors, leading to Notch signalling (Rand et al., 2000; Raya et al., 2004). CSL-independent Notch signalling is also known to occur, and is dependent on GSK3β (Brennan et al., 1997; Brennan et al., 1999b). This and other findings suggest a functional connection between the Notch and Wnt signalling pathways exists within cells (discussed further in section 1.4.3). In summary, interpretation of the molecular control of Notch signalling is much more complex than originally perceived as many underlying regulatory mechanisms in this pathway remain unknown.

1.4.2 The mechanisms of action of the Notch signalling pathway

Despite knowledge of the complexity of the Notch signalling pathway being a major focus in current research, our aim was not to uncover new details regarding the molecular control and effects of Notch signalling, but rather to understand a mechanism by which the Notch signalling pathway regulates pronephrogenesis, or pronephric patterning.

During development the cell-cell action of the Notch signalling pathway is utilised by tissues in three different ways; lateral inhibition, asymmetrical inheritance, and boundary formation (Fig 1.10). Lateral inhibition is the best characterized mechanism by which Notch signalling acts, and is a process that spatially assigns particular cell fates in many developing tissues. It is based around the idea that cross-talk between neighbouring cells through Notch-ligand interactions ensures one cell acquires a particular cell fate, due to active CSL-mediated transcription, but the opposing cell is inhibited to acquire the same fate as its CSL transcription complex remains repressive. The spatial arrangement of neural progenitors,

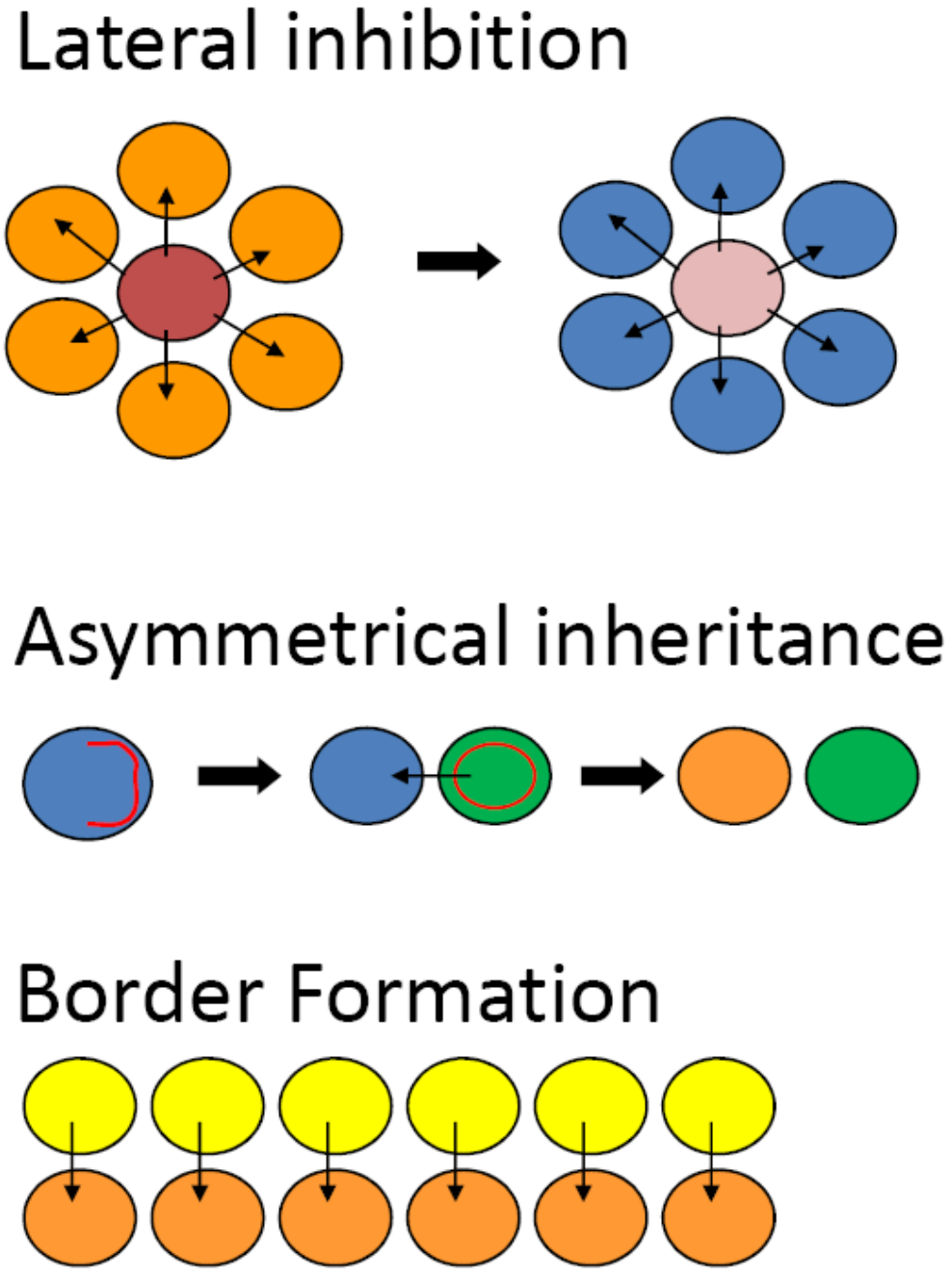

Figure 1.10 The three different modes of action of the Notch signalling pathway. *Lateral Inhibition* – small changes in a particular cell allow it to present Notch receptors that DSL ligands on neighbouring cells can interact with. Consequently this cell acquires a specific cell fate, a fate that this cell inhibits in surrounding cells due to their binding of Notch receptors, rather than presentation of Notch receptors on the cell surface. *Asymmetrical inheritance* – Localisation of particular maternal proteins involved in regulation of Notch signalling permits a one daughter cell to signal to the second daughter cell, and inhibit it acquiring a similar cell fate. *Boundary Formation* – Components of the Notch signalling pathway are expressed at the boundary between two distinct cell populations. Cell-cell interactions at this boundary are mediated by Notch and its various DSL ligands, ensuring maintenance (or establishment) of the boundary and thus permitting the cells on either side to proceed along defined lineages.

epidermal ciliated cells (Deblandre et al., 1999; Marnellos et al., 2000; Liu et al., 2007), inner ear hair cells (Kiernan et al., 2005), butterfly wing scales (Reed, 2004), distinct hormone secreting cell types in endocrine glands (Dutta et al., 2008), and sensory cells in the ear (Haddon et al., 1998) are just a small number of the many examples of lateral inhibition being utilised during development.

The principle of asymmetrical inheritance is similar to lateral inhibition, whereby one cell inhibits its neighbour from acquiring a particular cell fate. However the differing protein content of each cell has been ordered by the parent cell, where asymmetric localization of cell fate determinants results in daughter cells acquiring specific proteins subsequent to cytokinesis. Asymmetrical division regulates Notch signalling in the sense organ precursor (SOP) cell lineage in *Drosophila* (Schober et al., 1999; Wodarz et al., 1999; Wodarz et al., 2000). The SOP cell gives rise to the pI cell, which goes through four asymmetric divisions that permit only one daughter cell to contain the Notch regulator proteins Numb and Neur. These asymmetric divisions are essential for production of glial, hair and external socket cells, as well as neurons in the *Drosophila* nervous system (Manning and Doe, 1999). Such asymmetric divisions during stem cell inheritance are not restricted to neural stem cells, haematopoietic (Chiba, 2006) and intestinal (Ohlstein and Spradling, 2007) stem cells also undergo asymmetric division to produce either Notch-presenting or signal-sending daughter cells that proceed to inhibit one another from acquiring the same cell fate.

The final mode of action of the Notch signalling pathway during development is the establishment of boundaries between distinct cell populations. This process is

common during development as there are frequently occasions in developing tissues or organs where boundaries between juxtaposed cell populations are required to be established. Three well characterised examples are the dorsal-ventral boundary in the *Drosophila* imaginal wing disc, the dorsal-ventral boundary in the vertebrate limb bud, and the demarcation of somitic boundaries during paraxial mesoderm segmentation.

Establishment of a dorsal-ventral boundary in the Drosophila imaginal wing disc

Drosophila melanogaster, has been, and continues to be a powerful model organism for understanding classical and molecular genetics. Flies have provided insights into many areas of developmental biology, indeed the Notch signalling pathway was first discovered in *Drosophila* by Dexter (1914), who described how a mutant of *notch* caused wing notching.

The Notch signalling pathway has been identified as essential in establishing the dorsal-ventral boundary of the *Drosophila* imaginal wing disc. Larval stage *Drosophila* form imaginal discs as a base to form appendages and organs such as the wing, leg, eye/ antenna, and haltere. The imaginal wing disc is derived from embryonic ectoderm and is patterned across both its anterior-posterior and dorsal-ventral axes to form an adult wing of specified size and orientation (Fig 1.11A). A hierarchy of regulatory genes subdivide the wing; *decapentaplegic*, *patched* and *hedgehog* regulate anterior-posterior patterning (Capdevila et al., 1994) and the Notch and Wnt signalling pathways regulate formation of a dorsal-ventral (d/ v) boundary (Irvine and Wieschaus, 1994; Rauskolb et al., 1999). *apterous* expression is restricted to the entire dorsal region of the wing disc by *wingless* (Williams et al., 1993). It acts to induce dorsal cell fates, as opposed to *vestigial*, which is expressed

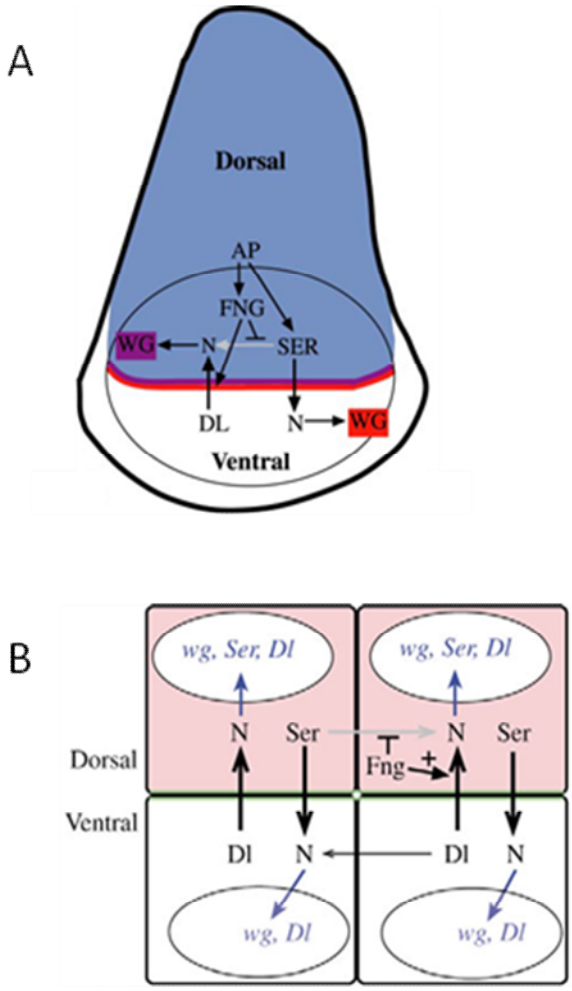

Figure 1.11 Dorsal/ Ventral compartmentalisation of the *Drosophila* imaginal wing disc. (A) Dorsal cells are blue, with dorsal *wingless* expression purple and ventral *wingless* expression red. Apterous (a dorsal specific gene) induces expression of *fringe* and *Serrate* in the dorsal compartment of the wing disc. Fringe acts to inhibit Notch-Serrate interactions, but at the wing margin Serrate is able to interact with Notch receptors on the ventral side (as these are not modified by Fringe). Notch-Delta interactions can occur on either side of the wing margin, however they are more prominent on the ventral side as there is no competition with Notch-Serrate interactions (additionally, later on *Delta* expression becomes restricted to the ventral side). (B) highlights these interactions at the cellular level. Notch-Serrate interactions cause gene expression that promotes dorsalisation in the ligand-presenting cell, but ventralisation in the receptor-presenting cell. Notch-Delta interactions induce the opposite effect. Abbreviations; AP- apterous, FNG- fringe, N- notch, SER- serrate, WG- wingless, DL- delta (Schematics adapted from Irvine and Rauskolb, 2001 (A); and Panin et al., 1997 (B))

in the ventral region of the wing disc and imparts ventral cell fates. At the boundary of *apterous* and *vestigial* expression lies the wing margin. Here *wingless, Delta, Serrate, Notch* and *fringe* are expressed and act to establish and maintain a boundary between the dorsal and ventral compartments. Initially Notch acts to promote *wingless* expression such that it straddles the d/ v boundary (Diaz-Benjumea and Cohen, 1995). This expression then becomes more refined due to the auto-inhibitory effect Wingless has on its own expression in neighbouring cells (Micchelli et al., 1997). Wingless also promotes expression of *delta* and *serrate* at the d/ v boundary (de Celis and Bray, 1997). Whilst *delta* is initially expressed on both sides of the boundary, *serrate* expression is only ever expressed on the dorsal side (Major and Irvine, 2005). The restriction of Notch ligands to either side of the border is the major contributory factor in establishment and maintenance of the d/ v boundary. Notch is expressed on either side of the boundary but Notch-ligand interactions are specifically modulated by Fringe (Panin et al., 1997). Fringe acts to post-translationally modify Notch receptors in the Golgi apparatus such that they preferentially bind Delta ligands. Fringe proteins are glycosyl transferases that extend carbohydrate chains from the initial fucose sugar added to EGF repeats on the Notch receptor by *O*-fucosyl transferase (Moloney et al., 2000; Haines and Irvine, 2003). *fringe* expressing cells in the dorsal compartment of the wing produce Notch receptors that have a higher affinity for Delta, whereas Notch receptors in the ventral compartment can bind both Serrate and Delta. Consequently the cells with Notch-Serrate interactions are ventralised and result in the expression of genes such as *wingless, delta* and *vestigial*, whereas Notch-Delta interactions are dorsalising and induce expression of genes such as *wingless, serrate* and *apterous* (Figure 1.11B). Fundamentally therefore, the Notch and Wnt signalling pathways and Fringe

establish positive feedback mechanisms that ultimately regulate d/ v boundary formation in the *Drosophila* imaginal wing disc.

Notch signalling regulates positioning of the Apical Ectodermal Ridge in the vertebrate limb bud

Vertebrate appendages arise from limb fields, which are specified to form in the correct position by the Hox genes (Zakany et al., 2004). Limb fields form from lateral plate and somitic mesoderm and are patterned across their dorsal-ventral (d/ v), proximal-distal (p/ d) and anterior-posterior (a/ p) axes to form correctly structured limb appendages (for reviews see Johnson and Tabin, 1997; Chen and Johnson, 1999; Niswander, 2003). In simplistic terms the limb bud constitutes mesenchyme tissue with an overlying ectodermal layer. Notch signalling has been identified in patterning the ectodermal layer of the limb bud.

At around the same time the mechanism for Fringe and Notch signalling regulation of d/ v boundary formation was being deciphered in the *Drosophila* imaginal wing disc, it was discovered, somewhat remarkably, that the same mechanism could be patterning the d/ v axis of the vertebrate limb bud (Irvine and Vogt, 1997). The apical ectoderm ridge (AER) is a specialised epithelial structure that runs along the a/ p axis of the limb bud at the d/ v interface (Carrington and Fallon, 1984). *Radical fringe*, a vertebrate homologue of *Drosophila fringe*, regulates AER formation and positioning in chick limb buds (Laufer et al., 1997; Rodriguez-Esteban et al., 1997). Surprisingly, this function is not conserved in the mouse limb bud, even though *Radical fringe* is expressed in a similar domain (Moran et al., 1999). In chick embryos, it is believed dorsal *Notch1*, *Serrate2* and *Radical fringe*-

expressing cells confront *Notch1* and *Delta1*-expressing ventral cells in the AER, thus regulating where the AER forms in a similar manner to regulation of the wing margin in *Drosophila* (Irvine and Vogt, 1997; Lewis, 1998). The AER is a critical component of vertebrate limb development as it produces growth factors of the FGF family that signal to the 'progress zone' directly beneath it, maintaining cell proliferation in the underlying mesenchyme and thus controlling the different skeletal anlagen that develop along the p/ d axis according to the progress zone model of vertebrate limb development (Wolpert, 2002). Engrailed-1 (En-1) restricts *Radical fringe* expression to dorsal ectoderm of the limb bud, and when *En-1* expression is inhibited, or *Radical fringe* is over-expressed, new AERs form at the boundary between *Radical fringe* expressing and non-expressing cells, causing additional limb outgrowth (Laufer et al., 1997; Rodriguez-Esteban et al., 1997). Despite these findings a definitive mechanism for positioning of the AER by the Notch signalling pathway, presumably regulated by Radical fringe, has not been elucidated. The early embryonic lethality of Notch-deficient mice (Conlon et al., 1995) and the inability to observe *Delta1* expression in the ventral portion of the AER are reasons for a mechanism not being defined. However it seems highly plausible to suggest the d/ v boundary in the vertebrate limb bud is established by the Notch signalling pathway by a similar mechanism to the *Drosophila* wing margin.

Notch signalling and the regulation of segmental boundaries

Segmentation of the vertebrate embryo begins when the paraxial (or presomitic) mesoderm immediately caudal to the otic vesicle subdivides into repeated epithelial structures called somites (Pourquie, 2001). Somites are important embryonic tissues as they proceed to form precursors of the axial skeleton, which

forms the ribs and vertebra, and dorsal dermamyotome, which contributes to the skeletal muscles and dermis of the back (Hirsinger et al., 2000). Somitogenesis requires boundaries to form between somitic and presomitic mesoderm, unsurprisingly, this process is regulated by the Notch signalling pathway (for reviews see Conlon et al., 1995; Irvine, 1999; Cinquin, 2007; Ozbudak and Pourquie, 2008). Periodic expression of genes involved in Notch signalling, regulate a molecular oscillator that initiates somitogenesis in an anterior to posterior wave across the presomitic mesoderm (Pourquie, 2001). The most widely acknowledged theoretical model of vertebrate segmentation is the 'clock and wave-front' model (Cooke and Zeeman, 1976; Cooke, 1998). Dynamic waves of expression of genes such as *hairy* and *Lunatic fringe* ensure periodically activated Notch signalling in the presomitic mesoderm (PSM) regulates the intermittent formation of somites (Palmeirim et al., 1997; Evrard et al., 1998; Prince et al., 2001; Dale et al., 2003). In addition to the Notch signalling pathway, the Wnt and FGF signalling pathways also instruct somitogenesis through a Wnt3a/ FGF8 gradient that regresses posteriorly and positions the 'determination front' where the next somite will form (Déqueant and Pourquíe, 2008). Despite this knowledge, exactly how oscillatory expression patterns of genes involved in these pathways are established and then generate somites remains unclear.

There are numerous review articles that attempt to explain the process of vertebrate segmentation, all of which differ with respect to the fine details of how gene expression patterns orchestrate somitogenesis (Cinquin, 2007; Déqueant and Pourquíe, 2008; these reviews highlight the differences in the current opinion of how segmentation is regulated). Indeed the mechanistic interactions between many of the

elements involved in somitogenesis remain poorly understood and controversial. Here, we will attempt to explain how the Notch signalling pathway is involved in the process of clock-regulated somite formation, emphasising the role of Lunatic fringe in this process (an additional role for Lunatic fringe in anterior-posterior patterning of the PSM is not discussed (see Shifley et al., 2008).

The molecular basis of the clock and wave-front model of segmentation is described in Figure 1.12. It is believed the Notch signalling pathway and the gene expression it induces acts as a 'clock' in the anterior PSM that permits somites of defined size and structure to form, although how such gene oscillations are generated remains unknown (Ozbudak and Pourquie, 2008). *Lunatic fringe* and a downstream mediator of Notch signalling, *hairy*, have a dynamic oscillating wave of gene expression across the posterior PSM, which upon localising to the anterior end of the PSM will form a somite (Fig 1.12). Notch-ICD directly up-regulates Fringe clock element 1 (FCE1), a 110 bp conserved region that acts as a cyclic promoter of *Lunatic fringe* in the posterior PSM (Cole et al., 2002), thus Notch signalling induces *Lunatic fringe* expression. However, how this establishes somitic boundaries is a controversial point. Originally it was argued the molecular oscillating 'clock' anterior to the determination front makes a cohort of cells permissive for somitogenesis. These cells express *Mesp2*, which activates *Lunatic fringe* expression and suppresses *Delta-like 1* expression (Morimoto et al., 2005). As *Mesp2* is expressed initially across the whole somite, the lack of *Delta-like 1* expression within the somite means that at somitic boundaries, Notch signalling is active. Indeed this Notch signalling instructs where the anterior and posterior extremities of the somite will form (Déqueant and Pourquíe, 2008). Initially it was argued that a negative

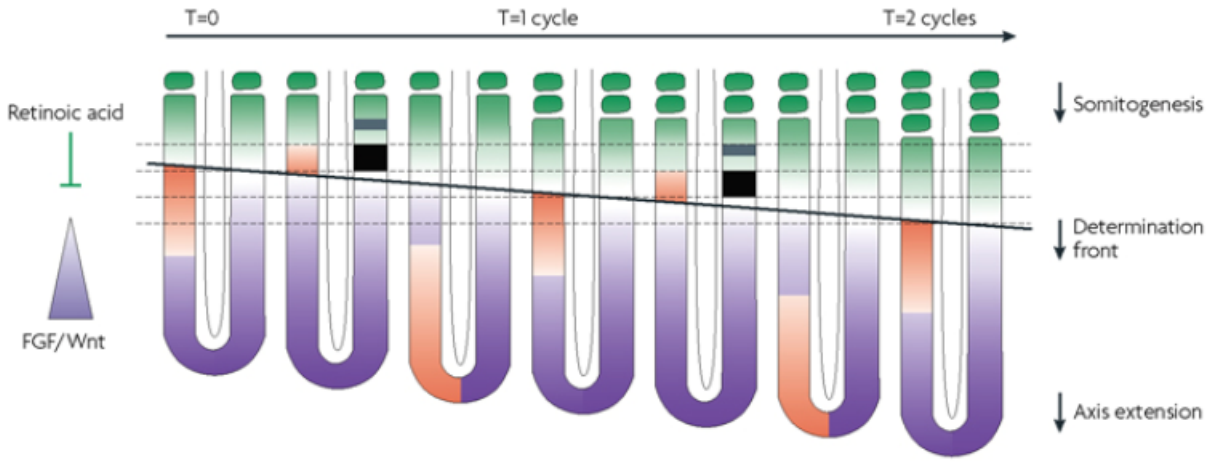

Figure 1.12 A model for somitogenesis. Vertebrate segmentation occurs as a consequence of boundaries set up by a molecular oscillatory clock in the anterior presomitic mesoderm (PSM) that is switched ON when a wave of gene expression from the posterior PSM moves anteriorly. This wave of expression is shown in red on the left side of the embryos shown in the figure. The posterior PSM is a mass of cells that are mesenchymal at the extreme posterior, yet undergo epithelialisation towards the anterior. This mesenchyme to epithelial transition is regulated by an anterior-posterior gradient of FGF8 and Wnt3a. Wnt3a induces expression of *FGF8*, and its subsequent signalling, which stimulates *Snai* gene expression. Snai proteins inhibit expression of genes involved in epithelialisation, such as *integrins*, *cadherins*, and genes involved in basal lamina formation, such as *laminin* and *fibronectin*, thus Snai proteins inhibit somitogenesis. The threshold whereby FGF and Wnt signalling permits epithelialisation coincides with the determination front, which is a virtual boundary, anterior to which somitogenesis can occur. The wave of expression of genes involved in the Notch signalling pathway, such as *Lunatic fringe* and *hairy*, eventually migrates anteriorly where they establish a stripe of *Mesp2* expression (anterior black block on the right of the embryo). The posterior boundary of *Mesp2* expression corresponds to the position of the determination front. It is proposed Mesp2 stabilises Lunatic fringe, permitting it to inhibit Notch activity. However in the regions anterior and posterior to the block of *Mesp2* expression there is no Lunatic fringe stabilisation, therefore Notch signalling is active. This produces and interface between two populations of cells, which is believed to define the boundaries within which a somite will form, consequently the wave of expression of *Lunatic fringe* and *hairy* from the posterior PSM to the anterior PSM, and the molecular clock in the anterior PSM that allows somitogenesis means a somite of defined size and structure will form. Retinoic acid (RA) is believed to inhibit FGF signalling in the anterior PSM and thus aid somitogenesis. Later Mesp2 becomes localised to the anterior region of the somite and specifies the anterior-posterior axis of each somite, again through its action on Lunatic fringe. (Déqueant and Pourquíe, 2008)

feedback loop existed whereby Mesp2 stabilised Lunatic fringe, which then inhibited Notch signalling by modifying Notch receptors such that they could not interact with Delta-like 1 (Morimoto et al., 2005). This theory is inconsistent with the effect Lunatic fringe has on Notch receptors in the vertebrate limb and the *Drosophila* imaginal wing disc (described above), where Fringe proteins have been implicated in promoting Notch interaction with Delta receptors, not inhibiting them. Despite this, it can be acknowledged that segmentation, whilst still exploiting the activities of Fringe proteins and the Notch signalling pathway, utilises a different mechanism to promote boundary formation to those observed in the *Drosophila* imaginal wing disc and vertebrate limb as there is no requirement for differential *Serrate*/ *Delta* expression. This is likely due to a number of factors; temporal control of expression of components of the Notch signalling pathway and additional regulation of Lunatic fringe are two possibilities. Segmentation therefore is a good example of how developing organisms utilise the Notch signalling pathway in dynamic ways to establish boundaries.

1.4.3 The 'Wntch' signalling pathway?

Many reports have indicated a recurrent and consistent relationship between the Notch and Wnt signalling pathways (Hayward et al., 2006; Hurlbut et al., 2007). It has been argued that these two pathways act as an integrated device that increases the probability a cell will acquire a specific cell fate (Hayward et al., 2008). Interpretation of these reports has led to the proposition that the Notch signalling pathway requires Wnt signalling during its signal transduction, suggesting that the Notch signalling pathway should be redefined as the 'Wntch' signalling pathway.

Wnt signalling consists of a complex pathway where cells excrete morphogenic Wnt glycoproteins that elicit responses on nearby cells by triggering three intracellular events (β-catenin-mediated, planar cell polarity and Ca^{2+}-related signalling) (Fig 1.13 describes the canonical Wnt signalling pathway in detail). In all three of the examples describing how the Notch signalling pathway regulates boundary formation, the Wnt signalling pathway is required. Furthermore lateral inhibition has been shown to absolutely require Wnt signalling (Couso et al., 1994), and there is a consistent requirement for Wnt signalling to pre-pattern cells, prior to Notch signalling activity (Hayward et al., 2008).

The mechanism by which the Wnt and Notch signalling pathways interact is still to be resolved. Knowledge from the development of the *Drosophila* imaginal wing disc has shown these two pathways can regulate each other's gene expression; Notch induces *wingless* expression (Diaz-Benjumea and Cohen, 1995), and, after refining its own expression (Rulifson et al., 1996), Wingless promotes expression of *Delta* and *Serrate* (Klein and Arias, 1998). Originally it was believed functional interaction between the Wnt and Notch signalling pathways was through negative cross-talk, perhaps through a 'presenilin hub' (De Strooper and Annaert, 2001). Presenilins mediate the degradation of β-catenin and are the catalytic subunit within γ-secretase that performs the S3 cleavage and releases Notch-ICD. Presenilin-mediated degradation of β-catenin requires a hydrophilic loop in the cytoplasmic domain of Presenilin (Saura et al., 2000). Interestingly, this cytoplasmic loop is not required for Notch processing, therefore the proteolysis of Notch and β-catenin by Presenilin is distinct (Soriano et al., 2001), indicating a possible role for Presenilin in inhibitory cross-talk between these two pathways. Further inhibitory cross-talk was

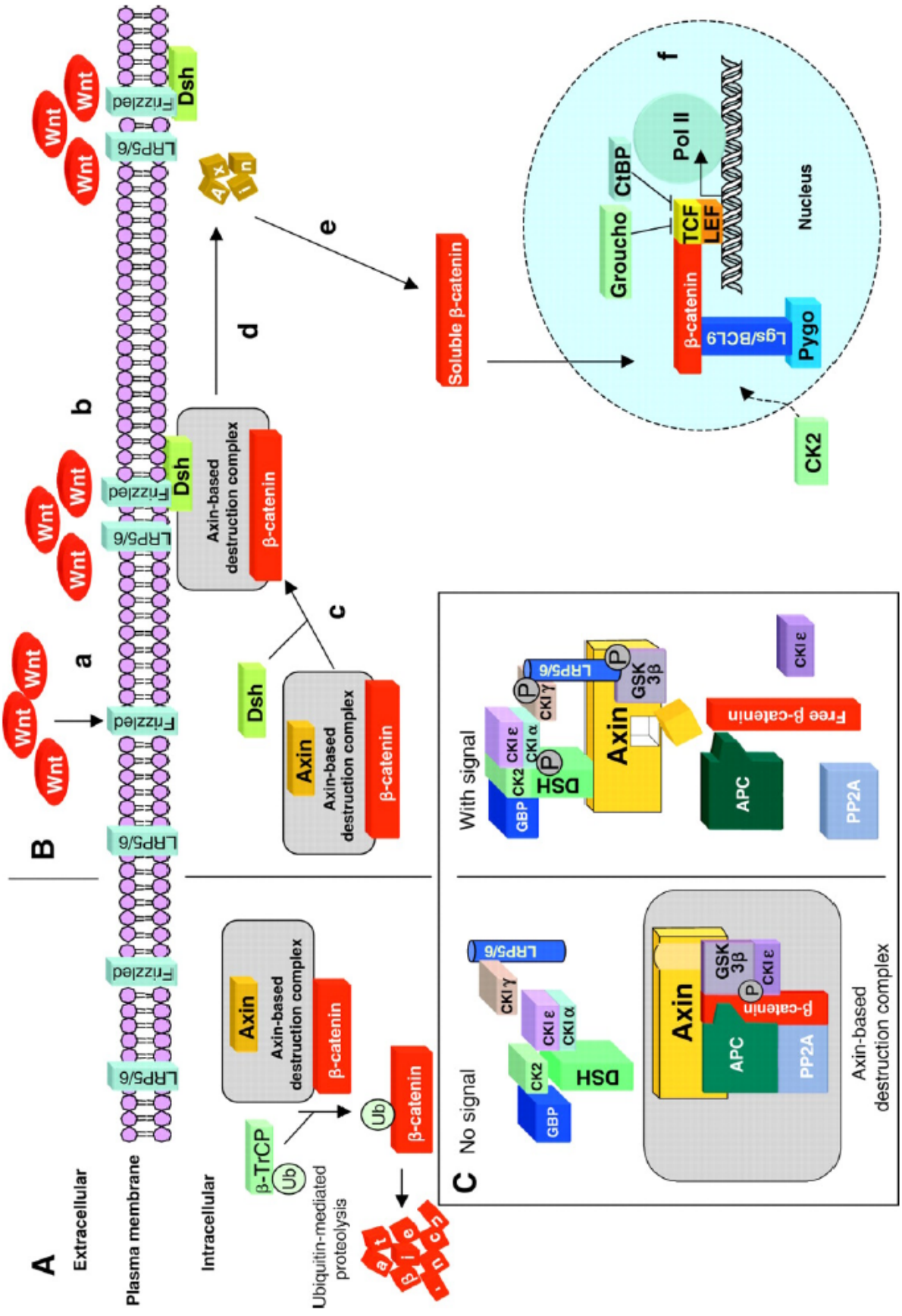
A
Extracellular
Plasma membrane
Intracellular
Ubiquitin-mediated proteolysis
B
a
b
c
d
e
f
Wnt
Frizzled
LRP5/6
Dsh
Axin-based destruction complex
β-catenin
β-TrCP
Ub
Axin
Soluble β-catenin
Nucleus
Groucho
CtBP
Pol II
TCF LEF
Lgs/BCL9
Pygo
CK2
C
No signal
With signal
GBP
CK2
CKI ε
CKI α
CKI γ
DSH
GSK 3β
APC
PP2A
P-catenin
Free β-catenin

Figure 1.13 The canonical Wnt signalling pathway. (A) When the Wnt signal is not present, Frizzled and LRP receptors in the plasma membrane cannot order the inactivation of the Axin-based destruction complex (see C, no signal). Consequently cytoplasmic β-catenin is inactivated by GSK3β-mediated phosphoryation, then poly-ubiquitinated and destroyed. As a consequence, β-catenin is unable to act as a transcription factor and specify particular cell fates. (B) Active Wnt signalling permits Dishevelled to inhibit the action of Axin-based destruction complex (the mechanism of how Dishevelled permits this remains unknown). Consequently cytoplasmic β-catenin concentrations rise and it can translocate to the nucleus where it interacts with the TCF/ LEF transcription complex, switching it to a transcriptional activator. The subsequent altered gene expression promotes specific cell fate decisions. Abbreviations; Dsh- Dishevelled, APC- adenomatous polyposis coli, PP2A- Protein Phosphatase-2A, CK- Casein Kinase, GBP- GSK-3β Binding Protein, LRP- Lipoprotein receptor-related protein, β-TrCP- Beta transducin repeat containing protein , Pygo- Pygopus (nuclear located protein), Pol II- DNA Polymerase II, CtBP- C-terminal Binding Protein (Schematic taken from Hayward et al., 2008)

observed by Axelrod et al (1996) who showed Dishevelled directly binds to the carboxy-terminus of the Notch receptor; an interaction they believed was antagonistic. The Notch signalling pathway can also suppress Wnt signalling. Notch has been shown to bind Armadillo (β-catenin) and complex functional interactions exist between Notch and Axin in *Drosophila* (Hayward et al., 2005; Hayward et al., 2006). Altogether these interactions highlight the integration of these two signalling pathways, yet do not explain the mechanics of how these interactions modulate signal transduction of either pathway. The fundamental importance of these pathways during development suggests these interactions are critical and future research will likely identify the significance of these interactions.

1.4.4 Regulation of nephrogenesis by the Notch signalling pathway

The Notch signalling pathway plays an integral role in development of all renal structures, from the Malpighian tubules in *Drosophila* to each renal form observed during development of the vertebrate kidney. Aberrant Notch signalling is a common cause of renal disease and cancer. Below, the role of Notch signalling in development of the various renal forms is described.

Notch signalling and the specification of the tip cell in Drosophila Malpighian tubules

In insects, excretion of nitrogenous waste and excess water is performed by the Malpighian tubules. Whilst the Malpighian tubules share little equivalence with vertebrate kidney forms, they are an excellent model of tubulogenesis thanks to their simplicity and the advantages of using *Drosophila* as a genetic model organism. The four Malpighian tubules are ectodermally derived from a posterior anlage (the

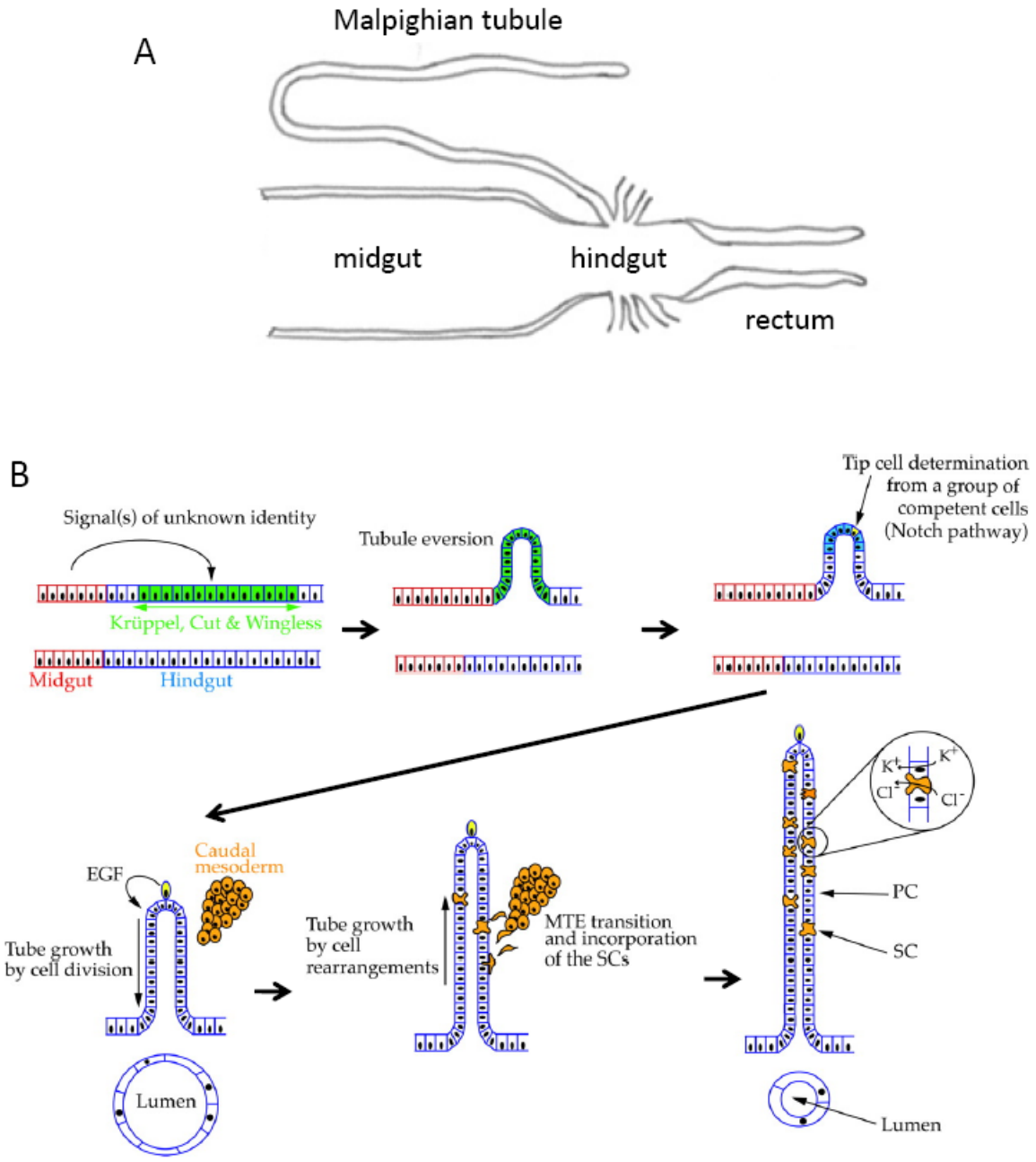

Figure 1.14 Development of the Malpighian tubules. (A) Schematic of a mature Malpighian tubule projecting out of the hindgut. (B) A signal between the mid- and hindgut, of unknown identity, establishes a region of cells in the ectoderm of the hindgut that will form a tubule. These cells are distinguished by their *kruppel*, *cut* and *wingless* expression. Soon after formation these cells initiate tubulogenesis. After eversion, the tubule requires a growth phase in order to elongate. In *Drosophila*, cell proliferation of developing Malpighian tubules is under the control of a tip cell. A tip cell will form within a group of competent cells through the process of Notch-mediated lateral inhibition. The tip cell then secretes epidermal growth factor (EGF) and induces cell proliferation, extending the tubule. Once cells have ceased dividing, complex re-arrangements and intercalation occurs to produce a mature and functional tubule. PC – Principal cells, SC – Stellate cells, MTE – Mesenchyme To Epithelial transition (Images adapted from Jung et al., 2005)

proctodeum, which will give rise to the hindgut) during early embryogenesis (Hoch et al., 1994). Subsequent cell proliferation establishes blind end tubules composed of approximately 120 epithelial cells (Wilkins, 1995). A domain of *kruppel*, *cut* and *wingless* expression allocates cells that will initiate tubule eversion (Fig 1.14) (Jung et al., 2005). The growth phase that commences is tightly controlled by a specialized tip cell. Within a group of competent cells around the tip of the extending tubule, Notch-mediated lateral inhibition will single out a specific cell that acquires a distinct cell fate; this cell is termed the tip mother cell. The two daughter cells that form after division of the tip mother cell inhibit each other acquiring the same cell fate through Notch-ligand interactions. Consequently, one will become the tip cell and the other will become an epidermal cell (Pugacheva and Mamon, 2005). Once the tip cell has differentiated it secretes epidermal growth factor, stimulating mitosis in neighbouring cells and enhancing cell proliferation of the tubule. In embryos that have mutant *notch*, *mastermind* or *neuralised* genes, the Malpighian tubules cease growing after the 17^{th} cell cycle and are half the size of wild type tubules (Pugacheva and Mamon, 2005). In conclusion the Notch signalling pathway plays an integral part in regulating the size of Malpighian tubules in insects through regulation of tip cell formation, which actively controls cell proliferation within each tubule.

Cilia formation in the zebrafish pronephros is regulated by Notch signalling

The zebrafish pronephros is similar in form and function to the *X. laevis* pronephros (Fig 1.15). However, the zebrafish pronephros is a closed system containing a bilateral pair of tubules directly connected to a midline fused glomerulus (Drummond et al., 1998). It does not have a functional coelom, or nephrostomes, as found in amphibian pronephroi. Furthermore the distribution of

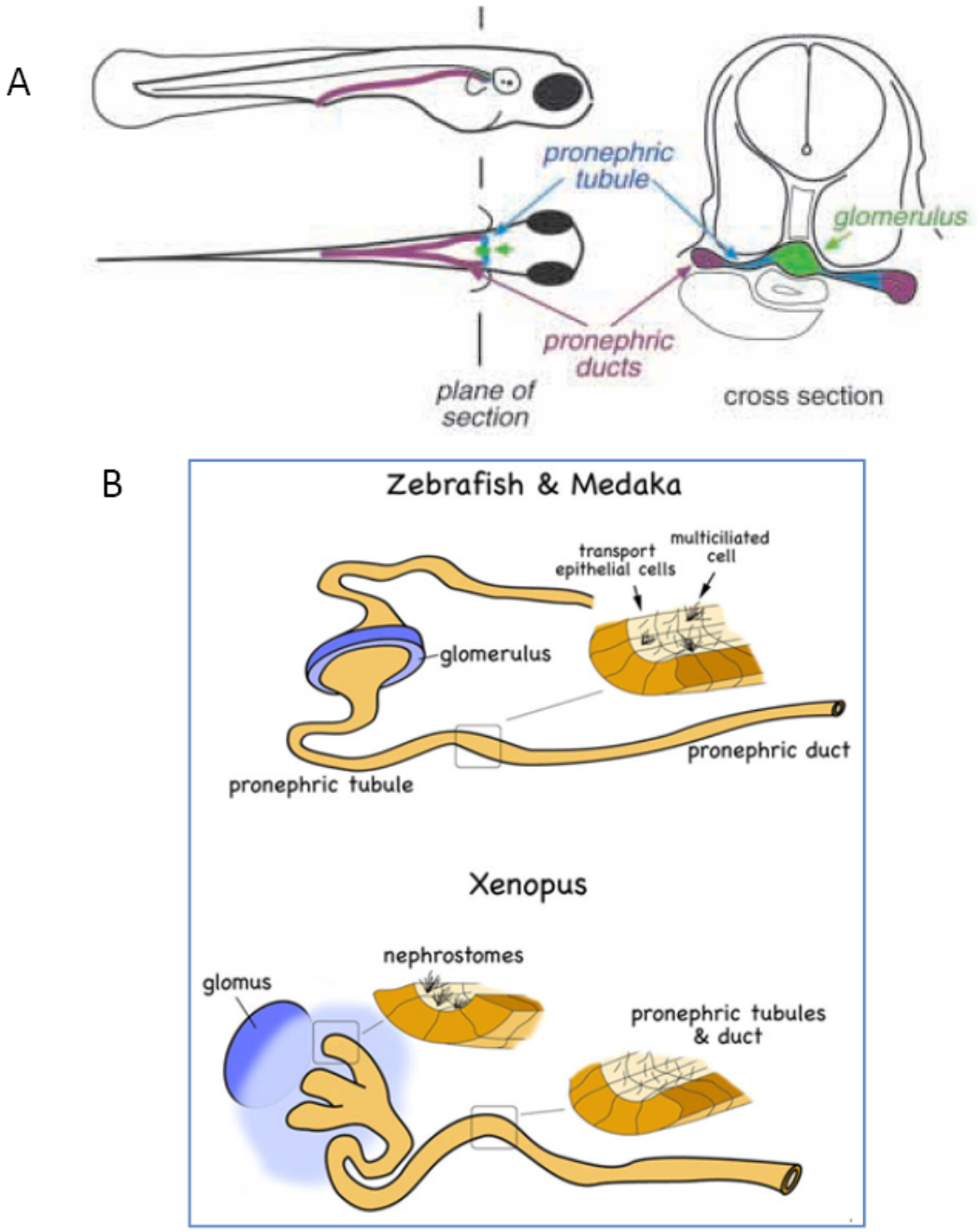

Figure 1.15 The zebrafish pronephros and how it differs from the *X. laevis* pronephros. (A) Lateral, dorsal and transverse views of the bilateral pronephric tubules and duct with a midline fused glomerulus. (B) Diagram illustrating the differences between teleost and amphibian pronephroi. The zebrafish pronephros is a closed system with a fused central glomerulus that both sets of tubules on either side of the embryo use to collect waste fluid. The pronephric system in zebrafish is closed as there is no coelomic cavity, the glomerulus is directly connected to the pronephric tubules. The pattern of ciliated cells in teleosts is in a 'salt and pepper' distribution, a pattern that is controlled by Notch-mediated lateral inhibition. The amphibian pronephros is an open pronephric system, with a single glomus for each of the two pronephroi found in a single embryo. Furthermore the distribution of ciliated cells differs to teleosts. All multicilliated cells in amphibian pronephroi are found in the nephrostomes. (Images adapted from Drummond et al., 1998; and Wessely and Obara, 2008)

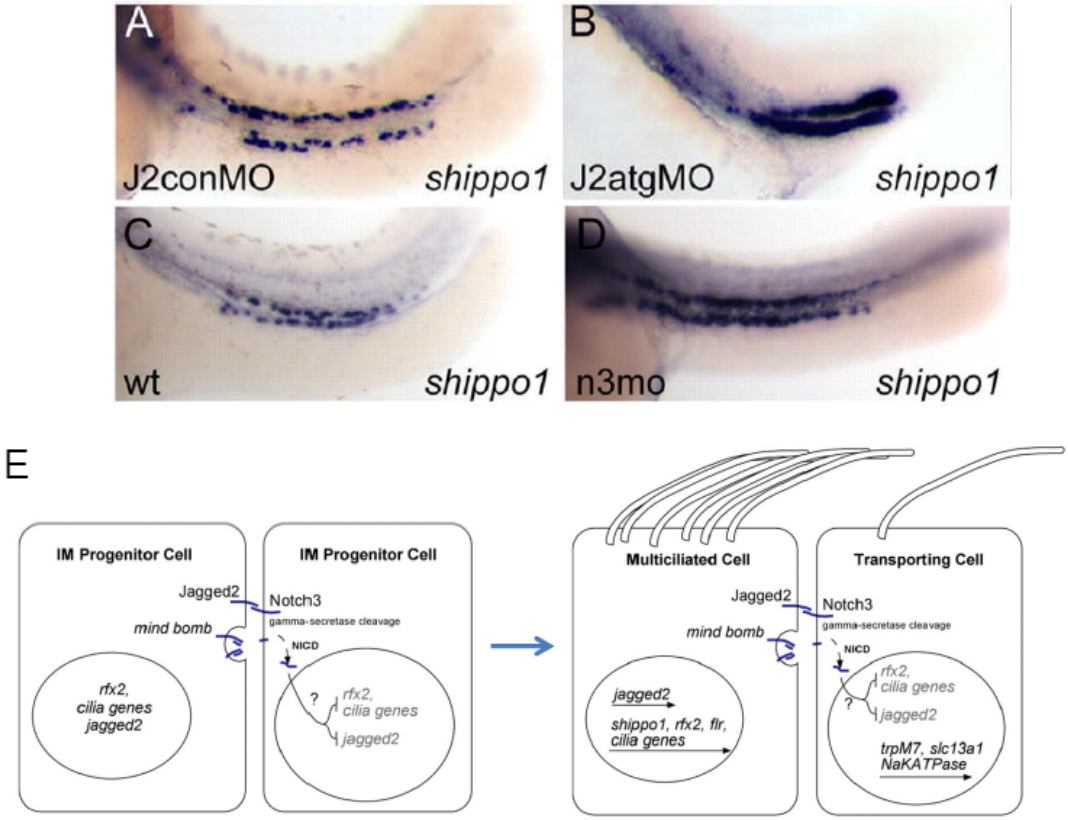

Figure 1.16 Notch signalling and pronephric patterning. A to D show lateral views of 34 hpf (hours post fertilisation) zebrafish pronephroi with the more dorsal stripe being the right sided pronephros duct and the more ventral stripe the left sided pronephros duct. A and C are control embryos that show wild type expression of *shippo-1*, an axonemal protein required for ciliogenesis (therefore a marker of multi-ciliated cells). B shows an embryo injected with a MO against *Jagged-2*. Inhibiting Notch signalling within the pronephros causes all cells to become multi-ciliated, as observed by ubiquitous expression of *shippo-1*. Injection of a MO against *Notch-3* had a similar effect (D). E represents the lateral inhibition mechanism by which Notch signalling mediates the patterning of multi-ciliated cells in the zebrafish pronephros. Cells within the intermediate mesoderm that will form the pronephros, signal to each other through the Notch signalling pathway. The ligand-presenting cell will induce expression of genes that promote ciliogenesis, whereas the receptor-presenting cell will promote expression of genes involved in electrolyte transport, thus is said to be a transporter cell and is only mono-ciliated. (Images adapted from Liu et al., 2007).

functionally distinct cells differs too. In zebrafish multi-ciliated and mono-ciliated (transporter) cells are present in a 'salt and pepper' distribution across the entire pronephric tubule and duct (Fig 1.15B) (Wessely and Obara, 2008). These multi-ciliated cells beat in a helical wave pattern and act as a 'screw pump', propelling fluid through the lumen (Kramer-Zucker et al., 2005). The 'salt and pepper' distribution of multi-ciliated cells intercalated with transporter cells suggests lateral inhibition is occurring. Expression of components of the Notch signalling pathway mimics the pattern of multi-ciliated cells in the pronephros of zebrafish; *Jagged-2* and *Notch-3* are expressed in a similar 'salt and pepper' distribution. Injection of morpholino oligonucleotides (MOs) that bind over the start codon of *Jagged-2* or *Notch-3* transcripts, thus inhibiting their translation and knocking down the effects of Jagged-2 or Notch-3 in the cell, caused all the cells in the pronephros to become multi-ciliated (Fig 1.16A-D) (Liu et al., 2007). Consequently in zebrafish, Notch signalling generates a cellular pattern in the pronephros through lateral inhibition (Fig 1.16E). Multi-ciliated cells within the *X. laevis* pronephros are not distributed in the same manner; they are only present in the nephrostomes. Thus it is unlikely that lateral inhibition is the mechanism by which the Notch signalling pathway is regulating *X. laevis* pronephros development.

Notch signalling regulates formation of the proximal-distal axis in the X. laevis pronephros

A role for Notch regulation of cell fate in the developing *X. laevis* pronephros was first identified by McLaughlin et al (2000). The authors of this paper showed *Notch-1*, *Delta-1* and *Serrate-1* are expressed in the pronephros anlagen in two distinct phases (Fig 1.17). Early phase expression of *Notch-1*, *Delta-1* and *Serrate-1*

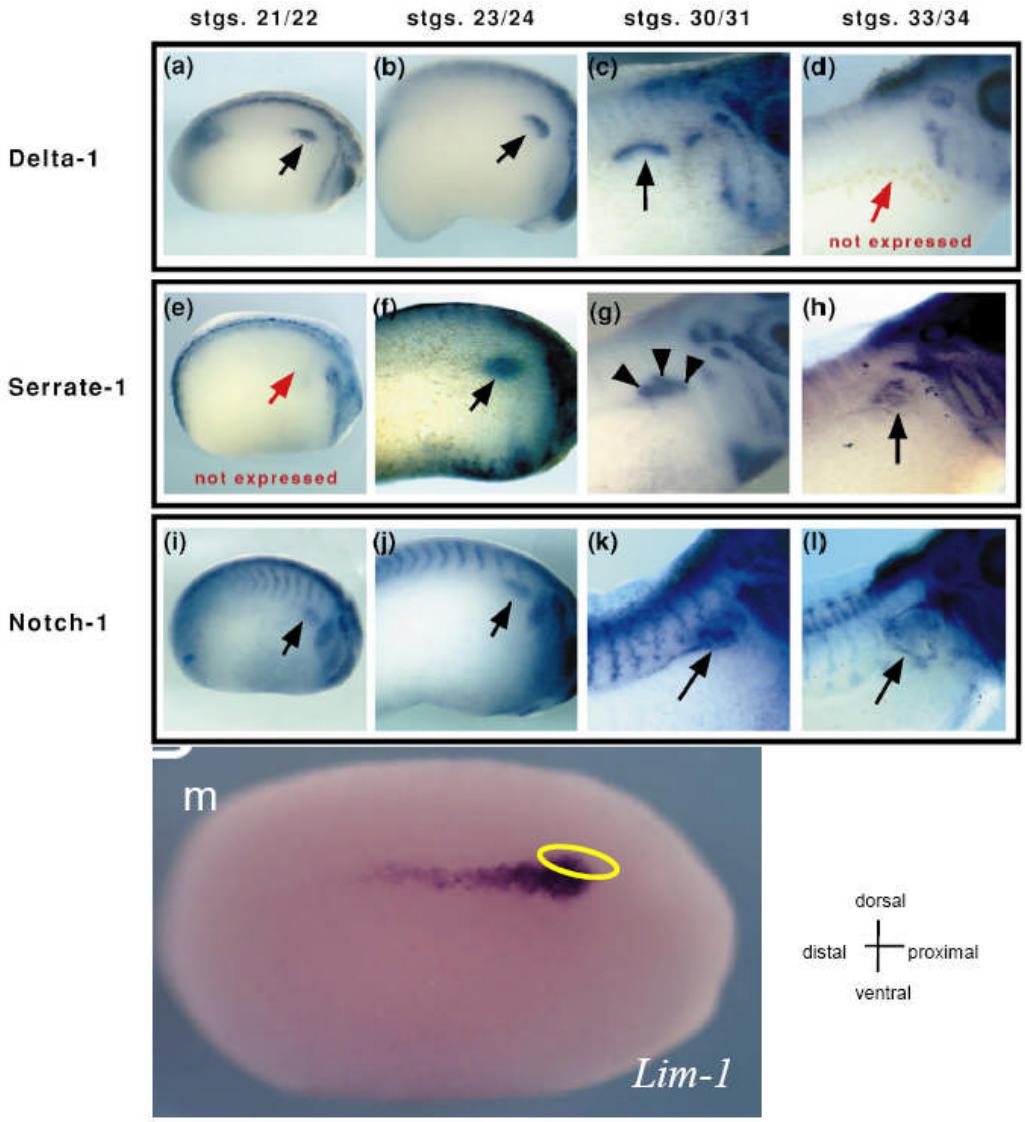

Figure 1.17 Expression profiles of *Notch-1, Serrate-1, Delta-1* and *Lim-1* in the pronephros anlagen of *X. laevis*. *Delta-1* is expressed in the dorsal-proximal region of the pronephros anlagen from stage 21/ 22 to stage 32, after which its expression in the pronephros anlagen ceases (a-d). *Serrate-1* expression in the pronephros begins slightly later in development, around stage 23/ 24, again in the dorsal-proximal region of the pronephros anlagen. *Serrate-1* expression persists in this region until stage 33/ 34 where its pronephric expression extends ventrally into the developing proximal tubules (e-h). *Notch-1* pronephric expression follows a similar pattern to *Serrate-1*; initially it is expressed in the dorsal-proximal region, then later in the tubules (i-l). *Notch-1* and *Serrate-1* therefore have two phases of pronephric expression, an early phase that, along with *Delta-1*, is restricted to the dorsal-proximal pronephric anlagen, and a late phase of pronephric expression within the proximal tubules. The entire pronephros anlagen at early tail bud stages of development can be distinguished by *in situ* hybridisation for the *Lim-1* transcription factor (m). The pronephros anlagen at these stages of development resembles a tear drop just ventral to the anterior somites. (m) emphasises the dorsal-proximal region where *Notch-1*, *Delta-1* and *Serrate-1* early phase pronephric expression is located. (Image of *Notch-1*, *Delta-1* and *Serrate-1* expression taken from McLaughlin et al., 2000)

is observed in the dorsal-proximal region of the pronephros anlagen during early tail bud stages of development. A second, late phase expression of *Notch-1* and *Serrate-1* in the proximal tubules is then observed, during which pronephric *Delta-1* expression has ceased. It is likely this periodic control of Notch signalling within the pronephros anlagen is necessary to direct distinct aspects of pronephrogenesis. This concept was confirmed by Taelman et al (2006), who showed activating Notch signalling in the pronephros, using an inducible and constitutively active Suppressor of Hairless construct (*Su(H)-VP16-hGR*), prior to stage 25 caused ectopic glomus formation. Induction of this construct post stage 25 had no effect on glomus development and in some cases induced ectopic proximal tubulogenesis. These results suggest early phase pronephric expression of components of the Notch signalling pathway is required for development of the glomus, and late phase expression is necessary for proximal tubule patterning.

An early Notch-related effect on glomus formation was first identified by McLaughlin et al (2000). They showed over-expression of inducible constitutively active *GR-Notch-ICD* and *GR-Su(H)-VP16* constructs increased expression of the glomus marker *WT-1*, but also proximal tubules immunostained with 3G8. These phenotypes were at the expense of distal tubule markers such as *c-ret* and 4A6 (Fig 1.18B and1.18F). Injection of an inducible dominant negative form of Su(H) (*GR-Su(H)*^{DBM}) had the opposite effect, inhibiting development of the proximal tubules and glomus and expanding the domain of expression of distal tubule markers (Fig 1.18D and 1.18H) (McLaughlin et al., 2000). Furthermore, over-expression and MO knock-down of the Notch-effector *HRT1* gene phenocopies the effects of Notch activation or suppression (Taelman et al., 2006).

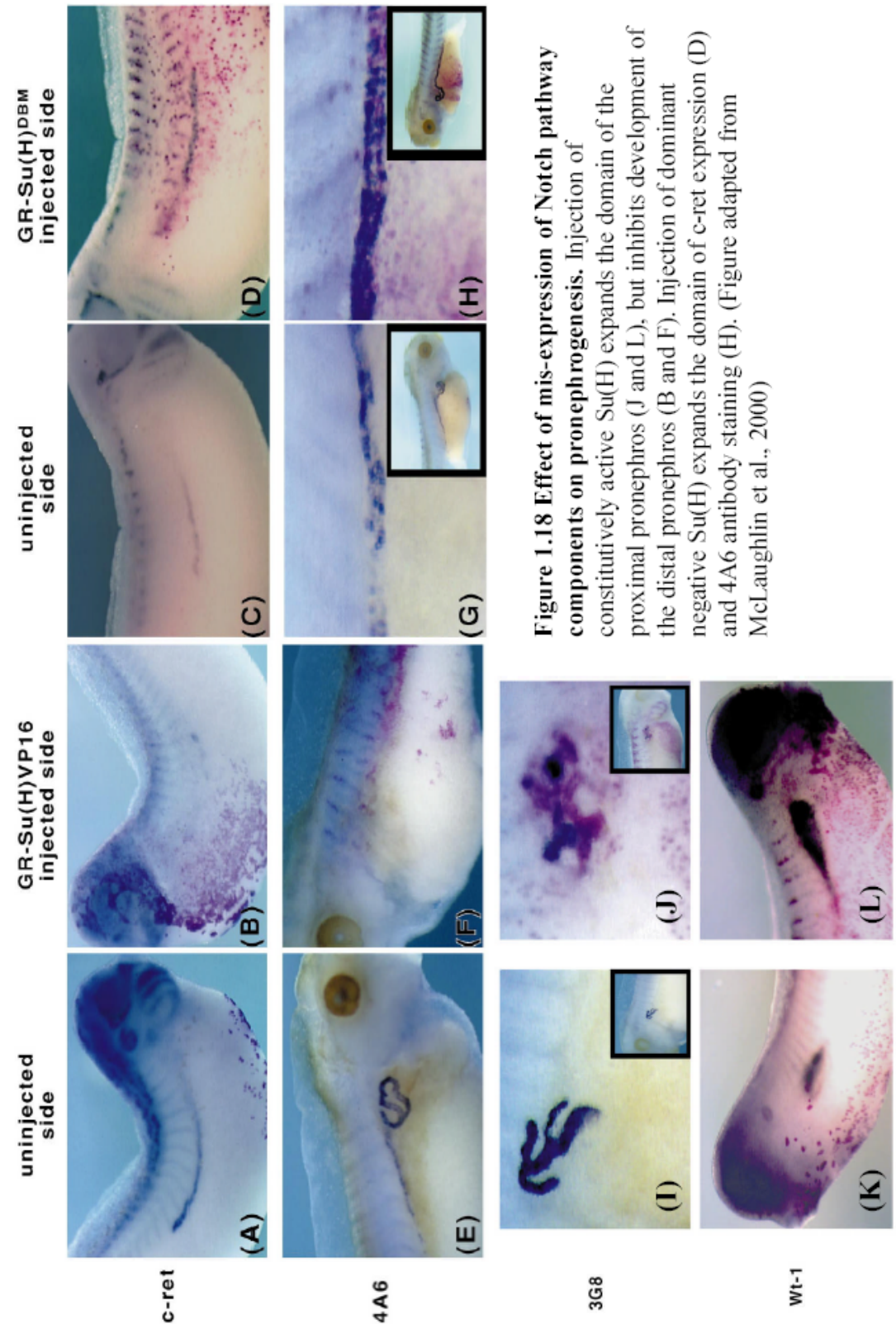

Figure 1.18 Effect of mis-expression of Notch pathway components on pronephrogenesis. Injection of constitutively active Su(H) expands the domain of the proximal pronephros (J and L), but inhibits development of the distal pronephros (B and F). Injection of dominant negative Su(H) expands the domain of c-ret expression (D) and 4A6 antibody staining (H). (Figure adapted from McLaughlin et al., 2000)

Further evidence to support proximal-distal control of pronephrogenesis by the Notch signalling pathway was observed by the differing effects Notch activation and suppression had on expression of the zinc finger oncogenic transcription factor *Evi1* (Van Campenhout et al., 2006). Evi1 is known to regulate proximal-distal development of the pronephros. It is expressed exclusively in the distal tubule and over-expression inhibits proximal tubule and glomus development, but has no effect on distal tubule development. This phenotype is indicative of a gene inhibiting proximal pronephric cell fates forming in the distal pronephros. Furthermore, an inducible dominant negative form of Evi1 (*Evi1-VP16-hGR*) induces ectopic glomus development at the expense of distal tubule markers such as *ClC-K* and *gremlin*, suggesting Evi1 acts to inhibit glomus development. Ectopic Notch activation in the pronephros inhibits *Evi1* expression (Van Campenhout et al., 2006), indicating early phase Notch signalling in the proximal pronephros is required to inhibit *Evi1* expression, and thus prevent distal pronephric cell fates in the proximal pronephros.

In conclusion, the Notch signalling pathway in *X. laevis* pronephros development is required for proximal-distal patterning. Importantly this effect is significantly different to Notch regulation of pronephrogenesis in zebrafish, and is similar to regulation of proximal-distal patterning of the mammalian nephron.

Notch signalling regulates the segmentation along the proximal-distal axis of the metanephric nephron

During metanephrogenesis epithelial outgrowth of the ureteric bud from the Wolffian duct initiates mesenchyme to epithelial transitions within the metanephric mesenchyme. The mesenchyme in turn induces branching morphogenesis in the

ureteric bud. The tips of these ureteric branches then protrude further into the metanephric mesenchyme and induce formation of the many nephrons that occupy the mature metanephros. Nephrogenic bodies develop in three stages; the renal vesicle, the comma-shaped body and finally the S-shaped body. A mature nephron then develops with a vasculature encapsulated by parietal epithelia, a proximal tubule, Henle's loop and a distal tubule connected to the collecting duct (Fig 1.19) (Dressler, 2006). The branching of the ureteric bud causes up-regulation of a number of Wnt genes in the surrounding mesenchyme. $Wnt9b^{-/-}$ embryos have arrested nephrogenesis, even though the ureteric bud has invaded the mesenchyme (Carroll et al., 2005). Wnt9b targets expression of *Wnt4*, which together can induce expression of the distal tubule marker *Lhx1* (Kobayashi et al., 2005). Indeed it has been proposed a morphogenic gradient of Wnt molecules across the renal vesicle is necessary for correct proximal-distal segmentation (Kopan et al., 2007). In addition to the Wnt signalling pathway, the Notch signalling pathway is required for proximal-distal patterning of the nephron (Fig 1.20). Mice homozygous for a hypomorphic Notch2 mutation have severe glomerular defects and die perinatally (McCright et al., 2001). Furthermore, dissected metanephroi taken from mice 11.5 days post-coitum and incubated for 6 days in the γ-secretase inhibitor DAPT, have inhibited podocyte and the proximal tubule development, but distal tubulogenesis is unaffected (Cheng et al., 2003). Despite this knowledge a mechanism for the Notch signalling pathway regulates proximal-distal segmentation of the nephron remains unclear (Fig 1.20 attempts to summarise current understanding).

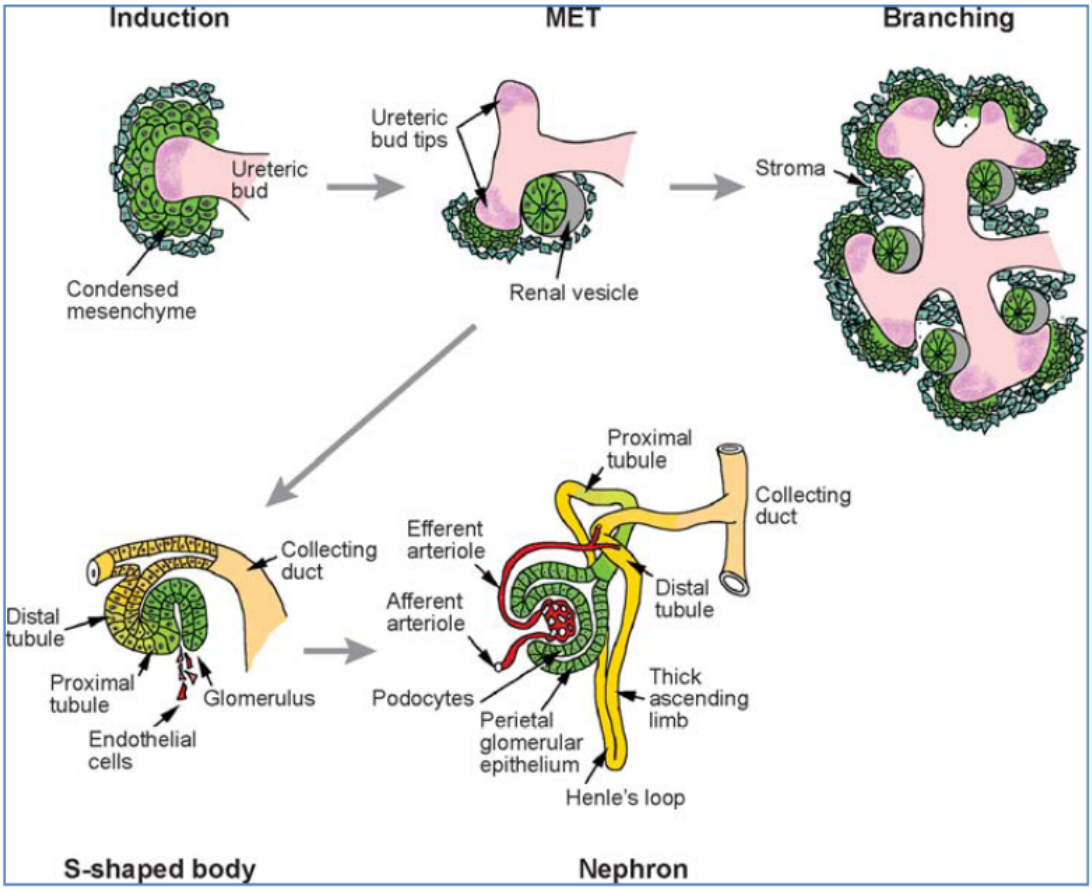

Figure 1.19 Metanephric nephron development. The ureteric bud invades the metanephric mesenchyme, which signals back to the bud, inducing branching morphogenesis - around these branches the renal vesicles develop. A renal vesicle will then develop into the S-shaped body, before developing a glomerulus and extending its tubules to form a mature nephron connected to the collecting duct. (Taken from Dressler, 2006)

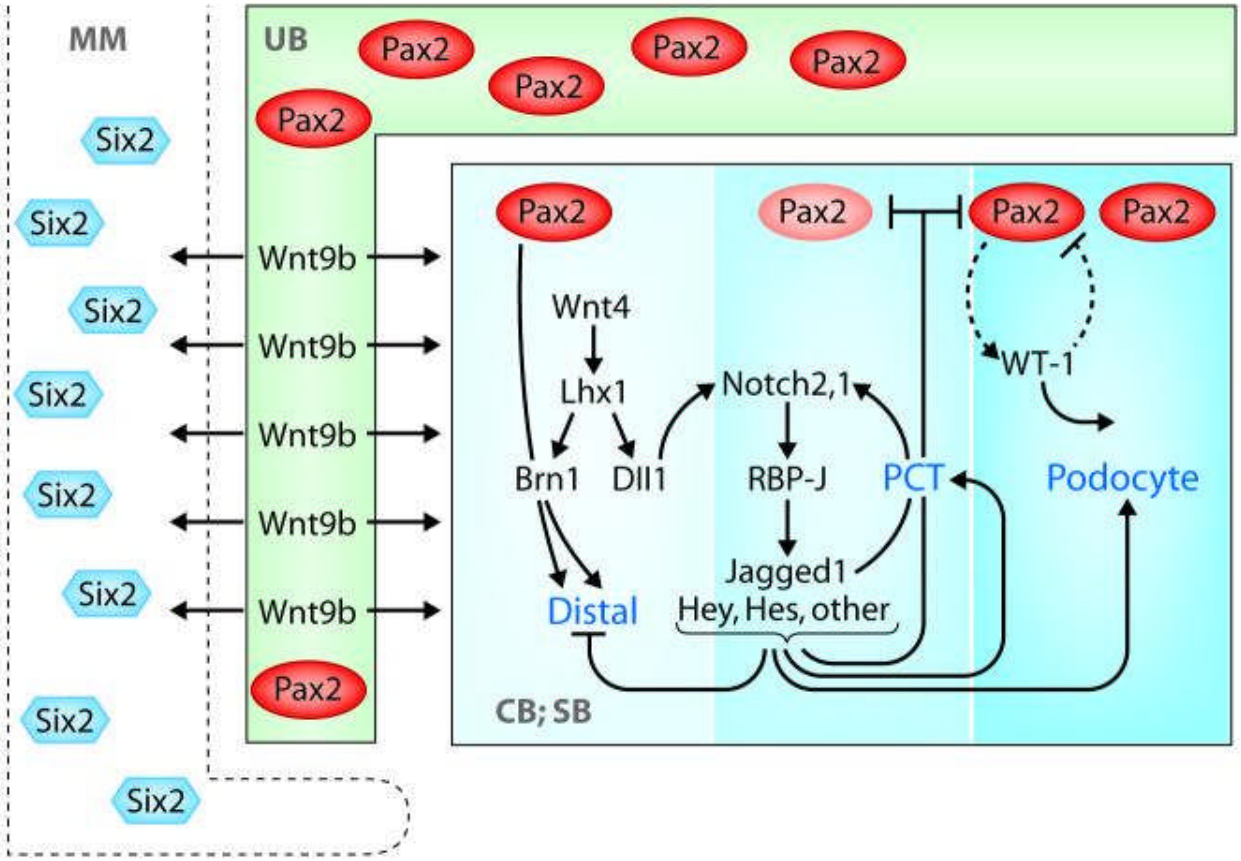

Figure 1.20 Schematic summarising the different signals that segment the developing nephron. Wnt9b is secreted from the ureteric bud to the renal vesicle, where it induces expression of *Wnt4* and *Lhx1* (*Lim-1*) (whose expression is also induced by Wnt4). Lhx1, along with Pax2, induces distal cell fates in the nephron. A morphogenic gradient of Wnt4 and Wnt9b, with highest concentration in the distal portion and lowest concentration in the proximal portion of the nephron, ensures *Lhx1* expression is strongest more distally. Lhx1 induces distal cell fates by promoting expression of *Brn1*, a POU domain-containing transcription factor. *Brn1*$^{-/-}$ mice have mature glomeruli and proximal tubules, yet nephron development is arrested prior to elongation of the loop of Henle, and the distal nephron segment fails to develop. Thus Brn1 is necessary for distal nephron development. Notch signalling is required for formation of the glomerulus and the proximal tubules. Inhibition of Notch signalling prevents proximal cell fates, and over-expression switches distal regions to proximal fates. In particular Notch2 and not Notch1 (research performed since the figure above was published) is involved in nephrogenesis. Exactly how the Notch signalling pathway segments the nephron is unknown, however the induction of *Delta-like 1* (*Dll1*) expression by Lhx1 suggests Notch interaction with this ligand promotes proximal cell fates in the receptor presenting cell, but inhibits it in the ligand presenting cell as *Dll1* is mainly expressed more distally. Six2 is also an important regulator of nephrogenesis. It is believed to maintain the multipotency of the metanephric mesenchyme, such that it can form renal vesicles of correct orientation. (PCT= Proximal Convoluted Tubule, MM= metanephric mesenchyme, UB= ureteric bud, C/SB= Common/S-shaped body) (Taken from Kopan et al., 2007)

1.4.5 Renal disease associated with aberrant Notch signalling

Aberrant Notch signalling during development is a major cause of nephropathy. The requirement of the Notch signalling pathway for formation of podocytes and the proximal tubules during the S-shape body phase means the most common diseases associated with irregular Notch signalling during nephrogenesis are glomerularopathies (Barisoni, 2008; Mertens et al., 2008). As already described, loss of Notch-2 function in mice is perinatally fatal due to defects in glomerulogenesis (McCright et al., 2001). Similarly, Presenilins play an important role in Notch receptor processing. The embryonic lethality of *Presenilin-1* and *Presenilin-2* double null mice embryos can be overcome by expression of a human *Presenilin-1* transgene, which permits survival to perinatal stages of development. In these embryos renal vesicles develop, but comma- and S-shaped bodies do not, due to a failure to pattern the glomerular and proximal tubule epithelium (Wang et al., 2003).

Renal diseases in adults are frequently caused by mis-activation of the Notch signalling pathway. Indeed, research into ectopic Notch signalling in adult kidneys has been a productive area of study in the past few years. Re-expression of Notch-1-ICD in mature mice podocytes caused massive proteinuria induced by glomerularsclerosis and loss of podocytes, observed by reduced *nephrin* and *WT-1* expression (Niranjan et al., 2008). In this remarkable paper, the authors show that active Notch-1 signalling induced p53-mediated apoptosis in podocytes and the proteinuria this podocyte apoptosis induced could be rescued by incubation with the γ-secretase inhibitor Dibenzazepine. Patients with Clear Cell Renal Cell Carcinoma (CCRCC) show elevated levels of *Notch-1* expression in their renal tissue. In human

CCRCC cell lines treated with the γ-secretase inhibitor DAPT, Notch signalling is reduced and attenuated proliferation is achieved by increased expression of $p27^{Kip1}$ and $p21^{Cip1}$ (Sjolund et al., 2008). CCRCC is believed to originate from the proximal tubule (Zambrano et al., 1999), thus mis-activation of Notch signalling in metanephroi once again causes disease of the proximal region of the kidney.

Whilst approaches to combating renal failure by inhibiting kidney-specific Notch signalling are being further investigated (Kretzler and Allred, 2008), it is obvious that the Notch signalling pathway is absolutely necessary for development of the proximal nephron segment, more accurately the glomerulus and the proximal convoluted tubule. Understanding how this development is controlled may elucidate knowledge of why mis-activated Notch signalling in the adult metanephros is a common cause of disease. As simplicity is a scientist's best friend, investigating pronephrogenesis may highlight a mechanism by which the Notch signalling pathway regulates formation of the proximal region of the metanephric nephron. The zebrafish pronephros does not require Notch signalling for formation of its proximal region (Liu et al., 2007), thus is unlikely to be an accurate model of mammalian nephron development. However, amphibian pronephros development requires Notch signalling for proximal-distal pronephric patterning (McLaughlin et al., 2000; Rones et al., 2002; Taelman et al., 2006; Van Campenhout et al., 2006). Investigation of the mechanism by which this process occurs could then be transposed to mammalian nephron segmentation. The simplicity of *X. laevis* pronephros development and the ease of using this model organism for research purposes suggests pronephrogenesis in *X. laevis* could be a more evolutionary relevant model of nephron development.

1.5 Aims of this thesis

The aims of this thesis are to describe and discuss experiments performed to further advance knowledge of the role that the cell cycle performs in regulation of organ size, and how the Notch signalling pathway regulates pronephrogenesis. Using *X. laevis* as a model organism, a wide range of techniques commonly used in the field of developmental biology have been utilised. MO knock-down of endogenous translation, over-expression by targeted micro-injection of *in vitro* synthesised mRNAs, animal cap assays, *in situ* hybridisation, antibody staining, Western blot analysis, site directed mutagenesis and RT-PCR are a sample of the powerful techniques used in this thesis.

Characterisation of the cell cycle inhibitor gene, $p27^{Xic1}$, in the pronephros was performed and is described in Chapter 3. As explained above, CKIs have diverse roles during development, and our initial aim was to observe if such roles were conserved in pronephros development. Initial results highlighted that it was unlikely that $p27^{Xic1}$ controls pronephrogenesis by means outside of its role in cell cycle regulation. However we did observe an effect on pronephric size, thus this aspect of $p27^{Xic1}$ function was further investigated. In Chapter 4 we further investigate the role of $p27^{Xic1}$ in cell differentiation, observing its interaction with growth-arrest-and-DNA-damage-induced gene gamma (Gadd45γ) and analysing how $p27^{Xic1}$ controls primary neurogenesis.

The Notch signalling pathway regulates cell proliferation, and our initial aim with the project was to understand how Notch signalling controls $p27^{Xic1}$ expression in the pronephros. Whilst doing these experiments we observed novel results that

hinted at a mechanism by which the Notch signalling pathway regulates patterning of the proximal-distal axis at tail bud stages of development, during the early phase of Notch signalling in the proximal-dorsal region of the pronephros anlagen (Chapters 5 and 6). The aim of this part of the thesis is therefore to describe this mechanism and discuss its conservation in nephrogenesis of higher eukaryotes.

Chapter 2

Materials and Methods

2.1 Materials

Supplier	***Material/ Reagent***
Ambion	mMESSAGE MACHINE SP6 Kit, Turbo DNase
Amersham	PVDF membrane
BDH Laboratory Supplies	Workbench chemicals
Biological Industries	EZ-ECL Chemilumiscence kit
Bioline	DNA hyperladder 1
Cambridge Biosciences	Protein G Sepharose beads
Cell Signalling	HA and Myc monoclonal antibodies
Fermentas	RNase Inhibitor
Fisher Scientific	DH5α Competent cells, Haematoxylin, Workbench chemicals
Fluka Biochemika	PMSF, Workbench chemicals
Fuji	X-ray film
Genetools	Morpholino oligonucleotides
Helena Biosciences	Workbench chemicals
Invitrogen	DNA oligonucleotides (primers) dNTPs, Restriction enzymes, *Taq*/ *Pfx* polymerases, T4 DNA ligase
Melford	CHAPS, Salmon Gal, X-gal
Mikrobiologie	Workbench chemicals
NEB	Pre-stained protein ladder
Promega	Rabbit reticulocyte lysate system
Roche	Alkaline Phosphatase, BM Purple, DNase 1, NBT/ BCIP, Proteinase K
Sigma-Aldrich	Antibodies (immunohistochemistry), Eosin, Fast Red, Gentamycin, Levamisole, Workbench chemicals
Qiagen	Gel extraction kit, mini-prep kit

2.2 Media and stock solutions

All general media and stock solutions were prepared according to Sambrook *et al.*, 1989.

2.3 *Escherichia coli* bacterial strains

DH5α	F^- *supE*44 Δ*lacU*169(∅80*lacZ*Δ*M*15) *hsdR*17 *recA*1 *gyrA*96 *thi*-1 *relA*1

2.4 Vectors

pBluescript KS+ vector contained clones for *$p27^{Xic1}$*, *Serrate, MyoD, Wnt-4, Lim-1, Lunatic fringe ORF* and *Radical fringe ORF*.

pBT vector contained clones for *Lunatic fringe Full Length* (*FL*), *Radical fringe FL*, and *Lunatic fringe Mature*

pCS2+ vector contained the clone for *Na^+ K^+ ATPase* and the original clones for *$p27^{Xic1}$*, *$p27^{Xic1}$ N*, *$p27^{Xic1}$ #2*, *$p27^{Xic1}$ C*, *$p21^{Cip1}$*, *HA-NGN, p35.1, Notch-ICD,* and *$Delta^{STU}$* that were kind gifts from Dr A. Philpott (Department of Oncology, University of Cambridge, Cambridge, CB2 2XY). Our *Gadd45γ-MT* clone was also in pCS2+ and was a kind gift from Dr Jose-Luis Gomez-Skarmeta (CABD, Seville, Spain).

pCMV Sport 6 vector contained purchased IMAGE clones for *Lunatic fringe, Radical fringe, Delta-1, slc5a2,* and *odf-3* and the original clone for *nephrin* which was a kind gift from Prof. Peter Vize (University of Calgary, Alberta, Canada)

2.5 DNA techniques

2.5.1 Agarose gel electrophoresis

1-1.5% agarose gels were prepared in 1X TBE buffer (90mM Tris-Borate ~pH 8.3, 2mM EDTA) in 0.5 μg/ml ethidium bromide. To load the samples accurately 6X glycerol loading buffer was used. 0.5 μg of DNA Hyperladder 1 was loaded to allow analysis of DNA size and concentration in samples. DNA/ RNA was separated by electrophoresis at 100volts (V) for small agarose gels (30 ml) and 150V for large agarose gels (100 ml). Nucleic acids were then detected and photographed under UV light. If needed, DNA was extracted from the gel using the Qiagen gel extraction kit according to manufacturer's instructions.

2.5.2 Restriction enzyme digests

Restriction digests were carried out according to the manufacturer's instructions. Following digestion of plasmids for ligation, treatment with phosphatase prevented plasmid re-ligation. 1 μl of calf intestinal alkaline phosphatase was added per 10 μl of reaction, and the reaction was incubated at 37°C for a further 30 minutes. An extraction using the Qiagen gel extraction kit removed the phosphatase prior to DNA ligation. DNA to be ligated was then purified with butanol. 100 μl of butanol was added for every 10 μl of sample, this was then mixed and vortexed before being spun at 13 200rpm for 10 minutes. The supernatant was removed and the sample pulsed at 13 200rpm. The residual supernatant was removed and the pure DNA re-suspended in 10 μl of sterilised water.

All other DNA digests were purified using the Qiagen gel extraction kit. However the gel extraction section of the protocol was not performed, instead 3 volumes of buffer QG and one volume of isopropanol were added.

2.5.3 DNA mini-preps

DNA was extracted from overnight cultures setup in 5 ml liquid broth containing 1 µl/ ml ampicillin using the Qiagen mini-prep kit procedure.

2.5.4 Ligation of DNA into plasmid vectors

25–50 ng of vector was mixed with insert digested with appropriate restriction enzymes (molar ratio 1:3) to make a final volume of 20 µl with 1 µl T4 DNA ligase (MBI Fermentas) and 4X ligation buffer. The ligation mix was incubated for a minimum of 1 hour at room temperature, or overnight to maximise the number of ligations.

2.5.5 Transformation of plasmid DNA into competent *Escherichia coli*

The *E. coli* strain DH5α competent cells were prepared for heat shock transformation according to Sambrook et al., (1989). 50 ng of the chilled ligation mix or 10 ng of plasmid was added to 50 µl of *E. coli* DH5α and incubated on ice for 30 minutes. Cells were then heat-shocked at 42°C for 30 seconds and incubated on ice for 2 minutes, before being diluted with 450 µl L-broth and incubated at 37°C for 45 minutes to recover. 50 µl of this mix was plated onto L-broth plates containing ampicillin at 100 µg/ ml. The remaining ligation mix cells were centrifuged for 5 minutes at 2 500 g, re-suspended in 50 µl L-broth and plated onto L-broth plates containing ampicillin at 100 µg/ml. Plates were incubated overnight at 37°C.

2.5.6 Primer Design

All primers were designed using Primer Designer (Scientific and Educational Software version 3.0)

2.5.7 Automated DNA Sequencing

Automated DNA sequencing was set up as follows. 500 ng of plasmid DNA or 100 ng of PCR product was added to 5.5 pmol of primer and made up to a total volume of 10 µl. Samples were then submitted to the departmental Molecular Biology Service for sequencing.

2.5.8 Site-directed mutagenesis

Mutagenesis to incorporate a point mutation into the $p27^{Xic1}$ clone was performed according to the manufacturers protocol (Stratagene – QuikChange® Site-Directed Mutagenesis Kit). Correct mutagenesis was confirmed by sequencing.

2.6 RNA Techniques

2.6.1 RNA extraction from embryos and animal caps

The volumes given below are for 5 animal caps or 1 whole embryo. Where different numbers of animal caps or whole embryos were used, the volumes were adjusted accordingly. A whole embryo was homogenized in 150 µl extraction buffer (300 mM NaCl, 20 mM Tris pH 7.5, 1 mM EDTA pH8, 1% SDS) with 3 µl of proteinase K (15 mg/ml) and incubated for 15 minutes at 37°C, samples could then be stored at -20°C.

Extraction was performed with addition of an equal volume of phenol and 5 μg of glycogen added to the upper phase. RNA was precipitated with two volumes of ethanol at –20°C for at least 30 minutes and centrifuged for 20 minutes at 13 200 rpm. The pellet was re-suspended in 30 μl of DNase I buffer (20 mM Tris pH8.3, 30 mM NaCl, 2.5 mM $MgCl_2$) containing 30 units of DNase I and 30 units of RNase inhibitor, and incubated for 20 minutes at 37°C. The samples were then extracted with an equal volume of phenol followed by phenol/ chloroform, with the aqueous layer being precipitated by adding 2 volumes of ethanol at room temperature for no longer than 30 minutes. This was centrifuged at 13 200 rpm for 20 minutes at 4°C, the pellet washed with 70% ethanol before being dried and re-suspended in 20 μl DEPC H_2O. 1 μl of RNA was analysed on a 1% agarose gel to check the integrity and yield.

2.6.2 Reverse Transcription PCR

RT-PCR was performed according to Barnett *et al.*, (1998). 0.5 μg of RNA extracted from animal caps or whole embryos was made up to a total volume of 21.1 μl with H_2O, heated at 75°C for 5 minutes before placing on ice. 7.9μl of reaction mix (3.3 μM random hexamers, 1X PCR buffer, 3 mM $MgCl_2$, 500 μM dNTPs, 1U/ μl RNase inhibitor) was added to each tube and incubated at 37°C for 5 minutes before addition of 2μl MMLV reverse transcriptase (200 u/μl) and further incubation at 37°C for 1 hour. Reactions were denatured at 95°C for 5 minutes and stored at –20°C. Samples lacking RNA and RT were added as negative controls.

The prepared cDNA was subjected to PCR analysis. 1 μl of cDNA + 1 μl H_2O was made up to a final volume of 25 μl with reaction mix containing 1X PCR buffer, 1.5

mM $MgCl_2$, 200 µM dNTPs, 1 µM of each primer, and 1U *Taq* polymerase. A sample lacking cDNA was checked for contamination in any of the components used and a linearity series (0.2 µl, 0.4 µl, 0.8 µl, 1.6 µl) of control cDNA was added to verify that the PCR was in the linear range and semi-quantitative. *ODC* was used as a loading control, with the amount of cDNA being added equalized with respect to this marker. Samples were amplified using standard PCR conditions; one denaturation cycle at 94°C for 3 minutes, one cycle at the appropriate annealing temperature for 1 minute followed by an elongation cycle at 72°C for 1 minute. Then, using the appropriate number of cycles for denaturation at 94°C for 30 seconds, the appropriate annealing temperature for 30 seconds, followed by elongation at 72°C for 30 seconds. The final elongation step was performed at 72°C for 5 minutes. 15 µl of sample was analysed on a 1.5% agarose gel. Primer sequences, number of cycles and the annealing temperatures are shown in table 2.1.

Marker	Primer Sequence (5'-3')	Annealing temperature (°C)	No. of cycles	Reference
p27^{XicI}	U-CATCGAGCTCAGCACTCACA	57	28	Rob Collins (thesis)
	D-GACAGTCGGACGCCTGGATT			
Radical fringe	U-CGACGTGCTGGATTCTGTAT	55	28	this work
	D-CAGGTTACTGTGCTGCATCT			
Lunatic fringe	U-CGGCACCTTCTCGGCTTATT	55	28	this work
	D-CATCGTTGGCGGTGATGTCT			
nephrin	U-GCAGCACCGCCTATAACTTCTCAG	57	28	this work
	D-CATATCCGCCCTCTTCCCAACCTT			
Na^+ K^+ ATPase	U-ATCACTGGTGTGGCGGTCTT	57	28	this work
alpha subunit	D-TCTCTGTGGTGTCGCGTTCA			
ODC	U-GGAGCTGCAAGTTGGAGA	55	20	Bassez et al, 1990
	D-TCAGTTGCCAGTGTGTGGTC			

Table 2.1. Primer sequences and RT-PCR molecular marker conditions.

2.6.3 Preparation of *in vitro* transcription of mRNA

Plasmid template DNA was linearised with the appropriate restriction enzyme and purified using a gel extraction kit. Capped mRNA was prepared using the

mMESSAGE mMACHINE® kit, Sp6, according to the manufacturer's instructions (Ambion®).

2.6.4 Wholemount *in situ* hybridisation

Plasmid templates were linearised with the appropriate restriction enzyme and purified using a gel extraction kit. Sense/ anti-sense RNA probes were prepared using digoxygenin (DIG) labelling kit (Boehringer-Mannheim), and single labelled whole-mount *in situ* hybridisation was carried out using a standard protocol adapted from Hemmati-Brivanlou *et al.*, 1990 and Harland, 1991. Pigmented embryos were bleached (1% H_2O_2, 5% formamide, 0.5 x SSC in H_2O) on a fluorescent light source following hybridisation for approximately 1–4 hours. Table 2.2 below alphabetically lists all the probes used in this study, giving the restriction digests and polymerases used to make the probes.

PROBE	PROBE TYPE	DIGEST	POLYMERASE	PLASMID
Delta	AS (3'UTR)	Nde1	T7	pCMVSport6
	S (FL)	Xho1	SP6	pCMVSport6
Lim-1	AS	Xho I	T7	pBS
	S	Sac I	T3	pBS
Lunatic Fringe	AS (3'UTR)	Nco I	T7	pCMVSport6
	S (FL)	Xho I	T3	pCMVSport6
MHC	AS	Nco I	SP6	Unknown
MyoD	AS	Hind III	T7	pBS
NaK ATPase	AS	Sma I	T7	pCS2
Nephrin	AS	Sma I	T7	pCMVSport6
Ntubulin	AS	Nco I	T3	pBS
odf3	AS	EcoR I	T7	pCMVSport6
Radical Fringe	AS (3'UTR)	BamH I	T7	pCMVSport6
	S (FL)	Xho I	T3	pCMVSport6
Serrate	AS (3'UTR)	Hind III	T7	pBS
Slc5a2	AS (FL)	EcoR I	T7	pCMVSport6
	S (FL)	Xho I	SP6	pCMVSport6
Wnt4	AS (3'UTR)	Xho1	T7	pBS
	S (FL)	Sac II	T3	pBS
Xic1	AS (FL)	Xho I	T7	pBS
	S (FL)	Sac II	T3	pBS

Table 2.2. Procedures for producing the *in situ* probes used in this thesis. (AS – anti-sense probe, S – sense probe, FL – full length probe, 3' UTR – probe specific for 3' UnTranslated Region sequence)

2.7 Protein techniques

2.7.1 Protein expression in oocytes

Oocytes were injected with 74 nl of mRNA at concentrations ranging 20-50 ng/µl and incubated at room temperature for 2 hours before transferring to 18°C overnight. If radio-labelling of proteins was carried out, the best 8 oocytes were selected after the 2 hour room temperature incubation. These oocytes were transferred to 100 µl Barth X containing 10 µCi ^{35}S-methionine and incubated overnight at 18°C.

2.7.2 Protein extraction from oocytes

Oocytes were washed twice in Barth X before being homogenised in protein extract buffer (150 mM NaCl, 1% NP40, 50 mM Tris-Cl pH8) and 1 mM PMSF. Samples were recovered by centrifugation at 13 000 rpm for 5 minutes to remove cell debris and the middle layer removed. These samples were then spun down at 13 200 rpm for an additional 30 minutes. If performing radio-labelling the entire protein extract was mixed with 2X protein loading buffer at a 1:1 ratio. 20 µl of protein was taken from the supernatant and mixed with 20 µl of protein loading buffer if Western blot analysis was to be performed. These extracts, either in loading buffer or protein extracted for immuno-precipitation (not in loading buffer) were stored at -80°C.

Protein samples denatured in protein loading buffer were heated for 3 minutes at 95°C and spun down for 5 minutes at 13 200 rpm before being loaded onto an SDS-PAGE gel. Samples were stacked through a 4% acrylamide stacking gel at 100V, followed by separation through a 10% acrylamide resolving gel in a tris-glycine

running buffer using the BioRad Mini Protean II system. Gels containing radio-labelled protein were dried for 1 hour at 80°C prior to autoradiography.

2.7.3 *In vitro* translation

In vitro translation of 1 µl *in vitro* transcribed mRNA was carried out using the nuclease treated rabbit reticulocyte lysate according to the manufacturer's instructions (Promega). Reaction products were radio-labelled using ^{35}S-methionine. Proteins were separated on a 10% acrylamide gel as described above.

2.7.4 Immuno-precipitation

Protein extracts were generated as explained in section 2.7.2. Extracts that were to be purified by immuno-precipitation were not denatured in protein loading buffer. Instead they were stored at -80°C. Protein extracts were defrosted on ice and at all times kept on ice. 200 µl protein extract was taken and placed in a new, already chilled, 1.5 ml Eppendorff tube. Primary antibody was added at the desired concentration. The extract with the primary antibody was mixed on a nutator (Eppendorff tubes on their side) at 4°C for 2 hours. Meanwhile beads (Protein G Sepharose used in this study) were swelled in protein extract buffer (150 mM NaCl, 1% NP40, 50 mM Tris-Cl pH8 and 1 mM PMSF). Typically 100 µl beads was swelled in 500 µl protein extract buffer. Beads were then washed 5 times in pre-chilled protein extract buffer, spun down at 5 000 rpm for 2 minutes each time. After final wash, 100 µl of beads were diluted into 500 µl protein extract buffer and stored at 4°C until required. For every 200 µl sample, 50 µl of swelled beads was added and mixed on a nutator at 4° for 2 hours. These mixes were then spun down at 5 000rpm for two minutes and washed 5 times in pre-chilled protein extract buffer. After the

final wash the beads were re-suspended in 30 µl protein loading buffer, placed on ice for 1 hour and then stored at -80°C. (Note: Incubation of protein extract for more than 2 hours in primary antibody or sepharose beads increases non-specific binding and results in failed immuno-precipitation of target protein).

2.7.5 Western blotting

Protein extractions were carried out as in section 2.7.2. Typically 10% of an oocyte or 50% of an IP was separated on a 10% SDS-PAGE gel at 100 volts for 2.5 hours. In preparation for Western transfer, the Western transfer buffer was made up (20% Methanol, 39 mM Glycine, 48 mM Tris-HCl pH 7.5, 0.037% SDS) and placed at 4°C whilst the protein gel ran. After 2 hours of running the protein gel the PVDF membrane (Amersham), filter paper and fibre pads were prepared for Western transfer. The PVDF membrane was soaked in Methanol for 30 seconds to ensure activation, and then washed in distilled water. Filter paper, PVDF membrane and fibre pads were then equilibrated in a bath of Western transfer buffer at 4°C. After 2.5 hours the protein gel was stopped, transferred onto filter paper and then incubated at 4°C in Western transfer buffer for 30 minutes. Western blot sandwiches were then made (Fibre pad – Filter paper – Gel – PVDF membrane – Filter paper – Fibre pad). Sandwiches were locked in a cassette, correctly orientated and then placed in Western blot transfer apparatus (Biorad). Transfer of protein to the PVDF membrane was carried out at 4°C at 30 volts overnight (14 hours at least). PVDF membranes were isolated and blocked in 50% Marvel milk in 1X TBST (TBS + 0.1% Tween-20) for 2 hours at room temperature rolling. Membranes were washed 3x 10 minutes in TBST before addition of the primary antibody at specific concentration (anti-HA 1:200, anti-Myc 1:1000) in 5% Marvel milk and 1X TBST, which was left to bind

overnight, rolling at 4°C. Membranes with primary antibody bound were washed 3x 10 minutes in 1X TBST. Secondary antibody was added at desired concentration (HA westerns used secondary at 1:2000, Myc westerns at 1:10 000) in 5% Marvel milk and 1X TBST for two hours, rolling at room temperature. Membranes were then washed 3x 10 minutes in 1X TBST and the signal developed using EZ-ECL kit according to manufacturer's instructions (Biological Industries).

2.8 Whole-mount immunohistochemistry

2.8.1 Whole-mount antibody staining

Embryos, fixed overnight at 4°C in MEMFA (0.5M MOPS pH7.4, 100mM EGTA, 1mM $MgSO_4$, 4% formaldehyde), were transferred to PBS for 5 minutes at room temperature before being dehydrated through serial dilutions of methanol / H_2O. Embryos were left in methanol for at least one night. Embryos were rehydrated with serial dilutions of PBS. They were then washed 2x with PBT (2mg/ml BSA, 0.1% Triton X-100 in PBS) blocked in PBT for at least 2 hours at 4°C on a nutator. Primary antibody was added (pronephric tubule specific monoclonal antibody 3G8 (1:40, diluted in PBS) and pronephric duct specific monoclonal antibody 4A6 (neat) (Vize et al., 1995)), and incubated rocking at 4°C overnight. Embryos were then washed with PBT, 5x 1 hour at 4°C on a nutator, and then secondary antibody, alkaline phosphatase conjugated goat anti-mouse (Sigma F-2012) (1:500), was added overnight at 4°C. Embryos were then washed 4x 1 hour with PBT at 4°C, followed by a 1 hour wash in colour buffer (0.1M Tris-Cl pH9, 25mM $MgCl_2$, 100mM NaCl, 0.1% Tween-20) at room temperature on a nutator. Embryos were transferred to a

24-well tissue culture plate with 500 µl of AP colour substrate (colour buffer with 1% v/v NBT/BCIP Boehringer-Mannheim). Staining was carried out in the dark, with the reaction stopped, typically after 15 minutes, with a PBS wash. Background staining was removed by alcohol washes (50% ethanol for 10 minutes, 2 x 100% Methanol for 10 minutes, 50% ethanol 10 minutes, before complete rehydration in PBS). The staining was fixed in MEMFA for 1 hour at room temperature. Where double staining was required, embryos were washed 3x 5 minutes with PBT to remove the MEMFA and blocked for 2 hours at 4°C on a nutator before undiluted 4A6 was added and incubated overnight at 4°C. Subsequent washes were repeated as for 3G8 except that the second colour reaction used Fast Red TR / Napthol AS/MX (Sigma) according to the manufacturer's instructions. Pigmented embryos were bleached (0.9% H_2O_2, 5% formamide, 0.5x SSC) on a fluorescent light box after the immunostaining had been performed (Note: prior bleaching significantly reduced 3G8 binding of epitope).

2.8.2 Whole-mount TUNEL staining

Embryos were fixed for 1 hour in MEMFA at 4°C, fixing for longer, results in a decline in the number of TUNEL positive cells. Embryos were rinsed 3x 10 minutes in PBS, dehydrated in serial dilutions of methanol / PBS (10 minutes each) before 2x 30 minute washes with 100% methanol on a nutator and stored at – 20°C overnight up to one week. Subsequent washes were performed on a nutator. Embryos were rehydrated in 5 minute serial dilution washes of methanol / PBS and PBS alone where half the solution would be replaced with the equivalent amount of PBS. They were then washed 2x 15 minutes in PBTw (PBS + 0.2% Tween-20) and then 2x 15 minutes in PBS at room temperature. Embryos were then put in TdT buffer (toxic)

for 30 minutes at room temperature in preparation for end labelling. This was replaced with TdT buffer containing 0.5 μM digoxigenin-dUTP (Boehringer-Mannheim) and 150 U/ml TdT (GibcoBRL) (250 μl / vial, volume brought up with 1x PBS to reduce background), and vials were held upright at room temperature overnight and then for 1 hour at 37°C. Embryos were transferred to a 24-well culture dish and washed 2x 1 hour in PBS / EDTA (1mM EDTA in PBS) at 65°C, followed by 4x 1 hour washes in PBS at room temperature. The embryo samples were washed in PBT for 15 minutes, and then for 1 – 2 hours in PBT + 20% goat serum at room temperature. They were transferred to vials and incubated upright, rocking, at 4°C overnight in PBT + 20% goat serum containing 1/2000 dilution of anti-digoxygenin coupled to alkaline phosphatase. Samples were transferred to a 24-well culture dish and washed 6x 1 hour in PBT at room temperature and put in fresh PBT overnight at 4°C. Embryos were washed 2x 5 minutes in alkaline phosphatase buffer (100mM Tris pH 9.5, 50 mM $MgCl_2$, 100 mM NaCl, 0.1% Tween 20) in preparation for the chromogenic reaction, and then in 500 μl alkaline phosphatase buffer containing 7.5 μl NBT / BCIP (15 mg/ml, Boehringer-Mannheim). When a sufficient colour signal had occurred, typically 20 minutes to 2 hours at room temperature in the dark, the reaction was stopped by washing for 30 minutes in MEMFA and fixation overnight at room temperature. Staining was visualised under a Nikon binocular microscope.

2.8.3 Whole-mount anti-phospho histone H3 staining

Embryos at desired stages of development were fixed overnight in MEMFA at 4°C. They were then dehydrated in serial dilutions of methanol / H_2O to 100% methanol and stored at –20°C for at least one night. Rehydration of embryos was performed in stepwise dilutions of 75%, 50%, 25% methanol / PBS and washed 2x 5 minutes in

PBS at room temperature. Samples were then washed with PBS for 5 minutes followed by 2x 10 minutes in PBST (0.2% BSA, 0.1% Triton X-100 in PBS). Embryos were incubated with 10% goat serum in PBST for 6 – 8 hours at room temperature, then incubated at 4°C with 5 μg/ml anti-phospho histone H3 (Upstate Technologies) in PBST overnight. Samples were then washed with 10% goat serum in PBST 4x 2 hours in PBST at room temperature. Embryos were then incubated with overnight with anti-rabbit-HRP in PBST + 10% goat serum. They were then washed with 10% goat serum in PBST 4x 2 hours at 4°C. Embryos were washed 2x 5 minutes in alkaline phosphatase buffer (100mM Tris pH 9.5, 50 mM $MgCl_2$, 100 mM NaCl, 0.1% Tween 20) in preparation for the chromogenic reaction. The colour reaction was performed with 500 μl alkaline phosphatase buffer containing 7.5 μl NBT / BCIP (15 mg/ml, Boehringer-Mannheim) at room temperature for 10 minutes. The staining was then fixed overnight in MEMFA at 4°C.

2.9 Histology

2.9.1 Wax sectioning

Embryos were transferred to glass Bijoux tubes and fixed in Bouin's fixative (5% Glacial Acetic acid, 25% Formaldehyde, 70% Picric acid) for two hours at room temperature. They were then rinsed in PBS multiple times and left in 70% Ethanol (diluted with PBS) at 4°C until wax embedding. Embryos were then transferred to fresh histo-clear clearing agent (National Diagnostics) for 20 minutes at room temperature. Histo-clear was replaced with pre-warmed 1:1 wax:histo-clear and left in the 59°C incubator for 20 minutes. This 1:1 solution was replaced with 100% fresh

wax (Paraplast embedding medium (Sigma)) and stored overnight at 59°C. Plastic plates were half filled and allowed to solidify the following morning. Embryos were positioned in a circle on the wax with their tail pointing outwards and a gap in between each embryo (6 embryos per dish maximum). Embryos were orientated using heated forceps (heated using an oil lamp). Embryos were then embedded in fresh wax, with their position marked on the dish with a marker pen. The wax was left to solidify for around 20 minutes (using an ice bucket if necessary). Blocks of wax, containing a correctly orientated embryo, were then cut out using a razor blade, ensuring the surface to be positioned on the block was perpendicular to the embryo. The size of these wax blocks were reduced sufficiently and placed on a wooden block using hot wax to hold the embedded embryo down. These mounted blocks were left overnight at room temperature, following which they were clamped into the microtome and embryos were sectioned at desired thickness (in this study 10-12 μm). To aid sectioning, wooden blocks were incubated for a short time (up to 60 seconds maximum) at 59°C to soften the wax. Ribbons of wax, containing sections, were transferred to a 42°C water bath and collected onto microscope slides. Sections were then left overnight at room temperature. Slides were then placed in a slide holder containing histo-clear for 10 minutes, before transfer to fresh histo-clear in a second slide holder for a further 10 minutes. The slides were left to dry for approximately 2 hours. Slides were then incubated in Xylene for 5 minutes before being transferred to fresh Xylene for a further 2 minutes to de-wax. Using a glass pipette a swab of Depex mounting solution was poured onto the slide and a cover slip was then placed on top without allowing any air bubbles to form underneath. These sections were then left overnight and analysed by light microscopy.

2.9.2 Histological staining

Dry slides, de-waxed in histo-clear, were prepared for haematoxylin and eosin staining. Slides were transferred to Xylene for 1 minute, fresh Xylene for an additional minute and then to slide holders containing serial dilutions of ethanol (100%, 90%, 80%.....10%, tap water). These slides were transferred to Harris Haematoxylin (Fisher Scientific) for 2 minutes 15 seconds, washed in tap water for 45 seconds, transferred to acid alcohol (70% Ethanol, 0.5% HCl) for 45 seconds, washed again in tap water for 45 seconds, washed in Scott's solution (166 mM $MgSO_4$ and 42 mM $NaHCO_3$ in two litres of tap water) for 90 seconds, then washed in water for 30 seconds. Slides were then incubated with 1% Eosin stain for 2 minutes 15 seconds before being washed for 45 seconds in tap water. The slides were again dehydrated in serial dilutions of water in Ethanol (50%, 60%.....100% Ethanol) and transferred to Xylene for 1 minute and then fresh Xylene for an additional minute. Slides were then mounted using Depex.

2.10 Embryo manipulations

2.10.1 *In vitro* fertilisation of *Xenopus* eggs

In vitro fertilisation was carried out on *Xenopus* eggs according to standard procedures. Embryos were dejellied in 2% (w/v) cysteine - HCl pH8, and washed two times with $1/10^{th}$ Barth X solution. Embryos were cultured to the desired stage in $1/10^{th}$ Barth X solution with 10 μg/ml gentamycin at 12–24°C. Staging was performed according to Nieuwkoop and Faber (1994).

2.10.2 Microinjection of embryos

For targeted microinjection of embryos, 18.4 nl of mRNA or morpholino oligonucleotide (MO) was injected into a two-cell or 8-cell stage embryo. *βgal* mRNA was injected as a lineage tracer and stained using the X-gal or Red-gal substrate to determine targeting to the pronephric region. Injections were performed in 5% Ficoll in Barth X.

2.10.3 Dissections

All dissections were performed using forceps and an eyebrow hair mounted in a hypodermic needle. Embryos were incubated until stage 8/9 where animal caps were dissected and grown to required stages according to un-dissected control embryos. Fine dissections of the presumptive pronephros were performed at various stages of development. Intermediate mesoderm was removed from presumptive pronephros and whole pronephros according to Brennan *et al.*, (1998).

2.10.4 Perturbation of gene expression using morpholino oligonucleotides

MO sequences are given in Figures 3.7A (*p27^{Xic1}* MO) and 6.5A (*Radical fringe* MO), 6.5B (*Lunatic fringe* MO1) and 6.5C (*Lunatic fringe* MO2). Standard Control morpholinos were designed and supplied by GeneTools, LLC (Corrallis, OR). All morpholinos were dissolved in ddH_2O to a stock concentration of 5 ng/nl. 5-20 ng was injected into V2 blastomere at the 8-cell stage alone or in combination with mRNA as specified earlier in section 2.10.2.

2.10.5 Chemical induction of cell cycle arrest using Hydroxyurea and Aphidicolin

Non-manipulated embryos were de-jellied and left to develop to stage 10.5 at 12°C in 1/10th Barth X. 20 µl 1M Hydroxyurea (made up fresh each time) and 10 µl of 15 mM Aphidicolin (stored in DMSO at -20°C) was then made up to 1 ml with 1/10th Barth X. Embryos were transferred to 24-well dishes (20 per well) containing this HUA/ 1/10th Barth X solution. Embryos were left to develop to desired stage at room temperature with the HUA/ 1/10th Barth X medium being changed twice daily. At the desired stage, embryos were fixed in MEMFA overnight at 4°C.

2.10.6 Lineage labelling for *βgal* mRNA injected embryos

Embryos at the desired stage were fixed for 1 hour in MEMFA (0.5M MOPS pH7.4, 100mM EGTA, 1mM $MgSO_4$, 4% formaldehyde). Meanwhile galactose substrate was prepared. For all embryos stained using 3G8 and 4A6 antibodies, the lineage label was stained blue using the X-gal substrate. For *in situ* hybridisations and all other antibody staining lineage labelled embryos were stained red using the Salmon/ Red-gal substrate. 0.075g X-gal (5-Bromo-4-Chloro-3-Inolyl-β-D-galactopyranoside) was weighed out in an Eppendorff and dissolved in 500 µl DMF (N,N-Dimethylformamide). The X-gal staining solution consisted of 15% X-gal, 5 mM Potassium ferricyanide, 5 mM Potassium ferrocyanide, and 2 mM $MgCl_2$ made up to 50 ml in PBS. Red-gal was made up in exactly the same way, but the Red-gal stock was in 20 mg/ml solution (dissolved in DMF, aliquoted and stored at -20°C). After 1 hour in MEMFA embryos were washed in PBS and then incubated in the X-gal or Red-gal substrate for 1 hour at 37°C. Embryos were washed in PBS and transferred back to MEMFA to be fixed overnight at 4°C.

2.10.7 Animal cap pronephros induction assays

Animal caps were dissected from stage 8/ 9 embryos as described in section 2.10.3. Caps were incubated in full strength Barth X medium containing 10 mg/ml BSA and a variety of growth factors; either no growth factor (untreated), 10^{-4}M Retinoic acid, 10 ng/ml Activin A, or 10^{-4}M Retinoic acid and 10 ng/ml Activin A. Caps were left for 2 hours in each solution before being transferred to 1/2 strength Barth X medium. Caps were left at room temperature in 1/2 strength Barth X medium until the desired stage of development was reached (whole embryos, fertilised at the same time as those embryos from which animal caps were taken, were used as stage determinants). Caps were placed in fresh media twice daily. RNA was then harvested from the caps using the protocol described in section 2.6.1.

Chapter 3

p27^{Xic1} controls pronephric organ size and somitogenesis through its cell cycle exit function during *Xenopus laevis* early development

3.1 Introduction

Development from fertilised egg to adult is a highly regulated process that is ultimately controlled by inter- and intra-cellular signals controlling cell proliferation, migration, differentiation and fate. We aimed to see how the cyclin-dependent kinase inhibitor p27^{Xic1} was involved in such processes during development of the *Xenopus laevis* embryonic kidney, the pronephros. To observe these activities we utilised a number of powerful techniques frequently used in the field of *Xenopus* research.

To observe if *p27^{Xic1}* is expressed in the pronephros we performed *in situ* hybridisation and RT-PCR analysis. These results determined whether *p27^{Xic1}* expression was spatially and temporally appropriate for it to have a role in nephrogenesis. In order to investigate the function of p27^{Xic1} in the pronephros we observed pronephric phenotypes upon over-expression and depletion of this gene product. To over-express *p27^{Xic1}*, we micro-injected *p27^{Xic1}* mRNA translated *in vitro* into a ventro-vegetal (V2) blastomere of an 8-cell stage embryo, as fate mapping has indicated these blastomeres give rise to cells that will form the pronephric anlagen on

either side of the embryo (Moody, 1987) (see Fig 3.1 for blastomere assignments). In order to monitor the targeting of the message, *βgal* mRNA was co-injected to act as a lineage tracer (Fig 3.2). Gene knockout is currently impossible in *Xenopus laevis* embryos as genetic studies cannot be performed due to the pseudo-tetraploid genome. However gene knock down studies can be performed using morpholino oligonucleotides (MO). These synthetic antisense oligos have morpholine rings that replace the ribose backbone making these oligos unrecognisable to the host cell. MOs can be designed to bind over the start codon or splicing site of particular gene transcript to inhibit translation or produce a truncated, and therefore inactive, protein product (Heasman et al., 2000; Corey and Abrams, 2001). Consequently protein expression of the gene is reduced. In *Xenopus* research this technique is repeatedly utilised and is a powerful tool to establish gene function.

As well as observing the pronephric phenotypes of over-expression and depletion of *p27*^{Xic1}, we wished to establish if there were any developmental effects on myogenesis, as V2 blastomere micro-injection targets the future myotome as well as pronephros. It is known that the paraxial mesoderm signals to the intermediate mesoderm to induce the pronephros anlagen (Seufert et al., 1999; Mauch et al., 2000; Mitchell et al., 2007). Thus if *p27*^{Xic1} over-expression or depletion affected myogenesis, the effects on nephrogenesis could be indirect, as a lack of (or disrupted) myogenesis may produce a pronephric phenotype. To test this we observed the effects of these injections on an early marker of differentiating muscle, *MyoD*, and a terminal marker of differentiated muscle, *MHC*, by *in situ* hybridisation.

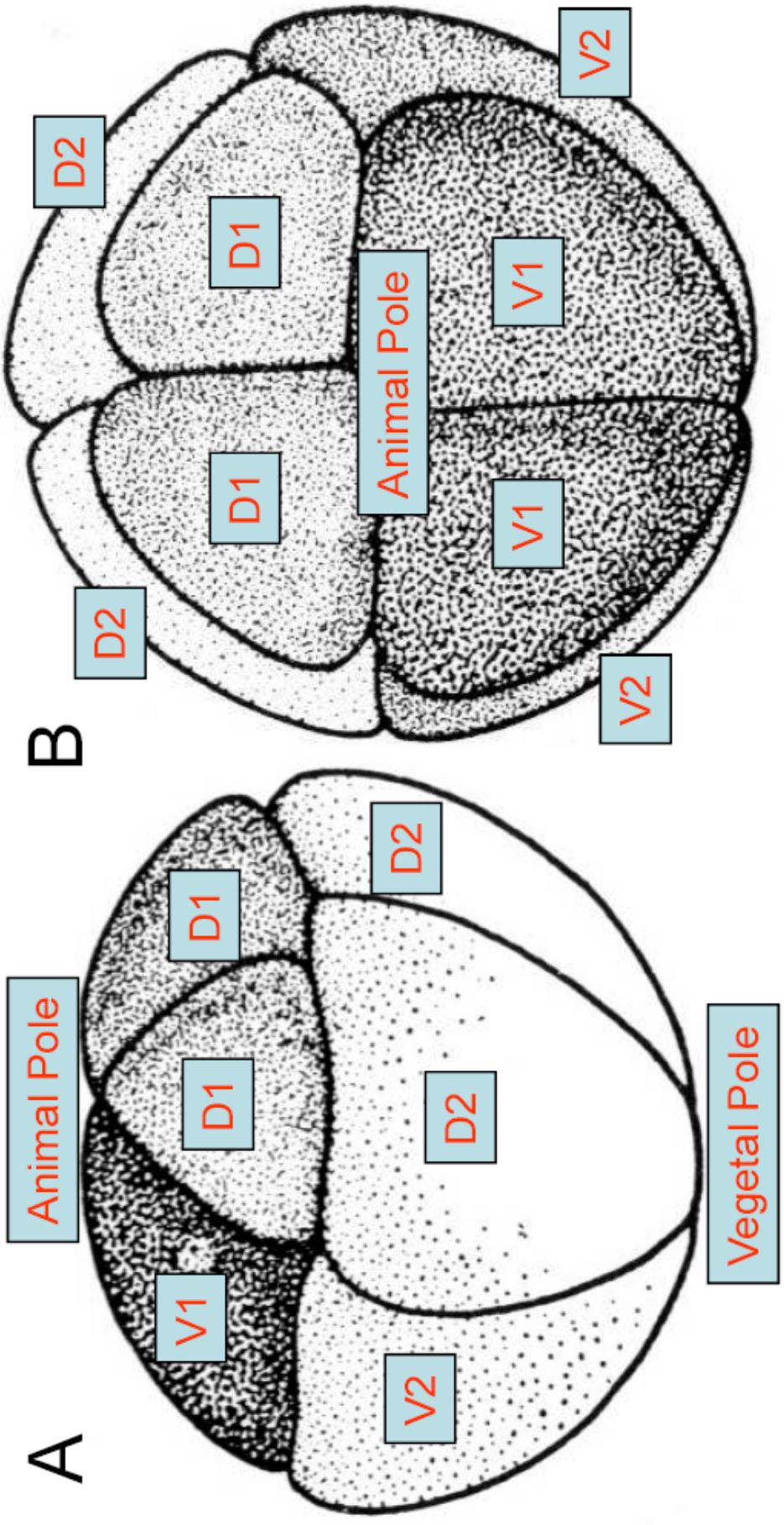

Figure 3.1 Nieuwkoop and Faber images of 8-cell stage *Xenopus laevis* embryos (acquired from xenbase.org). (A) Lateral view of an 8-cell stage embryo. (B) Animal pole view of an 8-cell stage embryo. All blastomeres are named and located according to assignments by Hirose and Jacobson (1979).

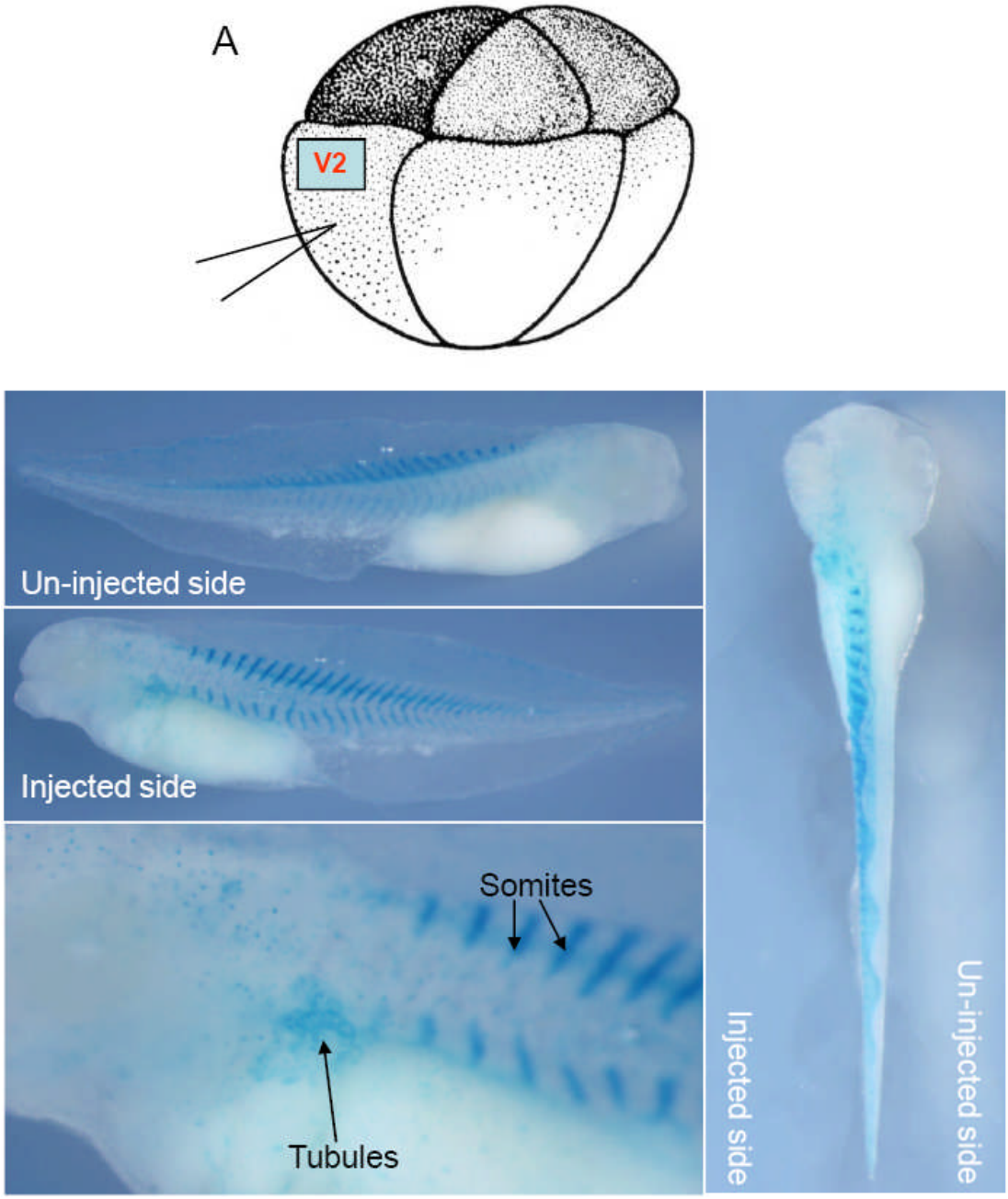

Figure 3.2 Targeting injected messages to the future pronephros and somites. (A) Lateral view of an 8-cell stage embryo indicating the V2 blastomere where message is injected to target the future pronephros. (B) Embryos were injected into the middle of a V2 blastomere with *βgal* mRNA, cultured to stage 41 and stained, by colour reaction using the X-gal substrate. Blue staining in the tubules and somites on only one side of the embryo indicate the injected message has been targeted correctly. NB: For *in situ* hybridisation analysis the injected *βgal* message was stained red, not blue, to improve visual distinction of lineage labelling and gene expression staining.

To observe the effects of p27^{Xic1} on cell division qualitative and quantitative approaches were adopted. p27^{Xic1} is a Cyclin-dependent Kinase Inhibitor (CKI); thus its injection will inhibit cell division. This effect can be observed at stage 8.5 by enlarged cells close to the site of injection. These enlarged cells recover normal cell division later on, but such observations allowed qualitative accounts of the level of cell cycle inhibitory activity of each injection to be monitored. To detail the effects of *p27^{Xic1}* over-expression or depletion on cell division quantitatively, we performed whole mount antibody staining for a marker of mitotic cells, phosphohistone H3 (pH3). Numerical comparison of positively stained cells on the injected and un-injected sides was observed, and statistical analysis of any effects was calculated.

Using these techniques we report that p27^{Xic1} is expressed within the developing pronephros by RT-PCR and detected within the functional pronephros at tadpole stages by *in situ* hybridisation. Over-expression of p27^{Xic1} reduces the size of the pronephric anlagen and results in disrupted somitogenesis. MO knock down also reduces the size of the pronephric anlagen, but completely inhibits myogenesis. The domain of the p27^{Xic1} protein responsible for the phenotypes was mapped to the N-terminus using p27^{Xic1} deletion constructs. These experiments identify previously unrecognised, functional roles for p27^{Xic1} in *X. laevis* pronephros development and somitogenesis and confirm the importance of this gene in diverse developmental processes.

3.2. Results

3.2.1 *p27^{Xic1}* expression in the pronephros

p27^{Xic1} expression has been previously shown in the notochord, neural plate, differentiating muscle and in the eye and brain but its distribution has not been reported past stage 33/34 in whole embryos (Ohnuma et al., 1999; Hardcastle and Papalopulu, 2000; Vernon et al., 2003; Vernon and Philpott, 2003). To analyse *p27^{Xic1}* expression in pronephric development, we investigated expression in later stage embryos using whole mount *in situ* hybridisation.

p27^{Xic1} expression in early stage and tail bud embryos followed similar domains to that previously reported (Collins. R, PhD Thesis, 2005), but was also detected in the pronephric region corresponding to the nephrostomes between stages 27 and 32 (Fig 3.3). Prior to and past these stages no pronephric expression of *p27^{Xic1}* was detected by *in situ* hybridisation.

To confirm the temporal expression of *p27^{Xic1}* in the pronephros, RT-PCR analysis was performed on dissected presumptive pronephroi (Fig. 3.4). Pronephric *p27^{Xic1}* expression was detected from stage 12.5 to stage 38. Thus RT-PCR analysis indicated expression of *p27^{Xic1}* in the presumptive pronephros precedes that detected by *in situ* hybridisation. Later, in pronephroi dissected from embryos at stage 35 and 38, expression of *p27^{Xic1}* was reduced compared to levels of expression earlier in development.

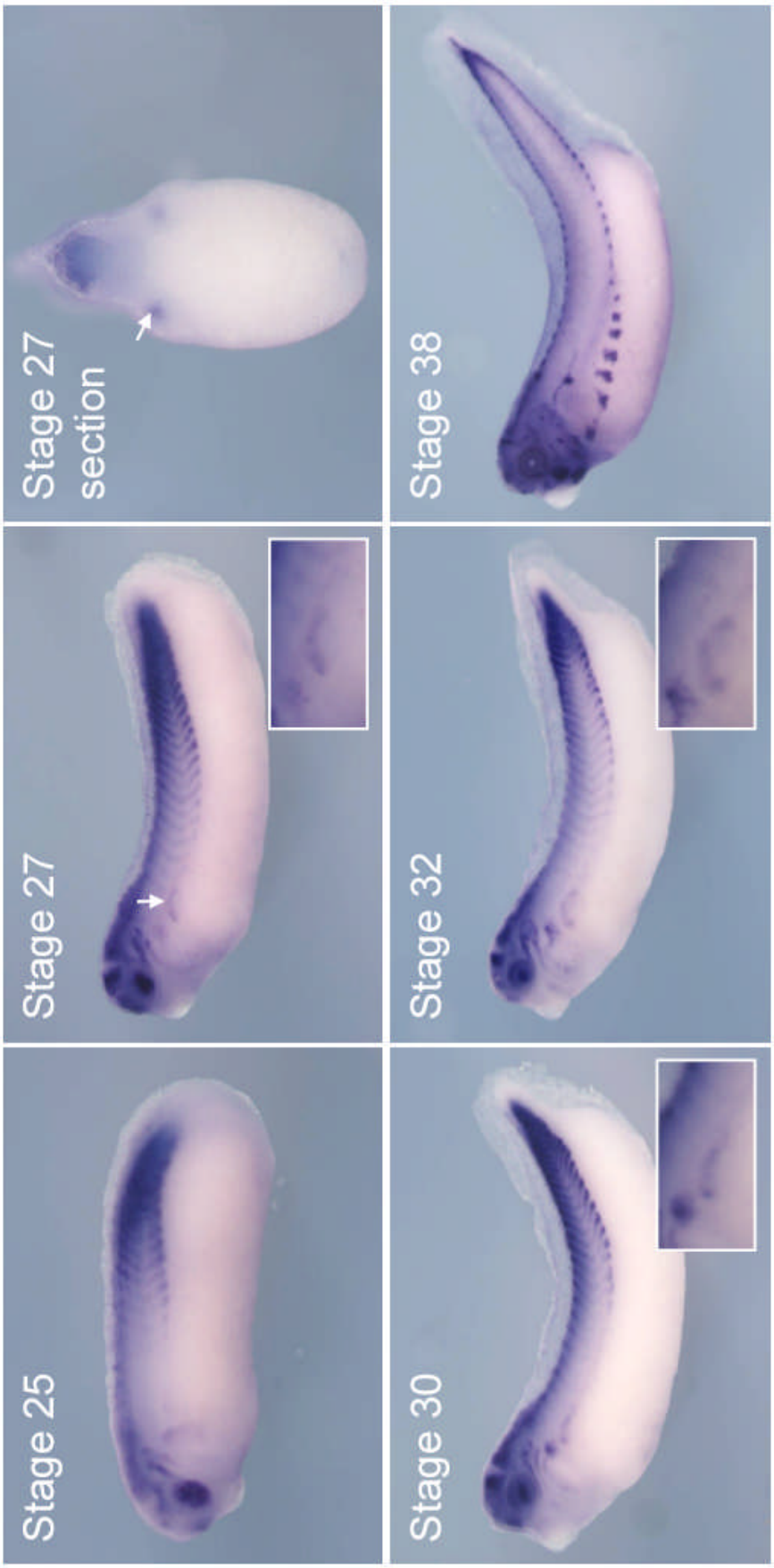

Figure 3.3 *p27Xic1* is expressed at late tail bud stages in the pronephros. Whole mount *in situ* hybridisation was carried out with a DIG-labelled anti-sense RNA probe for *p27Xic1*. Prior to and including stage 25, *p27Xic1* expression in the presumptive pronephros is not detected by *in situ* hybridisation. At stage 27 *p27Xic1* expression is clearly evident in the dorso-anterior region of the presumptive pronephros (white arrow). Pronephric staining is confirmed in transverse sections at stage 27 through the anterior pronephros anlagen; *p27Xic1* expression is visible in the pronephric tubules (white arrow). At stage 30 a similar pattern of *p27Xic1* expression to that seen at stage 27 is observed in the dorsal anterior pronephros anlagen. By stage 32 *p27Xic1* expression is concentrated in the nephrostomes and proximal tubules. No pronephric expression of *p27Xic1* is detected by *in situ* hybridisation at stage 38.

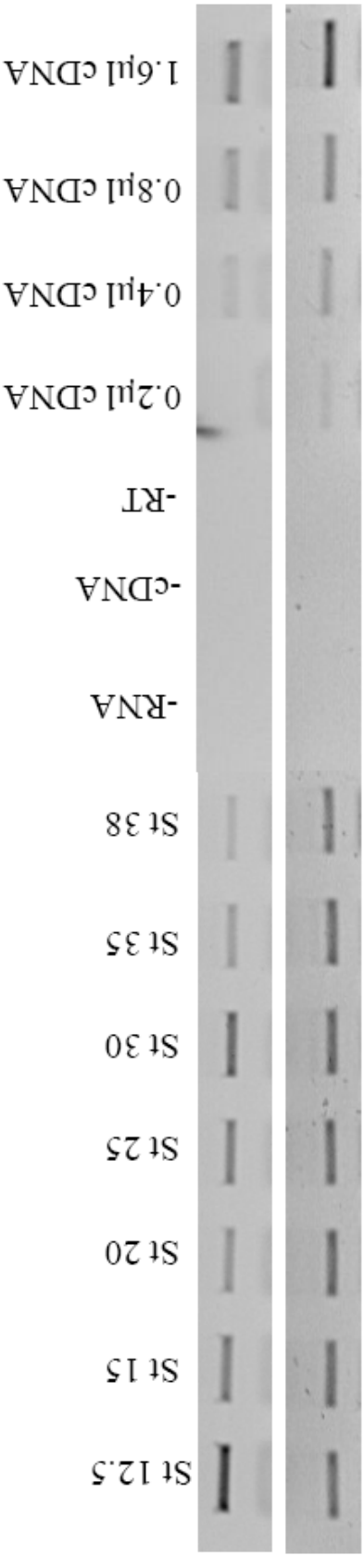

Figure 3.4 RT-PCR analysis confirms the expression profile of *p27Xic1* within presumptive pronephros tissue. The whole pronephric anlage was dissected from multiple embryos at stage 12.5, 15, 20, 25, 30, 35 and 38. mRNA and cDNAs were prepared by standard procedures and RT-PCR carried out for *p27Xic1* and the loading control *ODC*. Linearity of the PCR was confirmed by doubling the input of cDNA from control stage 20 embryos. Negative controls used were absence of RNA during the reverse transcription (-RNA), absence of reverse transcriptase (-RT), and absence of cDNA in the PCR (-cDNA). *p27Xic1* is expressed in the presumptive pronephric anlagen from stage 12.5, when the pronephric tubules are specified; through to stage 38, indicating *p27Xic1* may have a role in pronephros development. The quality of the dissected material has been confirmed elsewhere (Haldin et al, 2008)

In conclusion, *p27^{Xic1}* expression is temporally and spatially appropriate for a role in pronephros formation at all stages of its development, from induction of the anlagen through to differentiation and morphogenesis into a functional pronephros. This expression pattern suggests p27^{Xic1} may play a role in early pronephrogenesis.

3.2.2 *p27^{Xic1}* and *p21^{Cip1}* mRNA over-expression inhibited pronephric development

In order to examine the over-expression phenotype of *p27^{Xic1}* mRNA *in vivo*, we injected 50 pg *p27^{Xic1}* mRNA or 20 pg *p21^{Cip1}* mRNA into ventro-vegetal blastomeres of embryos at the 8-cell stage, with *βgal* mRNA to act as a lineage tracer. In each case the largest amount of mRNA that did not cause gross developmental defects was injected. The injected embryos were cultured to stage 41, correctly targeted embryos were sorted for pronephric expression via *βgal* staining and then subjected to whole mount antibody staining with 3G8, which detects proximal pronephric tubules and nephrostomes, and 4A6, which detects intermediate and distal pronephric tubules (Vize et al., 1995). The effects on pronephric structure were scored by comparing the lineage labelled injected side against the control, un-injected side, of the same embryo. Injecting control embryos with *βgal* mRNA alone did not affect proximal tubule (2% reduced, n=58) or intermediate and distal tubule (0% effected, n=58) morphology (Fig 3.5A). *p27^{Xic1}* mRNA injection gave a clear effect on pronephric morphology. The contribution to the proximal tubules was reduced on the injected side in 91% of embryos (n=23) (Fig 3.5B). Inspection of the intermediate and distal tubules revealed that *p27^{Xic1}* mRNA also reduced their size to a similar degree (83%, n=23) (Fig 3.5B). To confirm the results were statistically

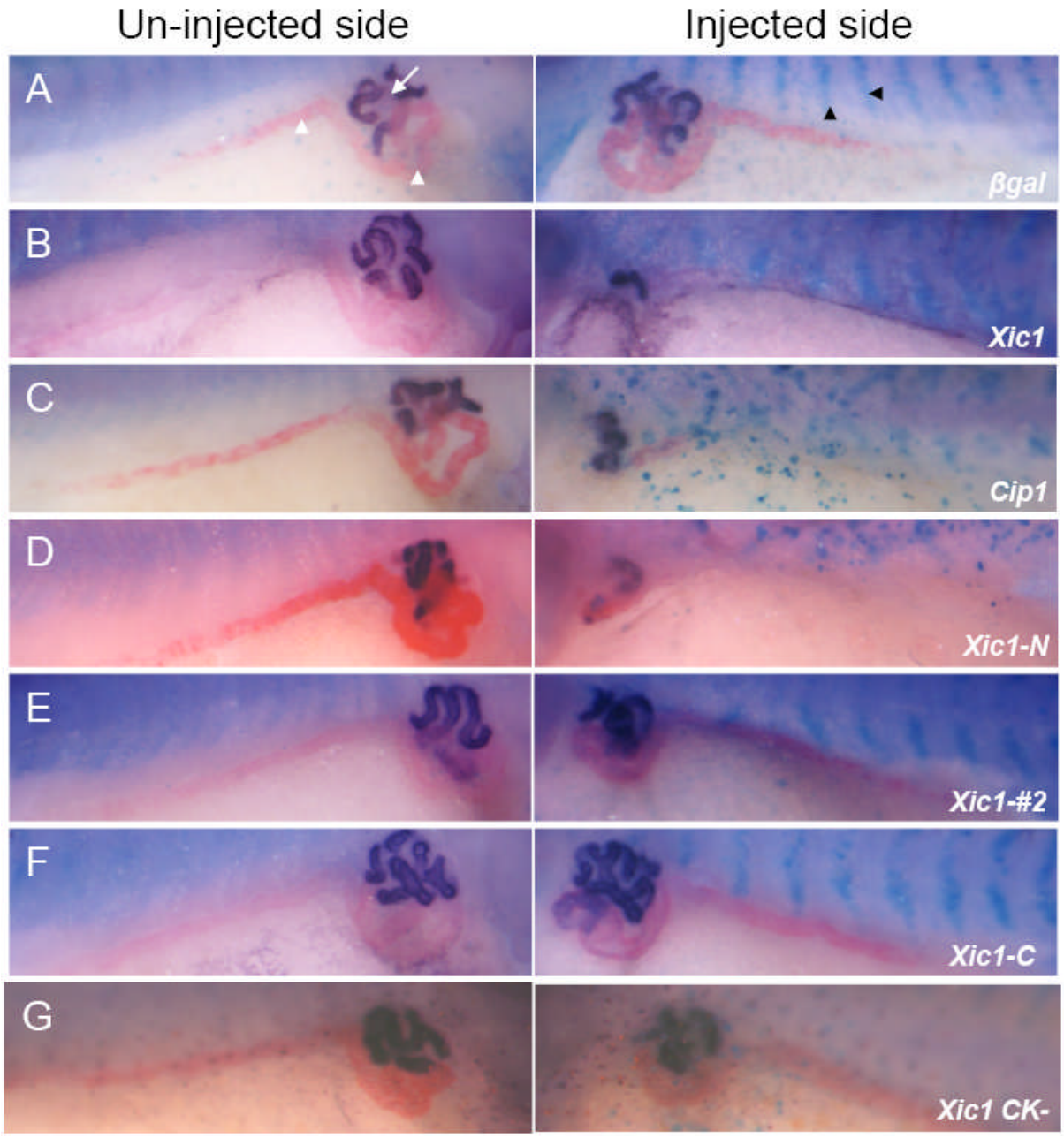

Figure 3.5 Over-expression of *p27Xic1* identifies a pronephric phenotype. *X. laevis* embryos were injected at the 8 cell stage into a ventro-vegetal blastomere to target the presumptive pronephric region. mRNA of the construct indicated was co-injected with *βgal* mRNA to act as a lineage tracer (blue staining, black arrowheads). Embryos were cultured till stage 41 and whole mount antibody stained with 3G8, to detect proximal pronephric tubules (white arrow, stained purple), and 4A6, to detect intermediate and distal pronephric tubules (white arrowheads, stained red). Control *βgal* mRNA injected embryos had normal pronephros development (A). *p27Xic1* mRNA, *p21Cip1* mRNA, and *p27Xic1 N* mRNA injections inhibited proximal, intermediate and distal tubule development on the injected side (B-D). *p27Xic1 #2* mRNA, *p27Xic1 C* mRNA and *p27Xic1 CK-* mRNA injections had no effect on pronephros development (E-G).

significant, Chi-squared analysis was performed. This analysis verified that the pronephros of *p27^{Xic1}* mRNA injected embryos was statistically significantly different in size when compared to *βgal* mRNA injected embryos ($p<0.05$).

p21^{Cip1} has functional and sequence homology with p27^{Xic1} and has been used to rescue the effect of the *p27^{Xic1}* MO (Vernon et al., 2003). Injecting *p21^{Cip1}* mRNA produced a similar phenotype to that of *p27^{Xic1}* mRNA (Fig 3.5C); the pronephric tubules were reduced in 82% of embryos (n=52). Chi-squared analysis was again performed on the results to reveal the phenotypes observed were statistically significant ($p<0.05$).

3.2.3 The *p27^{Xic1}* pronephric phenotype is dependent on the N terminus of the protein

p27^{Xic1} possesses three characteristic domains (Fig 3.6). The N-terminal half contains a Cyclin/ Cdk binding domain, highly conserved between p21^{Cip1}, p27^{Kip1}, and p57^{Kip2}. The C-terminal half possesses a PCNA-binding domain, also found in p21^{Cip1}, and a QT-domain, a potential cdc2 phosphorylation site that occurs in p27^{Kip1} (Polyak et al., 1994; Chen et al., 1995). Similar to full length p27^{Xic1}, p27^{Xic1} N (amino acids 1-96) inhibits Cdk kinase activity and stops cell division before MBT. p27^{Xic1} C (amino acids 97-210) can inhibit PCNA driven replication but cannot stop cell division before MBT (Ohnuma et al., 1999). A third construct, p27^{Xic1} #2 (amino acids 35-96), possesses Cdk2 inhibitory activity but has been shown to lack the Müller cell inductive activity observed with p27^{Xic1} N in the *Xenopus* retina (Ohnuma et al., 1999) and lack the ability to promote primary

Key

Cyclin binding site
Cdk binding site
PCNA binding site
QT domain

Xic1

MAAFHIALQEEMIVASPAALPRLSLGTGRGACRNLFGPIDHDELRSELKRQLKEIQASDCQRW
NFDFESGTPLKGTFCWEPVETKDVPSFYSPSRSLAANTTPQSRQQQPLLVSRQPEPREEAP
VDTVRNVPNPPCAKENAEKIIKRCQGVKGPTKASANTSTQRRKREITTPITDYFPKRKKI
LSAKPDATKGVHLLCPLEQTPRKKIR

Human Cip1

MSEPAGDVRQNPCGSKACRRLFGPVDSEQLSRDCDALMAGCIQEARERWNFDFVTETPL
EGDFAWERVRGLGLPKLYLPTGPRRGRDELGGGRRPGTSPALLQGTAEEDHVDLSLSCTLVPRSG
EQAEGSPGGPGDSQGRKRRQTSMTDFYHSKRRLIFSKRKP

Xic1-N (1-96)

MAAFHIALQEEMIVASPAALPRLSLGTGRGACRNLFGPIDHDELRSELKRQLKEIQASDCQRW
NFDFESGTPLKGTFCWEPVETKDVPSFYSPSRS

Xic1-#2 (35-96)

LFGPIDHDELRSELKRQLKEIQASDCQRWNFDFESGTPLKGTFCWEPVETKDVPSFYS
PSRS

Xic1-C (97-210)

LAANTTPQSRQQQPLLVSRQPEPREEAPVDTVRNVPNPPCAKENAEKIIKRCQGVKGPTKASANTSTQ
RRKREITTPITDYFPKRKKILSAKPDATKGVHLLCPLEQTPRKKIR

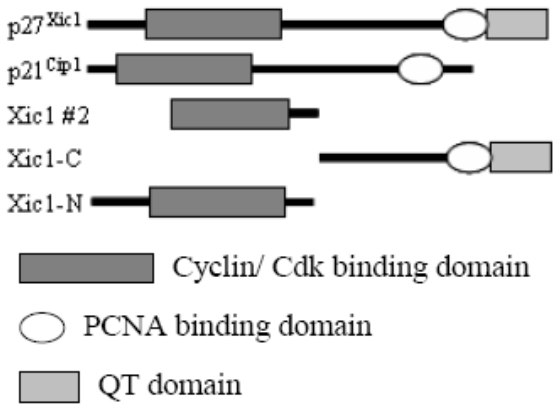

Figure 3.6 Amino acid sequences and **s**chematic illustration of human p21Cip1, p27Xic1 and the p27Xic1 constructs used in this study. (Note: PCNA binding domain and QT domain overlap, as illustrated by intercalated coloured letters in amino acid sequences.)

neurogenesis (Vernon et al., 2003). In order to investigate the effect these constructs had on pronephric development, we injected 50 pg *p27^{Xic1} N* mRNA, 80 pg *p27^{Xic1} C* mRNA and 80 pg *p27^{Xic1} #2* mRNA into a ventro-vegetal blastomere of 8 cell stage embryos and cultured till stage 41. Whole mount antibody staining was performed as previously described with 3G8/ 4A6. Inspection of *p27^{Xic1} N* mRNA injected embryos, revealed a clear effect on proximal tubule (68% reduced, n=22) and intermediate and distal tubule (68% reduced, n=22) morphology similar to full length *p27^{Xic1}* mRNA when compared against the control, un-injected side (Fig 3.5D). Chi-squared analysis of the results was performed as for *p27^{Xic1}* mRNA, which determined there was a statistically significant reduction in size of pronephric tubules ($p<0.05$). Therefore, p27^{Xic1} N, like the full length protein, affects pronephric development. In contrast, analysis of pronephric tubule morphology after *p27^{Xic1} #2* mRNA (n=34) and *p27^{Xic1} C* mRNA (n=23) injections showed 0% effect on the pronephric development, similar to control embryos injected with *βgal* mRNA (Fig 3.5E and F). Multiple repetitions of these over-expression experiments yielded similar data.

3.2.4 *p27^{Xic1}* MO depleted translation of *p27^{Xic1}* mRNA, but not *p21^{Cip1}* mRNA *in vitro*

To investigate whether depletion of p27^{Xic1} affects pronephric development, we utilised a previously characterised anti-sense morpholino oligonucleotide (MO, Fig 3.7A) designed to be complementary to *p27^{Xic1}*, and shown to specifically knock down *p27^{Xic1}* translation *in vivo* by Western blot analysis (Vernon et al., 2003; Movassagh and Philpott, 2008). The MO was tested *in vitro* to confirm its specificity. In order to control MO knock down experiments, rescue of any

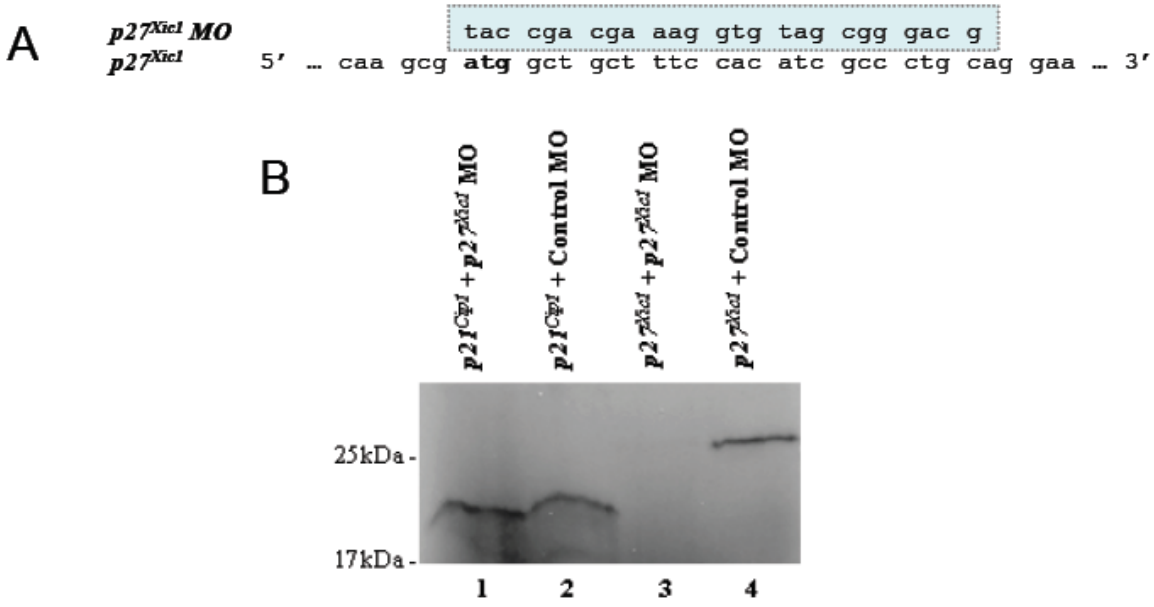

Figure 3.7 The *p27Xic1* MO does not inhibit translation of *p21Cip1* mRNA *in vitro*. The sequence of the *p27Xic1* MO and the region of the endogenous transcripts it binds to is shown in A (the start codon is in bold). (B) *p27Xic1* mRNA was co-translated *in vitro* with a related mRNA, *p21Cip1* mRNA, to identify if p21Cip1 was suitable to rescue the effects of the *p27Xic1* MO. Radio-labelled p27Xic1 and p21Cip1 were separated on an SDS-PAGE gel and detected by autoradiography. 4.8 µg *p21Cip1* mRNA was translated in the presence of either 10 µg *p27Xic1* MO (lane 1) or 10 µg *Control* MO (lane 2). 5.2 µg *p27Xic1* mRNA was translated in the presence of either 10 µg *p27Xic1* MO (lane 3) or 10 µg *Control* MO (lane 4). *p27Xic1* MO successfully knocks down translation of *p27Xic1* mRNA (lane 3) but not *p21Cip1* mRNA (lane 1). Thus *p21Cip1* mRNA is a suitable message to use to rescue the effects of the *p27Xic1* MO as p21Cip1 has functional homology with p27Xic1 but translation of *p21Cip1* mRNA is not inhibited by the *p27Xic1* MO.

phenotype observed needs to be achieved. To rescue the effects of the *p27^{Xic1}* MO in developing embryos we co-injected *p21^{Cip1}* (see section 3.2.6). Thus to assess whether *p21^{Cip1}* translation was inhibited by the *p27^{Xic1}* MO, and to ensure specificity of the *p27^{Xic1}* MO, an *in vitro* translation was performed using a rabbit reticulocyte lysate system with ^{35}S-Methionine. 4.8 µg *p21^{Cip1}* mRNA or 5.2µg *p27^{Xic1}* mRNA was incubated in combination with either 10 µg *p27^{Xic1}* MO or 10µg *Control* MO. The lysates were subjected to SDS-PAGE and analysed by autoradiography (Fig 3.7B). We observed no knock down of *p21^{Cip1}* mRNA translation *in vitro* (lane 1), but almost complete knock down of *p27^{Xic1}* mRNA translation *in vitro* (lane 3). This result indicated the *p27^{Xic1}* MO specifically knocks down translation of *p27^{Xic1}* mRNA, and *p21^{Cip1}* mRNA is a suitable message to use to rescue the effects of the *p27^{Xic1}* MO, since the Philpott laboratory has already demonstrated that it behaves in a functionally similar manner (Vernon et al., 2003).

3.2.5 p27^{Xic1} depletion using *p27^{Xic1}* MO reduced the size of the pronephric tubules

To determine if p27^{Xic1} depletion affected development of the pronephros, we injected 20 ng *p27^{Xic1}* MO with *βgal* mRNA into a ventro-vegetal blastomere of 8-cell stage embryos and cultured till stage 41. Embryos were selected for pronephric expression and whole mount antibody stained using 3G8 and 4A6 antibodies. Injection of a *Control* MO had 0% effect on the morphology of the pronephric tubules (n=24), confirming that the process of injecting a random sequence MO does not adversely effect pronephric development (Fig 3.8A). Inspection of *p27^{Xic1}* MO injected embryos revealed a clear effect on proximal tubule morphology when compared against the control, un-injected side. The proximal tubules were reduced

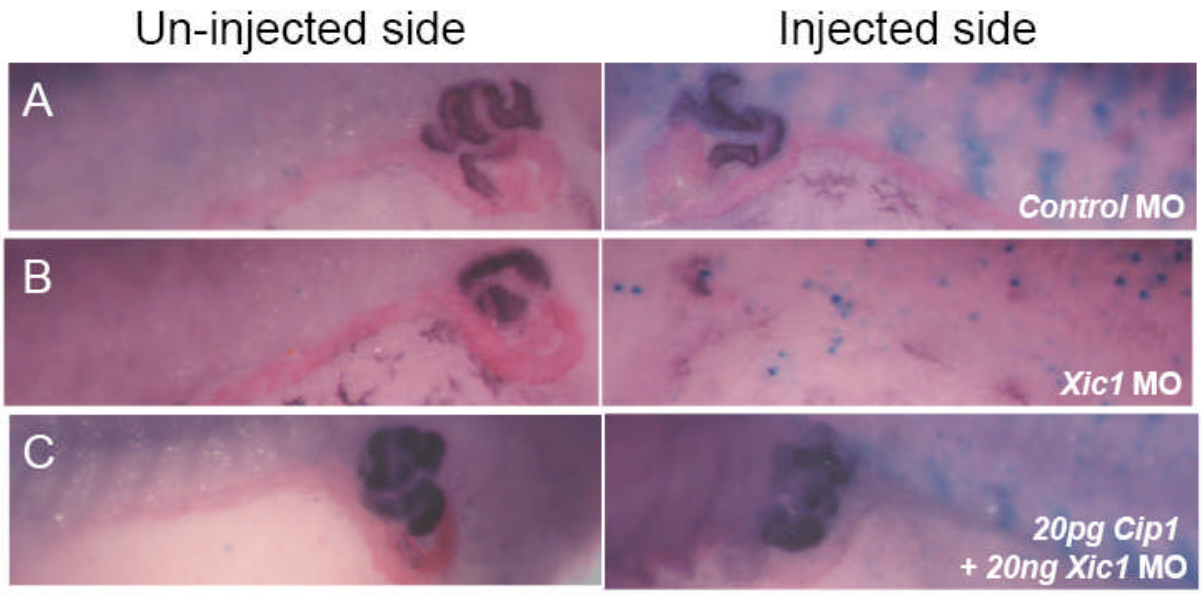

Figure 3.8 Inhibition of endogenous *p27Xic1* mRNA translation using a MO identifies a pronephros phenotype. *X. laevis* embryos were injected at the 8 cell stage into a ventro-vegetal blastomere to target the presumptive pronephric region. *βgal* mRNA was co-injected to act as a lineage tracer. Embryos were cultured till stage 41 and whole mount antibody stained with 3G8, to detect proximal pronephric tubules, and 4A6, to detect intermediate and distal pronephric tubules. *Control* MO-injected embryos had normal pronephros development (A). Injection of *p27Xic1* MO inhibited formation of the proximal, intermediate and distal tubules on the injected side (B). *p21Cip1* mRNA almost completely rescued development of the pronephros when co-injected with *p27Xic1* MO (C).

on the injected side of 93% of embryos (n=27) (Fig 3.8B). Analysis of the intermediate and distal tubule morphologies revealed *p27^{Xic1}* MO reduced their size in 81% of embryos (n=27). Chi-squared analysis on the results confirmed there was a statistically significant difference in pronephros morphology ($p<0.05$), thus we conclude *p27^{Xic1}* is required for normal nephrogenesis. Multiple repetitions of this knock down experiment yielded similar data.

3.2.6 Co-injecting *p21^{Cip1}* with *p27^{Xic1}* MO rescued development of the pronephros

We next attempted to rescue the *p27^{Xic1}* MO phenotype by co-injecting *p21^{Cip1}* with the *p27^{Xic1}* MO into a ventro-vegetal blastomere of an 8-cell stage embryo. p21^{Cip1} has functional homology with p27^{Xic1}, as described above, but is not translationally inhibited by the *p27^{Xic1}* MO (Fig 3.7B), thus enabling us to observe the specificity of the *p27^{Xic1}* MO we injected. Embryos were co-injected with 20 ng *p27^{Xic1}* MO, 20 pg *p21^{Cip1}* mRNA, and *βgal* mRNA to act as a lineage tracer, and cultured to stage 41. Correctly targeted embryos were selected and whole mount antibody stained using 3G8 and 4A6. Alongside these co-injections, single injections of 20 ng *p27^{Xic1}* MO and 20 pg *p21^{Cip1}* mRNA were also performed to act as controls. Both *p27^{Xic1}* MO and *p21^{Cip1}* mRNA single injections reduced the size of the pronephros to similar degrees previously observed (Fig 3.8B and 3.5C, respectively). However when 20 ng *p27^{Xic1}* MO was co-injected with 20 pg *p21^{Cip1}* mRNA a statistically insignificant number of embryos had a reduced pronephros (9%, n=23) (Fig 3.8C) ($p>0.05$). In these embryos nephrogenesis is almost completely rescued, thus the *p27^{Xic1}* MO specifically inhibits the translation of endogenous *p27^{Xic1}* mRNA.

3.2.7 The anti-apoptotic protein Bcl_{XL} had no effect on pronephric phenotypes observed when *p27^{Xic1}* is over-expressed or depleted using a MO

Programmed cell death (PCD) is a key developmental process required by multi-cellular organisms to eliminate unwanted cells. In *Xenopus laevis* apoptotic cells are distributed in a relatively defined pattern during early development indicating that PCD plays an important role in embryogenesis (Hensey and Gautier, 1998). Recently molecular connections between cell cycle exit and PCD have begun to be established (as reviewed in Greenwood and Gautier, 2005). Thus we wished to see if increased or decreased expression of *p27^{Xic1}* gave reduction phenotypes in the pronephros as a result of ectopic apoptosis. In order to establish this, we inhibited apoptosis by co-injecting the apoptotic inhibitor Bcl_{XL} with *p27^{Xic1}* mRNA or the *p27^{Xic1}* MO. Injecting *Bcl_{XL}* mRNA with *βgal* mRNA into one cell of a two cell stage embryo statistically significantly reduced apoptosis in 36% of embryos assayed by TUNEL analysis at stage 22 (n=55, $p<0.05$, Fig 3.9). We injected *p27^{Xic1}* mRNA and *p27^{Xic1}* MO with or without *Bcl_{XL}* mRNA into one cell of a two cell stage embryo and left the embryos to develop to stage 24. Expression of *Lim-1*, an early marker for the pronephros anlagen, was then detected by *in situ* hybridisation (Fig 3.10). The pronephros anlagen was reduced in 92% of embryos injected with the *p27^{Xic1}* MO (n=24) (Fig 3.10B) and 74% of embryos injected with *p27^{Xic1}* mRNA (n=38) (Fig 3.10D). The same phenotypes with similar degrees of severity were observed when *Bcl_{XL}* was co-injected with the *p27^{Xic1}* MO (97% reduced, n=41) (Fig 3.10C) and *p27^{Xic1}* mRNA (84% reduced, n=37) (Fig 3.10E). Chi-squared analysis on the results revealed there was no statistically significant difference in pronephros anlagen size between the single injections when compared to co-injected embryos ($p>0.05$). In

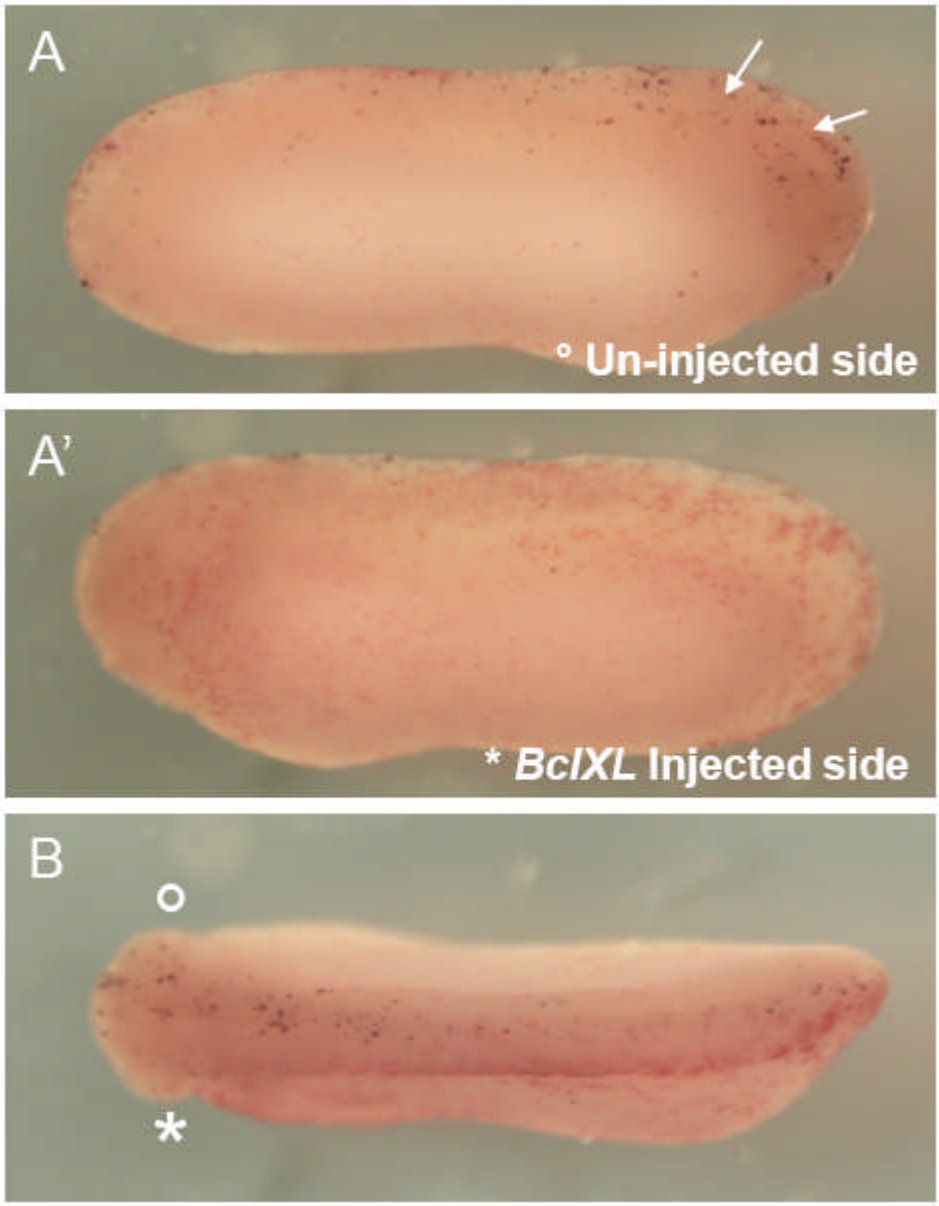

Figure 3.9 *BclXL* over-expression apoptosis, as observed by TUNEL analysis. *X. laevis* embryos were injected into one cell of a 2 cell stage embryo to target one side of the embryo. *βgal* mRNA was co-injected to act as a lineage trace. Embryos were cultured till stage 24 and assayed for apoptotic cells (white arrows) by whole mount TUNEL analysis. 1 ng *BclXL* mRNA reduced the number of apoptotic cells on the injected side (A), when compared to the un-injected side (A'). This phenotype is clearly highlighted when the embryo is observed from a dorsal view (B). * denotes injected side, ^{0} denotes un-injected side.

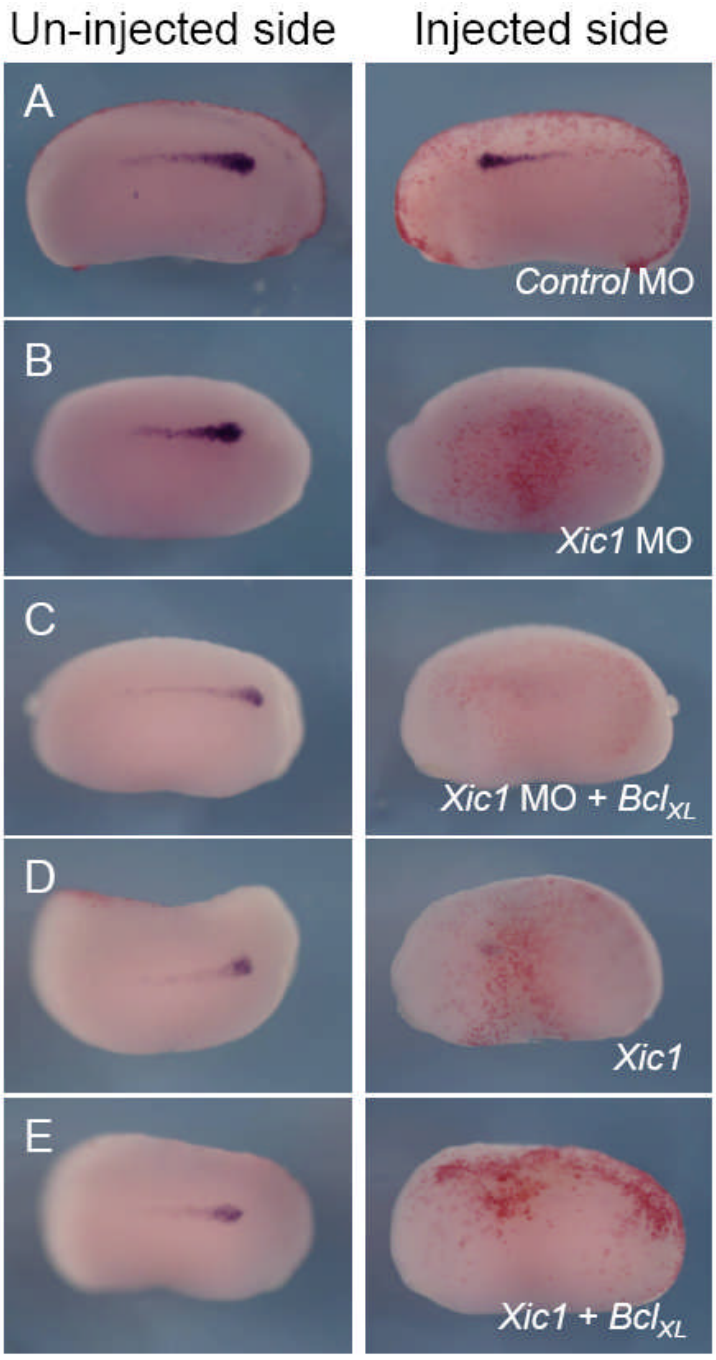

Figure 3.10 *p27Xic1* over-expression and depletion, using a MO, inhibited pronephros anlagen formation with the same severity in the presence or absence of the apoptotic inhibitor *BclXL*. *X. laevis* embryos were injected at the 8 cell stage into a ventro-vegetal blastomere to target the presumptive pronephric region. *βgal* mRNA was co-injected to act as a lineage trace. Embryos were cultured till stage 22 and whole mount *in situ* hybridised for expression of *Lim-1*, an early marker of the pronephros anlagen. Injection of the *Control* MO had no effect on *Lim-1* expression (A). *p27Xic1* mRNA, *p27Xic1* MO, *p27Xic1* mRNA/ *BclXL* mRNA, and *p27Xic1* MO/ *BclXL* mRNA all reduced expression of *Lim-1* on the injected side (B-E). Injection of *p27Xic1* mRNA and *p27Xic1* MO had effects on muscle development (see section 2.9); hence curling of the embryos towards the injected side was frequently observed, such as in the *p27Xic1*/ *BclXL* injected embryo shown here (panel E).

conclusion PCD caused by injection of *p27^{Xic1}* mRNA and *p27^{Xic1}* MO is not the mechanism by which nephrogenesis is inhibited.

3.2.8 Over-expression of *p27^{Xic1}* reduced cell division, but MO depletion of p27^{Xic1} had no effect

p27^{Xic1} is a well defined cell cycle inhibitor, thus over-expressing *p27^{Xic1}* could be expected to reduce the number of cells that can contribute to the pronephros anlagen when it is induced at stage 12-14, thus generating a pronephros of reduced size. To test whether an effect on cell cycle could explain the pronephric phenotype, we injected *p27^{Xic1}* mRNA and *p27^{Xic1}* MO into one cell of a two cell stage embryo and allowed development to stage 20. Following fixation and *βgal* staining *Lim-1 in situ* hybridisations and anti-phosphohistone H3 (pH3, a marker of dividing cells) immunostains were performed on the same embryos. As previously observed, over-expressing *p27^{Xic1}* mRNA reduced *Lim-1* expression in 75% of scored embryos (n=24) (Fig 3.11B), similarly 84% of embryos injected with the *p27^{Xic1}* MO had reduced *Lim-1* expression (n=31) (Fig 3.11C). However depleting *p27^{Xic1}* translation with the anti-sense MO had no statistically significant effect on pH3 immunostaining, on average there was a 1% increase in the number of dividing cells on the injected side of 11 embryos randomly selected and numerically scored for pH3 immunostained cells. Predictably, injection of *p27^{Xic1}* mRNA reduced the total number of pH3 immunostained cells on the injected side by 63% on average (n=11) (Fig 3.11E). Injection of *Control* MO had no significant effect on either *Lim-1* expression (2% reduced, n=55) or pH3 immunostaining (4% average reduction, n=10) (Fig 3.11A). Cell cycle effects after injection of components of the cell cycle

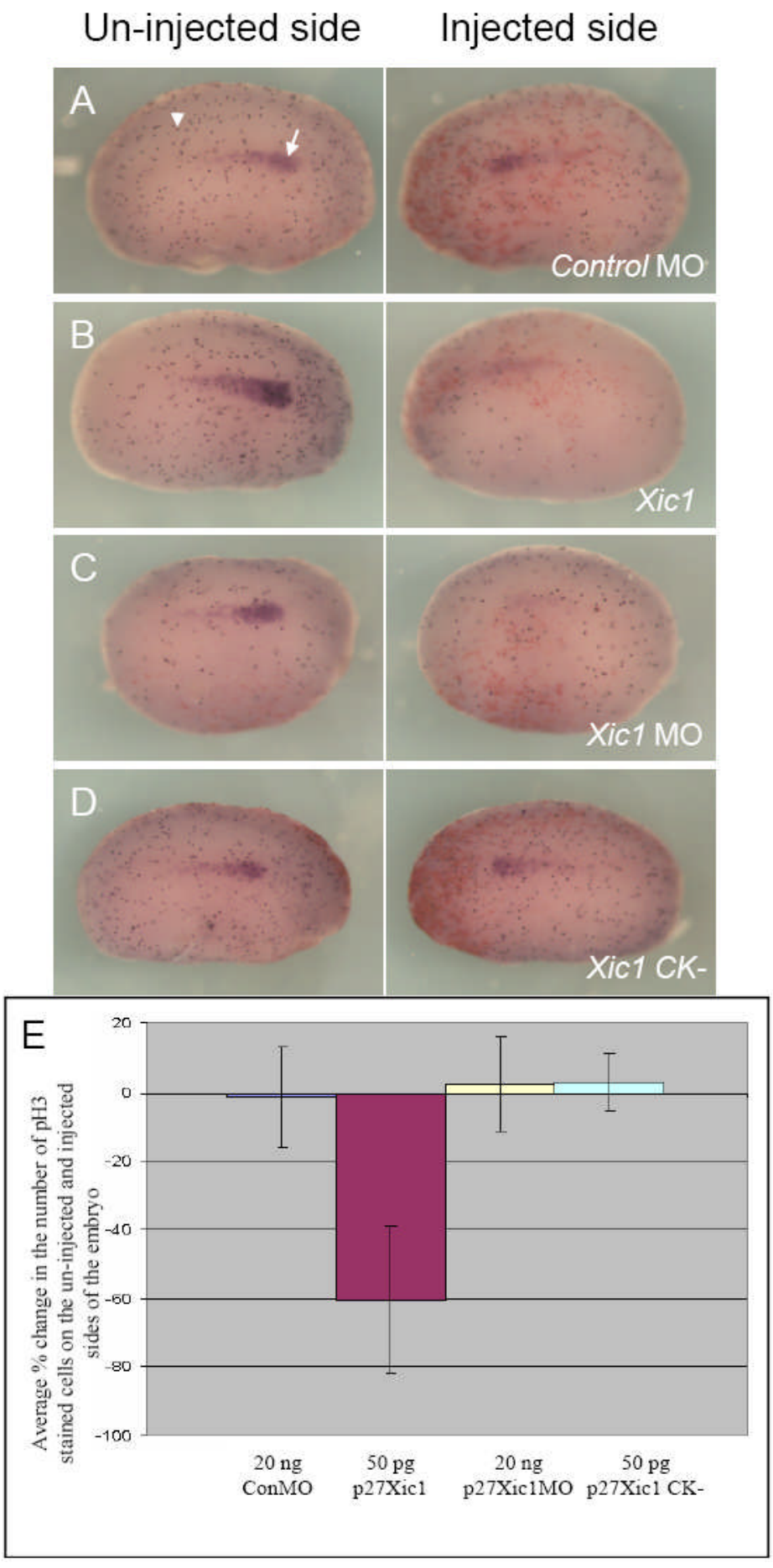
Un-injected side
Injected side
A
Control MO
B
Xic1
C
Xic1 MO
D
Xic1 CK-
E
Average % change in the number of pH3 stained cells on the un-injected and injected sides of the embryo
20
0
-20
-40
-60
-80
-100
20 ng ConMO
50 pg p27Xic1
20 ng p27Xic1MO
50 pg p27Xic1 CK-

Figure 3.11 Over-expression of *p27Xic1* mRNA reduced cell division, whereas depletion of endogenous *p27Xic1* mRNA translation using a MO had no effect on cell division. *X. laevis* embryos were injected into one cell of a two cell stage embryo with *βgal* mRNA to act as a lineage trace. Embryos were cultured till stage 22 and whole mount *in situ* hybridised for expression of *Lim-1*, and antibody stained for phosphohistone H3 (pH3, a marker of dividing cells). The *Control* MO had no effect on *Lim-1* expression (white arrow) or pH3 immunostaining (white arrowhead) (A). *p27Xic1* mRNA reduced both *Lim-1* expression and pH3 immunostaining (B). *p27Xic1* MO had no effect on pH3 immunostaining but reduced *Lim-1* expression (C). *p27Xic1 CK-* mRNA had no effect on either *Lim-1* expression or pH3 staining (D). * denotes injected side. To quantify the effect of these injections on cell division, positively pH3 immunostained cells on the injected and un-injected side of the embryos were numerically scored. The difference in the number of pH3 immunostained cells on the injected and un-injected sides of the embryos were numerically scored, calculated as percentages and are presented as a bar chart here (E) (see appendix for empirical data). The *Control* MO, *p27Xic1* MO, and *p27Xic1 CK-* mRNA had no statistically significant effect on pH3 immunostaining. *p27Xic1* mRNA statistically significantly reduced pH3 immunostaining on the injected side on average by 63% when compared to the un-injected side.

can often be observed at stage 8.5 where early translation of the injected message reduces cell division after CKI mRNA injection. Figure 3.12 highlights these effects, and reinforces the results obtained in this section as only *p27^{Xic1}* mRNA injection increased cell size as a consequence of reduced cell division (Fig 3.12C), whereas *Control* MO (Fig. 3.12A) and *p27^{Xic1}* MO (Fig 3.12B) had no effect. In conclusion these results suggest over-expressing *p27^{Xic1}* reduced the size of the pronephros due to premature cell cycle exit reducing the number of cells contributing to the anlagen. In contrast, reduction in size of the pronephros following MO knock down could not be attributed to this effect.

3.2.9 Loss of *p27^{Xic1}* inhibits myogenesis, which secondarily inhibits nephrogenesis

The signal instructing presumptive pronephric mesoderm to form the pronephros comes from the anterior somites (Seufert et al., 1999; Mauch et al., 2000; Mitchell et al., 2007). Thus myogenesis is required for pronephros anlagen induction. Injection into a ventro-vegetal blastomere targets both the future somites and pronephros. Hence we may be observing a pronephric phenotype at stage 41 due to alterations in myogenesis during earlier development. To test this hypothesis we injected *p27^{Xic1}* mRNA, *p27^{Xic1}* MO and *Control* MO with *βgal* mRNA to act as a lineage tracer into a ventro-vegetal blastomere of embryos at the 8-cell stage. The embryos were left to develop to stage 24, then fixed and subjected to double *in situ* hybridisation for *MyoD* and *Lim-1* expression. Over-expressing *p27^{Xic1}* caused an expected reduction in *Lim-1* expression in 78% of embryos (n=27) (Fig 3.13B). 76% of these affected embryos had disrupted segmentation in the somites, illustrated by *MyoD* expression being non-segmented. Depletion of *p27^{Xic1}* by antisense MO

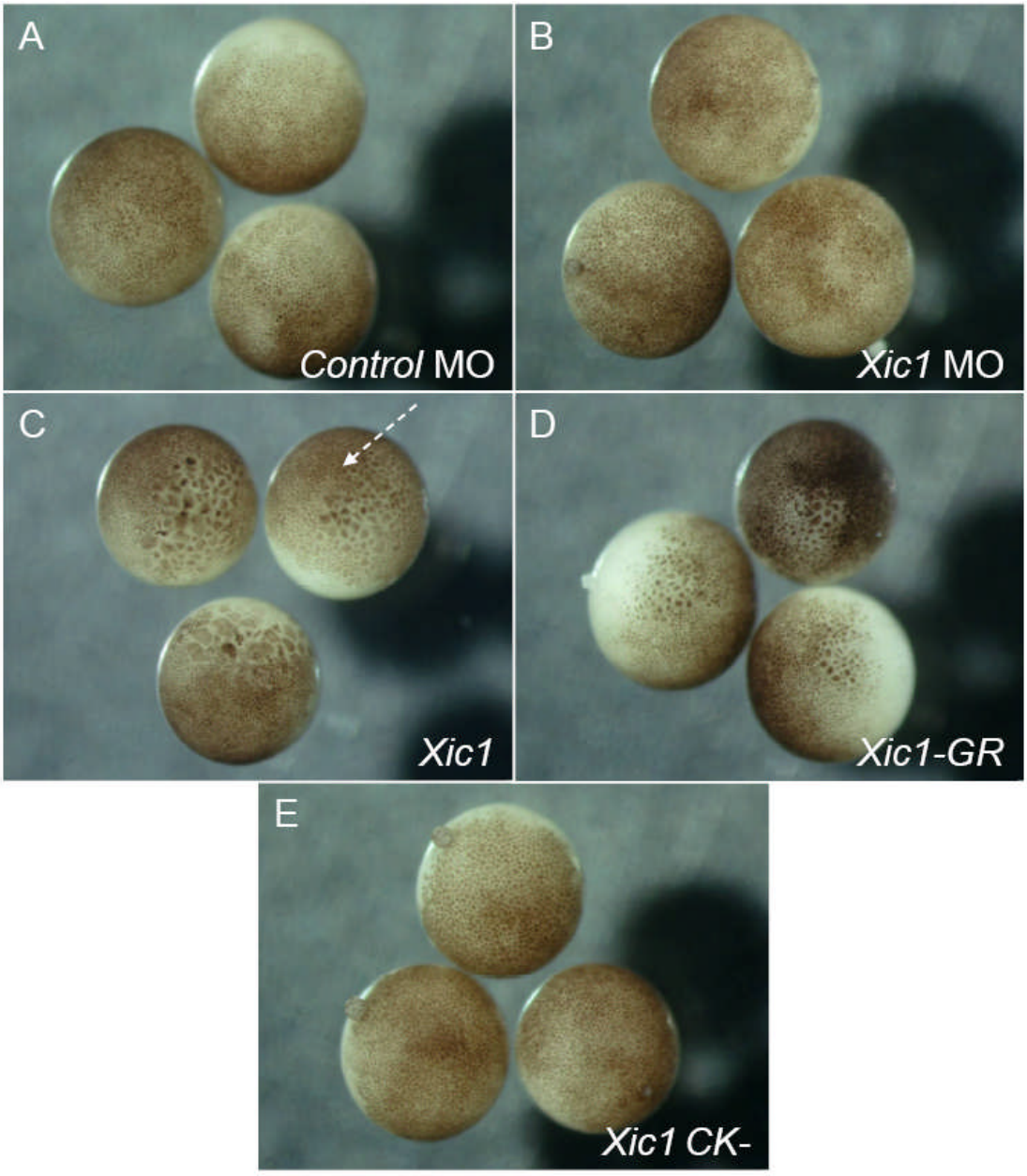

Figure 3.12 Mis-expression of *p27Xic1* caused cell division defects that could be observed at stage 8.5. *X. laevis* embryos were injected at the 8 cell stage into a ventro-vegetal blastomere to target the presumptive pronephric region. Embryos were cultured till stage 8.5 and the effect on cell cycle observed under the microscope. The *Control* MO had no effect on cell division (A). *p27Xic1* MO also had no effect on cell cycling (B). *p27Xic1* mRNA significantly reduced cell cycling (dashed white arrow) (C). *p27Xic1-GR* mRNA also reduced cell cycling at the same concentration as non-inducible *p27Xic1* mRNA, albeit with reduced potency, indicating this construct was leaky and experimentally invalid (D). p27Xic1 CK- had no observable effect on cell division at stage 8.5 (E).

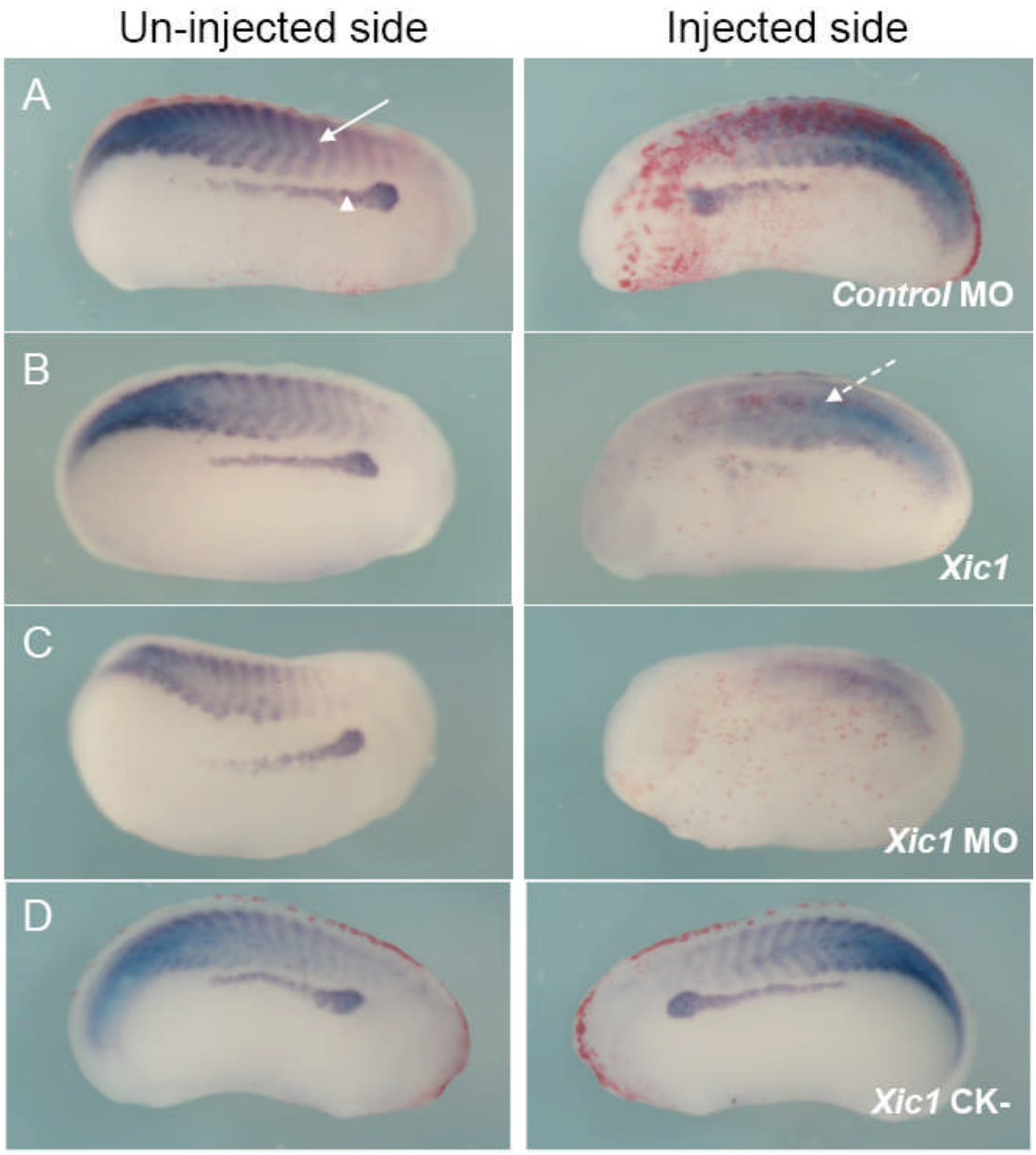

Figure 3.13 Mis-expression of *p27Xic1* disrupted somite morphology and muscle differentiation. *X. laevis* embryos were injected at the 8 cell stage into a ventro-vegetal blastomere to target the presumptive pronephric region. *βgal* mRNA was co-injected to act as a lineage trace. Embryos were cultured till stage 24 and whole mount *in situ* hybridised for expression of both *Lim-1* and *MyoD* (a marker of differentiating muscle). The *Control* MO had no effect on either *Lim-1* (as marked by the white arrowhead) or *MyoD* expression (as marked by the white arrow) (A). *p27Xic1* mRNA reduced *Lim-1* expression and disrupted *MyoD* expression (dashed white arrow), causing non-segmentation of the somites (B). *p27Xic1* MO reduced expression of both *Lim-1* and *MyoD* (C). *p27Xic1 CK-* had no effect on either *Lim-1* or *MyoD* expression (D).

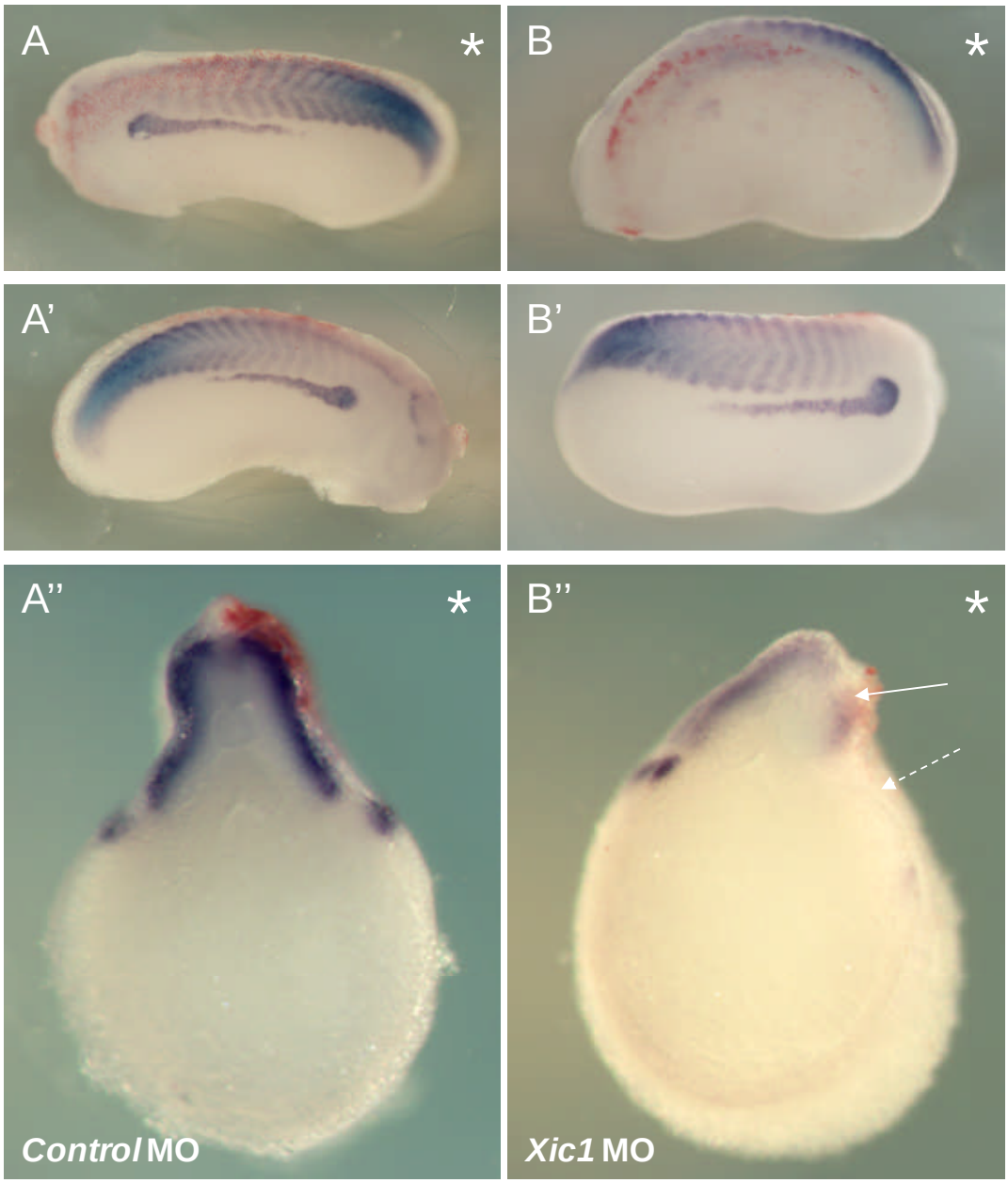

Figure 3.14 Sectioning highlights the reduction in *MyoD* expression on the injected side after injection of *p27Xic1* MO. *X. laevis* embryos were injected at the 8 cell stage into a ventro-vegetal blastomere to target the presumptive pronephric region. *βgal* mRNA was co-injected to act as a lineage trace. Embryos were cultured till stage 24 and whole mount *in situ* hybridised for expression of both *Lim-1* and *MyoD*. Embryos were then transverse sectioned with a razor blade to observe internal expression of both *Lim-1* and *MyoD*. Whole mount injected (A and B) and un-injected (A' and B') sides of the embryos are also shown. The *Control* MO had no observable effect on either *MyoD* or *Lim-1* expression (A''). *p27Xic1* MO clearly reduced expression of both *MyoD* (white arrow) and *Lim-1* (dashed white arrow) on the injected side (B''). Due to the lack of muscle on the injected side it was very common to observe embryos curling towards the injected side, and the dorsal side of the embryo frequently folded over the injected side. This can be clearly seen in B'' where the lack of muscle on the injected side has caused muscle on the un-injected side to fold over. * denotes injected side

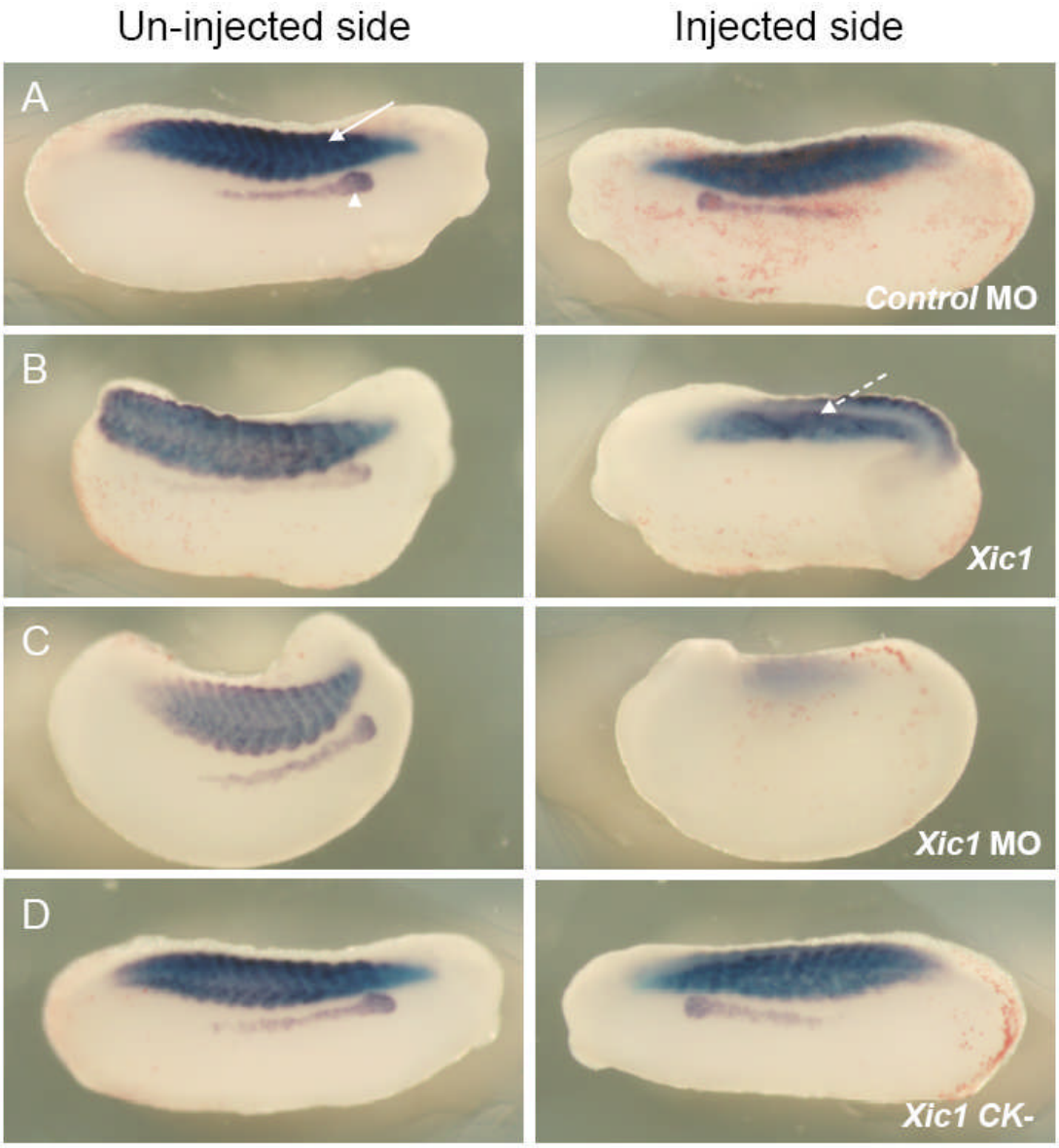

Figure 3.15 Mis-expression of *p27Xic1* disrupted somite morphology and muscle differentiation. *X. laevis* embryos were injected at the 8 cell stage into a ventro-vegetal blastomere to target the presumptive pronephric region. *βgal* mRNA was co-injected to act as a lineage tracer. Embryos were cultured till stage 24 and whole mount *in situ* hybridised for expression of both *Lim-1* and *MHC* (a marker of differentiated muscle). The *Control* MO had no effect on either *Lim-1* (as marked by the white arrowhead) or *MHC* expression (as marked by the white arrow) (A). *p27Xic1* mRNA reduced *Lim-1* expression and disrupted *MHC* expression (dashed white arrow), causing non-segmentation of the somites (B). *p27Xic1* MO reduced expression of both *Lim-1* and *MHC* (C). *p27Xic1 CK-* had no effect on either *Lim-1* or *MHC* expression (D).

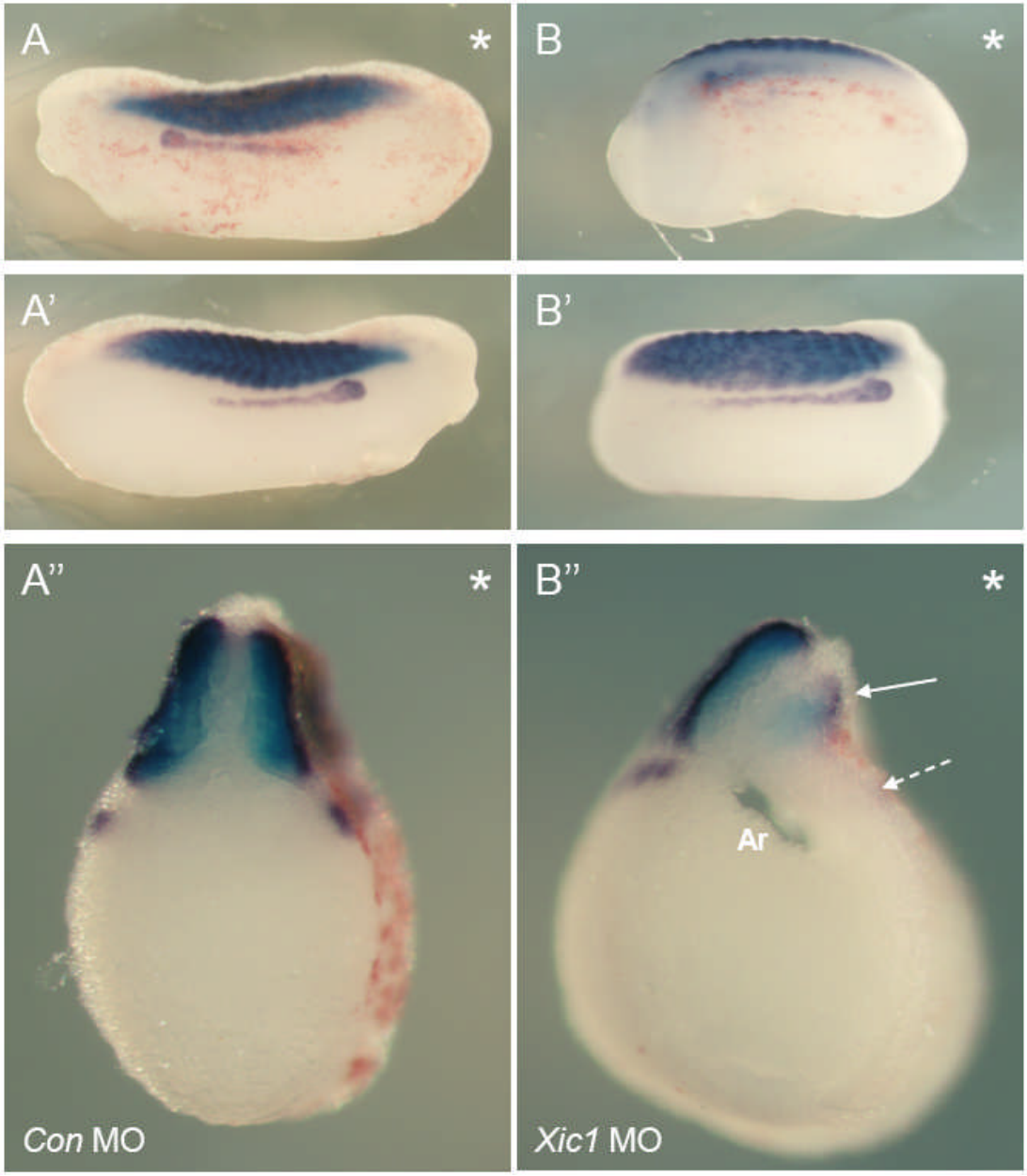

Figure 3.16 Sectioning highlights the reduction in *MHC* expression on the injected side after injection of *p27Xic1* MO. Injections and incubations were the same as in Fig 3.14; however *MHC* was used as a marker of the myotome. The phenotypes observed were very similar; the *p27Xic1* MO inhibited *MHC* and *Lim-1* expression on the injected side and caused the embryos to curl towards the injected side due to the lack of muscle. * denotes the injected side, Ar = Archenteron

injection severely reduced expression of *MyoD* and *Lim-1* in 79% of the embryos scored (n=33) (Fig 3.13C and Fig 3.14B). Injection of the *Control* MO had no effect on *MyoD*/ *Lim-1* (n=36) or *MHC/ Lim-1* (n=42) expression (Fig 3.13A and Fig 3.14A). Analysis of the effect of *p27^{Xic1}* depletion on *MHC/ Lim-1* expression gave an identical phenotype with 89% of embryos scored having reduced expression of these markers (n=27) (Fig 3.15C and 3.16B). Over-expression of *p27^{Xic1}* disrupted *MHC* expression in the same manner it effected *MyoD* expression, 66% of embryos had disrupted somitogenesis (n=35) (Fig 3.15B). We conclude p27^{Xic1} is required for myogenesis as loss of *p27^{Xic1}* expression inhibited *MyoD* and *MHC* expression. Furthermore we found that p27^{Xic1} is required for normal somitogenesis as over-expressing p27^{Xic1} disrupts this process, producing fused, un-segmented somites.

3.2.10 A mutant of *p27^{Xic1}* with inactive cyclin and cdk binding domains had no effect on pronephros formation or somitogenesis

To overcome the effects of *p27^{Xic1}* over-expression on the cell cycle prior to induction of the pronephros, and to identify if later effects on differentiation occurred, we initially used an inducible form of *p27^{Xic1}* that had an N-terminus glucocorticoid receptor tag. With this construct, injected message could be activated at different stages of development upon incubation of embryos in dexamethasone. However, in our hands, this construct proved to be leaky since we obtained phenotypes in the absence of dexamethasone (Fig 3.12D). As an alternative approach, a mutant of *p27^{Xic1}* was used that had inactivated cyclin and cdk binding domains, we term this mutant p27^{Xic1} CK- (Fig 3.17 illustrates sites of mutagenesis, this mutant was a kind gift from Mehregan Movassagh, Cambridge University). This

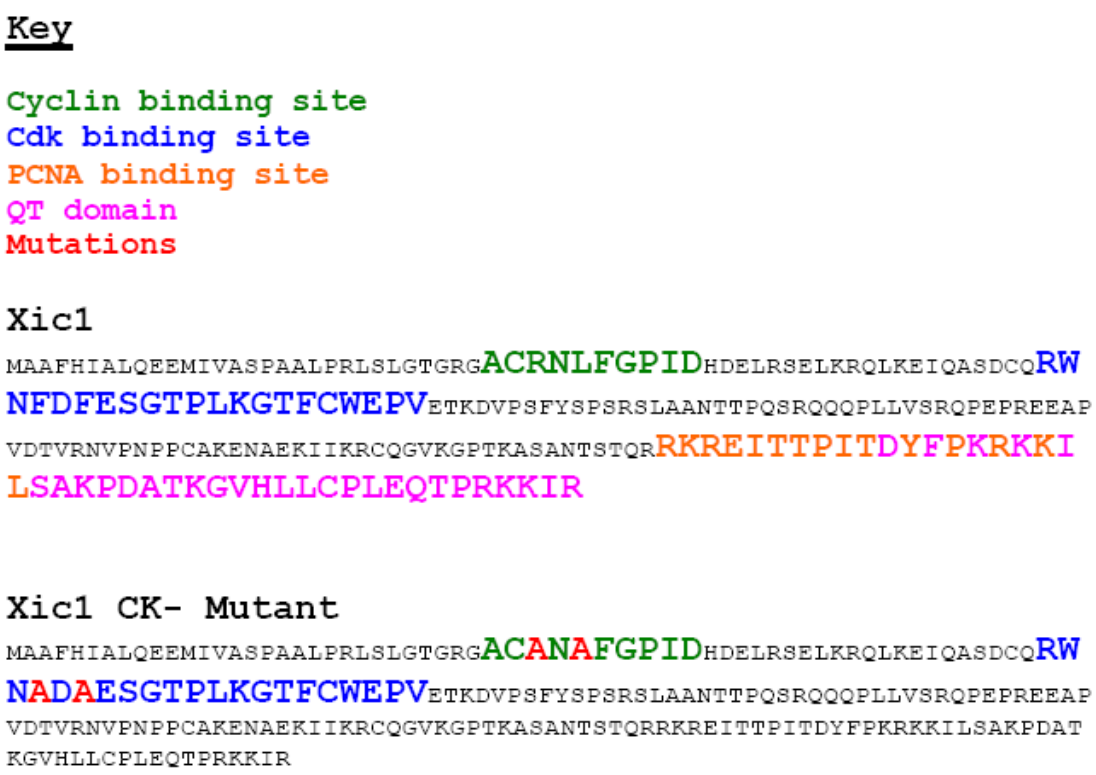

Figure 3.17 The amino acid sequence of the conserved cyclin and cdk binding site region within wild type p27Xic1 compared to that of the cyclin and cdk binding mutant p27Xic1 CK- (amino acids 31-82 displayed) (C). Mutations are in red, PCNA binding site and QT domain are also shown for completeness.

mutant enabled us to see if the effect on the pronephros we observed following *p27*^{Xic1} over-expression was due to premature cell cycle exit due to decreased cyclin/ cdk kinase activity. After injecting *p27*^{Xic1} *CK*- mRNA, at stage 8.5 we failed to observe enlarged cells usually seen following *p27*^{Xic1} mRNA injection, suggesting this mutant had successfully disabled the cell cycle exit function of p27^{Xic1} (Fig 3.12E). To confirm that this mutant had lost its cell cycle exit function we performed pH3 immunostaining on embryos injected into one cell of a two cell stage embryo with *p27*^{Xic1} *CK*- mRNA and *βgal* mRNA to act as a lineage tracer. On average out of 10 embryos numerically scored for total pH3 immunostained cells there was a statistically insignificant increase of 3.44% on the injected side ($P>0.05$) (Fig 3.11D and 3.11E). This result confirmed the lack of cell cycle inhibitory function in this mutant.

Injection of *p27*^{Xic1} *CK*- mRNA along with *βgal* mRNA lineage tracer into a ventro-vegetal blastomere of 8-cell stage embryos caused a statistically insignificant effect on pronephros formation at stage 41, as observed by whole mount 3G8/ 4A6 immunostaining (8% reduced, n=28, $P>0.05$) (Fig 3.5G). At stage 24 the same injection showed no significant effect on the pronephros anlagen formation or myogenesis, as seen by *Lim-1*/ *MyoD* (5% reduced *Lim-1*, 0% disrupted *MyoD*, n=43) (Fig 3.13D) or *Lim-1*/ *MHC* (2% reduced *Lim-1*, 0% disrupted *MHC*, n=52) (Fig 3.15D) double *in situ* hybridisations. Thus we suggest that the reduced pronephros phenotype and the non-segmented somite phenotype we observed when we over-expressed *p27*^{Xic1} were due to premature cell cycle exit through inhibition of cyclin/ cdk kinase activity. Injection of 5 ng GST tagged *p27*^{Xic1} *#2* protein has been shown to halt the cell cycle prior to MBT (Hartley et al., 1997). This construct

retains the ability to inhibit cyclin E/ cdk2, but has a reduced ability to inhibit cyclin A2/cdk2 (Movassagh and Philpott, 2008). Thus we might expect to observe a pronephric phenotype with *p27^{Xic1} #2* injection. However when *p27^{Xic1} #2* mRNA was injected no effect on pH3 staining was observed (see Chapter 4), suggesting to us that the concentrations of *p27^{Xic1} #2* we injected (80 pg) had no cell cycle effect, and hence no pronephric phenotype.

3.2.11 Inhibiting cell cycle using hydroxyurea and aphidicolin inhibited formation of the pronephros and disrupted segmentation of the somites

To ensure the reduction in the size of the pronephros we observed that when we over-expressed *p27^{Xic1}* mRNA could be due to premature cell cycle exit we interfered with normal cell division by incubating embryos from stage 10.5 in the cell division inhibitors Hydroxyurea and Aphidicolin (HUA) (Harris and Hartenstein, 1991). The embryos were left to develop to stage 23, where pH3 immunostains and *Lim-1*/ *MyoD* and *Lim-1*/ *MHC* whole mount double *in situ* hybridisations were performed, and to stage 41 where we carried out 3G8/ 4A6 whole mount immunostains. HUA treatment inhibited cell division, as observed by an average 82% reduction in the number of positively stained pH3 cells on the left side of the embryos treated with HUA compared to the controls (Fig 3.18, n=10). At stage 41 3G8/ 4A6 antibody staining was reduced in all embryos treated with HUA, with 4A6 staining completely absent (n=14) (Fig 3.19A). At these later stages embryos incubated in HUA had severely perturbed and delayed development, with rostral neural development affected in particular. At stage 23, development was somewhat delayed, but the phenotype was not as severe as in embryos incubated to later stages. HUA treatment, like *p27^{Xic1}* mRNA over-expression, inhibited pronephros anlagen

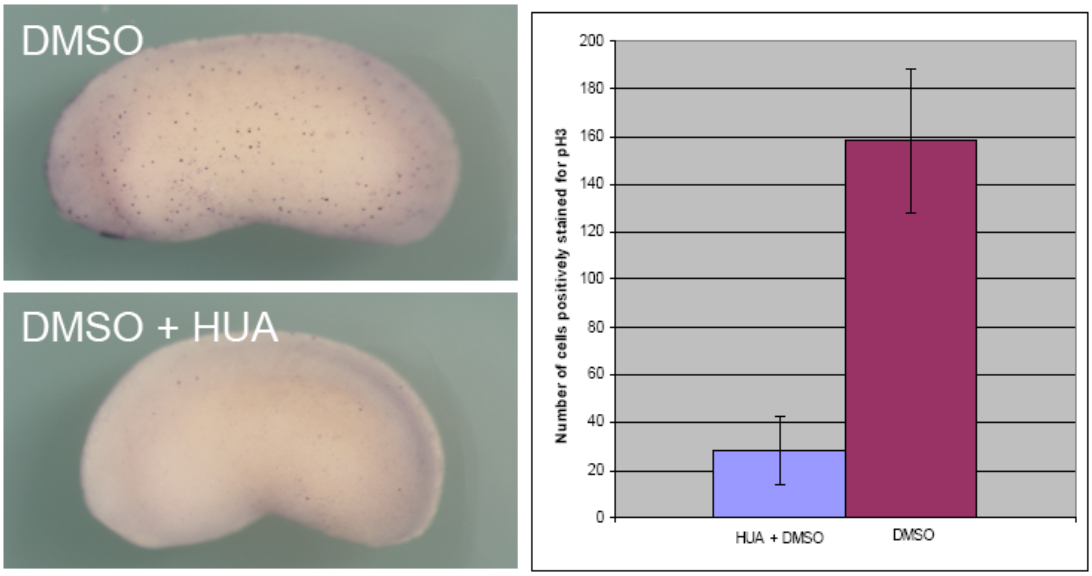

Figure 3.18 Incubation of embryos in Hydroxyurea and Aphidicolin (HUA) from stage 10.5 reduced cell division. Stage 10.5 *X. laevis* embryos were incubated in either HUA and DMSO or DMSO alone (control) and left to develop to stage 23 (staged according to control embryos). Whole mount pH3 antibody staining was then performed to detect cell division. The number of cells dividing was reduced in those embryos incubated with HUA compared to the controls (A). Of ten embryos randomly selected and scored for pH3 immunostaining on the left hand side of the embryo, all had less dividing cells than the ten randomly selected controls. On average there were 82% fewer dividing cells after HUA treatment (A').

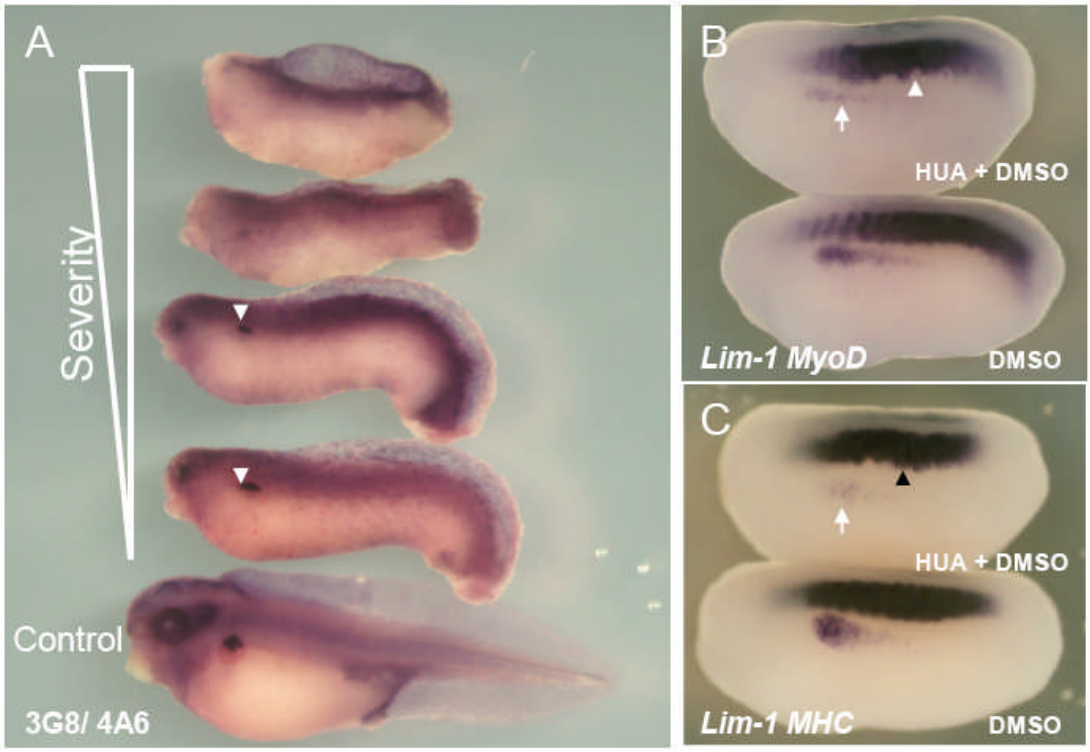

Figure 3.19 HUA treatment severely perturbs pronephric and muscle development. Stage 10.5 *X. laevis* embryos were incubated in either HUA and DMSO or DMSO only (control) and left to develop to stage 41 where whole mount 3G8/ 4A6 antibody staining was performed to detect the mature pronephros. All embryos treated with HUA had delayed development and reduced 3G8/ 4A6 staining (arrowheads). The control embryo showed normal development at stage 41 (A). Stage 10.5 *X. laevis* embryos were incubated in either HUA and DMSO or DMSO alone (control) and left to develop to stage 23 where whole mount *in situ* hybridisation for *Lim-1*/ *MyoD* (B) and *Lim-1*/ *MHC* (C) expression was performed. The HUA treated embryo is shown above the control untreated embryo in B and C. HUA treatment clearly inhibited pronephros anlagen formation, as seen by reduced *Lim-1* expression (white arrow), and disrupted the normally segmented *MyoD* expression (B) (white arrowhead) and MHC expression (C) (black arrowhead).

formation and disrupted somite segmentation in all the embryos treated (n=17) (Fig 3.19B and Fig 3.19C), a phenotype almost identical to the effect of *p27^{Xic1}* mRNA over-expression.

3.2.12 p35.1 disrupts muscle differentiation but had no effect on mature pronephros development

p35.1 is a member of the *p35* family, a group of proteins that bind to and activate cdk5. Philpott et al, showed *p35.1* mRNA over-expression disrupted muscle organisation in a similar manner to the *p27^{Xic1}* mRNA over-expression phenotype (Philpott et al., 1997). Reduced muscle development is known to inhibit nephrogenesis (Seufert et al., 1999; Mauch et al., 2000; Mitchell et al., 2007), but to observe if disrupted muscle organisation effects pronephros development we injected *p35.1* mRNA and observed its effects on both muscle and pronephros markers. *p35.1* mRNA was injected into a ventro-vegetal blastomere of the 8-cell stage embryo and cultured to stage 24, where *Lim-1*/ *MyoD* and *Lim-1*/ *MHC* double *in situ* hybridisations were performed. Whole mount 3G8/ 4A6 immunostaining was carried out on embryos cultured to stage 41. At stage 24 we observed a similar muscle phenotype to that of over-expression of *p27^{Xic1}* mRNA, 69% of *Lim-1*/ *MyoD* stained embryos had disrupted somite segmentation (n=23). However, in 75% of embryos with disrupted somite segmentation *Lim-1* expression was disorganised, but not reduced (Fig 3.20A). Similar results were obtained with *Lim-1*/ *MHC* stained embryos. 50% had disrupted somite segmentation, with 61% having disorganised pronephros anlagen development (n=46, Fig 3.20B). At stage 41, *p35.1* mRNA over-expression had no statistically significant effect on 3G8/ 4A6 staining ($P>0.05$, n=24, Fig 3.20C), only one embryo showed a reduced pronephros phenotype. Thus the

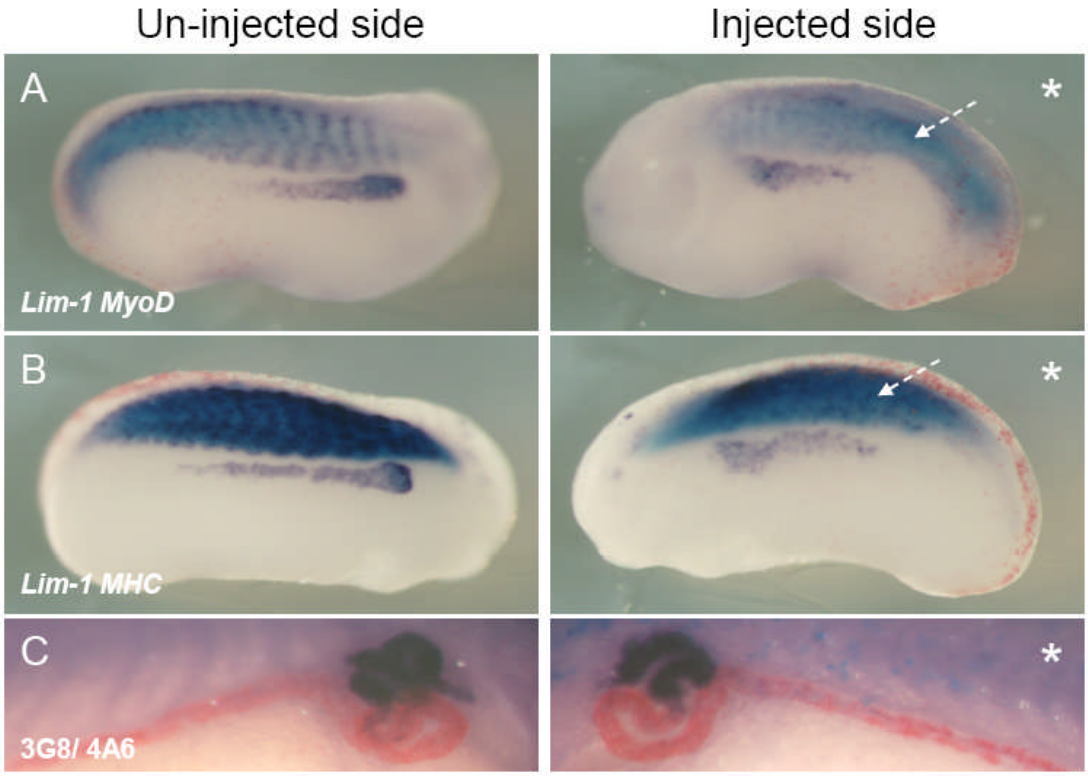

Figure 3.20 p35.1 disrupted somitogenesis and pronephros anlagen formation, but not mature pronephros development. *X. laevis* embryos were injected at the 8 cell stage into a ventro-vegetal blastomere to target the presumptive pronephric region. *βgal* mRNA was co-injected to act as a lineage trace. Embryos were cultured till stage 24, where whole mount *in situ* hybridisation for expression of *Lim-1*/ *MyoD* (A) and *Lim-1*/ *MHC* (B) was carried out, and to stage 41, where whole mount 3G8/ 4A6 antibody staining was performed (C). *p35.1* mRNA over-expression disrupted development of the myotome and pronephros anlagen (A and B). Both *MyoD* and *MHC* expression were abnormal on the injected side, with segmentation of the somites apparently lacking. *Lim-1* expression was also disrupted and mildly reduced on the injected side. However at stage 41 *p35.1* mRNA over-expression had no effect on the size of the mature pronephros (C).

early disorganised state of the pronephros anlagen induced by *p35.1* mRNA injection was insufficient to inhibit formation of a mature pronephros in later stage embryos.

In conclusion, correct somite organisation is not essential for pronephros development; it only temporarily disorganises the pronephros anlagen. These effects are seemingly insufficient to completely inhibit nephrogenesis and recovery of a relatively normal pronephros at later stages of development is possible. This result implies that *p27^{Xic1}* mRNA over-expression has an effect on nephrogenesis in addition to that of disruption of normal muscle formation, since the pronephros anlagen failed to develop. From our cell division assays (Fig 3.11), we believe this is probably due to inhibited cell cycling prior to and post formation of the pronephros anlagen.

3.3. Discussion

The expression of *p27^{Xic1}* has been previously shown in the differentiating muscle and notochord at neurula stages and at lower levels in the neural plate and heart (Ohnuma et al., 1999; Vernon et al., 2003; Movassagh and Philpott, 2008). We show for the first time *p27^{Xic1}* is expressed within the pronephros during development (Fig 3.3 and Fig 3.4). Strong expression in the dorso-anterior region of the pronephros between stages 27 and 32, suggest p27^{Xic1} could have a role in pronephric development. To ascertain whether p27^{Xic1} is required for pronephros development, over-expression and depletion studies were performed.

Over-expressing *p27^{Xic1}* affected development of the pronephros, reducing its size compared with the control, un-injected side at stage 22 and stage 41 (Fig 3.11B and Fig 3.5B). Injection of different domains of p27^{Xic1} mapped the N-terminus (amino acids 1-96) as the effector region inhibiting nephrogenesis (Fig 3.5D). Moreover, depleting endogenous p27^{Xic1} using a MO also inhibited development of the pronephros at stage 22 and stage 41 (Fig 3.11C and Fig 8B). We have demonstrated that over-expression and MO knock down of *p27^{Xic1}* inhibited formation of the pronephros by different mechanisms. Ectopic apoptosis was not a mechanism by which pronephros development was inhibited as co-injection of the apoptotic inhibitor *Bcl$_{XL}$* with *p27^{Xic1}* mRNA or *p27^{Xic1}* MO did not alter the frequency of pronephric phenotypes observed (Fig 3.10).

3.3.1 *p27^{Xic1}* over-expression inhibited pronephros development as premature cell cycle exit reduced the number of cells in the anlagen

Over-expressing *p27^{Xic1}* inhibited cell division, as observed by reduced pH3 immunostaining (Fig 3.11B). Injection of a mutant of p27^{Xic1} that had inactive cyclin and cdk binding domains, *p27^{Xic1} CK-*, had no effect on cell division (Fig 3.11D and Fig 3.11E) or pronephros development (Fig 3.5G and Fig 3.13D). Thus injection of *p27^{Xic1}* mRNA inhibited nephrogenesis by inhibiting cyclinA2/ cdk2 kinase activity. Organogenesis requires directed cell cycle exit and differentiation to form organs of desired size and structure. We have over-expressed *p27^{Xic1}* and found it reduced the size of the pronephros due to premature cell cycle exit, thus p27^{Xic1} is a regulator of organ size as a consequence of its function in controlling cell cycle exit.

3.3.2 Knock down of *p27*^{Xic1} expression using a MO inhibited pronephros development most likely due to inhibiting myogenesis

One of the earliest signals to the intermediate mesoderm to form pronephros originates from the anterior somites (Seufert et al., 1999; Mauch et al., 2000; Mitchell et al., 2007). Thus inhibition of myogenesis by *p27*^{Xic1} MO may be sufficient to inhibit pronephros formation. This theory is supported by our observation that *p27*^{Xic1} depletion reduced expression of *MyoD* and *MHC*, in particular in the anterior somites, at stage 22 (Fig 3.13C, and Fig 3.15C). On the same embryos *Lim-1* expression was also characterised and we observed total loss of pronephros anlagen formation when *p27*^{Xic1} depletion inhibited myogenesis. We conclude *p27*^{Xic1} is required for *MyoD* and *MHC* expression and, as previously reported, myogenesis, which results in a consequent inhibition of nephrogenesis. Furthermore we show over-expression of *p27*^{Xic1} inhibited segmented *MyoD* and *MHC* expression (Fig 13B and Fig 3.15B); however *p27*^{Xic1} *CK*- over-expression had no effect (Fig 13D and Fig 3.15D). Thus we conclude that this segmentation phenotype after injection of *p27*^{Xic1} mRNA was due to aberrant cell cycling.

3.3.3 p27^{Xic1} is necessary for co-ordinating cell cycle exit to aid segmentation of the somites

The clock and wavelength model of segmentation (Cooke and Zeeman, 1976) requires synchronous cell division to aid allocation of somites within the presomitic mesoderm. In the myotome, *p27*^{Xic1} expression overlaps with *MyoD* expression from stage 15 (Vernon and Philpott, 2003). Thus expression of *p27*^{Xic1} is temporally and spatially appropriate to have a role in directing cell cycle exit, and therefore somitogenesis. Chick embryos incubated for 24 hours in S-phase inhibitors such as

hydroxyurea display fused somites as a consequence of undirected cell cycle exit (Primmett et al., 1989). p27^{Xic1} is a cell cycle inhibitor, thus the non-segmentation pattern observed when *p27^{Xic1}* is over-expressed is not surprising. Nevertheless, this result establishes a previously unrecognised role for p27^{Xic1} in somite segmentation in *X. laevis*. Furthermore we have incubated embryos in HUA from stage 10.5 and disrupted somitogenesis in the same manner as *p27^{Xic1}* mRNA over-expression (Fig 3.19B and Fig 3.19C), thus confirming the role of cell cycle exit in somite allocation.

3.3.4 Muscle formation is required for pronephros development, but correct organization is not

p27^{Xic1} MO reduced the size of the muscle, as observed by reduced *MyoD* (Fig 3.13C and Fig 3.14B) and *MHC* expression (Fig 3.15C and Fig 3.16B). However, when *p27^{Xic1}* mRNA was over-expressed the muscle formed, but segmentation was disrupted (Fig 3.13B and Fig.3.15B). In these embryos the pronephros anlagen also failed to form, thus we required to know if this was a consequence of disrupted muscle development or an additional effect. To see if this was the case we over-expressed *p35.1*, a gene known to disrupt muscle organization but which is not expressed in the pronephros (Philpott et al., 1997). We observed disruption of muscle development when *p35.1* was over-expressed, and also disorganised pronephros anlagen formation (Fig 3.20A and Fig 3.20B). Interestingly disorganisation of the pronephros anlagen had no effect on formation of a mature pronephros as at stage 41 3G8/ 4A6 antibody staining was normal (Fig 3.20C). Thus we favour the hypothesis that disrupted somitogenesis is insufficient to affect development of a mature pronephros as *p35.1* mRNA over-expression did not affect mature pronephros development despite its effects on segmentation. *p27^{Xic1}* mRNA

did reduce mature pronephros development as well as affecting muscle segmentation, thus p27^{Xic1} has an additional effect on nephrogenesis. From our cell division studies (Fig 3.11), we suggest this additional effect is premature cell cycle exit reducing the number of cells that can contribute to the pronephros anlagen prior to and post its induction at stage 12.5, and hence p27^{Xic1} is controlling the size of the pronephros through its ability to regulate the cell cycle.

Chapter 4

p27^{Xic1} interaction with Gadd45γ and a speculative analysis of its role in primary neurogenesis

4.1 Introduction

Cyclin-dependent Kinase Inhibitors (CKIs) are multifunctional proteins that act to primarily promote cell cycle exit by inhibitory interactions with cyclin/ cdk complexes. Additionally, CKIs regulate diverse processes such as cell adhesion, migration, survival, transcription and fate determination (Besson et al., 2008). p27^{Xic1} has been reported to be important in regulating cell fate determination in the retina, heart, myotome and nervous system through an activity distinct from its well-characterised cell cycle exit function (Ohnuma et al., 1999; Ohnuma et al., 2002; Vernon et al., 2003; Vernon and Philpott, 2003; Movassagh and Philpott, 2008). These roles have, at least in part, been suggested to involve interactions with tissue-specific transcription factors. In mice, MyoD has been shown to interact with a mammalian homologue of p27^{Xic1}, p57^{Kip2} (Reynaud et al., 1999; Reynaud et al., 2000). Specifically, this interaction occurs in a region of p57^{Kip2} corresponding to an α-helix that spans the conserved cyclin and cdk binding sites (Fig 4.1A). p27^{Xic1} synergises with MyoD to promote muscle formation in *X. laevis* (Vernon and Philpott, 2003). Comparison of the amino acid sequence in the domain of p57^{Kip2} that interacts with mouse MyoD, and the analogous domain of p27^{Xic1}, identifies

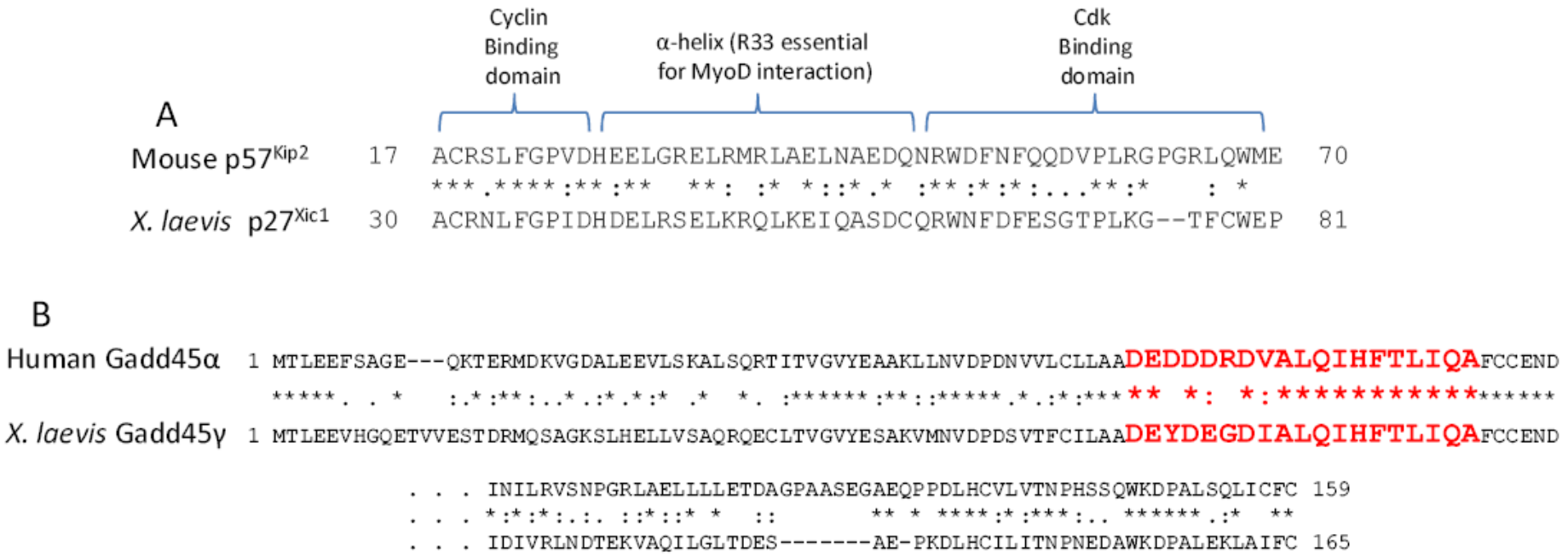

Figure 4.1 Sequence comparison between mouse p57^{Kip2} and *X. laevis* p27^{Xic1} and human Gadd45α and *X. laevis* Gadd45β (A) The conserved cyclin and cdk binding sites of p57^{Kip2} and p27^{Xic1} are indicated. An α-helix connects these two domains (helical structures determined using secondary structure prediction software, see figure 4.2). In p57^{Kip2}, this helix has been implicated in binding MyoD. The conservation of this 21 amino acid α-helix is high with 43% exact homology and 81% homology if amino acids with similar functional side chains are included. (B) The entire length of human Gadd45α and *X. laevis* Gadd45γ are compared and shows high percentage conservation in amino acid sequence. Highlighted in red is the domain of human Gadd45α that binds p21^{Cip1}. The homologous domain on *X. laevis* Gadd45γ is also highlighted in red. This high percentage conservation between the two sequences (89%), suggests Gadd45γ could interact with p27^{Xic1}, a functional homolog of p21^{Cip1}.

sufficient conservation to suggest p27^{Xic1} may also be capable of interacting with MyoD (Fig 4.1A). Furthermore, p27^{Xic1} stabilises neurogenin (X-NGNR-1) *in vivo*, with the N-terminus domain of p27^{Xic1} essential for this stabilisation (Vernon et al., 2003). The authors of this paper postulated this interaction could be a direct or indirect, with the latter more likely as p27^{Xic1} is able to inhibit cyclinA2/ cdk2, which has been shown to perturb neurogenesis, perhaps by destabilising neurogenin through inhibitory phosphorylation (Richard-Parpaillon et al., 2004). In addition, attempts to identify direct interactions between p27^{Xic1} and X-NGNR-1 have failed by co-immunoprecipitation (personal communication with Anna Philpott, Cambridge University). However, it remains possible p27^{Xic1} is capable of interacting directly with MyoD and X-NGNR-1, and we predicted this interaction would be within this conserved α-helix.

p27^{Xic1} has also been suggested to be a binding partner of the growth-arrest-and-DNA-damage-induced gene gamma (Gadd45γ) (de la Calle-Mustienes et al., 2002). The Gadd45 family of genes consists of *Gadd45α* (*Gadd45*), *Gadd45β* (*Myd118*), and *Gadd45γ* (*CR6*) (Hoffman and Liebermann, 2009). These genes encode proteins that are important regulators of environmental and physiological stress responses in the cell (Zhang et al., 2001; Hoffman and Liebermann, 2007; Liebermann and Hoffman, 2008). In addition, each Gadd45 gene product has been shown to be involved in cell cycle arrest, DNA repair and cell survival and apoptosis (Zhan et al., 1994; Zhang et al., 1999; Gupta et al., 2005; Hoffman and Liebermann, 2009). Gadd45 proteins have such diverse roles as they are able to interact with, and regulate the activity of a wide range of proteins (summarised in Fig 4.2). A gain-of-function screen performed in the Jones laboratory, using mRNA pools, made from a

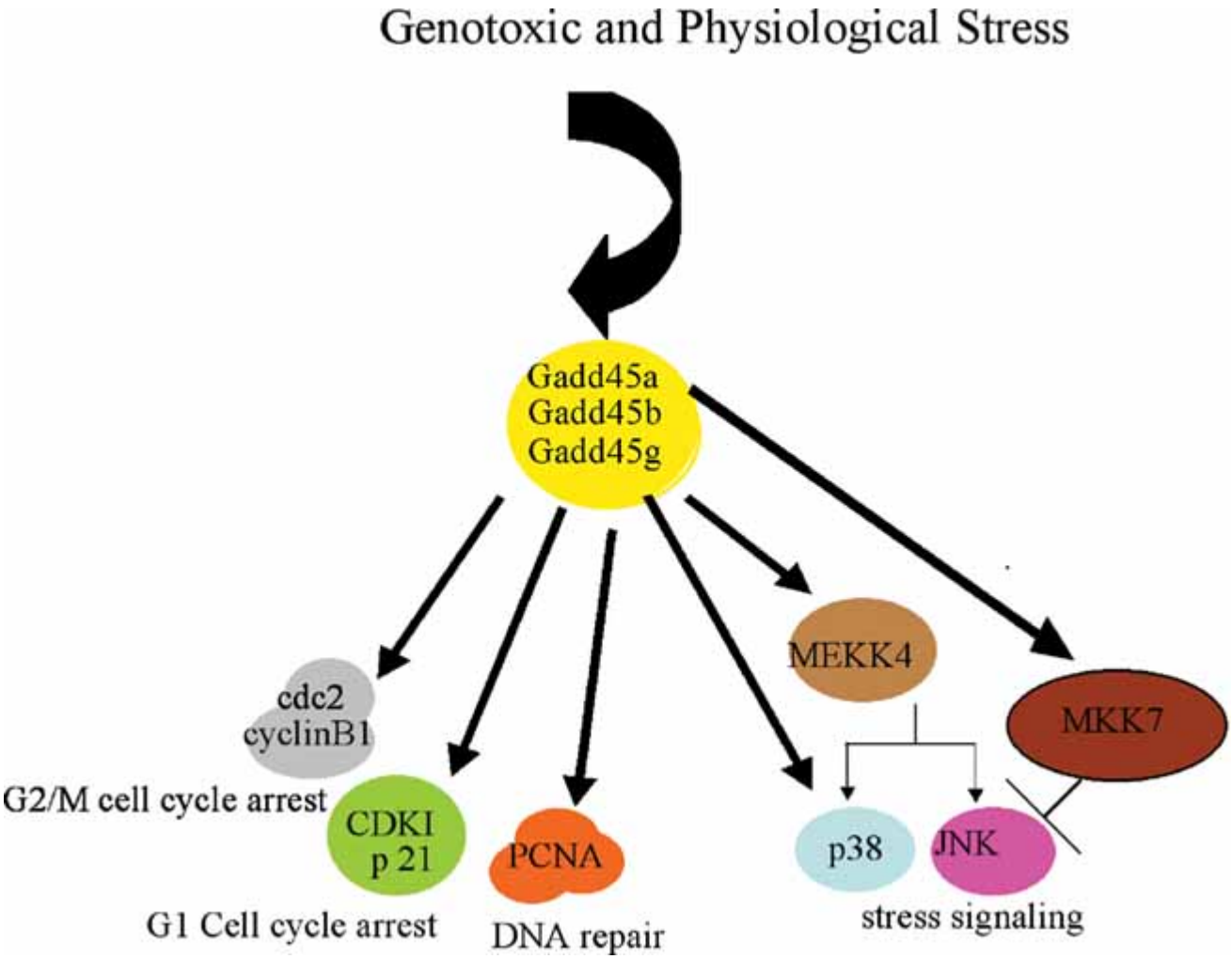

Figure 4.2 Gadd45 interactions with other cellular proteins. All Gadd45 proteins are capable of binding a variety of proteins within the cell, making them important regulators of diverse cellular processes. Gadd45α is able to bind to cdk1 in a p53-dependent manner, and inhibit the activity of CyclinB1/ cdk1, establishing a G2/M checkpoint and cell cycle arrest. Gadd45α has also been shown to interact with p21Cip1, augmenting its inhibition of the G1/S transition. Gadd45 proteins can also interact with Proliferating Cell Nuclear Antigen (PCNA) to promote nuclear excision DNA repair. Perhaps most importantly, Gadd45 proteins bind a number of proteins involved in cellular stress responses. Heat shock-induced stress responses cause expression of MEKK4, a mitogen-activating protein kinase kinase kinase (MAP3K) that phosphorylates the MAP2Ks MKK3 and MKK6 (which regulate the MAPK p38) and MKK4 and MKK7 (which regulate the activity of c-Jun NH2-terminal kinase, JNK). The kinase domain in MEKK4 is located in its C-terminus domain. MEKK4 is self-inhibiting, as its N-terminus can bind to the kinase domain in the C-terminus and inhibit enzyme activity. Gadd45 binds to the N-terminus of MEKK4, promoting its kinase activity. In addition, Gadd45 promotes dimerization of MEFF4, further enhancing its activity in the cell. (Image taken from Hoffman and Liebermann, 2009)

non-redundant *X. tropicalis* full-length plasmid cDNA library, injected into *X. laevis* embryos, followed by sib-selection to identify the single clone that caused abnormal phenotypes in the pronephros, found that over-expression of *Gadd45γ* produced a pronephric phenotype (Kyuno et al., 2008). The central region of human Gadd45α (amino acids 65-84) has been shown to directly interact with p21^{Cip1} in mammalian cells and in a yeast two hybrid screen (Kearsey et al., 1995; Zhao et al., 2000). The amino acid domain of mouse Gadd45α identified as interacting with p21^{Cip1} is almost completely conserved in *X. laevis* Gadd45γ (Fig 4.1B). Given this, we concur with de la Calle-Mustienes et al (2002) and believe p27^{Xic1} could be a binding partner of Gadd45γ. Such an interaction would, as has been postulated with Gadd45α interaction with p21^{Cip1} (Fan et al., 1999; Liebermann and Hoffman, 2007), aid G1 cell cycle arrest, promoting exit to a quiescent state. Moreover, *Gadd45γ* shares an almost identical whole mount *in situ* hybridisation expression pattern to *p27^{Xic1}* (Fig 4.3) (de la Calle-Mustienes et al., 2002).

The experiments performed in this chapter, aimed to attempt to identify direct interactions between p27^{Xic1} and Gadd45γ and further understand the suggested secondary function of p27^{Xic1} in cell fate determination. Understanding if p27^{Xic1} is able to interact with a wide variety of proteins in the cell could be the first step in determining how this CKI acts as a multi-functional molecule. Co-immunoprecipitation experiments identified if p27^{Xic1} interacted with Gadd45γ, either by direct binding or with a complex also bound to Gadd45γ, and co-injection over-expression experiments were performed to understand if such interactions were synergistic or additive. The results of these experiments and our inability, following multiple repetitions, to reproduce published data that investigated the role p27^{Xic1}

Figure 4.3 Comparison of the *in situ* hybridised expression patterns for *p27^{Xic1}* and *Gadd45γ* at similar stages of development. The similarity in the expression profiles of *Gadd45γ* and *p27^{Xic1}* suggest there may be cross-talk between their activities, similar to what is observed in mammals where p21^{Cip1} interacts directly with Gadd45α. Expression in the eye, brain, neural tube, somites, branchial arches and pronephros (indicated by a red arrow) is very similar. (Top image taken from Fig 3.3 of Chapter 3 from this thesis, bottom image taken from de la Calle-Mustienes, 2002).

plays in primary neurogenesis, throw doubt on the published view that p27^{Xic1} is a multi-functional protein capable of binding multiple substrates. Further experimentation yielding more definitive data is required to fully understand these processes, if indeed such activities are part of p27^{Xic1} function.

4.2 Results

4.2.1 Injection of *Gadd45γ* mRNA augments the cell cycle exit function of p27^{Xic1}

To determine if Gadd45γ was capable of aiding the cell cycle exit function of p27^{Xic1}, in the same manner as has been shown for Gadd45α and p21^{Cip1}, we performed single injections of *Gadd45γ* mRNA and *p27^{Xic1}* mRNA and analysed how the pronephric phenotypes caused by these single injections compared to embryos co-injected with *Gadd45γ* mRNA and *p27^{Xic1}* mRNA. RNAs were injected into the V2 blastomere of 8-cell stage embryos with either 500 pg *Gadd45γ* mRNA, 50 pg *p27^{Xic1}* mRNA or a combination of 500 pg *Gadd45γ* mRNA and 50 pg *p27^{Xic1}* mRNA. 400 pg *βgal* mRNA was co-injected to act as a lineage tracer. Embryos were then left to develop to stage 24 and 41 where markers for the pronephros were detected either by *in situ* hybridisation for expression of *Lim-1* (at stage 24) or whole mount antibody staining using 3G8, which detects the nephrostomes and proximal tubule, and 4A6, which detects the intermediate and distal tubules (at stage 41). All results described in this section have been repeated at least twice, yielding similar phenotypes, and statistically significant phenotypes were determined within 95% confidence limits.

From these injections we expected to observe more severe pronephric phenotypes upon co-injection of *Gadd45γ* mRNA and *p27^{Xic1}* mRNA compared to the single injections of either message. The first indication suggesting our expectations were accurate was observed by the cell cycle effect such injections have at stage 8.5 (Fig 4.4). After injection of *p27^{Xic1}* mRNA and translation of the exogenous message, the concentration of p27^{Xic1} within the cell is sufficient to inhibit cell division, a phenomenon observable by enlarged cells in embryos up to stage 9/ 10. We observed no cell cycle effect after injection of *βgal* mRNA alone (Fig 4.4A) or in combination with *Gadd45γ* mRNA (Fig 4.4C). Injection of *p27^{Xic1}* mRNA, as previously described, produced a cell cycle effect with enlarged cells around the site of injection (Fig 4.4B). However, co-injection of *Gadd45γ* mRNA with *p27^{Xic1}* mRNA had the most severe cell cycle effect (Fig 4.4D); the injected messages produced substantially larger cells around the site of injection than the single *p27^{Xic1}* mRNA injection. Though entirely non-quantitative, this observation suggests the cell cycle exit function of p27^{Xic1} is augmented by Gadd45γ.

p27^{Xic1} over-expression reduced formation of the pronephros anlagen at stage 24 at a similar frequency to the data presented and interpreted in Chapter 3. 51% of embryos had reduced *Lim-1* expression, with 20% having completely absent pronephric anlagen (n=49, Fig 4.5B). Injection of *Gadd45γ* mRNA also decreased pronephros anlagen development in 62% of embryos (n=47, Fig 4.5C). Co-injection of *p27^{Xic1}* mRNA and *Gadd45γ* mRNA significantly increased the prevalence of pronephric phenotypes at stage 24 with 84% of embryos having reduced *Lim-1* expression and 50% having completely absent *Lim-1* expression (n=31, Fig 4.5D). In conclusion early pronephrogenesis is inhibited by over-expression of either *p27^{Xic1}* or

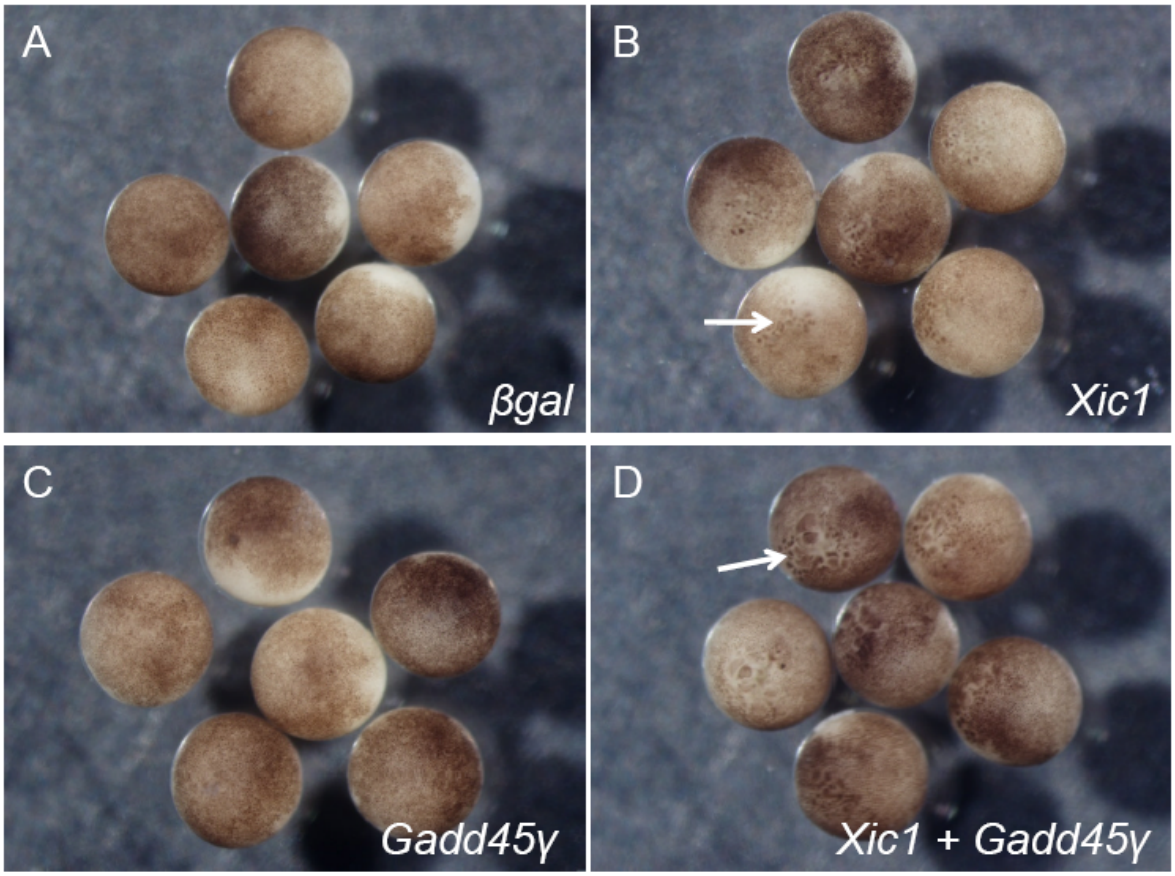

Figure 4.4 St 8.5 embryos displaying cell cycle effects after injection of *p27^{Xic1}* mRNA Injection of the *βgal* mRNA lineage tracer into the V2 blastomere of an 8-cell stage embryo had no effect on cell division (A). The same injection of 50 pg *p27^{Xic1}* mRNA caused a repeatable cell cycle effect, cells around the site of injection were larger than normal (B). Injection of 500 pg *Gadd45γ* mRNA had no obvious effect on cell division at stage 8.5 despite its well characterised ability to inhibit the cell cycle (C). Co-injection of 50 pg *p27^{Xic1}* mRNA and 500 pg *Gadd45γ* mRNA had a severe effect on cell division, inhibiting the cell cycle and producing much larger cells than occur during normal development. This co-injection suggests Gadd45γ is capable of augmenting the cell cycle exit function of p27^{Xic1}(D).

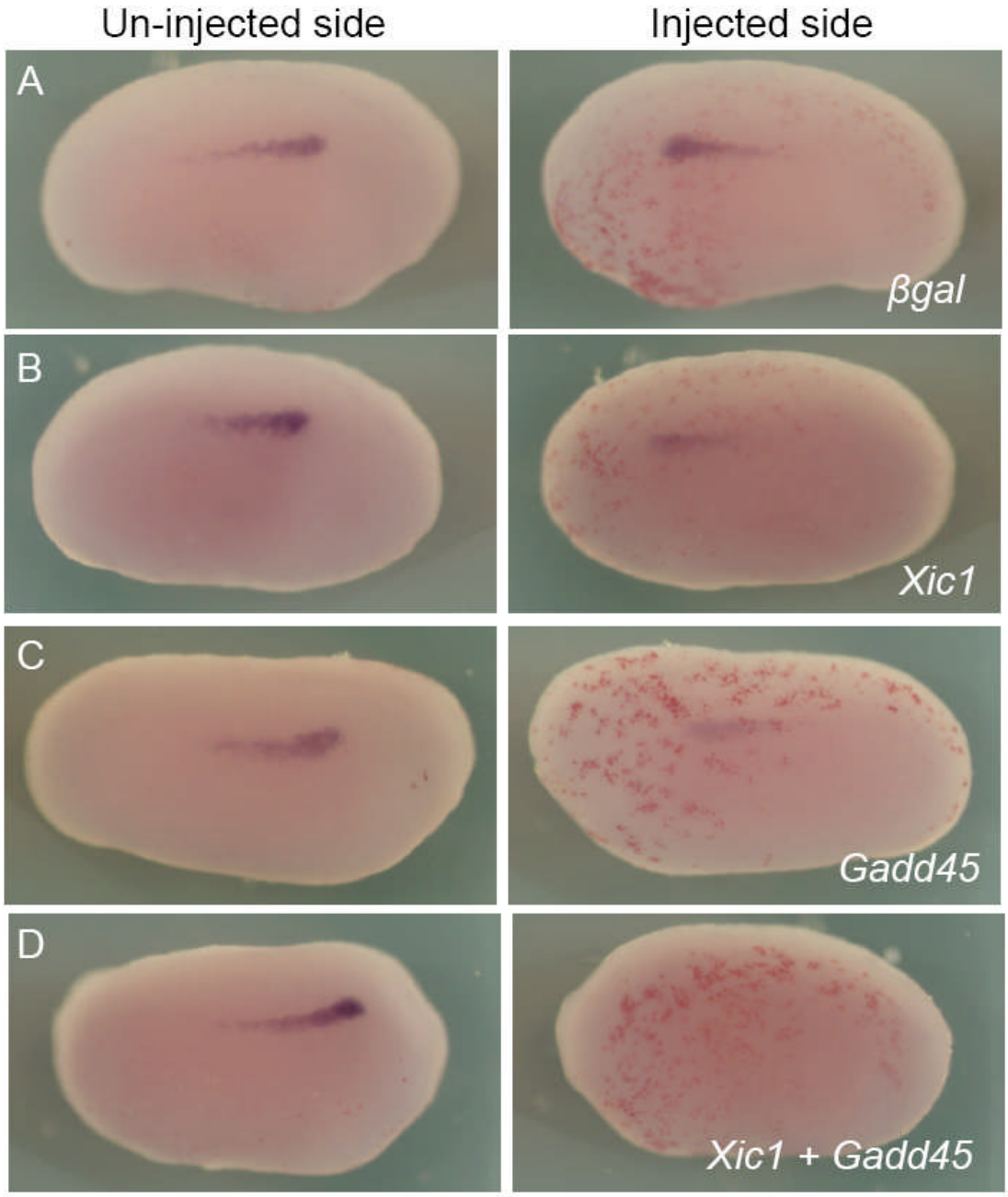

Figure 4.5 Over-expression of *p27^{Xic1}* and *Gadd45γ* inhibits pronephros anlagen formation. Embryos were injected into the V2 blastomere of an 8-cell stage embryo with 400 pg *βgal* mRNA to act as a lineage tracer. Embryos were then left to develop to stage 24 where they were fixed, sorted for correct targeting and whole mount in situ hybridised for *Lim-1*, a marker of the early pronephros anlagen. Injection of *βgal* mRNA had no effect on pronephros anlagen formation (A). Injection of 50 pg *p27^{Xic1}* mRNA, as described in Chapter 3, reduced *Lim-1* expression on the injected side (B). Injection of 500 pg *Gadd45γ* mRNA also reduced the size of the pronephros anlagen, with similar severity to *p27^{Xic1}* over-expression (C). Co-injection of *p27^{Xic1}* mRNA and *Gadd45γ* mRNA reduced the size of the pronephros with a higher frequency than either the single injections of p27^{Xic1} or Gadd45γ (D).

Gadd45γ, and co-injection of *p27^{Xic1}* mRNA/ *Gadd45γ* mRNA produced a more severe reduction in pronephros anlagen formation than the single injections.

At stage 41 *p27^{Xic1}* over-expression, as described in Chapter 3, reduced the size of the pronephros detectable with 3G8 and 4A6 antibodies. Here *p27^{Xic1}* mRNA single injections reduced 3G8/ 4A6 antibody staining in 59% of embryos (n=54, Fig 4.6B). We also observed a marginal, but still statistically significant, reduction of 3G8/ 4A6 antibody staining in 12% of embryos injected with *Gadd45γ* mRNA (n=68, Fig 4.6C). Co-injection of *p27^{Xic1}* mRNA and *Gadd45γ* mRNA reduced 3G8/ 4A6 antibody staining in 64% of embryos (n=58, Fig 4.6D). This increase in frequency is not of statistical significance to confirm Gadd45γ has an additive effect on p27^{Xic1} cell cycle exit function. However comparative analysis of the number of embryos that had completely absent pronephroi after single injections of *p27^{Xic1}* mRNA or co-injections of *p27^{Xic1}* mRNA/ *Gadd45γ* mRNA suggested that the co-injected embryos acquired a more severe pronephic phenotype (Appendix 2). Only one embryo (3% of those scored) had a completely absent pronephros in the single *p27^{Xic1}* mRNA injected sample of embryos. Co-injection of *p27^{Xic1}* mRNA/ *Gadd45γ* mRNA completely prevented 11 embryos (30% of those scored) developing a pronephros. In conclusion we are unable to confirm whether Gadd45γ acts synergistically or additively with p27^{Xic1} to promote cell cycle exit.

To directly and quantitatively observe if Gadd45γ is able to promote the cell cycle exit function of p27^{Xic1} we injected one cell of a two cell embryo with *p27^{Xic1}* mRNA, *Gadd45γ* mRNA and a combination of *p27^{Xic1}* mRNA/ *Gadd45γ* mRNA, left the embryos to develop to approximately stage 17, when they were fixed, stained for

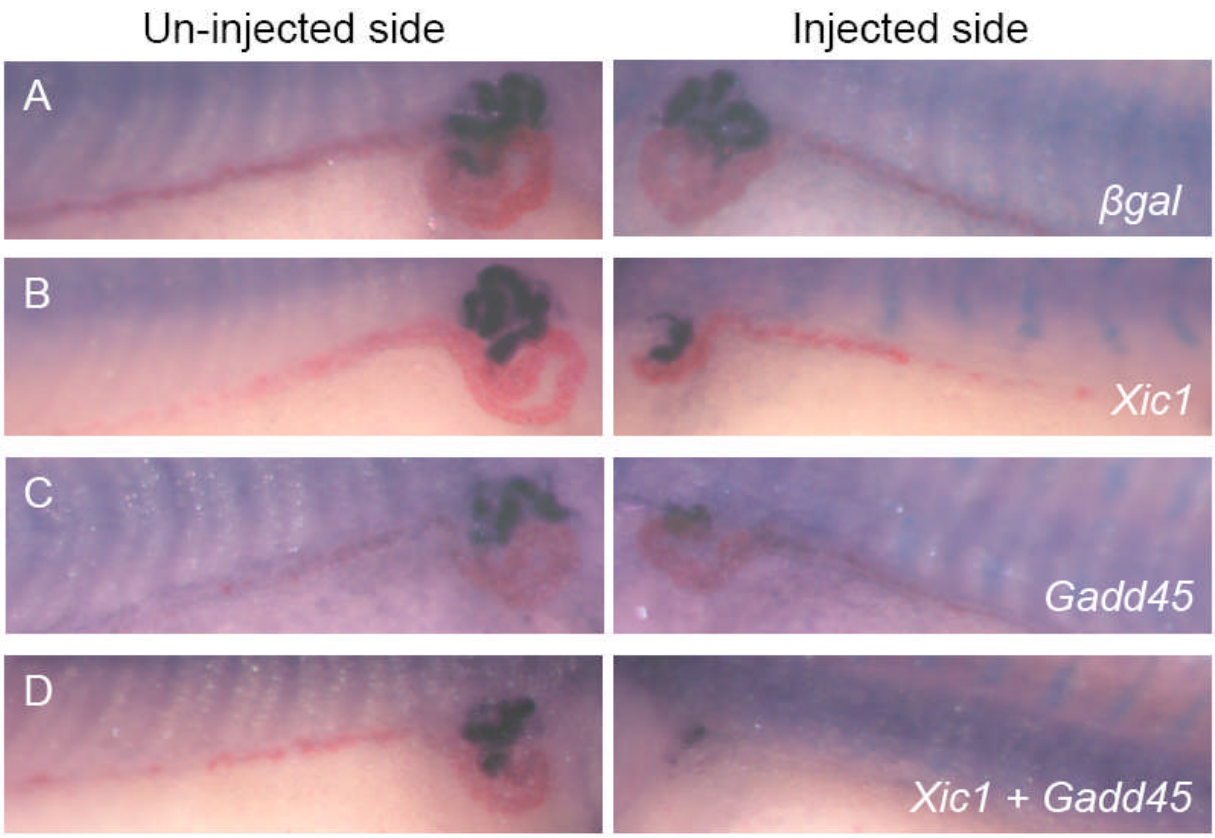

Figure 4.6 Over-expression of *p27^{Xic1}* and *Gadd45γ* inhibits pronephros development. Embryos were injected into the V2 blastomere of an 8-cell stage embryo with 400 pg *βgal* mRNA to act as a lineage tracer. Embryos were then left to develop to stage 41 where they were fixed, sorted for correct targeting and whole mount antibody stained using antibodies 3G8, which detects the nephrostomes and proximal tubules, and 4A6, which detects the intermediate and distal tubules. Injection of *βgal* mRNA had no effect on pronephrogenesis (A). Injection of 50 pg *p27^{Xic1}* mRNA, as described in Chapter 3, reduced 3G8/ 4A6 antibody staining on the injected side (B). Injection of 500 pg *Gadd45γ* mRNA also reduced the size of the pronephros at stage 41, but with less severity than *p27^{Xic1}* over-expression (C). Co-injection of *p27^{Xic1}* mRNA and *Gadd45γ* mRNA reduced the size of the pronephros with a frequency higher than either the single injections of p27^{Xic1} or Gadd45γ (D).

the βgal lineage label and then whole mount antibody stained for phosphohistone H3 (pH3, a marker of dividing cells). 12-14 embryos of each injection were scored and the difference between the number of positively stained pH3 cells on the injected and un-injected sides was compared. Injection of just the *βgal* mRNA lineage tracer had a statistically insignificant effect on cell division with an average 13% more pH3 stained cells on the un-injected side (n=12, Fig 4.7A). Injection of *p27^{Xic1}* mRNA reduced the number of positively stained pH3 cells on the injected side by 60% on average (n=13, Fig 4.7B). *Gadd45γ* over-expression reduced the number of pH3 positive cells by 27% on average on the injected side, although this result is surprisingly statistically insignificant (n=14, Fig 4.7C). Co-injection of *p27^{Xic1}* mRNA and *Gadd45γ* mRNA reduced pH3 staining on the injected side by 62% on average (n=14, Fig 4.7D). In conclusion, this result suggests Gadd45γ is unable to promote the cell cycle exit function of p27^{Xic1}, despite our previous observation at stage 8.5 that suggested Gadd45γ does augment the cell cycle exit function of p27^{Xic1}.

4.2.2 Gadd45γ function only enhances the activity of full length p27^{Xic1}

We next aimed to observe which domain of p27^{Xic1} gave an enhanced pronephric phenotype with Gadd45γ when these two messages were co-injected. Single injections of *p27^{Xic1}* mRNA, *p27^{Xic1} N* mRNA, *p27^{Xic1} #2* mRNA, *p27^{Xic1} C* mRNA and *Gadd45γ* mRNA and co-injections of *p27^{Xic1}*/ *Gadd45γ* mRNA, *p27^{Xic1} N*/ *Gadd45γ* mRNA, *p27^{Xic1} #2*/ *Gadd45γ* mRNA, and *p27^{Xic1} C* mRNA/ *Gadd45γ* mRNA were targeted to the future pronephros by injection into the V2 blastomere as previously described. Embryos were left to develop to stage 22, when they were fixed, stained for *βgal* lineage label and then *in situ* hybridised for *Lim-1* expression

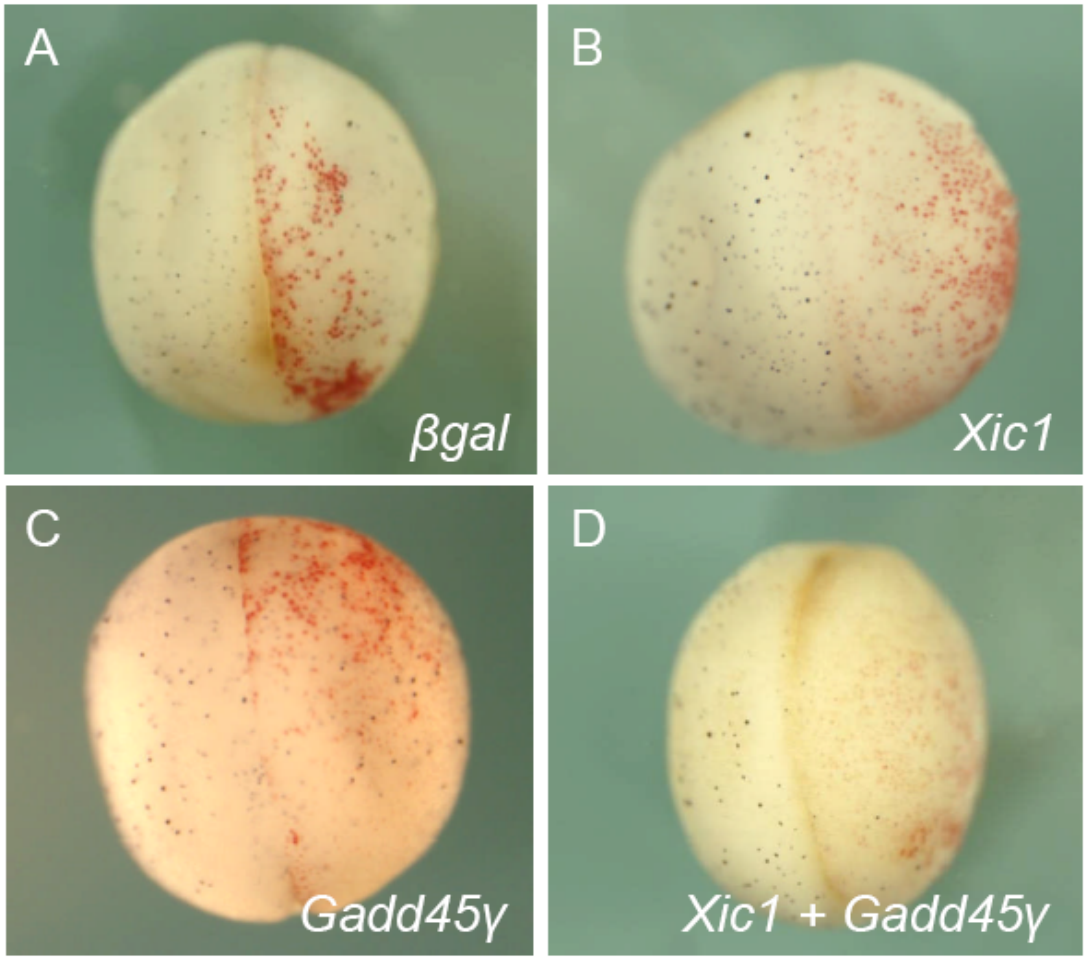

Figure 4.7 Over-expression of *p27^{Xic1}* and *Gadd45γ* inhibits cell division. Embryos were injected into one cell of a two-cell stage embryo with 400 pg *βgal* mRNA to act as a lineage tracer (injected side shown to the right). Embryos were then left to develop to stage 17 where they were fixed, sorted for correct targeting and whole mount antibody stained for phosphohistone H3 (pH3), a marker of dividing cells. Injection of *βgal* mRNA had no effect on cell division (A). Injection of 50 pg *p27^{Xic1}* mRNA, as described in Chapter 3, reduced pH3 antibody staining on the injected side (B). Injection of 500 pg *Gadd45γ* mRNA had an insignificant effect on pH3 staining on the injected side (C). Co-injection of *p27^{Xic1}* mRNA and *Gadd45γ* mRNA significantly reduced the frequency of dividing cells on the injected side (D).

to observe their effect on pronephros anlagen formation. We determined the presence of a pronephric phenotype by comparing the injected side with the un-injected side.

Injection of the *βgal* mRNA lineage tracer had no significant effect on pronephros anlagen formation (6% reduced, n=71, Fig 4.8A). Injection of *Gadd45γ* mRNA inhibited *Lim-1* expression in 25% of embryos scored (n=63, Fig 4.8B). *p27^{Xic1}* over-expression again inhibited pronephros anlagen formation, reducing *Lim-1* expression in 70% of embryos (n=24, Fig 4.8C). In this experiment, co-injection of *p27^{Xic1}* mRNA and *Gadd45γ* mRNA did not produce a more severe phenotype than the single *p27^{Xic1}* mRNA injection; a statistically significant 41% of embryos had reduced *Lim-1* expression (n=29, Fig 4.8D). *p27^{Xic1} N* over-expression reduced *Lim-1* expression in 81% of embryos (n=22, Fig 4.8E), and when co-injected with *Gadd45γ* mRNA gave an almost identical phenotypic prevalence (78% reduced, n=22, Fig 4.8F). Injection of *p27^{Xic1} #2* mRNA caused a statistically insignificant reduction of *Lim-1* expression in 10% of embryos scored (n=30, Fig 4.8G). Co-injecting *p27^{Xic1} #2* mRNA and *Gadd45γ* mRNA inhibited *Lim-1* expression on the injected side with a similar prevalence to the single *Gadd45γ* mRNA injection (26%, n=47, Fig 4.8H). Finally, injection of *p27^{Xic1} C* mRNA had no statistically significant effect on pronephros anlagen formation, reducing *Lim-1* expression on the injected side of only 14% of embryos (n=41, Fig 4.8I). Surprisingly, co-injecting *p27^{Xic1} C* mRNA and *Gadd45γ* mRNA also had no statistically significant effect on *Lim-1* expression, with only 8% of embryos possessing reduced *Lim-1* expression (n=24, Fig 4.8J). In conclusion, in this experiment, it was not possible to identify a specific domain of p27^{Xic1} that interacted in an additive or synergistic manner with Gadd45γ.

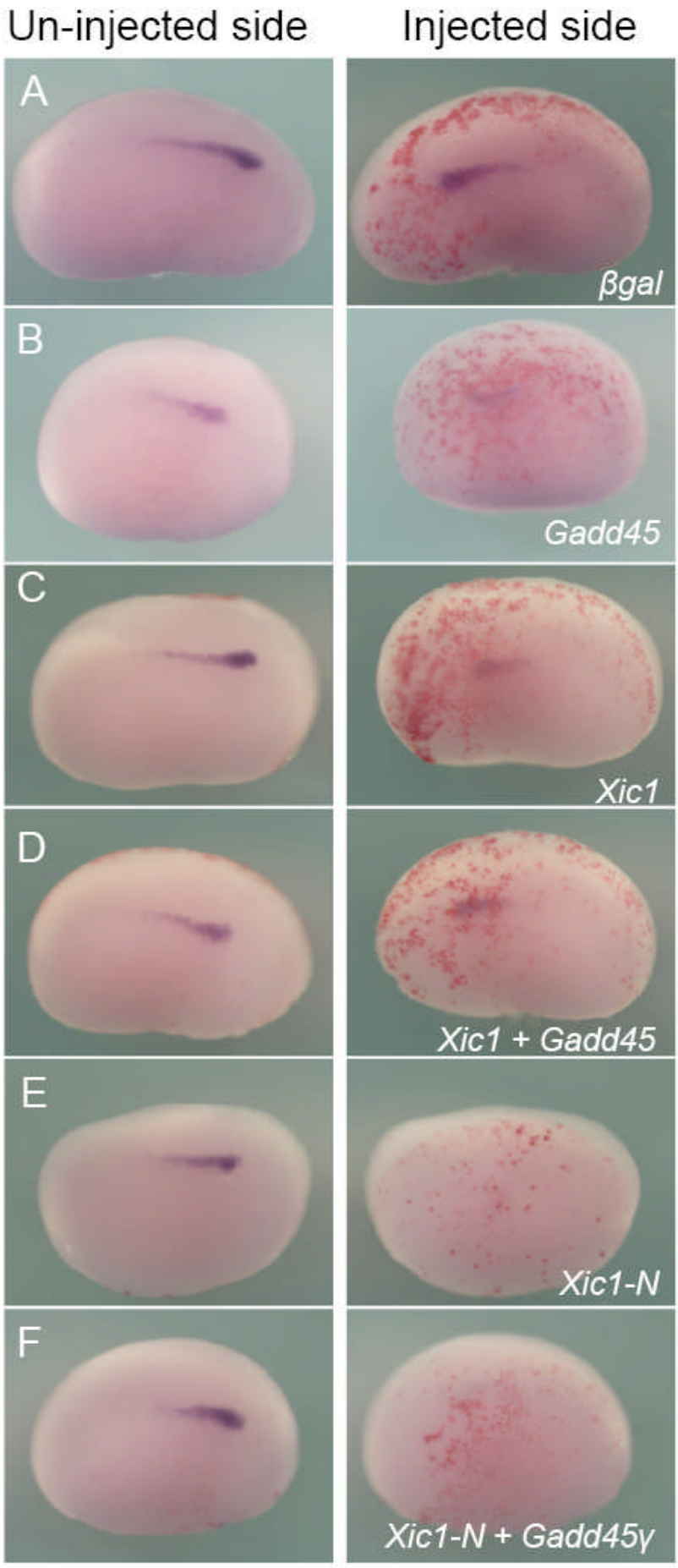
Un-injected side
Injected side
A
βgal
B
Gadd45
C
Xic1
D
Xic1 + Gadd45
E
Xic1-N
F
Xic1-N + Gadd45γ

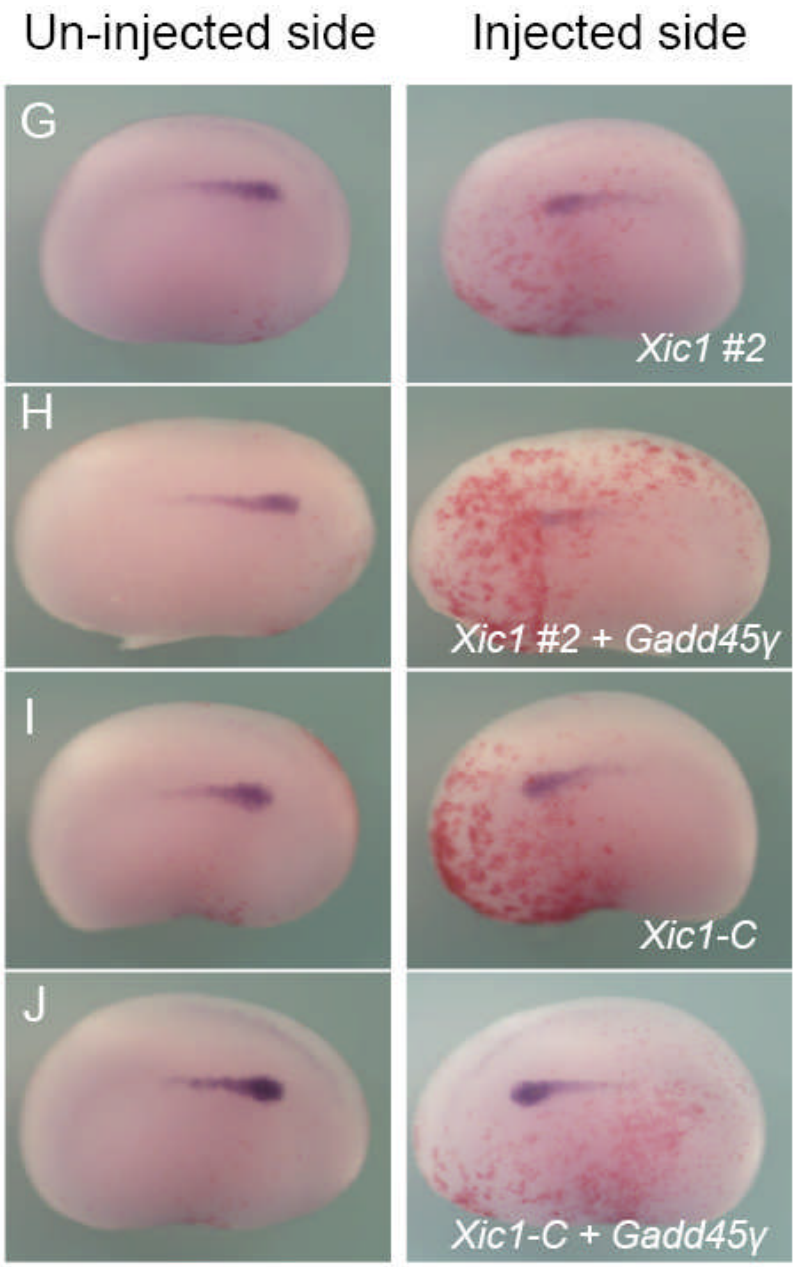

Figure 4.8 Over-expression of the various domains of *p27Xic1* with *Gadd45γ*. *X. laevis* embryos were injected at the 2-cell stage into one cell to target one side of the midline. *βgal* mRNA was co-injected to act as a lineage tracer. Embryos were cultured till stage 22 and whole mount *in situ* hybridised for expression of *Lim-1*, an early marker of the pronephros anlagen. Injection of the *βgal* mRNA had no effect on *Lim-1* expression (A). *p27^{Xic1}* mRNA and *Gadd45γ* mRNA single injections and *p27^{Xic1}* mRNA/ *Gadd45γ* mRNA co-injection, as already described, reduced pronephros anlagen formation (B-D). Both single injections of *p27^{Xic1}-N* mRNA and co-injection of *p27^{Xic1}-N* mRNA and *Gadd45γ* mRNA reduced *Lim-1* expression (E and F). Single injection of *p27^{Xic1}#2* mRNA had no effect on pronephros anlagen formation, but co-injection of *p27^{Xic1}#2* mRNA and *Gadd45γ* mRNA inhibited *Lim-1* expression (G and H). Neither single injections of *p27^{Xic1}-C* mRNA nor co-injection of *p27^{Xic1}-C* mRNA/ *Gadd45γ* mRNA inhibited pronephros anlagen formation (I and J).

4.2.3 Gadd45γ co-immunoprecipitates with p27^{Xic1} with a low affinity

In order to test if Gadd45γ is able to interact with p27^{Xic1} in similar manner to Gadd45α interacts with p21^{Cip1}; we performed a protein interaction study. Co-immunoprecipitation is technique that uses antibodies to first purify a specific antigen, and also any proteins bound to that antigen, from a protein extract, and then a second antibody is used to detect the presence of binding partners by Western blot analysis. The gold standard of co-immunoprecipitation experiments is the use of antibodies that detect endogenous protein as opposed to over-expressed or tagged proteins. Here, we were unable to perform co-immunoprecipitations on endogenous proteins as we did not possess antibodies for Gadd45γ or p27^{Xic1}. Instead we obtained tagged proteins (C-terminus Myc tagged (MT) Gadd45γ and N-terminus Haemagglutinin tagged (HA) p27^{Xic1}) and over-expressed these constructs in oocytes. Oogenesis in *X. laevis* is separated into six stages based on size and yolk content (Dumont, 1972). Stage VI oocytes are the most mature and will only enter meiosis after incubation in progesterone, and can be utilised as translation factories. Injected oocytes were left to translate the exogenous message overnight before being homogenised and processed for protein extraction.

To test if our injected messages were being translated we performed Western blot analysis on the protein extracts to identify translated HA- or Myc-tagged proteins. Figure 4.9A shows an anti-HA Western blot performed on these protein extracts. Lane 1 was our negative control; Western blot analysis using an antibody specific for the HA epitope did not identify any proteins in un-injected oocytes, thus there is no non-specific binding of the HA antibody used in the Western blot analysis. Lane 2 shows Western blot analysis on protein extracted from oocytes injected with

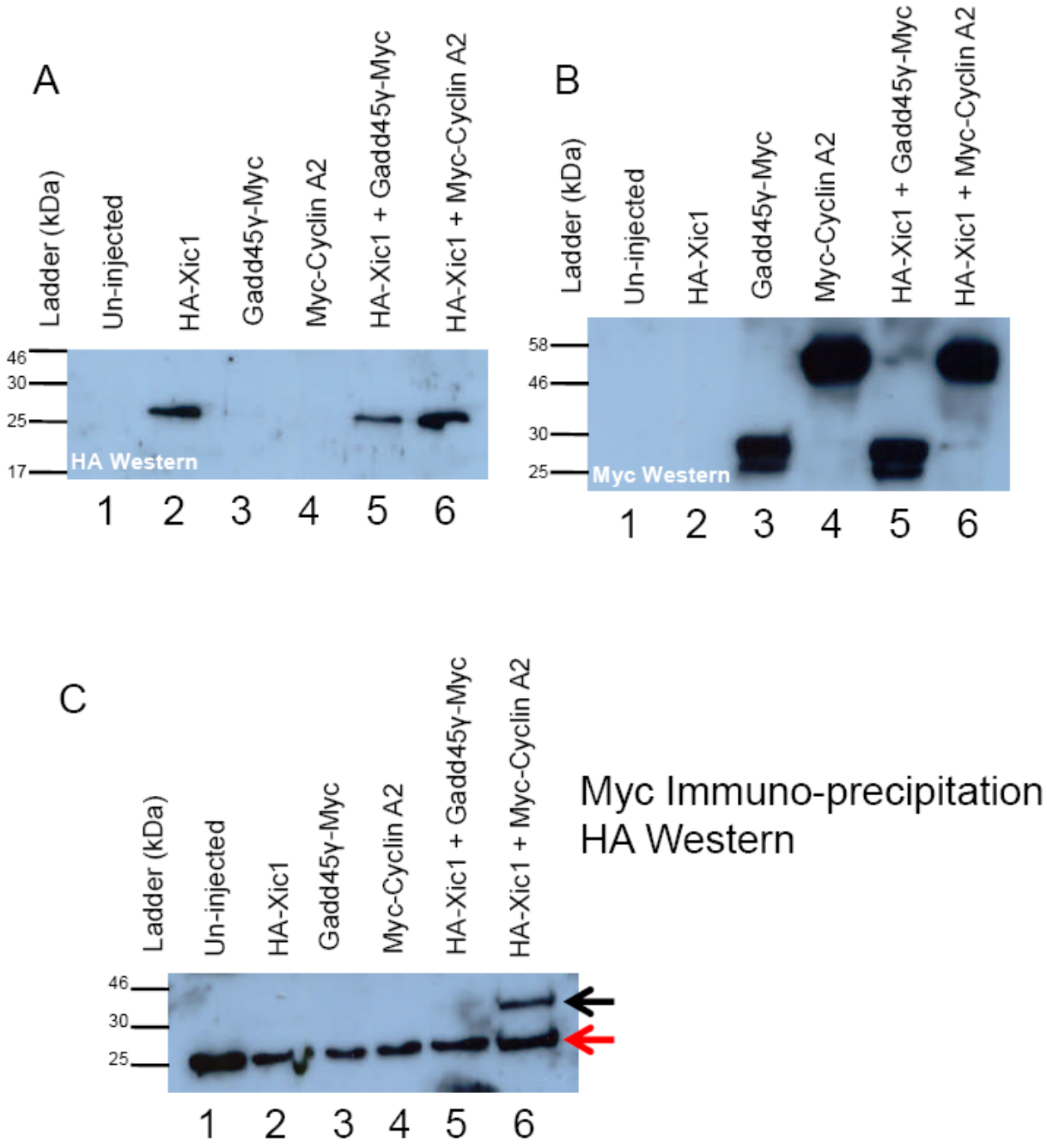
A
Ladder (kDa)
Un-injected
HA-Xic1
Gadd45γ-Myc
Myc-Cyclin A2
HA-Xic1 + Gadd45γ-Myc
HA-Xic1 + Myc-Cyclin A2
46
30
25
17
HA Western
1 2 3 4 5 6
B
Ladder (kDa)
Un-injected
HA-Xic1
Gadd45γ-Myc
Myc-Cyclin A2
HA-Xic1 + Gadd45γ-Myc
HA-Xic1 + Myc-Cyclin A2
58
46
30
25
Myc Western
1 2 3 4 5 6
C
Ladder (kDa)
Un-injected
HA-Xic1
Gadd45γ-Myc
Myc-Cyclin A2
HA-Xic1 + Gadd45γ-Myc
HA-Xic1 + Myc-Cyclin A2
Myc Immuno-precipitation
HA Western
46
30
25
1 2 3 4 5 6

Figure 4.9 Gadd45γ interacts with p27^{Xic1} with a low affinity. Oocytes were injected with 100 ng of various mRNA messages (as indicated), left to translate overnight, then harvested for protein extraction 24 hours after injection. Protein extracts were then exposed to Western blotting to observe translation of injected messages. (A) Haemagglutinin (HA) epitopes were detected using an anti-HA antibody. A *p27^{Xic1}* ORF cDNA clone was tagged with the HA epitope (YPYDVPDYA) by PCR cloning. mRNA synthesised *in vitro* from this clone translated *in vivo*, as observed by a band at approximately 27 kDa in lane 2. HA-p27^{Xic1} was also detected in lanes 5 and 6 where it was co-injected with Myc tagged (MT) *Gadd45*γ mRNA and *Cyclin A2* mRNA. (B) *Gadd45γ-MT* was a kind gift from Jose-Luis Gomez-Skarmeta, CABD Seville, and *MT-Cyclin A2* was a kind gift from Anna Philpott, University of Cambridge. Oocytes injected with *in vitro* synthesised *Gadd45γ-MT* mRNA successfully translated this message to produce Gadd45γ, as indicated by a distinct band in lane 3. *MT-Cyclin A2* mRNA also translated successfully (lane 4). After co-injection with *HA-p27^{Xic1}* mRNA, both *Gadd45γ-MT* (lane 5) and *MT-Cyclin A2* (lane 6) again successfully translated. Taken together A and B showed translation of *HA-p27^{Xic1}* mRNA, *Gadd45γ-MT* mRNA and *MT-Cyclin A2* mRNA was successful and therefore co-immunoprecipitations could be performed. (C) Immunoprecipitation of each protein extract was performed using an anti-Myc antibody. This procedure purified the protein extract by isolating only proteins with the Myc epitope (EQKLISEEDL), or those bound to protein containing the Myc epitope. A western using an anti-HA primary antibody was then performed to observe if HA-p27^{Xic1} co-immunoprecipitated with, and therefore bound (directly or indirectly) to, Gadd45γ-MT and MT-Cyclin A2. All six lanes of the Western blot shown in C contain bands highlighting non-specific binding. These bands (as indicated by the red arrow) have a molecular weight of approximately 20-25 kDa and are most probably the small subunit of the Myc antibody that for unknown reasons is bound to by the HA antibody. Nevertheless, we believe that there are bands present in this Co-IP that represent real protein interactions (black arrow). In lane 6, our positive control shows HA-p27^{Xic1} is present in anti-Myc purified protein extracts, showing, as has already been well characterised, that p27^{Xic1} directly interacts with Cyclin A2. Lanes 1-4 do not contain bands for HA-p27^{Xic1}, as expected. But there is a weak band of appropriate size, present in lane 5; suggesting HA-p27^{Xic1} interacts with Gadd45γ-MT, albeit with much lower affinity than p27^{Xic1} and Cyclin A2 interactions.

HA-p27^{Xic1} mRNA. A clear band at approximately 27 kDa is visible; and is most likely HA-p27^{Xic1}. Lane 3 and lane 4 are Western blot analyses on protein extracts taken from *Gadd45γ-MT* mRNA and *MT-Cyclin* A2 mRNA injected oocytes. Both lanes are negative for protein detectable with the HA antibody. To observe interactions between Gadd45γ and p27^{Xic1} we co-injected *Gadd45γ-MT* mRNA and *HA-p27^{Xic1}* mRNA and performed a co-immunoprecipitation (Fig 4.9C, lane 5). Figure 4.9A, lane 5 shows the presence of HA-p27^{Xic1} in the protein extract. As a positive control co-immunoprecipitation to show the interaction between p27^{Xic1} and Cyclin A2, which are known to interact and cause cell cycle exit (Philpott and Yew, 2008), was performed. Lane 6 shows the protein extracted from oocytes injected with *HA-p27^{Xic1}* mRNA and *MT-Cyclin A2* mRNA, with HA-p27^{Xic1} clearly present. In conclusion anti-HA Western blot analysis on each protein extract shows HA-p27^{Xic1} is present and there is no non-specific binding of this antibody during Western blot analysis.

Figure 4.9B shows Western blot analysis on the same protein extracts, but using an antibody that detects the Myc epitope. This Western blot aimed to detect successful translation of the over-expressed Myc-tagged messages. The negative control, un-injected oocyte protein extract (lane 1) and the *HA-p27^{Xic1}* mRNA injected oocyte protein extract (lane 2) contained no Myc tagged proteins. Gadd45γ-MT was detected in oocytes injected with *Gadd45γ-MT* mRNA (lanes 3 and 5). The protein product of *Gadd45γ* has an actual size of 18 kDa (Hoffman and Liebermann, 2009). However, the protein detected by the Myc antibody used here has an apparent molecular mass that is much larger, approximately 25-30 kDa. We believe this protein is Gadd45γ-MT, as there is no non-specific binding in the negative control

(lane 1). We are unable to explain why this protein runs at an anomalous position relative to non-tagged Gadd45γ, although it is likely to be a consequence of this protein being Myc-tagged. Lanes 4 and 6 identify the presence of appropriately sized MT-Cyclin A2 (untagged Cyclin A2 is estimated to be 46.5 kDa) in the oocytes injected with *MT-Cyclin A2* mRNA. In conclusion Figure 4.8B shows all Myc-tagged mRNA constructs translated appropriately.

We next performed a co-immunoprecipitation on the oocyte protein extracts described above, using the Myc antibody to purify the extracts, and the HA antibody for Western blot analysis (Fig 4.9C). No proteins were present in the un-injected control sample or the single injection controls (lanes 1-4). Our positive control with *HA-p27^{Xic1}* mRNA co-injected with *MT-Cyclin A2* mRNA (lane 6), showed p27^{Xic1} is able to bind Cyclin A2 as a band for HA-p27^{Xic1} at the appropriate size (27 kDa) is present (black arrow). This result shows HA-p27^{Xic1} is bound to MT-Cyclin A2 when MT-Cyclin A2 is immunoprecipitated with the Myc antibody. Co-immunoprecipitation of Gadd45γ-MT with HA-p27^{Xic1} was less successful. A weak band of appropriate size can be observed (lane 5, white arrow) suggesting p27^{Xic1} is able to bind Gadd45γ, but with a much lower affinity than Cyclin A2, although this has not been confirmed biochemically.

4.2.4 p27^{Xic1} over-expression did not cause ectopic primary neurogenesis

Over-expression of *p27^{Xic1}* has previously been shown to cause ectopic primary neurogenesis (Vernon et al., 2003; Vernon et al., 2006). In mouse, p27^{Kip2} has been shown to directly interact with Neurogenin-2, an interaction that promotes neuronal differentiation and migration in the cerebral cortex (Nguyen et al., 2006).

Thus it is possible p27^{Xic1} caused ectopic primary neurogenesis in *X. laevis* by interacting and stabilising X-NGNR-1 in the neural plate where primary neurons form in three stripes during neural tube formation (stages 13-18). Initially we aimed to repeat the results of Vernon et al (2003) and then use this model to further investigate the role of p27^{Xic1} as a regulator of cell fate determination. RNAs were injected into one cell of a two-cell stage embryo with 50 pg *p27^{Xic1}* mRNA or 20 ng of the *p27^{Xic1}* MO, and *βgal* mRNA to act as a lineage tracer. Embryos were left to develop to stage 15, where they were fixed, stained for the lineage label and then whole mount *in situ* hybridised for *Nβ-tubulin*, a marker of lateral, intermediate and medial primary neurons. Embryos were scored by eye to compare the number of primary neurons on the injected and un-injected sides.

20 ng of the *Control* MO caused a statistically insignificant 3% reduction in the number of primary neurons on the injected side when compared to the number of primary neurons on the un-injected side (n=62, Fig 4.10A). Injection of 20 ng *p27^{Xic1}* MO inhibited primary neurogenesis in 82% of embryos scored (n=49, Fig 4.10B). We observed no statistically significant difference in the number of primary neurons on the injected side of embryos injected with 50 pg *p27^{Xic1}* mRNA (12% reduced, n=24, Fig 4.10C), even though in each experimental repeat, the mRNA was tested for its ability to translate in a rabbit reticulocyte lysate system (data not shown). In conclusion p27^{Xic1} is required for primary neurogenesis; however over-expression did not cause ectopic primary neuron formation. These results throw doubt on the published interpretation of a role for p27^{Xic1} in the differentiation of primary neurons.

For p27^{Xic1} to promote primary neurogenesis, it has been suggested p27^{Xic1} binds directly to X-NGNR-1, a basic Helix-Loop-Helix (bHLH) transcription factor, thus stabilising it and promoting its activity. A mammalian homologue of p27^{Xic1}, p57^{Kip2}, has been reported to stabilise the muscle bHLH transcription factor MyoD, by direct interaction with its basic region (Reynaud et al., 1999; Reynaud et al., 2000). The authors of these papers showed arginine 33, located within an α-helix that spans the cyclin and cdk binding domains, was required for this interaction. Secondary protein structure software highlighted this α-helix was conserved in p27^{Xic1}, and sequence comparison indicated a high level of conservation (Fig 4.1A). Consequently we performed site-directed mutagenesis on the *p27^{Xic1}* cDNA clone to make three mutants; *p27^{Xic1} L48P*, *p27^{Xic1} S46A* and *p27^{Xic1} E54A*. These mutants were chosen with reference to the effect they would have on the helical structure (Fig 4.11). We mutated leucine 48 to a proline to break the helix, and thus disrupt any protein-protein interactions that possibly occur through this helix. We also mutated serine 46 to an alanine, as this mutation was the closest match to the R33L mutation performed in p57^{Kip2}, which prevented MyoD binding (Reynaud et al., 2000). Finally, we mutated glutamic acid 54 to an alanine. This mutation was an attempt to disrupt an acidic domain on one side of the helix. Analysis of the helical wheel (Fig 4.11) identified a domain of glutamic acids that could be involved in protein-protein interactions, especially as p57^{Kip2} was shown to bind to the basic region of MyoD. Injection of 200 pg *p27^{Xic1} L48P* mRNA (13% reduced, n=23, Fig 4.10D), 100 pg of *p27^{Xic1} S46A* mRNA (2% reduced, n=58, Fig 4.10E), or 100 pg of *p27^{Xic1} E54A* mRNA (0% affected, n=41, Fig 4.10F) had no statistically significant effect on primary neurogenesis.

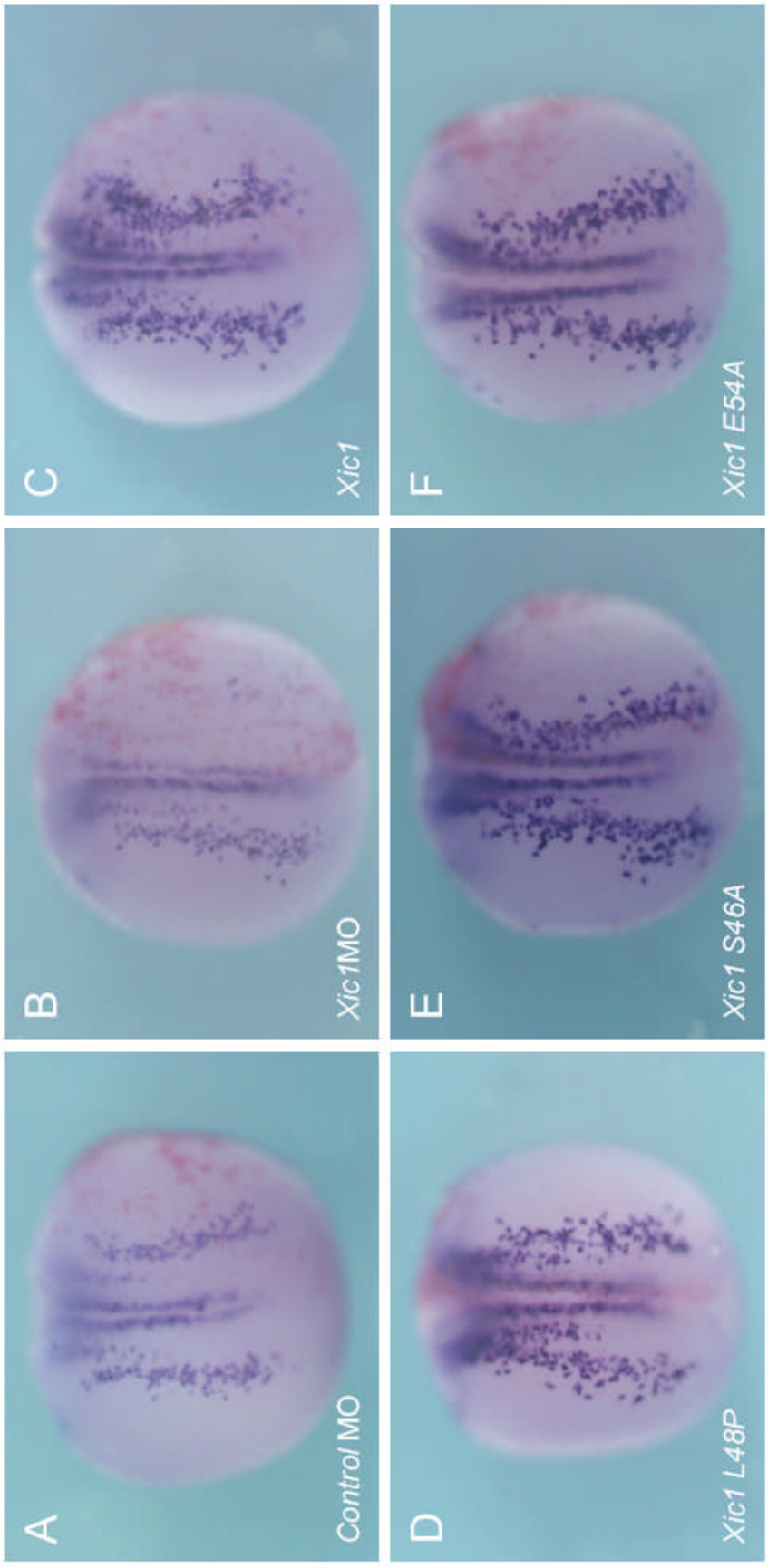

Figure 4.10 $p27^{Xic1}$ over-expression did not increase primary neurogenesis in our hands. One cell of two-cell stage embryos were injected with the experimental message and *βgal* mRNA to act as a lineage tracer. Embryos were left to develop to stage 15, when they were fixed and stained for the lineage label to observe which side of the embryo had been injected. Embryos were then *in situ* hybridised for a marker of primary neurons, *N-βtubulin*. Injection of 20 ng *Control* MO had no effect on primary neurogenesis, indicating injection of a random morpholino oligonucleotide does not perturb normal development (A). Injection of 20 ng $p27^{Xic1}$ MO inhibited primary neurogenesis (B). Injection of wild type $p27^{Xic1}$ mRNA, $p27^{Xic1}$ *L48P* mRNA, $p27^{Xic1}$ *S46A* mRNA, and $p27^{Xic1}$ *E54A* mRNA had no effect on primary neurogenesis (C-F). NB: Injected side shown on the right.

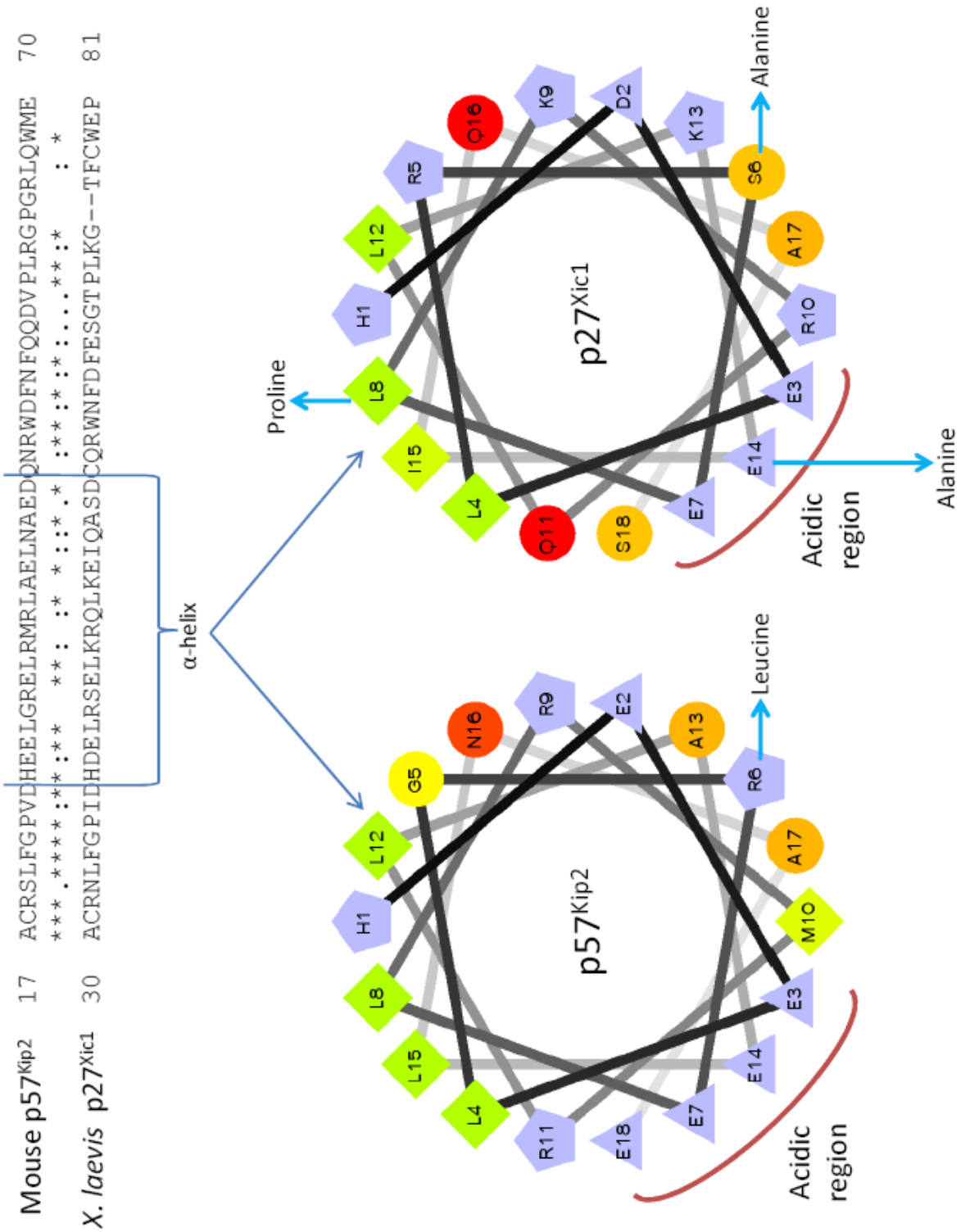
Mouse p57Kip2 17 ACRSLFGPVDHEELGRELRMRLAELNAEDQNRWDFNFQQDVPLRGPGRLQWME 70
X. laevis p27Xic1 30 ACRNLFGPIDHDELRSELKRQLKEIQASDCQRWNFDFESGTPLKG--TFCWEP 81
α-helix
Proline
Alanine
Alanine
Leucine
p27Xic1
p57Kip2
Acidic region
Acidic region
Q16
K9
D2
K13
S6
A17
R10
E3
E14
E7
S18
Q11
L4
I15
L8
H1
L12
R5
N16
R9
E2
A13
R6
A17
M10
E3
E14
E7
E18
R11
L4
L15
L8
H1
L12
G5

Figure 4.11 Helical wheels for an N-terminus alpha helix conserved in p57Kip2 and p27Xic1. Amino acid sequences encoding the alpha helix that spans the conserved cyclin and cdk binding regions of p57Kip2 and p27Xic1 inputted to software to calculate the distribution of amino acids around the helix. The two helical wheels therefore show the positioning of amino acids in the alpha helix viewed longitudinally, with the 5' end closest. Analysis of the helical wheels for p57Kip2 and p27Xic1 show there are similarities in amino acid distribution. Most strikingly, an acidic domain is present in both helices (as indicated in the figure). We chose to disrupt this acidic region by replacing one glutamic acid residue with an alanine that has a short, non-functional side-chain (E54A). In addition we introduced a proline residue, relatively near the start of the helix, to replace a leucine (L48P). This mutation would break the helix the proline side chain occupies the helical backbone region, specifically its methylene group disrupts the hydrogen-bonding required to maintain a helical secondary structure. Thus, this mutant should completely prevent any protein-protein interactions as the helical structure is probably lost, an certainly disrupted. We also mutated serine 46 to an alanine as this residue is in the position mutated by Reynaud et al (2000), and shown to prevent p57Kip2 binding MyoD (S46A). The software used to produce the helical wheels for p57Kip2 and p27Xic1 presents the hydrophilic residues as circles, hydrophobic residues as diamonds, potentially negatively charged as triangles, and potentially positively charged as pentagons. Hydrophobicity is colour coded as well: the most hydrophobic residue is green, and the amount of green is decreasing proportionally to the hydrophobicity, with zero hydrophobicity coded as yellow. Hydrophilic residues are coded red with pure red being the most hydrophilic (uncharged) residue, and the amount of red decreasing proportionally to the hydrophilicity. The potentially charged residues are light blue. Helical wheel software was created by Don Armstrong and Raphael Zidovetzki.

4.2.5 Cyclin A2 is required for pronephrogenesis, but is not essential for primary neurogenesis

Cyclin A2, as shown in Figure 4.9C, is a primary binding target of p27^{Xic1}. Consequently it is possible the presence of Cyclin A2 would sequester endogenous p27^{Xic1}, denying a cell fate determination function of p27^{Xic1} being utilised within the cell. We designed a morpholino oligonucleotide that could bind over the start codon of endogenous *Cyclin A2* transcripts to prevent its translation (Fig 4.12A). To test the activity of this MO we observed whether it could inhibit *in vitro* translation of ^{35}S-Methionine labelled *Cyclin A2* mRNA in a rabbit reticulocyte lysate system (Fig 4.12B). Translation of *Cyclin A2* mRNA was knocked down when this message was incubated with the *Cyclin A2* MO (Fig 4.12B, lane 2). To test the effectiveness of the Cyclin A2 MO *in vivo*, we injected stage VI oocytes with *Cyclin A2* mRNA in the presence or absence of the *Cyclin A2* MO, incubated the oocytes in medium containing ^{35}S-Methionine, and then extracted the protein and performed autoradiography as previously described (Fig 4.12C). A band of appropriate size representing over-expressed Cyclin A2 is present in oocytes injected with *Cyclin A2* mRNA in the absence of the *Cyclin A2* MO (Fig 4.12C, lane 1). In the presence of the *Cyclin A2* MO this band is not present (Fig 4.12C, lane 2). In conclusion the *Cyclin A2* MO is able to inhibit translation of over-expressed *Cyclin A2* mRNA *in vitro* and *in vivo*.

Depletion of Cyclin A2 produced a severe cell cycle effect at stage 8.5 (Fig 4.13). Injection of 10 ng, 20 ng or 40 ng of *Cyclin A2* MO inhibited cell division, producing large cells around the site of injection. This phenotype is expected, as the Cyclin A group of Cyclins are required for progression into the S-phase.

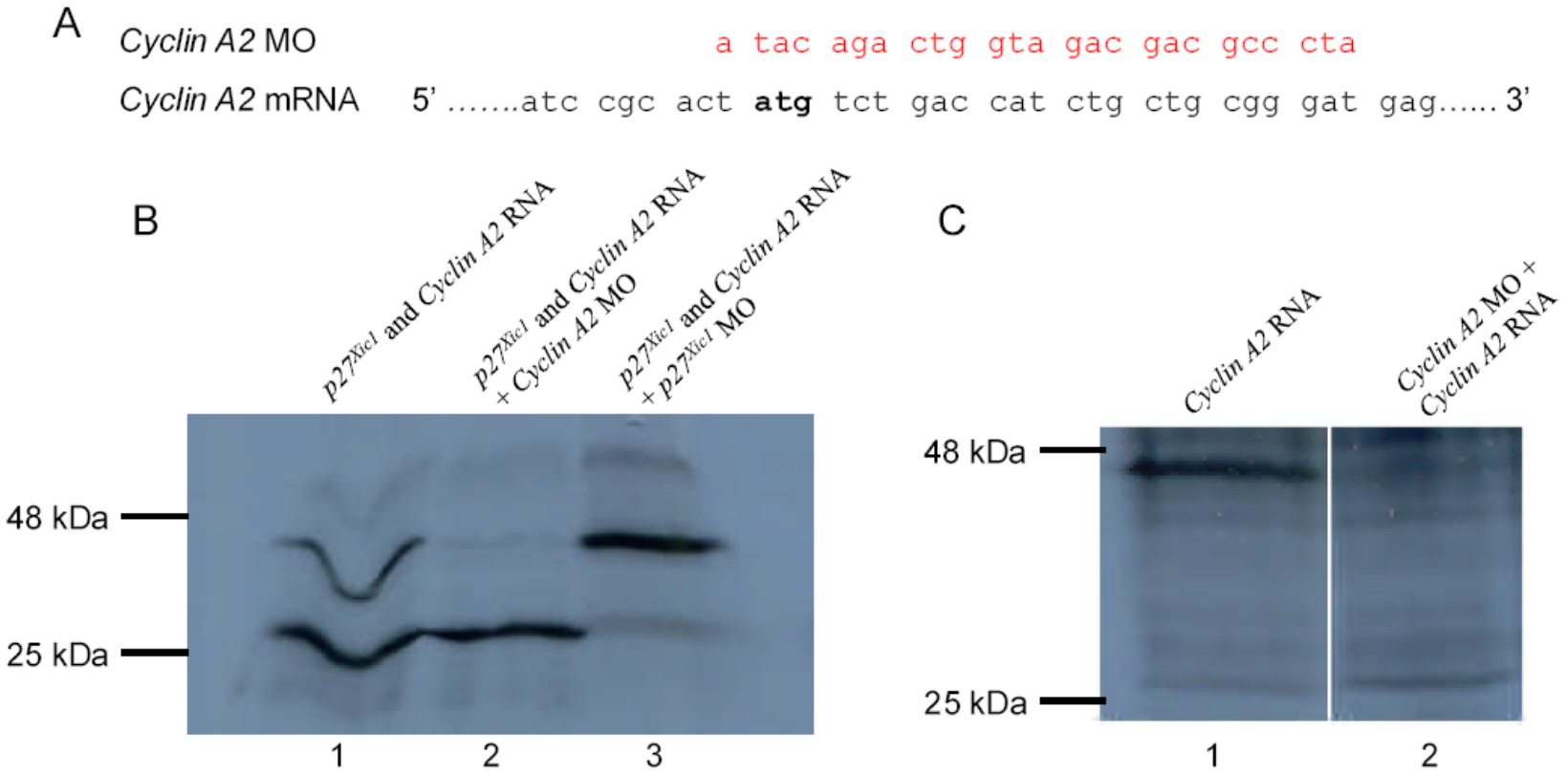

Figure 4.12 The *Cyclin A2* MO inhibits translation of *Cyclin A2* mRNA *in vitro* and *in vivo*. (A) Sequence of Cyclin A2 against which the MO was designed, to inhibit translation (atg start codon shown in bold). (B) Radio-labelled *p27Xic1* and *Cyclin A2* were separated on an SDS-PAGE gel and detected by autoradiography. p27Xic1 and Cyclin A2 mRNA translated successfully and produced proteins of predicted size (p27Xic1 = 27 kDa, Cyclin A2 = 46.5 kDa). 2.6 µg of *p27Xic1* mRNA co-translated *in vitro* with 1.8 µg *Cyclin A2* mRNA in the absence of MOs (lane 1), the presence of 5 µg *Cyclin A2* MO (lane 2), and but not in the presence of 5 µg *p27Xic1* MO (lane 3). 5 µg *Cyclin A2* MO successfully knocked down translation of 1.8 µg *Cyclin A2* mRNA, but not 2.6 µg *p27Xic1* mRNA *in vitro* (lane 2). (C) Oocytes were injected with *Cyclin A2* mRNA in the absence (lane 1) or presence of the *Cyclin A2* MO (lane 2) and left overnight in media containing ^{35}S-Met to process the exogenous message. Oocyte protein content was then separated on an SDS-PAGE gel and detected by autoradiography. *Cyclin A2* mRNA translation is clearly observed in lane 1. This translation is inhibited by the *Cyclin A2* MO (lane 2). In conclusion *Cyclin A2* mRNA translation has been shown to be specifically inhibited *in vitro*, and *in vivo*.

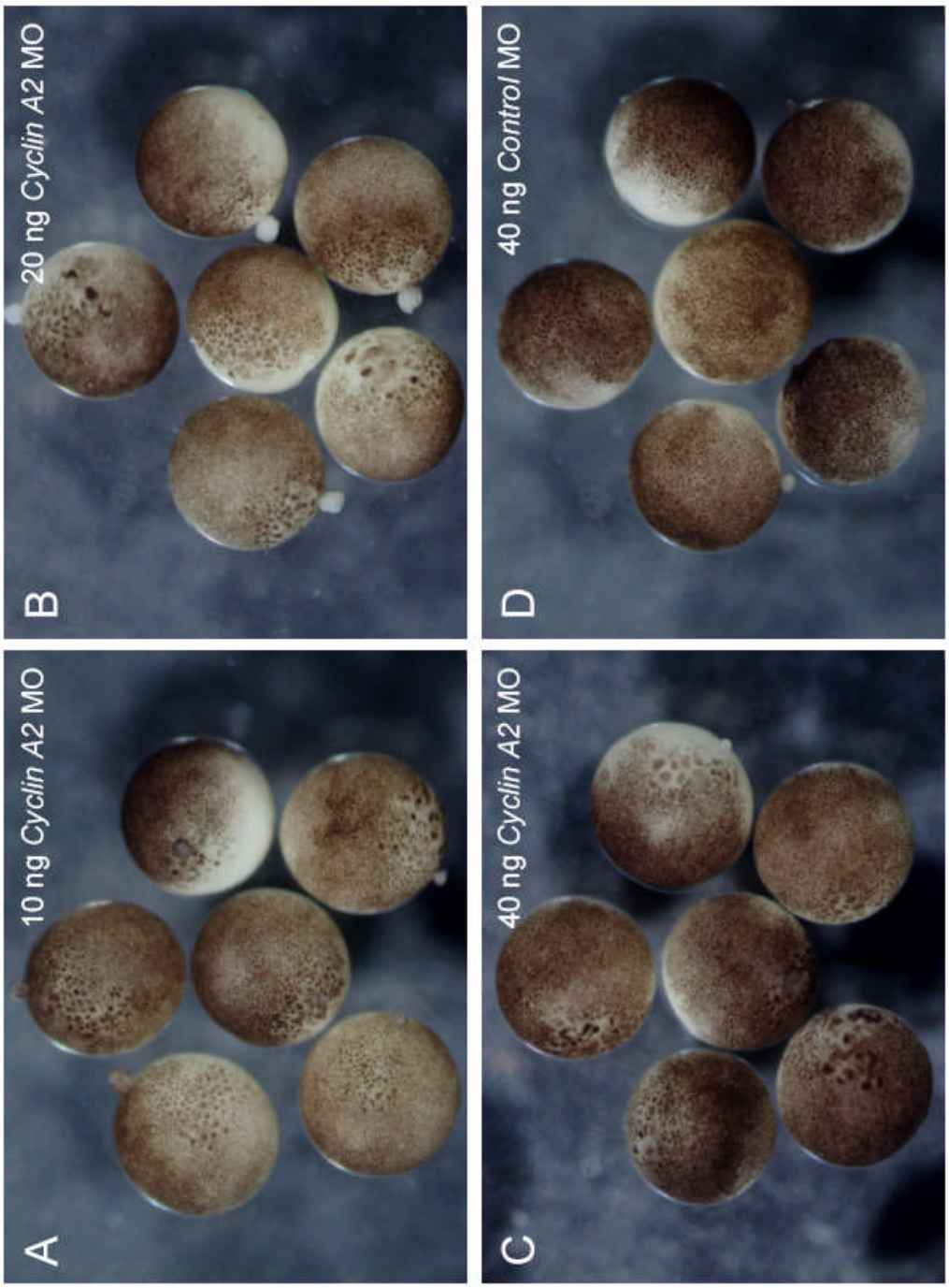

Figure 4.13 The Cyclin A2 MO affects cell cycle in vivo Embryos were injected into one cell of a 2-cell stage embryos with 10 ng, 20 ng, 40 ng of Cyclin A2 MO and 40 ng Control MO and left to develop to stage 8. Enlarged cells are apparent in all the Cyclin A2 MO injections, a phenotype that is indicative of premature cell cycle exit (A-C). The Control MO had no effect on cell cycle (D).

Consequently, loss of Cyclin A2 may be sufficient to inhibit cell cycle progression. Thus depletion of endogenous Cyclin A2 produced a similar phenotype at stage 8.5 to *p27^{Xic1}* over-expression. We therefore expected the pronephric phenotype of Cyclin A2 depletion to be the same as *p27^{Xic1}* over-expression. This result is what we observed, in embryos injected into the V2 blastomere at the 8-cell stage with 20 ng *Cyclin A2* MO to target the future pronephros (Fig 4.14). 49% of embryos had reduced 3G8/ 4A6 antibody staining when Cyclin A2 is depleted (n=39). In conclusion the effect the *Cyclin A2* MO has at stage 8.5 suggests it is capable of knocking down Cyclin A2 expression in developing embryos, and the pronephric phenotype produced when Cyclin A2 is depleted suggests Cyclin A2, through its role in cell cycle, is required for pronephrogenesis.

We next attempted to see the effect Cyclin A2 knock-down had on primary neurogenesis in order to understand if Cyclin A2 is involved in regulation of this process. As described above, we injected our message, along with *βgal* mRNA to act as a lineage tracer, into one cell of a two-cell stage embryo to target one side of the midline. Embryos were left to develop to stage 15, when they were fixed, stained for the lineage tracer, and the whole mount *in situ* hybridised for expression of *Nβ-tubulin*, a marker of differentiated primary neurons. 20 ng of the *Control* MO caused a statistically insignificant 3% reduction in primary neurogenesis on the injected side of injected embryos (n=62, Fig 4.15A). Depletion of Cyclin A2 after injection of 20 ng *Cyclin A2* MO had no statistically significant effect on *Nβ-tubulin* expression (13% reduced, n=52, Fig 4.15B). Over-expression of *Cyclin A2* reduced the number of primary neurons on the injected side of 83% of embryos scored (n=35, Fig 4.15C). Similarly, injection of 1 ng *Cdk2* mRNA inhibited primary neurogenesis in 92% of

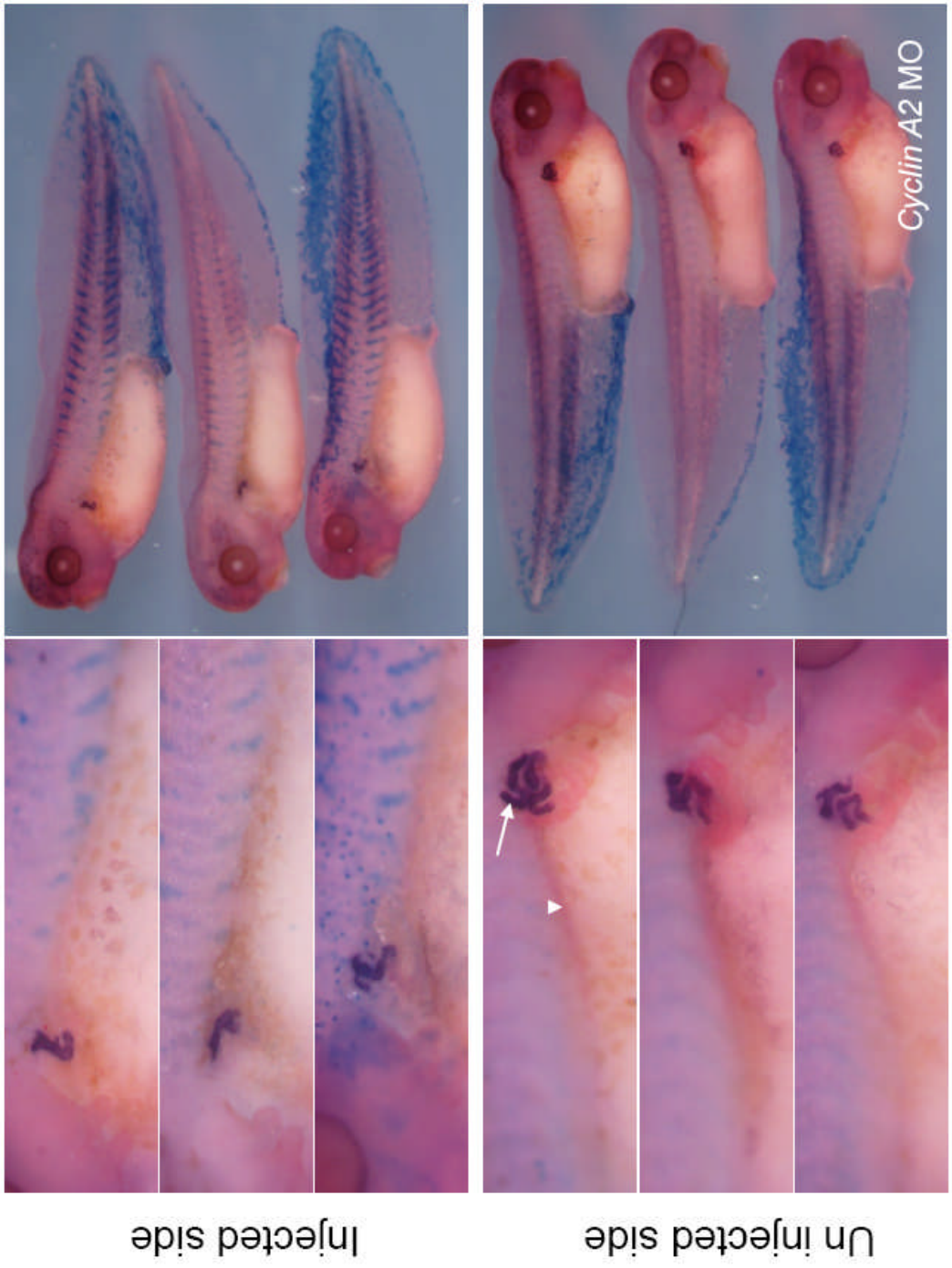

Figure 4.14 Injection of Cyclin A2 MO inhibits pronephrogenesis. *X. laevis* embryos were injected at the 8 cell stage into a ventro-vegetal blastomere to target the presumptive pronephric region. mRNA was co-injected with 400 pg *βgal* mRNA to act as a lineage tracer (blue staining). Embryos were cultured till stage 41 and whole mount antibody stained with 3G8, to detect nephrostomes and proximal pronephric tubules (white arrow, stained purple), and 4A6, to detect intermediate and distal pronephric tubules (white arrowheads, stained red). Injection of 20 ng Cyclin A2 MO reduced 3G8/ 4A6 staining on the injected side, indicating pronephrogenesis was inhibited.

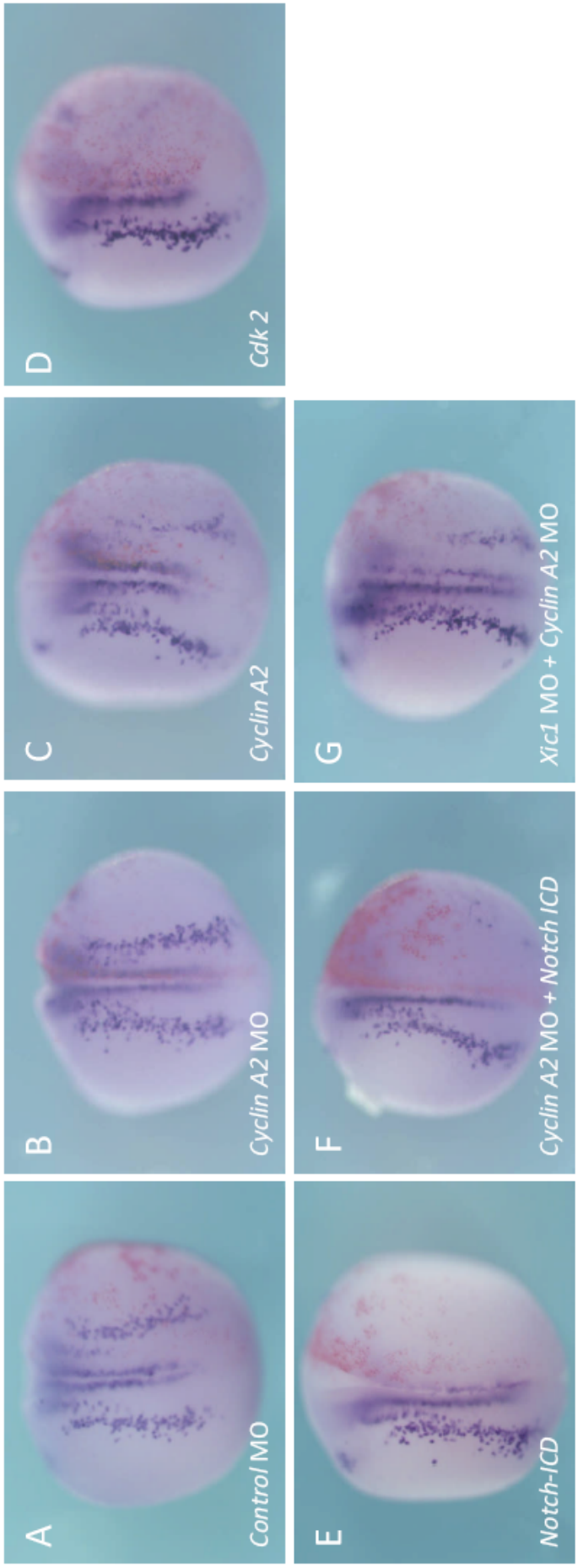

Figure 4.15 Depletion of Cyclin A2 has no effect on primary neurogenesis, but over-expression inhibits primary neurogenesis. One cell of two-cell stage embryos were injected with the experimental message and 400 pg *βgal* mRNA to act as a lineage tracer. Embryos were left to develop to stage 15, when they were fixed and stained for the lineage label to observe which side of the embryo had been injected. Embryos were then *in situ* hybridised for a marker of primary neurons, *N-βtubulin*. Injection of 20 ng *Control* MO had no effect on primary neurogenesis, indicating injection of a random morpholino oligonucleotide does not perturb normal development (A). Injection of 20 ng *Cyclin A2* MO had no effect on primary neurogenesis (B). Injection of 1 ng *Cyclin A2* mRNA, 1 ng *Cdk2* mRNA, and 600 pg *Notch-ICD* mRNA all inhibited primary neurogenesis on the injected side (C-E). Co-injections of 20 ng *Cyclin A2* MO/ 600 pg *Notch-ICD* and 20 ng *p27^{Xic1}* MO/ 1 ng *Cyclin A2* MO also inhibited primary neurogenesis (F and G). NB: Injected side shown to the right.

embryos scored (n=37, Fig 4.15D). As previously reported in published literature, over-expression of *Notch-ICD* caused a dramatic reduction in primary neurogenesis of 78% of embryos scored (n=58, Fig 4.15E). As *Cyclin A2* over-expression also inhibits primary neurogenesis, we aimed to observe if depletion of Cyclin A2 rescued in any way the effect of *Notch-ICD* mRNA injection. Co-injection of 20 ng *Cyclin A2* MO with 600 pg *Notch-ICD* mRNA inhibited formation of primary neurons to a similar degree observed after single injections with 600 pg *Notch-ICD* mRNA (96% reduced, n=48, Fig 4.15F). Likewise, we aimed to observe if knock-down of *Cyclin A2* expression had any effect on primary neurogenesis when p27^{Xic1} is depleted, as *p27^{Xic1}* knock-down could be causing a reduced primary neurogenesis phenotype as its absence would increase the cellular levels of free Cyclin A2/ cdk2, which could promote the inhibitory action of Cyclin A2 on X-NGNR-1 function. Co-injection of 20 ng *Cyclin A2* MO and 20 ng *p27^{Xic1} MO* failed to rescue the reduction phenotype observed after single injections of 20 ng *p27^{Xic1} MO* (88% reduced, n=16, Fig 4.15G). In conclusion Cyclin A2 is not required for primary neurogenesis.

4.3 Discussion

Previous publications have reported p27^{Xic1} is a multi-functional protein involved in cell fate determination in addition to cell cycle exit (Ohnuma et al., 1999; Ohnuma et al., 2002; Vernon et al., 2003; Vernon and Philpott, 2003; Nguyen et al., 2006; Movassagh and Philpott, 2008). The aims of this chapter were to identify if Gadd45γ is an interacting partner of p27^{Xic1} and evaluate the role p27^{Xic1} plays in primary neurogenesis in order to further understand this proposed multi-functionality.

Results we have obtained suggest p27^{Xic1} may be able to interact with growth-arrest-and-DNA-damage-induced gamma (Gadd45γ). However, we were unable to repeat the fundamental result of Vernon et al (2003) who showed *p27^{Xic1}* over-expression increased the number of cells fated to form primary neurons, reportedly by the stabilisation of X-NGNR-1. This negative result is important as if *p27^{Xic1}* over-expression enhances primary neurogenesis, this is a fundamental demonstration of a role in differentiation for p27^{Xic1}. Our inability to observe this phenotype suggests data reported in the literature is inaccurate (see Chapter 7 for further discussion).

4.3.1 p27^{Xic1} is a potential binding partner of Gadd45γ

Gadd45γ has been shown to be expressed in cells fated to form primary neurons at stage 16 (de la Calle-Mustienes et al., 2002). This expression profile suggests a link between cell differentiation and cell cycle arrest as Gadd45γ is able to antagonize cell division (de la Calle-Mustienes et al., 2002). We were unable to repeat this published result since we only observed a statistically insignificant reduction in the number of cells antibody stained for the mitotic marker pH3 (Fig 4.7C). Despite our result being statistically insignificant, there was a 27% reduction in positively stained pH3 cells on the injected side of embryos compared to the un-injected side. Thus we suggest Gadd45γ, as reported in the literature, might be capable of promoting cell cycle exit. This suggestion is bolstered by a study that showed Gadd45α can interact with p21^{Cip1}, augmenting its cell cycle exit function (Zhao et al., 2000). Furthermore, when *Gadd45γ* mRNA is co-injected with *p27^{Xic1}* mRNA the cell cycle exit function of p27^{Xic1} was promoted (Figs 4.4D). Thus Gadd45γ may be able to promote cell cycle exit through direct or indirect interaction with p27^{Xic1}.

The effect of over-expressing *Gadd45γ* and *p27^{Xic1}* increased the severity of the pronephric phenotypes observed at stage 24 and 41 compared to single injections of either *Gadd45γ* mRNA or *p27^{Xic1}* mRNA (Fig 4.5 and 4.6). In Chapter 3 we showed the cell cycle exit function of p27^{Xic1} inhibited myogenesis, which is likely to be the cause of the reduced pronephric phenotype when this gene is over-expressed. As we believe Gadd45γ augments the cell cycle exit function of p27^{Xic1}, it is likely the cause of pronephric phenotypes after *Gadd45γ* over-expression is disruption of the signal from the somites to the intermediate mesoderm to induce pronephrogenesis. We did not investigate this possibility further as the aim of this chapter was not to understand why *Gadd45γ* over-expression produced a pronephric phenotype, but to decipher if co-injecting *Gadd45γ* mRNA and *p27^{Xic1}* mRNA increased the severity of these pronephric phenotypes as a consequence of interaction between these two proteins. This interaction, we postulated, would perhaps stabilise p27^{Xic1} and augment its cell cycle exit function. To observe if such a protein-protein interaction is occurring we attempted to co-immunoprecipitate Gadd45γ bound to p27^{Xic1} (Fig 4.9). As previously reported, we showed Cyclin A2 binds with a high affinity to p27^{Xic1} (Fig 4.9C, lane 6). Co-immunoprecipitation of p27^{Xic1} and Gadd45γ we believe did occur, as observed by a weak band of appropriate size in lane 5 of Figure 4.9C. The weakness of this band is a possible sign of lower affinity between p27^{Xic1} and Gadd45γ, or maybe due to less HA-p27^{Xic1} present in this protein extract (as observed in Fig 4.9A, lane 5) compared to the amount of HA-p27^{Xic1} in the *HA-p27^{Xic1}* mRNA/ *MT-Cyclin* A2 mRNA co-injected protein extract (Fig 4.9A, lane 6). Future repeats of this experiment may yield more definitive data. Alternatively there are a number of approaches that we could perform in order to improve the data. Over-expressing gene products *in vitro*, such as in a rabbit reticulocyte lysate system;

would reduce the amount of non-specific binding, especially of yolk proteins present in oocytes. Over-expression in cell cultures may also help to eradicate this problem and maximise the number of specific antibody-antigen and antibody-bead interactions. In addition there are many other protocols, other than co-immunoprecipitation, that could be utilised, such as Bimolecular Fluorescent Complementation (BiFC), Fluorescent resonance energy transfer (Fret), Biacore® analysis (which could be used to test the affinity of p27^{Xic1} for Gadd45γ compared to the p27^{Xic1} and Cyclin A2 interaction) and yeast-two hybrid screens. We have also generated tagged constructs of different domains of p27^{Xic1} and Gadd45γ, which could be over-expressed and analysed for protein-protein interactions to map the regions of p27^{Xic1} and Gadd45γ required for binding. Whilst we have shown there is a possibility of interaction between p27^{Xic1} and Gadd45γ, further experimentation, using the above protocols, needs to be performed to yield more conclusive evidence of an important functional interaction.

4.3.2 *p27^{Xic1}* over-expression does not promote primary neurogenesis

The proneural protein neurogenin (X-NGNR-1) is a bHLH transcription factor that induces a differentiation program in cells fated to form primary neurons (Ma et al., 1996). In addition, primary neuron differentiation requires sequential activation of other proneural bHLH and zinc finger transcription factors, such as XMyt1 (Bellefroid et al., 1996), Xash3 (Zimmerman et al., 1993) and NeuroD (Lee et al., 1995). In neural tissue it has been reported p27^{Xic1} stabilises X-NGNR-1, enhancing neurogenesis (Vernon et al., 2003). As an α-helix spanning the cyclin and cdk binding domains in p57^{Kip2} has been shown to directly bind MyoD (Reynaud et al., 1999; Reynaud et al., 2000), and this same helix is conserved in p27^{Xic1} (Fig

4.1A), we aimed to observe if p27^{Xic1} stabilised X-NGNR-1 by direct binding to this conserved α-helix. As already reported, knock-down of *p27^{Xic1}* inhibited primary neurogenesis (Fig 4.10B); therefore p27^{Xic1} is required for primary neuron formation. We showed in Chapter 3 that the *p27^{Xic1}* MO had little effect on cell division (Fig 3.11C), thus it can be assumed that cell division in these embryos is normal. In conclusion, p27^{Xic1} is directly required for cell fate determination during primary neurogenesis. Vernon et al (2003) showed co-injecting the *p27^{Xic1}* MO and *X-NGNR-1* mRNA inhibited primary neurogenesis, but co-injecting the *p27^{Xic1}* MO and *NeuroD* mRNA did not prevent formation of primary neurons. Thus, during the sequential activation of transcription factors that ultimately leads to primary neuron differentiation, p27^{Xic1} is required to promote X-NGNR-1 activity. We designed an experiment to test whether this conserved α-helix spanning the cyclin and cdk binding domains of p27^{Xic1} was perhaps responsible for binding and stabilising X-NGNR-1 in the neural system. We performed site-directed mutagenesis, generating three mutants; p27^{Xic1} L48P (introducing a proline to act as a 'helix breaker'), p27^{Xic1} S46A (the nearest homolog to p57^{Kip2} R33L that was unable to bind MyoD) and p27^{Xic1} E54A (to eliminate an acidic domain on one side of the helix). When over-expressed in one side of the embryo, none of these mutants caused ectopic primary neurogenesis (Fig 4.10D-F). Vernon et al (2003) had reported over-expressing wild type *p27^{Xic1}* enhanced primary neurogenesis on the injected side. Thus we expected to see no statistically significant effect on primary neuron formation between the injected and un-injected sides after injection of our mutant mRNAs. However, when we injected wild type *p27^{Xic1}* mRNA we repeatedly had no statistically significant effect on primary neurogenesis (Fig 4.10C). The reproducibility of this result was such that we propose over-expression of *p27^{Xic1}* is unable to enhance primary

neurogenesis. As a consequence we were unable to conclude whether injection of our mutants of p27^{Xic1} could inhibit the proposed differentiation function of p27^{Xic1} in primary neurogenesis.

A possible explanation for why *p27^{Xic1}* over-expression did not enhance primary neurogenesis is that only cells containing X-NGNR-1 will form primary neurons. The gene expression pattern of *X-NGNR-1* is not regulated by p27^{Xic1}, but is regulated by lateral inhibition through the Notch signalling pathway (Fig 4.16) (Chitnis et al., 1995; Vernon et al., 2006). Neural plate cells containing Notch-ICD are maintained in an undifferentiated state, but cells containing activated Notch ligands are fated to form primary neurons. Vernon et al (2006) showed over-expression of a constitutively active form of *Notch*, *Notch-ICD*, inhibited expression of *X-NGNR-1* and *p27^{Xic1}*, and so prevented formation of primary neurons (a result we have repeated in Fig 4.15E). Ultimately, p27^{Xic1} can only stabilise X-NGNR-1 in those cells in which X-NGNR-1 is present. Thus, over-expressing *p27^{Xic1}* ensures exogenous *p27^{Xic1}* mRNA is, theoretically, in all the cells of the neural plate, but will only enhance primary neurogenesis in those cells containing X-NGNR-1 and already fated to form primary neurons. To overcome this issue and observe if our mutants are able or unable to affect differentiation, a rescue experiment could be performed. MOs are unable to bind over sequences that are not exactly complementary. p27Xic1 could be mutated in the region where the *p27^{Xic1}* MO binds, making this clone suitable to generate mRNA to rescue any phenotype produced after depletion of *p27^{Xic1}*. We could perform site-directed mutagenesis on this mutant *p27^{Xic1}* cDNA clone to produce our L48P, S46A and E54A mutants. Co- injection of mRNAs synthesised from these mutant clones with the *p27^{Xic1}* MO could be performed

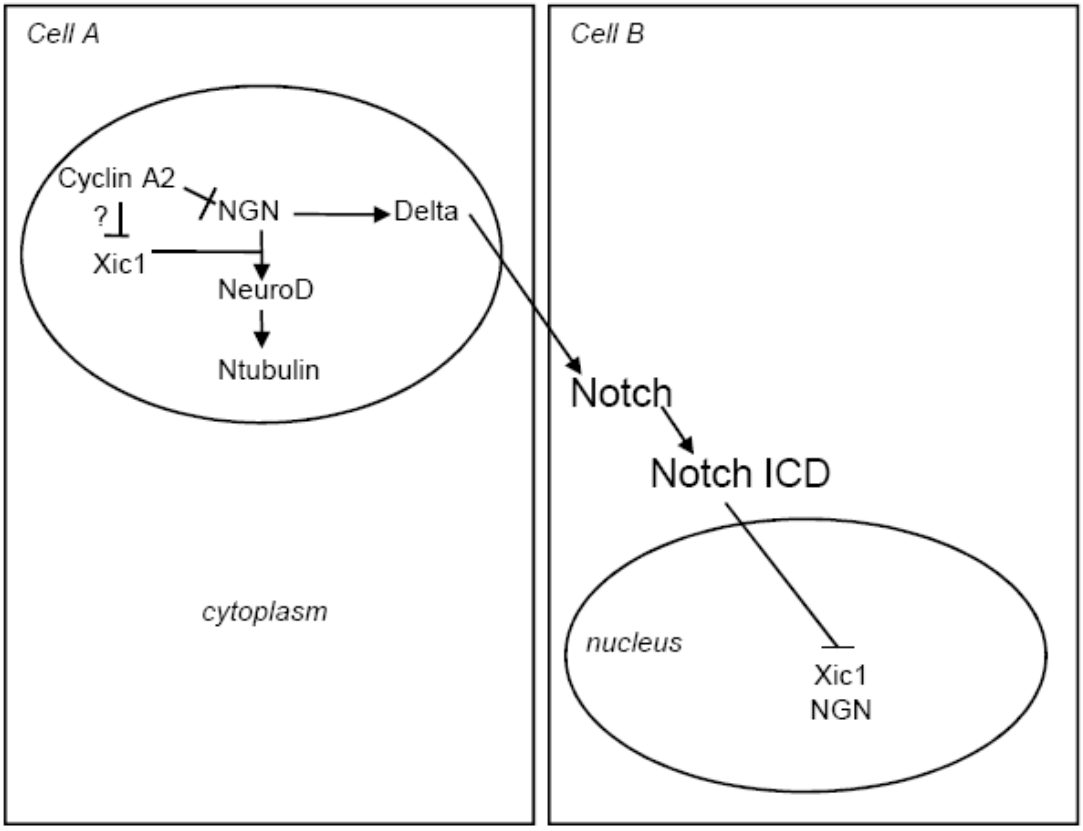

Figure 4.16 Lateral inhibition via the Notch signalling pathway regulates primary neuron differentiation by controlling expression of both p27^{Xic1} and Neurogenin (NGN) In early neural stages NGN, which is stabilised by p27^{Xic1} (mechanism unknown), acts to induce a signalling cascade that ultimately leads to the establishment of primary neurons in the neural plate. NGN is a transcription factor that, as well as inducing this signalling cascade, will increase expression of *Delta*. This induction of *Delta* expression allows for the Notch signalling pathway to regulate cell fate decisions through the process of lateral inhibition. Delta in cells expressing NGN will bind to Notch receptors on neighbouring cells, activating the Notch-ICD dependent pathway. In cells where the Notch-ICD dependent pathway is active, gene expression will differ to those cells expressing *Delta*. *NGN* and *p27^{Xic1}* expression is inhibited, thus these cells cannot form primary neurons. p27^{Xic1} is a cyclin dependent kinase inhibitor that primarily interacts with Cyclin A2. The levels of Cyclin A2 in the cytoplasm could affect the level of stabilisation of NGN by p27^{Xic1}, and therefore be an additional checkpoint in primary neurogenesis. (Schematic adapted from Vernon et al, 2006)

and the effect on primary neurogenesis observed. We would predict the wild type *p27^{Xic1}* mRNA to rescue the *p27^{Xic1}* MO phenotype, but the mutants would not rescue the phenotype as endogenous X-NGNR-1 remained unstable. In addition to this co-immunoprecipitations could be performed in a similar manner to the p27^{Xic1}/ Gadd45γ co-immunoprecipitation described above to observe if any protein-protein interactions occur. This study however falls out of the scope of this thesis.

4.3.3 Cyclin A2 is not required for primary neurogenesis, but depletion inhibits pronephrogenesis

Co-immunoprecipitation experiments to investigate X-NGNR-1 and p27^{Xic1} interaction have already been attempted using extracts from stage 20 embryos, and showed these two proteins are unable to co-immunoprecipitate (personal communication with Anna Philpott, Cambridge University). These negative preliminary results therefore suggest p27^{Xic1} and X-NGNR-1 are unable to interact. If p27^{Xic1} and X-NGNR-1 do not interact directly, an alternative mechanism by which p27^{Xic1} could prevent X-NGNR-1 degradation is through sequestering Cyclin A2/ cdk2. Supporting this theory, over-expression of *Cyclin A2* or c*dk2* inhibited primary neurogenesis (Fig 4.15C and 4.15D). Surprisingly, injection of the *Cyclin A2* MO had no effect on primary neurogenesis (Fig 4.15B). We interpret this result as being likely to occur for the same reasons *p27^{Xic1}* over-expression did not yield a phenotype; i.e. lateral inhibition regulated by the Notch signalling pathway determines which cells possess X-NGNR-1 and therefore depletion of Cyclin A2 will only affect those cells already capable of expressing X-NGNR-1 and fated to form primary neurons. We have observed depleting *Cyclin A2* and over-expressing *Notch-ICD* cannot rescue the reduced primary neurogenesis phenotype of single injections of *Notch-*

ICD mRNA (Fig 4.15F), therefore Cyclin A2 acts downstream of the Notch signalling pathway in primary neurogenesis, that is after specification of the primary neuron precursors.

These results, although novel, have not indicated a major role for Cyclin A2 in primary neurogenesis. Evidence to suggest Cyclin A2 has only a minor role in primary neurogenesis is supported by our result showing depletion of Cyclin A2 had no effect on embryos also injected with the *p27^{Xic1}* MO, primary neurogenesis was still inhibited. If Cyclin A2 is a major regulator of X-NGNR-1 degradation then co-depletion of Cyclin A2 and p27^{Xic1}, which has already been shown to stabilise X-NGNR-1, should at least partially rescue the phenotype. In the epidermis, over-expressing Cyclin A2/ cdk2 increased proliferation and inhibited differentiation (Richard-Parpaillon et al., 2004). Thus over-expressing *Cyclin A2*/ *cdk2* in the neural plate could prevent differentiation of primary neurons indirectly by preventing cells entering a quiescent state, which is required for terminal differentiation. In conclusion we propose Cyclin A2/ cdk2 does not directly regulate differentiation in neural tissue and acts only to regulate the amount of division in the neural plate.

Injection of the *Cyclin A2* MO inhibited pronephrogenesis (Fig 4.14). The *Cyclin A2* MO clearly inhibited cell division (Fig 4.13) and therefore any pronephric phenotype may be a product of inhibited muscle development reducing a signal from the somites to the intermediate mesoderm initiating pronephrogenesis, as we observed when *p27^{Xic1}* was over-expressed (Chapter 3). This result highlights a repeating issue with observing organogenesis in model organisms. Frequently, effects on early development, in this case development of the mesoderm, have a

subsequent effect on later development. Experiments where mRNA translation is knocked down (*Xenopus* and zebrafish) or gene expression is unconditionally knocked out (mouse) are unsuitable for accurate interpretation without proper controls. In the study of pronephros development, reduction phenotypes must be interpreted with respect to any effect the injected message or MO has on myotome development. Conditional transgenics in *X. tropicalis*, or inducible constructs in *X. laevis* could overcome this issue and target ectopic gene expression in the pronephros at a certain time during development. However, conditional knock-down using MOs is not achievable currently, thus the use of MOs to observe pronephrogenesis should only be scrutinised if that MO has a minimal effect on both early mesoderm formation and myogenesis.

Chapter 5

A role for the “Wntch” signalling pathway in development of the proximal region of the *Xenopus laevis* pronephros

5.1 Introduction

The animal kingdom utilises a strikingly small number of signalling pathways to ensure appropriate development. These signalling pathways are conserved between and utilised by all species with differing degrees of complexity. One such example is the Notch signalling pathway, which is used during development to control cell fates, cell proliferation and cell death (for reviews see Lewis, 1998; Kadesch, 2004; Bray, 2006; Hayward et al, 2008).

During development the Notch signalling pathway is expressed in two phases in the pronephros (McLaughlin et al., 2000). Early phase expression of *Notch-1*, *Delta-1* and *Serrate-1* between stages 22 and 30 is restricted to the proximal dorsal portion of the pronephros anlagen, where the future glomus, nephrostomes and most dorsal proximal tubules will develop. A second, late phase of expression of *Notch-1* and *Serrate-1* is observed between stages 30 and 38. The domain of this late phase *Notch-1* and *Serrate-1* expression differs from early phase expression of *Notch-1* and

Serrate-1 as it occurs more ventrally across the entire proximal tubules, and seems necessary for the patterning of the tubules (Taelman et al., 2006).

This chapter concentrates on the effects early phase pronephric Notch signalling has on pronephrogenesis, which has previously been identified to be integral in establishing the proximal-distal axis of the pronephros (McLaughlin et al., 2000). Mis-activation of early phase Notch signalling induces ectopic glomus and proximal tubule development, at the expense of distal tubulogenesis. However suppression of Notch signalling inhibits proximal pronephrogenesis, and induces ectopic distal tubule formation (McLaughlin et al., 2000; Taelman et al., 2006). These results displayed a role for the Notch signalling pathway in development of the pronephros, but they did not propose a mechanism for how Notch signalling regulates pronephrogenesis.

Initially, we aimed to understand how Notch signalling regulates $p27^{Xic1}$ expression in the pronephros. Despite promising preliminary results, our findings were inconclusive as both mis-activation and suppression of Notch signalling inhibited $p27^{Xic1}$ expression in the somites and the pronephros (see appendix 5). However these experiments inadvertently produced novel phenotypes for the regulation of proximal pronephrogenesis by the Notch signalling pathway, results that refined the data in the literature. Thus we pursued this line of research, analysing how the Notch signalling pathway, and subsequently also the Wnt signalling pathway, regulate development of the proximal pronephros.

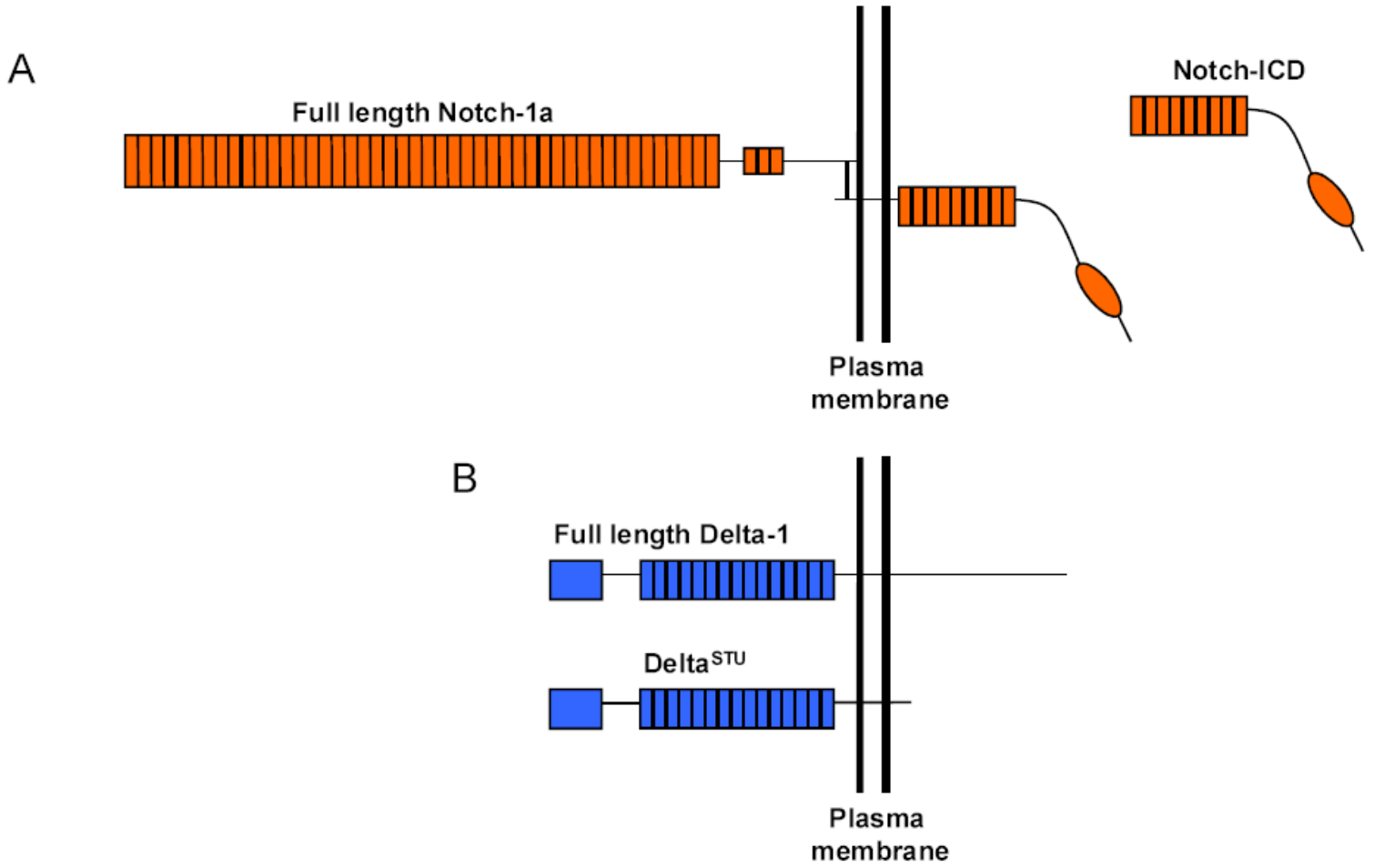

Figure 5.1 Schematic representation of the Notch and Delta constructs over-expressed in this study. Full length Notch-1a is 2524 amino acids in length. Notch-ICD, a truncated constitutively active form of the Notch receptor, consists of the final 774 amino acids of the intracellular domain of the full length Notch-1a protein (A). Full length Delta-1 is 721 amino acids long. Chitnis et al (1995) created a truncated dominant negative form of Delta-1, Delta^{STU}, which has its C-terminal 139 amino acids missing, thus its intracellular domain is omitted (B). * Note: this figure is not to scale.

To mis-activate the Notch signalling pathway we injected *Notch-ICD* mRNA, a truncated form of the Notch receptor that is constitutively active (Chitnis et al., 1995; Vernon et al., 2006). To suppress Notch signalling we injected mRNA encoding a dominant negative form of the Delta ligand, Delta^{STU} (Chitnis et al., 1995). Figure 5.1 illustrates the regions of Notch-1 and Delta-1 the Notch-ICD and Delta^{STU} constructs represent. Injection of *Notch-ICD* mRNA into the V2 blastomere ensures all cells within the pronephros anlagen potentially contain exogenous *Notch-ICD* mRNA. Consequently the Notch-ICD dependent pathway, where Notch-ICD binds to the CSL transcription complex and activates transcription of target genes, will be constitutively active across the entire pronephric anlagen. Delta^{STU} is a truncated Delta-1 construct that lacks the intracellular domain of this ligand. Accordingly, interaction with Notch receptors does not induce downstream signalling (Chitnis et al., 1995). In the nervous system Delta^{STU} acts as an anti-morph, perhaps by competing with endogenous Delta-1 for Notch receptors on neighbouring cells, preventing them receiving the signal.

Here we initially observed the effects of mis-activation and suppression of Notch signalling during pronephrogenesis, and refine the data in the literature to show early phase pronephric Notch/ Wnt-4 signalling promotes glomus and nephrostome formation. This refinement allowed us to propose a mechanism by which the Notch signalling pathway, together with the Wnt signalling pathway, sets up a boundary between the lateral and medial pronephric mesoderms that allows these two cell populations to diverge and develop independently. This is the first account of this mechanism operating in pronephric kidney formation.

5.2 Results

5.2.1 The Notch signalling pathway promotes formation of the nephrostomes and glomus

To observe pronephric phenotypes, approximately 600 pg *Notch-ICD* mRNA and 1 ng *Delta*^{STU} mRNA was injected into a ventro-vegetal (V2) blastomere of embryos at the 8-cell stage (see Chapter 3, Fig 3.1 for blastomere assignments), with 400 pg *βgal* mRNA to act as a lineage tracer. Embryos were cultured to various stages of development, fixed and stained for the lineage label. Correctly targeted embryos were selected and effects of *Notch-ICD* mRNA and *Delta*^{STU} mRNA injection on different markers of distinct regions of the pronephros was observed. All the phenotypes described in this section were statistical significant ($p<0.05$) and were repeated multiple times, yielding similar results (see Appendix 3).

Whole mount antibody staining with 3G8, which detects nephrostomes and proximal pronephric tubules, and 4A6, which detects intermediate and distal pronephric tubules (Vize et al., 1995), at stage 41 showed injecting *Notch-ICD* mRNA increased the size of the proximal region of the pronephros at the expense of the distal pronephric region. 76% of embryos had increased 3G8 staining, whilst 4A6 staining was reduced in 97% of embryos (n=34, Fig 5.2B). Injection of *Delta*^{STU} mRNA inhibited proximal pronephros formation but had no effect on distal pronephros development. 33% of embryos had reduced 3G8 staining, with only 5% having reduced 4A6 staining (n=36, Fig 5.2C). Injection of *βgal* mRNA alone had 0% effect on 3G8/ 4A6 staining (n=43, Fig 5.2A). As mis-activation of the Notch

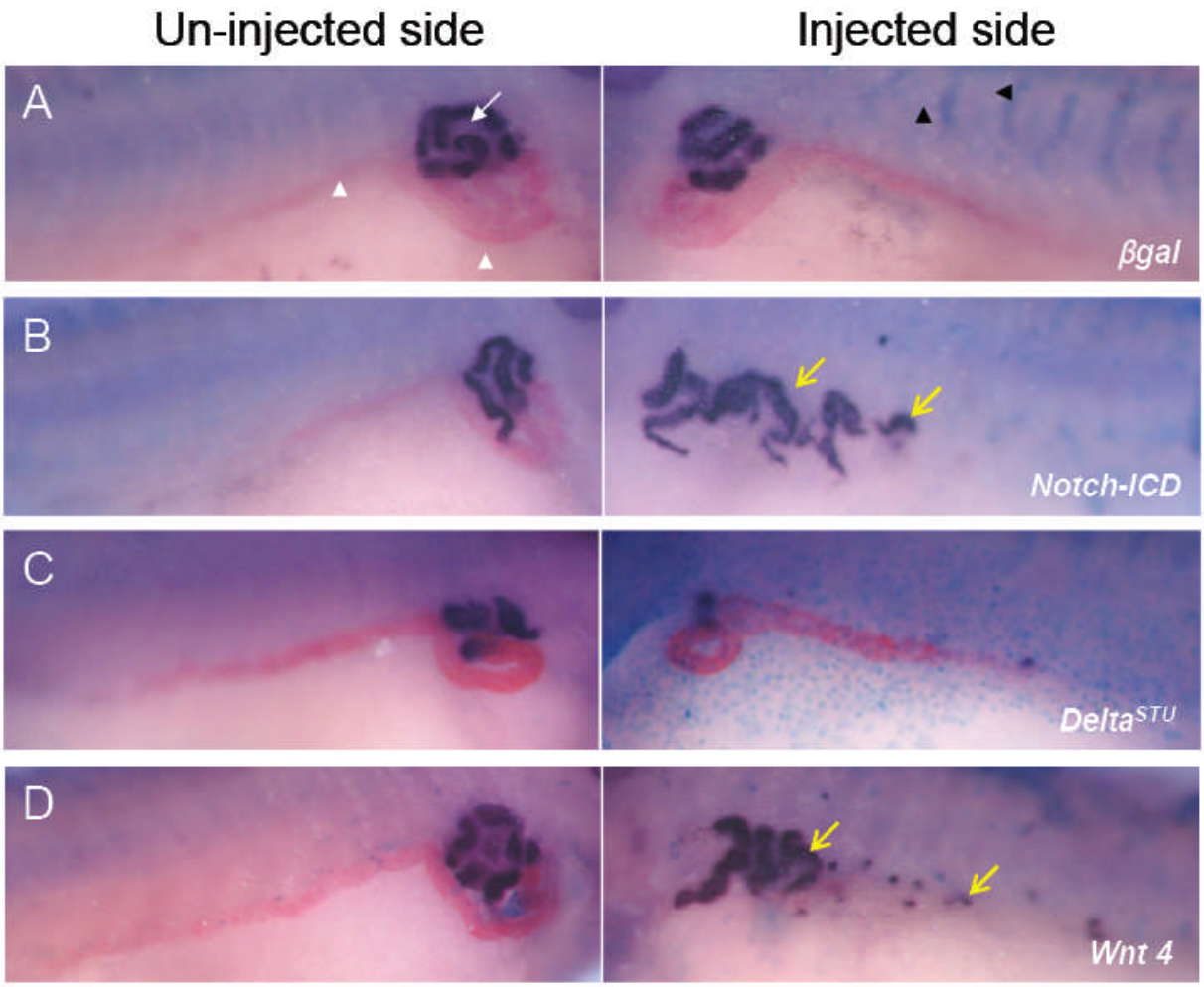

Figure 5.2 Mis-expression of the Notch and Wnt signalling pathways gives a pronephric phenotype. *X. laevis* embryos were injected at the 8 cell stage into a ventro-vegetal blastomere to target the presumptive pronephric region. mRNA was co-injected with *βgal* mRNA to act as a lineage tracer (blue staining, black arrowheads). Embryos were cultured till stage 41 and whole mount antibody stained with 3G8, to detect nephrostomes and proximal pronephric tubules (white arrow, stained purple), and 4A6, to detect intermediate and distal pronephric tubules (white arrowheads, stained red). Control *βgal* mRNA injected embryos had normal pronephros development (A). *Notch-ICD* mRNA injections induced ectopic 3G8 staining (yellow arrows), but inhibited distal tubule development on the injected side (B). *Delta*^{STU} *mRNA* reduced 3G8 staining, but had no effect on 4A6 staining (C). *Wnt 4* mRNA gave an identical phenotype to *Notch-ICD* mRNA, inducing ectopic 3G8 staining(yellow arrows) at the expense of 4A6 staining (D).

signalling pathway in the distal pronephric region promoted proximal pronephric cell fates at the expense of distal pronephric cell fates, early phase Notch signalling acts only to promote proximal pronephric cell fates.

To clarify these conclusions we repeated the injections of *Notch-ICD* mRNA and *Delta*^{STU} mRNA, cultured the embryos to stage 34 and performed *in situ* hybridisation for two markers of pronephric tubules; *Na*$^{+}$*K*$^{+}$ *ATPase*, an ion transporter expressed in the proximal, intermediate and distal tubules, and s*lc5a2*, a solute carrier expressed solely in the proximal tubules (Reggiani et al., 2007; Raciti et al., 2008). Injection of the *βgal* lineage tracer alone had a statistically insignificant effect on either marker ($p>0.05$). *Na*$^{+}$*K*$^{+}$ *ATPase* expression was reduced in 4% of embryos injected with *βgal* mRNA alone (n=24, Fig 5.3A). *slc5a2* expression was reduced in 3% of embryos injected with *βgal* mRNA alone (n=63, Fig 5.4A). Surprisingly, injection of *Notch-ICD* mRNA reduced *Na*$^{+}$*K*$^{+}$ *ATPase* expression in 96% of embryos (n=24, Fig 5.3B), and similarly reduced s*lc5a2* expression in 95% of embryos analysed (n=38 Fig 5.4B). Thus tubulogenesis was completely inhibited, a result not previously described since molecular markers to allow the distinction between different pronephric compartments were not utilised. Injection of *Delta*^{STU} mRNA inhibited s*lc5a2* expression in 76% of embryos (n=34, Fig 5.4C), but had a localised effect on *Na*$^{+}$*K*$^{+}$ *ATPase* expression. In 23% of embryos *Na*$^{+}$*K*$^{+}$ *ATPase* expression was completely reduced, however the most prominent phenotype, observed in 47% of embryos, was a reduction in only the proximal region of normal *Na*$^{+}$*K*$^{+}$ *ATPase* expression pattern (n=43, Fig 5.3C). Thus, like the result of

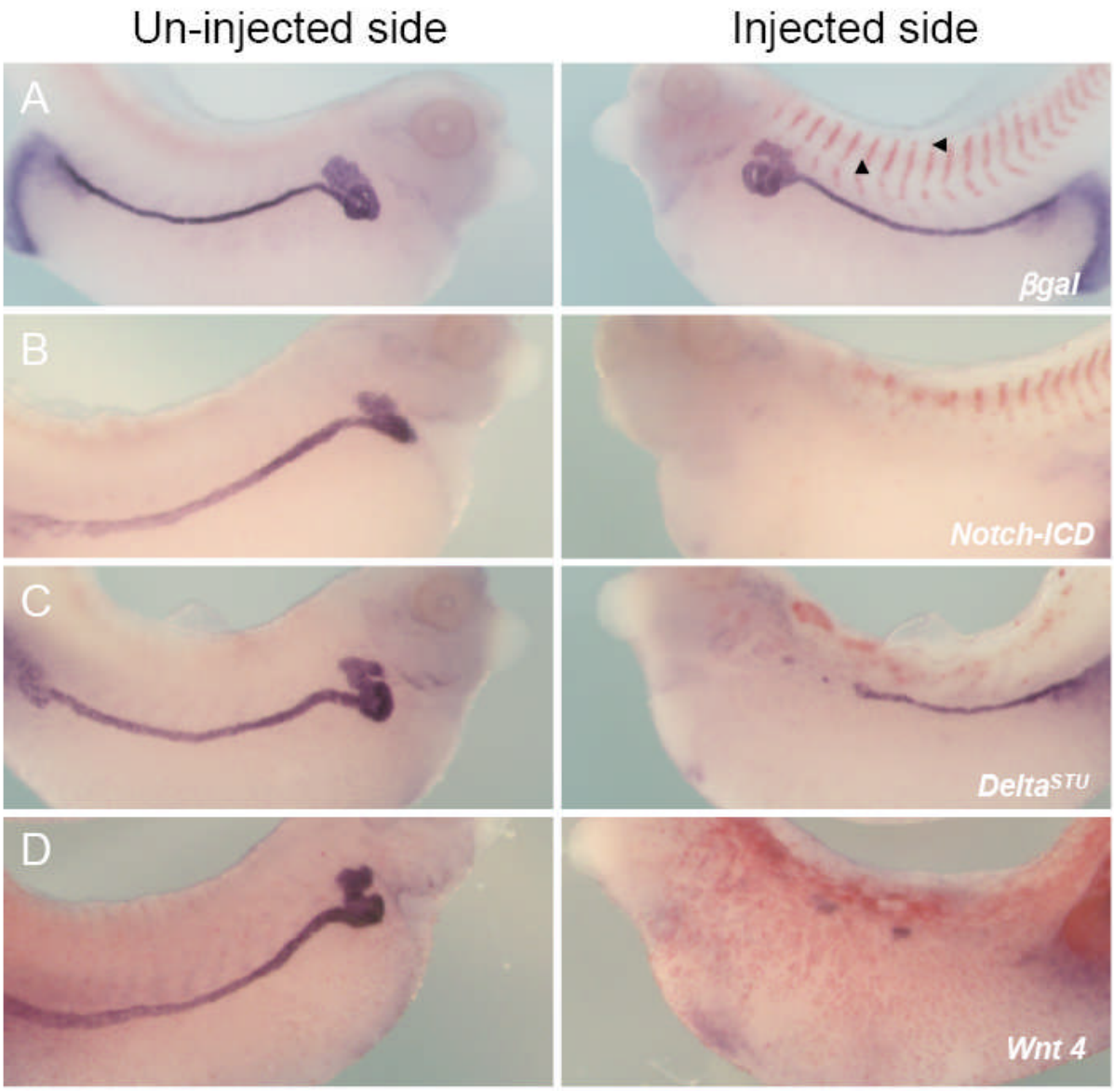

Figure 5.3 Mis-expression of the Notch and Wnt signalling pathways completely inhibits tubulogenesis. *X. laevis* embryos were injected at the 8 cell stage into a ventro-vegetal blastomere to target the presumptive pronephric region. mRNA was co-injected with *βgal* mRNA to act as a lineage tracer (red staining, black arrowheads). Embryos were cultured till stage 38 and then fixed. Whole mount *in situ* hybridisation was performed to detect expression of Na^+ K^+ *ATPase*, a marker of differentiated proximal, intermediate and distal tubules. Control *βgal* mRNA injected embryos had normal tubulogenesis (A). *Notch-ICD* mRNA injections completely inhibited tubulogenesis on the injected side (B). $Delta^{STU}$ *mRNA* reduced proximal tubulogenesis, but distal tubulogenesis persisted (C). *Wnt 4* mRNA gave an identical phenotype to *Notch-ICD* mRNA, completely inhibiting Na^+ K^+ *ATPase* expression on the injected side (D).

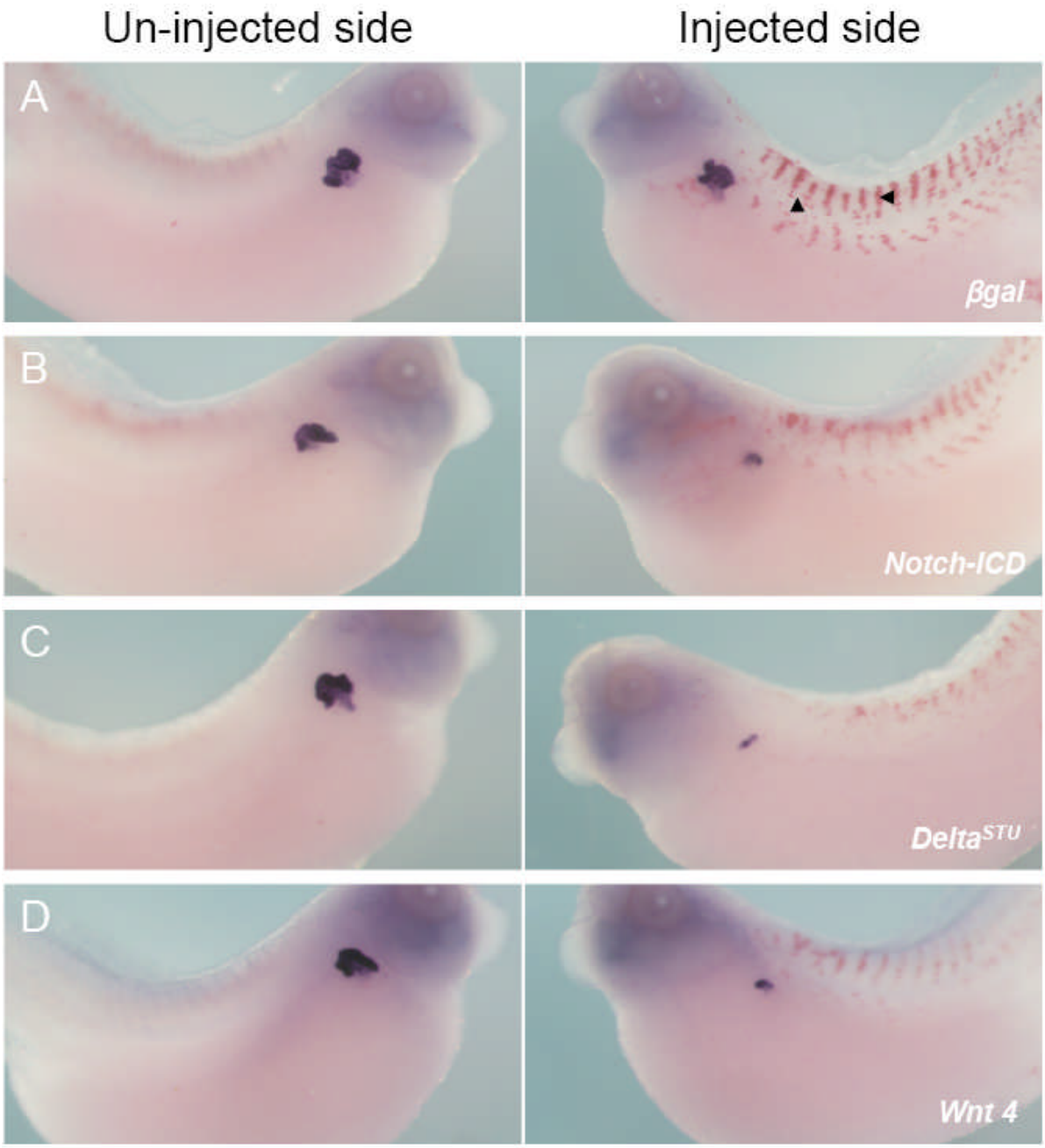

Figure 5.4 Mis-expression of the Notch and Wnt signalling pathways inhibits proximal tubulogenesis. *X. laevis* embryos were injected at the 8 cell stage into a ventro-vegetal blastomere to target the presumptive pronephric region. mRNA was co-injected with *βgal* mRNA to act as a lineage tracer (red staining, black arrowheads). Embryos were cultured till stage 38 and then fixed. Whole mount *in situ* hybridisation was performed to detect expression of s*lc5a2*, a marker of differentiated proximal tubules. Control *βgal* mRNA injected embryos had normal proximal tubulogenesis (A). *Notch-ICD* mRNA, *Delta*^{STU} *mRNA*, and *Wnt 4* mRNA gave identical phenotypes, inhibiting proximal tubulogenesis on the injected side (D).

the 3G8/ 4A6 antibody stain, Delta^{STU} disruption of pronephric development was predominantly in the proximal region.

In zebrafish the *odf3-like* gene, also known as *shippo1*, is expressed in a ‘salt and pepper’ pattern across the pronephric tubules. *odf3-like* is an axonemal structural protein that regulates cilia formation. Its expression pattern in zebrafish helped Liu et al (2007) conclude that the Notch signalling pathway regulates cell fate determination in the pronephros by the process of lateral inhibition. We performed a search for the *X. laevis* homolog of zebrafish *odf3-like* and identified the IMAGE clone 4682535 (GenBank accession number BC041210) that encodes *X. laevis odf3*. The spatial expression pattern of *odf3* was detected by *in situ* hydridisation and we showed it is expressed in ciliated cells in the epidermis and nephrostomes (see Fig 5.5A un-injected side), an expression pattern that is identical to other *X. laevis* markers of ciliated cells, such as *β4a-Tubulin* (Jones, 2005). This expression pattern underlines the likelihood that in *X. laevis*, lateral inhibition is not the process by which the Notch signalling pathway is patterning the developing pronephros as a ‘salt and pepper’ distribution of ciliated cells does not exist in the distal pronephric tubule as it does in zebrafish. Since injection of *Notch-ICD* mRNA inhibited proximal tubule formation, but induced ectopic 3G8 staining, we concluded this 3G8 staining must be completely nephrostomal. To test this hypothesis we injected *Notch-ICD* mRNA and *Delta^{STU}* mRNA as previously described, cultured the embryos to stage 34 and performed *in situ* hybridisation for *odf3* expression to observe the effects of these injections on nephrostome development. Controls injected with *βgal* mRNA caused 9% of embryos to have a reduced number of nephrostomes (n=53, Fig 5.5A). *Delta^{STU}* inhibited nephrostomal *odf3* expression in 89% of embryos (n=28,

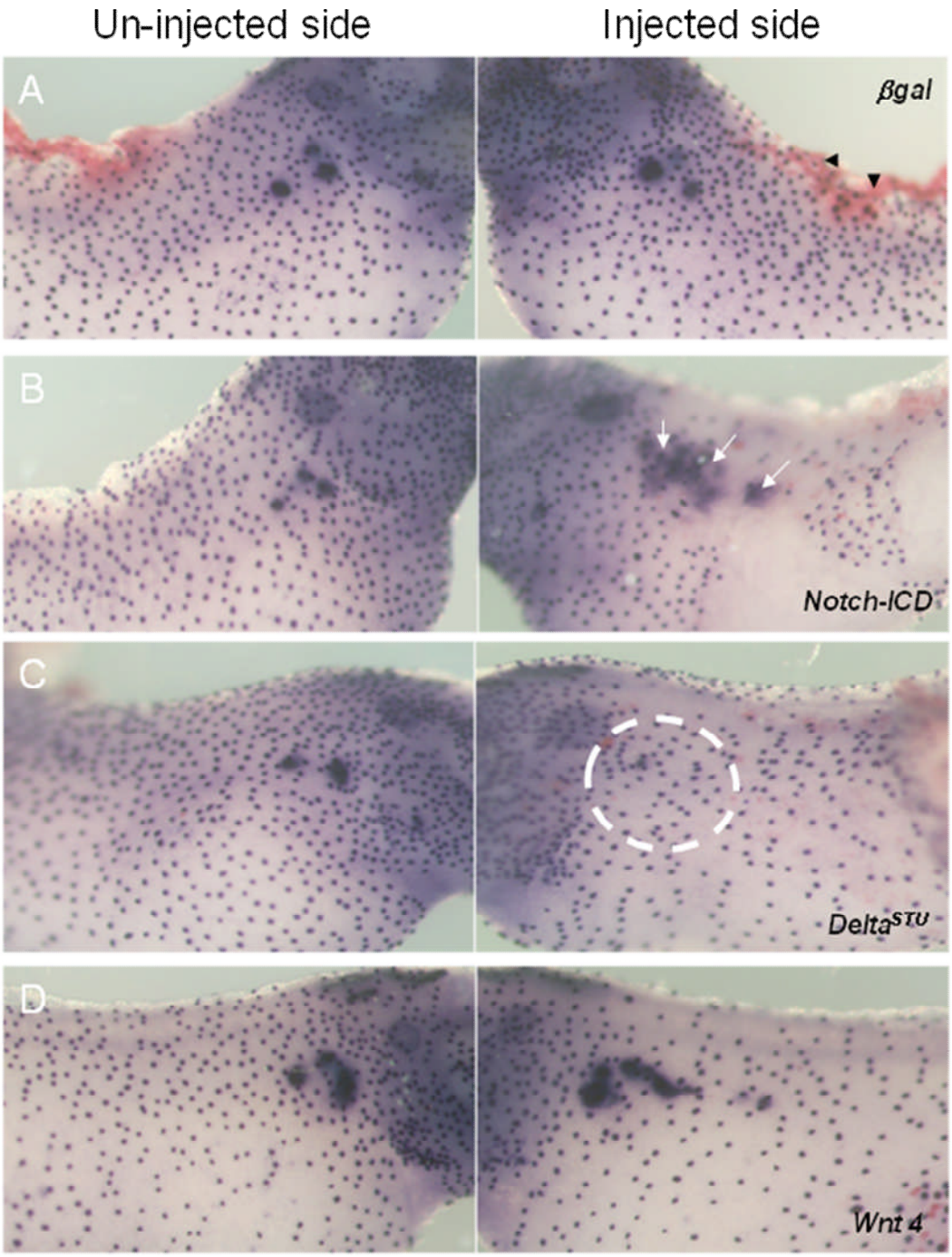

Figure 5.5 Mis-expression of the Notch and Wnt signalling pathways disrupts nephrostome development. *X. laevis* embryos were injected at the 8 cell stage into a ventro-vegetal blastomere to target the presumptive pronephric region. mRNA was co-injected with *βgal* mRNA to act as a lineage tracer (red staining, black arrowheads). Embryos were cultured till stage 38 and then fixed. Whole mount *in situ* hybridisation was performed to detect expression of *odf3*, a marker of differentiated nephrostomes. Control *βgal* mRNA injected embryos had normal nephrostome development (A). *Notch-ICD* mRNA injections induced ectopic nephrostome formation (B). *Delta*^{STU} *mRNA* inhibited nephrostome development (C). *Wnt 4* mRNA gave an identical phenotype to *Notch-ICD* mRNA, inducing ectopic nephrostome formation (D).

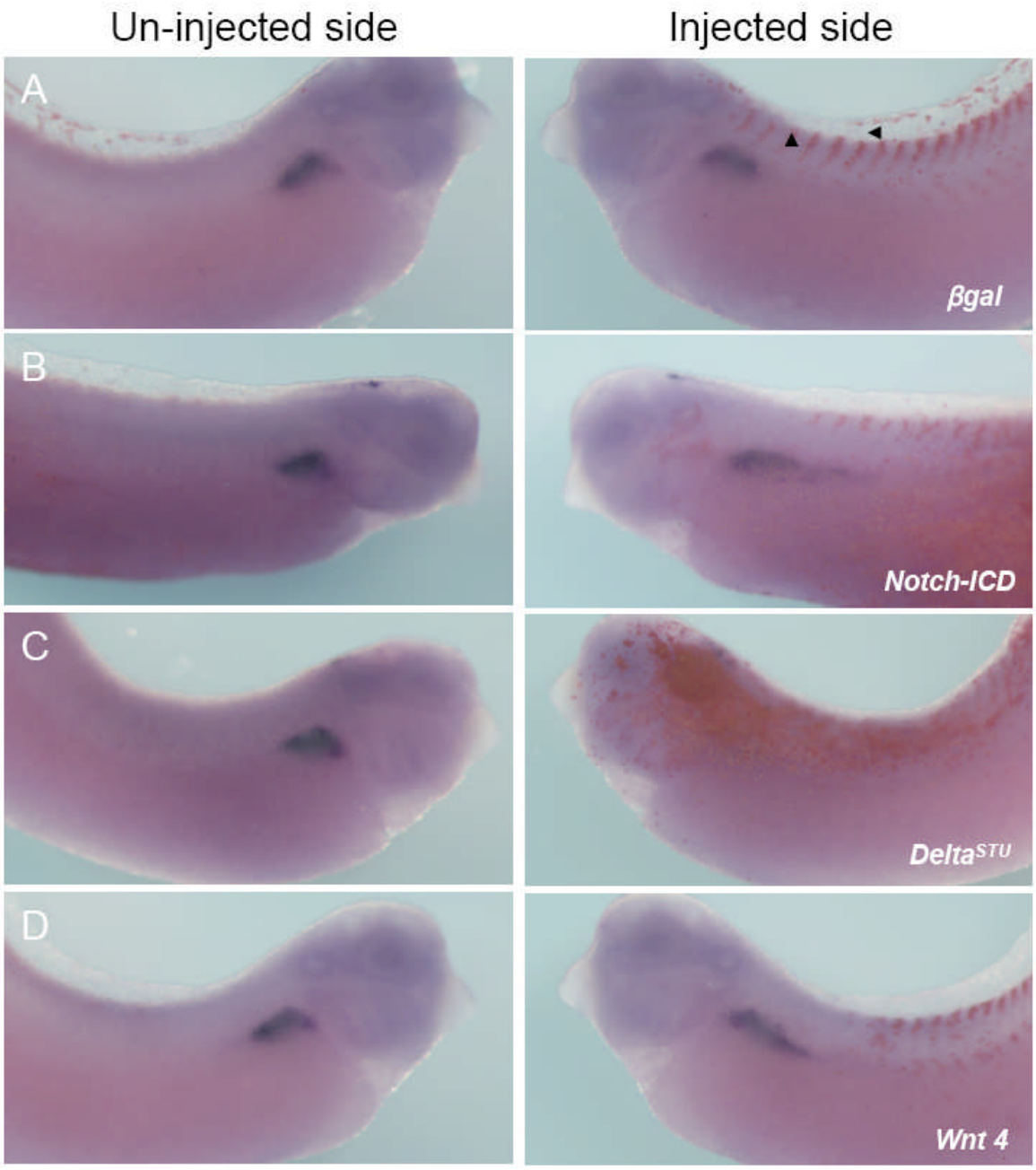

Figure 5.6 Mis-expression of the Notch and Wnt signalling pathways promotes glomus development. *X. laevis* embryos were injected at the 8 cell stage into a ventro-vegetal blastomere to target the presumptive pronephric region. mRNA was co-injected with *βgal* mRNA to act as a lineage tracer (red staining, black arrowheads). Embryos were cultured till stage 32 and then fixed. Whole mount *in situ* hybridisation was performed to detect expression of *Nephrin*, a marker of the glomus. Control *βgal* mRNA injected embryos had normal glomus development (A). *Notch-ICD* mRNA injections induced ectopic glomus formation on the injected side (B). *Delta*^{STU} *mRNA* inhibited glomus development (C). *Wnt 4* mRNA gave an identical phenotype to *Notch-ICD* mRNA, inducing larger glomus formation (D).

Fig 5.5C). However, and as expected, we observed ectopic nephrostomal *odf3* expression in 74% of embryos injected with *Notch-ICD* mRNA (n=27, Fig 5.5B). As the increase in *odf3* expression was equivalent to the increase in 3G8 staining we conclude ectopic 3G8 staining observed after *Notch-ICD* over-expression is completely nephrostomal. Increased nephrostomal formation at the expense of tubulogenesis has not previously been observed as markers such as 3G8, *Lim-1* and *Pax 2* were used (McLaughlin et al., 2000; Rones et al., 2002), all of which do not distinguish between nephrostomes and proximal tubules.

McLaughlin et al (2000) and Taelman et al (2006) both showed mis-activation of the Notch signalling pathway induced larger glomus formation, a result we have repeated; 81% of embryos injected with *Notch-ICD* mRNA had increased staining of the glomus marker *nephrin*, as observed by *in situ* hybridisation (n=27, Fig 5.6B). *Delta*^{STU} inhibited *nephrin* expression in 88% of embryos (n=34, Fig 5.6C). Controls injected with *βgal* mRNA alone had 0% effect on glomus formation (n=45, Fig 5.6A). In conclusion early phase Notch signalling in the proximal dorsal region of the pronephros anlagen inhibited tubulogenesis and promoted glomus and nephrostome formation.

5.2.2 The Wnt signalling pathway also promotes formation of the nephrostomes and glomus

During development the Notch signalling frequently, if not always, requires the Wnt signalling pathway to promote specific cell fates (Hayward et al., 2008). The Wnt gene *Wnt-4* is expressed in the proximal tubules and nephrostomes during the stages of development where the Notch signalling pathway is inducing nephrostome

and glomus cell fate decisions (Saulnier et al., 2002). We hypothesised these two pathways could be integrated and thus aid cell fate decisions in the proximal dorsal region of the pronephros anlagen.

In order to investigate this possibility, *Wnt-4* mRNA was injected into a ventro-vegetal blastomere of embryos at the 8-cell stage. *βgal* mRNA was co-injected to act as a lineage tracer. These embryos were then cultured to various stages of development to determine the effect of *Wnt-4* over-expression on different markers of distinct regions of the pronephros.

Wnt-4 mRNA induced ectopic 3G8 staining in 69% of embryos, with 4A6 staining reduced in 77% of embryos (n=26, Fig 5.2D). Expression of the tubule markers *Na^+K^+ ATPase* and *slc5a2* was reduced in 83% (n=23, Fig 5.3D) and 92% (n=36, Fig 5.4D) of embryos, respectively. *Wnt-4* mRNA induced ectopic nephrostomal *odf3* expression in 76% of embryos (n=34, Fig 5.5D) and increased the domain of *nephrin* expression in 75% of embryos (n=32, Fig 5.6D). All control *βgal* mRNA injected embryos had no statistically significant effects on pronephros development ($p>0.05$). In conclusion *Wnt-4* over-expression induced ectopic nephrostome and glomus formation at the expense of tubules, an identical phenotype to *Notch-ICD* over-expression. Thus it is possible these two signalling pathways are integrated in this region of the pronephros anlagen in order to direct nephrostome and glomus cell fate decisions.

5.2.3 Mis-activation of Notch signalling induced *Wnt-4* expression

We next aimed to see if *Notch-ICD* mRNA and *Delta*^{STU} mRNA targeted to the developing pronephros affected *Wnt-4* expression, in order to understand if there was positive or negative regulation of gene expression by either pathway upon the other. To observe this we targeted injections of *Notch-ICD* mRNA and *Delta*^{STU} mRNA to the future pronephros, as previously described, and cultured the embryos to stage 28, where they were fixed and stained for the lineage label. Correctly targeted embryos were selected and *in situ* hybridisation detecting expression of *Wnt-4* was performed. Injection of *βgal* mRNA alone caused a statistically insignificant 4% reduction in *Wnt-4* expression on the injected side when compared to the un-injected side ($p>0.05$, n=25). 47% of *Notch-ICD* mRNA injected embryos had ectopic *Wnt-4* expression (n=32). This increased *Wnt-4* expression was indicative of ectopic 3G8 staining or ectopic *odf3* and *nephrin* expression discussed earlier. The domain of *Wnt-4* expression increased distally, and looked tubular in appearance (Fig 5.7A). Injection of *Delta*^{STU} mRNA inhibited *Wnt-4* expression on the injected side in 78% of embryos, and in these affected embryos 94% had completely absent *Wnt-4* expression on the injected side highlighting the severity of the phenotype (n=23, Fig 5.7B). In conclusion, activation of the *Notch-ICD* dependent pathway induced *Wnt-4* expression. Conversely suppression of Notch signalling inhibited *Wnt-4* expression.

5.2.4 Over-expression of *Wnt-4* had no obvious effect on *Delta-1* or *Serrate-1* expression

Wnt-4 expression is induced by *Notch-ICD* mRNA injection, thus we wanted to observe if pronephric *Wnt-4* over-expression could induce expression of components of the Notch signalling pathway. We injected *Wnt-4* mRNA into

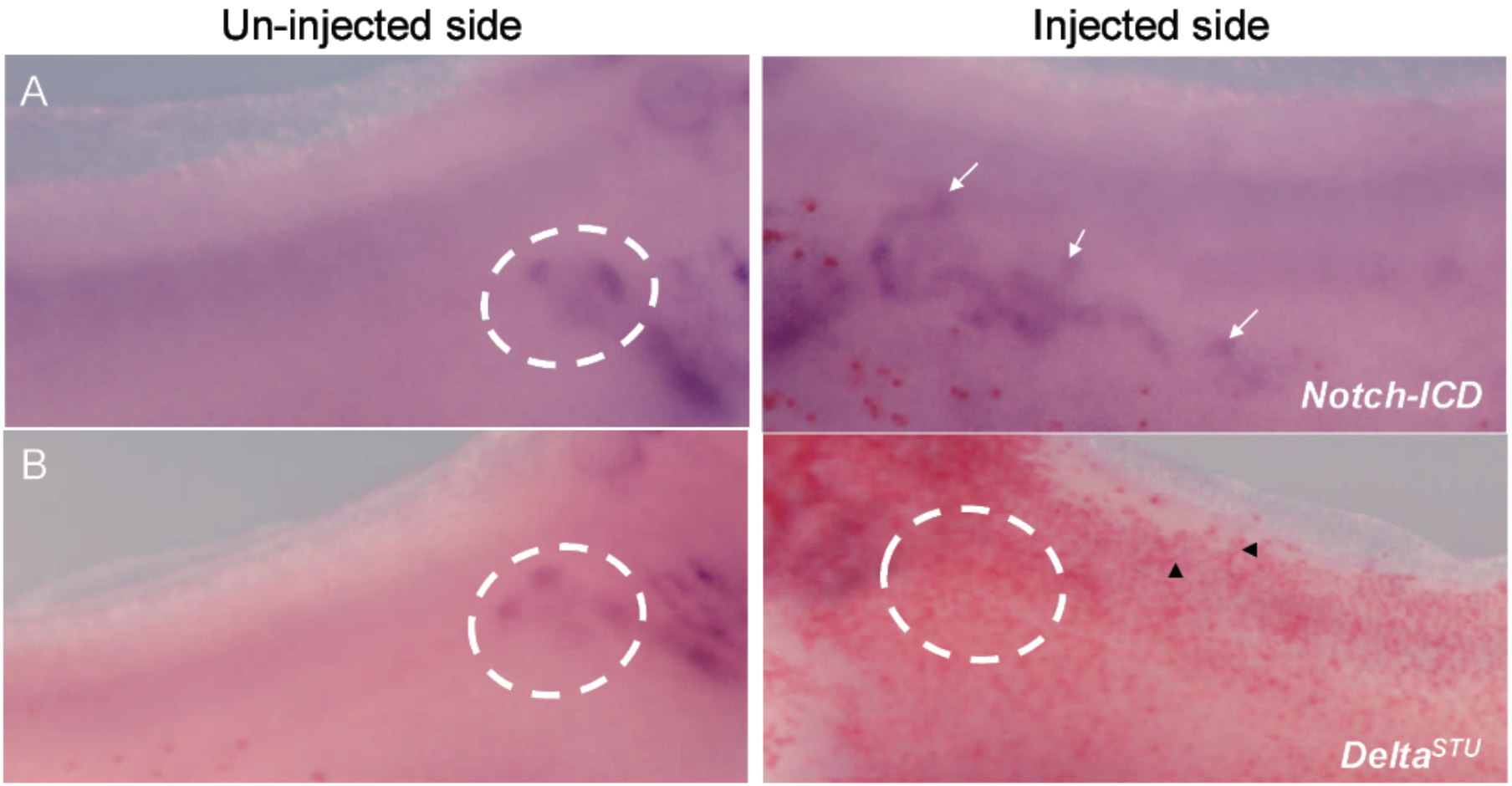

Figure 5.7 Mis-expression of the Notch signalling pathways alters pronephric Wnt signalling. *X. laevis* embryos were injected with *Notch-ICD* and *Delta*^{STU} mRNA at the 8 cell stage into a ventro-vegetal blastomere to target the presumptive pronephric region. Samples were co-injected with *βgal* mRNA to act as a lineage tracer (red staining, black arrowheads). Embryos were cultured till stage 28, fixed and whole mount *in situ* hybridised to detect *Wnt 4* expression. *Notch-ICD* mRNA injections induced ectopic pronephric *Wnt 4* expression on the injected side (A). *Delta*^{STU} mRNA inhibited pronephric *Wnt 4* expression (B).

a ventro-vegetal blastomere of embryos at the 8-cell stage, with *βgal* mRNA to act as a lineage tracer. Embryos were cultured to stage 28, fixed and stained for the lineage label, and correctly targeted embryos were selected and tested for expression of *Delta-1* and *Serrate-1* by *in situ* hybridisation.

Wnt-4 over-expression did not have a dramatic effect on *Delta-1* and *Serrate-1* expression levels, relative to the effect *Notch-ICD* mRNA had on *Wnt-4* expression. *Delta-1* expression was reduced in only 6% of embryos (n=32, Fig 5.8B), likewise *Serrate-1* expression was reduced in 14% of embryos (n=36, Fig 5.9B). However we did observe a change in both *Delta-1* and *Serrate-1* expression. 84% of *Delta-1 in situ* hybridised embryos and 61% of *Serrate-1 in situ* hybridised embryos had disorganised gene expression. Frequently expression would be more distal (see Fig 5.8B and Fig 5.9B, marked with asterix), and would not resemble *Delta-1* or *Serrate-1* expression on the un-injected side. Sometimes there would be scattered expression on the injected side, which could be described as ectopic expression (see white arrows on Fig 5.8B). This infrequent ectopic expression was never of the magnitude of *Wnt-4* ectopic expression observed after *Notch-ICD* mRNA. In conclusion *Wnt-4* over-expression disrupted expression of *Delta-1* and *Serrate-1*, but did not seemingly inhibit or induce expression of these genes.

5.2.5 *Notch-ICD* and *Wnt-4* over-expression inhibits formation of the lateral pronephric mesoderm

Wnt-4 and *Notch-ICD* over-expression caused gross pronephric phenotypes, increasing the size of the glomus and nephrostomes at the expense of the tubules. As

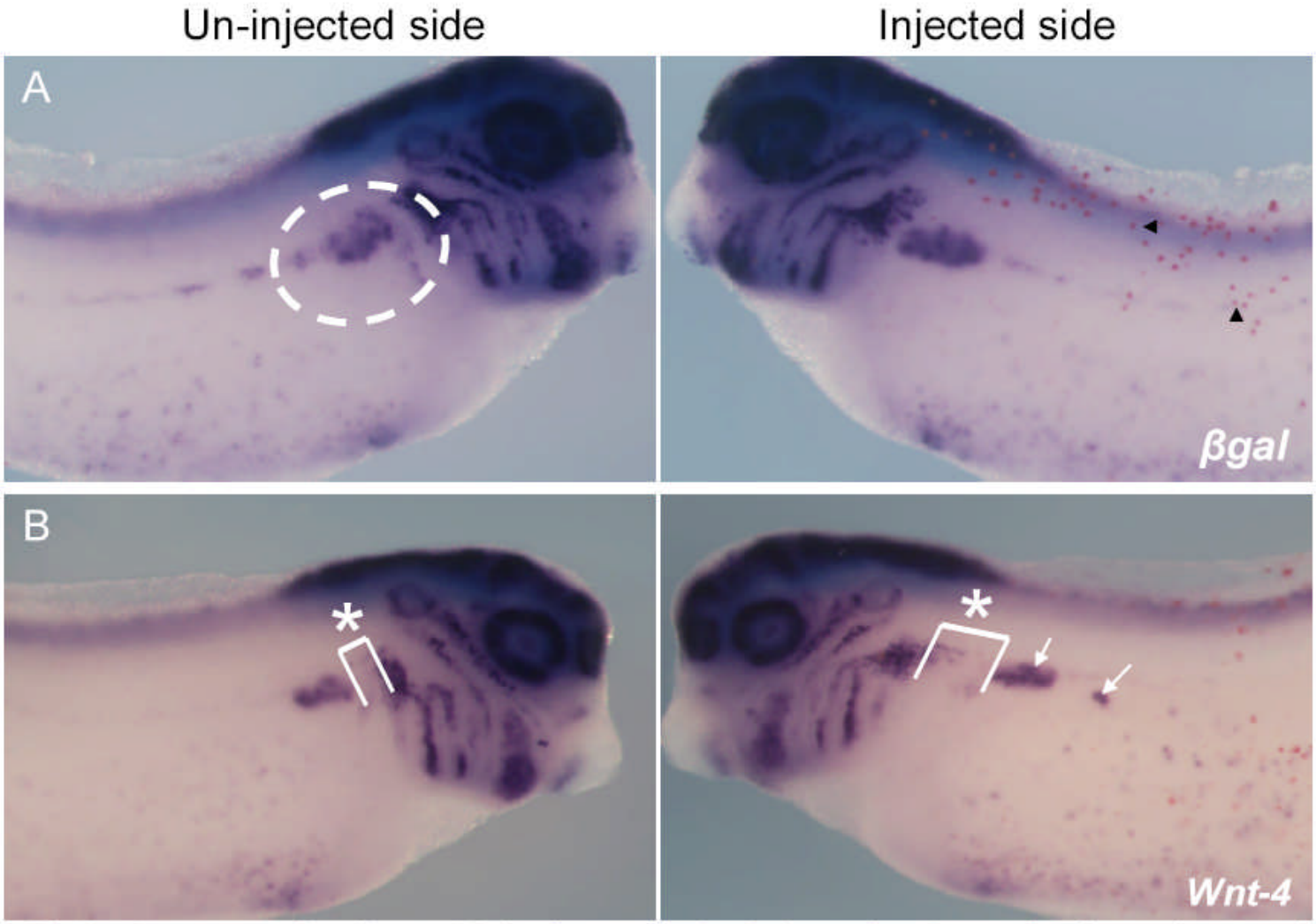

Figure 5.8 *Wnt-4* over-expression disrupted *Delta-1* expression but had no major phenotypic effects on its expression. *X. laevis* embryos were injected with *Wnt-4* mRNA at the 8 cell stage into a ventro-vegetal blastomere to target the presumptive pronephric region. Samples were co-injected with *βgal* mRNA to act as a lineage tracer (red staining, black arrowheads). Embryos were cultured till stage 28, fixed and whole mount *in situ* hybridised to detect *Delta-1* expression. *βgal* mRNA injections had no effect on *Delta-1* expression on the injected side (A). *Wnt-4* mRNA disrupted the expression pattern, but not the level of *Delta-1* (white arrows), frequently its expression was more distal (B). * Highlights the expression of *Delta-1* is more distal on the injected side when compared to the un-injected side.

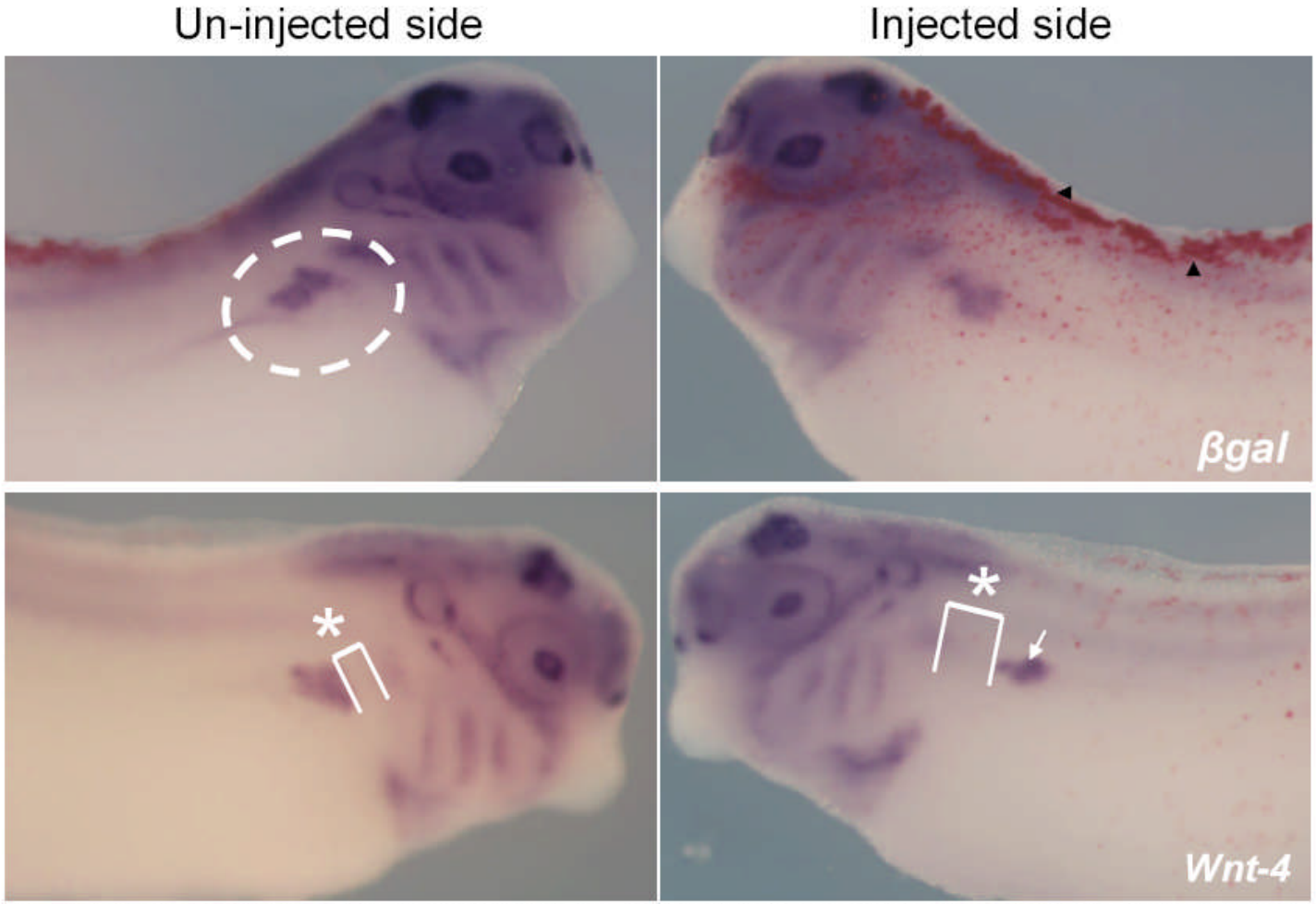

Figure 5.9 *Wnt-4* over-expression disrupted *Serrate-1* expression but had no major phenotypic effects on its expression. *X. laevis* embryos were injected with *Wnt-4* mRNA at the 8 cell stage into a ventro-vegetal blastomere to target the presumptive pronephric region. Samples were co-injected with *βgal* mRNA to act as a lineage tracer (red staining, black arrowheads). Embryos were cultured till stage 28, fixed and whole mount *in situ* hybridised to detect *Serrate-1* expression. *βgal* mRNA injections had no effect on *Serrate-1* expression on the injected side (A). *Wnt-4* mRNA disrupted *Serrate-1* expression (white arrow), as with the effect on *Delta-1* expression, frequently its expression was more distal (B). * Note the increase in distance of *Serrate-1* expression from the head region on the injected side compared to the un-injected side.

the pronephros anlagen is a three dimensional structure, we aimed to observe the effect these injections had on the layout of the pronephros in section.

Embryos injected with *Wnt-4* mRNA and *Notch-ICD* mRNA targeted to future pronephros, and stained for *nephrin* expression by *in situ* hybridisation at stage 32, were sectioned using a razor blade (Fig 5.10). A clear phenotype was observed in these sectioned embryos. The medial pronephric mesoderm, the region of the pronephros anlagen where the glomus develops, extended into the lateral pronephric mesoderm after both *Wnt-4* mRNA (Fig 5.10A) and *Notch-ICD* mRNA (Fig 5.10B) injection. The only marker of the lateral pronephric mesoderm whose expression is increased after over-expression of *Wnt-4* and *Notch-ICD* is *odf-3*, a marker of the nephrostomes. Despite their position in the lateral pronephric mesoderm, nephrostomes are induced to form by a signal originating from the medial pronephric mesoderm (Howland, 1916). Thus it is perhaps unsurprising ectopic glomus formation is accompanied with ectopic nephrostome formation. In conclusion we suggest the lateral pronephric mesoderm does not form correctly in embryos over-expressing *Notch-ICD* and *Wnt-4*, and the entire anlagen switches to medial pronephric mesoderm.

To further investigate these findings we performed wax sectioning on *Notch-ICD* mRNA injected embryos. Embryos were co-injected with *GFP* mRNA and sorted into left and right injected sides at stage 26 (Fig 5.11A). Embryos were left to develop to stage 41, when they were fixed and wax embedded. 12 μm wax sections were then cut and analysed histologically by staining with haematoxylin and eosin to mark cell nuclei and cytoplasms. Strong phenotypes were again observed

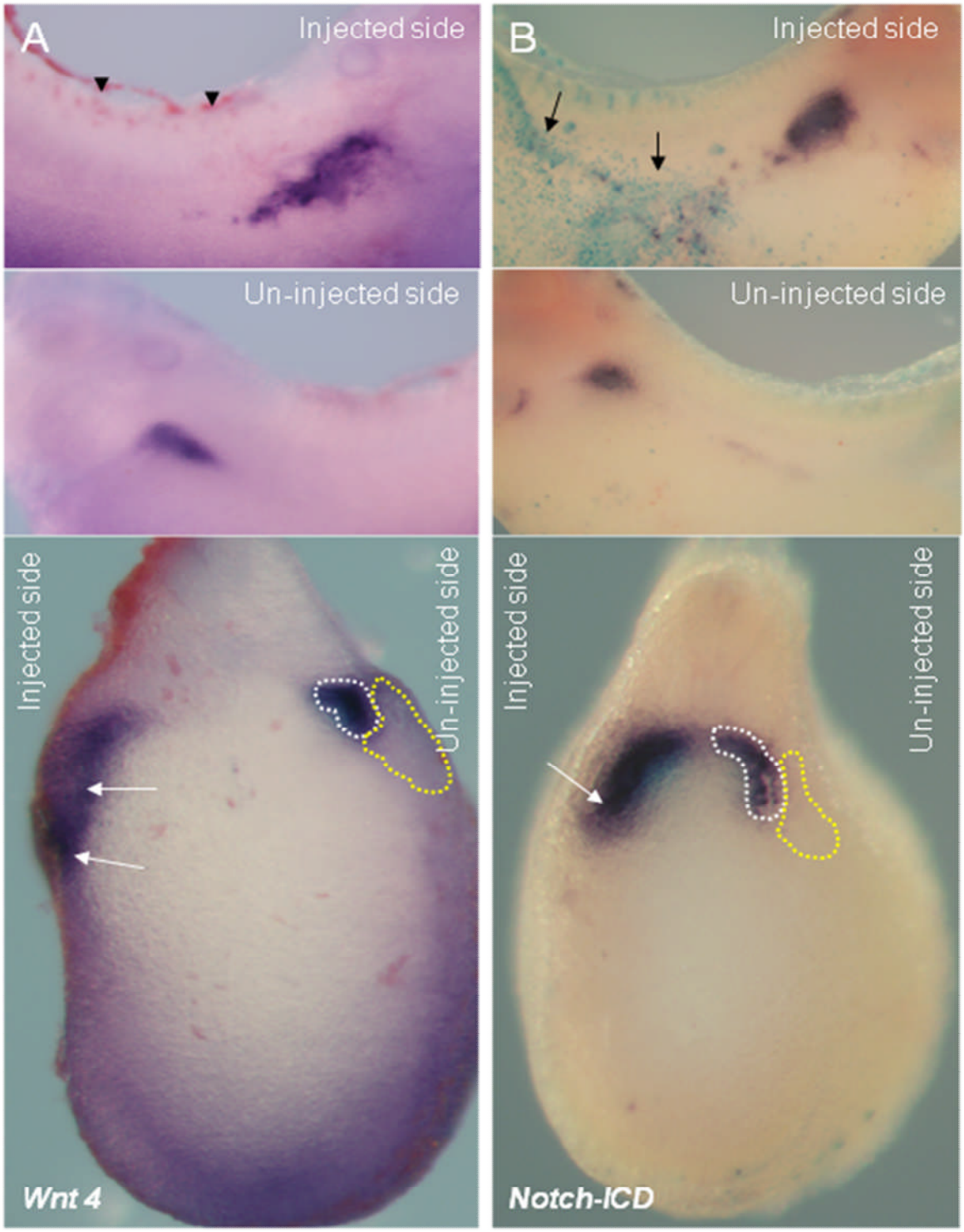
A
Injected side
Un-injected side
Injected side
Un-injected side
Wnt 4
B
Injected side
Un-injected side
Injected side
Un-injected side
Notch-ICD

Figure 5.10 Sectioning of embryos injected with *Wnt-4* mRNA and *Notch-ICD* mRNA suggests the lateral and medial mesoderms do not form in separation. Embryos were injected into a ventro-vegetal blastomere with *Wnt-4* mRNA and *Notch-ICD* mRNA at the 8-cell stage with *βgal* mRNA to act as a lineage tracer. Embryos were left to develop to stage 32, when they stained for the lineage tracer and fixed. *In situ* hybridisation for *nephrin* expression was then performed to observe the size of the glomus. *Wnt-4* mRNA injected embryos had, as previously observed, an enlarged glomus on the injected side. Upon sectioning these embryos using a razor blade it was discovered that the expression of *nephrin* extended into the lateral mesoderm on the injected side (white arrows). The un-injected side of these embryos has been annotated to show the normal positioning of the lateral and medial pronephric mesoderms (dashed white lines indicate the medial pronephric mesoderm where the glomus develops, and the yellow dashed lines highlight the lateral pronephric mesoderm where the nephrostomes and proximal tubules develop). Clearly the injected side has abnormal allocation of distinct pronephric regions (A). *Notch-ICD* mRNA injection induces the same phenotype observed with *Wnt-4* mRNA injection, the medial pronephric mesoderm has extended into the lateral pronephric mesoderm (B). Note the lineage label is stained red for the Wnt-4 injection (marked with black arrowheads on the injected side) but for the Notch-ICD injection the lineage label is stained blue (marked with black arrows on the injected side).

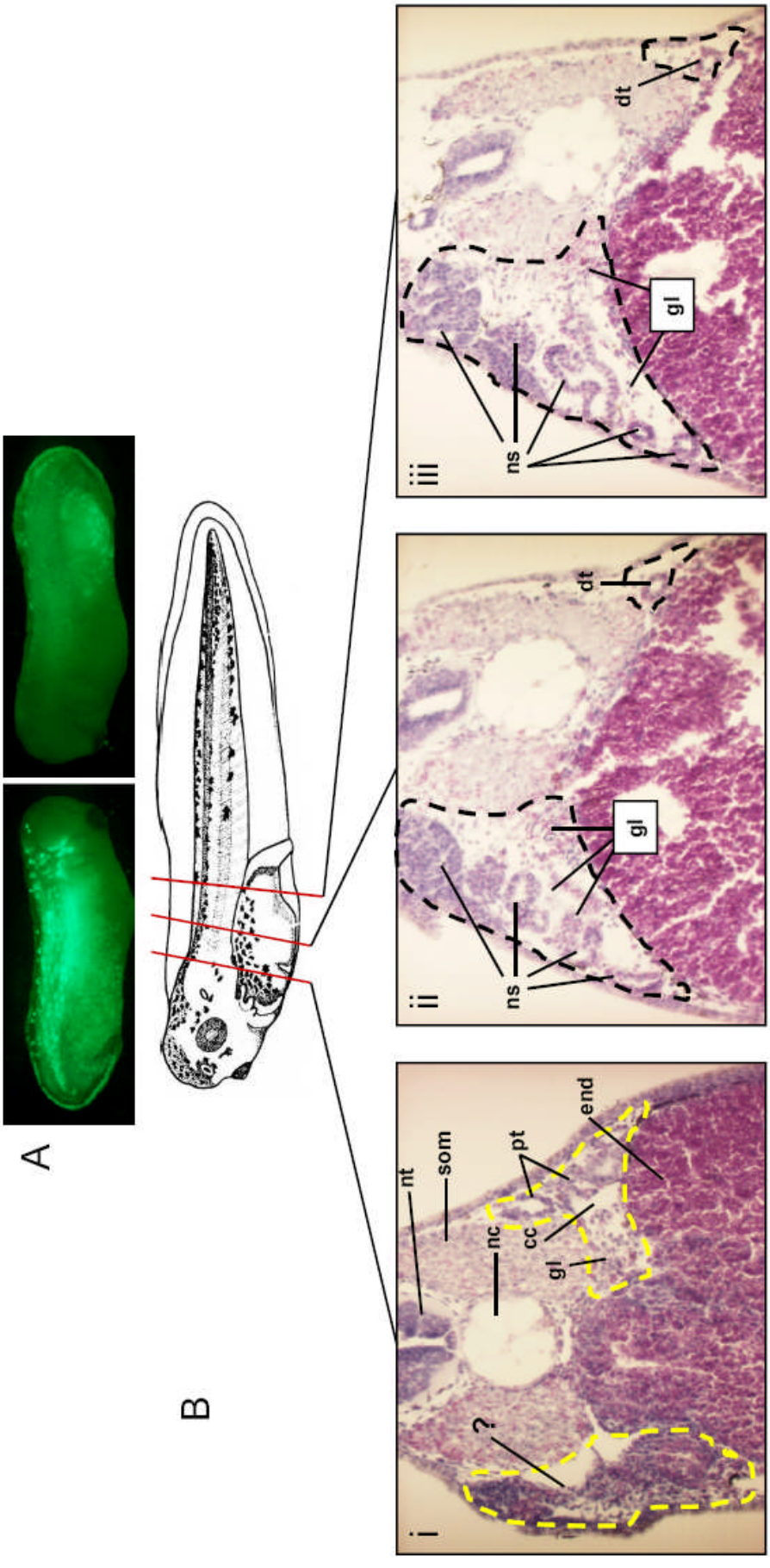
A
B
i
ii
iii
nt
som
nc
cc
pt
gl
end
?
ns
gl
dt
ns
gl
dt

Figure 5.11 Sectioning of *Notch-ICD* mRNA injected embryos. Embryos were injected with *Notch-ICD* mRNA into a ventro-vegetal blastomere at the 8-cell stage with GFP mRNA to act as a lineage tracer. They were left to develop to stage 26 where they were sorted for pronephric expression of GFP under a fluorescent microscope. Correctly targeted embryos were split into left and right injected sides and cultured to stage 41 when they were fixed in Bouin's fixative, embedded in wax and finally sectioned at 12 µm intervals. To help understand the histology of the sections haematoxylin and eosin staining was performed on the sectioned material to identify the nuclei and cytoplasm of the sectioned cells. GFP targeting to the pronephric anlagen is shown in (A). Histological analysis of *Notch-ICD* mRNA injected embryos illustrates massive alterations in pronephric structure on the injected side (left in each image) (B). The proximal pronephros on the injected side resembles a mass of un-patterned and morphologically non-distinct cells which we cannot distinguish as any particular cell type (Bi). More distally in the region of the distal tubulogenesis (see un-injected side), there is ectopic tubulogenesis on the injected side, which appears to form more dorsally than in wild-type embryos. From whole-mount *in situ* hybridisation (see Fig 5.5) these tubules are nephrostomal. The glomus and tubules are not correctly localised and the pronephric landscape is wholly abnormal (Bii). Extending more distally the pronephros on the injected side is similar to Bii, highlighting the extent to which the phenotype extends into the distal region of the pronephros (Biii). (nc= notochord, nt= neural tube, som= somites, gl = glomus, cc= coelomic cavity, pt= proximal tubules, end= endoderm, ns= nephrostomes, dt= distal tubules).

after *Notch-ICD* mRNA injection (Fig 5.11B). In the proximal pronephric region a mass of unidentifiable and non-distinct cells can be observed forming not only in the pronephric region but more dorsally around the somites. We cannot identify these cells although there could be some tubulogenesis and podocytes occurring within this cell mass (Fig 5.11Bi). In these sections, normal pronephric development of the proximal region can be clearly seen on the un-injected side. The glomus, indicated by dispersed podocytes, the coelomic cavity, and the proximal tubules have all formed in their correct positions.

In the distal pronephric region, sections exhibit the phenotypes we expected from *in situ* hybridisation analysis of *Notch-ICD* mRNA injected embryos already described (Section 5.2.2). There is ectopic glomus and tubule formation (Fig 5.11Bii), with the latter previously identified as nephrostomal tubules (Fig 5.5B). The glomus is dispersed throughout the region where the abnormal pronephros is developing and nephrostomal tubules are forming in dorsal regions around the somites. There are numerous cavities in these sections; it is possible these cavities formed as a consequence of abnormal pronephric development, or as a result of separation of ectopic nephrostomes from ectopic glomus, a process that occurs in normal pronephrogenesis. We observed these same phenotypes upon observation of sections at more distal points along the pronephros anlagen (Fig 5.11Biii), thus highlighting the extent to which the mature pronephros is altered upon injection of *Notch-ICD* mRNA.

5.2.6 Over-expression of *Delta-1* induces ectopic medial pronephrogenesis

As Notch-mediated boundaries are established as a consequence of differential Notch-ligand interactions, we wanted to observe if over-expression of *Delta-1* and *Serrate-1* produced pronephric phenotypes. We injected 1 ng of *Delta-1* or *Serrate-1* mRNA, with *βgal* mRNA to act as a lineage tracer, into a ventro-vegetal blastomere to target the presumptive pronephros. Embryos were left to develop to stage 28, where *in situ* hybridisation for expression of a medial pronephric mesoderm (*nephrin*) and lateral pronephric mesoderm (*slc5a2*) marker was detected. Surprisingly, injection of *Serrate-1* mRNA repeatedly induced no pronephric phenotype (images of injected embryos not shown, see appendix 3 for empirical data), even after injection of larger amounts of mRNA (up to 6 ng). Thus Serrate-1 is seemingly not involved in pronephrogenesis. Over-expression of *Delta-1* did produce a pronephric phenotype, inducing ectopic *nephrin* expression in 61% of embryos (Fig 5.12A, n=28) and inhibiting *slc5a2* expression in 86% of embryos (Fig 5.12B, n=29). This phenotype is identical to the effect *Notch-ICD* over-expression had on pronephrogenesis.

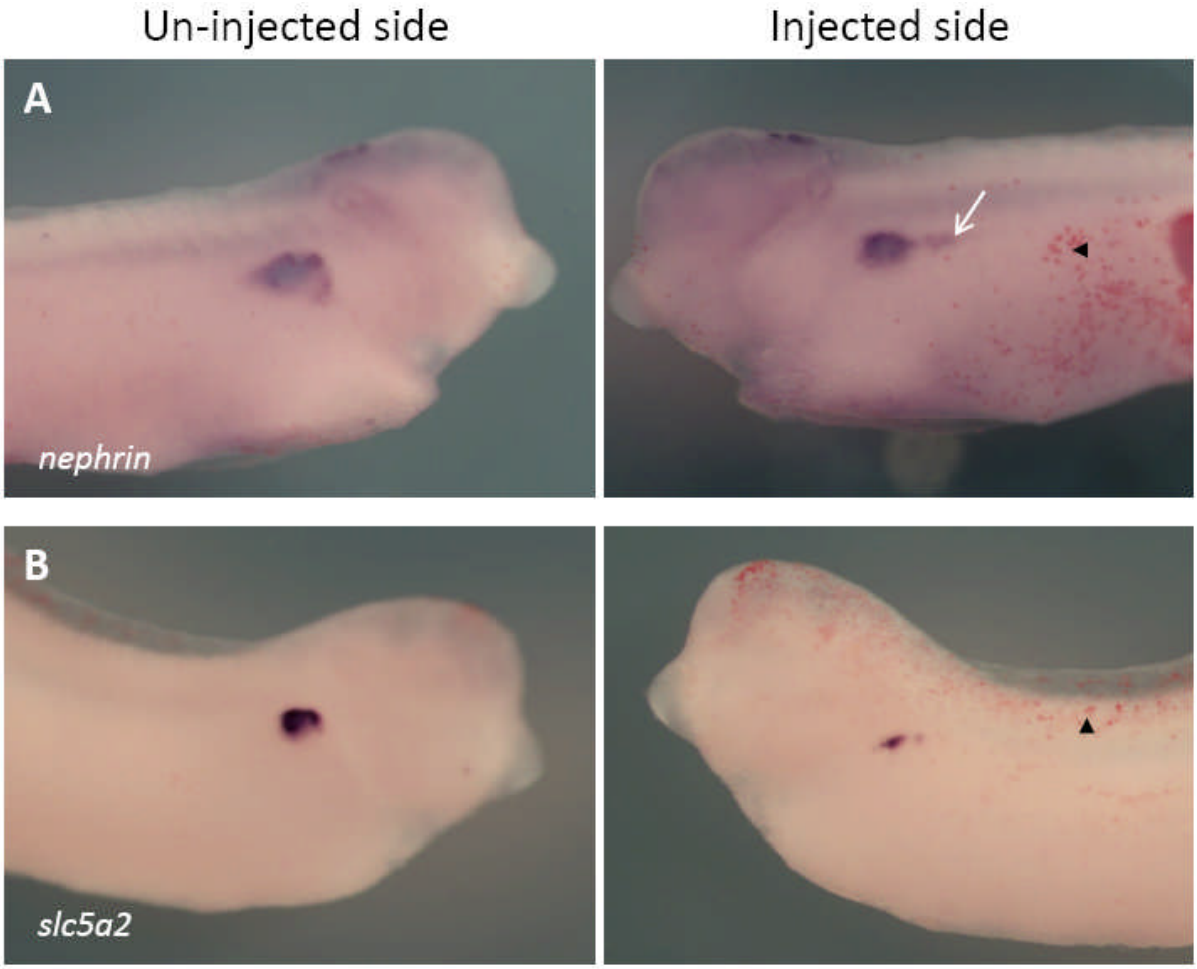

Figure 5.12 *Delta-1* over-expression yields the same effects on pronephrogenesis as *Notch-ICD* over-expression. *X. laevis* embryos were injected with *Delta-1* mRNA at the 8 cell stage into a ventro-vegetal blastomere to target the presumptive pronephric region. Samples were co-injected with *βgal* mRNA to act as a lineage tracer (red staining, black arrowheads). Embryos were cultured till stage 28, fixed and whole mount *in situ* hybridised to detect expression of *nephrin*, a marker of the glomus, and *slc5a2*, a marker of the proximal tubules. Injection of *Delta-1* mRNA caused ectopic glomus formation (A, white arrow), but inhibited proximal tubule development (B).

5.3 Discussion

Previous studies in the amphibian pronephros showed the Notch signalling pathway regulates development of this organ by establishing a proximal-distal axis across the entire length of the pronephros (McLaughlin et al., 2000; Rones et al., 2002; Taelman et al., 2006). We have refined these results and propose mis-activation of the Notch signalling pathway induces ectopic formation of the medial pronephric mesoderm at the expense of the lateral pronephric mesoderm. Furthermore we have demonstrated a novel role for the Wnt signalling pathway in pronephrogenesis, which we suggest is integrated with the Notch signalling pathway, and together this “Wntch” pathway establishes a boundary that defines the point of separation of the lateral and medial pronephric mesoderms.

5.3.1 Mis-activation of the Notch signalling pathway induced ectopic nephrostome and glomus development, but inhibited proximal tubulogenesis

Mis-activation of the Notch signalling pathway in the pronephros, by injection of *Notch-ICD* mRNA, caused increased nephrostomal and glomus formation (Fig 5.5B and Fig 5.6B), but inhibited tubulogenesis completely (Fig 5.3B). This phenotype has not been observed previously as pronephric markers used to indicate the effects of mis-expressing components of the Notch signalling pathway failed to distinguish between nephrostomes and tubules. Examples of pronephros markers that have been used in published studies are the 3G8 antibody, which identifies both the nephrostomes and proximal tubules (Vize et al., 1995), and *Lim-1* and *Pax-2*, which are both expressed across the entire lateral pronephric mesoderm, thus mark the nephrostomes as well as proximal, intermediate and distal tubules

(Carroll and Vize, 1999; Chan et al., 2000). McLaughlin et al (2000) reasoned the increase in 3G8 staining and *Lim-1* and *Pax-2* expression they observed after mis-activation of the Notch signalling pathway was an increase in proximal pronephric development (glomus, nephrostomes and proximal tubules). Our interpretation of the effects *Notch-ICD* mRNA injection had on 3G8/ 4A6 antibody staining (Fig 5.2) led us to the same conclusion. However, complete inhibition of tubulogenesis, indicated by loss of Na^+ K^+ *ATPase* expression, suggested the ectopic 3G8 staining observed after *Notch-ICD* over-expression was completely nephrostomal. This theory is supported by *Notch-ICD* mRNA injection inducing ectopic nephrostome formation, as observed by increased *odf-3* expression (Fig 5.5B). In conclusion we refine the results currently in the literature to show ectopic activation of the Notch signalling pathway induces ectopic glomus and nephrostome development at the expense of tubules.

Suppression of the Notch signalling pathway using $Delta^{STU}$ had no effect on distal tubulogenesis (Fig 5.2C and Fig 5.3C), but it did inhibit glomus, nephrostome and proximal tubule development (Fig 5.6C, Fig 5.5C, Fig 5.4C and Fig 5.3C). Components of the Notch signalling pathway are expressed in the proximal pronephric region in two phases during development, however no expression of *Notch-1*, *Delta-1* or *Serrate-1* is observed in the intermediate or distal tubules (McLaughlin et al., 2000; Rones et al., 2002; Taelman et al., 2006). Therefore, it is not surprising suppression of the Notch signalling pathway inhibited proximal pronephros development, with little or no effect on distal tubulogenesis. Notch signalling is integral to formation of the glomus and nephrostomes during tail bud stages of pronephrogenesis (as described here), and also proximal tubule

development during later stages of pronephrogenesis (Taelman et al., 2006). Thus inhibiting early and late phase Notch signalling by injecting *Delta*^{STU} mRNA would be expected to completely inhibit proximal pronephrogenesis. Our results differ slightly from published findings, as McLaughlin et al (2000) showed suppression of Notch signalling increased the size of the distal tubules, a phenotype we were unable to reproduce after injection of *Delta*^{STU} mRNA. No components of the Notch signalling pathway are expressed in this region of the pronephros, hence we cannot explain the findings of McLaughlin et al (2000), as there are no Notch receptors present in the distal tubules for Notch signalling inhibitors such as Delta^{STU} to suppress; we therefore believe exogenous mRNA cannot have an effect in this region, and suggest this published effect on distal tubule width is an artefact. Furthermore, if suppression of the Notch signalling pathway promoted development of the distal pronephros we would expect to observe ectopic distal tubulogenesis in the proximal region of the pronephros, a phenotype neither ourselves nor McLaughlin et al (2000) observed.

5.3.2 Over-expressing *Wnt-4* reproduced the phenotypes observed after *Notch-ICD* over-expression

Over-expressing *Wnt-4* highlighted a role for the Wnt signalling pathway in pronephrogenesis that is potentially integrated with the Notch signalling pathway. *Wnt-4* is expressed in the nephrostomes and proximal tubules during early tail bud stages of development (Saulnier et al., 2002). We have over-expressed *Wnt-4* and shown it caused identical phenotypes to *Notch-ICD* over-expression; ectopic nephrostome (Fig 5.5D) and glomus (Fig 5.6D) formation was accompanied by inhibited tubulogenesis (Fig 5.3D and Fig 5.4D). Intriguingly Saulnier et al (2000)

showed over-expression of *Wnt-4* disrupted nephrostome formation, producing fused structures, and proximal tubulogenesis without affecting more distal tubule development. These findings are similar to our own, but they did not observe ectopic nephrostome formation or inhibition of distal tubule development. We suggest this is due to the amount of exogenous message present in these embryos. We injected 1 ng of *Wnt-4* mRNA compared to 0.25 ng *Wnt-4* mRNA injected by Saulnier et al (2000). Hence the phenotypes Saulnier et al (2000) observed were less severe. Saulnier et al (2000) knocked down translation of endogenous *Wnt-4* mRNA using a MO and showed this inhibited proximal tubule development but left distal tubulogenesis largely unaffected, an identical phenotype to $Delta^{STU}$ over-expression described here. In conclusion the Wnt signalling pathway is required for the formation of glomus and nephrostomes during pronephrogenesis and the correlation between the phenotypes observed after over-expression of both *Wnt-4* and *Notch-ICD*, and likewise $Delta^{STU}$ mRNA and *Wnt-4* MO injection, suggest these two pathways may be integrated.

5.3.3 *Notch-ICD* mRNA induced the Wnt signalling pathway, but exogenous *Wnt-4* mRNA had no obvious effect on components of the Notch signalling pathway

We aimed to see if the Notch and Wnt signalling pathways were integrated by observing the effect mis-activation of either pathway had on expression of components of the other pathway. We found injection of *Notch-ICD* mRNA caused ectopic *Wnt-4* expression on the injected side (Fig 5.7A). The pattern of ectopic *Wnt-4* expression was similar to ectopic 3G8 antibody staining and *odf-3* and *nephrin* expression we had observed previously. As Wnts are secreted proteins, it is possible cells expressing *Wnt-4* induce neighbouring cells to form medial pronephric

mesoderm. Suppression of the Notch signalling pathway by injection of *Delta*^{STU} mRNA had the opposite effect, inhibiting *Wnt-4* expression on the injected side (Fig 5.7B), a phenotype that correlates with the effects over-expressing *Delta*^{STU} had on proximal pronephrogenesis discussed previously.

Injection of *Wnt-4* mRNA did not have an obvious effect on *Delta-1* or *Serrate-1* expression. There was no significant inhibition or induction of expression of either *Delta-1* or *Serrate-1*, rather their expression was disrupted to the extent it was abnormal when compared to the un-injected side. We suggest this abnormality is perhaps a product of the overall effect *Wnt-4* mRNA injection had on pronephrogenesis, rather than a direct affect *Wnt-4* over-expression had on *Serrate-1* and *Delta-1* expression. We know from results described above that *Wnt-4* over-expression will cause ectopic glomus and nephrostome development at the expense of tubulogenesis. Thus the pronephroi stained for *Delta-1* and *Serrate-1* expression by *in situ* hybridisation would have abnormal development. In conclusion the lack of a distinctive phenotypic effect on pronephric *Delta-1* and *Serrate-1* expression after *Wnt-4* mRNA injection indicates Wnt-4 does not induce or suppress expression of components of the Notch signalling pathway. This result is informative as it suggests there is no positive feedback loop between the Notch and Wnt signalling pathways in the proximal pronephros. Rather the Notch-ICD dependent pathway is required upstream for *Wnt-4* expression, but expression of components of the Notch signalling pathway do not require Wnt signalling. Thus we can position pronephric Wnt-4 signalling downstream from the Notch signalling pathway. Wnt-4 therefore may act as a morphogen, inducing formation of the medial pronephric mesoderm in the proximal pronephros.

5.3.4 Histological analysis of the pronephros after *Wnt-4* and *Notch-ICD* over-expression indicated the lateral pronephric mesoderm does not form

The pronephros is a simple organ to study, but for accurate examination pronephrogenesis needs to be observed in three dimensions. This is due to the fact the pronephros anlagen separates down its midline during tail bud stages of development to produce the lateral and medial pronephic mesoderms, which are later separated by the coelom. Glomus development is medial to the proximal tubules, not directly above as some schematics suggest. One way to observe the pronephros in three dimensions is by histological sectioning.

Initially we used a razor blade to section embryos stained for *nephrin* expression after injection of *Notch-ICD* mRNA and *Wnt-4* mRNA. We were surprised to observe expression of *nephrin*, a marker of the glomus (the proximal medial pronephric mesoderm), in the region of the pronephros anlagen where the lateral pronephric mesoderm normally develops (Fig 5.10). In these embryos ectopic glomus and nephrostome development occurred across the whole pronephric anlagen, and was not restricted to the medial pronephros. This finding suggests cells normally fated to form tubules had switched to glomus and nephrostomal cell fates. In conclusion *Notch-ICD* and *Wnt-4* over-expression caused the pronephros anlagen to ubiquitously develop as medial pronephric mesoderm. As the glomus develops from the medial pronephric mesoderm it induces the nephrostomes to develop at the tips of the proximal tubules. Therefore the nephrostomes, despite functioning on the lateral/ tubules side of the coelomic cavity, require the medial pronephric mesoderm to be

induced (Howland, 1916), thus accounting for the presence of ectopic nephrostome formation.

Paraplast wax sectioning was performed on stage 41 embryos injected with *Notch-ICD* mRNA targeted to the pronephros (Fig 5.11B). Haematoxylin and eosin staining identified cell nuclei and cytoplasm and allowed for histological analysis of the embryos to be performed. The un-injected side of Figure 5.11Bi illustrates the normal organisation of the proximal pronephros in section. The glomus can be identified by dispersed podocytes, and the coelomic cavity separates the glomus from the proximal tubules, which are clearly seen as cross-sectioned tubes. More distally in Figure 5.11Bii and Figure 5.11Biii the un-injected side shows cross-sections of the distal tubule. The injected side of this embryo clearly identified the phenotypes we expected having performed whole mount *in situ* hybridisation for markers of the glomus and nephrostomes after *Notch-ICD* over-expression. Podocytes and nephrostomal tubules are dispersed throughout the entire pronephric region (Fig 5.11Bii injected side). Cavities are also present across the entire pronephric region, which may have arisen as a result of sectioning or abnormal pronephrogenesis, or could have formed as a consequence of ectopic glomus tissue separating from ectopic nephrostomes.

Better understanding of the effects of *Wnt-4*, *Delta*^{STU} or *Notch-ICD* over-expression requires technical improvements in pronephric labelling. For example the production of transgenic embryos with a *GFP* driven kidney reporter would label the entire pronephros. The effects of injected messages could then be easily analysed in real-time under a fluorescent microscope; and in three dimensions by confocal analysis. This labelling technique would allow us to follow the effects of injections

across the entire pronephros, which by stage 35 is clearly compartmented into the glomus, coelom, nephrostomes, and tubules. Furthermore the separation of the lateral and medial pronephric mesoderms around stage 28, to form the coelomic cavity, would be observable, and we could detect if *Wnt-4*, *Delta*^{STU} or *Notch-ICD* over-expression inhibited this process. At present this technique is not possible to carry out, but would advance studies into pronephrogenesis.

5.3.5 The Notch and Wnt signalling pathways may setup a boundary between the lateral and medial pronephric mesoderms

Previous studies suggested proximal tubulogenesis, as well as glomus formation was increased after mis-activation of the Notch signalling pathway. This made it difficult to hypothesise a mechanism by which the Notch signalling pathway was regulating development of the proximal pronephros as the two main mechanisms of action by which the Notch signalling pathway regulates organogenesis, lateral inhibition and boundary formation, could not explain how the Notch signalling pathway formed a proximal-distal axis across the pronephros. We have discovered *Notch-ICD* and *Wnt-4* over-expression caused ectopic formation of the medial pronephric mesoderm, at the expense of the lateral pronephric mesoderm; a result that enables conclusions to be made that differ from previous studies. Rather than establishing a proximal-distal axis across the entire pronephros, we propose the Notch and Wnt signalling pathways setup a lateral-medial axis across the proximal-dorsal region of the pronephros anlagen. Moreover, we suggest this lateral-medial axis is established by the Notch signalling pathway through the formation of a boundary between the lateral and medial pronephric mesoderms during tail bud

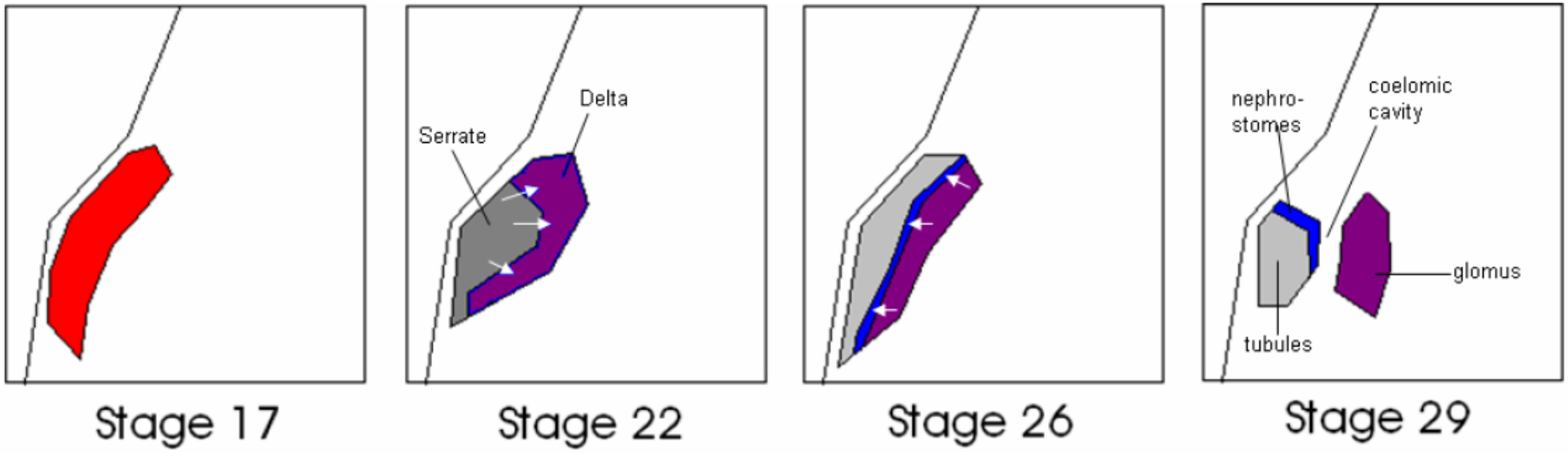

Schematic adapted from Vize et al (1995)

Figure 5.13 Schematic of one model for the separation of the lateral and medial pronephric mesoderms based on the *Drosophila* imaginal wing disc At stage 17 the pronephros anlagen is a mass of un-differentiated and un-patterned cells located in the intermediate mesoderm lateral to the anterior somites. By stage 22 *Delta-1*, *Serrate-1* and *Notch-1* expression is observed in the proximal-dorsal region of the pronephros anlagen. We propose the Notch signalling pathway acts to setup a boundary in this region of the pronephros to separate the lateral (grey) from the medial (purple) pronephric mesoderms. By this stage *Wnt-4* is also highly expressed in this region and acts downstream of the Notch signalling pathway to induce medial pronephric mesoderm cell fate decisions (white arrows). By stage 26 the medial pronephric mesoderm has been induced and a signal within the medial pronephric mesoderm induces nephrostome cell fate decisions in the medial pronephric mesoderm at the boundary with the lateral pronephric mesoderm. As this layer of mesoderm is distinct we will term it the medio-lateral pronephric mesoderm (blue). By late tail bud stages of development the medial pronephric mesoderm has physically dissociated from the rest of the pronephros anlagen to form the glomus, with the cavity formed by this split becoming the coelom. The medio-lateral pronephric mesoderm, despite originating in the medial pronephric mesoderm, stays on the tubule side of the coelom and will form the nephrostomes.

stages of development. Vize et al (1997) illustrated these are the developmental stages when the lateral and medial pronephric mesoderms form, thus expression of components of the Notch signalling pathway are temporally and spatially appropriate to have a role in separation of the lateral and medial pronephric mesoderms. Once a boundary is formed, Wnt-4, which is also temporally and spatially expressed appropriately, could act as a morphogen, directing cell fate decisions in the medial pronephric mesoderm (see Fig 5.13 for schematic).

As this theoretical model is identical to the establishment of the dorsal-ventral boundary in *Drosophila*, there is a requirement for differential Notch-ligand binary cell interactions. In *Drosophila* it is believed Notch-Serrate and Notch-Delta interactions induce differential transcription cascades that ultimately produce two distinct populations of cells either side of the boundary (Irvine and Wieschaus, 1994; Johnston et al., 1997; Irvine and Rauskolb, 2001). Here, *Delta-1* over-expression induced ectopic medial pronephric mesoderm at the expense of lateral pronephric mesoderm, an identical phenotype to *Notch-ICD* over-expression (Fig 5.12). However, we did not observe any pronephric phenotype after injection of *Serrate-1* mRNA. This non-phenotype is surprising as *Notch-ICD* mRNA injection has previously been shown to promote *Serrate-1* expression (McLaughlin et al., 2000). It is possible mRNA synthesised from our cDNA clone for *Serrate-1* was not able to translate *in vivo*, although we have tested the translatability of this construct in a rabbit reticulocyte lysate system and obtained high levels of Serrate-1 protein (data not shown). Further experimentation, such as the use of MOs to knock-down pronephric *Serrate* expression, is required to observe if this lack of a phenotype after *Serrate-1* over-expression is the real effect of this message. *Serrate-1* over-

expression has been shown to inhibit primary neurogenesis (Kiyota et al., 2001); therefore we could test the ability of our message to induce an *in vivo* phenotype by attempting to reproduce this result.

A pronephric phenotype after over-expression of *Serrate-1* is necessary to support the model we propose in Figure 5.13 for how the Notch signalling pathway regulates patterning of the pronephros anlagen. If our model is accurate, we would expect *Serrate-1* over-expression to cause ectopic proximal tubule formation and inhibit glomus development; given *Delta-1* over-expression produced the opposite pronephric phenotype, promoting glomus formation at the expense of proximal tubulogenesis. However, injection of *Notch-ICD* mRNA increases *Serrate-1* expression (McLaughlin et al., 2000), therefore Notch-Serrate interactions are, at least in part, a cause of ectopic medial pronephric mesoderm formation and inhibited lateral pronephric mesoderm development. Collectively therefore, our data and the results from McLaughlin et al (2000) suggest over-expressing *Delta-1* and *Serrate-1* produces the same pronephric phenotype. If these phenotypes are accurate, transposing the mechanism of dorsal-ventral boundary formation in the wing of *Drosophila* to the pronephros is not possible, and the mechanism we propose in Figure 5.13 is inaccurate. Rather, a novel and undoubtedly more complex mechanism would be required to define exactly how the Notch signalling pathway regulates proximal pronephrogenesis.

Despite this, our findings, when analysed in tandem with published research describing how the Notch signalling pathway establishes developmental boundaries, strongly suggest that a boundary is formed between the lateral and medial pronephric

mesoderms. To the best of our knowledge this finding is completely novel in terms of kidney development and may be conserved in mesonephros and mammalian metanephros development. Interestingly, most mammalian renal diseases caused by aberrant Notch signalling are glomerular diseases such as sclerosing glomerular disease (Mertens et al., 2008). Thus *X. laevis* pronephrogenesis, as a simple and easily manipulated system, is potentially a powerful model for advancing our knowledge of how the Notch signalling pathway regulates kidney organogenesis.

Chapter 6

Expression analysis and functional characterisation of Radical fringe and Lunatic fringe in the Xenopus laevis pronephros

6.1 Introduction

The Notch signalling pathway plays an important role in development of the proximal region of the *X. laevis* pronephros (McLaughlin et al., 2000; Rones et al., 2002; Taelman et al., 2006). From our results discussed in Chapter 5 we suggested that the Notch signalling pathway regulates proximal pronephrogenesis through formation of a boundary. This hypothesis, not proposed in any previous publications, suggested early phase pronephric Notch signalling during tail bud stages of development is integral to the establishment of the medial and lateral pronephric mesoderms. For this hypothesis to be supported, the mechanism by which the Notch signalling pathway is regulated in this region of the pronephros needed to be elucidated.

Previous studies that uncovered the role of the Notch signalling pathway in establishing developmental boundaries repeatedly identified one class of proteins as essential in the regulation of Notch receptors to permit boundary formation. This class of glycosyl transferases are termed the Fringe proteins, which act to post-translationally modify Notch receptors by glycosylation (Johnston et al., 1997; Irvine,

1999; Bruckner et al., 2000; Okajima and Irvine, 2002; Visan et al., 2006). Such modification increases affinity of Notch receptors for Delta ligands, but reduces Notch-Serrate interactions (Haines and Irvine, 2003). The formation of the dorsal-ventral boundary in the *Drosophila* imaginal wing disc (Irvine and Wieschaus, 1994; Rauskolb et al., 1999), the demarcation of segmental boundaries (Dearden and Akam, 2000; Prince et al., 2001; Dale et al., 2003; Gomez et al., 2008), and the establishment of a dorsal-ventral boundary in the vertebrate limb bud (Rodriguez-Esteban et al., 1997) are just a few examples of Fringe acting to establish developmental boundaries between discrete populations of cells. If the Notch signalling pathway is regulating proximal pronephrogenesis by establishing a boundary between the lateral and medial pronephric mesoderms, we would expect to observe expression of *fringe* genes in this proximal pronephric region and detect pronephric phenotypes upon mis-expression of these genes.

In this chapter we observe the expression patterns, and effects of pronephric mis-expression of two homologues of the *Drosophila fringe* gene in *Xenopus laevis*, *Lunatic fringe* and *Radical fringe*. We use over-expression and MO knock-down techniques to uncover a role for *Lunatic fringe* in regulation of proximal pronephrogenesis that supports our hypothesis that the Notch signalling pathway functions to separate the lateral and medial pronephric mesoderms during early tail bud stages of development.

6.2 Results

6.2.1 *Radical* and *Lunatic fringe* are expressed in the pronephros during tail bud stages of development

To observe the expression patterns of *Lunatic* and *Radical fringe* we performed *in situ* hybridisations using DIG-labelled anti-sense and sense RNA probes (Figs 6.1 and 6.2). The aim of this experiment was to identify pronephric expression of *Lunatic* and *Radical fringe* as previous studies had failed to observe such spatial expression (Wu et al., 1996). The results obtained improve the data in the literature as previously unrecorded lower level expression of *Lunatic* and *Radical fringe*, across the whole embryo, was identified due to improved protocols.

Lunatic fringe expression was first detected in the pronephros at stage 22, and persisted until stage 32/33 (Fig 6.1). At stage 22 expression in the hindbrain, midbrain, eye vesicle, somites, middle lateral line and antero-dorsal line was also detected (Fig 6.1A). By stage 27 strong expression of *Lunatic fringe* was detected in the proximal dorsal pronephric region, the ventral muscle anlagen, and the eye (Fig 6.1B). In the brain, expression of *Lunatic fringe* remained in the rhombencephalon, but was no longer expressed in the midbrain; instead expression was stronger in the forebrain. A region of *Lunatic fringe* expression was also detected in extreme ventral region of the embryo. This area is too distal to be heart or liver, thus we propose this expression is in an anterior blood island. Expression of *Lunatic fringe* at stage 30 was similar to the expression detected at stage 27, apart from additional expression within the branchial arches and expression in the eye being more prevalent in the retina (Fig 6.1C). Dissection of this stage 30 embryo identified internal

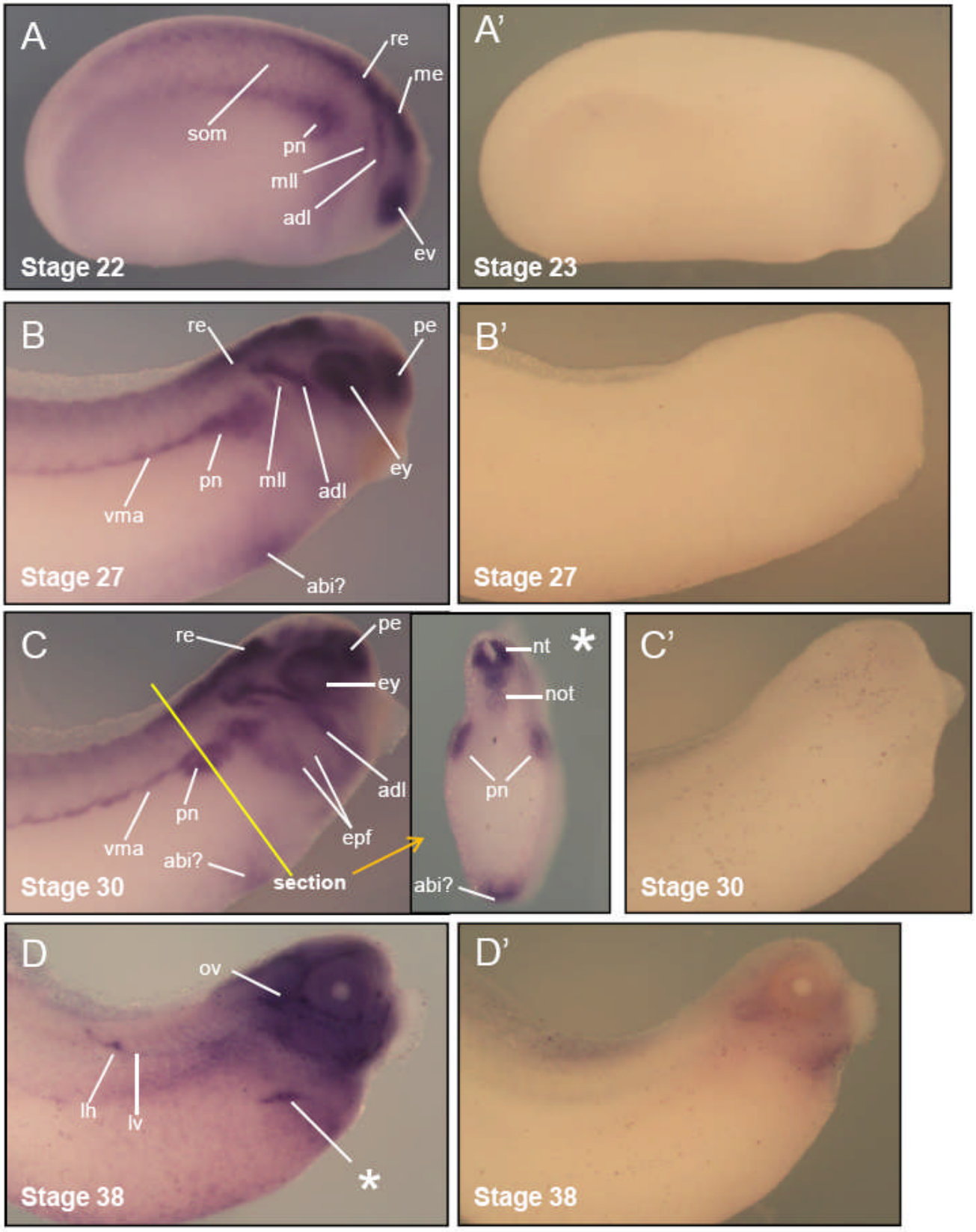
A
re
me
som
pn
mll
adl
ev
Stage 22
A'
Stage 23
B
re
pe
pn
mll
adl
ey
vma
abi?
Stage 27
B'
Stage 27
C
re
pe
ey
adl
pn
vma
abi?
epf
section
Stage 30
nt
not
pn
abi?
C'
Stage 30
D
ov
lh
lv
Stage 38
D'
Stage 38

Figure 6.1 Lateral views of embryos stained for *Lunatic fringe* expression by *in situ* hybridisation. A range of embryonic stages are shown hybridised with *Lunatic fringe* DIG-labelled anti-sense probe (A-D), with the corresponding sense probe-treated embryos shown opposite (A'-D'). (A) At stage 22 *Lunatic fringe* is expressed in the hindbrain, midbrain, eye vesicle, pronephros, middle lateral line and anterodorsal line. (B) Stage 27 *Lunatic fringe* expression is similar to the expression pattern at stage 22. However expression in the midbrain is lost. Instead, expression of *Lunatic fringe* in the forebrain and ventral migrating muscle anlagen can clearly be observed. Furthermore, expression in the eye is being restricted to the retina, and a ventral domain of expression can be observed, which is too posterior to be defined as heart or liver, thus we conclude this expression is in an anterior blood island. (C) At stage 30 expression is similar to that observed at stage 27. *Lunatic fringe* expression in the head region is more distinct, branchial arches are stained, as is the anteroventral line, and expression in the retina is more pronounced. Pronephric expression is also more clear, and not masked by the ventral muscle anlagen expression. In section this pronephric expression of *Lunatic fringe* is clearly evident. (D) By stage 38 *Lunatic fringe* expression is restricted to the head region and small areas of the rest of the body. Expression in an extending lymphatic vessel and lymphatic heart is observed. A peculiar, yet repeatable expression pattern is observed in the anterior region of the belly (highlighted by *), the region this expression marks is unknown. A'-D' show little staining with the sense DIG-labelled RNA probe for *Lunatic fringe*, suggesting all staining observed in A-D is specific (abi – anterior blood island, adl – anterodorsal line, avl – anteroventral line, epf – epibranchial facial placodes, ev – eye vesicle, ey – eye, lh – lymphatic heart, lv – lymphatic vesicle, me – mesencephalon (midbrain), mll – middle lateral line, not – notochord, nt – neural tube, ov – otic vesicle, pe – proencephalon (forebrain), pn – pronephros, re – rhombencephalon (hindbrain), som – somites, vma – ventral muscle anlagen)

expression of *Lunatic fringe*, with pronephric expression, which in the lateral view was masked by ventral muscle anlagen expression, clearly identifiable. As well as expression in the hindbrain, which in section may be posterior enough to be the neural tube, *Lunatic fringe* expression was detected at low levels in the notochord (Fig 6.1C*). By stage 38 expression of *Lunatic fringe* in the pronephros was lost (Fig 6.1D). Apart from the head region the only detectable expression patterns were in a dorsal lymphatic vessel and heart, and a peculiar area of expression in the anterior gut region, which we are unable to define. All sense *in situ* hybridisations for *Lunatic fringe* were negative and are shown opposite equivalently staged anti-sense stained embryos (Fig 6.1A'- D').

Radical fringe expression in the pronephros was detected between stages 25 and 34 (Fig 6.2), slightly later than *Lunatic fringe* pronephric expression. Expression of *Radical fringe* at stage 22 was detected in the somites, eye vesicle, branchial arches and all regions of the brain (Fig 6.2A). At stage 28 pronephric and otic vesicle expression of *Radical fringe* can clearly be observed in addition to indistinguishable expression in the head region (Fig 6.2B). By stage 32, *Radical fringe* expression was predominantly in the head region and pronephros (Fig 6.2C). As with *Lunatic fringe*, all sense *in situ* hybridisations for *Radical fringe* were negative and are shown below the anti-sense stained embryos (Fig 6.2A'- C').

To ensure the pronephric expression of *Lunatic* and *Radical fringe* detected by *in situ* hybridisation was not an artefact, we performed RT-PCR analysis on pronephroi dissected from various stages of development. Both *Lunatic* and *Radical fringe* are expressed in the pronephros from stage 12.5 to stage 38 (Fig 6.3).

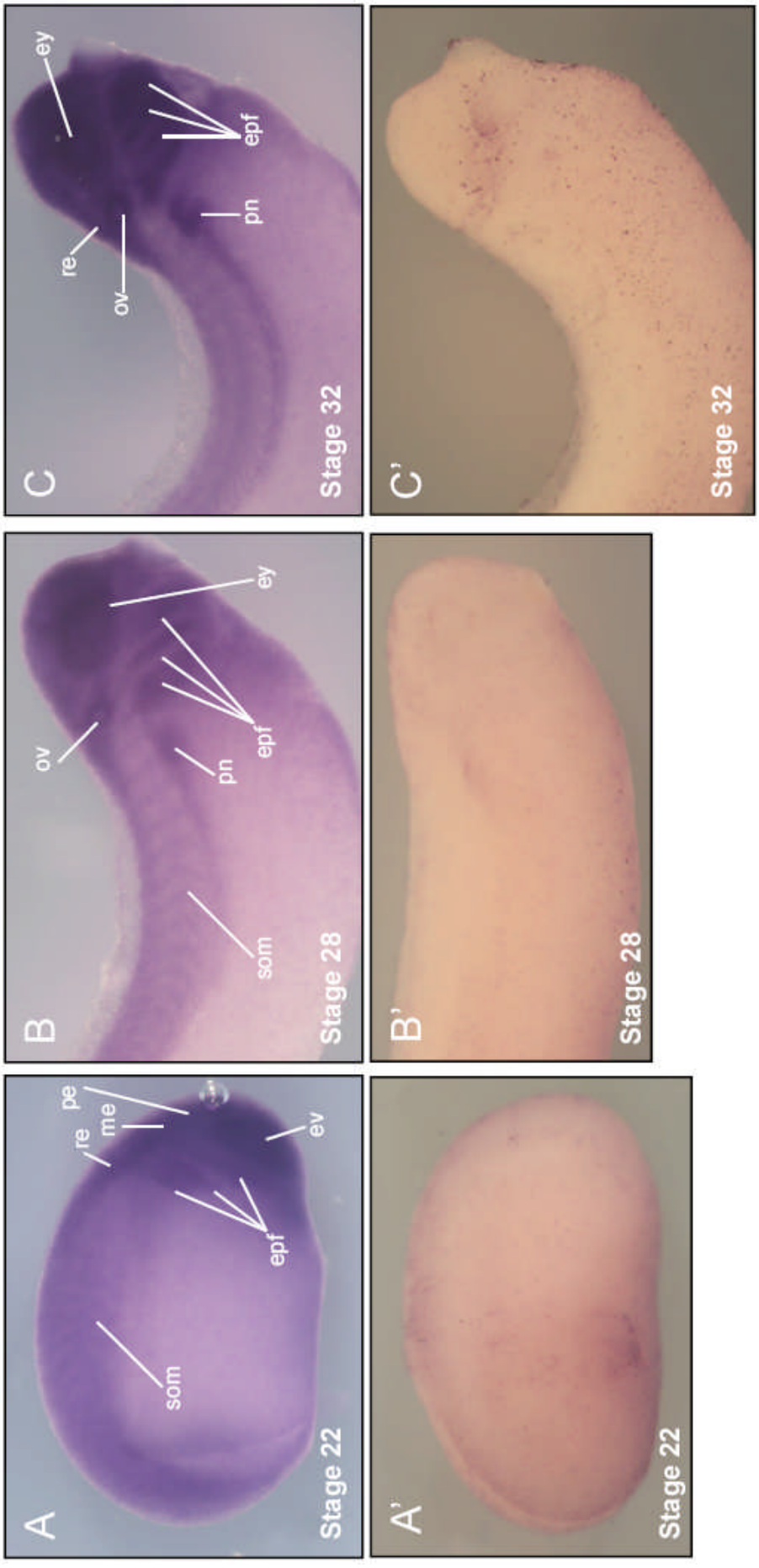
A
pe
me
re
ev
epf
som
Stage 22
A'
Stage 22
B
ey
ov
epf
pn
som
Stage 28
B'
Stage 28
C
ey
re
ov
epf
pn
Stage 32
C'
Stage 32

Figure 6.2 Lateral views of embryos stained for *Radical fringe* expression by *in situ* hybridisation. A range of embryonic stages are shown hybridised with *Radical fringe* DIG-labelled anti-sense probe, with the corresponding sense probe-treated embryos (A'-C') shown beneath. (A) At stage 22 *Radical fringe* is expressed in the hindbrain, midbrain, eye vesicle, and branchial arches. (B) Stage 28 *Radical fringe* expression in the brain is reduced, but expression in the eye, like *Lunatic fringe* expression, is beginning to be restricted to the retina. Pronephric *Radical fringe* expression is also detected (C) At stage 32 expression is similar to that observed at stage 27. (epf – epibranchial facial placodes, ev – eye vesicle, ey – eye, me – mesencephalon (midbrain), ov – otic vesicle, pe – proencephalon (forebrain), pn – pronephros, re – rhombencephalon (hindbrain), som – somites)

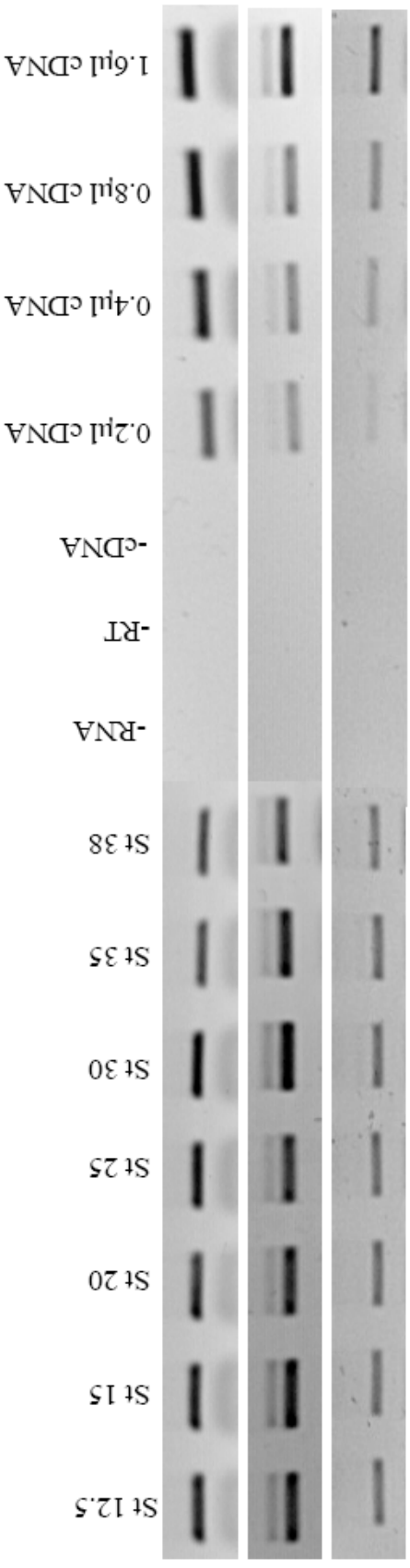

Figure 6.3 RT-PCR analysis confirms the expression of *Lunatic* and *Radical fringe* within presumptive pronephros tissue. The whole pronephric anlage was dissected from multiple embryos at stage 12.5, 15, 20, 25, 30, 35 and 38. mRNA and cDNAs were prepared by standard procedures and RT-PCR carried out for *Lunatic fringe*, *Radical fringe* and the loading control *ODC*. Linearity of the PCR was confirmed by doubling the input of cDNA from control stage 20 embryos. Negative controls used were absence of RNA during the reverse transcription (-RNA), absence of reverse transcriptase (-RT), and absence of cDNA in the PCR (-cDNA). *Lunatic* and *Radical fringe* are expressed in the presumptive pronephric anlagen from stage 12.5, when the pronephric tubules are specified; through to stage 38, indicating they may have a role in pronephros development. The quality of the dissected material has been confirmed elsewhere (Haldin et al, 2008)

These results confirm *Lunatic* and *Radical fringe* expression are both temporally and spatially appropriate for a role in pronephrogenesis. Furthermore they are expressed in the same region and at the same time during development as components of the Notch signalling pathway and *Wnt-4*.

6.2.2 Over-expression of *Radical fringe* caused ectopic pronephros development, over-expression of *Lunatic fringe* inhibited pronephros development

We next attempted to over-express *Radical* and *Lunatic fringe* in the pronephros by injecting mRNA into a ventro-vegetal (V2) blastomere of embryos at the 8-cell stage, with *βgal* mRNA to act as a lineage tracer. We initially injected mRNA encoded from the full length cDNA clones of both *Lunatic* and *Radical fringe*, but neither produced a phenotype *in vivo* (Appendix 6). To test if these mRNAs were translating we performed an *in vitro* translation assay in a rabbit reticulocyte lysate system. Translated protein was radio-labelled with ^{35}S-Methionine, separated on an SDS-PAGE gel and detected by autoradiography (Fig 6.4D). We found *Radical fringe* mRNA transcribed from the full length cDNA clone did not translate *in vitro* (Fig 6.4D, lane 1), but *Lunatic fringe* mRNA did (Fig 6.4D, lane 2). Thus *Radical fringe* mRNA is likely not to be translated *in vivo*, explaining its inability to produce a phenotype, whereas *Lunatic fringe* mRNA is likely to be translated *in vivo*, but the protein must be inactive as it has no effect on development of the pronephros.

Commonly the 5' and 3' UTRs of full length cDNA clones contain regulatory sequences that disrupt the production of active protein from injected mRNA. Thus we decided to PCR clone the open reading frame (ORF) of *Lunatic* and *Radical*

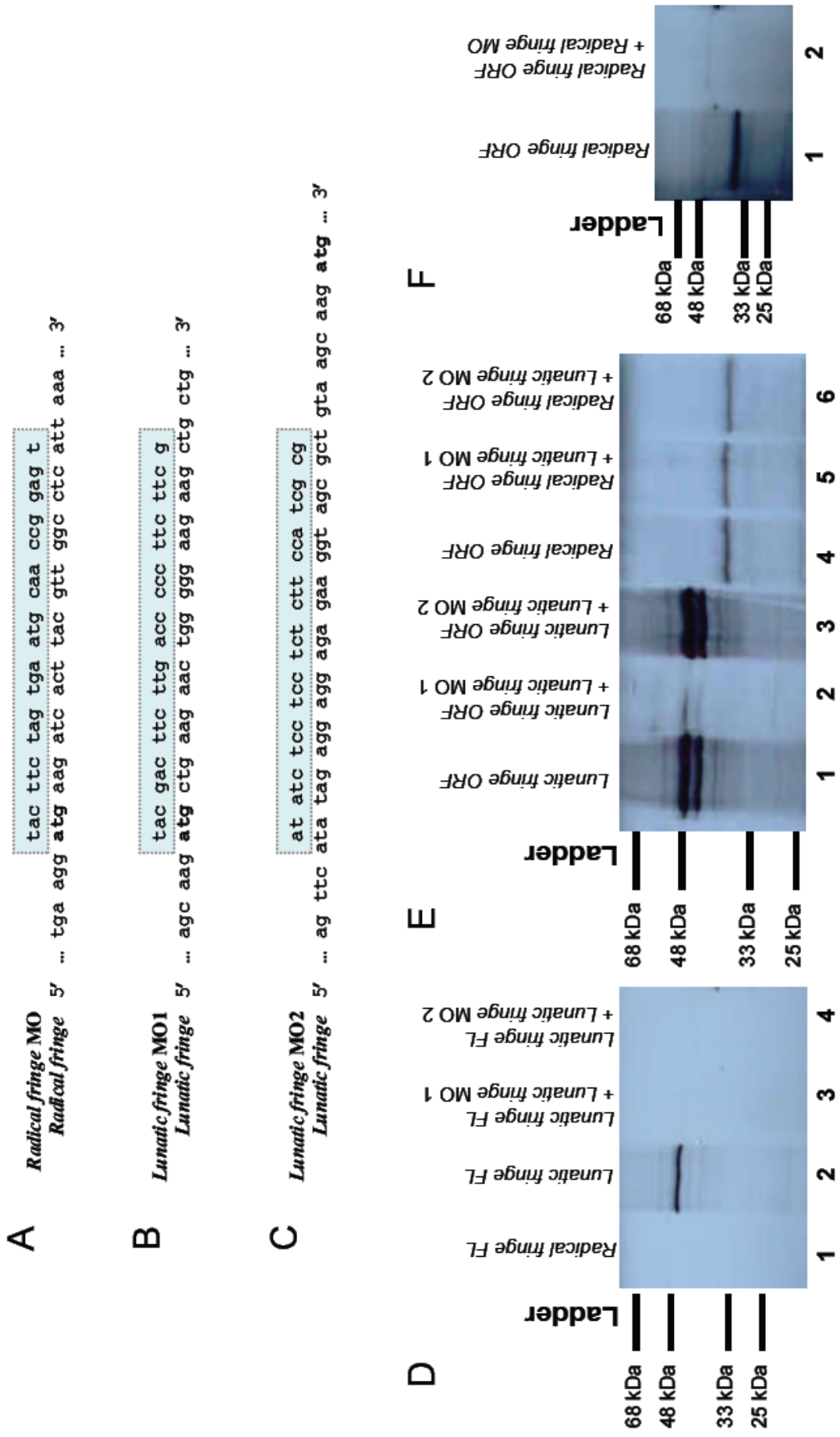
A
Radical fringe MO
Radical fringe
5′ … tga agg atg aag atc act tac gtt ggc ctc att aaa … 3′
tac ttc tag tga atg caa ccg gag t
B
Lunatic fringe MO1
Lunatic fringe
5′ … agc aag atg ctg aag aac tgg ggg aag aag ctg ctg … 3′
tac gac ttc ttg acc ccc ttc ttc g
C
Lunatic fringe MO2
Lunatic fringe
5′ … ag ttc ata tag agg agg aga gaa ggt agc gct gta agc aag atg … 3′
at atc tcc tcc tct ctt cca tcg cg
D
Ladder
68 kDa
48 kDa
33 kDa
25 kDa
Radical fringe FL
Lunatic fringe FL
Lunatic fringe FL + Lunatic fringe MO 1
Lunatic fringe FL + Lunatic fringe MO 2
1 2 3 4
E
Ladder
68 kDa
48 kDa
33 kDa
25 kDa
Lunatic fringe ORF
Lunatic fringe ORF + Lunatic fringe MO 1
Lunatic fringe ORF + Lunatic fringe MO 2
Radical fringe ORF
Radical fringe ORF + Lunatic fringe MO 1
Radical fringe ORF + Lunatic fringe MO 2
1 2 3 4 5 6
F
Ladder
68 kDa
48 kDa
33 kDa
25 kDa
Radical fringe ORF
Radical fringe ORF + Radical fringe MO
1 2

Figure 6.4 Rabbit reticulocyte lysates detecting *in vitro* translation of mRNAs and activity of the different *Lunatic and Radical fringe* MOs used in this study. Morpholino oligonucleotides were designed to inhibit translation of endogenous *Radical* and *Lunatic fringe* transcripts. The *Radical fringe* MO extends over the start codon (highlighted in bold) (A). Two MOs for *Lunatic fringe* were designed, MO1 binds over the start codon (highlighted in bold) (B). *Lunatic fringe* MO2 binds over a region of the 5'UTR sequence of this transcript, the start codon has been highlighted in bold to show its proximity to the region this MO binds to (C). To detect if our *in vitro* synthesised messages translated we performed an *in vitro* translation in a rabbit reticulocyte system using ^{35}S-Methionine labelled mRNA, radio-labelled protein was then separated on by SDS-PAGE and detected by autoradiography (D-F). 3.2 µg *Radical fringe Full Length* (*FL*) mRNA did not translate *in vitro* (lane 1). 2.9 µg *Lunatic fringe FL* mRNA did translate *in vitro* (lane 2) and two MOs designed to knockdown endogenous *Lunatic fringe* expression inhibited *Lunatic fringe mRNA* translation *in vitro* (lane 3 (5 µg of MO1) and lane 4 (5 µg MO2)) (D). Phenotypes were not observed after injection of mRNA into embryos for *Lunatic fringe* and *Radical fringe* encoded from full length cDNA clones, most likely due to regulatory elements in the UTRs. Thus we PCR cloned the open reading frame (ORF) from cDNA clones of full length *Lunatic* and *Radical fringe* into the pCS2+ vector. 2.6 µg *Lunatic fringe ORF* translated *in vitro* (lane 1). Its translation was blocked by 5 µg *Lunatic fringe* MO1 (lane 2), but not by 5 µg *Lunatic fringe* MO2 (lane 3). Thus *Lunatic fringe ORF* mRNA is a suitable message to rescue the pronephric phenotype of *Lunatic fringe* MO2. 0.8 µg *Radical fringe ORF* mRNA also translated *in vitro* (lane 4). Thus regulatory sequences must reside in the 5' and/ or 3' un-translated regions (UTRs) of the full length cDNA clone for *Radical fringe* that prevents its translation *in vitro*, and very probably *in vivo* too. In the presence of 5 µg *Lunatic fringe* MO1 and MO2, 0.8 µg *Radical fringe ORF* mRNA still translated. Thus *Radical fringe ORF* mRNA is a suitable message to rescue the effects of both *Lunatic fringe* MO1 and MO2 (E). *Radical fringe ORF* mRNA produces a protein 38 kDa in size (lane 1) and its translation is inhibited by the *Radical fringe* MO (lane 2) (F). Note: In the text the description of the phenotypes produced by *Radical* and *Lunatic fringe* over-expression is of over-expression of mRNA produced from the cDNA clones that encode only the ORF.

fringe into the pCS2+ vector. Translation of these mRNAs *in vitro* was again tested using a rabbit reticulocyte lysate system (Fig 6.4E). ^{35}S-Methionine radio-labelled Lunatic fringe (Fig 6.4E, lane 1) and Radical fringe (Fig 6.4E, lane 4) produced from mRNAs encoding only the ORFs of these genes, was detected by autoradiography, confirming the presence of inhibitory sequences in the full length *Radical fringe* cDNA clone. Over-expression of these clones *in vivo* yielded pronephric phenotypes.

The morpholino oligonucleotides (MO) used in this chapter are also displayed in Figure 6.4. Figure 6.4A gives the *Radical fringe* MO sequence and Figures 6.4B and 6.4C display the sequences of the two *Lunatic fringe* MOs used. To test whether the MOs were inhibiting translation of *Lunatic* and *Radical fringe* transcripts, we performed an *in vitro* translation using a rabbit reticulocyte lysate system as described above. Translation from mRNA synthesised from the full length *Lunatic fringe* cDNA clone was inhibited by both *Lunatic fringe* MO1 and MO2 (Fig 6.4D, lanes 3 and 4). *Lunatic fringe* MO2 inhibits translation of *Lunatic fringe* transcripts by binding to a region of the 5' UTR upstream from the start codon (Fig 6.4C). *Lunatic fringe* mRNA encoded from the ORF cDNA clone should not be inhibited by *Lunatic fringe* MO2. This is indeed the case as *Lunatic fringe* MO1, but not *Lunatic fringe* MO2 inhibits translation of *Lunatic fringe* (ORF) mRNA (Fig 6.4E, lanes 2 and 3). Radical fringe was not synthesised from the full length clone *in vitro*, thus we could not test the effectiveness of the *Radical fringe* MO on this clone. However mRNA synthesised from the cDNA clone encoding only the ORF of *Radical fringe* did translate (Fig 6.4F lane 1), and the *Radical fringe* MO inhibited its translation *in vitro* (Fig 6.4F lane 2). In conclusion the *Radical fringe* MO and both

Lunatic fringe MOs are able to specifically inhibit translation of endogenous *Radical* and *Lunatic fringe* transcripts, respectively.

For over-expression of *Radical fringe*, embryos were injected into a ventro-vegetal (V2) blastomere at the 8-cell stage with *Radical fringe* mRNA (transcribed from the ORF clone) and *βgal* mRNA, to act as a lineage tracer. Embryos were then cultured to various stages of development, where different regions of the pronephros were stained either by *in situ* hybridisation for expression markers, or antibody staining of pronephric epitopes. The embryos tolerated injection of large amounts of *Radical fringe* mRNA, up to 5 ng. We decided to inject 2 ng *Radical fringe* mRNA as this yielded statistically significant data without causing gross developmental defects. Pronephric phenotypes were detected by comparing the pronephric structure on the injected and un-injected sides. All results have been repeated multiple times yielding similar data and only results calculated as statistically significant within 95% confidence limits were defined as inducing a phenotype.

Radical fringe over-expression caused ectopic formation of every region of the pronephros. Expression of tubule markers *Na^+ K^+ ATPase* (Fig 6.5B, n=23) and *slc5a2* (Fig 6.6E, n=22) was increased in 67% and 59% of embryos, respectively. Ectopic formation of the glomus was observed in 81% of embryos *in situ* hybridised for *nephrin* expression (Fig 6.6B, n=21). Nephrostomal formation was also ectopic, with the domain of *odf-3* expression increased in 62% of embryos (Fig 6.6H, n=21). Antibody staining of the functional pronephros at stage 41 with 3G8, a marker of the proximal tubules and nephrostomes, and 4A6, a marker of the intermediate and distal tubules, highlighted the extreme nature of the pronephric phenotype produced upon

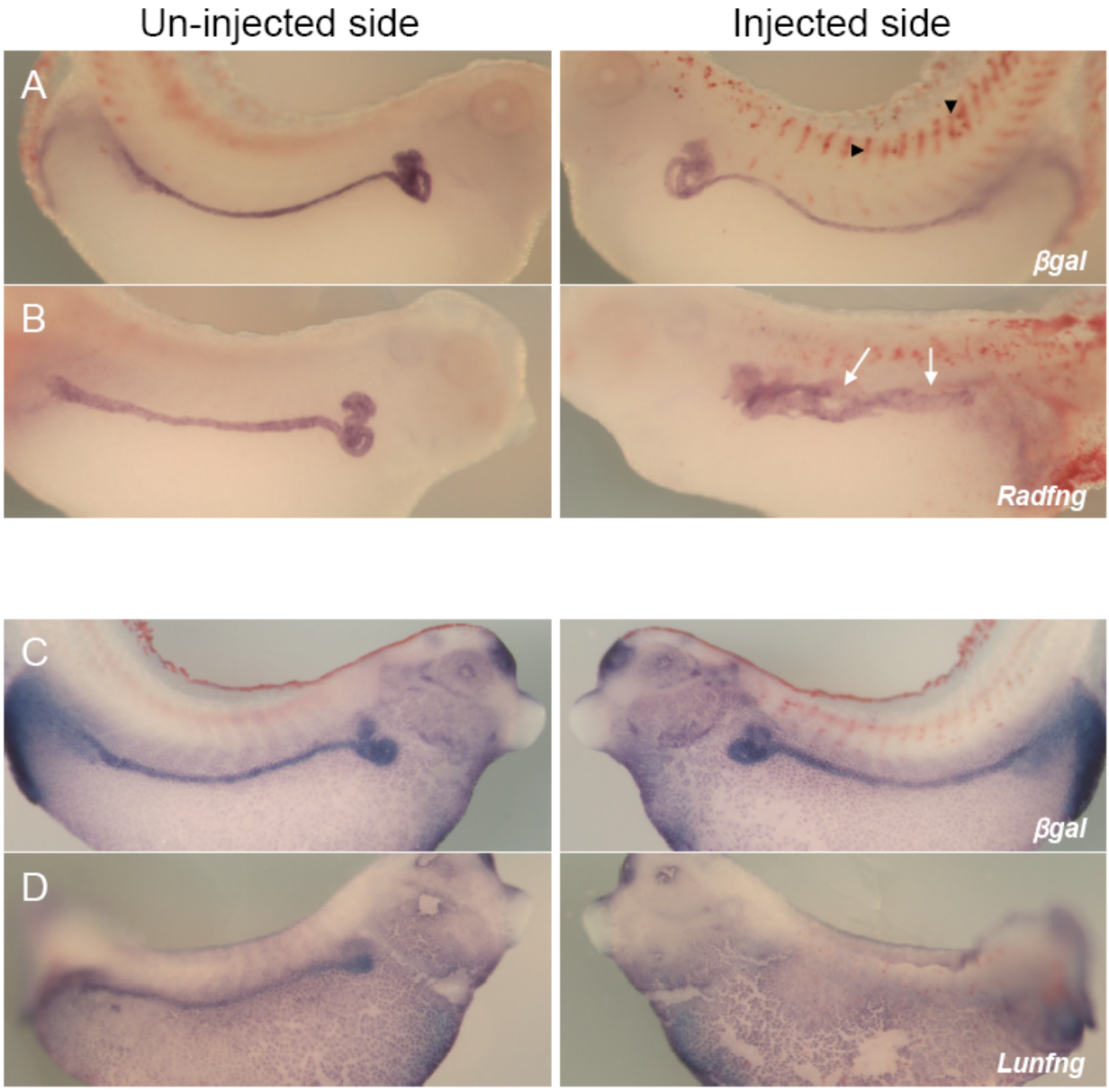
Un-injected side
Injected side
A
βgal
B
Radfng
C
βgal
D
Lunfng

Figure 6.5 Over-expression of *Lunatic* and *Radical fringe* affected tubulogenesis. *X. laevis* embryos were injected at the 8 cell stage into a ventro-vegetal blastomere to target the presumptive pronephric region. mRNA was co-injected with *βgal* mRNA to act as a lineage tracer (red staining, black arrowheads). Embryos were cultured till stage 36 and then fixed. Whole mount *in situ* hybridisation was performed to detect expression of Na^+ K^+ *ATPase*, a gene expressed in the proximal, intermediate and distal tubules. Control *βgal* mRNA injected embryos had normal tubule development (A and C). Injection of 2 ng *Radical fringe* mRNA severely disrupted development of the tubules, causing ectopic tubulogenesis (highlighted with white arrows) (B). Over-expression of 1 ng *Lunatic fringe* mRNA had the opposite effect, inhibiting tubulogenesis completely (D).

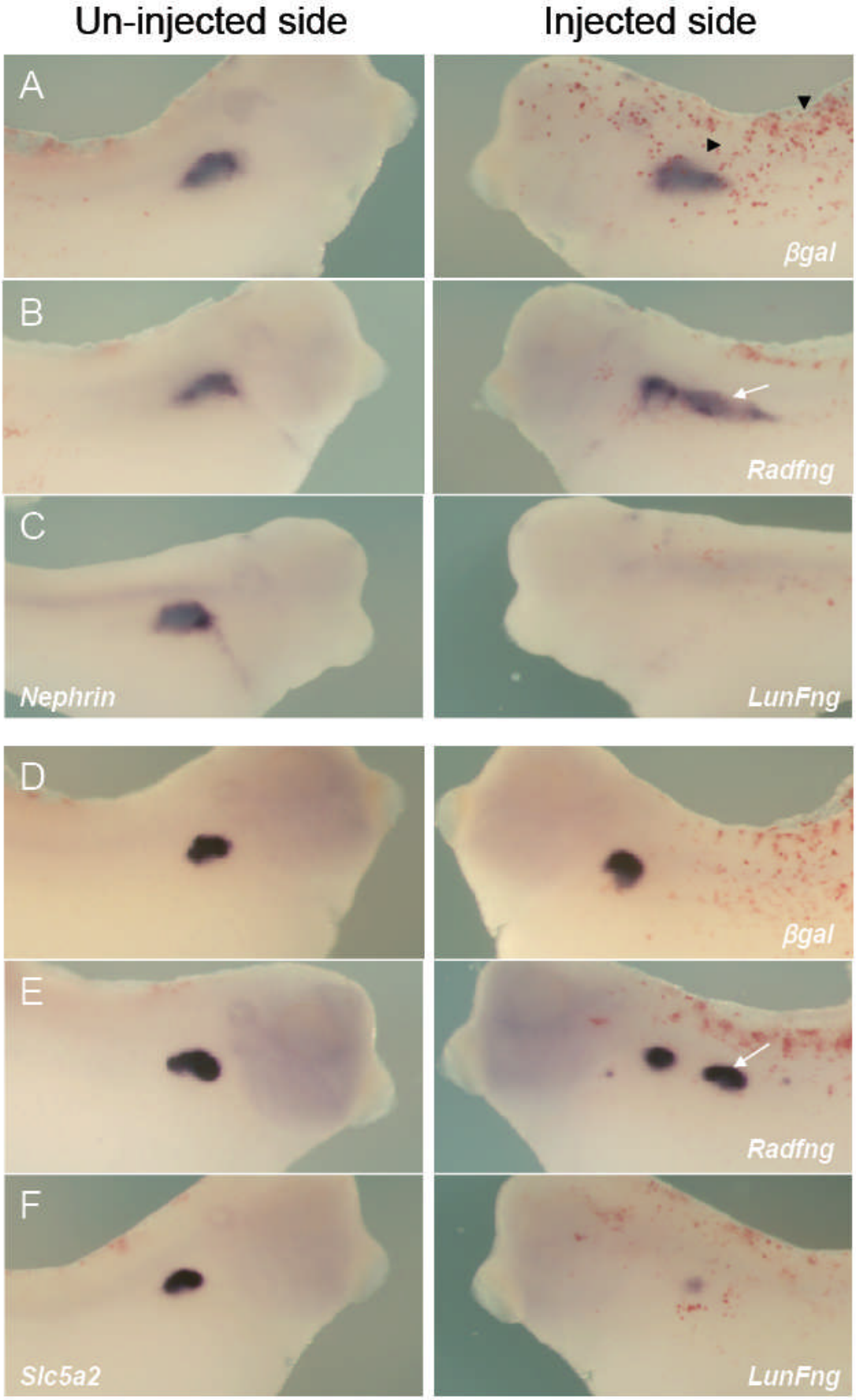
Un-injected side
Injected side
A
βgal
B
Radfng
C
Nephrin
LunFng
D
βgal
E
Radfng
F
Slc5a2
LunFng

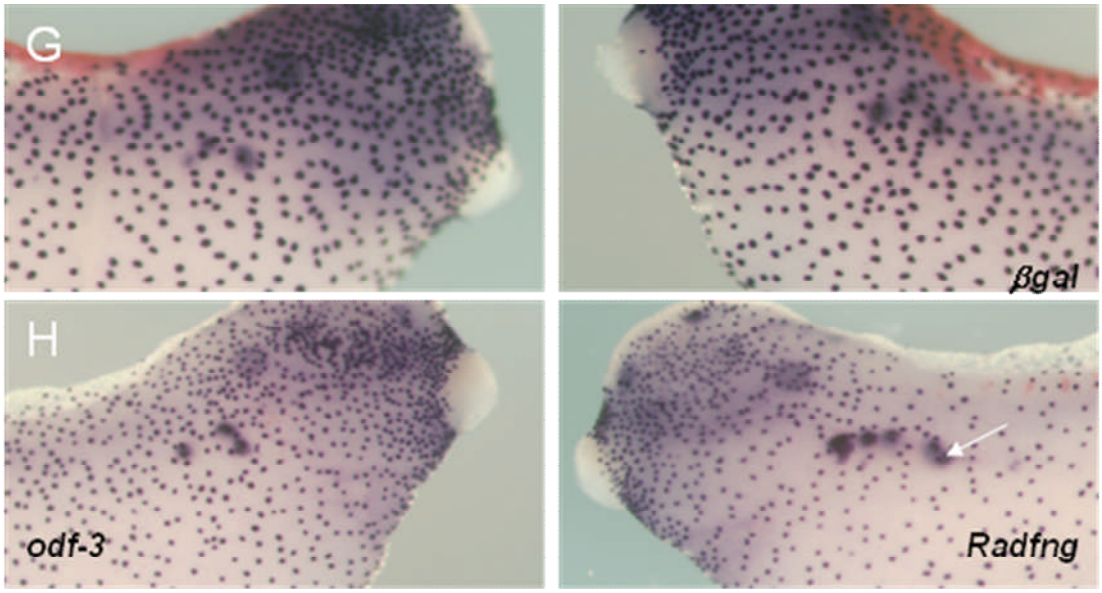

Figure 6.6 Over-expression of *Radical fringe* caused ectopic glomus, nephrostome and proximal tubule formation. Over-expression of *Lunatic fringe* inhibited formation of the glomus and proximal tubules. *X. laevis* embryos were injected at the 8 cell stage into a ventro-vegetal blastomere to target the presumptive pronephric region. mRNA was co-injected with *βgal* mRNA to act as a lineage tracer (red staining, black arrowheads). Embryos were cultured till stage 32 and then fixed. Whole mount *in situ* hybridisation was performed to detect expression of *nephrin*, a marker of the glomus, *slc5a2*, a marker of the proximal tubules, and *odf-3*, a marker of the nephrostomes. Control *βgal* mRNA injected embryos had normal tubule development (A, D and G). Injection of 2 ng *Radical fringe* mRNA severely disrupted development of the pronephros. Ectopic glomus (B), proximal tubule (E) and nephrostome (H) formation was observed (highlighted with white arrows). Injection of 500 pg *Lunatic fringe* mRNA inhibited expression of *nephrin* (C) and *slc5a2* (F).

over-expression of *Radical fringe*. Unlike injection of *Notch-ICD* mRNA, *Radical fringe* mRNA caused ectopic staining of 4A6 (63%, n=41), as well as 3G8 (93%, n=41). Frequently the proximal pronephric domain would be duplicated in the distal region (Fig 6.7Bi-iii). The most extreme phenotype is shown in Figure 6.7Biv where a large amount of ectopic proximal and distal pronephric structures across the entire length of the pronephros was present. Additionally, we never observed ectopic 3G8 staining ventral to ectopic 4A6 staining, suggesting that, despite the Notch signalling pathway being involved in regulation of the lateral-medial axis of the proximal pronephros, it is not required for formation of the dorsal-ventral boundary in the lateral pronephric mesoderm. Injection of the *βgal* lineage tracer had no effect on the development of any region of the pronephros (see Figures and appendix 4).

Over-expression of *Lunatic fringe* would be expected to yield identical phenotypes to *Radical fringe* over-expression as both proteins have homologous function and share 63% amino acid sequence identity (81% of amino acids have functionally similar side chain identities). Furthermore apart from *Lunatic fringe* having a higher affinity for fucosylated EGF repeats on the Notch receptor (Rampal et al., 2005), no difference in function between the three mammalian *fringe* genes, *Lunatic*, *Radical* and *Manic fringe*, has been discerned. Surprisingly, we observed complete inhibition of pronephrogenesis after over-expression of *Lunatic fringe*. Embryos were less tolerant of injected *Lunatic fringe* mRNA than *Radical fringe* mRNA. Injection of more than 500 pg of *Lunatic fringe* mRNA was lethal during neurogenesis (stages 12-18). Overall development in these embryos was severely disrupted, frequently the embryos would curl towards the injected side and somitogenesis appeared grossly abnormal on the injected side.

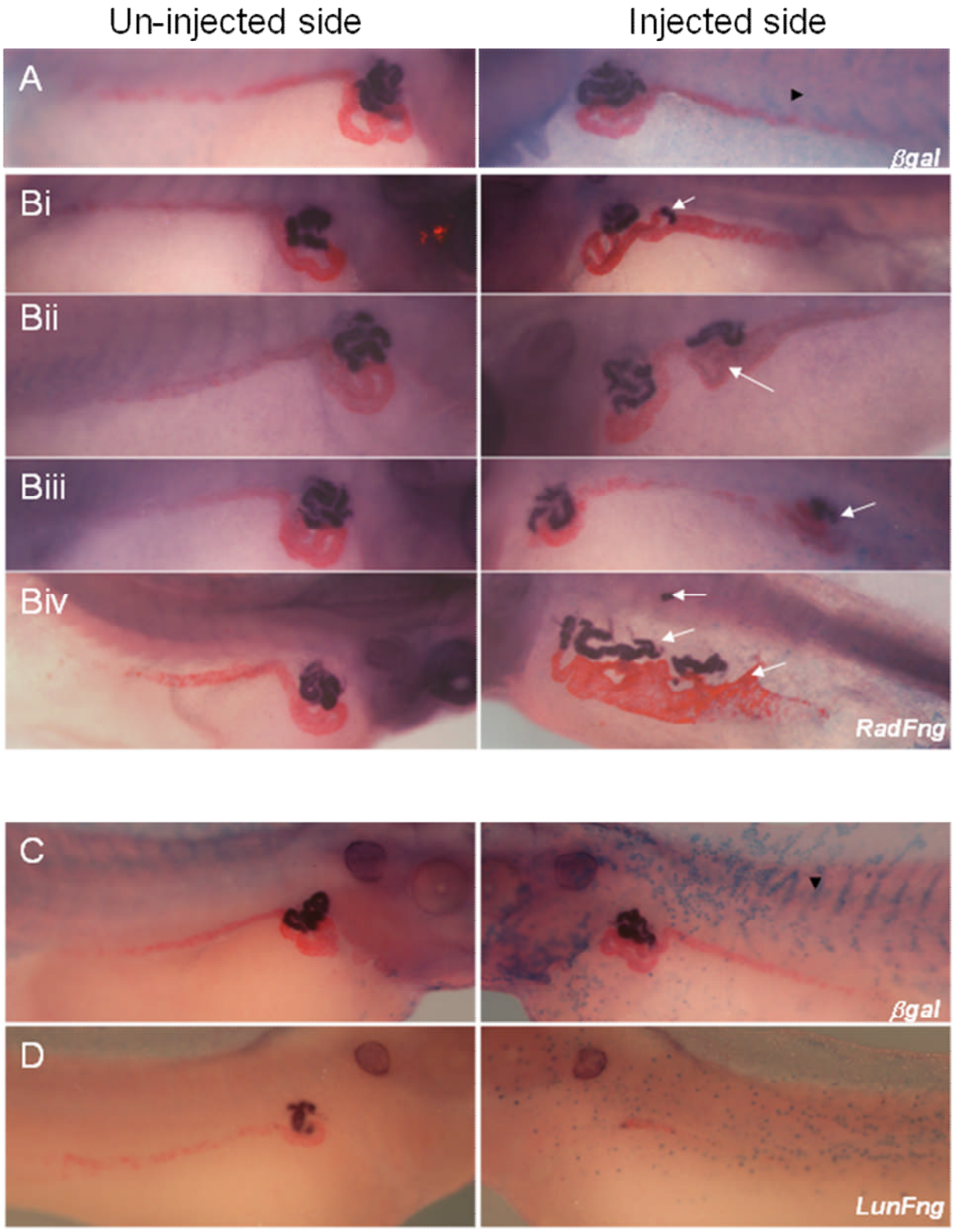
Un-injected side
Injected side
A
βgal
Bi
Bii
Biii
Biv
RadFng
C
βgal
D
LunFng

Figure 6.7 Over-expression of *Lunatic* and *Radical fringe* affected pronephrogenesis. *X. laevis* embryos were injected at the 8 cell stage into a ventro-vegetal blastomere to target the presumptive pronephric region. mRNA was co-injected with *βgal* mRNA to act as a lineage tracer (blue staining, black arrowheads). Embryos were cultured till stage 41 and then fixed. Whole mount antibody staining was performed to detect epitopes bound by 3G8 (proximal tubules and nephrostomes) and 4A6 (intermediate and distal tubules). Control *βgal* mRNA injected embryos had normal tubule development (A and C). Injection of 2 ng *Radical fringe* mRNA severely disrupted development of the pronephros, causing ectopic 3G8 and 4A6 staining (highlighted with white arrows) (Bi-iv). Over-expression of 1 ng *Lunatic fringe* mRNA had the opposite effect, inhibiting pronephrogenesis completely (D).

Pronephric over-expression of *Lunatic fringe* mRNA inhibited formation of the tubules. 85% of embryos had reduced *Na^+ K^+ ATPase* expression (Fig 6.5D, n=26), and 95% of embryos had reduced *slc5a2* expression (Fig 6.6F, n=19). Glomus formation, detected by *nephrin in situ* hybridisation, was reduced in 88% of embryos (Fig 6.6C, n=17). At stage 41, 3G8/ 4A6 staining highlighted nephrostome and tubule formation was reduced in 75% of embryos (Fig 6.7D, n=36). A more severe effect on 3G8 staining was detected, 51% of the embryos affected had completely absent 3G8 staining, whereas only 19% of affected embryos had completely absent 4A6 staining. In conclusion over-expression of *Lunatic fringe* inhibited formation of all regions of the pronephros.

6.2.3 Knock-down of *Radical fringe* had no effect on pronephros development, knock-down of *Lunatic fringe* inhibited pronephros development

Loss-of-function phenotypes prove that a gene is required for a specific process. Gain-of-function phenotypes do not as they may induce a developmental effect that does not occur naturally, thus the phenotype is a false-positive. Therefore we designed MOs to knock-down expression of *Radical* and *Lunatic fringe* and observe the effects this had on pronephrogenesis.

We injected 20 ng of each MO into a ventro-vegetal blastomere to target the future pronephros (see Figure 6.4A-C for MO sequences). Embryos were injected along with *βgal* mRNA to act as a lineage tracer and controls were injected with 20 ng of a random *Control* MO. Embryos were cultured to various stages of development, fixed, stained for the lineage tracer, sorted for those embryos that were correctly targeted and then stained by either *in situ* hybridisation or antibody staining

for markers of distinct regions of the pronephros. Pronephric phenotypes were detected by comparing the pronephric structure on the injected and un-injected sides. All results described as producing a phenotype were calculated as statistically significant within 95% confidence limits.

Injection of 20 ng of *Radical fringe* MO had no statistically significant effect on development of any region of the pronephros. 20 ng *Radical fringe* MO caused 3% of embryos to have reduced *Na^+ K^+ ATPase* expression (Fig 6.8B, n=35), no embryos had reduced *nephrin* (Fig 6.9B, n=23) or *slc5a2* (Fig 6.9F, n=21) expression and whilst 20% of embryos had reduced *odf-3* expression (Fig 6.9J, n=25), this was a statistically insignificant difference from the *Control* MO injected embryos. Furthermore immunostaining of the mature pronephros with 3G8/ 4A6 antibodies was not affected by injection of the *Radical fringe* MO (Fig 6.10B). A statistically insignificant 6% decrease in 3G8 staining and 2% decrease in 4A6 staining was observed (n=47). Analysis of embryos showed no gross developmental defects after injection of the *Radical fringe* MO, the embryos developed normally and there was nearly no death as a consequence of injection. In conclusion *Radical fringe* is not required for normal development of the pronephros during embryogenesis.

Injection of both *Lunatic fringe* MO1 and MO2 inhibited formation of all compartments of the pronephros. Injection of more than 5 ng of either MO was lethal, highlighting the importance of *Lunatic fringe* during development. *Na^+ K^+ ATPase* expression was reduced in every embryo injected with either *Lunatic fringe* MO1 (Fig 6.8D, n=21) or MO2 (Fig 6.8E, n=18). 3G8 antibody staining was reduced in 93% embryos injected with MO1 (Fig 6.10D) and 77% of embryos injected with

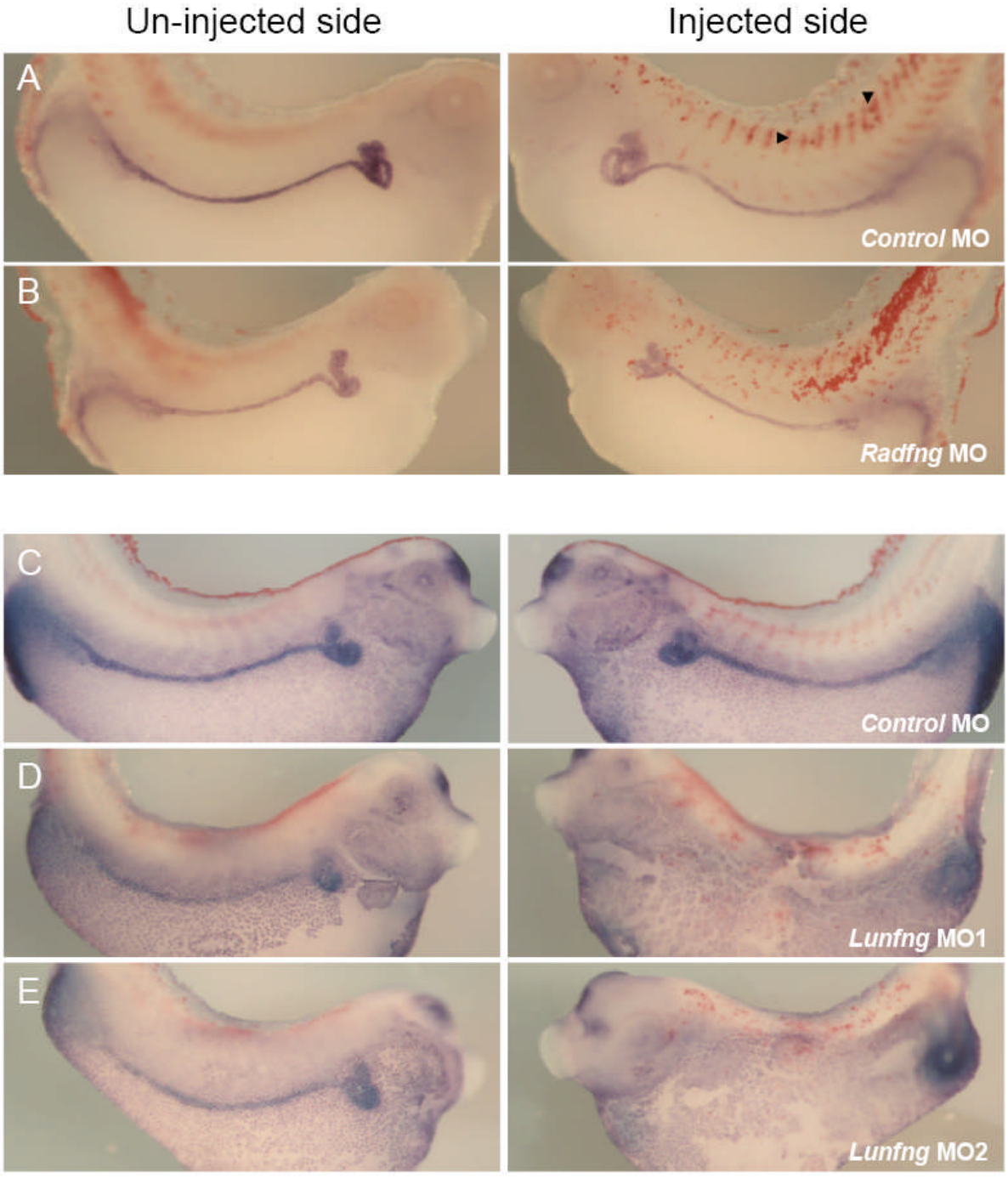
Un-injected side
Injected side
A
Control MO
B
Radfng MO
C
Control MO
D
Lunfng MO1
E
Lunfng MO2

Figure 6.8 Knock-down of *Lunatic* and *Radical fringe* endogenous translation using MOs had differing effects on pronephrogenesis. *X. laevis* embryos were injected at the 8 cell stage into a ventro-vegetal blastomere to target the presumptive pronephric region. MOs were co-injected with *βgal* mRNA to act as a lineage tracer (red staining, black arrowheads). Embryos were cultured till stage 36 and then fixed. Whole mount *in situ* hybridisation was performed to detect expression of Na^+ K^+ *ATPase*, a gene expressed in the proximal, intermediate and distal tubules. 20 ng *Control* MO injected embryos had normal tubule development (A and C). Injection of 20 ng *Radical fringe* MO had no effect on development of the tubules (B). Knock-down of endogenous *Lunatic fringe* mRNA after injection of either 5 ng *Lunatic fringe* MO1 (D) or 5 ng *Lunatic fringe* MO2 inhibited tubulogenesis completely (E).

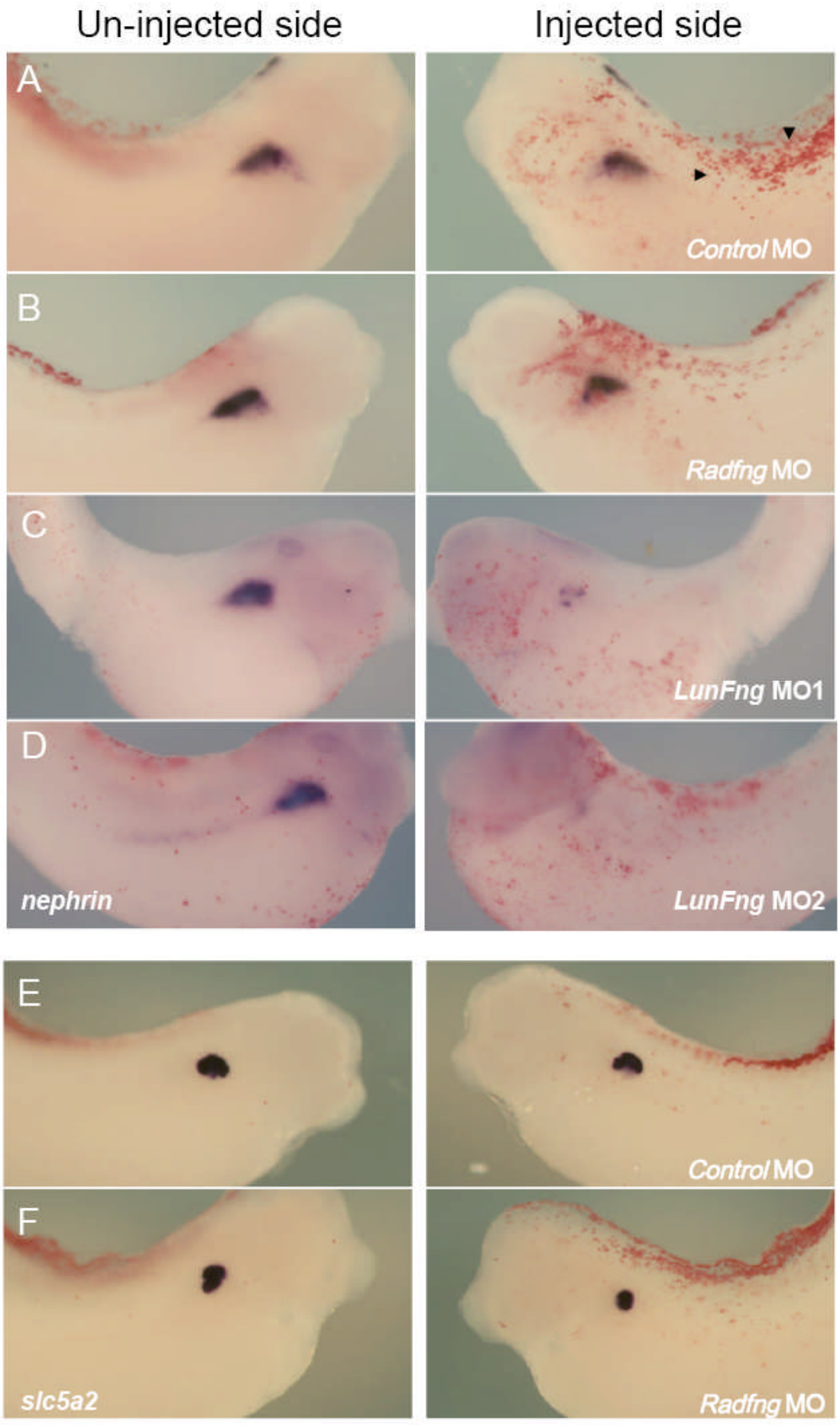
Un-injected side
Injected side
A
Control MO
B
Radfng MO
C
LunFng MO1
D
nephrin
LunFng MO2
E
Control MO
F
slc5a2
Radfng MO

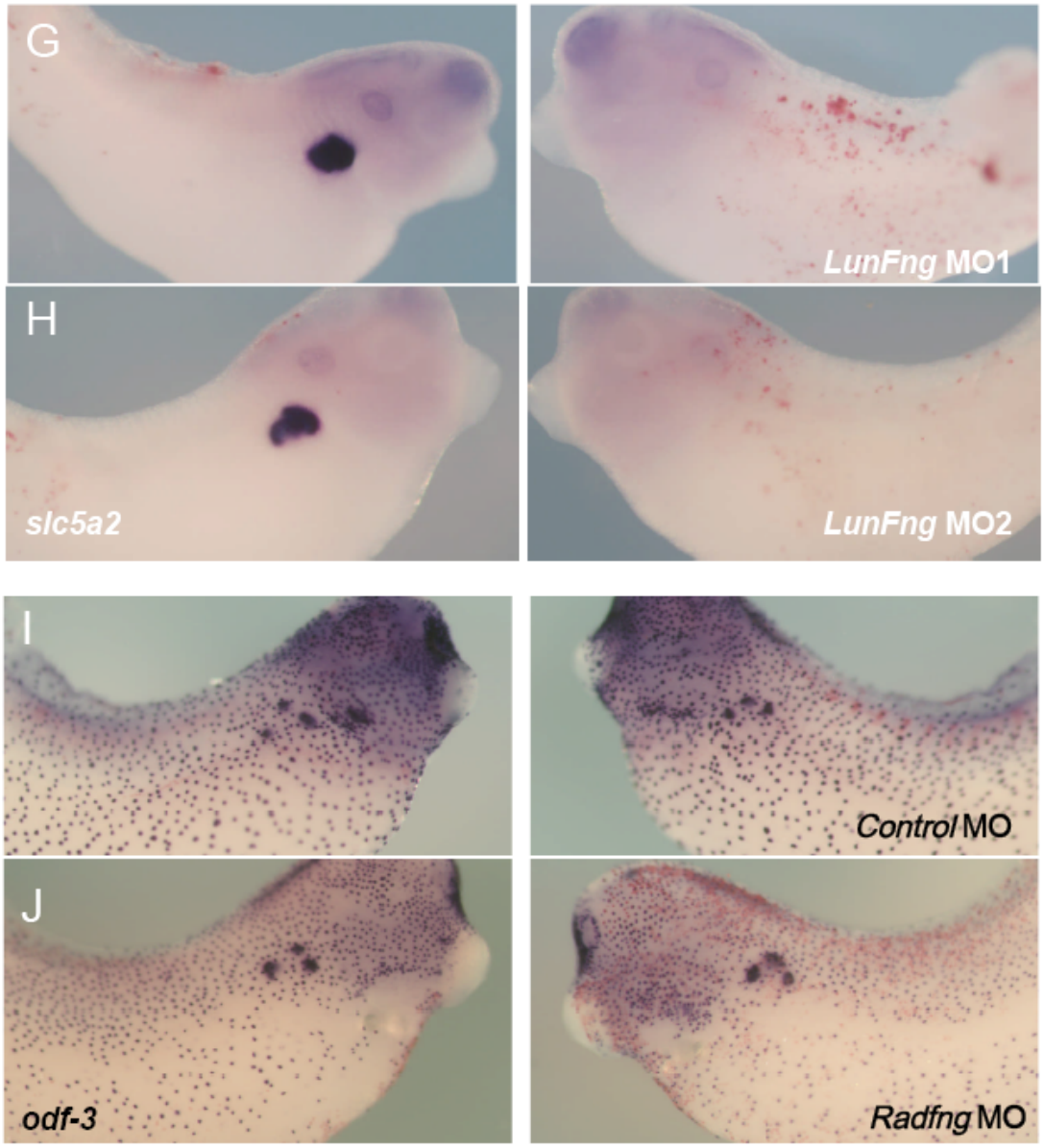

Figure 6.9 MO knock-down of endogenous *Radical fringe* mRNA translation had no effect on glomus, nephrostome or proximal tubule formation. Depletion of Lunatic fringe inhibited formation of all regions of the pronephros *X. laevis* embryos were injected at the 8 cell stage into a ventro-vegetal blastomere to target the presumptive pronephric region. MOs were co-injected with *βgal* mRNA to act as a lineage tracer (red staining, black arrowheads). Embryos were cultured till stage 32 and then fixed. Whole mount *in situ* hybridisation was performed to detect expression of *nephrin*, a marker of the glomus, *slc5a2*, a marker of the proximal tubules, and *odf-3*, a marker of the nephrostomes. *Control* MO injected embryos had normal tubule development (A, E and I). Injection of 20 ng *Radical fringe* MO had no statistically significant effect on glomus (B), proximal tubule (F) or nephrostome (K) development. Injection of 5 ng of either *Lunatic fringe* MO inhibited glomus (C and D) and proximal tubule (G and H) development. (NB: C and D are taken from Fig 6.13 and G and H from Fig 6.14, they have been reproduced in this figure for continuity in the text.)

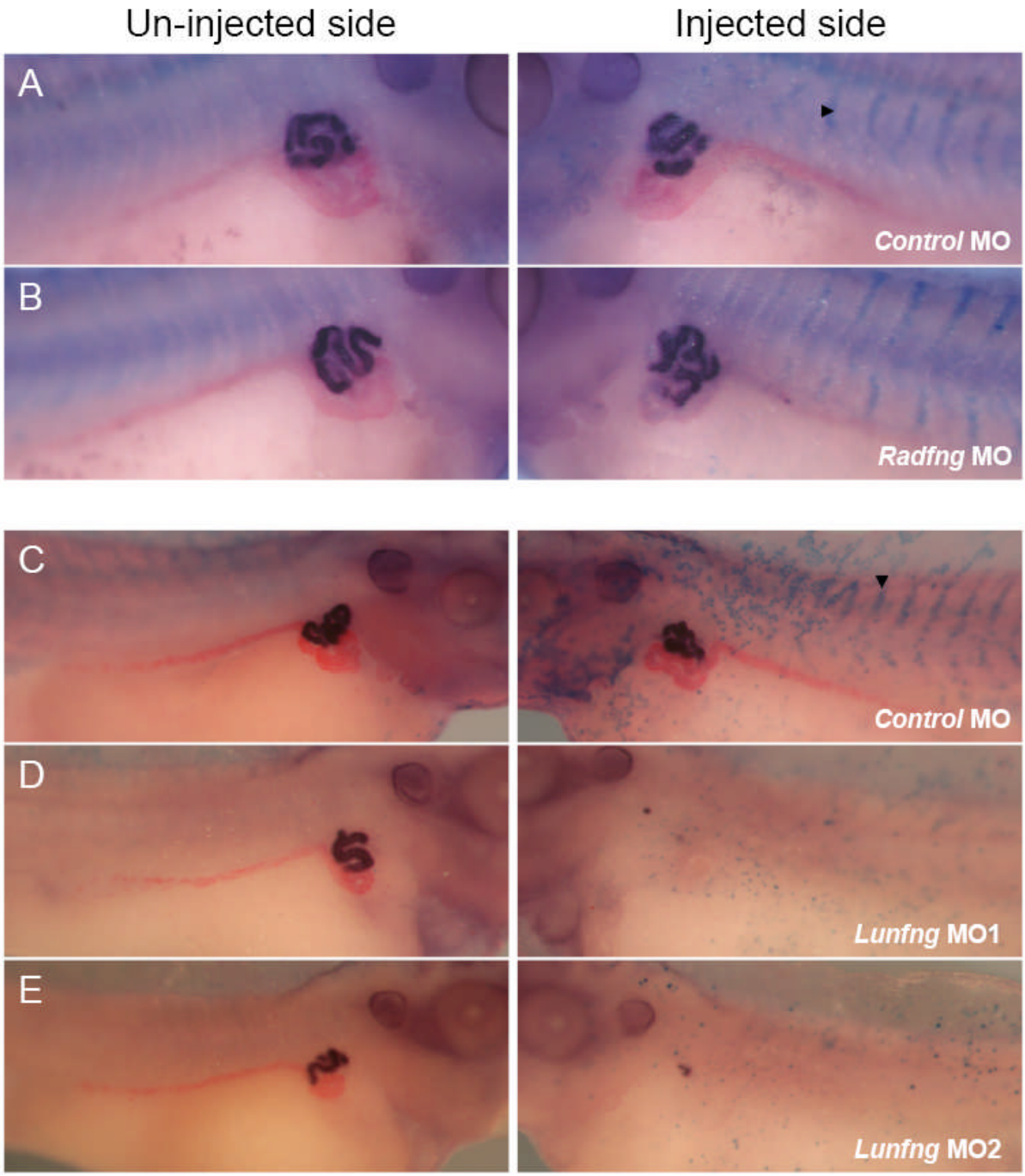
Un-injected side
Injected side
A
Control MO
B
Radfng MO
C
Control MO
D
Lunfng MO1
E
Lunfng MO2

Figure 6.10 Knock-down of *Lunatic* and *Radical fringe* endogenous translation using MOs had differing effects on pronephrogenesis. *X. laevis* embryos were injected at the 8 cell stage into a ventro-vegetal blastomere to target the presumptive pronephric region. MOs were co-injected with *βgal* mRNA to act as a lineage tracer (blue staining, black arrowheads). Embryos were cultured till stage 41 and then fixed. Whole mount antibody staining was performed using 3G8/ 4A6, which detect epitopes in the proximal tubules and nephrostomes (3G8, stained purple) and the intermediate and distal tubules (4A6, stained red). 20 ng *Control* MO injected embryos had normal pronephros development (A and C). Injection of 20 ng *Radical fringe* MO had no effect on development of the pronephros (B). Knock-down of endogenous *Lunatic fringe* mRNA after injection of either 5 ng *Lunatic fringe* MO1 (D) or 5 ng *Lunatic fringe* MO2 inhibited tubulogenesis completely (E).

MO2 (Fig 6.10E). Similarly, 4A6 staining was reduced in 85% of embryos injected with MO1 and 81% of embryos injected with MO2. *nephrin* expression was reduced in 95% of embryos injected with *Lunatic fringe* MO1 (Fig 6.9C, n=19) and 78% of embryos injected with *Lunatic fringe* MO2 (Fig 6.9D, n=18). Likewise proximal tubulogenesis, detected by *in situ* hybridisation for *slc5a2*, was reduced in 93% of embryos injected with *Lunatic fringe* MO1 (Fig 6.9F, n=14) and 58% of embryos injected with *Lunatic fringe* MO2 (Fig 6.9G, n=19). Gross development of embryos injected with either MO was severely affected; the embryos were malformed, frequently curled towards the injected side and failed to form an appropriately structured tail (see Fig 6.9G as an example of an abnormal embryo observed after *Lunatic fringe* MO2 injection).

6.2.4 Pronephric phenotypes induced by the *Lunatic fringe* MOs can be rescued

In order to observe the specificity of a MO, rescue of any phenotype must be achieved. From our *in vitro* translation analysis of the *Lunatic fringe* MOs, we observed translation of *Lunatic fringe* mRNA, synthesised from the ORF encoding cDNA clone, was not inhibited by *Lunatic fringe* MO2 (Fig 6.4E, lane 3). Furthermore, neither *Lunatic fringe* MO1 nor *Lunatic fringe* MO2 inhibited translation of *Radical fringe* mRNA (Fig 6.4E, lanes 5 and 6). In conclusion *Lunatic fringe* mRNA can be used to attempt rescue of the *Lunatic fringe* MO2 phenotype, and *Radical fringe* mRNA, as Radical fringe shares functional homology with Lunatic fringe, can be used to rescue the phenotypes caused by both *Lunatic fringe* MOs. In order to see if rescue was achievable, 5 ng of either *Lunatic fringe* MO1 or MO2 was co-injected with 2 ng *Radical fringe* mRNA, and 5 ng *Lunatic fringe* MO2 was co-injected with 0.5 ng *Lunatic fringe* mRNA. Embryos were injected into a V2

blastomere, to target the future pronephros, at the 8-cell stage along with *βgal* mRNA, to act as a lineage tracer. Embryos were left to develop to stage 32, fixed, stained for the lineage tracer, sorted for correct targeting to the pronephros and then *in situ* hybridised for *nephrin* (a marker of the medial pronephric mesoderm) and *slc5a2* (a marker of the lateral pronephric mesoderm).

As observed in section 6.2.2, injection of *Lunatic fringe* mRNA caused 86% of embryos to have reduced *nephrin* expression (Fig 6.11B, n=21). Similarly, *Lunatic fringe* MO2 inhibited *nephrin* expression in 87% of embryos (Fig 6.11C, n=24). These phenotypes were statistically significantly different from the *Control* MO injected embryos, where only 5% of embryos had reduced *nephrin* expression ($p<0.05$, Fig 6.11A, n=19). Upon co-injection of *Lunatic fringe* mRNA with *Lunatic fringe* MO2, 40% of embryos had reduced *nephrin* expression (Fig 6.11D, n=20). Whilst this result remains a statistically significant reduction in *nephrin* expression when compared to the *Control* MO injected embryos, it represents a reduction in the prevalence of the phenotype induced by either *Lunatic fringe* mRNA or *Lunatic fringe* MO2 single injections. In conclusion there is a partial rescue of the phenotype of *Lunatic fringe* MO2 upon co-injection with *Lunatic fringe* mRNA.

As well as observing if *Lunatic fringe* mRNA is able to rescue the effects of *Lunatic fringe* MO2 on *nephrin* expression, we also observed if *slc5a2* expression could be rescued (Fig 6.12). Injection of 20 ng *Control* MO reduced *slc5a2* expression in 12% of embryos (Fig 6.12A, n=17). Injection of either *Lunatic fringe* mRNA (100% reduced, Fig 6.12B, n=12) or *Lunatic fringe* MO2 (95% reduced, Fig 6.12C, n=20) had a severe effect on proximal tubule formation indicated by almost

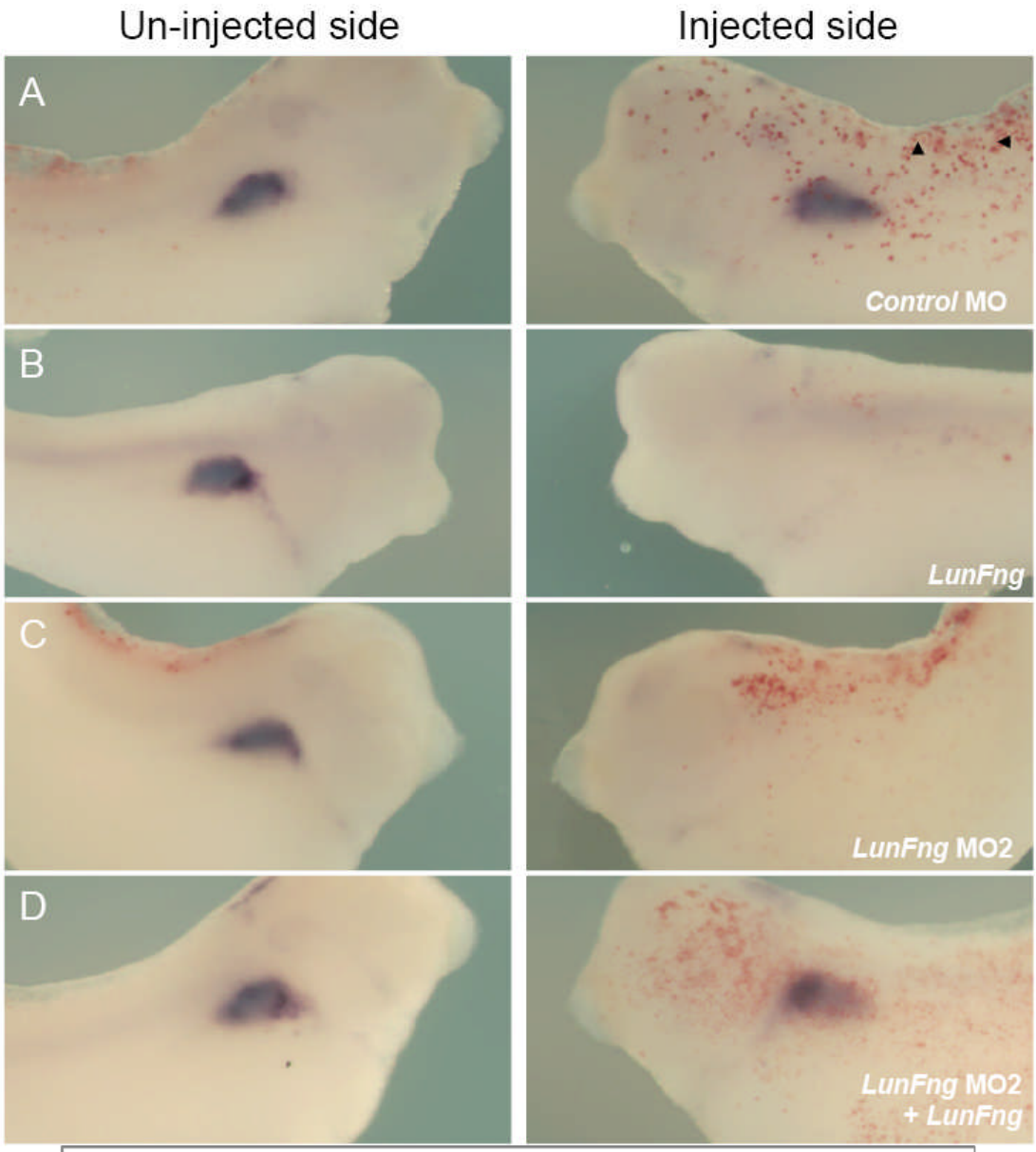
Un-injected side
Injected side
A
Control MO
B
LunFng
C
LunFng MO2
D
LunFng MO2
+ LunFng

E

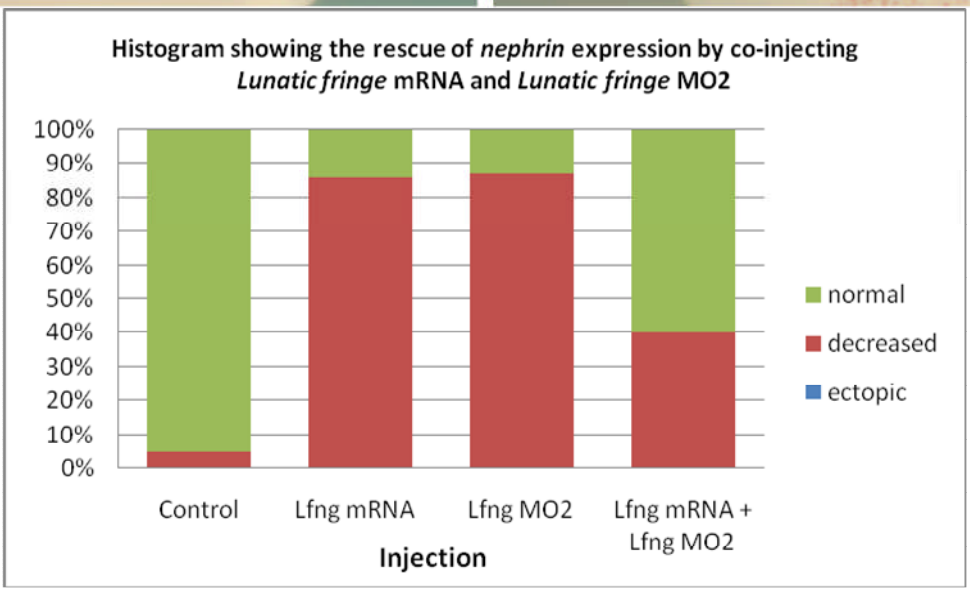
Histogram showing the rescue of nephrin expression by co-injecting Lunatic fringe mRNA and Lunatic fringe MO2
100%
90%
80%
70%
60%
50%
40%
30%
20%
10%
0%
Control
Lfng mRNA
Lfng MO2
Lfng mRNA + Lfng MO2
Injection
normal
decreased
ectopic

Figure 6.11 Phenotypic effects of depletion of *Lunatic fringe* expression can be rescued. *X. laevis* embryos were injected at the 8 cell stage into a ventro-vegetal blastomere to target the presumptive pronephric region. mRNA was co-injected with *βgal* mRNA to act as a lineage tracer (red staining, black arrowheads). Embryos were cultured till stage 34 and then fixed. Whole mount *in situ* hybridisation was performed to detect expression of *nephrin*, a marker of the glomus. *Control* MO injected embryos had normal glomus development (A). Injection of the *Lunatic fringe* mRNA (encoded from the ORF cDNA clone, hence does not have its translation inhibited by *Lunatic fringe* MO2) and *Lunatic fringe* MO2 inhibited glomus formation (B and C). Injection of *Lunatic fringe* mRNA with *Lunatic fringe* MO2 rescued the phenotypes observed in single injections, glomus development was restored (D). A histogram representing the spread of phenotypes after each injection is shown in E.

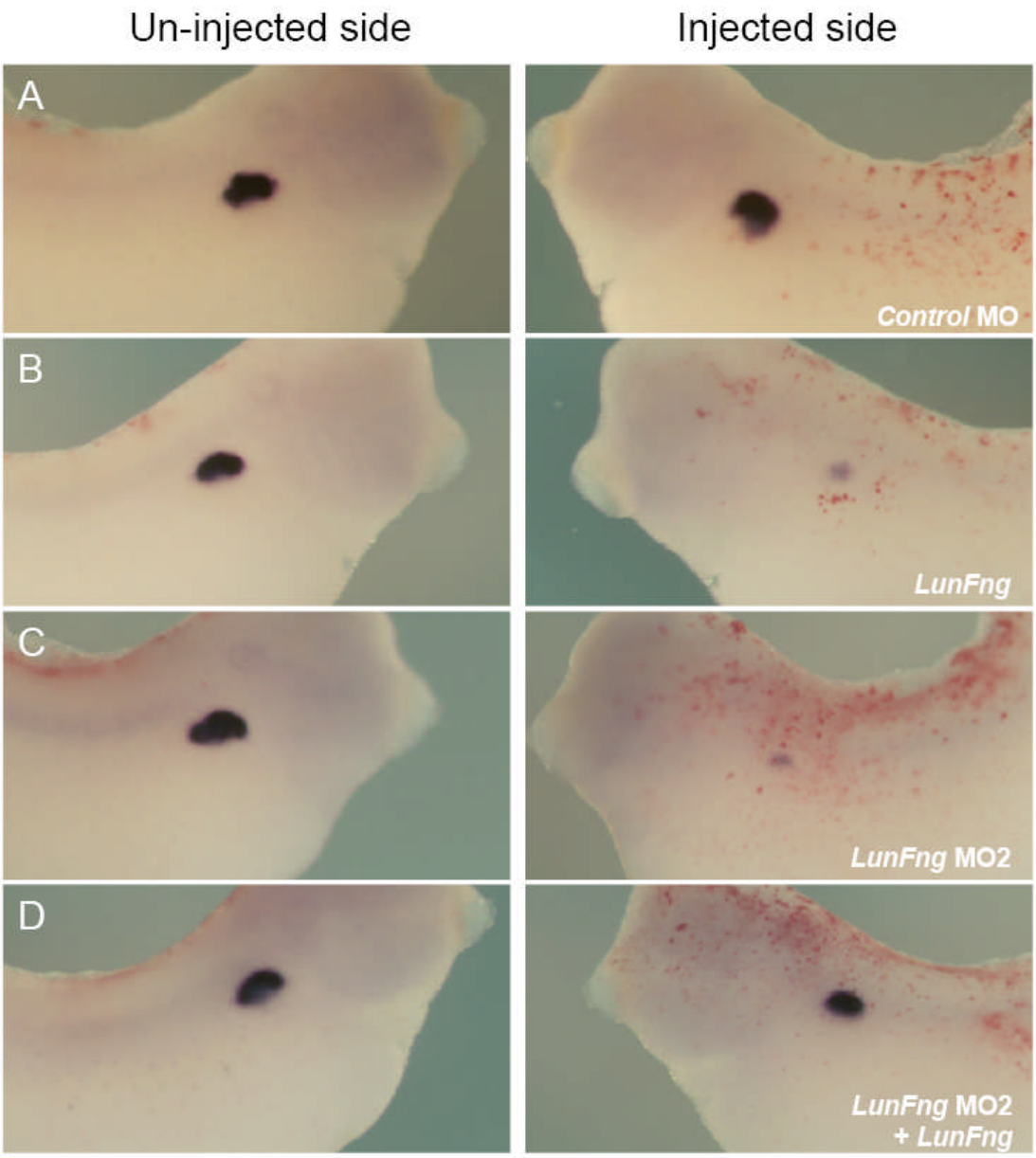
Un-injected side
Injected side
A
Control MO
B
LunFng
C
LunFng MO2
D
LunFng MO2
+ LunFng

E

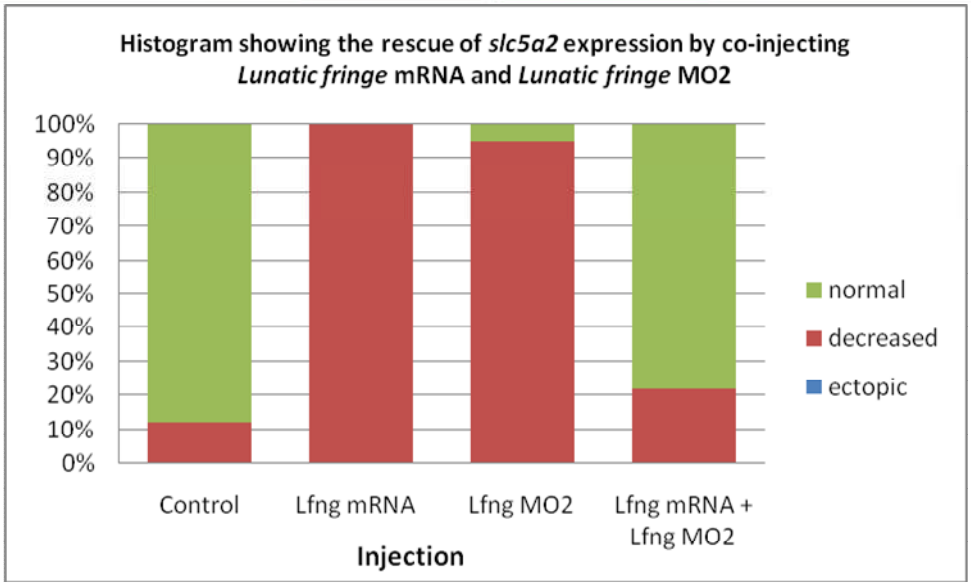
Histogram showing the rescue of slc5a2 expression by co-injecting Lunatic fringe mRNA and Lunatic fringe MO2
100%
90%
80%
70%
60%
50%
40%
30%
20%
10%
0%
Control
Lfng mRNA
Lfng MO2
Lfng mRNA + Lfng MO2
Injection
normal
decreased
ectopic

Figure 6.12 Phenotypic effects of depletion of *Lunatic fringe* expression on proximal tubulogenesis can be rescued. *X. laevis* embryos were injected at the 8 cell stage into a ventro-vegetal blastomere to target the presumptive pronephric region. mRNA was co-injected with *βgal* mRNA to act as a lineage tracer (red staining, black arrowheads). Embryos were cultured till stage 34 and then fixed. Whole mount *in situ* hybridisation was performed to detect expression of *Slc5a2*, a marker of the proximal tubules. *Control* MO injected embryos had normal proximal tubulogenesis (A). Injection of the *Lunatic fringe* mRNA (encoded from the ORF cDNA clone, hence does not have its translation inhibited by *Lunatic fringe* MO2) and *Lunatic fringe* MO2 inhibited proximal tubule formation (B and C). Injection of *Lunatic fringe* mRNA with *Lunatic fringe* MO2 rescued the phenotypes observed in single injections, proximal tubulogenesis was restored (D). A histogram representing the spread of phenotypes after each injection is shown in E.

complete loss of *slc5a2* expression on the injected side. Co-injection of 5 ng *Lunatic fringe* MO2 and 0.5 ng *Lunatic fringe* mRNA did not have a statistically significant effect on proximal tubulogenesis when compared to the control embryos, 22% of embryos had reduced *slc5a2* expression (Fig 6.12D, n=18). In conclusion, *slc5a2* expression can be almost completely rescued by co-injection of *Lunatic fringe* mRNA and *Lunatic fringe* MO2.

Co-injection of *Radical fringe* mRNA with either *Lunatic fringe* MO1 or MO2 rescued expression of *nephrin* (Fig 6.13). *Radical fringe* mRNA caused ectopic *nephrin* expression in 68% of embryos (Fig 6.13B, n=28), whereas *Lunatic fringe* MO1 inhibited *nephrin* expression in 95% of embryos (Fig 6.13C, n=19) and *Lunatic fringe* MO2 inhibited *nephrin* expression in 78% of embryos (Fig 6.13D, n=18). Co-injection of *Radical fringe* mRNA with *Lunatic fringe* MO1 reduced the number of embryos that had a smaller domain of *nephrin* expression to 42% (Fig 6.13E, n=33). Moreover, 27% of the embryos co-injected with *Radical fringe* mRNA and *Lunatic fringe* MO1 had ectopic *nephrin* expression. In conclusion, *Radical fringe* mRNA rescued the glomus phenotype induced by *Lunatic fringe* MO1; and in some cases caused an over-rescue of the phenotype, inducing ectopic glomus formation. Co-injection of *Radical fringe* mRNA with *Lunatic fringe* MO2 caused 51% of embryos to have reduced *nephrin* expression (Fig 6.13F, n=24). This is a smaller proportion to the number of embryos that had reduced *nephrin* expression after single injection of *Lunatic fringe* MO2, suggesting a partial rescue of the phenotype. As with the co-injection of *Radical fringe* mRNA and *Lunatic fringe* MO1, co-injection of *Radical fringe* mRNA and *Lunatic fringe* MO2 induced ectopic *nephrin* expression in a significant number of embryos (33%), suggesting *Radical fringe* mRNA over-

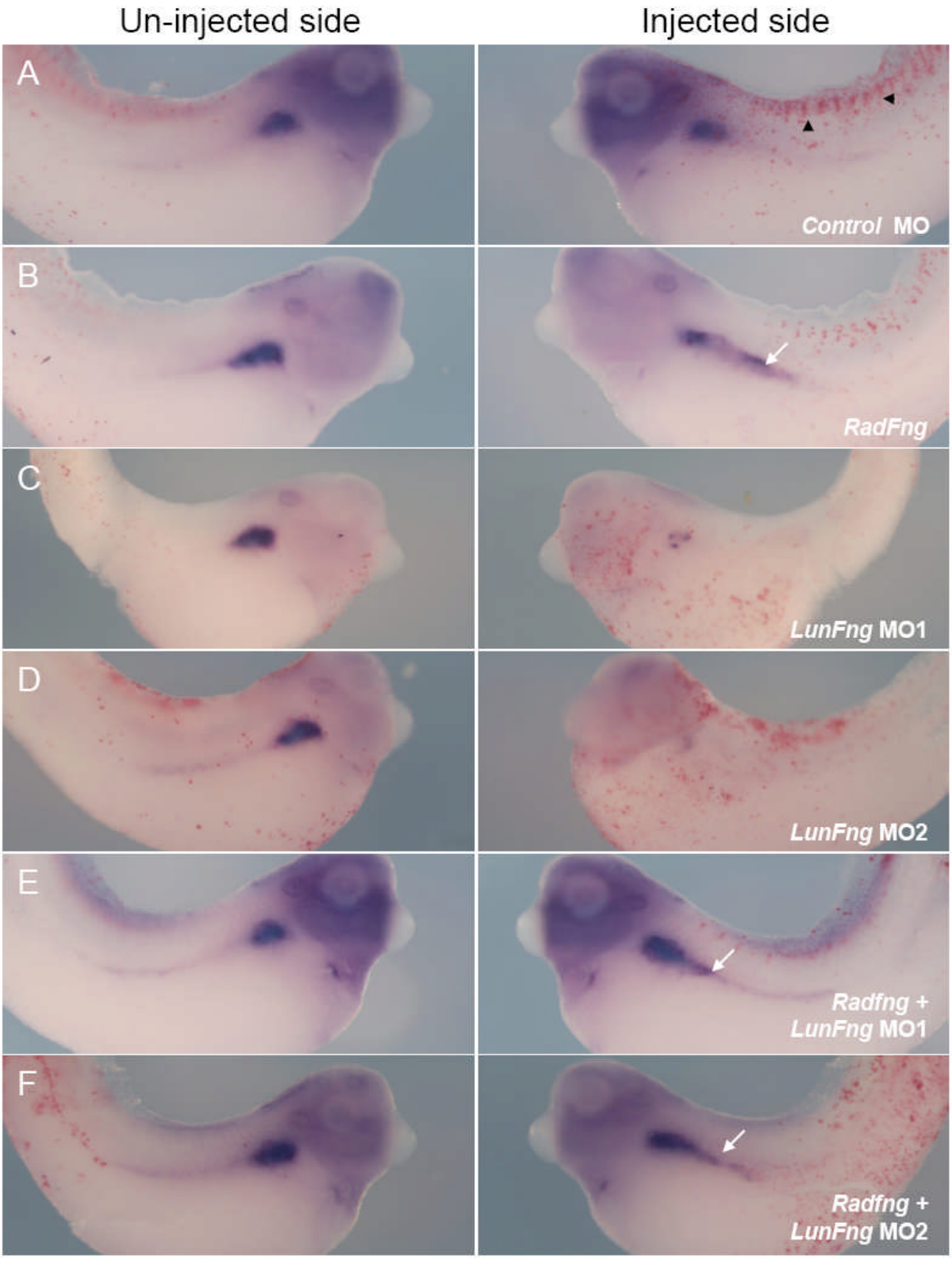
Un-injected side
Injected side
A
Control MO
B
RadFng
C
LunFng MO1
D
LunFng MO2
E
Radfng +
LunFng MO1
F
Radfng +
LunFng MO2

G

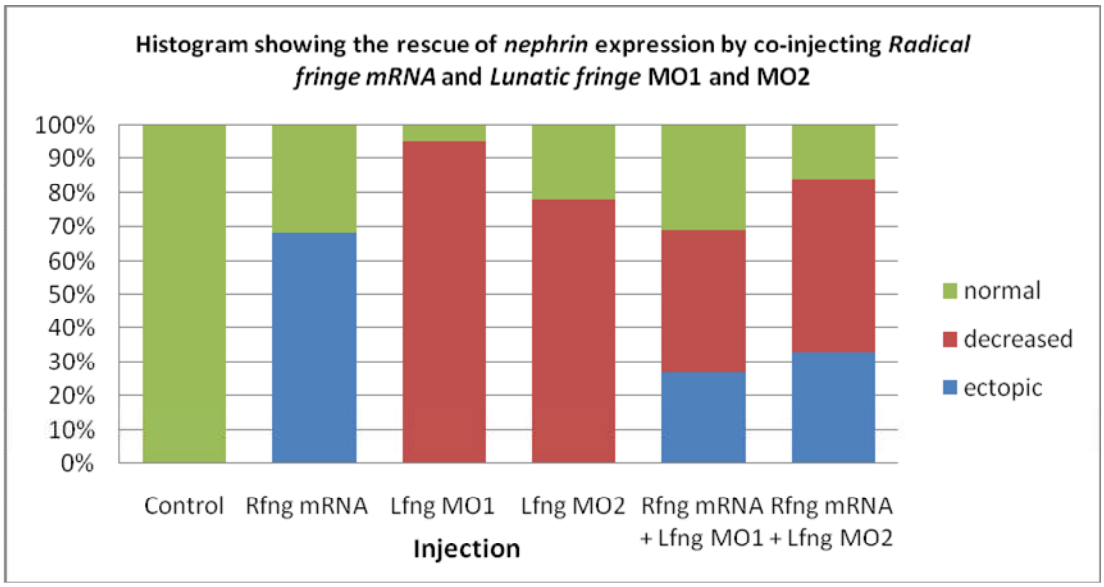

Figure 6.13 Phenotypic effects of depletion of *Lunatic fringe* expression on glomus formation can be rescued with exogenous *Radical fringe* mRNA. *X. laevis* embryos were injected at the 8 cell stage into a ventro-vegetal blastomere to target the presumptive pronephric region. mRNA was co-injected with *βgal* mRNA to act as a lineage tracer (red staining, black arrowheads). Embryos were cultured till stage 32 and then fixed. Whole mount *in situ* hybridisation was performed to detect expression of *Nephrin*, a marker of the glomus. *Control* MO injected embryos had normal glomus development (A). Injection of the 2 ng *Radical fringe* mRNA caused ectopic glomus formation (white arrows) (B). Injection of 5 ng *Lunatic fringe* MO1 or MO2 inhibited glomus formation (C and D). Co-injection of 2 ng Radical fringe mRNA with 5 ng *Lunatic fringe* MO1 or MO2 rescued the phenotypes observed in single MO injections, indeed ectopic glomus development was still observed (white arrows) (E and F). A histogram representing the spread of phenotypes after each injection is shown in G.

rescued the phenotype. General observation of the embryos co-injected with *Radical fringe* mRNA and either *Lunatic fringe* MO1 or MO2 showed that development was not so grossly affected as the single injections of the *Lunatic fringe* MOs. Additionally, no embryos had absent *nephrin* expression when co-injected with *Radical fringe* mRNA, highlighting a reduction in the severity of the phenotypes caused by the single injections of *Lunatic fringe* MOs (a third of embryos scored with reduced *nephrin* expression after injection of *Lunatic fringe* MO1 had completely absent glomus formation). In conclusion *Radical fringe* mRNA is able to rescue the effects of either *Lunatic fringe* MO on *nephrin* expression.

We next observed if co-injection of *Radical fringe* mRNA with either *Lunatic fringe* MO1 or MO2 could rescue expression of *slc5a2*, a marker of the lateral pronephric mesoderm (Fig 6.14). Single injection of *Radical fringe* mRNA caused ectopic expression of *slc5a2* on the injected side of 78% of embryos (Fig 6.14B, n=49). Injection of *Lunatic fringe* MO1 (Fig 6.14C, 93% reduced, n=14) and *Lunatic fringe* MO2 (Fig 6.14D, 58% reduced, n=19) inhibited expression of *slc5a2*. Co-injection of *Radical fringe* mRNA with *Lunatic fringe* MO1 almost completely rescued the reduction phenotype of the single *Lunatic fringe* MO1 injection, only 3% of embryos had reduced *slc5a2* expression (Fig 6.14E, n=30). As was observed with *nephrin* expression, *slc5a2* expression was ectopic in 27% of embryos co-injected with *Radical fringe* mRNA and *Lunatic fringe* MO1. This result suggests *Radical fringe* over-expression completely rescued the *slc5a2* phenotype of embryos injected with *Lunatic fringe* MO1, indeed in some embryos there was an over-rescue. *Radical fringe* mRNA co-injected with *Lunatic fringe* MO2 also rescued the phenotype of the single *Lunatic fringe* MO2 injection. 37% of embryos had reduced *slc5a2* expression

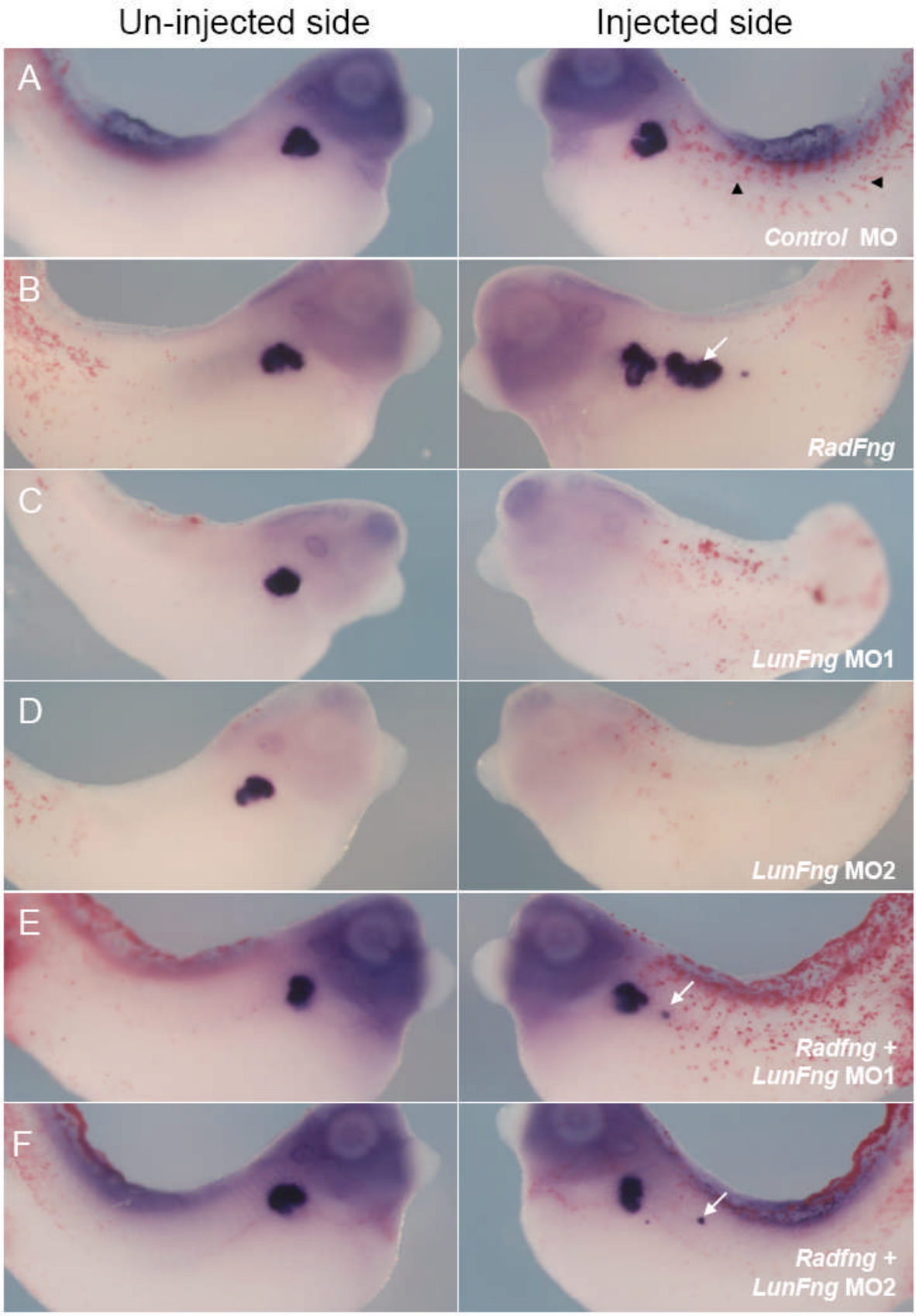
Un-injected side
Injected side
A
Control MO
B
RadFng
C
LunFng MO1
D
LunFng MO2
E
Radfng +
LunFng MO1
F
Radfng +
LunFng MO2

G

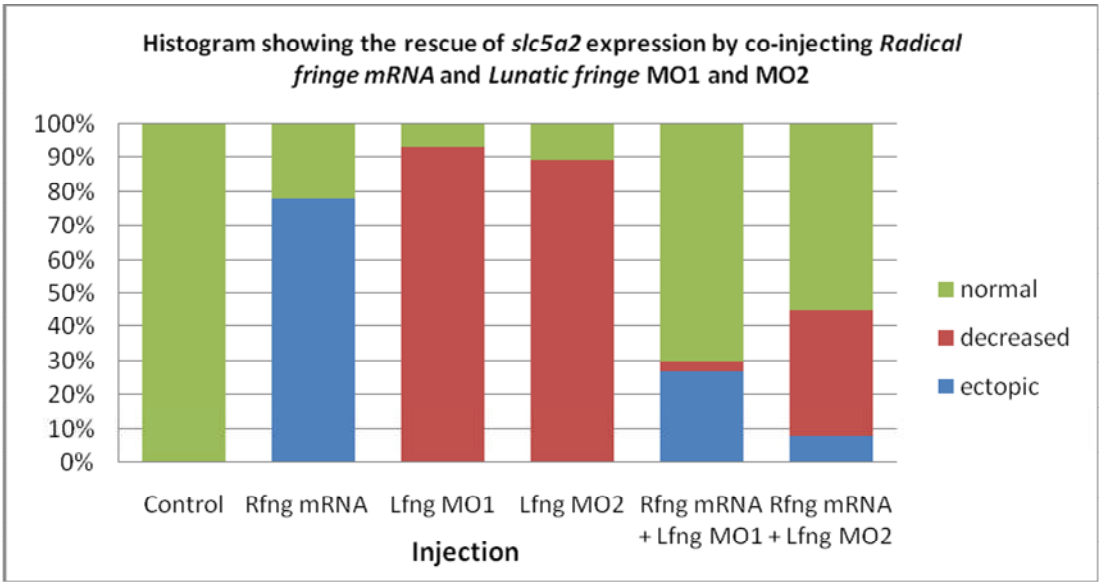

Figure 6.14 Phenotypic effects of depletion of *Lunatic fringe* expression proximal tubule formation can be rescued with exogenous mRNA. *X. laevis* embryos were injected at the 8 cell stage into a ventro-vegetal blastomere to target the presumptive pronephric region. mRNA was co-injected with *βgal* mRNA to act as a lineage tracer (red staining, black arrowheads). Embryos were cultured till stage 32 and then fixed. Whole mount *in situ* hybridisation was performed to detect expression of *Slc5a2*, a marker of the proximal tubules. *Control* MO injected embryos had normal proximal tubulogenesis (A). Injection of the 2 ng *Radical fringe* mRNA caused ectopic proximal tubule formation (white arrows) (B). Injection of 5 ng *Lunatic fringe* MO1 or MO2 inhibited proximal tubule development (C and D). Co-injection of 2 ng Radical fringe mRNA with 5 ng *Lunatic fringe* MO1 or MO2 rescued the phenotypes observed in single MO injections, indeed ectopic proximal tubule development was still observed (white arrows) (E and F). A histogram representing the spread of phenotypes after each injection is shown in G.

(Fig 6.14F, n=38), which is significantly different to the 58% of embryos that had reduced *slc5a2* expression in the single *Lunatic fringe* MO2 injection. Furthermore 8% of embryos had ectopic *slc5a2* expression. In conclusion there is a partial rescue of the effect *Lunatic fringe* MO2 has on proximal tubulogenesis when this MO is co-injected with *Radical fringe* mRNA.

We conclude that all phenotypes produced from injection of either *Lunatic fringe* MO1 and MO2 can be rescued by *Radical fringe* mRNA co-injection. Furthermore co-injection of *Lunatic fringe* mRNA is sufficient to partially rescue the effects of injecting *Lunatic fringe* MO2. Analysis of the empirical data, and general observation whilst scoring the experiments in the laboratory, highlighted a significant improvement in survival and development of embryos co-injected with *Lunatic fringe* MO1 or MO2 and *Radical*/ *Lunatic fringe* mRNA compared to single injections of *Lunatic fringe* MO1 and MO2. Taken together we believe the results we have attained strongly suggest both *Lunatic fringe* MOs specifically bind to and inhibit translation of endogenous *Lunatic fringe* transcripts *in vivo*.

6.2.5 Pronephric phenotypes induced by the *Lunatic fringe* MOs and over-expression may be due to inhibited myogenesis

We next aimed to see the effects *Lunatic* and *Radical fringe* over-expression and MO knock-down had on muscle formation, as myogenesis is necessary for pronephrogenesis (Seufert et al., 1999; Mauch et al., 2000; Mitchell et al., 2007). To observe this we repeated the ventro-vegetal (V2) blastomere injections described previously, let the embryos develop to stage 24 and then performed double *in situ*

hybridisation for expression of genes marking differentiated muscle (*MHC*) and pronephros anlagen (*Lim-1*).

Injection of the *Control* MO (n=43), *Radical fringe* MO (n=51) and *Radical fringe* mRNA (n=48) had 0% affect on *MHC* expression (Fig 6.15 A-C). 64% of embryos injected with *Lunatic fringe* mRNA had reduced *MHC* expression (n=25, Fig 6.16B), and every embryo injected with *Lunatic fringe* MO1 (n=19, Fig 6.16C) and *Lunatic fringe* MO2 (n=17, Fig 6.16D) had reduced *MHC* expression. In conclusion neither *Radical fringe* mRNA injection nor MO knock-down of *Radical fringe* expression had an effect on myogenesis. However, both over-expressing *Lunatic fringe* and knocking down translation of endogenous *Lunatic fringe* mRNA inhibited myogenesis.

Injection of the *Control* MO reduced expression of *Lim-1* expression on the injected side of 5% of embryos, compared to the un-injected side (Fig 6.15A). Similarly, the *Radical fringe* MO insignificantly reduced *Lim-1* expression in 2% of embryos (Fig 6.15C). *Radical fringe* over-expression disrupted formation of the pronephros anlagen, causing ectopic *Lim-1* expression in 27% of embryos (Fig 6.15B, white arrow). *Lunatic fringe* over-expression inhibited *Lim-1* expression in 76% of embryos (Fig 6.16B). As with their effect on *MHC* expression, every embryo injected with either *Lunatic fringe* MO1 or MO2 had reduced *Lim-1* expression, indeed every embryo scored had completely absent *Lim-1* expression on the injected side, indicating the severity of the phenotype (Fig 6.16B and 6.16C).

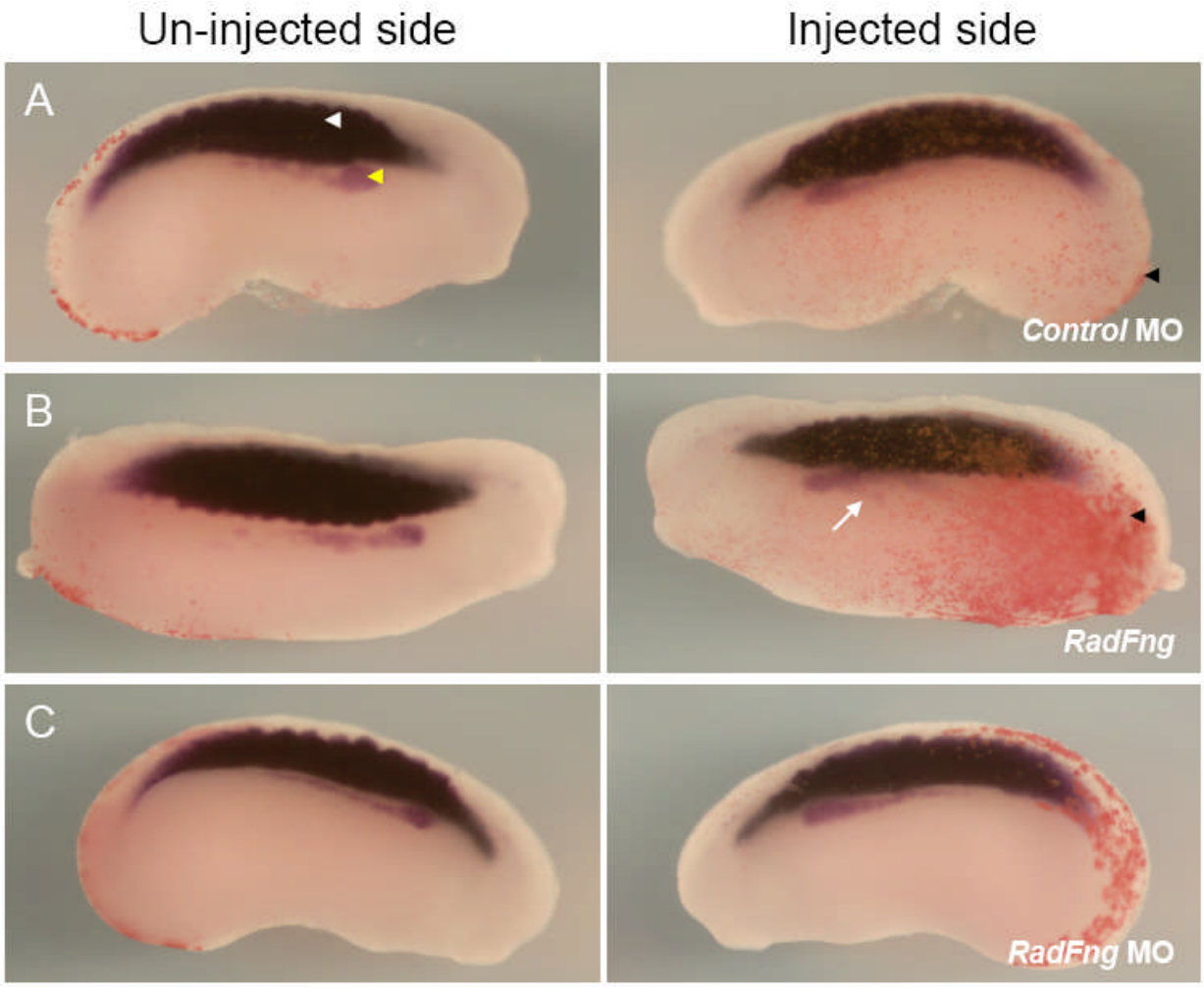

Figure 6.15 Knock-down of *Radical fringe* endogenous translation using a MO had no effect on somite formation or pronephros anlagen induction, but over-expression disrupted pronephros anlagen development. *X. laevis* embryos were injected at the 8 cell stage into a ventro-vegetal blastomere to target the presumptive pronephric region. MOs and mRNA were co-injected with *βgal* mRNA to act as a lineage tracer (red staining, black arrowheads). Embryos were cultured till stage 24 and then fixed. Whole mount double *in situ* hybridisation was performed to detect expression of *MHC* (white arrowhead), a gene expressed in differentiated somites, and *Lim-1* (yellow arrowhead), a gene expressed in the pronephros anlagen. 20 ng *Control* MO injected embryos had normal muscle and pronephros anlagen development (A). 2 ng *Radical fringe* mRNA had no obvious effect on muscle differentiation, but disrupted *Lim-1* expression, in some cases causing ectopic pronephros anlagen formation (white arrows) (B). Injection of 20 ng *Radical fringe* MO had no effect on development of the pronephros anlagen or muscle (C).

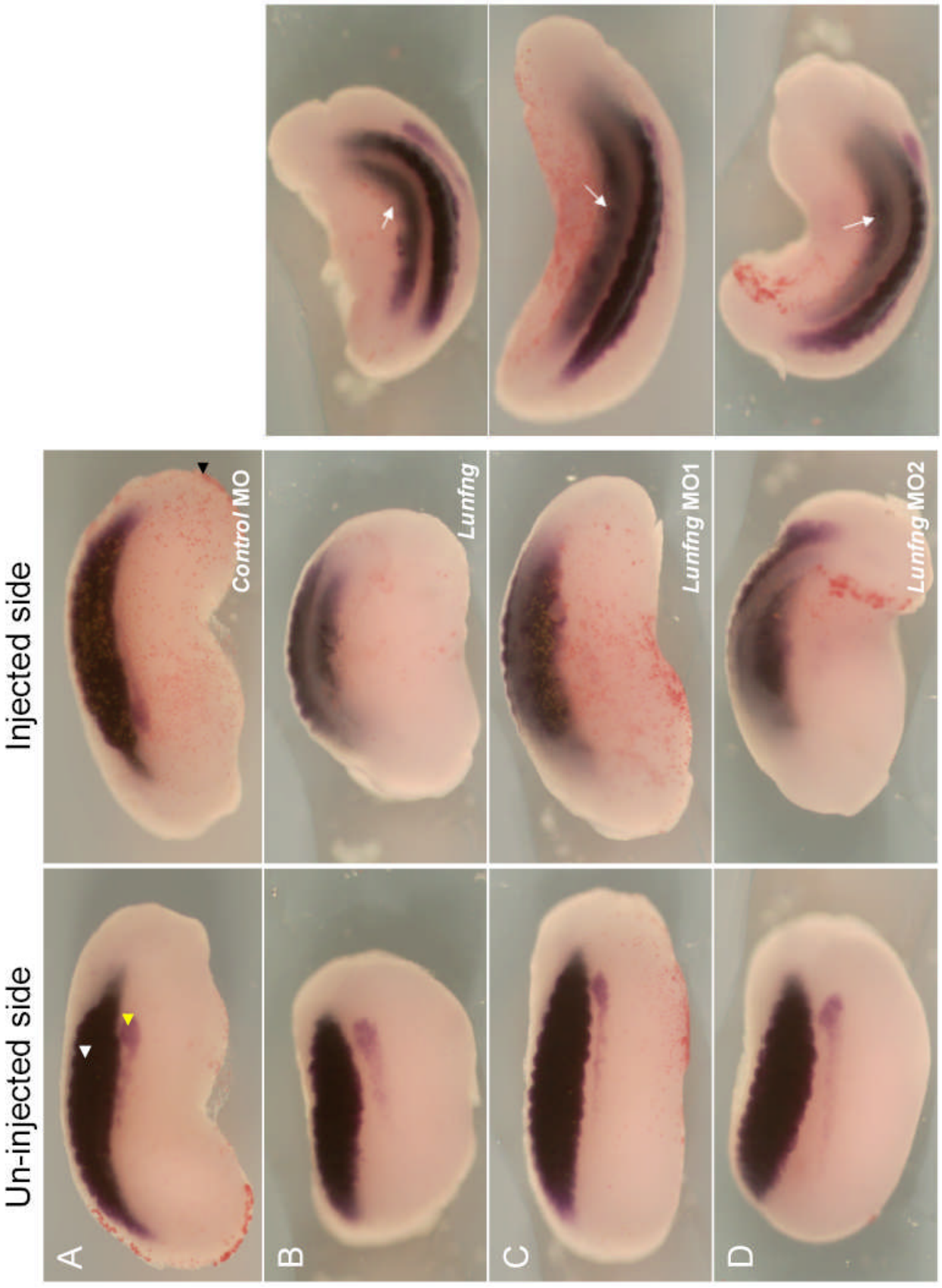
Un-injected side
Injected side
A
B
C
D
Control MO
Lunfng
Lunfng MO1
Lunfng MO2

Figure 6.16 Knock-down of *Lunatic fringe* endogenous translation using two different MOs and over-expression of *Lunatic fringe* mRNA reduced somite formation and completely inhibited pronephros anlagen induction. *X. laevis* embryos were injected at the 8 cell stage into a ventro-vegetal blastomere to target the presumptive pronephric region. MOs and mRNA were co-injected with *βgal* mRNA to act as a lineage tracer (red staining, black arrowheads). Embryos were cultured till stage 24 and then fixed. Whole mount double *in situ* hybridisation was performed to detect expression of *MHC* (white arrowhead), a gene expressed in differentiated somites, and *Lim-1* (yellow arrowhead), a gene expressed in the pronephros anlagen. 20 ng *Control* MO injected embryos had normal muscle and pronephros anlagen development (A). 1 ng *Lunatic fringe* mRNA, 5 ng *Lunatic fringe* MO1 and 5 ng *Lunatic fringe* MO2 all inhibited Lim-1 expression and severely reduced MHC expression (white arrows) on the injected side (B-C). The inhibition of pronephros development may be as a result of an effect on myogenesis.

In conclusion, we suggest the effect of *Radical fringe* mRNA on pronephrogenesis, described in section 6.2.2, is a direct effect of this message on pronephros development as *Radical fringe* over-expression had no gross somite effect. However the effect of *Lunatic fringe* over-expression and MO knock-down on pronephrogenesis is likely to be indirect as both injections inhibit myogenesis, and thus may prevent the signal from the somites inducing intermediate mesoderm to form pronephros, explaining why both over-expression and MO knock-down generate such extreme reduction phenotypes.

6.2.6 *Lunatic fringe* mRNA does not inhibit pronephros development in growth factor incubated animal caps

Treatment of isolated *X. laevis* blastula stage presumptive ectoderm with 10 ng/ ml Activin and 10^{-4} M Retinoic acid causes differentiation of pronephros at a high frequency (Fig 6.17). This *in vitro* induction of pronephric compartments presents a system whereby myogenesis and somitogenesis are not required for pronephros development. We proceeded to inject both cells of a two cell stage embryo with 1 ng each of *Lunatic fringe* mRNA. The embryos were left overnight to develop to blastula stage 8.5, at which point animal caps were dissected and placed in growth factors (as indicated in Fig 6.19) for two hours. Caps were then transferred to media not containing growth factors, and left to develop to stage 35 (whole embryos, fertilised at the same time as embryos from which animal caps were dissected, were used for staging). Caps were then photographed, for analysis of morphology (Fig 6.18), and processed for RNA extraction and reverse transcription to obtain cDNA. In un-injected caps not treated with any growth factors, no

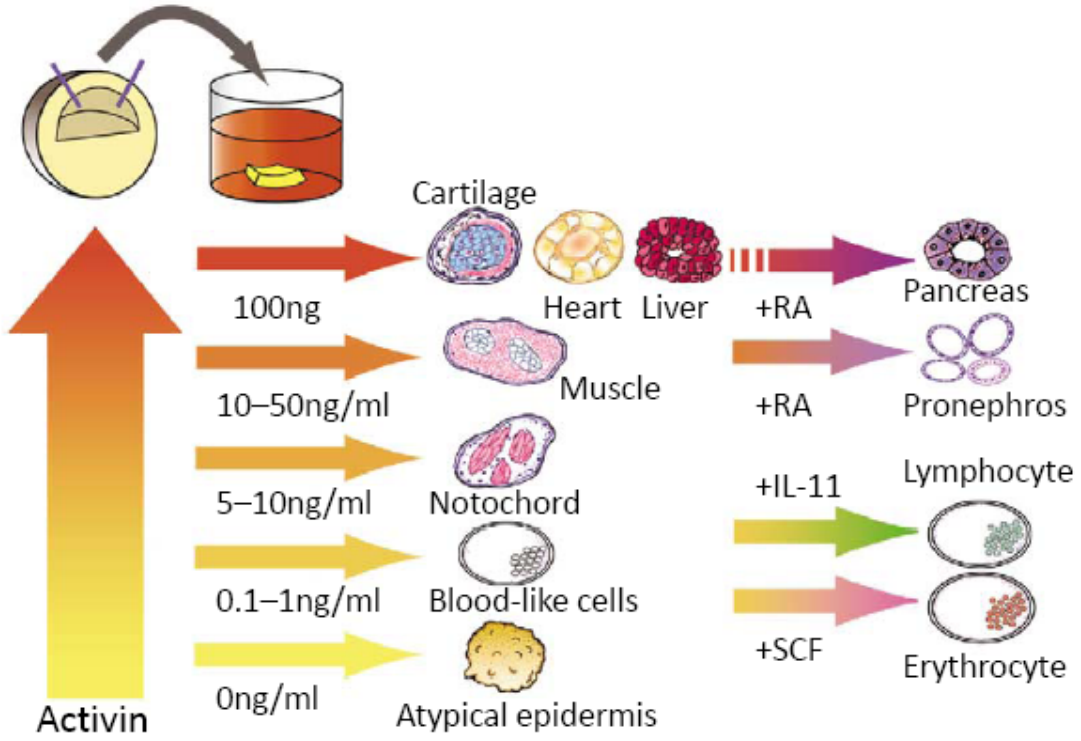

Figure 6.17 Schematic illustrating the different tissues that can be induced with different concentrations and combinations of growth factors. Animal caps are dissected from blastula stage embryos and incubated for approximately 2 hours in growth factors. Caps are then left to develop to a specific stage in development, when they can be processed and analysed for specific markers of a variety of tissues by RT-PCR. To induce pronephros dissected animal caps were incubated in 10 ng//ml Activin and 10^{-4} M Retinoic acid. (Schematic taken from Okabayashi and Asashima, 2003)

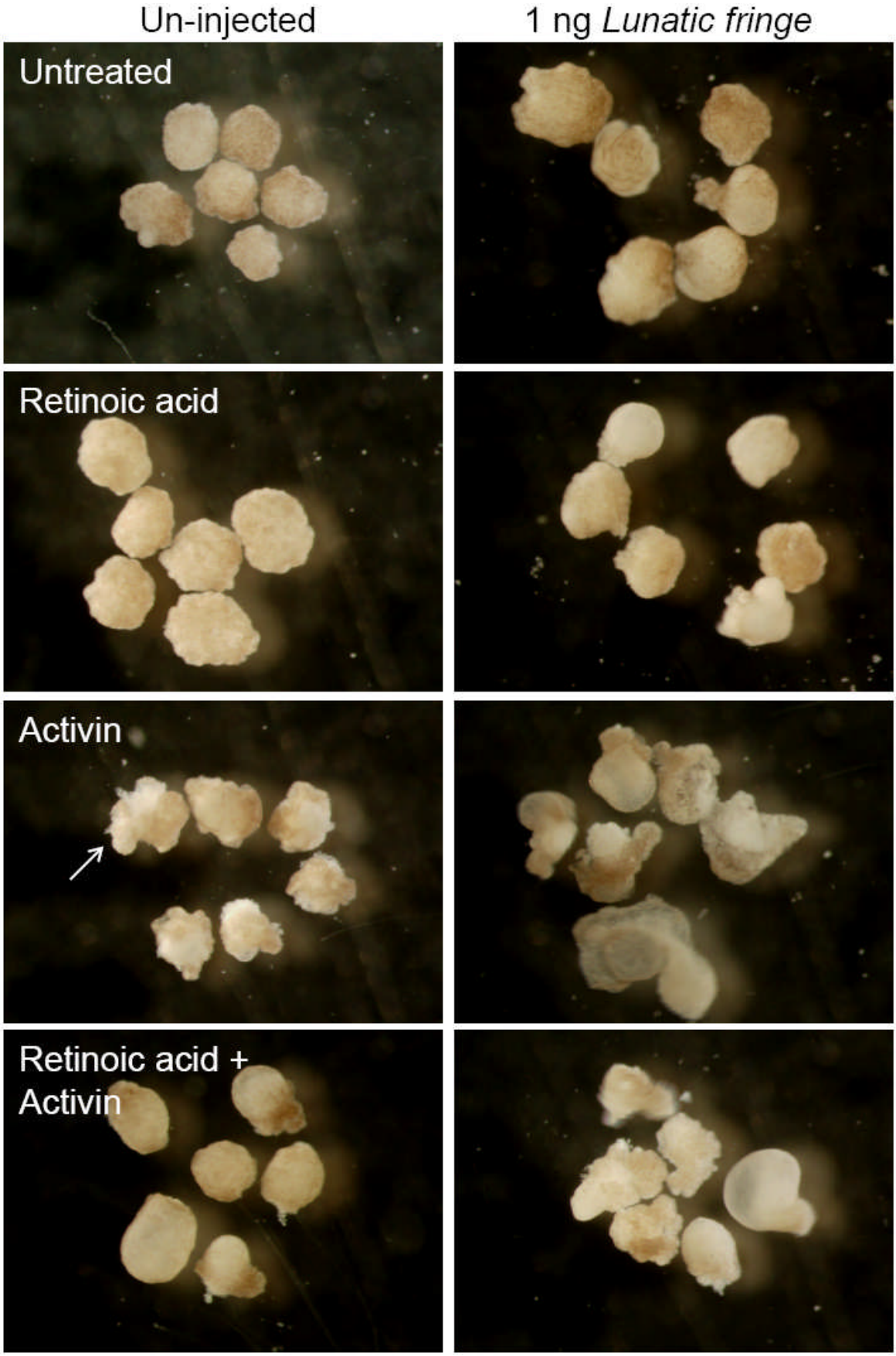
Un-injected
1 ng *Lunatic fringe*
Untreated
Retinoic acid
Activin
Retinoic acid +
Activin

Figure 6.18 Effects of growth factors in un-injected and *Lunatic fringe* mRNA injected animal caps. Activin, Retinoic acid and Lunatic fringe are mesoderm inducers, thus we expected to observe growths in the dissected caps. Untreated un-injected and *Lunatic fringe* mRNA injected caps developed normally, and Retinoic acid had little effect on cap morphology in either set of samples. Treatment of un-injected caps in Activin had an effect on cap morphology, with mesodermal extensions being observed (white arrow). Similar, yet more severe extensions were observed in Activin treated caps that were injected with *Lunatic fringe* mRNA, suggesting Lunatic fringe promotes mesoderm induction. Cap morphology upon incubation of un-injected and *Lunatic fringe* mRNA injected caps in both Retinoic acid and Activin was similar to the Activin only treatment, mesoderm extensions were again observed.

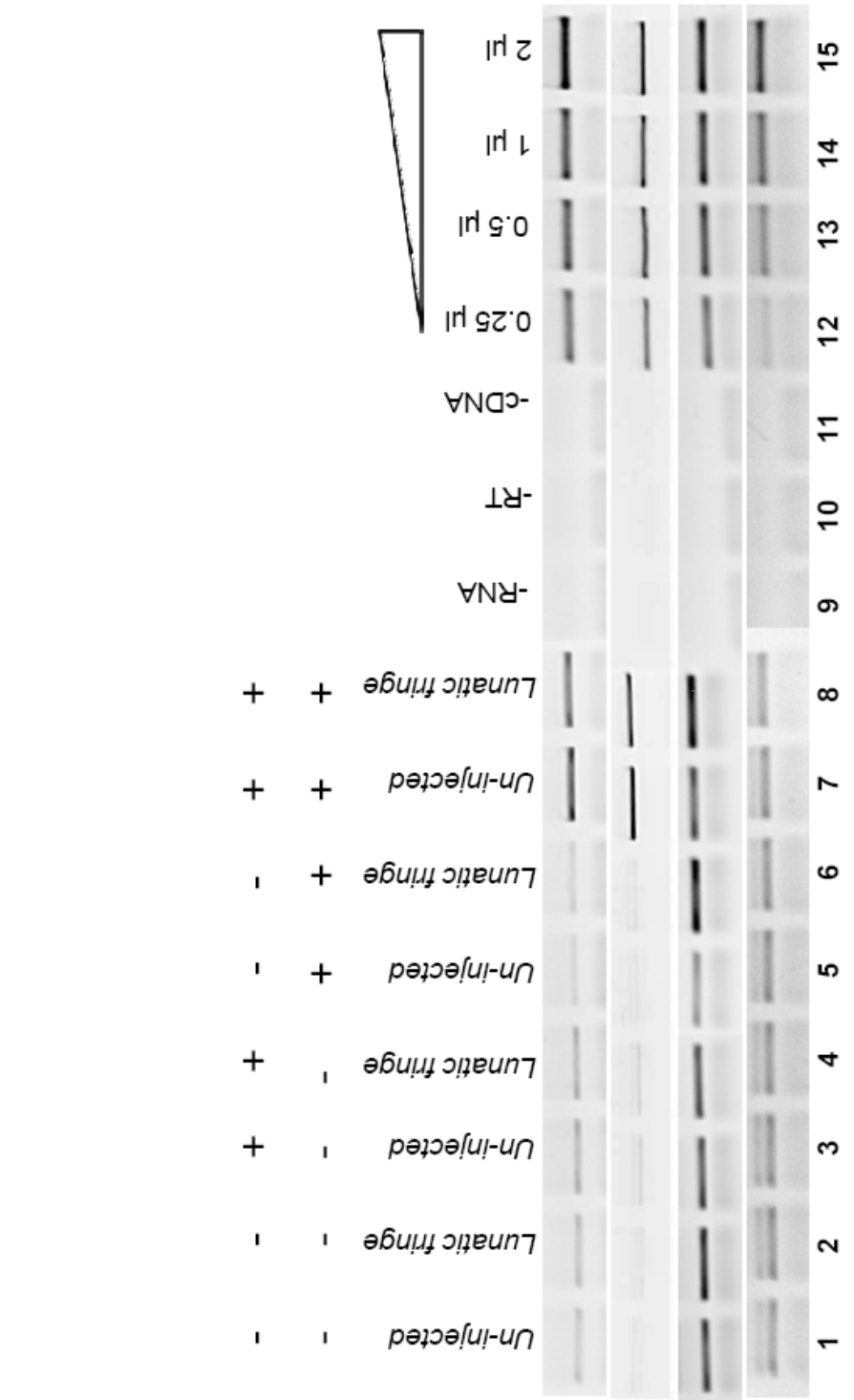

Figure 6.19 RT-PCR on dissected animal cap material suggests *Lunatic fringe* mRNA does not inhibit pronephros development. Animal caps were dissected at blastula stages of development, then incubated for 2 hours in the indicated growth factors before being cultured to stage 35. mRNA and cDNAs were prepared by standard procedures and RT-PCR carried out for the medial pronephric marker *nephrin*, the lateral pronephric marker *Na⁺ K⁺ ATPase γ* subunit, *Lunatic fringe* and the loading control *ODC*. Linearity of the PCR was confirmed by doubling the input of cDNA from caps taken from un-injected embryos and cultured in both Retinoic acid and Activin. Negative controls used were absence of RNA during the reverse transcription (-RNA), absence of reverse transcriptase (-RT), and absence of cDNA in the PCR (-cDNA). *nephrin* and *Na⁺ K⁺ ATPase γ* expression were observed only in un-injected and *Lunatic fringe* mRNA injected caps incubated in both growth factors (lanes 7 and 8). *Lunatic fringe* expression was observed in all cap samples (lanes 1-8), but was more highly expressed in *Lunatic fringe* mRNA injected caps than un-injected caps (for example compare lane 8 with lane 7), indicating exogenous mRNA was present in the caps taken from *Lunatic fringe* mRNA injected embryos. These results show that *Lunatic fringe* mRNA does not inhibit pronephric induction or differentiation of medial or lateral pronephric markers in this *in vitro* system.

induction of the medial pronephric mesoderm marker *nephrin* or the lateral pronephric mesoderm marker *Na^+ K^+ ATPase* (lane 1) was observed. Likewise, untreated caps dissected from *Lunatic fringe* mRNA injected embryos, did not express these pronephric markers (lane 2). Similar results were observed in un-injected and *Lunatic fringe* mRNA injected caps treated with either Retinoic acid (lanes 3 and 4) or Activin (lanes 5 and 6). However upon incubation of caps in media containing both growth factors, animal caps were induced to form pronephros, as observed by *nephrin* and *Na^+ K^+ ATPase* expression in the un-injected sample (lane 7). Importantly, injection of *Lunatic fringe* mRNA did not prevent this pronephric induction and differentiation (lane 8), expression of *nephrin* and *Na^+ K^+ ATPase* was also induced in these caps.

In conclusion, whilst this *in vitro* induction of pronephrogenesis does not reflect exactly the processes that occur *in vivo*, the observation that *Lunatic fringe* over-expression does not inhibit development of the pronephros in this system suggests inhibited pronephros development in whole embryos was a consequence of an effect on muscle development, as described in section 6.2.5. This result is important as it suggests the conclusion that *Lunatic fringe* over-expression directly inhibits pronephros development is inaccurate.

6.2.7 Over-expression of *Radical fringe* resulted in ectopic *Wnt-4*, *Delta-1* and *Serrate-1* expression

Fringe proteins are enzymes that require the presence of a substrate to be active. Consequently, it is difficult to ascertain scientific reasoning for why *Radical fringe* over-expression induced ectopic formation of all compartments of the

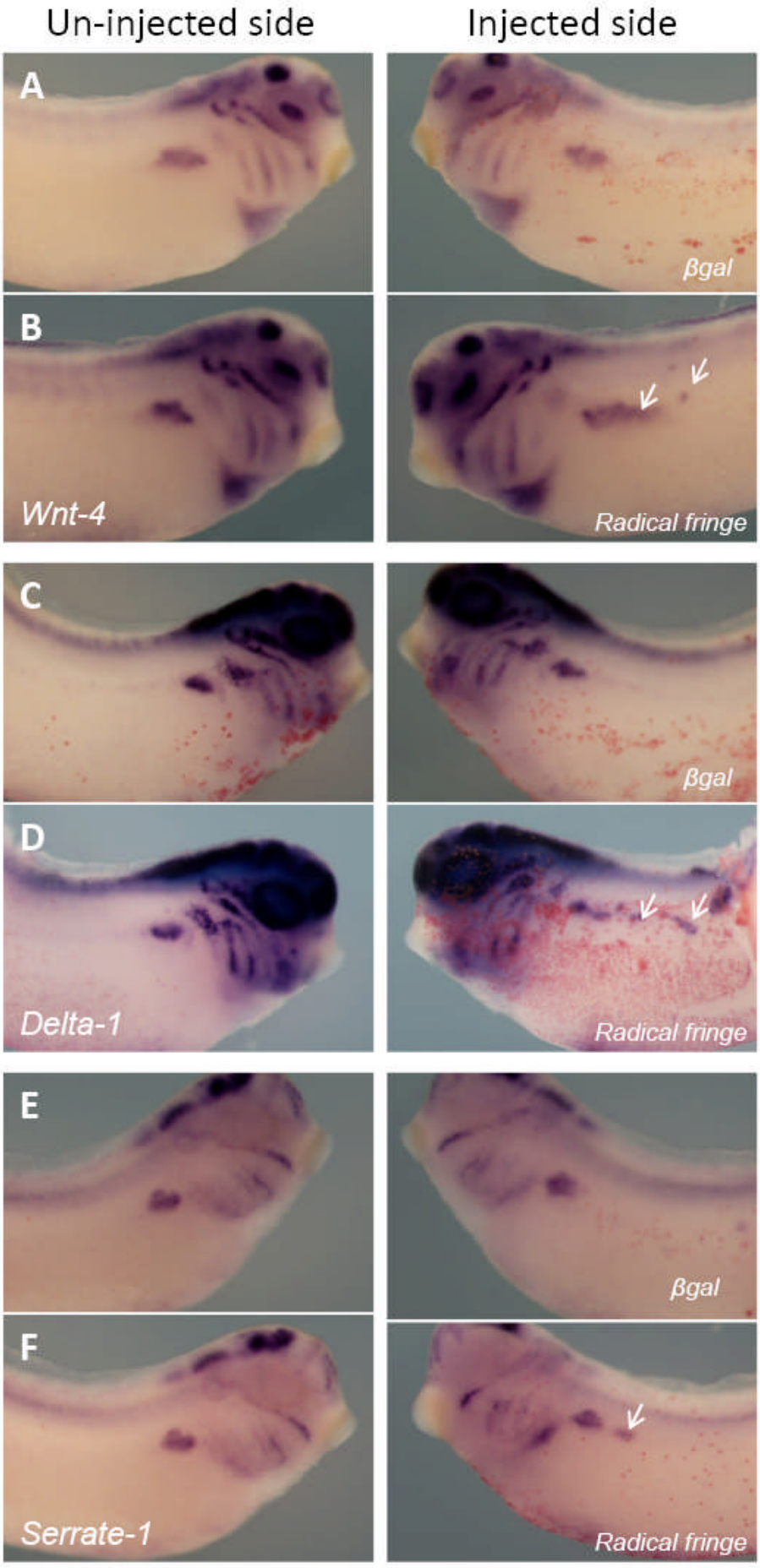
Un-injected side
Injected side
A
βgal
B
Wnt-4
Radical fringe
C
βgal
D
Delta-1
Radical fringe
E
βgal
F
Serrate-1
Radical fringe

Figure 6.20 *Radical fringe* over-expression induces ectopic expression of *Wnt4, Delta-1* and *Serrate-1*. . *X. laevis* embryos were injected at the 8 cell stage into a ventro-vegetal blastomere to target the presumptive pronephric region. *βgal* mRNA mRNA was co-injected to act as a lineage tracer (red staining). Embryos were cultured till stage 32 and then fixed. Whole mount *in situ* hybridisation was performed to detect expression of *Wnt4*, *Delta-1* and *Serrate-1*. Pronephric *Wnt4* (A), *Delta-1* (C) or *Serrate-1* (E) expression was not affect by injection of the *βgal* lineage tracer. Injection of 2 ng *Radical fringe* mRNA caused ectopic expression of *Wnt4* (B), *Delta-1* (D) and *Serrate-1* (F) (indicated by white arrows).

pronephros as Radical fringe is not a transcription factor capable of altering gene expression. To observe how Radical fringe is inducing this ectopic pronephrogenesis we injected 2 ng *Radical fringe* mRNA into a V2 blastomere of an 8-cell stage embryo, cultured the embryos to stage 32 and performed *in situ* hybridisation for expression of *Wnt-4* and components of the Notch signalling pathway, *Delta-1* and *Serrate-1* (Fig 6.20). Over-expression of *Radical fringe* caused ectopic *Wnt-4* expression in 73% of embryos (Fig 6.20B, n=62). *Serrate-1* expression was ectopic in 80% of embryos injected with *Radical fringe* mRNA (Fig 6.20D, n=65). Similarly, *Delta-1* expression was ectopic in 84% of embryos when *Radical fringe* was over-expressed (Fig 6.20F, n=51). Injection of the βgal lineage tracer alone had no effect on expression of *Wnt-4*, *Delta-1* or *Serrate-1* (see appendix 6). In conclusion *Radical fringe* over-expression caused ectopic pronephrogenesis as Wnt-4 and the Notch signalling pathway are ectopically active.

6.3 Discussion

6.3.1 *Radical* and *Lunatic fringe* expression is temporally and spatially appropriate for a role in regulating the Notch signalling pathway in the proximal-dorsal region of the pronephros

Our hypothesis that the Notch signalling pathway is regulating early pronephrogenesis by establishing a boundary between the lateral and medial pronephric mesoderms required appropriate temporal and spatial expression of *X. laevis* homologues of the *Drosophila fringe* gene; *Lunatic fringe* and *Radical fringe*.

Fringe is essential for regulating the ligand specificity of Notch receptors (Irvine, 1999). In boundary formation this is necessary as Notch-Delta and Notch-Serrate interactions induce differential downstream transcription cascades. Consequently cell fate decisions in cells where Notch receptors are bound to Serrate will differ to those in cells where Notch receptors are bound to Delta. Thus if two populations of cells have different Notch-ligand interactions they will acquire different cell fates. Fringe increases the affinity of Notch receptors to the Delta ligand, thus its presence only on one side of a boundary ensures those cells will be directed towards a cell fate that differs to cells on the opposite side of the boundary. In these terms, it is Fringe that is the fundamental regulator of Notch-mediated developmental boundary formation (Irvine, 1999).

We observed expression of both *Lunatic* and *Radical fringe* in the dorsal-proximal region of the pronephros anlagen. *Lunatic fringe* was expressed in this region between stages 22 and 32/ 33, whereas *Radical fringe* expression began slightly later, from stage 25 to 32/ 33. Importantly, both gene expression profiles are temporally and spatially similar to *Notch-1*, *Delta-1*, *Serrate-1* and *Wnt-4*, indicating *fringe* genes may have a role in regulation of Notch signalling in this region of the pronephros. As with components of the Notch pathway and *Wnt-4*, we were unable to properly establish if *Lunatic* and *Radical fringe* expression is within the lateral or medial pronephric mesoderms. The presence of *fringe* genes in this pronephric region adds to evidence that a boundary in the dorsal-proximal region of the pronephros anlagen is being established.

6.3.2 *Radical* fringe has no role in pronephrogenesis

Given the dorsal-proximal localisation of *Radical* and *Lunatic fringe* expression in the pronephros, we would expect to observe disrupted glomus, nephrostome and proximal tubule development upon knock-down of either *Radical* or *Lunatic fringe* expression. However, MO knock-down of *Radical fringe* expression had no effect on development of the pronephros (Figs 6.8B, 6.9B, 6.9D and 6.10B) or myogenesis (Fig 6.15B). Such results suggest Radical fringe is not required for development of the pronephros or myotome. This conclusion is further enhanced by the grossly normal development of these embryos, which looked similar to the *Control* MO injected embryos. Radical fringe has been shown to be important in AER positioning in the chick wing bud (Johnson and Tabin, 1997; Laufer et al., 1997; Chen and Johnson, 1999), and directs Notch activation in boundaries between adjacent rhombomeres in the zebrafish hindbrain (Blair, 2004; Cheng et al., 2004). Despite these findings, it has been suggested Radical fringe plays no role in mouse development (Visan et al., 2006). This claim is supported by *Radical fringe*-deficient mice showing no obvious phenotypic defects during development (Zhang et al., 2002). In the same paper, *Lunatic fringe*-deficient mice displayed severe developmental defects, most notably in segmentation. Furthermore, *Lunatic fringe*/ *Radical fringe*-deficient mice do not have phenotypic defects above the severity of single *Lunatic fringe*-deficient mice (Zhang et al., 2002). These results are very similar to our data. We observed severe developmental defects when over-expressing or knocking down *Lunatic fringe*, but *Radical fringe* knock-down had no effect on development. In addition co-injection of *Lunatic fringe* MO1 with the *Radical fringe* MO did not alter the frequency of pronephric phenotypes detected after single injections of *Lunatic fringe* MO1 (Appendix 6). Thus endogenous Radical fringe is

unable to compensate for loss of *Lunatic fringe* expression in *X. laevis* muscle and pronephros development, even though it is expressed in both regions. Despite this we were able to rescue the pronephric phenotypes induced by *Lunatic fringe* MO1 and MO2 by co-injection with high levels of *Radical fringe* mRNA. This result suggests Radical fringe is capable of compensating for loss of endogenous Lunatic fringe, but the endogenous levels of *Radical fringe* expression are too low.

The three vertebrate *fringe* genes *Lunatic*, *Radical* and *Manic fringe* are all glycosyl transferases, and all have been shown to modify Notch receptors by addition of N-acetylglucosamine to fucose sugars on EGF repeats (Rampal et al., 2005). The presence of three different forms of Fringe in vertebrates seems to be redundant in development; all mammalian fringe genes have very similar biochemical behaviour and their enzymatic properties do not differ with respect to time, temperature, metal ion requirements or pH (Rampal et al., 2005). Indeed, the only difference between the three mammalian Fringes is the catalytic activity of Lunatic fringe is much higher than either Radical or Manic fringe (Rampal et al., 2005). EGF repeats are conserved regions of sequence roughly 40 bp in length. They contain six cysteine residues that form three evenly spaced disulphide bonds (van de Poll et al., 2000). Lunatic, Radical and Manic fringe all preferentially modify EGF repeats that have a glutamic acid residue at position 24 and a proline residue at position 28 within the EGF repeat, again highlighting their conserved activity (Rampal et al., 2005). Additionally early genetic studies in *Drosophila* showed all three mammalian Fringes complemented *fringe* mutants (Johnston et al., 1997). From these findings we conclude there is no experimental evidence of major functional differences between Lunatic and Radical fringe. Therefore, we suggest the ectopic formation of all pronephric compartments

observed after *Radical fringe* over-expression (Figs 6.5B, 6.6B, 6.6D, 6.6E, and 6.7B) is representative of over-expression of any *fringe* gene in the pronephros. As Fringes are essential for Notch-mediated boundary formation by regulation of Notch-ligand interactions, over-expression of *fringe* in the pronephros would be expected to establish multiple boundaries across the entire anlagen. We have proposed Notch signalling establishes a boundary across the proximal pronephros, separating the lateral and medial pronephric mesoderms, thus we would expect to observe ectopic proximal tubule, nephrostome and glomus formation as boundaries could be established more distally due to the presence of exogenous *Radical fringe* mRNA in the entire pronephros anlagen. These expected phenotypes were what we observed. We detected ectopic *nephrin* (Fig 6.6B) and *odf-3* expression (Fig 6.6E), similar to phenotypes observed after *Notch-ICD* mRNA injection. Additionally, and unlike *Notch-ICD* over-expression, we observed ectopic *slc5a2* expression (Fig 6.6D), thus *Radical fringe* over-expression induced ectopic proximal tubulogenesis. These striking phenotypes are supported by antibody staining for the mature pronephros at stage 41 with 3G8/ 4A6 (Fig 6.7B). We clearly observed ectopic 3G8 and 4A6 staining, and repeatedly obtained embryos that appeared to have duplicated proximal pronephric regions in the distal pronephros (Fig 6.7Bi-iii). Furthermore, in these 3G8/ 4A6 immunostained embryos, we never observed 3G8 staining ventral to 4A6 staining, thus the dorsal-ventral axis of the pronephros is maintained in these embryos (a result clearly identifiable in Fig 6.7Biv). It is unlikely therefore that the Notch signalling pathway regulates a molecularly defined dorsal-ventral axis in the lateral pronephric mesoderm. In relation to this finding, the pattern of ectopic 4A6 staining was different to ectopic 3G8 staining. During normal pronephrogenesis the most distal point of the proximal tubule is connected to the intermediate tubule, by

definition this is the point where 3G8 stained tubules are connected to 4A6 stained tubules. In *Radical fringe* mRNA injected embryos, ectopic 3G8 antibody staining in the distal pronephros was repeatedly connected to a 4A6 stained tubule. Such 4A6 staining we characterised as ectopic, although it is likely this is intermediate tubule staining and represents a complete duplication of the entire proximal pronephros. This observation is important as it suggests distal tubulogenesis was not ectopic, and therefore this pronephric phenotype is an expansion of proximal pronephros into the distal pronephric region. In conclusion, we propose *Radical fringe* over-expression duplicates the entire proximal pronephros in distal pronephric regions, though this needs to be confirmed by the use of additional markers, such as *ClC-K* (a marker of the intermediate tubule) and *c-ret* (a marker of the distal tubule).

These results provide evidence that Fringe is modulating boundary formation between the proximal lateral and medial pronephric mesoderms as the phenotype produced is as expected if Notch-mediated boundary formation is occurring. However, these results are difficult to interpret with respect to the function of Fringe. As previously explained, Fringe proteins act to modify Notch receptors by addition of N-acetylglucosamine to fucose sugars added to EGF repeats by *O*-fucosyl transferase (Haines and Irvine, 2003). Thus Fringe activity, exogenous or endogenous, is dependent on the availability of Notch receptors in the pronephros anlagen. *Notch-1* is expressed in the dorsal-proximal region of the pronephros anlagen from stage 22 to stage 30, then later is expressed in the proximal tubules (McLaughlin et al., 2000). Hypothetically, exogenous Radical fringe can only function in these cells. This is not what is happening in the embryos we injected as ectopic pronephros formation is occurring distal to the normal domain of *Notch-1*

expression. It is possible low levels of *Notch-1*, not detectable by the *in situ* hybridisation technique, are expressed throughout the pronephros anlagen, and Radical fringe acts upon these receptors to promote Notch signalling more distally. Alternatively, the phenotype we observed could be due exogenous *Radical fringe* mRNA enhancing normal Notch signalling in the pronephros anlagen, which leads to a transcription cascade that causes expression of genes such as *Wnt4*, whose gene product is secreted and could induce expression of *Notch* ectopically. Wingless has been shown to induce expression of components of the Notch signalling pathway in the *Drosophila* imaginal wing disc (de Celis and Bray, 1997), although we have shown *Wnt4* over-expression had no significant effect on *Delta-1* or *Serrate-1* expression in the pronephros (section 5.2.4). Figure 6.20 shows over-expressing *Radical fringe* induced ectopic *Wnt4, Delta-1* and *Serrate-1* expression. Therefore pronephric anlagen that contain exogenous *Radical fringe* mRNA are able to induce ectopic Wnt and Notch signalling, which is likely to be the cause of the increased expression and staining of differentiated pronephros markers (*nephrin*, *slc5a2*, and 3G8). Whilst this result gives a possible reason as to why ectopic pronephrogenesis is occurring, further experimentation is required to fully understand the mechanism by which exogenous *Radical fringe* mRNA induces such gene expression, as the protein product of this message is an enzyme and not a transcription factor.

The mechanism by which Fringe regulates dorsal-ventral patterning of the wing margin in *Drosophila* is through directing differential Notch-ligand interactions. In the pronephros, non-differential Notch-ligand interactions should be induced after *Radical fringe* mRNA injection. Given the data in the literature, Notch-ligand interactions in the pronephros anlagen of these *Radical fringe* mRNA injected

embryos will theoretically be ubiquitously Notch-Delta in nature. When such a molecular environment is created, ectopic glomus, nephrostomes, and proximal tubules occurs. This phenotype does not fit with the mechanistic explanation for Fringe modulated dorsal-ventral patterning in the imaginal wing disc. If what was occurring in the fly wing margin is transposable to the pronephros, we would expect to observe a phenotype where there was ectopic formation of one side of the boundary, the side whose cell fate is orchestrated by Notch-Delta interactions. Instead we observed ectopic formation of both sides of the proposed boundary. Thus, the phenotypes observed in this chapter do not correlate with phenotypes observed in the literature. However, it is extremely unlikely that every cell within the pronephros anlagen will translate the exogenous message at the same level. What is more likely is that there is an inequality in the amount of exogenous *Radical fringe* mRNA translated by each cell in the anlagen, and thus differential Notch-ligand interactions are liable to persist. Indeed, it is likely such ectopic differential Notch-ligand interactions are the cause of the ectopic pronephric phenotypes we observed.

6.3.3 *Lunatic fringe* is likely to be the mediator of Notch-ligand interactions during pronephros development in *X. laevis*

Lunatic fringe is the best described vertebrate *fringe* gene. As well as regulating somitic boundaries within the presomitic mesoderm (Pourquie, 2003), Lunatic fringe has been shown to be involved in other events during development, such as establishing boundaries within developing mouse teeth (Pouyet and Mitsiadis, 2000). As already discussed, Lunatic fringe is the major functional Fringe during vertebrate development, Radical and Manic fringe seem to be involved in discrete processes during development (Rampal et al., 2005). These findings are consistent

with our results. Injection of *Lunatic fringe* mRNA or either MO was much more toxic than injection of *Radical fringe* mRNA or the *Radical fringe* MO. Embryos could not tolerate more than 0.5 ng *Lunatic fringe* mRNA, and gross developmental defects were observed after injection of only 5 ng *Lunatic fringe* MO1 or MO2.

Even though both *Lunatic fringe* MOs were very toxic, upon injection we expected to observe a phenotype where markers for the proximal pronephros were disrupted. However, depletion of Lunatic fringe inhibited formation of all compartments of the pronephros. In Chapter 3 we argued the $p27^{Xic1}$ MO reduced pronephros size as a consequence of inhibited myogenesis, preventing a signal, from the somites to the intermediate mesoderm, inducing pronephros anlagen formation (Figures 3.13-3.16) (Seufert et al., 1999; Mauch et al., 2000; Mitchell et al., 2007). Injection of *Lunatic fringe* MO1 or MO2 also inhibited formation of the myotome at a high frequency (Fig 6.16). The reduction in *MHC* expression observed upon injection of either *Lunatic fringe* MO1 or MO2 (Fig 6.16C and 6.16D) suggests that the somitic signal to the intermediate mesoderm is not being sent due to muscle development being perturbed.

The biochemical and functional similarities between Lunatic fringe and Radical fringe meant we expected to observe ectopic pronephrogenesis upon over-expression of *Lunatic fringe*, as was observed after *Radical fringe* over-expression. However, injection of *Lunatic fringe* mRNA inhibited formation of all compartments of the pronephros. *MHC* expression was reduced in *Lunatic fringe* mRNA injected embryos (Fig 6.16B). Thus, as with *Lunatic fringe* MO knock-down, we propose the pronephric phenotype induced after *Lunatic fringe* over-expression is indirect and

most likely a consequence of inhibited myogenesis. Whilst inhibited muscle formation is an indication of why pronephros development is reduced, an explanation for how both *Lunatic fringe* over-expression and knock-down prevented myogenesis is difficult to establish. The toxicity of *Lunatic fringe* mRNA and MOs suggests gross effects on early development are likely to occur. For example, ectopic apoptosis or interference with cell cycle regulation, which could disrupt gastrulation, early mesoderm induction, and paraxial mesoderm formation are possible reasons for how *Lunatic fringe* mRNA and MO messages have similar effects on development of the pronephros and somitogenesis. Further experimentation, for instance observing the effects *Lunatic fringe* over-expression or depletion has on early mesoderm markers, such as *goosecoid* or *Brachyury*, and antibody staining for pH3 and Caspase-3 to detect cell division and apoptotic effects of such injections, would need to be carried out in order to see if additive developmental defects are the cause of inhibited myogenesis in *Lunatic fringe* gain- and loss-of-function experiments.

Pronephrogenesis in an *in vitro* induction system was not inhibited by over-expression of *Lunatic fringe* mRNA. Animal caps taken from blastula stage embryos injected with 2 ng *Lunatic fringe* mRNA and incubated in 10 ng/ ml Activin and 10^{-4} M Retinoic acid did not inhibit expression of *nephrin* or Na^+ K^+ *ATPase*. Therefore formation of the lateral and medial pronephric mesoderms was not inhibited by *Lunatic fringe* mRNA injection, as observed in whole embryos. This result suggests the effect on myogenesis we identified after over-expression of *Lunatic fringe* was the reason for an effect on pronephrogenesis, and if we were able to induce *Lunatic fringe* expression in the pronephros of whole embryos we would not observe a reduction phenotype. One approach to get around this problem in whole embryos

could be to manufacture an inducible *Lunatic fringe* construct. Such a construct could be injected into the V2 blastomere and then induced around stage 18. By this stage the pronephros anlagen has been induced, thus exogenous *Lunatic fringe* mRNA in the myotome would not effect pronephrogenesis. In this circumstance we would expect to observe a similar phenotype to *Radical fringe* over-expression. Given this experiment has not been performed, and Lunatic fringe did not inhibit pronephrogenesis in animal caps induced by growth factors to differentiate into pronephros, we suggest the phenotype observed after *Radical fringe* over-expression is representative of the effect *Lunatic fringe* would have on pronephrogenesis.

6.3.4 Concluding remarks

Knock-down of *Radical fringe* had no effect on pronephrogenesis, therefore Radical fringe plays no role in development of the pronephros. Over-expressing *Radical fringe* did produce a pronephric phenotype, and this phenotype was indicative of an effect on Notch signalling. Given this result, and the fact *Lunatic fringe* is appropriately expressed both temporarily and spatially, we suggest Fringe proteins play a role in pronephrogenesis, and this role is the regulation of Notch receptors to establish a boundary in the proximal pronephros anlagen that separates the lateral and medial pronephric mesoderms during early tail-bud stages of development. If our hypothesis is accurate, Lunatic fringe is the best candidate for performing this function. However, the only way this proposal can be proven is by observation of a proximal pronephros phenotype after knock-down of *Lunatic fringe*, something we have been unable to achieve, in the absence of a muscle phenotype. In the future it may be possible to inject a blastomere at the 32-cell stage to target the pronephros more specifically, thus reduce the effect the *Lunatic fringe* MO has on

myogenesis. However, the toxicity of this MO suggests to us MO knock-down of *Lunatic fringe* translation seriously perturbs early development, and so is unlikely to be usable in the study of pronephrogenesis.

Chapter 7

General Discussion

The aims of this thesis were to describe and discuss data collected that established roles for certain cell cycle regulators and the Notch signalling pathway in development of the pronephros in *X. laevis*. We have identified a role for the cyclin dependent kinase inhibitor $p27^{Xic1}$ in regulating organ size and propose a mechanism by which the Notch signalling pathway patterns the proximal pronephros anlagen to enable separation of the lateral and medial pronephric mesoderms.

7.1 A role for cell cycle regulation in pronephrogenesis

7.1.1 $p27^{Xic1}$ is a regulator of pronephros organ size and somitogenesis

We have shown that $p27^{Xic1}$ is strongly expressed in the nephrostomal region of the pronephros by *in situ* hybridisation, a result previous studies had not observed (Ohnuma et al., 1999; Hardcastle and Papalopulu, 2000; Ohnuma et al., 2002; Vernon et al., 2003; Vernon and Philpott, 2003). $p27^{Xic1}$ has been implicated as a regulator of cell fate determination in addition to promoting cell cycle exit (Ohnuma et al., 1999; Vernon et al., 2003; Vernon and Philpott, 2003). As $p27^{Xic1}$ is expressed in the nephrostomes from stage 28 to stage 33, it was possible it could be regulating cell fate determination in this pronephric compartment as these are the stages when

the nephrostomes are differentiating (Nieuwkoop and Faber, 1994). Moreover, we detected pronephric expression of *p27^{Xic1}* in the tubules and glomus by RT-PCR. Therefore, as has been observed in primary neurogenesis, myogenesis and cardiogenesis (Vernon et al., 2003; Vernon and Philpott, 2003; Movassagh and Philpott, 2008), we expected to observe increased pronephrogenesis upon over-expression of *p27^{Xic1}* and reduced pronephrogenesis upon depletion of pronephric p27^{Xic1} by injection of a MO previously shown to specifically knock-down endogenous *p27^{Xic1}* translation (Vernon et al., 2003). This was not what we observed, both *p27^{Xic1}* over-expression and depletion inhibited development of the pronephros.

A possible explanation for a reduced pronephric phenotype after over-expression and depletion of *p27^{Xic1}* was the effect these messages had on *X. laevis* development prior to the induction of the pronephros anlagen. It is known the somites signal to the intermediate mesoderm, inducing the pronephros anlagen to develop (Seufert et al., 1999; Mauch et al., 2000; Mitchell et al., 2007). The nature of this signal remains unknown, although recent research in the Jones laboratory implicates the Wnt signalling pathway, possibly Wnt11, as a potential candidate for this signal (Tételin thesis, 2008). Injection of mRNA or MOs into the V2 blastomere of 8-cell stage embryos targets the future somites as well as pronephros. We believed over-expressing and depleting *p27^{Xic1}* in this blastomere could have an effect on myogenesis that subsequently inhibited the signal from the somites to the intermediate mesoderm to induce pronephrogenesis. To test this theory we observed the effect such injections had on expression of two markers of the myotome, *Myosin Heavy Chain* (*MHC*, a marker of differentiated muscle) and *MyoD* (an early marker of differentiating muscle). The *p27^{Xic1}* MO almost completely inhibited myogenesis,

reducing expression of both *MHC* and *MyoD* to an extent that implies the pronephric phenotype caused by *p27^{Xic1}* depletion could be the intermediate mesoderm not being induced by a somitic signal to undergo pronephrogenesis. A reduced pronephros was the expected phenotype of a lack of *p27^{Xic1}* expression in the pronephros as previous studies have shown cell cycle exit and differentiation are unable to occur without *p27^{Xic1}* in *X. laevis* (Ohnuma et al., 1999; Hardcastle and Papalopulu, 2000; Ohnuma et al., 2002; Vernon et al., 2003; Vernon and Philpott, 2003; Vernon et al., 2006; Movassagh and Philpott, 2008), and in vertebrates lacking expression of Cip/ Kip CKIs homologous to p27^{Xic1}, such as p21^{Cip1} (Zezula et al., 2001), p27^{Kip1} (Nguyen et al., 2006) and p57^{Kip2} (Reynaud et al., 1999; Reynaud et al., 2000). However, as the *p27^{Xic1}* MO inhibited myogenesis, we believe any pronephric phenotype after *p27^{Xic1}* depletion is quite likely to be an indirect consequence of reduced myogenesis, rather than a direct effect on differentiation of the pronephros.

Over-expressing *p27^{Xic1}* also produced a muscle phenotype; although this phenotype was not an effect on myogenesis, rather a disruption of somitogenesis. Somites appeared fused and segmentation was severely disrupted, but expression of *MyoD* and *MHC* persisted. We aimed to understand if such disrupted segmentation affected pronephros induction. p35.1 is a member of a family of proteins that bind to and activate cdk5 and has been shown to disrupt somitogenesis in a similar manner to *p27^{Xic1}* when over-expressed (Philpott et al., 1997). We reproduced this phenotype, observing disrupted somitogenesis on the side of embryos injected with *p35.1* mRNA. We also performed *in situ* hybridisation for expression of *Lim-1*, a marker of the pronephros anlagen, at stage 24, and also antibody staining with 3G8 and 4A6 to detect epitopes in the mature pronephros at stage 41. p35.1 did not inhibit expression

of *Lim-1* or reduce 3G8/ 4A6 antibody staining. This result suggested to us disrupted somitogenesis is unlikely to prevent the somitic signal to the intermediate mesoderm that induces pronephrogenesis. Therefore, p27^{Xic1} over-expression must have been inhibiting pronephros development by another mechanism. We propose this is a consequence of the cell cycle exit function of p27^{Xic1}. Two pieces of evidence support this claim. Firstly, injection of a mutant of *p27^{Xic1}* that has an inactive cyclin A2/ cdk2 binding region (*p27^{Xic1} CK*-) did not disrupt somitogenesis or produce a pronephros phenotype. Secondly, we showed *p27^{Xic1}* over-expression severely reduced cell division on the injected side of embryos, as observed by reduced pH3 antibody staining. Thus the ability of p27^{Xic1} to bind cyclinA2/ cdk2 complexes and inhibit cell cycle progression was the cause of disrupted segmentation and inhibited pronephrogenesis later. It is most likely pronephrogenesis was prevented by premature cell cycle exit reducing the number of cells that could contribute to the pronephros anlagen prior to its formation, thus we have discovered a novel role for p27^{Xic1} as an important regulator of organ size. Disruption of somitogenesis as a consequence of premature cell cycle exit is a not surprising phenotype; co-ordinated cell division is required for somitogenesis as the 'clock and wavelength' model of segmentation requires synchronous cell division to allocate the somites (Cooke and Zeeman, 1976; Primmett et al., 1989). Even so, this phenotype highlights a novel role for p27^{Xic1} in early development, that of correct allocation of somites within the paraxial mesoderm.

7.1.2 Is p27^{Xic1} a multi-functional CKI?

Many studies have implicated CKIs homologous to p27^{Xic1} as multi-functional proteins involved in a diverse array of cellular processes in addition to

their well characterised cell cycle exit function (Besson et al., 2008). We initially aimed to see if p27^{Xic1} was involved in regulation of cell fates in the pronephros, although the effect depletion of p27^{Xic1} had on myogenesis and the premature cell cycle exit over-expressing this gene caused in early development, meant we were unable to observe directly if cell fate determination in the pronephros was controlled by p27^{Xic1}. However, p27^{Xic1} has been shown to have a role in cell fate determination during primary neurogenesis (Vernon et al., 2003). As neurogenesis is a primary induction, the early effects of *p27^{Xic1}* over-expression and depletion on the cell cycle, or development in general, should be minimised. We were able to reproduce the published reduced primary neurogenesis phenotype induced by the *p27^{Xic1}* MO (Vernon et al., 2003). This phenotype showed that p27^{Xic1} is required for differentiation of primary neurons. Vernon et al (2003) went on to show this requirement was through the stabilisation of X-NGNR-1. The authors of this paper also observed p27^{Xic1} over-expression increased primary neurogenesis, a phenotype we were unable to reproduce. Rather, we suggest *p27^{Xic1}* over-expression is unable to promote primary neuron formation as its proposed role during primary neurogenesis permits it only to stabilise X-NGNR-1, not dictate which cells express *X-NGNR-1*. The Notch signalling pathway acts through lateral inhibition to pattern the neural plate and define which cells become primary neurons (Vernon et al., 2006). Thus exogenous p27^{Xic1} will only stabilise X-NGNR-1 in cells that are expressing this gene, and cannot induce primary neurogenesis in cells not containing X-NGNR-1. In conclusion, evidence to support a role for p27^{Xic1} in directly promoting primary neurogenesis is not definitive, in our hands.

p27^{Xic1} has also been shown to be important in gliogenesis (Ohnuma et al., 2002). Differentiation in the retina occurs in a conserved histogenic order, which is controlled by the Notch signalling pathway and p27^{Xic1}. *p27^{Xic1}* expression in the ciliary marginal zone (CMZ) is strongest in the central retina (Ohnuma et al., 1999). When over-expressed, *p27^{Xic1}* promotes differentiation of Müller glial cells at the expense of bipolar cells by promoting premature cell cycle exit in the region where bipolar cells normally form. Thus, although p27^{Xic1} promotes Müller glial cell differentiation, there is no evidence to suggest this is a direct effect on cell fate determination. Indeed, as retinogenesis occurs in a conserved histogenic order, premature cell cycle exit ensures a different cell fate is chosen, rather than directly promoting differentiation.

In addition to this, we observed a strong reduction in *MyoD* expression after p27^{Xic1} depletion at stage 24. A previous study investigating the role p27^{Xic1} plays in myogenesis concluded p27^{Xic1} stabilises MyoD/ Myf5, and this activity is a mechanism by which p27^{Xic1} promotes myogenesis (Vernon and Philpott, 2003). The authors of this paper arrived at this conclusion as depletion of p27^{Xic1} inhibited expression of *Muscle Actin* (a terminal marker of differentiated muscle) but not *MyoD* or *Myf5*, at stage 15. Thus, in the sequential transcription cascade that permits myogenesis, p27^{Xic1} must be acting on early bHLH transcription factors to promote their stabilisation. We have not depleted p27^{Xic1} and observed *MyoD* expression at stage 15, but we have shown at stage 24 *MyoD* expression is severely reduced. Given this phenotype, we predict it is unlikely *MyoD* expression at stage 15 would not be unaffected by p27^{Xic1} depletion. Thus, the *p27^{Xic1}* MO, despite our evidence that it specifically knocks-down only endogenous *p27^{Xic1}* translation, is an

inappropriate experimental tool to observe effects on later development, due to its effects on early embryonic patterning.

In conclusion, strong evidence linking $p27^{Xic1}$ directly to cell differentiation has yet to be presented. The data in the literature does not clearly show $p27^{Xic1}$ acts as a multi-functional protein, and it is our belief that further experimentation yielding more definitive data is required to prove this additional activity.

Evidence supporting mammalian CKIs acting as multi-functional proteins is much stronger than data proposing the ability of $p27^{Xic1}$ to promote differentiation. *p21*$^{-/-}$ mice cannot undergo oligodendrocyte differentiation, even though no cell cycle effect is observable (Zezula et al., 2001). Mice homozygous for a cell cycle mutant allele of $p27^{Kip1}$, *p27*$^{CK-}$, can stabilise Neurogenin-2 and still undergo primary neurogenesis (Nguyen et al., 2006). In mammalian cell lines $p57^{Kip2}$ has been shown to directly bind MyoD, stabilising this bHLH transcription factor and thus promoting myogenesis (Reynaud et al., 2000). These results suggest that, despite the weak evidence gathered so far, $p27^{Xic1}$ may be able to act as a multi-functional protein as there is functional and sequence homology between $p27^{Xic1}$ and mammalian Cip/ Kip CKIs. If $p27^{Xic1}$ is a multi-functional protein capable of directly promoting cell differentiation independently of its cell cycle exit function, we assume it will have multiple binding partners to enable it to perform this function. To investigate if $p27^{Xic1}$ is able to interact with multiple binding partners, we initially attempted to co-immunoprecipitate $p27^{Xic1}$ bound to growth-arrest-and-DNA-damage-induced gamma (Gadd45γ). Gadd45γ has previously been shown to produce a pronephros phenotype and is the most likely candidate protein capable of binding to $p27^{Xic1}$ as

the sequence of mammalian Gadd45α shown to interact with $p21^{Cip1}$ is almost completely conserved in Gadd45γ (Kearsey et al., 1995; Zhao et al., 2000; de la Calle-Mustienes et al., 2002; Kyuno et al., 2008). We have shown these two proteins may interact, but with a much lower affinity than $p27^{Xic1}$ interaction with Cyclin A2. Further investigation may provide stronger evidence for this interaction, and if $p27^{Xic1}$ is able to bind to Gadd45γ, it is possible it could interact with multiple proteins such as the bHLH transcription factors X-NGNR-1 and MyoD. If such interactions were established, this would yield definitive data that proved $p27^{Xic1}$ is a multi-functional protein.

7.2 The Notch signalling pathway establishes a boundary between the proximal lateral and medial pronephric mesoderms

7.2.1 Evidence for the Notch signalling pathway regulating pronephrogenesis

We have proposed a novel mechanism by which the Notch signalling pathway acts during early tail bud stages of development to separate the lateral and medial pronephric mesoderms in the proximal region of the pronephros anlagen by means of establishing a boundary. This boundary permits the lateral and medial pronephric mesoderms to develop in isolation and therefore allows the glomus, coelom, nephrostome and proximal tubule compartments to form appropriately. The most definitive example of the Notch signalling pathway establishing a developmental boundary is in the *Drosophila* imaginal wing disc (Johnston et al., 1997). Two findings showed the dorsal-ventral boundary of the imaginal wing disc was formed as a consequence of Notch signalling. Firstly the expression profiles of

apterous, *vestigial*, *serrate*, *delta*, *notch* and *wingless* provided evidence that two distinct cell populations existed that opposed each other and maintained the boundary (Couso et al., 1994; Diaz-Benjumea and Cohen, 1995; de Celis and Bray, 1997). In particular, Serrate acts as a signal from dorsal cells that activates Notch receptors on the ventral side of the wing margin, whereas Delta acts as a signal from ventral cells that activates Notch receptors on the dorsal side of the wing margin. This asymmetric positioning of *delta* and s*errate* expression across the dorsal-ventral border of the wing margin is regulated by a positive feedback loop between Delta and Serrate. Investigations into how this positive feedback loop is established and maintained led to the second major finding; the glycosyl transferase Fringe modulates Notch receptors, enhancing their affinity for the Delta ligand (Johnston et al., 1997; Panin et al., 1997). The expression of *fringe* solely on the dorsal side of the wing margin means Notch receptors on this side specifically bind to Delta ligands. As *delta* is expressed on the ventral side of the wing margin, Fringe modified Notch receptors can only be activated in the dorsal cells juxtaposed to the ventral side. Notch receptor activation in these dorsal cells induces expression of dorsalising genes such as *apterous*, and also *serrate*. Ultimately, differential gene expression caused by Notch-Delta and Notch-Serrate interactions on either side of the dorsal-ventral wing margin maintains the boundary. As Fringe orchestrates the positioning of Notch-ligand interactions, it is the fundamental regulator of developmental boundary formation regulated by the Notch signalling pathway.

We initially expected the above differential Notch-ligand interaction mechanism for Notch-mediated boundary formation to be conserved in the pronephros anlagen. This hypothesis was strengthened by our novel observation of

Lunatic fringe expression in this dorsal-proximal compartment. However, the discrete spatial expression of *Delta* and *Serrate* observed in the imaginal wing disc is not present across the medial-lateral axis of the pronephros anlagen. Previous studies have outlined expression profiles for *Wnt4* (Saulnier et al., 2002), *Delta-1*, *Serrate-1*, *Notch-1* (McLaughlin et al., 2000), *HRT1* (a downstream mediator of Notch signalling) and *Serrate-2* (Taelman et al., 2006). All these genes are expressed in the dorsal-proximal region of the pronephros anlagen during lateral and medial pronephric mesoderm separation (early tail bud stages, see Figure 1.4). Surprisingly, all these genes (apart from *HRT1*, which is initially expressed in both the lateral and medial pronephric mesoderms, before localising to the lateral pronephric mesoderm around stage 25) are expressed on the lateral side of the proximal-dorsal pronephric mesoderm. None of these genes are expressed in the medial pronephric mesoderm where the future glomus develops. This lack of medial expression of genes involved in Notch signalling does not favour the differential Notch-ligand interaction mechanism that establishes the dorsal-ventral boundary in the *Drosophila* imaginal wing disc is conserved during separation of the lateral and medial pronephric mesoderms in *X. laevis*. If such a mechanism was conserved, we would expect to see expression of *Delta* and *Serrate* on opposing sides of the medial-lateral axis. In addition to this we have over-expressed *Delta-1* and observed a phenotype similar to injection of *Notch-ICD* mRNA; ectopic glomus formation at the expense of tubulogenesis. *Notch-ICD* over-expression has previously been shown to promote *Serrate-1* expression (McLaughlin et al., 2000). Thus, it is likely that injection of *Serrate-1* mRNA will also produce ectopic medial pronephrogenesis and inhibit lateral pronephrogenesis. If a mechanism of differential Notch-ligand interactions promoted medio-lateral patterning of the pronephros anlagen, we would expect over-

expression of *Delta-1* to induce ectopic formation of one side of this axis, with *Serrate-1* over-expression inducing expansion of the opposite side. As this does not occur, an alternative mechanism for medio-lateral patterning by the Notch signalling pathway must be in place.

In addition to these findings, we have shown that mis-activation of the Notch and Wnt signalling pathways induced ectopic medial pronephrogenesis. Although *Wnt4* is known to be expressed solely in the lateral pronephric mesoderm, the exact medio-lateral positioning of *Notch-1* expression relative to medial-lateral pronephric patterning is unknown. It is likely *Notch-1* expression is specific to the lateral pronephic mesoderm as later in development it is expressed in the tubules and the lateral views of stage 22-24 embryos *in situ* hybridised for *Notch-1* are similar to *Delta-1* and *Serrate-1* expression profiles. If *Wnt4* and *Notch-1* are both expressed in the lateral pronephric mesoderm during early tail bud stages, then why, when they are over-expressed, do they inhibit lateral pronephric mesoderm development? An explanation for this in terms of the action of Wnt4 is easier to explain as Wnts are secreted proteins that can act as morphogens. Wnt4 over-expression induced ectopic medial pronephrogenesis, but is expressed solely in the lateral pronephric mesoderm (Saulnier et al., 2002). We suggest Wnt4 is secreted to the medial side, where it induces glomus cell fates. For this to be the case a receptor for Wnt4 must be expressed in the medial pronephros. To date, no Frizzled receptors have been shown to be expressed specifically in the medial pronephric mesoderm at the appropriate stage, although to our knowledge a purposeful search for such *Frizzled* expression in this particular pronephric compartment has not been undertaken. It is possible in the future a Frizzled receptor may be shown to be expressed in the medial pronephric

mesoderm. The ectopic formation of medial pronephros and inhibited lateral pronephrogenesis after over-expression of *Notch-ICD* is more difficult to explain as Notch signalling involves paracrine binary-cell interactions. If, as is most likely, *Notch-1* is expressed solely in the lateral pronephros, mis-activation of Notch signalling by injection of *Notch-ICD* mRNA would be expected to increase expression of markers of the proximal lateral pronephric mesoderm, for example *slc5a2* and proximal *Na^+ K^+ ATPase* expression. Likewise, we would expect over-expression of *Delta-1* and *Serrate-1* to cause increased proximal tubulogenesis. However, we have shown proximal and distal tubulogenesis is inhibited by injection of *Notch-ICD* mRNA and *Delta-1* mRNA. Instead markers of the glomus (medial pronephric mesoderm) and nephrostomes are increased. We propose this finding can only be explained by consideration of the role of Wnt4. We have shown *Notch-ICD* mRNA can induce *Wnt4* expression and *$Delta^{STU}$* mRNA injection inhibited *Wnt4* expression. Conversely, *Wnt4* over-expression has little effect on *Delta-1* or *Serrate-1* expression. Thus, we can position *Wnt4* expression downstream of Notch signalling. This finding suggests expression of components of the Notch signalling pathway in the lateral pronephric mesoderm during early tail bud stages of development act to promote *Wnt4* expression in this region. Subsequently Wnt4 is secreted to and acts upon the medial pronephric mesoderm to provoke glomus formation. The ectopic nephrostome development we observed is likely to be a consequence of increased medial pronephrogenesis as the medial pronephric mesoderm induces formation of the nephrostomes (Howland, 1916).

This suggestion that Wnt4 is a major regulator of proximal pronephros medial-lateral patterning fits our findings, although more experiments need to be

performed to support the evidence shown here. Detailed medial-lateral expression patterns for *Notch-1*, *Serrate-1* and *Wnt4* from stage 20 to stage 28 need to be performed to establish the exact lateral position of these genes expression profiles. Expression of a *Frizzled* receptor in the medial portion of the pronephros must also be discovered in order to establish the medial pronephric mesoderm as a receiver of the Wnt4 signal. In addition to expression profiling, further experimentation with Wnt4 is required. Co-injection of *Notch-ICD* mRNA with the *Wnt4* MO should prevent formation of all regions of the pronephros, if Wnt4 does act downstream of Notch signalling. Implanting beads soaked in Wnt4 protein in distal regions of the pronephros anlagen we suggest would provoke ectopic glomus development at the expense of distal tubulogenesis. This experiment would be important as it would show Wnt4 acts in a region where there is no detectable Notch signalling, but still would be able to induce medial pronephogenesis.

Fundamentally, we conclude that a Notch-mediated boundary like the one formed during development of the *Drosophila* imaginal wing disc is not capitulated during medio-lateral patterning in the pronephros anlagen. We believe a molecularly defined boundary is established in this region of the pronephros by the Notch signalling pathway, but by a different mechanism (Fig 7.1). A pool of cells in the dorsal-proximal region of the lateral pronephric mesoderm, between stage 20 and stage 28, signal to each other through the Notch-ligand paracrine interactions. This signalling permits expression of *Wnt4*, whose gene product is secreted by this pool of cells to the medial side of the pronephic mesoderm where it induces and maintains expression of genes such as *WT-1* and *Lmx1b* that inhibit expression of lateral pronephric mesoderm specific genes, such as *Lim-1* and *Pax-2*, in the medial

pronephros. The consequence of this signalling is the medial and lateral pronephric mesoderms can develop in isolation, and ultimately develop pronephric compartments with distinct functions. Thus, Notch signalling is present in the lateral pronephric region to induce glomus cell fates in the medial pronephric mesoderm.

If the Notch signalling pathway functions to induce Wnt4 secretion to the medial side, a question arises as to why components of the Notch and Wnt signalling pathway are expressed in the lateral pronephric mesoderm, and not in the medial pronephric mesoderm? We suggest this could be due to Notch signalling inhibiting medial cell fates and promoting proximal tubulogenesis in this region of the lateral pronephros. In support of this theory, Taelman et al (2006) showed specific temporal effects of Notch signalling during pronephrogenesis. When Notch signalling is mis-activated from stage 15, *WT-1* expression was increased in over 90% of embryos, and expression of a marker of the proximal lateral pronephros, *SMP-30*, was reduced in 98% of embryos. However, induction of this message at stage 27 increased *WT-1* expression in only 10% of embryos and approximately 30% of embryos had ectopic *SMP-30* expression. Taelman et al (2006) concluded the Notch signalling pathway and specifically a downstream mediator of Notch signalling (HRT1), first regulate development of the glomus, and later favour development of the proximal tubules. During pronephrogenesis there is specific requirement for an ordered developmental approach. Firstly, induction to form the pronephros anlagen occurs, then the anlagen undergoes patterning, and finally differentiation and morphogenesis results in a mature, functional pronephros. More specifically, the second step in this process, patterning of the pronephros, may also occur in sequential steps. Firstly, the medial-lateral axis is established, then later the proximal-distal axis that patterns the tubules

is formed. Evidence to support these claims include the later specification of the distal pronephros (Brennan et al., 1998; Brennan et al., 1999), the spatially different early and late phase of expression of *Notch-1* and *Serrate-1* (McLaughlin et al., 2000), the earlier expression of differentiating glomus markers such as *WT-1* (Wallingford et al., 1998), *nephrin* (Gerth et al., 2005) and *Pod-1* (Simrick et al., 2005), compared to proximal tubule markers such as *slc5a2* (Reggiani et al., 2007), *SMP-30* (Sato et al., 2000) and *PDZK-1* (Taelman et al., 2006) and the results described above from Taelman et al (2006). It is tempting to speculate that the Notch signalling pathway in the early phase of pronephros development has a dual role; establishing the glomus by initiating a Wnt4 signal to the medial pronephros, and maintaining the lateral pronephric mesoderm in a relatively un-patterned and un-differentiated state. Later in development, the Notch signalling pathway enables patterning of the lateral pronephric mesoderm, promoting proximal tubulogenesis.

7.2.2 A role for fringe during pronephrogenesis

We have shown *Lunatic fringe* and *Radical fringe* are expressed in the lateral pronephric mesoderm of the dorsal-proximal pronephros anlagen between stage 22 and stage 32/ 33. Fringe proteins are glycosyl transferases that, as explained above, post-translationally modify Notch receptors. In *Drosophila*, this glycosylation gives Notch receptors a higher affinity for Delta ligands (Johnston et al., 1997). As Fringes determine Notch-ligand interactions and are essential for boundary formation, we initially perceived the expression of *Lunatic fringe* in this pronephric region was to establish a boundary by a similar mechanism as fringe has been shown to establish a boundary in the *Drosophila* imaginal wing disc. However, as discussed above, differential Notch-ligand interaction is not the mechanism by which the medio-lateral

axis of the dorsal-proximal pronephros is patterned by the Notch signalling pathway. Consequently, the expression of *fringe* genes in this region of the pronephros is confusing as Fringe function is believed to promote Notch-Delta interactions. Functional analysis of Lunatic and Radical fringe in the pronephros was hindered by the relative toxicity of *Lunatic fringe* mRNA and MOs. We were unable to interpret the role of Lunatic fringe in the pronephros due to the gross defects its mis-expression had on myogenesis. Despite this, we have shown that *Radical fringe* over-expression caused ectopic formation of all regions of the pronephros. Radical fringe is not involved in pronephrogenesis as translational knock-down of this gene had no effect on development of any region of the pronephros. However, we believe the functional homology of all fringe proteins enables us to suggest over-expression of *Radical fringe* produces a pronephric phenotype representative of over-expression of *Lunatic fringe*, if this experiment were possible.

Over-expressing high levels of *Radical fringe* produced striking phenotypes, inducing ectopic formation of glomus, nephrostome, and tubule pronephric compartments in the absence of any morphological defects in the embryos. We propose this ectopic pronephrogenesis is a product of enhanced Notch signalling that, as we have shown, caused ectopic expression of genes such as *Wnt4*, *Delta-1* and *Serrate-1*. This phenotype is confusing when compared to the pronephric effects of *Wnt4* and *Notch-ICD* over-expression. Lateral pronephrogenesis was completely inhibited by injection of *Notch-ICD* mRNA and *Wnt4* mRNA. Therefore enhanced Notch signalling caused by *Radical fringe* over-expression, and the increased Wnt4 signal it produces, might be predicted to inhibit lateral pronephrogenesis also. As this phenotype was not what we observed we believe the phenotypes produced by

injection of *Notch-ICD* mRNA does not reflect the effect of Notch signalling overall being mis-activated. The Notch signalling pathway is complex, with Notch-ICD activated gene expression only one part of the signal transduced by Notch-ligand interactions. Notch-ICD induces expression of genes by switching the CSL-transcription factor complex from a transcriptional repressor to a transcriptional activator (Jarriault et al., 1995), and is undoubtedly an important product of Notch signal transduction. However, other processes occur as a consequence of Notch-ligand interactions, such as altered gene expression in the ligand-presenting cell, Notch-ICD independent pathways, and ubiquitination and cleavage of DSL ligands (Kadesch, 2004; Bray, 2006). In tissues injected with *Notch-ICD* mRNA all the cells will entertain solely the Notch-ICD-dependent pathway and negate any other aspect of Notch signalling. We suggest injection of *Radical fringe* mRNA enhanced Notch signalling as a whole, rather than just the Notch-ICD pathway, by permitting more Notch-ligand interactions. Consequently, the phenotype of *Radical fringe* over-expression represents a phenotype caused by enhanced Notch signalling in its entirety, in the pronephros. Notch-ICD has been used repeatedly, including in this thesis, as a tool to 'mis-activate' Notch signalling. However, this mis-activation is only of a specific part of the overall signal transduced by the Notch signalling pathway and given the recent understanding of the complexity of this pathway, the use of Notch-ICD to mis-activate the entire Notch signal is inaccurate, instead this construct only mis-activates one part of the many signals induced by Notch signalling.

There are a number of recent publications that support the idea Fringe proteins enhance Notch-ligand interactions and so the phenotypes present are

representative of globally enhanced Notch signalling rather than an increase in a specific aspect of this pathway. Enhanced *Lunatic fringe* expression increases neurogenesis in the trunk neural tube of chicken embryos, as a consequence of Notch/ Delta modulation (ME et al., 2007). Similarly, *Lunatic fringe* over-expression enhances T cell development (Tsukumo et al., 2006). The authors of this paper identified high expression of *Lunatic fringe* strengthened Notch-signalling by reporter gene assay, and during T cell development a particular subset of T cells ($CD4^{-}CD8^{+}$) have high levels of *Lunatic fringe* expression, which enhances Notch signalling and imparts their cell fate. In these cases, fringe is not acting to establish a boundary; rather it promotes all aspects of Notch signalling. In addition, the influence of Fringe on Notch signalling in vertebrates may not be directly parallel to the situation in *Drosophila*. For example, Notch2-Jagged1 interactions have been shown to be enhanced by Lunatic fringe (Hicks et al., 2000). Consequently, the effect mammalian fringes have on Notch-ligand interactions is different to that observed in *Drosophila*, where only Notch-Delta interactions are enhanced, and Notch-Serrate (Jagged) interactions are unaffected. Rather, it may be that Fringe activity in vertebrates depends on the Notch receptor, as well as the Notch ligand (Haines and Irvine, 2003), indicating another level of complexity to this pathway. In conclusion, we suggest fringe proteins (most likely Lunatic fringe) promote Notch signalling in a pool of cells in the dorsal-proximal region of the lateral pronephric mesoderm. This Notch signalling provokes the Wnt4 signal to the medial pronephros and ensures correct development of the proximal tubules (Fig 7.1). This function of Fringe supports our findings as it explains the reason we obtain both ectopic lateral and medial pronephrogenesis as *Radical fringe* over-expression recruits groups of cells along the entire pronephros anlagen length to acquire similar cell fate inducing

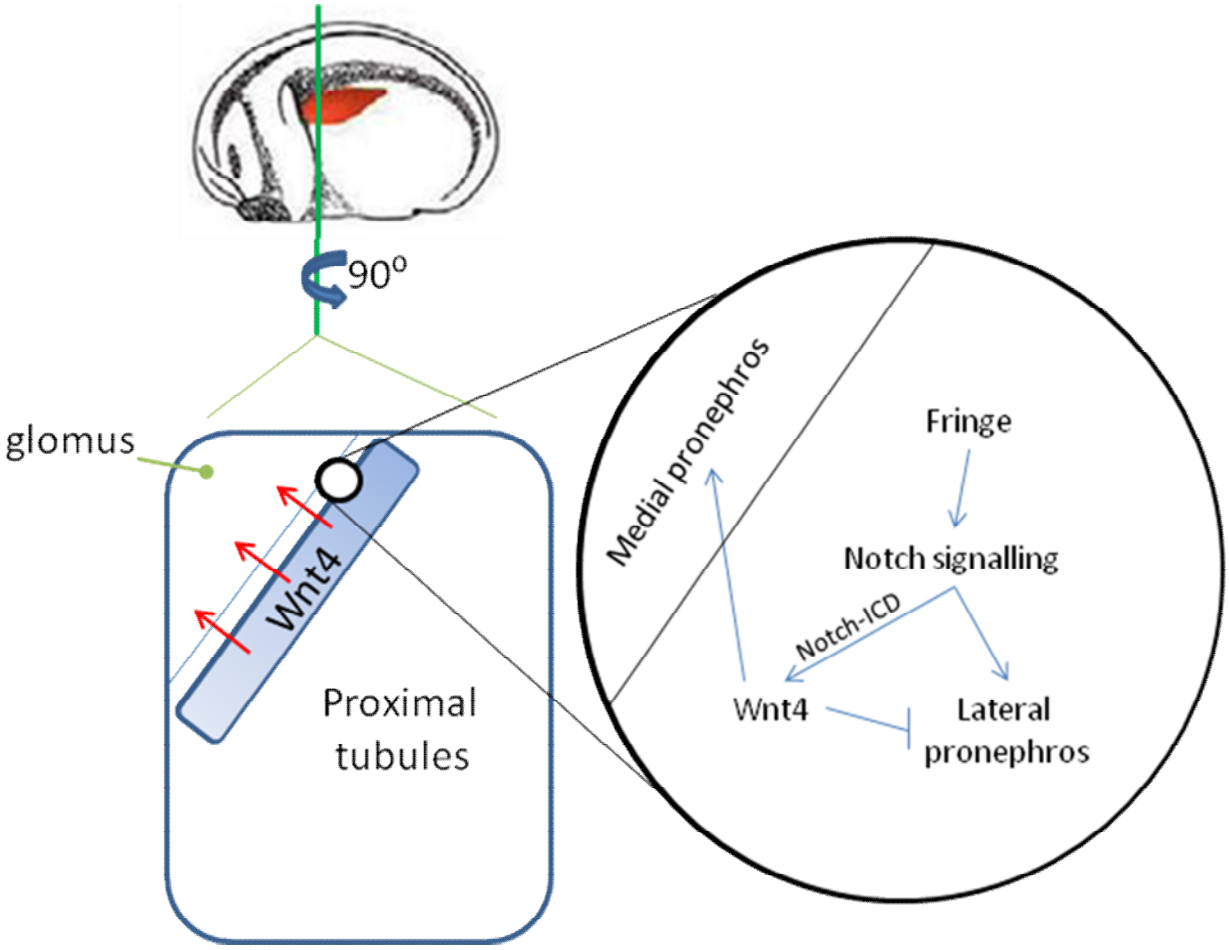

Figure 7.1 A model for Notch-mediated medio-lateral patterning of the proximal pronephros anlagen. Observing the proximal pronephros anlagen at early tail bud stages in cross-section, we propose the pool of cells in the proximal-dorsal region of the lateral pronephros mesoderm juxtaposed to the medial pronephros that undergo Notch signalling, act to promote medial pronephrogenesis by inducing the secretion of Wnt4 to the medial side. This signal seems to be activated by the Notch-ICD-dependent pathway and the gene expression it induces. The overall effect of binary cell interactions through Notch-ligand binding, promotes differentiation of the lateral pronephros in the correct position. Ectopic expression of Wnt4 prevents this lateral pronephrogenesis. Thus this pool of cells establishes a boundary that prevents extension of medial pronephros cell fates (those cells that express molecules like WT-1) into the lateral pronephric mesoderm (where cells expressing Lim-1 and Pax-8 are located).

capabilities as is observed in the pool of cells expressing Wnt4 and components of the Notch signalling pathway in the proximal-dorsal lateral region.

7.2.3 Is *X. laevis* pronephrogenesis a good model of metanephric nephron segmentation?

The metanephric nephron is comprised of specialised segments that perform unique solute transport functions (Jacobson, 1981). Recent investigation into zebrafish and *X. laevis* pronephros patterning has shown the proximal-distal axis is a strictly segmented structure with regions of analogous solute carrier composition to those observed in mammalian nephrons (Nichane et al., 2006; Van Campenhout et al., 2006; Reggiani et al., 2007; Raciti et al., 2008). Consequently Wingert and Davidson (2008) have written a mini review article collating all these results and comparing the mammalian nephron and zebrafish and *Xenopus* pronephros in terms of tubule identity along the proximal distal axis (Fig 7.2) (Wingert and Davidson, 2008). The authors of this article argue anamniote vertebrate pronephros models will be invaluable to dissect the developmental pathways that establish segmentation of the tubules as experimental analysis of these organisms is much easier than in the study of metanephrogenesis. From our results we agree with this conclusion. Interpretation of results in zebrafish initially led us to believe this system was not a very good model to understand metanephric nephron development as certain aspects of this renal system are different to *X. laevis* pronephrogenesis and mammalian metanephrogenesis. Notable differences include, the Notch signalling pathway in zebrafish is necessary to regulate patterning of multi-ciliated and non-ciliated cells rather than the proximal pronephric region (Liu et al., 2007; Ma and Jiang, 2007), and the renal progenitors of all regions of the zebrafish pronephros are induced

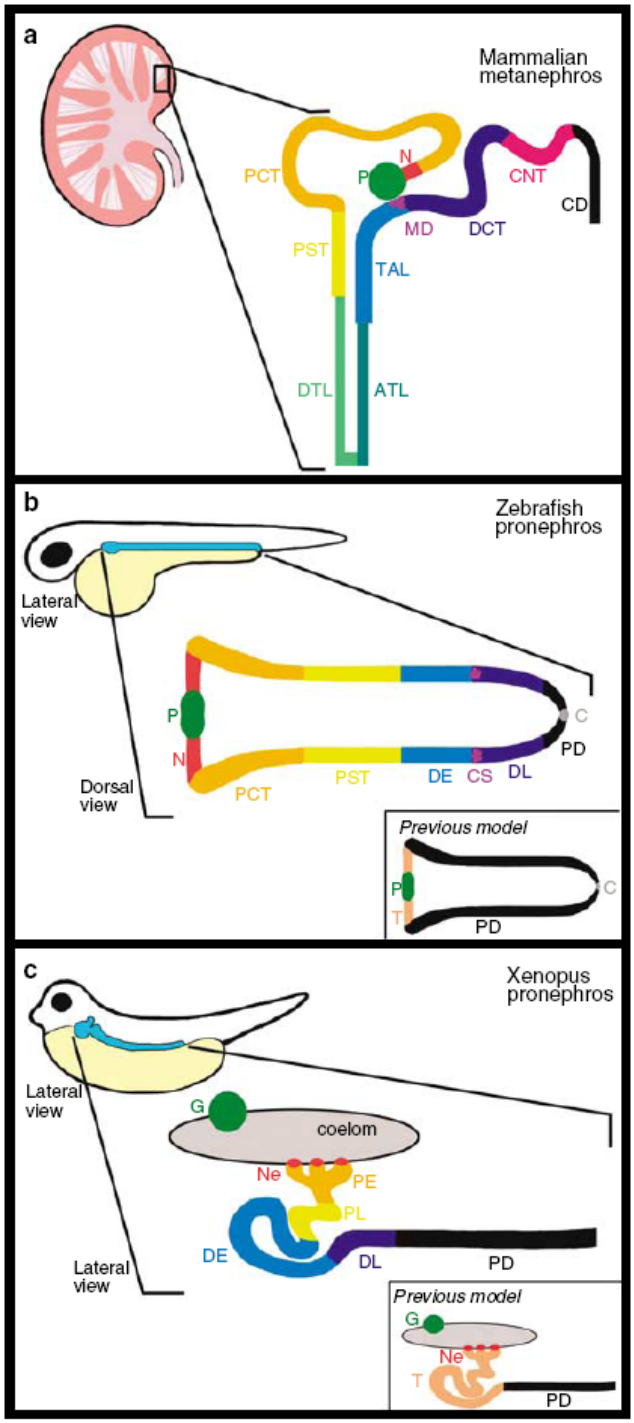

Figure 7.2 Conservation of the proximal/ distal segmentation of the mammalian metanephric nephron and the zebrafish and *Xenopus* pronephroi. The pronephros found in zebrafish and *Xenopus* is representative of a single nephron found in the mammalian metanephros. Significant similarities in tubular structure and molecular composition are present. Abbreviations: ATL, ascending thin limb; C, cloaca; CD, collecting duct; CNT, connecting tubule; CS, corpuscle of Stannius; DCT, distal convoluted tubule; DE, distal early; DL, distal late; DTL, descending thin limb; G, glomus; MD, macula densa; N, neck; Ne, nephrostome; P, podocytes of renal corpuscle; PCT, proximal convoluted tubule; PD, pronephric duct; PE, proximal early; PL, proximal late; PST, proximal straight tubule; T, tubule; TAL, thick ascending limb. (Figure taken from Wingert and Davidson, 2008)

simultaneously, rather than the nephric duct extending caudally towards the cloaca as is observed in *X. laevis* and as happens in mammals (Drummond, 2005; Wingert and Davidson, 2008). These differences are frustrating as zebrafish has the potential to be a genetic model of pronephrogenesis where transgenic lines can be made to target over-expression of particular genes temporally in the intermediate mesoderm. Given the difficulties we have had with the *Lunatic fringe* MO in our experiments in *X. laevis*, we hoped zebrafish may provide a better model system to analyse the hypotheses presented in this thesis. However, whilst most experimentation on how the Notch signalling pathway regulates zebrafish pronephrogenesis has concentrated on patterning of multi-ciliated cells, *in situ* hybridisation analysis of *Notch3* (Liu et al., 2007) and *Jagged2a* (Ma and Jiang, 2007) at earlier stages of development may suggest Notch signalling during early zebrafish pronephrogenesis is required to form the glomus and subsequently pattern the tubules. In support of this, the pattern of *Notch-1* and *Serrate-1* expression post stage 30 in *X. laevis* is mosaic in appearance and may be indicative of lateral inhibition patterning cell fates in this region at this time of development (McLaughlin et al., 2000). Whilst intercalated multi-ciliated and mono-ciliated cells are not present in the tubules of *X. laevis*, 4A6 staining does appear mosaic and may mark cells containing an epitope not present in certain cells along the distal tubule (Vize et al., 1995). Additionally, mammalian collecting ducts have been shown to be composed of principal cells, involved in specific solute transport, intercalated with different cell lineages (Aigner et al., 1995).

7.2.4 Concluding remarks

Many molecules involved in development of the pronephros are required for development of the metanephric nephron (such as *WT-1*, *Wnt9b*, *Wnt4*, *Notch-1*, *Pax-*

2, *Pax-8* and many more). Despite there being subtle differences, for example Wnt4 in nephron development is required for distal differentiation rather than proximal differentiation, *X. laevis* pronephrogenesis is certainly a more than adequate model of metanephric development. In terms of Notch-mediated regulation of nephrogenesis, research into *X. laevis* pronephros development may yield important data on glomerulus diseases that are frequently induced as a consequence of mis-expression of components of the Notch pathway (Mertens et al., 2008). In particular, we suggest future directions to study how Notch signalling regulates pronephros development should concentrate on the role Fringe and Wnt4 play as we have distinguished these two genes as important factors controlling the effects of Notch signalling in pronephrogenesis in *X. laevis*.

Appendices

Empirical Data and Statistical Analysis (1-4)

Effect of *Notch-ICD* and *Delta*^{STU} over-expression on *p27*^{Xic1} expression (5)

Fringe translation is regulated by UTR sequences and co-injection of the *Radical* and *Lunatic Fringe* MOs does not alter the single *Lunatic fringe* MO1 phenotype (6)

Appendix One

Empirical Data and Statistical Analysis for Chapter 3

The Chi-squared test to determine the statistical significance of my data

To test the significance of my results I chose to use the Chi-squared test. With this test all my data was analysed statistically.

Formulas required for the Chi-squared (χ^2) test analysis:

H_0 = null hypothesis

Chi-squared (χ^2) = $\Sigma \frac{(O - E)^2}{E}$ Where O = Observed frequency
E = Expected frequency

Expected value (E) = (row total x column total) / grand total

degrees of freedom (d f) = (number of rows – 1) (number of columns – 1)

p = probability of error threshold

if χ^2 > p = data presents a statistically significant relationship between the variables. Therefore, the null hypothesis is rejected.

Example:

400 pg *βgal* mRNA was injected with or without 2 ng *Radical fringe* mRNA into ventro-vegetal (V2) blastomere of an 8-cell stage embryo, cultured to stage 41 and the effect on 3G8 antibody staining was scored relative to the control un-injected side (appendix Table 1).

Injection	Ectopic	Decrease	Normal
400pg β-gal	0	1	19
2ng Radical fringe + 400pg β-gal	38	0	3

Ap Table 1 Results from 3G8 antibody stained embryos injected with *p27^{Xic1}* MO

Chi-squared (χ^2) test.

Null Hypothesis: "There is no difference in pronephric 3G8 staining between 2 ng *Radical fringe* mRNA and control *βgal* mRNA injected *Xenopus* embryos".

Step 1: Determine the threshold of tolerance for error. I will use a 1 in 20 probability of error threshold, or p< 0.5.

Step 2: Add up the row and column totals, and determine the grand total of all the scored phenotypes.

Injection	Ectopic	Decrease	Normal	Totals
400pg β-gal	0	1	19	20
2ng Radical fringe + 400pg β-gal	38	0	3	41
TOTALS	38	1	22	61

row totals

column totals

grand total

Step 3: Calculation of the expected frequencies as follows:

For 2 ng *Radical fringe* with ectopic pronephrogenesis,

O = 38

E = (row total x column total) / grand total

E = (20 x 38) / 61 = **12.46**

For 2 ng *Radical fringe* with decreased ectopic pronephrogenesis,

O = 0

E = (row total x column total) / grand total

E = (20 x 1) / 61 = **0.33**…….. etc

This generates the following expected frequencies,

Injection	Ectopic	Decrease	Normal
400pg β-gal	12.46	0.33	7.21
2ng Radical fringe + 400pg β-gal	25.54	0.67	14.79

Step 4: Calculation of χ^2 value for each variable combination;

$$\chi^2 = \frac{(O - E)^2}{E}$$

For each variable the value of χ^2 is generated,

e.g. 2 ng *Radical fringe* / Ectopic = $\frac{(0 - 12.46)^2}{12.46}$ = **12.46** (to 2 d.p.)

2ng $p27^{Xic1}$ / Narrowed = $\frac{(1 - 0.33)^2}{0.33}$ = **1.36** (to 2 d.p.)

and so on for each row and column…

Step 5: Total χ^2 value

$$\chi^2 = \frac{\Sigma (O - E)^2}{E} = \mathbf{49.31}$$

Step 6: Calculating the degrees of freedom,

d.f. = (number of rows – 1) (number of columns – 1)

therefore, d.f. = (2 – 1) (3 – 1) = **2**

Step 7: Looking up the critical value for χ^2 at 2 d.f., $p< 0.5 = 5.991$

The χ^2 value is 16.70 which is significant because it is above the critical value for the probability of error threshold, $p< 0.5$. Therefore the null hypothesis can be rejected, and affirms the claim that 2 ng *Radical fringe* mRNA and control *βgal* mRNA injected into *Xenopus* embryos gives different phenotypes in the pronephros.

This was performed for each experiment analysed.

Over-expression of *p27^{Xic1}*, *p21^{Cip1}* and *p27^{Xic1}-N* affects kidney development

Empirical data for Figure 3.5

Proximal Tubules (3G8 antibody staining)

Injection	Reduced	Absent	Widened	Normal	Totals	Significance
Uninjected	0 (0)	0 (0)	0 (0)	48 (100)	48	0.38
400pg β-galactosidase (β-gal)	1 (1.7)	0 (0)	0 (0)	57 (98.3)	58	n/a
10pg p21Cip1 + 400pg β-gal	16 (48.5)	3 (9.1)	0 (0)	14 (42.4)	33	38.14
20pg p21Cip1 + 400pg β-gal	26 (50)	17 (32.6)	0 (0)	9 (17.4)	52	74.86
25pg p27Xic1 + 400pg β-gal	20 (37)	7 (13)	0 (0)	27 (50)	54	34.76
50pg p27Xic1 + 400pg β-gal	13 (56.5)	8 (34.8)	0 (0)	2 (8.7)	23	43.75
25pg p27Xic1-N + 400pg β-gal	14 (42.2)	0 (0)	0 (0)	19 (57.8)	33	25.29
50pg p27Xic1-N + 400pg β-gal	8 (36.4)	7 (31.8)	0 (0)	7 (31.8)	22	71.1
40pg p27Xic1-#2 + 400pg β-gal	2 (5.9)	0 (0)	0 (0)	32 (94.1)	23	1.17
80pg p27Xic1-#2 + 400pg β-gal	0 (0)	0 (0)	0 (0)	13 (100)	34	0
40pg p27Xic1-C + 400pg β-gal	0 (0)	0 (0)	0 (0)	23 (100)	23	0
80pg p27Xic1-C + 400pg β-gal	0 (0)	0 (0)	0 (0)	32 (100)	32	0
50pg p27Xic1 CK- 400pg β-gal	2 (7.1)	0 (0)	0 (0)	26 (92.9)	28	1.61

Note: In text 'absent' has been included in score for reduced pronephros phenotype
% are shown in brackets next to empirical data

Intermediate and Distal Tubules (4A6 antibody staining)

Injection	Reduced	Absent	Widened	Normal	Totals	Significance
Uninjected	0 (0)	0 (0)	0 (0)	48 (100)	48	0
400pg β-galactosidase (β-gal)	0 (0)	0 (0)	0 (0)	58 (100)	58	n/a
10pg p21Cip1 + 400pg β-gal	15 (45.5)	3 (9)	0 (0)	15 (45.5)	33	44.57
20pg p21Cip1 + 400pg β-gal	29 (55.8)	14 (26.9)	0 (0)	9 (17.3)	52	109.97
25pg p27Xic1 + 400pg β-gal	16 (29.6)	7 (13)	0 (0)	31 (57.4)	54	31.07
50pg p27Xic1 + 400pg β-gal	12 (52.1)	7 (30.4)	0 (0)	4 (17.4)	23	62.57
25pg p27Xic1-N + 400pg β-gal	13 (39)	0 (0)	0 (0)	20 (61)	33	22.9
50pg p27Xic1-N + 400pg β-gal	7 (31.8)	8 (36.4)	0 (0)	7 (31.8)	22	48.7
40pg p27Xic1-#2 + 400pg β-gal	0 (0)	0 (0)	0 (0)	34 (100)	23	0
80pg p27Xic1-#2 + 400pg β-gal	0 (0)	0 (0)	0 (0)	13 (100)	34	0
40pg p27Xic1-C + 400pg β-gal	0 (0)	0 (0)	0 (0)	23 (100)	23	0
80pg p27Xic1-C + 400pg β-gal	0 (0)	1 (0.5)	0 (0)	31 (99.5)	32	0.49
50pg p27Xic1 CK- 400pg β-gal	2 (7.1)	0 (0)	0 (0)	26 (92.9)	28	4.235

Key

Significant value	$p \leq 0.05 = 5.991$
Non-significant value	

Null hypothesis: "There is no difference in pronephric tubule phenotype between x pg *p27^{Xic1}* / *p21^{Cip1}* / *p27^{Xic1} N*/ *p27^{Xic1} #2*/ and *p27^{Xic1} C* mRNA and 400pg *βgal* mRNA injected *Xenopus* embryos"

Knockdown of *p27^{Xic1}* endogenous translation using a Morpholino Oligonucleotide (MO) affects kidney development and can be rescued with *p21^{Cip1}* mRNA

Empirical data for Figure 3.8

Proximal Tubules (3G8 antibody staining)

Injection	Increase	Decrease	Absent	Normal	Totals	Significance
Uninjected	0 (0)	0 (0)	0 (0)	19 (100)	19	0
20ng Control MO + 400pg β-gal	0 (0)	0 (0)	0 (0)	23 (100)	23	n/a
5ng p27Xic1 MO + 400pg β-gal	0 (0)	5 (13.5)	0 (0)	32 (86.5)	37	3.27
10ng p27Xic1 MO + 400pg β-gal	0 (0)	8 (53.3)	1 (6.6)	6 (40.1)	15	18.08
20ng p27Xic1 MO + 400pg β-gal	0 (0)	16 (59.2)	9 (33.3)	2 (7.5)	27	46
10pg p21Cip1 + 400pg β-gal	0 (0)	16 (37.1)	0 (0)	26 (62.9)	42	52.67
20pg p21Cip1 + 400pg β-gal	0 (0)	18 (52.9)	13 (38.2)	3 (8.9)	34	54.66
10pg p21Cip1 + 20ng p27Xic1 MO + 400pg β-gal	0 (0)	11 (68.75)	4 (25)	1 (6.25)	16	36.56
20pg p21Cip1 + 20ng p27Xic1 MO + 400pg β-gal	0 (0)	2 (8.7)	0 (0)	21 (91.3)	23	2.08

Intermediate and Distal Tubules (4A6 antibody staining)

Injection	Increase	Decrease	Absent	Normal	Totals	Significance
Uninjected	0 (0)	0 (0)	0 (0)	19 (100)	19	0
20ng Control MO + 400pg β-gal	0 (0)	0 (0)	0 (0)	23 (100)	23	n/a
5ng p27Xic1 MO + 400pg β-gal	0 (0)	5 (13.5)	0 (0)	32 (86.5)	37	3.27
10ng p27Xic1 MO + 400pg β-gal	0 (0)	9 (60)	0 (0)	6 (40)	15	18.08
20ng p27Xic1 MO + 400pg β-gal	0 (0)	21 (77.7)	1 (3.8)	5 (18.5)	27	33.47
10pg p21Cip1 + 400pg β-gal	0 (0)	14 (33.3)	2 (4.8)	26 (61.9)	42	52.67
20pg p21Cip1 + 400pg β-gal	0 (0)	18 (52.9)	13 (38.2)	3 (8.9)	34	54.66
10pg p21Cip1 + 20ng p27Xic1 MO + 400pg β-gal	0 (0)	13 (81.25)	2 (12.5)	1 (6.25)	16	36.56
20pg p21Cip1 + 20ng p27Xic1 MO + 400pg β-gal	0 (0)	2 (8.7)	0 (0)	21 (91.3)	23	2.08

Key

Significant value	$p \leq 0.05 = 5.991$
Non-significant value	

Null hypothesis: "There is no difference in tubule phenotypes observed after *Xenopus* embryos were injected with x ng *p27^{Xic1}* MO and/ or x pg *p21^{Cip1}* mRNA and x pg *Control* MO"

The Apoptotic inhibitor *Bcl_{XL}* has no effect on the pronephric phenotypes induced by *$p27^{Xic1}$* mRNA and *$p27^{Xic1}$* MO

Empirical data for Figure 3.10

Pronephros Anlagen (*Lim-1 in situ* hybridisation)

Injection	Increase	Decrease	Absent	Normal	Totals	Significance
Uninjected	0 (0)	0 (0)	0	23 (100)	23	1.56
20ng ConMO + 400pg β-gal	0 (0)	1 (7)	0	14 (93)	15	n/a
20ng p27Xic1 MO + 1ng BclXL+ 400pg β-gal	0 (0)	18 (44)	23 (56)	0 (0)	41	126.25
20ng p27Xic1 MO+ 400pg β-gal	0 (0)	16 (66)	6 (25)	2 (9)	24	19.5
50pg p27Xic1 + 1ng BclXL + 400pg β-gal	0 (0)	14 (38)	17 (45)	6 (17)	37	26.9
50pg p27Xic1 + 400pg β-gal	0 (0)	21 (55)	7 (18)	10 (27)	38	19.47

Key

Significant value	$p \leq 0.05 = 5.991$
Non-significant value	

Null hypothesis: "There is no difference in the *Lim-1* expression pattern between x pg *$p27^{Xic1}$* / *$p27^{Xic1}$* MO / *Bcl_{XL}* mRNA and 20 ng *Control* MO injected *Xenopus* embryos"

p27^{Xic1} mRNA decreases cell division in addition to inhibiting pronephros development, *p27*^{Xic1} MO and *p27*^{Xic1} CK- have no effect on cell division

Empirical data for Figure 3.11

Pronephros Anlagen (*Lim-1 in situ* hybridisation)

Injection	Increase	Decrease	Normal	Totals	Significance
20ng ConMO + 400pg β-gal	0 (0)	1 (1.8)	54 (98.2)	55	n/a
20ng p27Xic1 MO + 400pg β-gal	0 (0)	26 (83.8)	5 (16.2)	31	61.99
50pg p27Xic1 + 400pg β-gal	0 (0)	18 (75)	6 (25)	24	48.98
50pg p27Xic1 CK- + 400pg β-gal	0 (0)	3 (4.5)	64 (95.5)	67	0.786

Key

Significant value	$p \leq 0.05 = 5.991$
Non-significant value	

Null hypothesis: "There is no difference in the *Lim-1* expression pattern between x pg *p27*^{Xic1} / *p27*^{Xic1} MO / *p27*^{Xic1} *CK*- mRNA and 20 ng *Con*trol MO injected *Xenopus* embryos"

Cell Division (pH3 antibody staining)

20 ng Control *MO*

Embryo	No. of cells injected side	No. of cells un-injected side	% difference
1	231	214	7.35
2	219	277	-20.9
3	205	225	-8.88
4	158	191	-17.2
5	213	209	1.57
6	180	232	-22.41
7	159	130	18.23
8	158	124	21.5
9	167	149	10.77
10	233	260	-10.4
11	120	114	5
st dev	36.69084602	56.30065396	-1.397272727
∑	2043	2125	14.74775674
mean	185.7272727	193.1818182	3.85% dec

20 ng p27^{Xic1} *MO*

Embryo	No. of cells injected side	No. of cells un-injected side	% difference
1	94	81	13.82
2	83	43	48.19
3	45	61	-26.23
4	51	128	-60.16
5	95	46	51.57
6	215	227	-5.28
7	36	47	-23.4
8	63	67	-5.29
9	52	48	7.69
10	84	81	3.57
11	88	67	23.8
st dev	48.73247937	54.06359891	2.570909091
∑	906	896	31.11417404
mean	82.36363636	81.45454545	1.1% inc

50 pg p27^{Xic1}

Embryo	No. of cells injected side	No. of cells un-injected side	% difference
1	46	245	-81.2
2	89	222	-59.9
3	34	204	-83.3
4	78	241	-67.6
5	38	108	-64.8
6	54	190	-71.57
7	77	215	-64.18
8	70	102	-31.4
9	110	65	-40.9
10	61	52	-14.7
11	40	247	-83.8
st dev	23.92184243	75.00460592	-60.30454545
∑	697	1891	21.37278872
mean	63.36363636	171.9090909	63.1% dec

50 pg p27^{Xic1} CK-

Embryo	No. of cells injected side	No. of cells un-injected side	% difference
1	46	245	-81.2
2	89	222	-59.9
3	34	204	-83.3
4	78	241	-67.6
5	38	108	-64.8
6	54	190	-71.57
7	77	215	-64.18
8	70	102	-31.4
9	110	65	-40.9
10	61	52	-14.7
11	40	247	-83.8
st dev	23.92184243	75.00460592	-60.30454545
∑	697	1891	21.37278872
mean	63.36363636	171.9090909	63.1% dec

p27^{Xic1} mRNA inhibited pronephros anlagen formation and disrupted somitogenesis, *p27^{Xic1}* MO inhibited both pronephros anlagen formation and myogenesis, and *p27^{Xic1}* CK- had no effect

Empirical data for Figure 3.13

Pronephros Anlagen (*Lim-1 in situ* hybridisation)

Injection	Increase	Decrease	Normal	Totals	Significance
20ng ConMO + 400pg β-gal	0 (0)	0 (0)	23 (100)	23	n/a
20ng p27Xic1 MO + 400pg β-gal	0 (0)	26 (78.8)	7 (21.2)	33	33.81
20ng p27Xic1 + 400pg β-gal	0 (0)	21 (77.7)	6 (22.3)	27	30.84
20ng p27Xic1 CK- + 400pg β-gal	0 (0)	2 (4.7)	41 (95.3)	43	1.1

Key

Significant value	$p \leq 0.05 = 5.991$
Non-significant value	

Null hypothesis: "There is no difference in the *Lim-1* expression pattern between x pg *p27^{Xic1}* / *p27^{Xic1}* MO / *p27^{Xic1} CK*- mRNA and 20 ng *Con*trol MO injected *Xenopus* embryos"

Muscle (*Myo-D in situ* hybridisation)

Injection	Increase	Decrease	Fused	Normal	Totals	Significance
20ng ConMO + 400pg β-gal	0 (0)	0 (0)	0 (0)	23 (100)	23	n/a
20ng p27Xic1 MO + 400pg β-gal	0 (0)	26 (78.8)	0 (0)	7 (21.2)	33	33.81
20ng p27Xic1 + 400pg β-gal	0 (0)	4 (14.8)	16 (59.2)	7 (26)	27	23.28
20ng p27Xic1 CK- + 400pg β-gal	0 (0)	0 (0)	0 (0)	43 (100)	43	0

Key

Significant value	$p \leq 0.05 = 5.991$
Non-significant value	

Null hypothesis: "There is no difference in the *MyoD* expression pattern between x pg *p27^{Xic1}* / *p27^{Xic1}* MO / *p27^{Xic1} CK*- mRNA and 20 ng *Con*trol MO injected *Xenopus* embryos"

*Note: Degrees of freedom have not changed despite an extra column as the "Fused" column was not included in the calculation of significance for *p27^{Xic1}* MO when compared to the *Control* MO as it was not a phenotype observed with the *p27^{Xic1}* MO. However the dominant phenotype after *p27^{Xic1}* mRNA injection was fused somites, thus the "Decrease" column was excluded from the calculation of significance for *p27^{Xic1}* mRNA compared to the *Control* MO, instead the "Fused" somite phenotype was compared as it was the dominant phenotype observed with *p27^{Xic1}* mRNA.*

p27^{Xic1} mRNA inhibited pronephros anlagen formation and disrupted somitogenesis, *p27^{Xic1}* MO inhibited both pronephros anlagen formation and myogenesis, and *p27^{Xic1}* CK- had no effect

Empirical data for Figure 3.15

Pronephros Anlagen (*Lim-1 in situ* hybridisation)

Injection	Increase	Decrease	Normal	Totals	Significance
20ng ConMO + 400pg β-gal	0 (0)	0 (0)	42 (100)	42	n/a
20ng p27Xic1 MO + 400pg β-gal	0 (0)	24 (88.9)	3 (11.1)	27	57.2
20ng p27Xic1 + 400pg β-gal	0 (0)	21 (77.7)	6 (22.3)	27	46.93
20ng p27Xic1 CK- + 400pg β-gal	0 (0)	1 (1.9)	51 (98.1)	52	0.825

Key

Significant value	$p \leq 0.05 = 5.991$
Non-significant value	

Null hypothesis: "There is no difference in the *Lim-1* expression pattern between x pg *p27^{Xic1}* / *p27^{Xic1}* MO / *p27^{Xic1} CK*- mRNA and 20 ng *Con*trol MO injected *Xenopus* embryos"

Muscle (*MHC in situ* hybridisation)

Injection	Increase	Decrease	Fused	Normal	Totals	Significance
20ng ConMO + 400pg β-gal	0 (0)	0 (0)	0 (0)	42 (100)	42	n/a
20ng p27Xic1 MO + 400pg β-gal	0 (0)	24 (88.9)	0 (0)	3 (11.1)	27	57.2
20ng p27Xic1 + 400pg β-gal	0 (0)	8 (22.9)	23 (65.7)	4 (11.4)	35	53.7
20ng p27Xic1 CK- + 400pg β-gal	0 (0)	0 (0)	0 (0)	52 (100)	52	0

Key

Significant value	$p \leq 0.05 = 5.991$
Non-significant value	

Null hypothesis: "There is no difference in the *Lim-1* expression pattern between x pg *p27^{Xic1}* / *p27^{Xic1}* MO / *p27^{Xic1} CK*- mRNA and 20 ng *Con*trol MO injected *Xenopus* embryos"

HUA treatment inhibited cell division

Empirical data for Figure 3.17

Cell Division (pH3 antibody staining)

Embryo	No. of cells (left side) HUA + DMSO	No. of cells (left side) DMSO
1	34	152
2	11	139
3	61	147
4	20	193
5	15	142
6	37	135
7	29	154
8	24	236
9	40	132
10	13	153
Σ	284	1583
mean	28.4	158.3
st dev	14.33290266	30.54193838

p35.1 mRNA disrupted both pronephros anlagen formation and somitogenesis, but this was insufficient to affect mature pronephros development

Empirical data for Figure 3.19

Pronephros Anlagen (*Lim-1 in situ* hybridisation)

(As part of Lim-1/ MyoD in situ *hybridisation)*

Injection	Increase	Decrease	Disrupted	Normal	Totals	Significance
400pg β-gal	0 (0)	0 (0)	0 (0)	26 (100)	26	n/a
2ng p35.1 + 400pg β-gal	0 (0)	2 (8.7)	12 (52)	9 (39.3)	23	19.96

Key

Significant value	p ≤ 0.05 = 5.991
Non-significant value	

Null hypothesis: "There is no difference in the *Lim-1* expression pattern between 2 ng *p35.1* mRNA and 400 pg βgal mRNA injected *Xenopus* embryos"

Muscle (*Myo-D in situ* hybridisation)

(As part of Lim-1/ MyoD in situ *hybridisation)*

Injection	Increase	Decrease	Fused	Normal	Totals	Significance
400pg β-gal	0 (0)	0 (0)	0 (0)	26 (100)	26	n/a
2ng p35.1 + 400pg β-gal	0 (0)	6 (26)	16 (69.5)	1 (4.5)	23	38.92

Key

Significant value	p ≤ 0.05 = 5.991
Non-significant value	

Null hypothesis: "There is no difference in the *Myo-D* expression pattern between 2 ng *p35.1* mRNA and 400 pg βgal mRNA injected *Xenopus* embryos"

Pronephros Anlagen (*Lim-1 in situ* hybridisation)
(As part of Lim-1/ MHC in situ *hybridisation)*

Injection	Increase	Decrease	Disrupted	Normal	Totals	Significance
400pg β-gal	0 (0)	0 (0)	0 (0)	19 (100)	19	n/a
2ng p35.1 + 400pg β-gal	0 (0)	10 (21.7)	28 (60.9)	8 (17.4)	46	26.86

Key

Significant value	p ≤ 0.05 = 5.991
Non-significant value	

Null hypothesis: "There is no difference in the *Lim-1* expression pattern between 2 ng *p35.1* mRNA and 400 pg βgal mRNA injected *Xenopus* embryos"

Muscle (*MHC in situ* hybridisation)
(As part of Lim-1/ MHC in situ *hybridisation)*

Injection	Increase	Decrease	Fused	Normal	Totals	Significance
400pg β-gal	0 (0)	0 (0)	0 (0)	19 (100)	19	n/a
2ng p35.1 + 400pg β-gal	0 (0)	4 (8.7)	23 (50)	19 (41.3)	46	16.69

Key

Significant value	p ≤ 0.05 = 5.991
Non-significant value	

Null hypothesis: "There is no difference in the *MHC* expression pattern between 2 ng *p35.1* mRNA and 400 pg βgal mRNA injected *Xenopus* embryos"

Tubules (3G8/ 4A6 Antibody Stain)

Injection	Increase	Decrease	Normal	Totals	Significance
400pg β-gal	0 (0)	1 (2.9)	34 (97.1)	35	n/a
2ng p35.1 + 400pg β-gal	0 (0)	1 (4.2)	7 (95.8)	24	0

Key

Significant value	p ≤ 0.05 = 5.991
Non-significant value	

Null hypothesis: "There is no difference in the 3G8/4A6 antibody staining between 2 ng *p35.1* mRNA and 400 pg βgal mRNA injected *Xenopus* embryos"

Appendix Two

Empirical Data and Statistical Analysis for Chapter 4

Over-expression of *p27Xic1 and Gadd45γ inhibits pronephros development*

Empirical data for Figure 4.4

Pronephros anlagen (*Lim-1 in situ* hybridisation)

Injection	Increase	Decrease	Absent	Normal	Total	Significance
400pg LacZ	0 (0%)	2 (7%)	0 *(0%)*	25 (93%)	27	n/a
50pg p27Xic1 + 400pg LacZ	0 (0%)	25 (51%)	5 *(20%)*	24 (49%)	49	11.25
500pg GADD45 + 400pg LacZ	0 (0%)	29 (62%)	4 *(14%)*	18 (38%)	47	20.76
50pg p27Xic1 + 500pg GADD45 + 400pg LacZ	0 (0%)	26 (84%)	13 *(50%)*	5 (16%)	31	33.78

Empirical data for Figure 4.5

Proximal tubules, Intermediate tubules and Distal tubules (3G8/ 4A6 antibody staining)

Injection	Increase	Decrease	Absent	Normal	Total	Significance
400pg LacZ	0 (0%)	1 (1%)	0 *(0%)*	72 (99%)	73	n/a
50pg p27Xic1 + 400pg LacZ	0 (0%)	32 (59%)	1 *(3%)*	22 (41%)	54	54.05
500pg GADD45 + 400pg LacZ	0 (0%)	8 (12%)	0 *(0%)*	60 (88%)	68	6.36
50pg p27Xic1 + 500pg GADD45 + 400pg LacZ	0 (0%)	37 (64%)	11 *(30%)*	21 (44%)	58	42.94

Key

Significant value	$p \leq 0.05 = 5.991$
Non-significant value	

Null hypothesis: "There is no difference in pronephric phenotype between x pg *p27Xic1, Gadd45γ or p27Xic1/ Gadd45γ* mRNA and 400pg *βgal* mRNA injected *Xenopus* embryos"

Over-expression of *p27Xic1 and Gadd45γ inhibits cell division*

Empirical data for Figure 4.6

Cell division (pH3 antibody stain)

well	1		2		3		4	
injection	XIC1		Gadd45g		Xic+Gadd45g		LacZ	
	inj. Side	uninj. Side	inj. Side	uninj. Side	inj. Side	uninj. Side	inj. Side	uninj. Side
	22	60	9	19	27	34	6	7
	8	69	0	2	6	17	40	14
	10	12	5	11	2	15	11	17
	14	66	18	13	7	29	11	7
	8	16	8	11	3	16	4	41
	12	18	15	6	1	4	57	65
	26	73	9	23	12	44	13	32
	1	6	8	15	5	32	11	9
	14	48	2	7	0	14	27	15
	7	7	15	11	20	8	24	28
	42	93	1	5	10	5	22	38
	56	71	15	30	3	27	26	17
	7	30	4	4	0	4		
			12	8	10	26		
mean	17.46153846	43.76923077	8.642857143	11.78571429	7.571428571	19.64285714	21	24.16666667
	Significant		Not Significant		Significant		Not significant	
stdev	15.704	30.061	5.773	7.827	7.861	12.549	15.392	17.393
sterror	4.355	8.338	1.543	2.092	2.101	3.354	4.443	5.021
mean difference		26.31		3.15		12.07		3.17
mean % difference		-60.10%		-26.71%		-61.46%		-13.10%

Null hypothesis: "There is no difference in the number of positively dividing cells between the injected side and un-injected side of *Xenopus* embryos injected with x pg *p27Xic1, Gadd45γ or p27Xic1/ Gadd45γ* mRNA and 400pg *βgal* mRNA"

Over-expression of *p27Xic1 domains and Gadd45γ inhibits pronephros anlagen formation*

Empirical data for Figure 4.7

Pronephros anlagen (*Lim-1 in situ* hybridisation)

Injection	Increased	Decreased	Normal	Totals	Significance
400pg βgal	0 (0)	4 (6)	67 (94)	71	n/a
500pg Gadd45 + 400pg βgal	0 (0)	16 (25)	47 (75)	63	10.2
50pg Xic1 + 400pg βgal	0 (0)	17 (70)	7 (30)	24	44.3
50pg Xic1 + 500pg Gadd45 + 400pg βgal	0 (0)	12 (41)	17 (59)	29	19.7
50pg Xic-1-N + 400pg βgal	0 (0)	18 (81)	4 (19)	22	54
50pg Xic-1-N + 500pg Gadd45 + 400pg βgal	0 (0)	17 (78)	5 (22)	22	49.2
80pg Xic1#2 + 400pg βgal	0 (0)	3 (10)	27 (90)	30	0.65
80pg Xic1#2 + 500pg Gadd45 + 400pg βgal	0 (0)	12 (26)	35 (74)	47	9.48
80pg Xic1-C + 400pg βgal	0 (0)	6 (14)	35 (86)	41	2.58
80pg Xic1-C + 500pg Gadd45 + 400pg βgal	0 (0)	2 (8)	22 (92)	24	0.23

Key

Significant value	$p \leq 0.05 = 5.991$
Non-significant value	

Null hypothesis: "There is no difference in *Lim-1* expression between x pg mRNA injected and 400pg *βgal* mRNA injected *Xenopus* embryos"

Effects of various MO and mRNAs on primary neurogenesis

Empirical data for Figure 4.9 and 4.13

Primary neurons (*Nß-tubulin in situ* hybridisation)

Injection	Increase	Decrease	Absent	Normal	Totals	Significance
20ng ConMO + 400pg βgal	0 (0)	2 (3)	0	60 (97)	62	n/a
20ng Xic1MO + 400pg βgal	0 (0)	40 (82)	1	9 (18)	49	71.4
50pg Xic1 + 400pg βgal	0 (0)	3 (12)	0	21 (88)	24	2.7
200pg Xic1-NT + 400pg βgal	0 (0)	9 (15)	0	49 (85)	58	5.44
200pg Xic1-#2 + 400pg βgal	0 (0)	7 (14)	0	44 (86)	51	4.2
200pg Xic1-CT + 400pg βgal	3 (5)	5 (9)	0	50 (86)	58	5.1
600pg Notch-ICD + 400pg βgal	0 (0)	45 (78)	41	14 (22)	58	67.9
1ng DeltaSTU + 400pg βgal	0 (0)	5 (10)	0	45 (90)	50	2.17
20ng A2 MO + 400pg βgal	0 (0)	7 (13)	0	45 (87)	52	4.09
70pg A2 6MT + 400pg βgal	0 (0)	29 (83)	0	6 (7)	35	65.2
20ng A2 MO + 70pg A2 6MT + 400pg βgal	0 (0)	19 (90)	0	2 (10)	21	64.7
200pg L48P + 400pg βgal	0 (0)	3 (13)	0	20 (87)	23	2.9
100pg S46A + 400pg βgal	0 (0)	1 (2)	0	57 (98)	58	0.3
100pg E54A + 400pg βgal	0 (0)	0 (0)	0	41 (100)	41	1.3
20ng Xic1MO + 20ng A2 MO + 400pg βgal	0 (0)	14 (88)	3	2 (12)	16	55.4
20ng A2 MO + 50pg Xic1 + 400pg βgal	1 (4)	3 (12)	2	22 (84)	25	4.3
20ng A2 MO + 50pg Xic1-NT + 400pg βgal	0 (0)	19 (90)	16	2 (10)	21	60.9
20ng A2 MO + 50pg Xic1-#2 + 400pg βgal	0 (0)	7 (14)	0	44 (86)	51	4.2
20ng A2 MO + 50pg Xic1-CT + 400pg βgal	0 (0)	0 (0)	0	38 (100)	38	1.3
20ng A2 MO + 600pg Notch-ICD + 400pg βgal	0 (0)	46 (96)	28	2 (4)	48	111.3
20ng A2 MO + 1ng DeltaSTU + 400pg βgal	3 (7)	7 (16)	0	33 (77)	43	8.1
20ng A2 MO + 200pg L48P + 400pg βgal	0 (0)	1 (4)	0	24 (96)	25	0.02
20ng A2 MO + 100pg S46A + 400pg βgal	0 (0)	1 (2)	0	44 (98)	45	0.01
20ng A2 MO + 100pg E54A + 400pg βgal	0 (0)	1 (3)	0	34 (97)	35	0.015

Key

Significant value	$p \leq 0.05 = 5.991$
Non-significant value	

Null hypothesis: "There is no difference in primary neurogenesis between x ng/ pg MO or mRNA injected and 20 ng *Control* MO/ 400pg *βgal* mRNA injected *Xenopus* embryos"

Depletion of Cyclin A2 inhibits pronephros development

Empirical data for Figure 4.12

Proximal tubules, Intermediate tubules and Distal tubules (3G8/ 4A6 antibody staining)

Injection	Narrowed	Absent	Widened	Normal	Totals	Significance
20ng Cyclin A2 MO + 400pg β-gal	19 (48.7)	0 (0)	2 (5.1)	18 (46.2)	39	34.43
40ng Cyclin A2 MO + 400pg β-gal	0 (0)	25 (80.6)	5 (16.1)	1 (3.3)	31	83.81
40ng Control MO + 400pg β-gal	1 (1.5)	2 (3)	0 (0)	63 (95.5)	66	n/a

Key

Significant value	$p \leq 0.05 = 5.991$
Non-significant value	

Null hypothesis: "There is no difference in pronephric phenotype between x ng *Cyclin A2* MO and 20 ng *Control* MO/ 400pg *βgal* mRNA injected *Xenopus* embryos"

Appendix Three

Empirical Data and Statistical Analysis for Chapter 5

Over-expression of *Notch-ICD*, *Delta*^{STU}, and *Wnt 4* affects 3G8/ 4A6 antibody staining

Empirical data for Figure 5.2

Proximal Tubules (3G8 antibody staining)

Injection	Ectopic	Decrease	Absence	Normal	Totals	Significance
Uninjected	0 (0)	0 (0)	0	51 (100)	51	0
400pg β-gal	0 (0)	0 (0)	0	43 (100)	43	n/a
600pg Notch-ICD + 400pg β-gal	26 (76)	3 (9)	0	5 (15)	34	55.67
1ng DeltaSTU + 400pg β-gal	0 (0)	12 (33)	1	24 (66)	36	16.9
1ng Wnt 4 + 400pg β-gal	18 (69)	2 (8)	0	6 (23)	26	46.57

Note: In text 'absent' has been included in score for reduced pronephros phenotype
% are shown in brackets next to empirical data

Intermediate and Distal Tubules (4A6 antibody staining)

Injection	Ectopic	Decrease	Absence	Normal	Totals	Significance
Uninjected	0 (0)	0 (0)	0	51 (100)	51	0
400pg β-gal	0 (0)	0 (0)	0	43 (100)	43	n/a
600pg Notch-ICD + 400pg β-gal	0 (0)	33 (97)	28	1 (3)	34	72.87
1ng DeltaSTU + 400pg β-gal	0 (0)	2 (5.5)	0	34 (94.5)	36	2.44
1ng Wnt 4 + 400pg β-gal	0 (0)	20 (77)	16	6 (23)	26	46.56

Key

Significant value	$p \leq 0.05 = 5.991$
Non-significant value	

Null hypothesis: "There is no difference in pronephric tubule phenotype between x pg *Notch-ICD*, *Delta*^{STU}, and *Wnt 4* mRNA and 400pg *βgal* mRNA injected *Xenopus* embryos"

Over-expression of *Notch-ICD, Delta^{STU}*, and *Wnt 4* affects *Na^+ K^+ ATPase* expression

Empirical data for Figure 5.3

Proximal, intermediate and distal tubules (*Na^+ K^+ ATPase*)

Injection	Ectopic	Decrease	Absence	Normal	Totals	Significance
Uninjected	0 (0)	0 (0)	0	25 (100)	25	0.49
400pg β-gal	0 (0)	1 (4)	0	27 (100)	28	n/a
600pg Notch-ICD + 400pg β-gal	0 (0)	23 (96)	17	1 (4)	24	44.23
1ng DeltaSTU + 400pg β-gal	0 (0)	*30 (70)	1	13 (30)	43	30.2
1ng Wnt 4 + 400pg β-gal	0 (0)	19 (83)	4	4 (17)	23	33.17

* This value identifies that Delta^{STU} reduced overall *Na^+ K^+ ATPase* expression; however the table does not acknowledge which regions of pronephric *Na^+ K^+ ATPase* were reduced. Delta^{STU} actually completely reduced *Na^+ K^+ ATPase* expression in 27% of embryos, but in 47% it only reduced proximal *Na^+ K^+ ATPase* expression. For all other injections (*Notch-ICD* and *Wnt 4*) *Na^+ K^+ ATPase* was reduced in both the proximal and distal regions

Key

Significant value	$p \leq 0.05 = 5.991$
Non-significant value	

Null hypothesis: "There is no difference in pronephric tubules phenotype between x pg *Notch-ICD, Delta^{STU}*, and *Wnt 4* mRNA and 400pg *βgal* mRNA injected *Xenopus* embryos"

Over-expression of *Notch-ICD*, *Delta*^{STU}, and *Wnt 4* inhibits *Slc5a2* expression

Empirical data for Figure 5.4

Proximal tubules (*Slc5a2*)

Injection	Ectopic	Decrease	Absence	Normal	Totals	Significance
Uninjected	0 (0)	0 (0)	0	0 (0)	0	n/a
400pg β-gal	0 (0)	2 (3)	0	61 (97)	63	n/a
600pg Notch-ICD + 400pg β-gal	0 (0)	36 (95)	27	2 (5)	38	92.66
1ng DeltaSTU + 400pg β-gal	0 (0)	26 (76)	14	8 (24)	34	57.79
1ng Wnt 4 + 400pg β-gal	0 (0)	33 (92)	19	3 (8)	36	78.38

Key

Significant value	$p \leq 0.05 = 5.991$
Non-significant value	

Null hypothesis: "There is no difference in pronephric proximal tubule phenotype between x pg *Notch-ICD*, *Delta*^{STU}, and *Wnt 4* mRNA and 400pg *βgal* mRNA injected *Xenopus* embryos"

Over-expression of *Notch-ICD*, *Delta*^{STU}, and *Wnt 4* affects *odf3* expression

Empirical data for Figure 5.5

Nephrostomes (*odf3*)

Injection	Ectopic	Decrease	Absence	Normal	Totals	Significance
Uninjected	0 (0)	0 (0)	0	0 (0)	0	n/a
400pg β-gal	0 (0)	6 (9)	0	47 (91)	53	n/a
600pg Notch-ICD + 400pg β-gal	20 (74)	2 (7)	0	0 (0)	27	56.54
1ng DeltaSTU + 400pg β-gal	0 (0)	25 (89)	22	3 (11)	28	47.27
1ng Wnt 4 + 400pg β-gal	26 (76)	3 (8)	0	5 (15)	34	59.35

Key

Significant value	$p \leq 0.05 = 5.991$
Non-significant value	

Null hypothesis: "There is no difference in pronephric nephrostome phenotype between x pg *Notch-ICD*, *Delta*^{STU}, and *Wnt 4* mRNA and 400pg *βgal* mRNA injected *Xenopus* embryos"

Over-expression of *Notch-ICD*, *Delta*^{STU}, and *Wnt 4* affects *Nephrin* expression

Empirical data for Figure 5.6

Glomus (*Nephrin*)

Injection	Ectopic	Decrease	Absence	Normal	Totals	Significance
Uninjected	0 (0)	0 (0)	0	0 (0)	0	n/a
400pg β-gal	0 (0)	0 (0)	0	45 (100)	45	n/a
600pg Notch-ICD + 400pg β-gal	22 (81)	5 (19)	0	0 (0)	27	56.88
1ng DeltaSTU + 400pg β-gal	0 (0)	30 (88)	19	4 (12)	34	63.96
1ng Wnt 4 + 400pg β-gal	24 (75)	3 (9)	0	5 (16)	32	70.55

Key

Significant value	$p \leq 0.05 = 5.991$
Non-significant value	

Null hypothesis: "There is no difference in pronephric glomus phenotype between x pg *Notch-ICD*, *Delta*^{STU}, and *Wnt 4* mRNA and 400pg *βgal* mRNA injected *Xenopus* embryos"

Over-expression of *Notch-ICD* and *Delta*^{STU} affects *Wnt 4* expression

Empirical data for Figure 5.7

Wnt 4 in situ hybridisation

Injection	Ectopic	Decrease	Absence	Normal	Totals	Significance
Uninjected	0 (0)	0 (0)	0	0 (0)	0	n/a
400pg β-gal	0 (0)	1 (4)	1	24 (96)	25	n/a
600pg Notch-ICD + 400pg β-gal	15 (47)	1 (3)	0	16 (50)	32	15.96
1ng DeltaSTU + 400pg β-gal	0 (0)	18 (78)	17	5 (15)	23	30.2

Key

Significant value	$p \leq 0.05 = 5.991$
Non-significant value	

Null hypothesis: "There is no difference in *Wnt 4* expression between x pg *Notch-ICD* and *Delta*^{STU} mRNA and 400pg *βgal* mRNA injected *Xenopus* embryos"

Over-expression of *Wnt 4* disrupts *Delta-1* and *Serrate-1* expression

Empirical data for Figure 5.8

Delta-1 in situ hybridisation

Injection	Disrupted	Ectopic	Decrease	Absence	Normal	Totals	Significance
Uninjected	0	0	0	0	0	0	n/a
400pg β-gal	0 (0)	0 (0)	0 (0)	0	21 (100)	21	n/a
1 ng Wnt-4 + 400pg β-gal	27 (84)	0 (0)	2 (6)	0	3 (10)	32	40.74

Empirical data for Figure 5.9

Serrate-1 in situ hybridisation

Injection	Disrupted	Ectopic	Decrease	Absence	Normal	Totals	Significance
Uninjected	0	0	0	0	0	0	n/a
400pg β-gal	0 (0)	0 (0)	0 (0)	0	19 (100)	19	n/a
1 ng Wnt-4 + 400pg β-gal	22 (61)	0 (0)	5 (14)	0	9 (25)	36	29.84

Key

Significant value	$p \leq 0.05 = 7.82$
Non-significant value	

Null hypothesis: "There is no difference in *Delta-1* or *Serrate-1* expression between 1 ng *Wnt-4* mRNA and 400pg *βgal* mRNA injected *Xenopus* embryos"

Over-expression of *Delta-1* caused ectopic glomus formation, but inhibited *slc5a2* expression

Empirical data for Fig 5.12

Glomus (*nephrin in situ* hybridisation)

Injection	Ectopic	Decrease	Absence	Normal	Totals	Significance
Uninjected	0 (0)	0 (0)	0	0 (0)	0	n/a
400pg β-gal	0 (0)	3 (9)	0	31 (91)	34	n/a
1ng Delta-1 + 400pg β-gal	17 (61)	1 (7)	0	10 (32)	28	28.43
1ng Serrate-1 + 400pg β-gal	0 (0)	4 (11)	0	31 (89)	35	0.11

Proximal tubule (*slc5a2 in situ* hybridisation)

Injection	Ectopic	Decrease	Absence	Normal	Totals	Significance
Uninjected	0 (0)	0 (0)	0	0 (0)	0	n/a
400pg β-gal	0 (0)	2 (4)	0	44 (96)	46	n/a
1ng Delta-1 + 400pg β-gal	0 (0)	25 (86)	9	4 (14)	29	51.73
1ng Serrate-1 + 400pg β-gal	0 (0)	6 (19)	0	25 (81)	31	4.47

Key

Significant value	$p \leq 0.05 = 5.991$
Non-significant value	

Null hypothesis: "There is no difference in *nephrin* or *slc5a2* expression between 1 ng *Delta-1* mRNA or 1 ng *Serrate-1* mRNA and 400pg *βgal* mRNA injected *Xenopus* embryos"

Appendix Four

Empirical Data and Statistical Analysis for Chapter 6

***Radical fringe* over-expression induced ectopic tubulogenesis, whereas *Lunatic fringe* over-expression inhibited tubulogenesis**

Empirical data for Figure 6.5

Tubules (*Na^+K^+ ATPase*)

Injection	Ectopic	Decrease	Absence	Normal	Totals	Significance
Uninjected	0 (0)	0 (0)	0	0 (0)	0	n/a
400pg β-gal	0 (0)	1 (2)	0	41 (98)	42	n/a
2ng Radical fringe + 400pg β-gal	18 (67)	4 (14)	0	5 (19)	27	43.46

Injection	Ectopic	Decrease	Absence	Normal	Totals	Significance
Uninjected	0 (0)	0 (0)	0	0 (0)	0	n/a
400pg β-gal	0 (0)	4 (8)	0	49 (92)	53	n/a
0.5ng Lunatic fringe 400pg β-gal	0 (0)	22 (92)	0	2 (2)	24	50.98

Key

Significant value	$p \leq 0.05 = 5.991$
Non-significant value	

Null hypothesis: "There is no difference in tubulogenesis between x ng *Radical fringe* mRNA and *Lunatic fringe* mRNA and 400 pg *βgal* mRNA injected *Xenopus* embryos"

Radical fringe over-expression induced ectopic glomus, nephrostome and proximal tubule formation

Empirical data for Figure 6.6

Glomus (*Nephrin*)

Injection	Ectopic	Decrease	Absence	Normal	Totals	Significance
Uninjected	0 (0)	0 (0)	0	0 (0)	0	n/a
400pg β-gal	0 (0)	1 (5)	0	19 (95)	20	n/a
2ng Radical fringe + 400pg β-gal	17 (81)	4 (19)	0	0 (0)	21	37.8

Proximal tubules (*slc5a2*)

Injection	Ectopic	Decrease	Absence	Normal	Totals	Significance
Uninjected	0 (0)	0 (0)	0	0 (0)	0	n/a
400pg β-gal	0 (0)	2 (12)	0	15 (88)	17	n/a
2ng Radical fringe + 400pg β-gal	13 (59)	6 (27)	0	3 (14)	22	22.72

Nephrostomes (*odf-3*)

Injection	Ectopic	Decrease	Absence	Normal	Totals	Significance
Uninjected	0 (0)	0 (0)	0	0 (0)	0	n/a
400pg β-gal	0 (0)	3 (16)	0	16 (84)	19	n/a
2ng Radical fringe + 400pg β-gal	13 (62)	8 (38)	0	0 (0)	21	31.23

Key

Significant value	$p \leq 0.05 = 5.991$
Non-significant value	

Null hypothesis: "There is no difference in glomus, nephrostome or proximal tubule formation between x ng *Radical fringe* mRNA and 400 pg *βgal* mRNA injected *Xenopus* embryos"

Radical fringe over-expression induced ectopic pronephrogenesis, *Lunatic fringe* over-expression inhibited pronephrogenesis

Empirical data for Figure 6.7

Proximal tubules and Nephrostomes (3G8 antibody)

Injection	Ectopic	Decrease	Absence	Normal	Totals	Significance
Uninjected	0 (0)	0 (0)	0	0 (0)	0	n/a
400pg β-gal	0 (0)	1 (5)	0	19 (95)	20	n/a
2ng Radical fringe + 400pg β-gal	38 (93)	0 (0)	0	3 (7)	41	49.31

Injection	Ectopic	Decrease	Absence	Normal	Totals	Significance
Uninjected	0 (0)	0 (0)	0	0 (0)	0	n/a
400pg β-gal	0 (0)	1 (2)	0	41 (98)	42	n/a
0.5ng Lunatic fringe + 400pg β-gal	0 (0)	27 (75)	14	9 (25)	36	44.5

Intermediate and Distal tubules (4A6 antibody)

Injection	Ectopic	Decrease	Absence	Normal	Totals	Significance
Uninjected	0 (0)	0 (0)	0	0 (0)	0	n/a
400pg β-gal	0 (0)	1 (5)	0	19 (95)	20	n/a
2ng Radical fringe + 400pg β-gal	26 (63)	2 (5)	0	13 (32)	41	23.99

Injection	Ectopic	Decrease	Absence	Normal	Totals	Significance
Uninjected	0 (0)	0 (0)	0	0 (0)	0	n/a
400pg β-gal	0 (0)	0 (0)	0	42 (100)	42	n/a
0.5ng Lunatic fringe + 400pg β-gal	0 (0)	27 (75)	5	9 (25)	36	48.14

Key

Significant value	$p \leq 0.05 = 5.991$
Non-significant value	

Null hypothesis: "There is no difference in 3G8/ 4A6 antibody staining between x ng *Radical fringe* mRNA/ *Lunatic fringe* mRNA and 400 pg *βgal* mRNA injected *Xenopus* embryos"

Radical fringe **knock-down had no effect on tubulogenesis, but *Lunatic fringe* MO1 and MO2 completely inhibited tubulogenesis**

Empirical data for Figure 6.8

Proximal, Intermediate and Distal tubules (*Na^+K^+ ATPase*)

Injection	Ectopic	Decrease	Absence	Normal	Totals	Significance
Uninjected	0 (0)	0 (0)	0	0 (0)	0	n/a
20ng Control MO + 400pg β-gal	0 (0)	2 (4)	0	50 (96)	52	n/a
20ng Radical fringe MO + 400pg β-gal	0 (0)	1 (3)	0	34 (97)	35	0.06

Injection	Ectopic	Decrease	Absence	Normal	Totals	Significance
Uninjected	0 (0)	0 (0)	0	0 (0)	0	n/a
20ng Control MO + 400pg β-gal	0 (0)	0 (0)	0	26 (100)	26	n/a
5ng Lunatic fringe MO1 + 400pg β-gal	0 (0)	21 (100)	14	0 (0)	21	47
5ng Lunatic fringe MO2 + 400pg β-gal	0 (0)	18 (100)	12	0 (0)	18	35

Key

Significant value	$p \leq 0.05 = 5.991$
Non-significant value	

Null hypothesis: "There is no difference in tubulogenesis between 20 ng *Radical fringe* MO/ *Lunatic fringe* MO1 and MO2 and 20 ng *Control* MO (+ 400 pg *βgal* mRNA) injected *Xenopus* embryos"

Depletion of *Lunatic fringe* expression, but not *Radical fringe* expression, by MO injection inhibited glomus development

Empirical data for Figure 6.9 and Ap 6 Fig 5

Glomus (Nephrin)

Injection	Ectopic	Decrease	Absence	Normal	Totals	Significance
Uninjected	0 (0)	0 (0)	0	0 (0)	0	n/a
20ng Control MO + 400pg β-gal	0 (0)	0 (0)	0	19 (100)	19	n/a
20ng Radical fringe MO + 400pg β-gal	0 (0)	0 (0)	0	23 (100)	23	0
5 ng Lunatic fringe MO1 + 400pg β-gal	0 (0)	18 (100)	17	0 (0)	18	50.68
5ng Lunatic fringe MO1 + 20ng Radical fringe MO + 400pg β-gal	0 (0)	21 (100)	15	0 (0)	21	40.16

Key

Significant value	$p \leq 0.05 = 5.991$
Non-significant value	

Null hypothesis: "There is no difference in glomus development between x ng *Radical fringe MO* and *Lunatic fringe MO1* mRNA and 20ng *Control* MO injected *Xenopus* embryos"

Depletion of *Lunatic fringe* expression, but not *Radical fringe* expression, by MO injection inhibited proximal tubulogenesis

Empirical data for Figure 6.9 and Ap 6 Fig 6

Proximal tubules (Slc5a2)

Injection	Ectopic	Decrease	Absence	Normal	Totals	Significance
Uninjected	0 (0)	0 (0)	0	0 (0)	0	n/a
20ng Control MO + 400pg β-gal	0 (0)	0 (0)	0	23 (100)	23	n/a
20ng Radical fringe MO + 400pg β-gal	0 (0)	0 (0)	0	21 (100)	21	0
5 ng Lunatic fringe MO1 + 400pg β-gal	0 (0)	21 (91)	22	2 (9)	23	38.64
5ng Lunatic fringe MO1 + 20ng Radical fringe MO + 400pg β-gal	0 (0)	27 (100)	26	0 (0)	27	44.43

Key

Significant value	$p \leq 0.05 = 5.991$
Non-significant value	

Null hypothesis: "There is no difference in proximal tubule development between x ng *Radical fringe MO* and *Lunatic fringe MO1* mRNA and 20ng *Control* MO injected *Xenopus* embryos"

Depletion of *Lunatic fringe* expression, but not *Radical fringe* expression, by MO injection inhibited nephrostome development

Empirical data for Figure 6.9 and Ap 6 Fig 7

Nephrostomes (odf3)

Injection	Ectopic	Decrease	Absence	Normal	Totals	Significance
Uninjected	0 (0)	0 (0)	0	0 (0)	0	n/a
20ng Control MO + 400pg β-gal	0 (0)	3 (11)	0	24 (89)	27	n/a
20ng Radical fringe MO + 400pg β-gal	0 (0)	5 (20)	0	20 (80)	25	0.53
5 ng Lunatic fringe MO1 + 400pg β-gal	0 (0)	21 (100)	21	0 (0)	21	40.87
5ng Lunatic fringe MO1 + 20ng Radical fringe MO + 400pg β-gal	0 (0)	20 (100)	20	0 (0)	20	36.31

Key

Significant value	$p \leq 0.05 = 5.991$
Non-significant value	

Null hypothesis: "There is no difference in nephrostome development between x ng *Radical fringe MO* and *Lunatic fringe MO1* mRNA and 20ng *Control* MO injected *Xenopus* embryos"

Depletion of *Lunatic fringe* expression, but not *Radical fringe* expression, by MO injection inhibited pronephrogenesis

Empirical data for Figure 6.10

Proximal tubules and Nephrostomes (3G8 antibody)

Injection	Ectopic	Decrease	Absence	Normal	Totals	Significance
Uninjected	0 (0)	0 (0)	0	0 (0)	0	n/a
20ng Control MO + 400pg β-gal	0 (0)	7 (8)	0	76 (92)	83	n/a
20ng Radical fringe MO + 400pg β-gal	0 (0)	3 (6)	0	44 (94)	47	0.17

Injection	Ectopic	Decrease	Absence	Normal	Totals	Significance
Uninjected	0 (0)	0 (0)	0	0 (0)	0	n/a
20ng Control MO + 400pg β-gal	0 (0)	2 (4)	0	44 (96)	46	n/a
5ng Lunatic fringe MO1 + 400pg β-gal	0 (0)	26 (93)	11	2 (7)	28	57.95
5ng Lunatic fringe MO2 + 400pg β-gal	0 (0)	24 (77)	4	7 (23)	31	44.18

Intermediate and Distal tubules (4A6 antibody)

Injection	Ectopic	Decrease	Absence	Normal	Totals	Significance
Uninjected	0 (0)	0 (0)	0	0 (0)	0	n/a
20ng Control MO + 400pg β-gal	0 (0)	2 (2)	0	81 (98)	83	n/a
20ng Radical fringe MO + 400pg β-gal	0 (0)	1 (2)	0	46 (98)	47	0.06

Injection	Ectopic	Decrease	Absence	Normal	Totals	Significance
Uninjected	0 (0)	0 (0)	0	0 (0)	0	n/a
20ng Control MO + 400pg β-gal	0 (0)	0 (0)	0	46 (100)	46	n/a
5ng Lunatic fringe MO1 + 400pg β-gal	0 (0)	24 (86)	3	4 (14)	28	58.37
5ng Lunatic fringe MO2 + 400pg β-gal	0 (0)	25 (81)	5	6 (19)	31	52.88

Key

Significant value	$p \leq 0.05 = 5.991$
Non-significant value	

Null hypothesis: "There is no difference in 3G8/ 4A6 antibody staining between x ng *Radical fringe* mRNA and 400 pg *βgal* mRNA injected *Xenopus* embryos"

Lunatic fringe mRNA rescues the pronephric phenotype of *Lunatic fringe* MO2

Empirical data for Figure 6.11

Glomus (*nephrin*)

Injection	Ectopic	Decrease	Absence	Normal	Totals	Significance
Uninjected	0 (0)	0 (0)	0	0 (0)	0	n/a
20ng Control MO + 400pg β-gal	0 (0)	1 (5)	0	18 (95)	19	n/a
0.5ng Lunatic fringe + 400pg β-gal	0 (0)	18 (86)	12	3 (14)	21	25.9
0.5ng Lunatic fringe + 5ng Lunatic fringe MO2 + 400pg β-gal	0 (0)	8 (40)	0	12 (60)	20	6.6
5ng Lunatic fringe MO2 + 400pg β-gal	0 (0)	21 (87)	20	3 (13)	24	28.7

Key

Significant value	$p \leq 0.05 = 5.991$
Non-significant value	

Null hypothesis: "There is no difference in *nephrin* expression between x ng *Lunatic fringe* mRNA/ *Lunatic fringe* MO2 and 400 pg *βgal* mRNA injected *Xenopus* embryos"

Lunatic fringe mRNA rescues the pronephric phenotype of *Lunatic fringe* MO2

Empirical data for Figure 6.12

Proximal tubules (*slc5a2*)

Injection	Ectopic	Decrease	Absence	Normal	Totals	Significance
Uninjected	0 (0)	0 (0)	0	0 (0)	0	n/a
20ng Control MO + 400pg β-gal	0 (0)	2 (12)	0	15 (88)	17	n/a
0.5ng Lunatic fringe + 400pg β-gal	0 (0)	12 (100)	11	0 (0)	12	21.71
0.5ng Lunatic fringe + 5ng Lunatic fringe MO2 + 400pg β-gal	0 (0)	4 (22)	2	14 (78)	18	0.67
5ng Lunatic fringe MO2 + 400pg β-gal	0 (0)	19 (95)	12	1 (5)	20	25.95

Key

Significant value	$p \leq 0.05 = 5.991$
Non-significant value	

Null hypothesis: "There is no difference in *slc5a2* expression between x ng *Lunatic fringe* mRNA/ *Lunatic fringe* MO2 and 400 pg *βgal* mRNA injected *Xenopus* embryos"

Radical fringe mRNA rescues the pronephric phenotype of *Lunatic fringe* MO1 and MO2

Empirical data for Figure 6.13

Proximal tubules (*slc5a2*)

Injection	Ectopic	Decrease	Absence	Normal	Totals	Significance
Uninjected	0 (0)	0 (0)	0	0 (0)	0	n/a
20ng Control MO + 400pg β-gal	0 (0)	0 (0)	0	15 (100)	15	n/a
2ng Radical fringe + 400pg β-gal	19 (68)	0 (0)	0	9 (32)	28	18.24
5ng Lunatic fringe MO1 + 400pg β-gal	0 (0)	18 (95)	6	1 (5)	19	30.21
5ng Lunatic fringe MO2 + 400pg β-gal	0 (0)	14 (78)	2	4 (22)	18	20.77
2ng Radical fringe + 5ng Lunatic fringe MO1 + 400pg β-gal	9 (27)	14 (42)	0	10 (31)	33	53.71
2ng Radical fringe + 5ng Lunatic fringe MO2 + 400pg β-gal	8 (33)	12 (51)	0	4 (16)	24	26.46

Key

Significant value	$p \leq 0.05 = 5.991$
Non-significant value	

Null hypothesis: "There is no difference in *slc5a2* expression between x ng *Radical fringe* mRNA/ *Lunatic fringe* MO2 and 400 pg *βgal* mRNA injected *Xenopus* embryos"

Radical fringe mRNA rescues the pronephric phenotype of *Lunatic fringe* MO1 and MO2

Empirical data for Figure 6.14

Proximal tubules (*slc5a2*)

Injection	Ectopic	Decrease	Absence	Normal	Totals	Significance
Uninjected	0 (0)	0 (0)	0	0 (0)	0	n/a
20ng Control MO + 400pg β-gal	0 (0)	0 (0)	0	26 (100)	26	n/a
2ng Radical fringe + 400pg β-gal	38 (78)	0 (0)	0	11 (22)	49	40.86
5ng Lunatic fringe MO1 + 400pg β-gal	0 (0)	13 (93)	13	1 (7)	14	35.77
5ng Lunatic fringe MO2 + 400pg β-gal	0 (0)	11 (58)	5	8 (7)	19	20.38
2ng Radical fringe + 5ng Lunatic fringe MO1 + 400pg β-gal	8 (27)	1 (3)	1	21 (70)	30	9.32
2ng Radical fringe + 5ng Lunatic fringe MO2 + 400pg β-gal	3 (8)	14 (37)	0	21 (55)	38	15.83

Key

Significant value	$p \leq 0.05 = 5.991$
Non-significant value	

Null hypothesis: "There is no difference in *slc5a2* expression between x ng *Radical fringe* mRNA/ *Lunatic fringe* MO2 and 400 pg *βgal* mRNA injected *Xenopus* embryos"

Lunatic fringe mRNA and MOs affect myogenesis, *Radical fringe* mRNA and MO has no effect on myogenesis

Empirical data for Figure 6.15 and Figure 6.16

Muscle (*MHC*)

Injection	Ectopic	Decrease	Absence	Normal	Totals	Significance
Uninjected	0 (0)	0 (0)	0	0 (0)	0	n/a
20ng Control MO + 400pg β-gal	0 (0)	0 (0)	0	43 (100)	43	n/a
2ng Radical fringe + 400pg β-gal	0 (0)	0 (0)	0	51 (100)	51	0
20ng Radical fringe MO + 400pg β-gal	0 (0)	0 (0)	0	48 (100)	48	0
0.5ng Lunatic fringe + 400pg β-gal	0 (0)	16 (64)	7	9 (36)	25	36.01
5ng Lunatic fringe MO1 + 400pg β-gal	0 (0)	19 (100)	14	0 (0)	19	38.06
5ng Lunatic fringe MO2 + 400pg β-gal	0 (0)	17 (100)	12	0 (0)	17	59.94

Pronephros anlagen (*Lim-1*)

Injection	Ectopic	Decrease	Absence	Normal	Totals	Significance
Uninjected	0 (0)	0 (0)	0	0 (0)	0	n/a
20ng Control MO + 400pg β-gal	0 (0)	2 (5)	0	41 (95)	43	n/a
2ng Radical fringe + 400pg β-gal	14 (27)	0 (0)	0	37 (73)	51	14.69
20ng Radical fringe MO + 400pg β-gal	0 (0)	1 (2)	0	47 (98)	48	0.47
0.5ng Lunatic fringe + 400pg β-gal	0 (0)	19 (76)	3	6 (24)	25	38.06
5ng Lunatic fringe MO1 + 400pg β-gal	0 (0)	18 (100)	18	0 (0)	19	52.37
5ng Lunatic fringe MO2 + 400pg β-gal	0 (0)	17 (100)	17	0 (0)	17	50.8

Key

Significant value	$p \leq 0.05 = 5.991$
Non-significant value	

Null hypothesis: "There is no difference in *MHC* or *Lim-1* expression between x ng *Radical fringe* mRNA/ *Radical fringe* MO/ *Lunatic fringe* mRNA/ *Lunatic fringe* MO1 or MO2 and *Control* MO injected *Xenopus* embryos"

Lunatic fringe **mRNA and MOs affect myogenesis, *Radical fringe* mRNA and MO has no effect on myogenesis**

Empirical data for Figure 6.20

Wnt-4

Injection	Ectopic	Decrease	Absence	Normal	Totals	Significance
Uninjected	0 (0)	0 (0)	0	0 (0)	0	n/a
400pg β-gal	0 (0)	3 (9)	0	46 (94)	49	n/a
2ng Radical fringe + 400pg β-gal	45 (73)	13 (21)	2	4 (6)	62	86.47

Serrate-1

Injection	Ectopic	Decrease	Absence	Normal	Totals	Significance
Uninjected	0 (0)	0 (0)	0	0 (0)	0	n/a
400pg β-gal	0 (0)	6 (11)	0	47 (89)	53	n/a
2ng Radical fringe + 400pg β-gal	52 (80)	11 (17)	1	2 (3)	65	94.65

Delta-1

Injection	Ectopic	Decrease	Absence	Normal	Totals	Significance
Uninjected	0 (0)	0 (0)	0	0 (0)	0	n/a
400pg β-gal	0 (0)	0 (0)	0	41 (100)	41	n/a
2ng Radical fringe + 400pg β-gal	43 (84)	8 (16)	4	0 (0)	51	91.95

Key

Significant value	$p \leq 0.05 = 5.991$
Non-significant value	

Null hypothesis: "There is no difference in *Wnt-4*, *Delta-1* or *Serrate-1* expression between 2 ng *Radical fringe* mRNA *βgal* mRNA injected *Xenopus* embryos"

Appendix Five

Effect of *Notch-ICD* and *Delta*^{STU} over-expression on *p27*^{Xic1} expression

Ap5.1 Introduction

Preliminary data performed in our laboratory suggested *Notch-ICD* over-expression increased pronephric expression of $p27^{Xic1}$. This work was performed by RT-PCR; embryos were injected with *Notch-ICD* mRNA at the one cell stage and left to develop to stage 13 or 20, presumptive pronephros was dissected and RNA extracted for RT-PCR analysis (Collins, thesis 2005). At stage 13 no discernable effect on $p27^{Xic1}$expression was observed, yet at stage 20 $p27^{Xic1}$expression was increased by about 30%. This result suggested one the gene targets of the Notch-ICD dependent pathway was $p27^{Xic1}$.

Ap5.2 Results

5.2.1 *Notch-ICD* and $Delta^{STU}$ inhibited $p27^{Xic1}$expression in animal caps

Embryos injected with *Notch-ICD* mRNA had severe pronephric phenotypes, as discussed in Chapter 4. Thus we believed it was difficult to isolate presumptive pronephroi from any stage of development without there being contamination with somatic or lateral plate mesoderm, as the pronephroi were grossly abnormal. Consequently we believed it would be difficult to repeat the results described above, as our dissected presumptive pronephroi would not be pure pronephric samples.

Instead we injected *Notch-ICD* mRNA and $Delta^{STU}$ mRNA into both cells of a 2-cell stage embryo, allow them to develop to stage 8 and then dissect animal caps from the embryos. Animal caps have proven to be an excellent experimental tissue in which a wide range of molecules have been tested (Green, 1999) (see Ap 5 Fig 1 for animal cap assay technique). Caps dissected here were allowed to develop

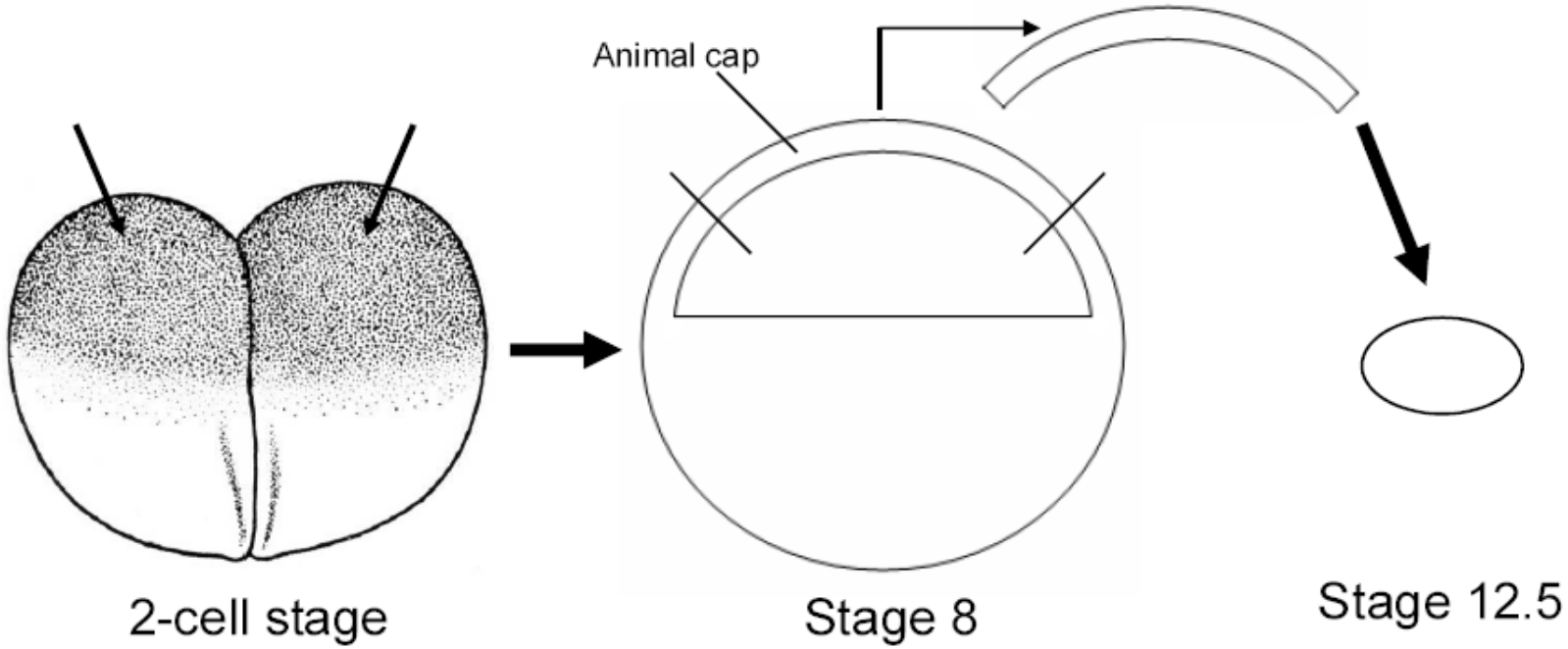

Appendix 5 Figure 1 Schematic of animal cap assay Embryos were injected into both cells of a 2-cell stage embryo and left to incubate to stage 8. At stage 8 the animal caps were dissected using forceps or a sharp ended hair (if many caps are required to be dissected a gastromaster can be used) and left to develop to stage 12.5, where RNA was extracted for RT-PCR analysis.

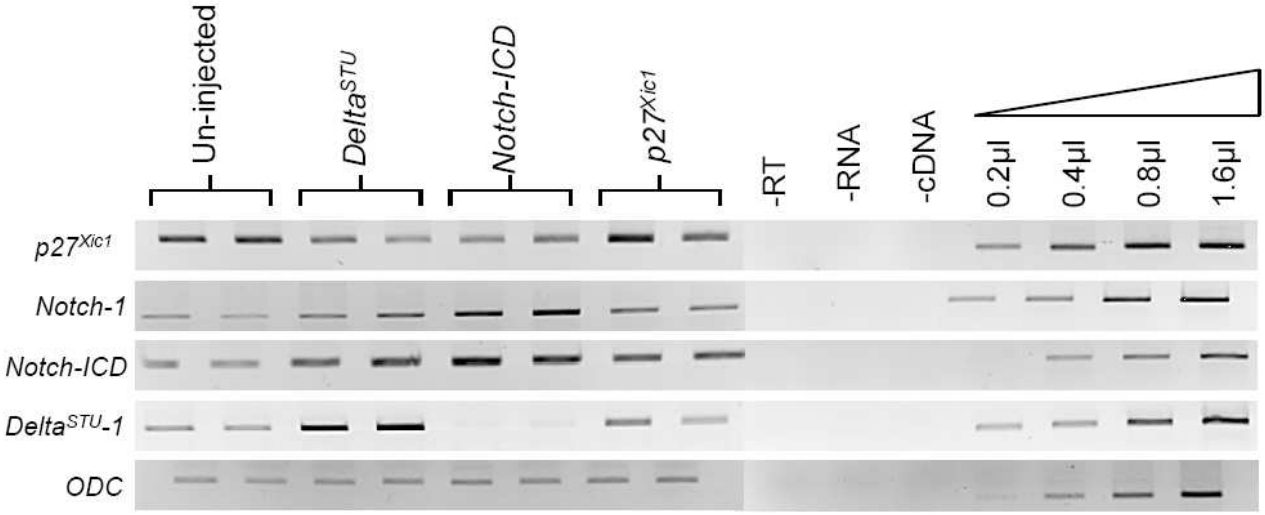

Appendix 5, Figure 2 PCR analysis identifying the effects *p27*^{Xic1} mRNA, *Notch-ICD* mRNA and *Delta*^{STU} mRNA injections have on each others expression in animal caps. Embryos were injected into both cells of a two-cell stage embryo with approximate final amounts of 600 pg *Notch-ICD* mRNA, 1 ng *Delta*^{STU} mRNA, and 50 pg *p27*^{Xic1} mRNA. Embryos were then cultured to stage 8, and animal caps were dissected using forceps. The caps were left to develop until stage 12.5 (using an un-injected whole embryo for stage definitions). mRNA and cDNAs were prepared by standard procedures and RT-PCR carried out for *p27*^{Xic1}, *Notch*, *Notch-ICD* and *Delta*^{STU} and the loading control *ODC*. Linearity of the PCR was confirmed by doubling the input of cDNA from un-injected stage 12.5 animal caps. Negative controls used were absence of RNA during the reverse transcription (-RNA), absence of reverse transcriptase (-RT), and absence of cDNA in the PCR (-cDNA). *Delta*^{STU} mRNA injection inhibited expression of *p27*^{Xic1} significantly, but increased expression of *Notch*. *Notch-ICD* mRNA injection also inhibited *p27*^{Xic1} but also completely inhibited *Delta* expression. Injection of *p27*^{Xic1} mRNA had no effect on *Notch* or *Delta* expression although seemed to increase the amount of *Notch* present as the cleaved intra-cellular domain (Notch-ICD).

to stage 12.5, where RNA was extracted for RT-PCR analysis. We found injection of *Notch-ICD* mRNA and $Delta^{STU}$ mRNA inhibited expression of $p27^{Xic1}$ in animal caps (Ap 5 Fig 2). Conversely, $p27^{Xic1}$ over-expression had no effect on *Notch-1* or *Delta-1* expression.

5.2.2 *Notch-ICD* and $Delta^{STU}$ inhibited expression of $p27^{Xic1}$ in whole embryos

To determine if these effects could be repeated in whole embryos 600 pg *Notch-ICD* mRNA and 1 ng $Delta^{STU}$ mRNA was injected into a ventro-vegetal (V2) blastomere of embryos at the 8-cell stage (see Chapter 3, Fig 3.1 for blastomere assignments), with 400 pg *βgal* mRNA to act as a lineage tracer. Embryos were cultured to stage 20 and analysed for effects on $p27^{Xic1}$ expression by *in situ* hybridisation for this gene.

After over-expression of both *Notch-ICD* and $Delta^{STU}$, $p27^{Xic1}$ expression was statistically significantly prevented when compared to the control *βgal* mRNA injected embryos (Ap 5 Fig 3A); mimicking the results of the animal cap assay. Injection into the V2 blastomere targets the future somites and pronephros anlagen. Somitic expression of $p27^{Xic1}$ was reduced in 83% of embryos injected with *Notch-ICD* mRNA (n=24, Ap 5 Fig 3B) and 59% of embryos injected with $Delta^{STU}$ mRNA (n=32) (Ap 5 Fig 3C). Control *βgal* injected embryos had 0% effect on $p27^{Xic1}$ expression (n=38).

In conclusion *Notch-ICD* and $Delta^{STU}$ over-expression inhibited expression of $p27^{Xic1}$ in both animal caps and whole embryos. We never observed any increase in $p27^{Xic1}$ expression.

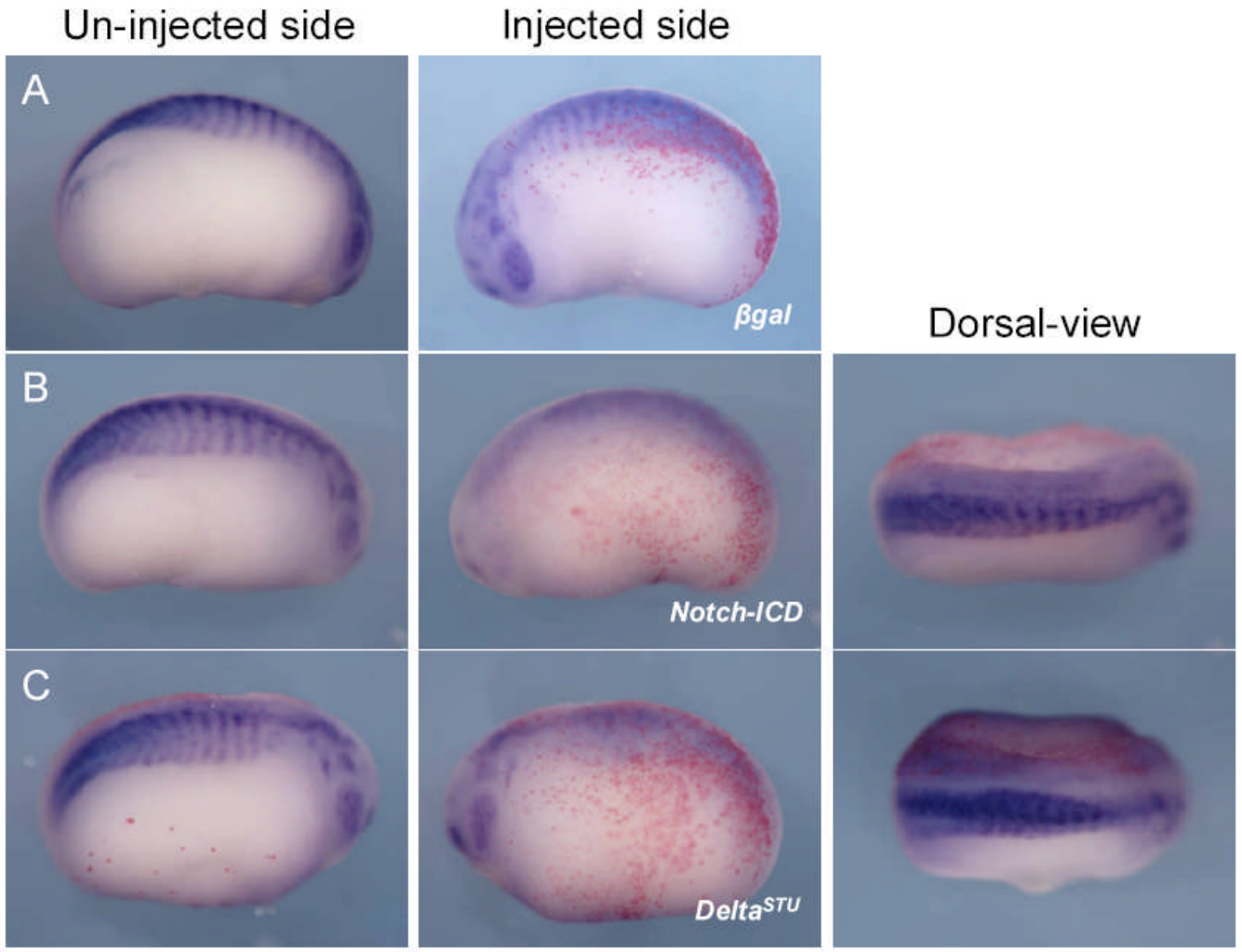

Appendix 5 Figure 3 Injection of *Notch-ICD* mRNA and *Delta*^{STU} mRNA reduced expression of *p27*^{Xic1}. *X. laevis* embryos were injected at the 8 cell stage into a ventro-vegetal blastomere to target the presumptive pronephric region. *βgal* mRNA was co-injected to act as a lineage tracer. Embryos were cultured till stage 20 and whole mount *in situ* hybridised for expression of *p27*^{Xic1}. Control *βgal* injected embryos had normal *p27*^{Xic1} expression (A). Injection of *Notch-ICD* and *Delta*^{STU} inhibited *p27*^{Xic1} expression in the somites (B and C).

Ap5.3 Discussion

The aim of these experiments was to show pronephric regulation of *p27^{Xic1}* expression by the Notch signalling pathway. However mis-activation and suppression of the Notch signalling pathway inhibited expression of *p27^{Xic1}* in animal cap assays (Ap 5 Fig 2) and whole embryos (Ap 5 Fig 3). As we could not repeat the results of Collins (these, 2005), we abandoned this line of research as no explanation for why both mis-activation and suppression of the Notch signalling pathway inhibited *p27^{Xic1}* expression could be ascertained. Performing these experiments was useful however as in addition to work shown in this appendix we injected *Notch-ICD* and *Delta^{STU}* to observe the effects on pronephric markers such as 3G8/ 4A6 and *Na^+ K^+ ATPase*, which led us to discover novel data suggesting a mechanism for how the Notch signalling pathway regulates development of the lateral and medial pronephric mesoderms, as discussed in Chapters 5 and 6.

Appendix Six

Fringe translation is regulated by UTR sequences and co-injection of the *Radical* and *Lunatic Fringe* MOs does not alter the single *Lunatic fringe* MO1 phenotype

Ap6.1 Introduction

This appendix presents data highlighting the inhibitory effect on translation of UTR sequences in mRNAs synthesised *in vitro* from full length cDNA clones for *Radical* and *Lunatic fringe*. This effect is shown *in vivo*, as embryos injected with mRNA encoded from full length cDNA clones for *Radical* and *Lunatic fringe* did not perturb pronephrogenesis in whole embryos. We also show that a truncated form of Lunatic fringe, termed Lunatic fringe Mature, has no effect on pronephrogenesis when over-expressed. Finally, we present data illustrating that co-injecting the *Lunatic* and *Radical fringe* MOs does not alter the effect of the single *Lunatic fringe* MO phenotype, providing further evidence for the non-functionality of Radical fringe during early *X. laevis* development.

Ap6.2 Results and Discussion

5.2.1 Injection of mRNAs synthesised from full length cDNA clones of *Lunatic* and *Radical fringe* had no effect on pronephros development

8-cell stage embryos were injected into a ventro-vegetal blastomere with 2 ng of *Lunatic fringe* mRNA or 2 ng *Radical fringe* mRNA and 400 pg *βgal* mRNA to act as a lineage tracer. Embryos were then left to develop to stage 34, when they were fixed, sorted for correct targeting according to lineage label staining, and then *in situ* hybridised for markers of the pronephros.

Injection of *Lunatic fringe* mRNA had no statistically significant effect on *nephrin* (Ap6 Fig 1B, 7% reduced, n=28), *slc5a2* (Ap6 Fig 2B, 3% reduced, n=34), or *odf-3* expression (Ap6 Fig 2B, 18% reduced, n=27, 14% of the control embryos

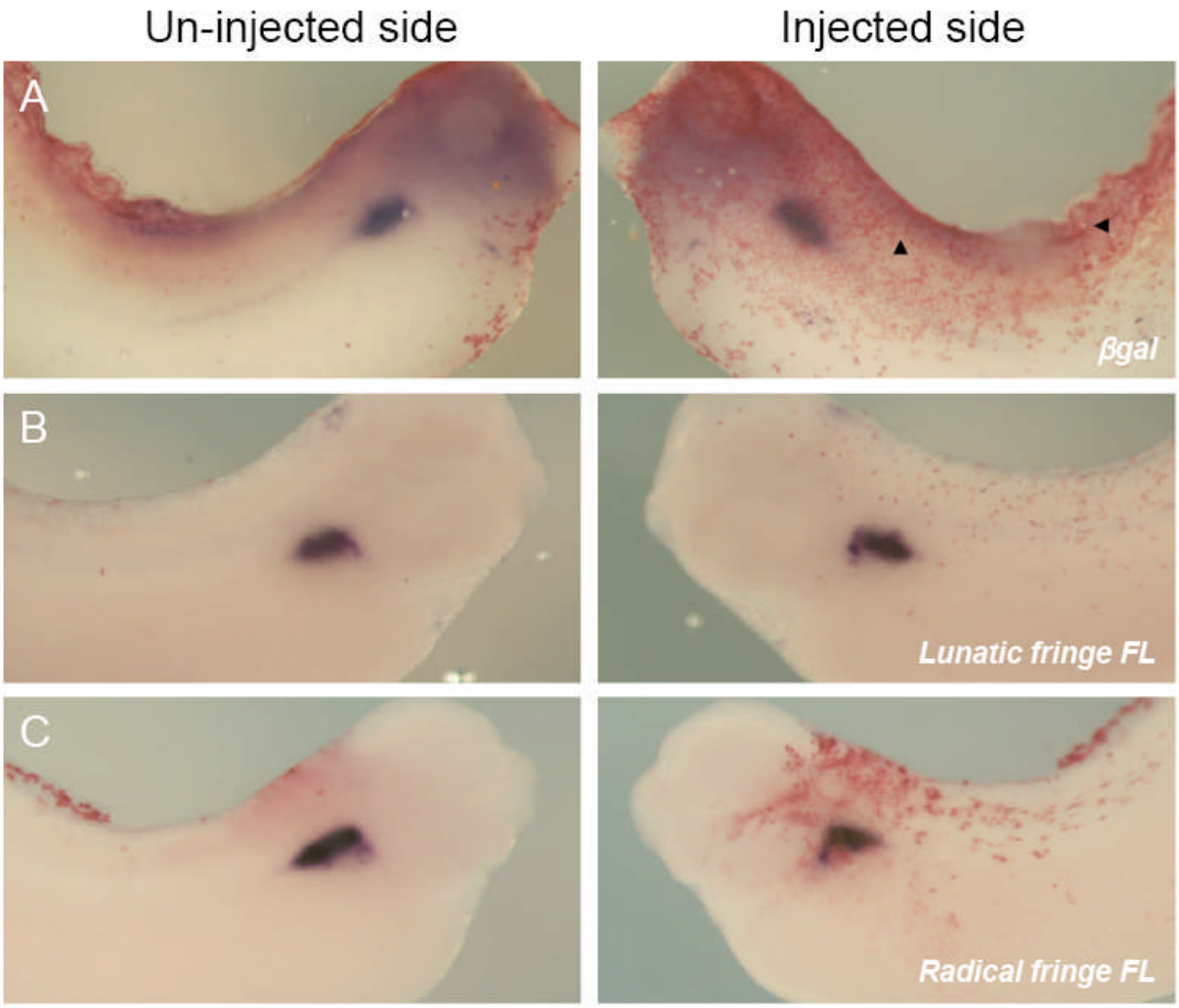

Appendix 6 Figure 1 Over-expression of full length (FL) *Lunatic* and *Radical fringe* has no effect on glomus formation. *X. laevis* embryos were injected at the 8 cell stage into a ventro-vegetal blastomere to target the presumptive pronephric region. mRNA was co-injected with *βgal* mRNA to act as a lineage tracer (red staining, black arrowheads). Embryos were cultured till stage 34 and then fixed. Whole mount *in situ* hybridisation was performed to detect expression of *Nephrin*, a marker of the glomus. Control *βgal* mRNA injected embryos had normal glomus development (A). Injection of neither *Lunatic fringe FL* mRNA nor *Radical fringe FL* mRNA affected development of the glomus (B and C).

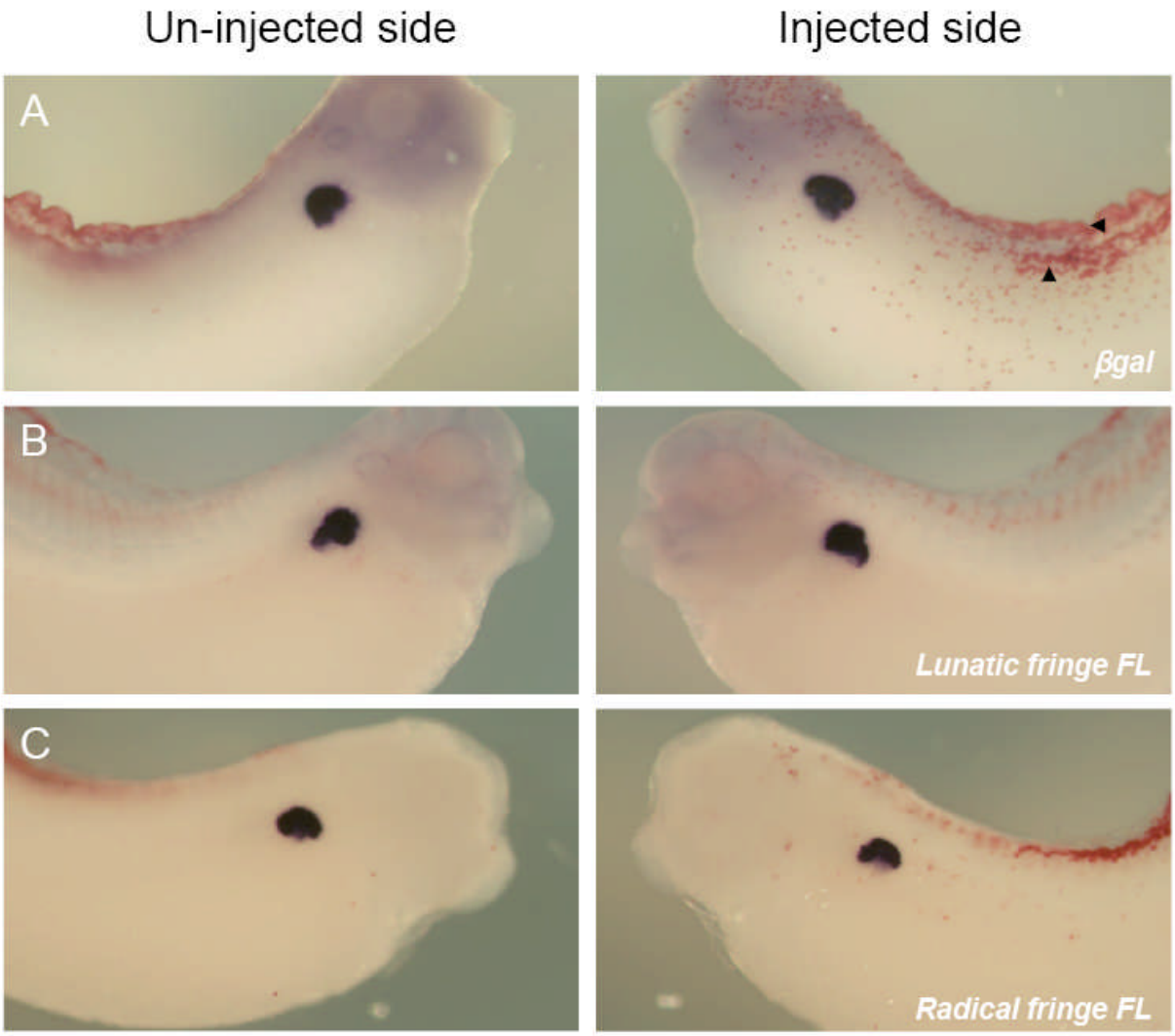

Appendix 6 Figure 2 Over-expression of full length (FL) *Lunatic* and *Radical fringe* has no effect on proximal tubulogenesis. *X. laevis* embryos were injected at the 8 cell stage into a ventro-vegetal blastomere to target the presumptive pronephric region. mRNA was co-injected with *βgal* mRNA to act as a lineage tracer (red staining, black arrowheads). Embryos were cultured till stage 34 and then fixed. Whole mount *in situ* hybridisation was performed to detect expression of *Slc5a2*, a marker of the proximal tubules. Control *βgal* mRNA injected embryos had normal proximal tubule development (A). Injection of neither *Lunatic fringe FL* mRNA nor *Radical fringe FL* mRNA affected development of the proximal tubules (B and C).

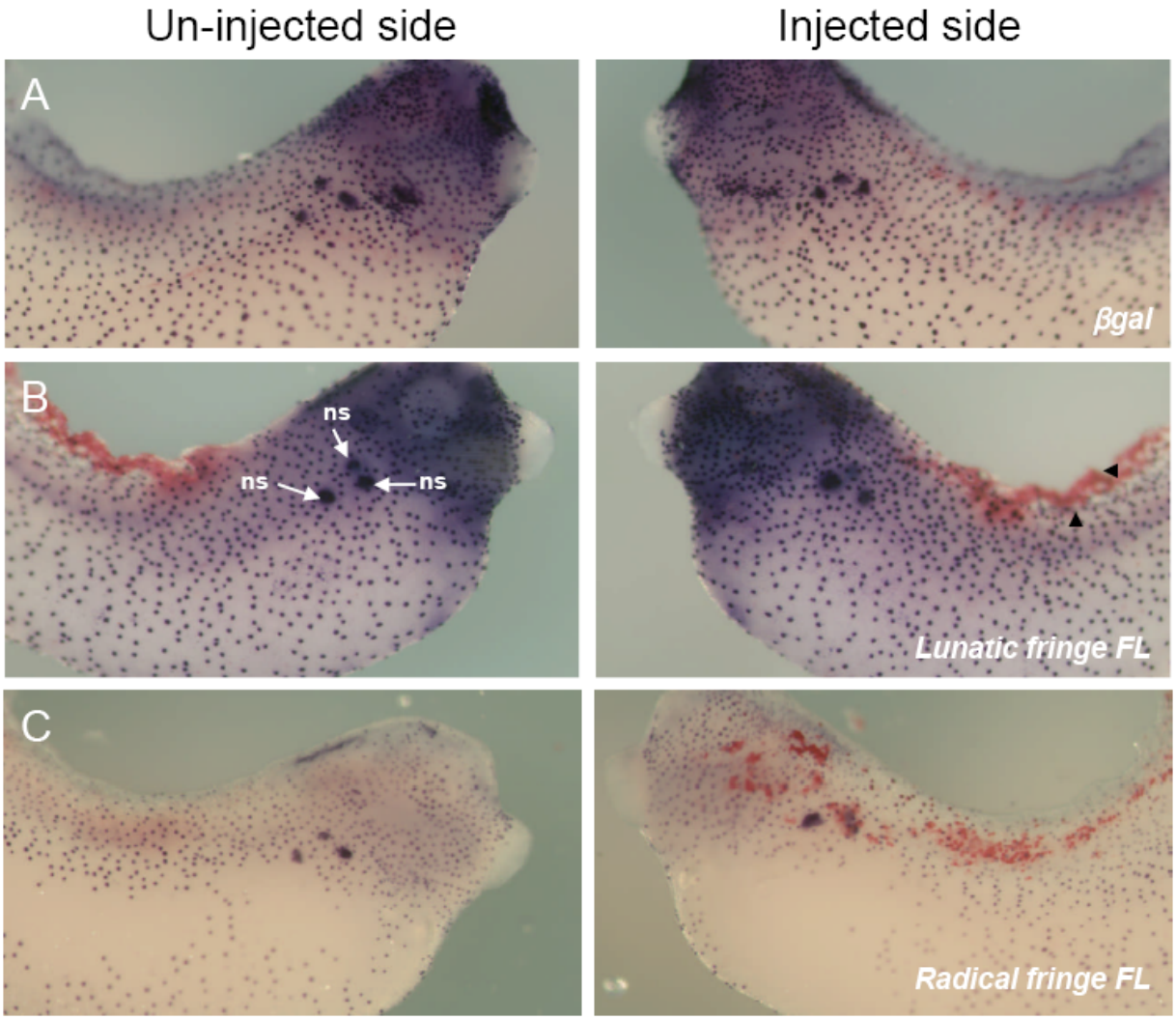

Appendix 6 Figure 3 Over-expression of full length (FL) *Lunatic* and *Radical fringe* has no effect on nephrostome formation. *X. laevis* embryos were injected at the 8 cell stage into a ventro-vegetal blastomere to target the presumptive pronephric region. mRNA was co-injected with *βgal* mRNA to act as a lineage tracer (red staining, black arrowheads). Embryos were cultured till stage 34 and then fixed. Whole mount *in situ* hybridisation was performed to detect expression of *odf3*, a gene expressed in the ciliated cells of the nephrostomes (see white arrows marked ns) and the epidermis. Control *βgal* mRNA injected embryos had normal nephrostome development (A). Injection of neither *Lunatic fringe FL* mRNA nor *Radical fringe FL* mRNA affected development of the nephrostomes (B and C).

had reduced *odf-3* expression) when compared to the control lineage label only injected embryos. Similar results were obtained after injection of *Radical fringe* mRNA synthesised from the full length cDNA clone. No embryos had reduced *nephrin* expression (Ap6 Fig 1C, n=29), 4% of embryos had reduced *slc5a2* expression (Ap6 Fig 2C, n=26) and 6% had reduced *odf-3* expression (Ap6 Fig 3C, n=33). Thus mRNA synthesised from the full length cDNA clones of *Lunatic* and *Radical fringe* have no effect on pronephrogenesis. In chapter 6 over-expression of *Lunatic* and *Radical fringe* mRNA synthesised from cDNA clones encoding only the ORF gave phenotypes upon over-expression. In conclusion the UTR sequences in both *Lunatic* and *Radical fringe* are likely to contain regulatory sequences that inhibit translation of these messages *in vivo*.

5.2.2 Over-expression of a truncated form of *Lunatic fringe* had no effect on pronephrogenesis

Drosophila fringe and mammalian *Lunatic fringe* are predicted to be pre-pro-protein precursors that require processing within the cell prior to becoming functionally active (Johnston et al., 1997). *X. laevis Lunatic fringe* also contains these conserved processing sites (Wu et al., 1996). We decided to PCR clone the mature region of the full length *Lunatic fringe* cDNA clone; deleting a 5' fragment that encoded the 5' UTR and the first 87 amino acids within the ORF, leaving the remaining 288 amino acids, encoding the mature Lunatic fringe region, and the 3' UTR. We initially believed this would be required when over-expressing *fringe* genes as the activity of the exogenous message would rely on the cellular apparatus that processed the cleavage sites. As this endogenous apparatus was not co-over-

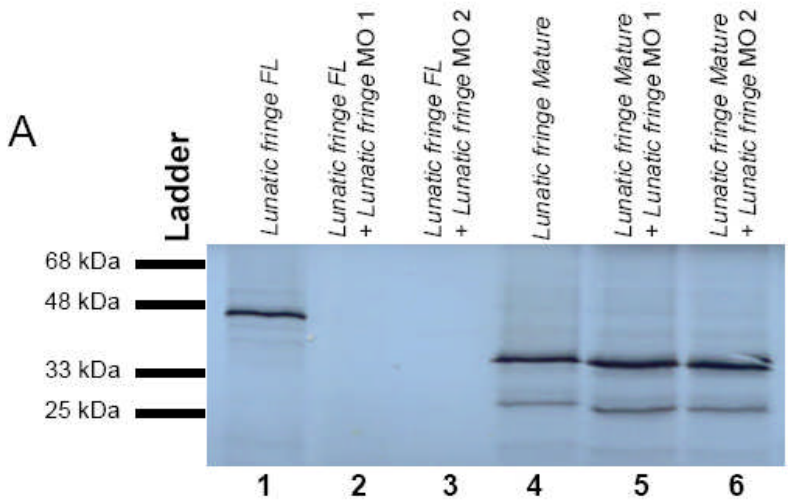
A
Ladder
Lunatic fringe FL
Lunatic fringe FL + Lunatic fringe MO 1
Lunatic fringe FL + Lunatic fringe MO 2
Lunatic fringe Mature
Lunatic fringe Mature + Lunatic fringe MO 1
Lunatic fringe Mature + Lunatic fringe MO 2
68 kDa
48 kDa
33 kDa
25 kDa
1
2
3
4
5
6

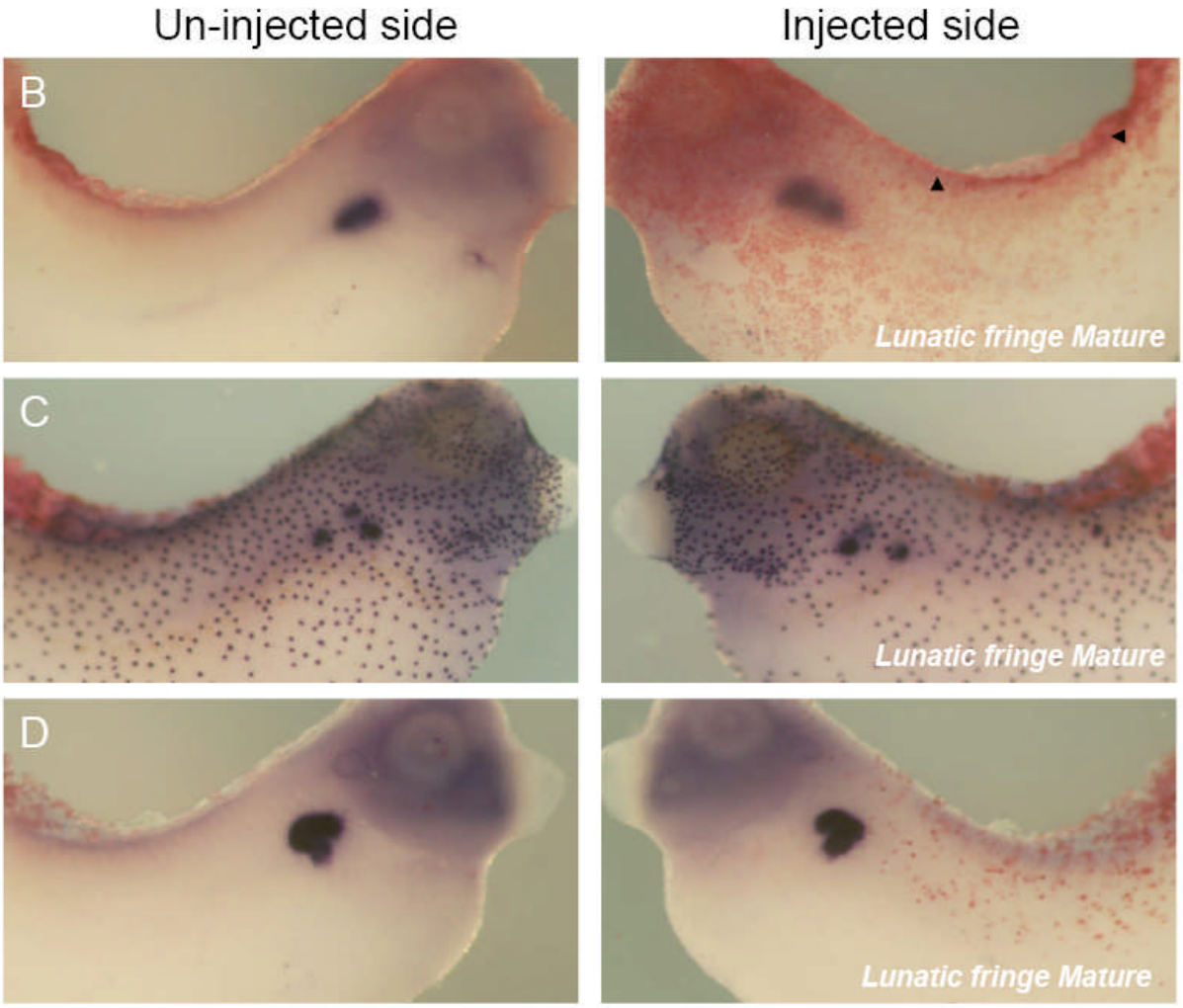
Un-injected side
Injected side
B
Lunatic fringe Mature
C
Lunatic fringe Mature
D
Lunatic fringe Mature

Appendix 6 Figure 4 Over-expression of *Lunatic fringe Mature* had no effect on pronephrogenesis despite its mRNA being translated strongly *in vitro* in a rabbit reticulocyte lysate system. (A) As described previously, *Lunatic fringe FL* mRNA did translate *in vitro* (lane 1) and two MOs designed to knockdown endogenous *Lunatic fringe* expression inhibited *Lunatic fringe mRNA* translation *in vitro* (lane 2 (MO1) and lane 3 (MO2)). *Lunatic fringe Mature* mRNA also translated *in vitro* (lane 5) and was not knocked down by *Lunatic fringe* MO1 (lane 5) or MO2 (lane 6). This result suggested *Lunatic fringe Mature* mRNA was suitable to rescue the effects of both *Lunatic fringe* MO1 and MO2. *X. laevis* embryos were injected at the 8 cell stage into a ventro-vegetal blastomere to target the presumptive pronephric region. mRNA was co-injected with *βgal* mRNA to act as a lineage tracer (red staining, black arrowheads). Embryos were cultured till stage 34 and then fixed. Whole mount *in situ* hybridisation was performed to detect expression of *nephrin*, a marker of the glomus, *odf3*, a marker of ciliated cells and thus the nephrostomes, and *slc5a2*, a marker of differentiated proximal tubules. Injection of *Lunatic fringe Mature* mRNA had no effect on development of any region of the pronephros analysed here (B-D).

expressed, it was possible we were not observing a phenotype after injection of the full length mRNAs due to saturation of the cellular processing apparatus.

To confirm mRNA synthesised from the *Lunatic fringe Mature* cDNA was able to translate we performed an *in vitro* translation using a rabbit reticulocyte lysate, as previously described. We attained a protein band of appropriate size according to molecular weight predictors after incubation of *Lunatic fringe* mRNA in the rabbit reticulocyte lysate (Ap6 Fig 4A, lane 4). Furthermore both *Lunatic fringe* MO1 and MO2 did not inhibit translation of *Lunatic fringe Mature* mRNA as this message did not contain sequence either MO could recognise (Ap6 Fig 4A, lane 5 and 6). In conclusion *Lunatic fringe Mature* mRNA was able to translate in vitro and could possibly be used to rescue the phenotypes of both *Lunatic fringe* MO1 and MO2.

We next over-expressed *Lunatic fringe Mature* in the pronephric region by micro-injection into a ventro-vegetal blastomere of an 8-cell stage embryo, as described above. *Lunatic fringe Mature* over-expression had no effect on *nephrin* expression (Ap6 Fig 4B, n=24) or *slc5a2* expression (Ap6 Fig 4D, n=31) and although 11% of embryos had reduced *odf-3* expression (Ap6 Fig 4C, n=19), this result was not statistically significantly different to the control *βgal* mRNA injected embryos. In conclusion *Lunatic fringe Mature* over-expression in whole embryos has no effect on pronephrogenesis.

5.2.3 Co-injection of *Lunatic fringe* MO1 with *Radical fringe* MO did not alter the phenotype observed

In chapter 6 we described how single injections of *Lunatic fringe* MO1 and MO2 severely inhibited pronephros development, most likely due to an effect on

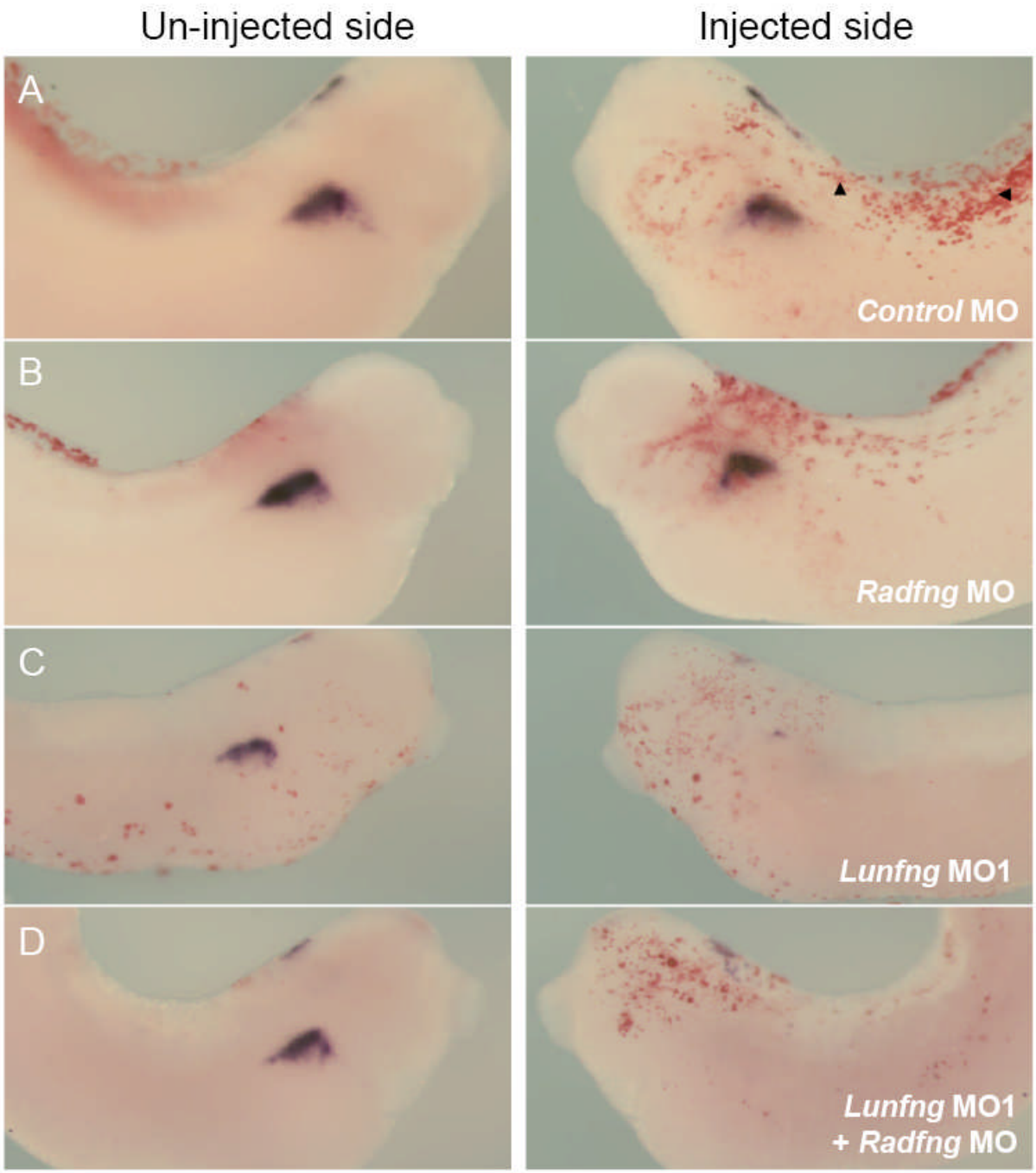

Appendix 6 Figure 5 Depletion of *Lunatic fringe* inhibits glomus formation, but *Radical fringe* knock down has no effect on glomus formation. *X. laevis* embryos were injected at the 8 cell stage into a ventro-vegetal blastomere to target the presumptive pronephric region. mRNA was co-injected with *βgal* mRNA to act as a lineage tracer (red staining, black arrowheads). Embryos were cultured till stage 34 and then fixed. Whole mount *in situ* hybridisation was performed to detect expression of *Nephrin*, a marker of the glomus. *Control* MO and Radical fringe MO injected embryos had normal glomus development (A and B). Injection of the *Lunatic fringe* MO1 inhibited glomus development (C). Similarly co-injection of the *Radical fringe* MO with the *Lunatic fringe* MO1 also inhibited glomus development (D).

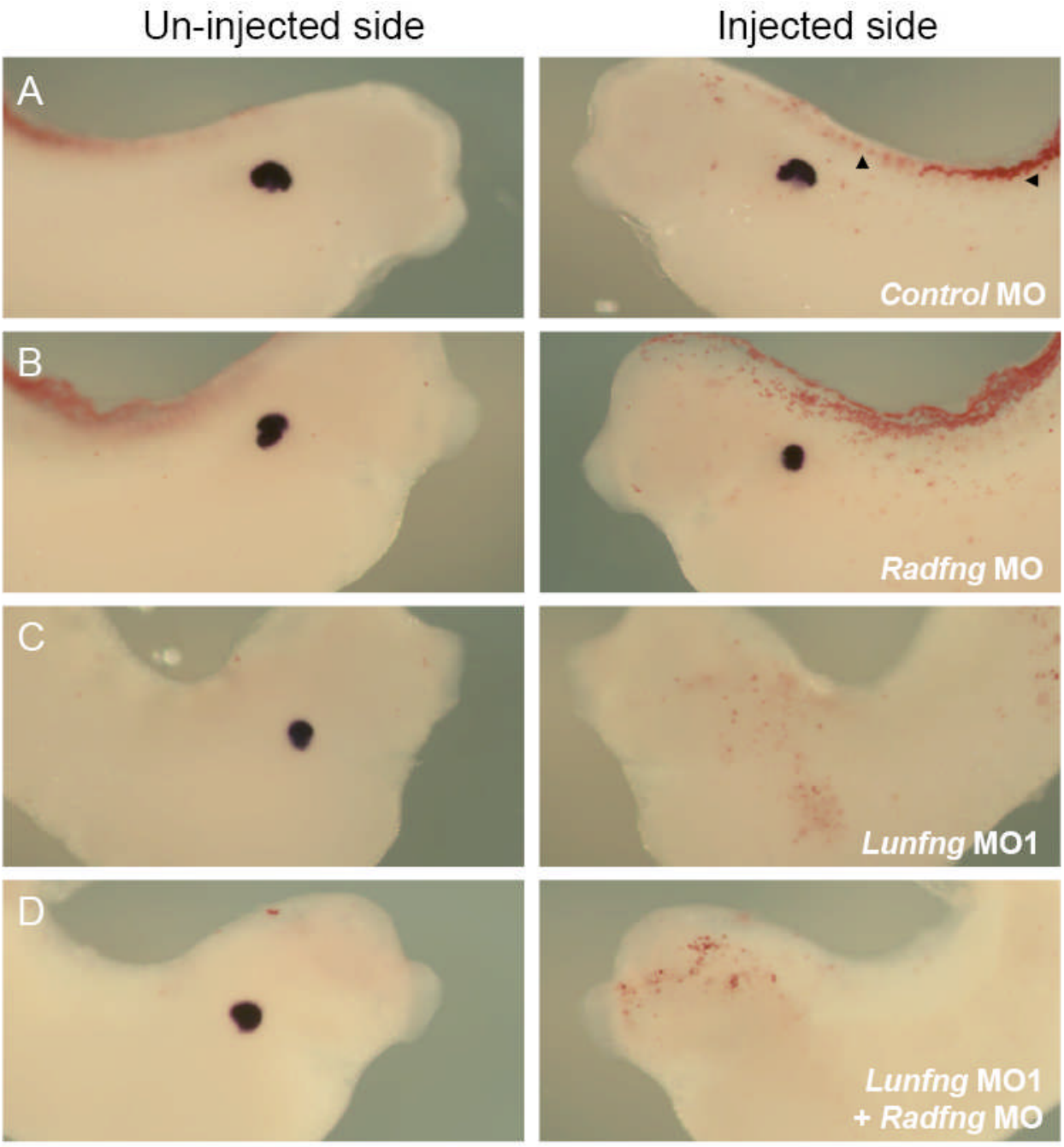

Appendix 6 Figure 6 Depletion of *Lunatic fringe* inhibits proximal tubule formation, but *Radical fringe* knock down has no effect. *X. laevis* embryos were injected at the 8 cell stage into a ventro-vegetal blastomere to target the presumptive pronephric region. mRNA was co-injected with *βgal* mRNA to act as a lineage tracer (red staining, black arrowheads). Embryos were cultured till stage 34 and then fixed. Whole mount *in situ* hybridisation was performed to detect expression of *slc5a2*, a marker of the proximal tubules. *Control* MO and Radical fringe MO injected embryos had normal proximal tubulogenesis (A and B). Injection of the *Lunatic fringe* MO1 inhibited proximal tubule development (C). Similarly co-injection of the *Radical fringe* MO with the *Lunatic fringe* MO1 also inhibited proximal tubule development (D).

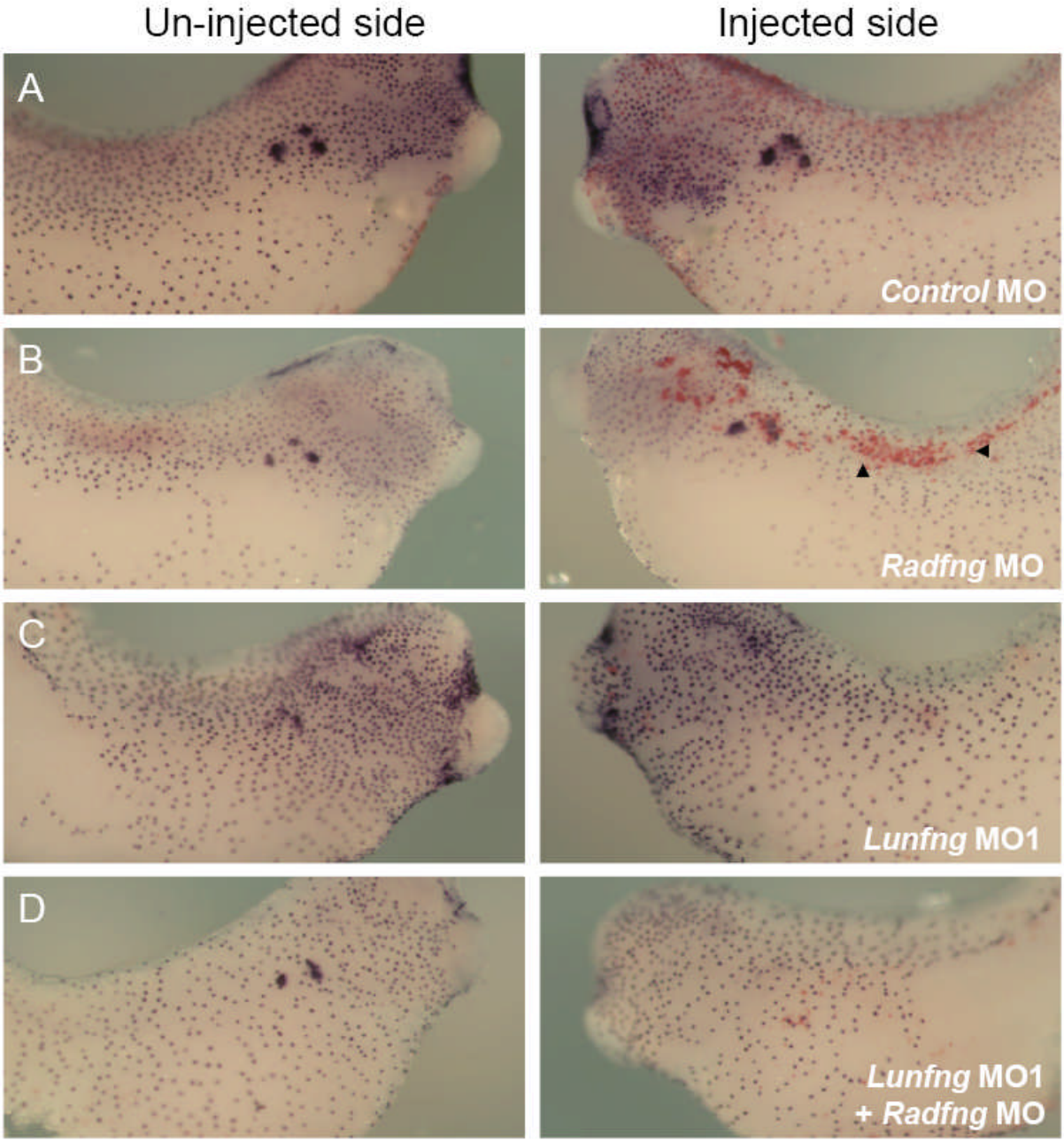

Appendix 6 Figure 7 Depletion of *Lunatic fringe* inhibits nephrostome formation, but *Radical fringe* knock down has no effect. *X. laevis* embryos were injected at the 8 cell stage into a ventro-vegetal blastomere to target the presumptive pronephric region. mRNA was co-injected with *βgal* mRNA to act as a lineage tracer (red staining, black arrowheads). Embryos were cultured till stage 34 and then fixed. Whole mount *in situ* hybridisation was performed to detect expression of *odf3*, a marker of ciliated cells and thus the three nephrostomes found at the tips of the proximal tubules projecting into the ceolomic cavity. *Control* MO and Radical fringe MO injected embryos had normal nephrostome development (A and B). Injection of the *Lunatic fringe* MO1 inhibited nephrostome formation (C). Similarly co-injection of the *Radical fringe* MO with the *Lunatic fringe* MO1 also inhibited nephrostome development (D).

myogenesis. Here we show co-injection of *Lunatic fringe* MO1 with *Radical fringe* MO does not alter this phenotype.

Single injections of *Lunatic fringe* MO1 almost completely inhibited pronephrogenesis in every embryo scored (see appendix 4). 100% of embryos had reduced *nephrin* and *odf-3* expression and 91% of embryos had reduced *slc5a2* expression. Consequently, analysis of whether the *Radical fringe* MO amplifies this phenotype after co-injection with *Lunatic fringe* MO1 cannot be observed. In mice knockouts of *Lunatic fringe* have perturbed segmentation, but *Radical fringe* knockouts develop normally (Zhang et al., 2002). Double knockout of *Lunatic* and *Radical fringe* in mice does not amplify the phenotype observed in the single *Lunatic fringe* knockout, suggesting Radical fringe plays a minor role during mouse development. The lack of a pronephric phenotype after single injections of *Radical fringe* MO and the similarity in the gross developmental defects observed between *Lunatic fringe* MO1 single injections and *Radical fringe* MO/ *Lunatic fringe* MO1 co-injections (for example compare Ap6 Fig 5-7C and 5-7D) suggests that Radical fringe is not required during *X. laevis* pronephros development.

References

Aigner, J., Kloth, S., Jennings, M. L. and Minuth, W. W. (1995). Transitional differentiation patterns of principal and intercalated cells during renal collecting duct development. *Epithelial Cell Biol* **4**, 121-30.

Arias, A. M., Brown, A. M. and Brennan, K. (1999). Wnt signalling: pathway or network? *Curr Opin Genet Dev* **9**, 447-54.

Axelrod, J. D., Matsuno, K., Artavanis-Tsakonas, S. and Perrimon, N. (1996). Interaction between Wingless and Notch signaling pathways mediated by dishevelled. *Science* **271**, 1826-32.

Barisoni, L. (2008). Notch signaling: a common pathway of injury in podocytopathies? *J Am Soc Nephrol* **19**, 1045-6.

Barnett, M. W., Old, R. W. and Jones, E. A. (1998). Neural induction and patterning by fibroblast growth factor, notochord and somite tissue in Xenopus. *Dev Growth Differ* **40**, 47-57.

Bassez, T., Paris, J., Omilli, F., Dorel, C. and Osborne, H. B. (1990). Post-transcriptional regulation of ornithine decarboxylase in Xenopus laevis oocytes. *Development* **110**, 955-62.

Bellefroid, E. J., Bourguignon, C., Hollemann, T., Ma, Q., Anderson, D. J., Kintner, C. and Pieler, T. (1996). X-MyT1, a Xenopus C2HC-type zinc finger protein with a regulatory function in neuronal differentiation. *Cell* **87**, 1191-202.

Besson, A., Dowdy, S. F. and Roberts, J. M. (2008). CDK inhibitors: cell cycle regulators and beyond. *Dev Cell* **14**, 159-69.

Blain, S. W. (2008). Switching cyclin D-Cdk4 kinase activity on and off. *Cell Cycle* **7**, 892-8.

Blair, S. S. (2004). Developmental biology: Notching the hindbrain. *Curr Biol* **14**, R570-2.

Brändli, A. W. (1999). Towards a molecular anatomy of the Xenopus pronephric kidney. *Int J Dev Biol* **43**, 381-95.

Bray, S. J. (2006). Notch signalling: a simple pathway becomes complex. *Nat Rev Mol Cell Biol* **7**, 678-89.

Brennan, H. C., Nijjar, S. and Jones, E. A. (1998). The specification of the pronephric tubules and duct in Xenopus laevis. *Mech Dev* **75**, 127-37.

Brennan, H. C., Nijjar, S. and Jones, E. A. (1999a). The specification and growth factor inducibility of the pronephric glomus in Xenopus laevis. *Development* **126**, 5847-56.

Brennan, K., Klein, T., Wilder, E. and Arias, A. M. (1999b). Wingless modulates the effects of dominant negative notch molecules in the developing wing of Drosophila. *Dev Biol* **216**, 210-29.

Brennan, K., Tateson, R., Lewis, K. and Arias, A. M. (1997). A functional analysis of Notch mutations in Drosophila. *Genetics* **147**, 177-88.

Brennan, K., Tateson, R., Lieber, T., Couso, J. P., Zecchini, V. and Arias, A. M. (1999c). The abruptex mutations of notch disrupt the establishment of proneural clusters in Drosophila. *Dev Biol* **216**, 230-42.

Brou, C., Logeat, F., Gupta, N., Bessia, C., LeBail, O., Doedens, J. R., Cumano, A., Roux, P., Black, R. A. and Israel, A. (2000). A novel proteolytic cleavage involved in Notch signaling: the role of the disintegrin-metalloprotease TACE. *Mol Cell* **5**, 207-16.

Bruckner, K., Perez, L., Clausen, H. and Cohen, S. (2000). Glycosyltransferase activity of Fringe modulates Notch-Delta interactions. *Nature* **406**, 411-5.

Bryant, P. J. and Schmidt, O. (1990). The genetic control of cell proliferation in Drosophila imaginal discs. *J Cell Sci Suppl* **13**, 169-89.

Burns, W. C., Kantharidis, P. and Thomas, M. C. (2007). The role of tubular epithelial-mesenchymal transition in progressive kidney disease. *Cells Tissues Organs* **185**, 222-31.

Capdevila, J., Estrada, M. P., Sanchez-Herrero, E. and Guerrero, I. (1994). The Drosophila segment polarity gene patched interacts with decapentaplegic in wing development. *EMBO J* **13**, 71-82.

Capdevila, J. and Izpisua Belmonte, J. C. (2001). Patterning mechanisms controlling vertebrate limb development. *Annu Rev Cell Dev Biol* **17**, 87-132.

Carrington, J. L. and Fallon, J. F. (1984). The stages of flank ectoderm capable of responding to ridge induction in the chick embryo. *J Embryol Exp Morphol* **84**, 19-34.

Carroll, T., Wallingford, J., Seufert, D. and Vize, P. D. (1999). Molecular regulation of pronephric development. *Curr Top Dev Biol* **44**, 67-100.

Carroll, T. J., Park, J. S., Hayashi, S., Majumdar, A. and McMahon, A. P. (2005). Wnt9b plays a central role in the regulation of mesenchymal to epithelial transitions underlying organogenesis of the mammalian urogenital system. *Dev Cell* **9**, 283-92.

Carroll, T. J. and Vize, P. D. (1996). Wilms' tumor suppressor gene is involved in the development of disparate kidney forms: evidence from expression in the Xenopus pronephros. *Dev Dyn* **206**, 131-8.

Carroll, T. J. and Vize, P. D. (1999). Synergism between Pax-8 and lim-1 in embryonic kidney development. *Dev Biol* **214**, 46-59.

Chan, T. C., Takahashi, S. and Asashima, M. (2000). A role for Xlim-1 in pronephros development in Xenopus laevis. *Dev Biol* **228**, 256-69.

Chen, H. and Johnson, R. L. (1999). Dorsoventral patterning of the vertebrate limb: a process governed by multiple events. *Cell Tissue Res* **296**, 67-73.

Chen, J., Jackson, P. K., Kirschner, M. W. and Dutta, A. (1995). Separate domains of p21 involved in the inhibition of Cdk kinase and PCNA. *Nature* **374**, 386-8.

Cheng, H. T., Miner, J. H., Lin, M., Tansey, M. G., Roth, K. and Kopan, R. (2003). Gamma-secretase activity is dispensable for mesenchyme-to-epithelium transition but required for podocyte and proximal tubule formation in developing mouse kidney. *Development* **130**, 5031-42.

Cheng, Y. C., Amoyel, M., Qiu, X., Jiang, Y. J., Xu, Q. and Wilkinson, D. G. (2004). Notch activation regulates the segregation and differentiation of rhombomere boundary cells in the zebrafish hindbrain. *Dev Cell* **6**, 539-50.

Chiba, S. (2006). Notch signaling in stem cell systems. *Stem Cells* **24**, 2437-47.

Chitnis, A. (2006). Why is delta endocytosis required for effective activation of notch? *Dev Dyn* **235**, 886-94.

Chitnis, A., Henrique, D., Lewis, J., Ish-Horowicz, D. and Kintner, C. (1995). Primary neurogenesis in Xenopus embryos regulated by a homologue of the Drosophila neurogenic gene Delta. *Nature* **375**, 761-6.

Cinquin, O. (2007). Understanding the somitogenesis clock: what's missing? *Mech Dev* **124**, 501-17.

Cole, S. E., Levorse, J. M., Tilghman, S. M. and Vogt, T. F. (2002). Clock regulatory elements control cyclic expression of Lunatic fringe during somitogenesis. *Dev Cell* **3**, 75-84.

Collins, R.J. (2005) Characterisation of *p27^{Xic1}* and its role in pronephros development in *Xenopus laevis*. PhD Thesis.

Combs, H. L., Shankland, S. J., Setzer, S. V., Hudkins, K. L. and Alpers, C. E. (1998). Expression of the cyclin kinase inhibitor, p27kip1, in developing and mature human kidney. *Kidney Int* **53**, 892-6.

Conlon, R. A., Reaume, A. G. and Rossant, J. (1995). Notch1 is required for the coordinate segmentation of somites. *Development* **121**, 1533-45.

Cooke, J. (1998). A gene that resuscitates a theory--somitogenesis and a molecular oscillator. *Trends Genet* **14**, 85-8.

Cooke, J. and Zeeman, E. C. (1976). A clock and wavefront model for control of the number of repeated structures during animal morphogenesis. *J Theor Biol* **58**, 455-76.

Corey, D. R. and Abrams, J. M. (2001). Morpholino antisense oligonucleotides: tools for investigating vertebrate development. *Genome Biol* **2**, REVIEWS1015.

Costantini, F. (2006). Renal branching morphogenesis: concepts, questions, and recent advances. *Differentiation* **74**, 402-21.

Couso, J. P., Bishop, S. A. and Martinez Arias, A. (1994). The wingless signalling pathway and the patterning of the wing margin in Drosophila. *Development* **120**, 621-36.

Crickmore, M. A. and Mann, R. S. (2008). The control of size in animals: insights from selector genes. *Bioessays* **30**, 843-53.

Croisille, Y. (1976). On some recent contributions to the study of kidney tubulogenesis in mammals and birds. In *Tests of teratogenicity in vitro* (ed. J. D. Ebert and M. Marois), pp. 149-170. North-Holland Publ. Co., Amsterdam.

Crowe, E., Halpin, D. and Stevens, P. (2008). Early identification and management of chronic kidney disease: summary of NICE guidance. *Bmj* **337**, a1530.

Dale, J. K., Maroto, M., Dequeant, M. L., Malapert, P., McGrew, M. and Pourquie, O. (2003). Periodic notch inhibition by lunatic fringe underlies the chick segmentation clock. *Nature* **421**, 275-8.

Dale, L. and Slack, J. M. (1987). Fate map for the 32-cell stage of Xenopus laevis. *Development* **99**, 527-51.

Daniels, M., Dhokia, V., Richard-Parpaillon, L. and Ohnuma, S. (2004). Identification of Xenopus cyclin-dependent kinase inhibitors, p16Xic2 and p17Xic3. *Gene* **342**, 41-7.

de Celis, J. F. and Bray, S. (1997). Feed-back mechanisms affecting Notch activation at the dorsoventral boundary in the Drosophila wing. *Development* **124**, 3241-51.

de la Calle-Mustienes, E., Glavic, A., Modolell, J. and Gomez-Skarmeta, J. L. (2002). Xiro homeoproteins coordinate cell cycle exit and primary neuron formation by upregulating neuronal-fate repressors and downregulating the cell-cycle inhibitor XGadd45-gamma. *Mech Dev* **119**, 69-80.

De Strooper, B. and Annaert, W. (2001). Where Notch and Wnt signaling meet. The presenilin hub. *J Cell Biol* **152**, F17-20.

Dearden, P. and Akam, M. (2000). A role for Fringe in segment morphogenesis but not segment formation in the grasshopper, Schistocerca gregaria. *Dev Genes Evol* **210**, 329-36.

Deblandre, G. A., Wettstein, D. A., Koyano-Nakagawa, N. and Kintner, C. (1999). A two-step mechanism generates the spacing pattern of the ciliated cells in the skin of Xenopus embryos. *Development* **126**, 4715-28.

Déqueant, M. L. and Pourquíe, O. (2008). Segmental patterning of the vertebrate embryonic axis. *Nat Rev Genet* **9**, 370-82.

Di Cunto, F., Topley, G., Calautti, E., Hsiao, J., Ong, L., Seth, P. K. and Dotto, G. P. (1998). Inhibitory function of p21Cip1/WAF1 in differentiation of primary mouse keratinocytes independent of cell cycle control. *Science* **280**, 1069-72.

Diaz-Benjumea, F. J. and Cohen, S. M. (1995). Serrate signals through Notch to establish a Wingless-dependent organizer at the dorsal/ventral compartment boundary of the Drosophila wing. *Development* **121**, 4215-25.

Doree, M. and Hunt, T. (2002). From Cdc2 to Cdk1: when did the cell cycle kinase join its cyclin partner? *J Cell Sci* **115**, 2461-4.

Dressler, G. R. (2006). The cellular basis of kidney development. *Annu Rev Cell Dev Biol* **22**, 509-29.

Dressler, G. R. (2008). Another niche for Notch. *Kidney Int* **73**, 1207-9.

Drummond, I. A. (2005). Kidney development and disease in the zebrafish. *J Am Soc Nephrol* **16**, 299-304.

Drummond, I. A., Majumdar, A., Hentschel, H., Elger, M., Solnica-Krezel, L., Schier, A. F., Neuhauss, S. C., Stemple, D. L., Zwartkruis, F., Rangini, Z. et al. (1998). Early development of the zebrafish pronephros and analysis of mutations affecting pronephric function. *Development* **125**, 4655-67.

Dumont, J. N. (1972). Oogenesis in Xenopus laevis (Daudin). I. Stages of oocyte development in laboratory maintained animals. *J Morphol* **136**, 153-79.

Dutta, S., Dietrich, J. E., Westerfield, M. and Varga, Z. M. (2008). Notch signaling regulates endocrine cell specification in the zebrafish anterior pituitary. *Dev Biol* **319**, 248-57.

Evrard, Y. A., Lun, Y., Aulehla, A., Gan, L. and Johnson, R. L. (1998). lunatic fringe is an essential mediator of somite segmentation and patterning. *Nature* **394**, 377-81.

Fales, D. (1935). Experiments on the development of the pronephros of *Amblystoma punctatum*. *J. Exp. Zool.* **72**, 147-173.

Fan, W., Richter, G., Cereseto, A., Beadling, C. and Smith, K. A. (1999). Cytokine response gene 6 induces p21 and regulates both cell growth and arrest. *Oncogene* **18**, 6573-82.

Fiuza, U. M. and Arias, A. M. (2007). Cell and molecular biology of Notch. *J Endocrinol* **194**, 459-74.

Gerth, V. E., Zhou, X. and Vize, P. D. (2005). Nephrin expression and three-dimensional morphogenesis of the Xenopus pronephric glomus. *Dev Dyn* **233**, 1131-9.

Gomez, C., Ozbudak, E. M., Wunderlich, J., Baumann, D., Lewis, J. and Pourquie, O. (2008). Control of segment number in vertebrate embryos. *Nature* **454**, 335-9.

Gordon, W. R., Vardar-Ulu, D., Histen, G., Sanchez-Irizarry, C., Aster, J. C. and Blacklow, S. C. (2007). Structural basis for autoinhibition of Notch. *Nat Struct Mol Biol* **14**, 295-300.

Green, J. (1999). The animal cap assay. *Methods Mol Biol* **127**, 1-13.

Greenwood, J. and Gautier, J. (2005). From oogenesis through gastrulation: developmental regulation of apoptosis. *Semin Cell Dev Biol* **16**, 215-24.

Gupta, M., Gupta, S. K., Balliet, A. G., Hollander, M. C., Fornace, A. J., Hoffman, B. and Liebermann, D. A. (2005). Hematopoietic cells from Gadd45a- and Gadd45b-deficient mice are sensitized to genotoxic-stress-induced apoptosis. *Oncogene* **24**, 7170-9.

Haddon, C., Jiang, Y. J., Smithers, L. and Lewis, J. (1998). Delta-Notch signalling and the patterning of sensory cell differentiation in the zebrafish ear: evidence from the mind bomb mutant. *Development* **125**, 4637-44.

Haines, N. and Irvine, K. D. (2003). Glycosylation regulates Notch signalling. *Nat Rev Mol Cell Biol* **4**, 786-97.

Haldin, C. E., Masse, K. L., Bhamra, S., Simrick, S., Kyuno, J. I. and Jones, E. A. (2008). The lmx1b gene is pivotal in glomus development in Xenopus laevis. *Dev Biol*.

Hara-Chikuma, M. and Verkman, A. S. (2006). Aquaporin-1 facilitates epithelial cell migration in kidney proximal tubule. *J Am Soc Nephrol* **17**, 39-45.

Hardcastle, Z. and Papalopulu, N. (2000). Distinct effects of XBF-1 in regulating the cell cycle inhibitor p27(XIC1) and imparting a neural fate. *Development* **127**, 1303-14.

Harland, R. M. (1991). In situ hybridization: an improved whole-mount method for Xenopus embryos. *Methods Cell Biol* **36**, 685-95.

Harlow, E. and Lane, D. (1988). Antibodies: A laboratory manual: Cold Spring Harbour Laboratory Press, Cold Spring Harbour, New York.

Harper, J. W., Adami, G. R., Wei, N., Keyomarsi, K. and Elledge, S. J. (1993). The p21 Cdk-interacting protein Cip1 is a potent inhibitor of G1 cyclin-dependent kinases. *Cell* **75**, 805-16.

Harris, W. A. and Hartenstein, V. (1991). Neuronal determination without cell division in Xenopus embryos. *Neuron* **6**, 499-515.

Hartley, R. S., Sible, J. C., Lewellyn, A. L. and Maller, J. L. (1997). A role for cyclin E/Cdk2 in the timing of the midblastula transition in Xenopus embryos. *Dev Biol* **188**, 312-21.

Hartwig, J. H., Brown, D., Ausiello, D. A., Stossel, T. P. and Orci, L. (1990). Polarization of gelsolin and actin binding protein in kidney epithelial cells. *J Histochem Cytochem* **38**, 1145-53.

Hayward, P., Balayo, T. and Martinez Arias, A. (2006). Notch synergizes with axin to regulate the activity of armadillo in Drosophila. *Dev Dyn* **235**, 2656-66.

Hayward, P., Brennan, K., Sanders, P., Balayo, T., DasGupta, R., Perrimon, N. and Martinez Arias, A. (2005). Notch modulates Wnt signalling by associating with Armadillo/beta-catenin and regulating its transcriptional activity. *Development* **132**, 1819-30.

Hayward, P., Kalmar, T. and Arias, A. M. (2008). Wnt/Notch signalling and information processing during development. *Development* **135**, 411-24.

Heasman, J., Kofron, M. and Wylie, C. (2000). Beta-catenin signaling activity dissected in the early Xenopus embryo: a novel antisense approach. *Dev Biol* **222**, 124-34.

Heitzler, P. and Simpson, P. (1993). Altered epidermal growth factor-like sequences provide evidence for a role of Notch as a receptor in cell fate decisions. *Development* **117**, 1113-23.

Henery, C. C., Bard, J. B. and Kaufman, M. H. (1992). Tetraploidy in mice, embryonic cell number, and the grain of the developmental map. *Dev Biol* **152**, 233-41.

Hensey, C. and Gautier, J. (1998). Programmed cell death during Xenopus development: a spatio-temporal analysis. *Dev Biol* **203**, 36-48.

Hicks, C., Johnston, S. H., diSibio, G., Collazo, A., Vogt, T. F. and Weinmaster, G. (2000). Fringe differentially modulates Jagged1 and Delta1 signalling through Notch1 and Notch2. *Nat Cell Biol* **2**, 515-20.

Hirose, G. and Jacobson, M. (1979). Clonal organization of the central nervous system of the frog. I. Clones stemming from individual blastomeres of the 16-cell and earlier stages. *Dev Biol* **71**, 191-202.

Hirsinger, E., Jouve, C., Dubrulle, J. and Pourquie, O. (2000). Somite formation and patterning. *Int Rev Cytol* **198**, 1-65.

Hoch, M., Broadie, K., Jackle, H. and Skaer, H. (1994). Sequential fates in a single cell are established by the neurogenic cascade in the Malpighian tubules of Drosophila. *Development* **120**, 3439-50.

Hoffman, B. and Liebermann, D. A. (2007). Role of gadd45 in myeloid cells in response to hematopoietic stress. *Blood Cells Mol Dis* **39**, 344-7.

Hoffman, B. and Liebermann, D. A. (2009). Gadd45 modulation of intrinsic and extrinsic stress responses in myeloid cells. *J Cell Physiol* **218**, 26-31.

Holley, S. A., Jackson, P. D., Sasai, Y., Lu, B., De Robertis, E. M., Hoffmann, F. M. and Ferguson, E. L. (1995). A conserved system for dorsal-ventral patterning in insects and vertebrates involving sog and chordin. *Nature* **376**, 249-53.

Holtfreter J (1933) Die totale Exogastrulation, eine Selbstablösung des Ektoderms vom Entomesoderm. Entwicklung und funktionelles Verhalten nervenloser Organe. Arch Entw Mech Org (Roux) 132:307–383

Horster, M. F., Braun, G. S. and Huber, S. M. (1999). Embryonic renal epithelia: induction, nephrogenesis, and cell differentiation. *Physiol Rev* **79**, 1157-91.

Howland, R. B. (1916). On the Effect of Removal of the Pronephros of the Amphibian Embryo. *Proc Natl Acad Sci U S A* **2**, 231-4.

Hughes, J., Brown, P. and Shankland, S. J. (1999). Cyclin kinase inhibitor p21CIP1/WAF1 limits interstitial cell proliferation following ureteric obstruction. *Am J Physiol* **277**, F948-56.

Hurlbut, G. D., Kankel, M. W., Lake, R. J. and Artavanis-Tsakonas, S. (2007). Crossing paths with Notch in the hyper-network. *Curr Opin Cell Biol* **19**, 166-75.

Irvine, K. D. (1999). Fringe, Notch, and making developmental boundaries. *Curr Opin Genet Dev* **9**, 434-41.

Irvine, K. D. and Rauskolb, C. (2001). Boundaries in development: formation and function. *Annu Rev Cell Dev Biol* **17**, 189-214.

Irvine, K. D. and Vogt, T. F. (1997). Dorsal-ventral signaling in limb development. *Curr Opin Cell Biol* **9**, 867-76.

Irvine, K. D. and Wieschaus, E. (1994). fringe, a Boundary-specific signaling molecule, mediates interactions between dorsal and ventral cells during Drosophila wing development. *Cell* **79**, 595-606.

Ishibe, S. and Cantley, L. G. (2008). Epithelial-mesenchymal-epithelial cycling in kidney repair. *Curr Opin Nephrol Hypertens* **17**, 379-85.

Jacobson, H. R. (1981). Functional segmentation of the mammalian nephron. *Am J Physiol* **241**, F203-18.

Jarriault, S., Brou, C., Logeat, F., Schroeter, E. H., Kopan, R. and Israel, A. (1995). Signalling downstream of activated mammalian Notch. *Nature* **377**, 355-8.

Jasinski, S., Riou-Khamlichi, C., Roche, O., Perennes, C., Bergounioux, C. and Glab, N. (2002). The CDK inhibitor NtKIS1a is involved in plant development, endoreduplication and restores normal development of cyclin D3; 1-overexpressing plants. *J Cell Sci* **115**, 973-82.

Jin, X., Kim, J. G., Oh, M. J., Oh, H. Y., Sohn, Y. W., Pian, X., Yin, J. L., Beck, S., Lee, N., Son, J. et al. (2007). Opposite roles of MRF4 and MyoD in cell proliferation and myogenic differentiation. *Biochem Biophys Res Commun* **364**, 476-82.

Johnson, R. L. and Tabin, C. J. (1997). Molecular models for vertebrate limb development. *Cell* **90**, 979-90.

Johnston, S. H., Rauskolb, C., Wilson, R., Prabhakaran, B., Irvine, K. D. and Vogt, T. F. (1997). A family of mammalian Fringe genes implicated in boundary determination and the Notch pathway. *Development* **124**, 2245-54.

Jones, E. A. (2005). Xenopus: a prince among models for pronephric kidney development. *J Am Soc Nephrol* **16**, 313-21.

Jones, E. A. and Woodland, H. R. (1986). Development of the ectoderm in Xenopus: tissue specification and the role of cell association and division. *Cell* **44**, 345-55.

Jung, A. C., Denholm, B., Skaer, H. and Affolter, M. (2005). Renal tubule development in Drosophila: a closer look at the cellular level. *J Am Soc Nephrol* **16**, 322-8.

Kadesch, T. (2004). Notch signaling: the demise of elegant simplicity. *Curr Opin Genet Dev* **14**, 506-12.

Kageyama, R., Ohtsuka, T., Shimojo, H. and Imayoshi, I. (2008). Dynamic Notch signaling in neural progenitor cells and a revised view of lateral inhibition. *Nat Neurosci* **11**, 1247-51.

Kearsey, J. M., Coates, P. J., Prescott, A. R., Warbrick, E. and Hall, P. A. (1995). Gadd45 is a nuclear cell cycle regulated protein which interacts with p21Cip1. *Oncogene* **11**, 1675-83.

Kidd, S. and Lieber, T. (2002). Furin cleavage is not a requirement for Drosophila Notch function. *Mech Dev* **115**, 41-51.

Kiernan, A. E., Cordes, R., Kopan, R., Gossler, A. and Gridley, T. (2005). The Notch ligands DLL1 and JAG2 act synergistically to regulate hair cell development in the mammalian inner ear. *Development* **132**, 4353-62.

Kim, Y. G., Alpers, C. E., Brugarolas, J., Johnson, R. J., Couser, W. G. and Shankland, S. J. (1999). The cyclin kinase inhibitor p21CIP1/WAF1 limits glomerular epithelial cell proliferation in experimental glomerulonephritis. *Kidney Int* **55**, 2349-61.

Kiyota, T., Jono, H., Kuriyama, S., Hasegawa, K., Miyatani, S. and Kinoshita, T. (2001). X-Serrate-1 is involved in primary neurogenesis in Xenopus laevis in a complementary manner with X-Delta-1. *Dev Genes Evol* **211**, 367-76.

Klein, T. and Arias, A. M. (1998). Interactions among Delta, Serrate and Fringe modulate Notch activity during Drosophila wing development. *Development* **125**, 2951-62.

Kobayashi, A., Kwan, K. M., Carroll, T. J., McMahon, A. P., Mendelsohn, C. L. and Behringer, R. R. (2005). Distinct and sequential tissue-specific activities of the LIM-class homeobox gene Lim1 for tubular morphogenesis during kidney development. *Development* **132**, 2809-23.

Koo, B. K., Lim, H. S., Song, R., Yoon, M. J., Yoon, K. J., Moon, J. S., Kim, Y. W., Kwon, M. C., Yoo, K. W., Kong, M. P. et al. (2005). Mind bomb 1 is essential for generating functional Notch ligands to activate Notch. *Development* **132**, 3459-70.

Kopan, R., Cheng, H. T. and Surendran, K. (2007). Molecular insights into segmentation along the proximal-distal axis of the nephron. *J Am Soc Nephrol* **18**, 2014-20.

Kopan, R. and Goate, A. (2000). A common enzyme connects notch signaling and Alzheimer's disease. *Genes Dev* **14**, 2799-806.

Kopp, J. B. (2002). BMP-7 and the proximal tubule. *Kidney Int* **61**, 351-2.

Kramer-Zucker, A. G., Olale, F., Haycraft, C. J., Yoder, B. K., Schier, A. F. and Drummond, I. A. (2005). Cilia-driven fluid flow in the zebrafish pronephros, brain and Kupffer's vesicle is required for normal organogenesis. *Development* **132**, 1907-21.

Kretzler, M. and Allred, L. (2008). Notch inhibition reverses kidney failure. *Nat Med* **14**, 246-7.

Kyuno, J., Masse, K. and Jones, E. A. (2008). A functional screen for genes involved in Xenopus pronephros development. *Mech Dev* **125**, 571-86.

Laufer, E., Dahn, R., Orozco, O. E., Yeo, C. Y., Pisenti, J., Henrique, D., Abbott, U. K., Fallon, J. F. and Tabin, C. (1997). Expression of Radical fringe in limb-bud ectoderm regulates apical ectodermal ridge formation. *Nature* **386**, 366-73.

Le Borgne, R., Bardin, A. and Schweisguth, F. (2005a). The roles of receptor and ligand endocytosis in regulating Notch signaling. *Development* **132**, 1751-62.

Le Borgne, R., Remaud, S., Hamel, S. and Schweisguth, F. (2005b). Two distinct E3 ubiquitin ligases have complementary functions in the regulation of delta and serrate signaling in Drosophila. *PLoS Biol* **3**, e96.

Lee, J. E., Hollenberg, S. M., Snider, L., Turner, D. L., Lipnick, N. and Weintraub, H. (1995). Conversion of Xenopus ectoderm into neurons by NeuroD, a basic helix-loop-helix protein. *Science* **268**, 836-44.

Leevers, S. J. and McNeill, H. (2005). Controlling the size of organs and organisms. *Curr Opin Cell Biol* **17**, 604-9.

Lewis, J. (1998). Notch signalling and the control of cell fate choices in vertebrates. *Semin Cell Dev Biol* **9**, 583-9.

Liebermann, D. A. and Hoffman, B. (2007). Gadd45 in the response of hematopoietic cells to genotoxic stress. *Blood Cells Mol Dis* **39**, 329-35.

Liebermann, D. A. and Hoffman, B. (2008). Gadd45 in stress signaling. *J Mol Signal* **3**, 15.

Liu, Y., Pathak, N., Kramer-Zucker, A. and Drummond, I. A. (2007). Notch signaling controls the differentiation of transporting epithelia and multiciliated cells in the zebrafish pronephros. *Development* **134**, 1111-22.

Logeat, F., Bessia, C., Brou, C., LeBail, O., Jarriault, S., Seidah, N. G. and Israel, A. (1998). The Notch1 receptor is cleaved constitutively by a furin-like convertase. *Proc Natl Acad Sci U S A* **95**, 8108-12.

Lundberg, A. S. and Weinberg, R. A. (1999). Control of the cell cycle and apoptosis. *Eur J Cancer* **35**, 531-9.

Ma, M. and Jiang, Y. J. (2007). Jagged2a-notch signaling mediates cell fate choice in the zebrafish pronephric duct. *PLoS Genet* **3**, e18.

Ma, Q., Kintner, C. and Anderson, D. J. (1996). Identification of neurogenin, a vertebrate neuronal determination gene. *Cell* **87**, 43-52.

Major, R. J. and Irvine, K. D. (2005). Influence of Notch on dorsoventral compartmentalization and actin organization in the Drosophila wing. *Development* **132**, 3823-33.

Manning, L. and Doe, C. Q. (1999). Prospero distinguishes sibling cell fate without asymmetric localization in the Drosophila adult external sense organ lineage. *Development* **126**, 2063-71.

Marnellos, G., Deblandre, G. A., Mjolsness, E. and Kintner, C. (2000). Delta-Notch lateral inhibitory patterning in the emergence of ciliated cells in Xenopus: experimental observations and a gene network model. *Pac Symp Biocomput*, 329-40.

Mauch, T. J., Yang, G., Wright, M., Smith, D. and Schoenwolf, G. C. (2000). Signals from trunk paraxial mesoderm induce pronephros formation in chick intermediate mesoderm. *Dev Biol* **220**, 62-75.

McCright, B., Gao, X., Shen, L., Lozier, J., Lan, Y., Maguire, M., Herzlinger, D., Weinmaster, G., Jiang, R. and Gridley, T. (2001). Defects in development of the kidney, heart and eye vasculature in mice homozygous for a hypomorphic Notch2 mutation. *Development* **128**, 491-502.

McLaughlin, K. A., Rones, M. S. and Mercola, M. (2000). Notch regulates cell fate in the developing pronephros. *Dev Biol* **227**, 567-80.

ME, D. E. B., Barembaum, M., Arman, O. and Bronner-Fraser, M. (2007). Lunatic fringe causes expansion and increased neurogenesis of trunk neural tube and neural crest populations. *Neuron Glia Biol* **3**, 93-103.

Mertens, P. R., Raffetseder, U. and Rauen, T. (2008). Notch receptors: a new target in glomerular diseases. *Nephrol Dial Transplant* **23**, 2743-5.

Micchelli, C. A., Rulifson, E. J. and Blair, S. S. (1997). The function and regulation of cut expression on the wing margin of Drosophila: Notch, Wingless and a dominant negative role for Delta and Serrate. *Development* **124**, 1485-95.

Michalopoulos, G. K. and DeFrances, M. (2005). Liver regeneration. *Adv Biochem Eng Biotechnol* **93**, 101-34.

Mitchell, T., Jones, E. A., Weeks, D. L. and Sheets, M. D. (2007). Chordin affects pronephros development in Xenopus embryos by anteriorizing presomitic mesoderm. *Dev Dyn* **236**, 251-61.

Mizukami, Y. and Fischer, R. L. (2000). Plant organ size control: AINTEGUMENTA regulates growth and cell numbers during organogenesis. *Proc Natl Acad Sci U S A* **97**, 942-7.

Moloney, D. J., Panin, V. M., Johnston, S. H., Chen, J., Shao, L., Wilson, R., Wang, Y., Stanley, P., Irvine, K. D., Haltiwanger, R. S. et al. (2000). Fringe is a glycosyltransferase that modifies Notch. *Nature* **406**, 369-75.

Moody, S. A. (1987). Fates of the blastomeres of the 32-cell-stage Xenopus embryo. *Dev Biol* **122**, 300-19.

Moody, S. A. and Kline, M. J. (1990). Segregation of fate during cleavage of frog (Xenopus laevis) blastomeres. *Anat Embryol (Berl)* **182**, 347-62.

Moran, J. L., Levorse, J. M. and Vogt, T. F. (1999). Limbs move beyond the radical fringe. *Nature* **399**, 742-3.

Morimoto, M., Takahashi, Y., Endo, M. and Saga, Y. (2005). The Mesp2 transcription factor establishes segmental borders by suppressing Notch activity. *Nature* **435**, 354-9.

Movassagh, M. and Philpott, A. (2008). Cardiac differentiation in Xenopus requires the cyclin-dependent kinase inhibitor, p27Xic1. *Cardiovasc Res*.

Nagahama, H., Hatakeyama, S., Nakayama, K., Nagata, M. and Tomita, K. (2001). Spatial and temporal expression patterns of the cyclin-dependent kinase (CDK) inhibitors p27Kip1 and p57Kip2 during mouse development. *Anat Embryol (Berl)* **203**, 77-87.

Neufeld, T. P., de la Cruz, A. F., Johnston, L. A. and Edgar, B. A. (1998). Coordination of growth and cell division in the Drosophila wing. *Cell* **93**, 1183-93.

Nevins, J. R. (1998). Toward an understanding of the functional complexity of the E2F and retinoblastoma families. *Cell Growth Differ* **9**, 585-93.

Newport, J. and Kirschner, M. (1982). A major developmental transition in early Xenopus embryos: II. Control of the onset of transcription. *Cell* **30**, 687-96.

Newport, J. W. and Kirschner, M. W. (1984). Regulation of the cell cycle during early Xenopus development. *Cell* **37**, 731-42.

Nguyen, L., Besson, A., Heng, J. I., Schuurmans, C., Teboul, L., Parras, C., Philpott, A., Roberts, J. M. and Guillemot, F. (2006). p27kip1 independently promotes neuronal differentiation and migration in the cerebral cortex. *Genes Dev* **20**, 1511-24.

Nichane, M., Van Campenhout, C., Pendeville, H., Voz, M. L. and Bellefroid, E. J. (2006). The Na+/PO4 cotransporter SLC20A1 gene labels distinct restricted subdomains of the developing pronephros in Xenopus and zebrafish embryos. *Gene Expr Patterns* **6**, 667-72.

Nieuwkoop, P. D. and Faber, J. (1994). Normal table of *Xenopus laevis* (Daudin) 4th ed.: Garland Publishing, Inc. New York.

Nigg, E. A. (1991). The substrates of the cdc2 kinase. *Semin Cell Biol* **2**, 261-70.

Nigg, E. A., Blangy, A. and Lane, H. A. (1996). Dynamic changes in nuclear architecture during mitosis: on the role of protein phosphorylation in spindle assembly and chromosome segregation. *Exp Cell Res* **229**, 174-80.

Niranjan, T., Bielesz, B., Gruenwald, A., Ponda, M. P., Kopp, J. B., Thomas, D. B. and Susztak, K. (2008). The Notch pathway in podocytes plays a role in the development of glomerular disease. *Nat Med* **14**, 290-8.

Niswander, L. (2003). Pattern formation: old models out on a limb. *Nat Rev Genet* **4**, 133-43.

Obaya, A. J. and Sedivy, J. M. (2002). Regulation of cyclin-Cdk activity in mammalian cells. *Cell Mol Life Sci* **59**, 126-42.

Ohlstein, B. and Spradling, A. (2007). Multipotent Drosophila intestinal stem cells specify daughter cell fates by differential notch signaling. *Science* **315**, 988-92.

Ohnuma, S., Hopper, S., Wang, K. C., Philpott, A. and Harris, W. A. (2002). Co-ordinating retinal histogenesis: early cell cycle exit enhances early cell fate determination in the Xenopus retina. *Development* **129**, 2435-46.

Ohnuma, S., Philpott, A., Wang, K., Holt, C. E. and Harris, W. A. (1999). p27Xic1, a Cdk inhibitor, promotes the determination of glial cells in Xenopus retina. *Cell* **99**, 499-510.

Okabayashi, K. and Asashima, M. (2003). Tissue generation from amphibian animal caps. *Curr Opin Genet Dev* **13**, 502-7.

Okajima, T. and Irvine, K. D. (2002). Regulation of notch signaling by o-linked fucose. *Cell* **111**, 893-904.

Ozato, K. (1969). Cell cycle in the primitive streak and the notochord of early chick embryos. *Embryologia (Nagoya)* **10**, 297-311.

Ozbudak, E. M. and Pourquie, O. (2008). The vertebrate segmentation clock: the tip of the iceberg. *Curr Opin Genet Dev* **18**, 317-23.

Palmeirim, I., Henrique, D., Ish-Horowicz, D. and Pourquie, O. (1997). Avian hairy gene expression identifies a molecular clock linked to vertebrate segmentation and somitogenesis. *Cell* **91**, 639-48.

Panin, V. M., Papayannopoulos, V., Wilson, R. and Irvine, K. D. (1997). Fringe modulates Notch-ligand interactions. *Nature* **387**, 908-12.

Philpott, A., Porro, E. B., Kirschner, M. W. and Tsai, L. H. (1997). The role of cyclin-dependent kinase 5 and a novel regulatory subunit in regulating muscle differentiation and patterning. *Genes Dev* **11**, 1409-21.

Philpott, A. and Yew, P. R. (2008). The Xenopus cell cycle: an overview. *Mol Biotechnol* **39**, 9-19.

Polyak, K., Lee, M. H., Erdjument-Bromage, H., Koff, A., Roberts, J. M., Tempst, P. and Massague, J. (1994). Cloning of p27Kip1, a cyclin-dependent kinase inhibitor and a potential mediator of extracellular antimitogenic signals. *Cell* **78**, 59-66.

Pourquie, O. (2001). The vertebrate segmentation clock. *J Anat* **199**, 169-75.

Pourquie, O. (2003). Vertebrate somitogenesis: a novel paradigm for animal segmentation? *Int J Dev Biol* **47**, 597-603.

Pouyet, L. and Mitsiadis, T. A. (2000). Dynamic Lunatic fringe expression is correlated with boundaries formation in developing mouse teeth. *Mech Dev* **91**, 399-402.

Primmett, D. R., Norris, W. E., Carlson, G. J., Keynes, R. J. and Stern, C. D. (1989). Periodic segmental anomalies induced by heat shock in the chick embryo are associated with the cell cycle. *Development* **105**, 119-30.

Prince, V. E., Holley, S. A., Bally-Cuif, L., Prabhakaran, B., Oates, A. C., Ho, R. K. and Vogt, T. F. (2001). Zebrafish lunatic fringe demarcates segmental boundaries. *Mech Dev* **105**, 175-80.

Pugacheva, O. M. and Mamon, L. A. (2005). [Genetic nature of abnormal larval development in the progeny of l(1)ts403(sbr10) females of Drosophila melanogaster]. *Tsitologiia* **47**, 623-36.

Raciti, D., Reggiani, L., Geffers, L., Jiang, Q., Bacchion, F., Subrizi, A. E., Clements, D., Tindal, C., Davidson, D. R., Kaissling, B. et al. (2008). Organization of the pronephric kidney revealed by large-scale gene expression mapping. *Genome Biol* **9**, R84.

Rampal, R., Li, A. S., Moloney, D. J., Georgiou, S. A., Luther, K. B., Nita-Lazar, A. and Haltiwanger, R. S. (2005). Lunatic fringe, manic fringe, and radical fringe recognize similar specificity determinants in O-fucosylated epidermal growth factor-like repeats. *J Biol Chem* **280**, 42454-63.

Rand, M. D., Grimm, L. M., Artavanis-Tsakonas, S., Patriub, V., Blacklow, S. C., Sklar, J. and Aster, J. C. (2000). Calcium depletion dissociates and activates heterodimeric notch receptors. *Mol Cell Biol* **20**, 1825-35.

Rauskolb, C., Correia, T. and Irvine, K. D. (1999). Fringe-dependent separation of dorsal and ventral cells in the Drosophila wing. *Nature* **401**, 476-80.

Raya, A., Kawakami, Y., Rodriguez-Esteban, C., Ibanes, M., Rasskin-Gutman, D., Rodriguez-Leon, J., Buscher, D., Feijo, J. A. and Izpisua Belmonte, J. C. (2004). Notch activity acts as a sensor for extracellular calcium during vertebrate left-right determination. *Nature* **427**, 121-8.

Reed, R. D. (2004). Evidence for Notch-mediated lateral inhibition in organizing butterfly wing scales. *Dev Genes Evol* **214**, 43-6.

Reggiani, L., Raciti, D., Airik, R., Kispert, A. and Brändli, A. W. (2007). The prepattern transcription factor Irx3 directs nephron segment identity. *Genes Dev* **21**, 2358-70.

Reynaud, E. G., Leibovitch, M. P., Tintignac, L. A., Pelpel, K., Guillier, M. and Leibovitch, S. A. (2000). Stabilization of MyoD by direct binding to p57(Kip2). *J Biol Chem* **275**, 18767-76.

Reynaud, E. G., Pelpel, K., Guillier, M., Leibovitch, M. P. and Leibovitch, S. A. (1999). p57(Kip2) stabilizes the MyoD protein by inhibiting cyclin E-Cdk2 kinase activity in growing myoblasts. *Mol Cell Biol* **19**, 7621-9.

Richard-Parpaillon, L., Cosgrove, R. A., Devine, C., Vernon, A. E. and Philpott, A. (2004). G1/S phase cyclin-dependent kinase overexpression perturbs early development and delays tissue-specific differentiation in Xenopus. *Development* **131**, 2577-86.

Robert, B. (2007). Bone morphogenetic protein signaling in limb outgrowth and patterning. *Dev Growth Differ* **49**, 455-68.

Rodriguez-Esteban, C., Schwabe, J. W., De La Pena, J., Foys, B., Eshelman, B. and Belmonte, J. C. (1997). Radical fringe positions the apical ectodermal ridge at the dorsoventral boundary of the vertebrate limb. *Nature* **386**, 360-6.

Rones, M. S., Woda, J., Mercola, M. and McLaughlin, K. A. (2002). Isolation and characterization of Xenopus Hey-1: a downstream mediator of Notch signaling. *Dev Dyn* **225**, 554-60.

Roth, S. (2003). The origin of dorsoventral polarity in Drosophila. *Philos Trans R Soc Lond B Biol Sci* **358**, 1317-29; discussion 1329.

Rulifson, E. J., Micchelli, C. A., Axelrod, J. D., Perrimon, N. and Blair, S. S. (1996). wingless refines its own expression domain on the Drosophila wing margin. *Nature* **384**, 72-4.

Sato, A., Asashima, M., Yokota, T. and Nishinakamura, R. (2000). Cloning and expression pattern of a Xenopus pronephros-specific gene, XSMP-30. *Mech Dev* **92**, 273-5.

Saulnier, D. M., Ghanbari, H. and Brandli, A. W. (2002). Essential function of Wnt-4 for tubulogenesis in the Xenopus pronephric kidney. *Dev Biol* **248**, 13-28.

Saura, C. A., Tomita, T., Soriano, S., Takahashi, M., Leem, J. Y., Honda, T., Koo, E. H., Iwatsubo, T. and Thinakaran, G. (2000). The nonconserved hydrophilic loop domain of presenilin (PS) is not required for PS endoproteolysis or enhanced abeta 42 production mediated by familial early onset Alzheimer's disease-linked PS variants. *J Biol Chem* **275**, 17136-42.

Saxén, L. (1987). Organogesis of the kidney. *Cambridge: Cambridge University Press*.

Saxen, L. and Sariola, H. (1987). Early organogenesis of the kidney. *Pediatr Nephrol* **1**, 385-92.

Schober, M., Schaefer, M. and Knoblich, J. A. (1999). Bazooka recruits Inscuteable to orient asymmetric cell divisions in Drosophila neuroblasts. *Nature* **402**, 548-51.

Schroeter, E. H., Kisslinger, J. A. and Kopan, R. (1998). Notch-1 signalling requires ligand-induced proteolytic release of intracellular domain. *Nature* **393**, 382-6.

Seufert, D. W., Brennan, H. C., DeGuire, J., Jones, E. A. and Vize, P. D. (1999). Developmental basis of pronephric defects in Xenopus body plan phenotypes. *Dev Biol* **215**, 233-42.

Seville, R. A., Nijjar, S., Barnett, M. W., Masse, K. and Jones, E. A. (2002). Annexin IV (Xanx-4) has a functional role in the formation of pronephric tubules. *Development* **129**, 1693-704.

Sherr, C. J. and Roberts, J. M. (1999). CDK inhibitors: positive and negative regulators of G1-phase progression. *Genes Dev* **13**, 1501-12.

Shifley, E. T., Vanhorn, K. M., Perez-Balaguer, A., Franklin, J. D., Weinstein, M. and Cole, S. E. (2008). Oscillatory lunatic fringe activity is crucial for segmentation of the anterior but not posterior skeleton. *Development* **135**, 899-908.

Shou, W. and Dunphy, W. G. (1996). Cell cycle control by Xenopus p28Kix1, a developmentally regulated inhibitor of cyclin-dependent kinases. *Mol Biol Cell* **7**, 457-69.

Simpson, P. (1990). Notch and the choice of cell fate in Drosophila neuroepithelium. *Trends Genet* **6**, 343-5.

Simrick, S., Masse, K. and Jones, E. A. (2005). Developmental expression of Pod 1 in Xenopus laevis. *Int J Dev Biol* **49**, 59-63.

Sjolund, J., Johansson, M., Manna, S., Norin, C., Pietras, A., Beckman, S., Nilsson, E., Ljungberg, B. and Axelson, H. (2008). Suppression of renal cell carcinoma growth by inhibition of Notch signaling in vitro and in vivo. *J Clin Invest* **118**, 217-28.

Smith, C. and Mackay, S. (1991). Morphological development and fate of the mouse mesonephros. *J Anat* **174**, 171-84.

Smith, D. M., Torres, R. D. and Stephens, T. D. (1996). Mesonephros has a role in limb development and is related to thalidomide embryopathy. *Teratology* **54**, 126-34.

Snow, M. H. L. (1977). Gastrulation in Mouse - Growth and Regionalization of Epiblast. *Journal of Embryology and Experimental Morphology* **42**, 293-303.

Soriano, S., Kang, D. E., Fu, M., Pestell, R., Chevallier, N., Zheng, H. and Koo, E. H. (2001). Presenilin 1 negatively regulates beta-catenin/T cell factor/lymphoid enhancer factor-1 signaling independently of beta-amyloid precursor protein and notch processing. *J Cell Biol* **152**, 785-94.

Stern, C. D. (1979). Re-Examination of Mitotic-Activity in the Early Chick-Embryo. *Anatomy and Embryology* **156**, 319-329.

Su, J. Y., Rempel, R. E., Erikson, E. and Maller, J. L. (1995). Cloning and characterization of the Xenopus cyclin-dependent kinase inhibitor p27XIC1. *Proc Natl Acad Sci U S A* **92**, 10187-91.

Taelman, V., Van Campenhout, C., Solter, M., Pieler, T. and Bellefroid, E. J. (2006). The Notch-effector HRT1 gene plays a role in glomerular development and patterning of the Xenopus pronephros anlagen. *Development* **133**, 2961-71.

Taniguchi, Y., Karlstrom, H., Lundkvist, J., Mizutani, T., Otaka, A., Vestling, M., Bernstein, A., Donoviel, D., Lendahl, U. and Honjo, T. (2002). Notch receptor cleavage depends on but is not directly executed by presenilins. *Proc Natl Acad Sci U S A* **99**, 4014-9.

Tételin, S. (2008) An analysis of wnt signalling molecules in Xenopus pronephros development. PhD Thesis

Thayer, M. J., Tapscott, S. J., Davis, R. L., Wright, W. E., Lassar, A. B. and Weintraub, H. (1989). Positive autoregulation of the myogenic determination gene MyoD1. *Cell* **58**, 241-8.

Tran, U., Pickney, L. M., Ozpolat, B. D. and Wessely, O. (2007). Xenopus Bicaudal-C is required for the differentiation of the amphibian pronephros. *Dev Biol* **307**, 152-64.

Tsukumo, S., Hirose, K., Maekawa, Y., Kishihara, K. and Yasutomo, K. (2006). Lunatic fringe controls T cell differentiation through modulating notch signaling. *J Immunol* **177**, 8365-71.

Van Campenhout, C., Nichane, M., Antoniou, A., Pendeville, H., Bronchain, O. J., Marine, J. C., Mazabraud, A., Voz, M. L. and Bellefroid, E. J. (2006). Evi1 is specifically expressed in the distal tubule and duct of the Xenopus pronephros and plays a role in its formation. *Dev Biol* **294**, 203-19.

van de Poll, M. L., van Rotterdam, W., Gadellaa, M. M., Stortelers, C., van Vugt, M. J. and van Zoelen, E. J. (2000). Non-linear antigenic regions in epidermal growth factor (EGF) and transforming growth factor alpha (TGF alpha) studied by EGF-TGF alpha chimaeras. *Biochem J* **349**, 267-74.

Vernon, A. E., Devine, C. and Philpott, A. (2003). The cdk inhibitor p27Xic1 is required for differentiation of primary neurones in Xenopus. *Development* **130**, 85-92.

Vernon, A. E., Movassagh, M., Horan, I., Wise, H., Ohnuma, S. and Philpott, A. (2006). Notch targets the Cdk inhibitor Xic1 to regulate differentiation but not the cell cycle in neurons. *EMBO Rep* **7**, 643-8.

Vernon, A. E. and Philpott, A. (2003). A single cdk inhibitor, p27Xic1, functions beyond cell cycle regulation to promote muscle differentiation in Xenopus. *Development* **130**, 71-83.

Visan, I., Yuan, J. S., Tan, J. B., Cretegny, K. and Guidos, C. J. (2006). Regulation of intrathymic T-cell development by Lunatic Fringe- Notch1 interactions. *Immunol Rev* **209**, 76-94.

Vize, P. D., Jones, E. A. and Pfister, R. (1995). Development of the Xenopus pronephric system. *Dev Biol* **171**, 531-40.

Vize, P. D., Seufert, D. W., Carroll, T. J. and Wallingford, J. B. (1997). Model systems for the study of kidney development: use of the pronephros in the analysis of organ induction and patterning. *Dev Biol* **188**, 189-204.

P.D. Vize, A.S. Woolf and Bard JBL, The Kidney From normal development to congenital disease, Academic Press, London (2003).

Wada, T., Matsushima, K. and Kaneko, S. (2008). The role of chemokines in glomerulonephritis. *Front Biosci* **13**, 3966-74.

Wallingford, J. B., Carroll, T. J. and Vize, P. D. (1998). Precocious expression of the Wilms' tumor gene xWT1 inhibits embryonic kidney development in Xenopus laevis. *Dev Biol* **202**, 103-12.

Wang, P., Pereira, F. A., Beasley, D. and Zheng, H. (2003). Presenilins are required for the formation of comma- and S-shaped bodies during nephrogenesis. *Development* **130**, 5019-29.

Wang, W. and Struhl, G. (2004). Drosophila Epsin mediates a select endocytic pathway that DSL ligands must enter to activate Notch. *Development* **131**, 5367-80.

Wang, W. and Struhl, G. (2005). Distinct roles for Mind bomb, Neuralized and Epsin in mediating DSL endocytosis and signaling in Drosophila. *Development* **132**, 2883-94.

Wang, Z., Wang, S., Fisher, P. B., Dent, P. and Grant, S. (2000). Evidence of a functional role for the cyclin-dependent kinase inhibitor p21CIP1 in leukemic cell (U937) differentiation induced by low concentrations of 1-beta-D-arabinofuranosylcytosine. *Differentiation* **66**, 1-13.

Weinberg, R. A. (1995). The retinoblastoma protein and cell cycle control. *Cell* **81**, 323-30.

Wessely, O. and Obara, T. (2008). Fish and frogs: models for vertebrate cilia signaling. *Front Biosci* **13**, 1866-80.

Wilkins, A. S. (1995). Singling out the tip cell of the Malpighian tubules--lessons from neurogenesis. *Bioessays* **17**, 199-202.

Williams, J. A., Paddock, S. W. and Carroll, S. B. (1993). Pattern formation in a secondary field: a hierarchy of regulatory genes subdivides the developing Drosophila wing disc into discrete subregions. *Development* **117**, 571-84.

Wingert, R. A. and Davidson, A. J. (2008). The zebrafish pronephros: a model to study nephron segmentation. *Kidney Int* **73**, 1120-7.

Wodarz, A., Ramrath, A., Grimm, A. and Knust, E. (2000). Drosophila atypical protein kinase C associates with Bazooka and controls polarity of epithelia and neuroblasts. *J Cell Biol* **150**, 1361-74.

Wodarz, A., Ramrath, A., Kuchinke, U. and Knust, E. (1999). Bazooka provides an apical cue for Inscuteable localization in Drosophila neuroblasts. *Nature* **402**, 544-7.

Wolpert, L. (2002). The progress zone model for specifying positional information. *Int J Dev Biol* **46**, 869-70.

Wu, J. Y., Wen, L., Zhang, W. J. and Rao, Y. (1996). The secreted product of Xenopus gene lunatic Fringe, a vertebrate signaling molecule. *Science* **273**, 355-8.

Wu, Y. and Zhou, B. P. (2008). New insights of epithelial-mesenchymal transition in cancer metastasis. *Acta Biochim Biophys Sin (Shanghai)* **40**, 643-50.

Yan, Y., Frisen, J., Lee, M. H., Massague, J. and Barbacid, M. (1997). Ablation of the CDK inhibitor p57Kip2 results in increased apoptosis and delayed differentiation during mouse development. *Genes Dev* **11**, 973-83.

Yoshioka, H., Ishimaru, Y., Sugiyama, N., Tsunekawa, N., Noce, T., Kasahara, M. and Morohashi, K. (2005). Mesonephric FGF signaling is associated with the development of sexually indifferent gonadal primordium in chick embryos. *Dev Biol* **280**, 150-61.

Zakany, J., Kmita, M. and Duboule, D. (2004). A dual role for Hox genes in limb anterior-posterior asymmetry. *Science* **304**, 1669-72.

Zambrano, N. R., Lubensky, I. A., Merino, M. J., Linehan, W. M. and Walther, M. M. (1999). Histopathology and molecular genetics of renal tumors toward unification of a classification system. *J Urol* **162**, 1246-58.

Zezula, J., Casaccia-Bonnefil, P., Ezhevsky, S. A., Osterhout, D. J., Levine, J. M., Dowdy, S. F., Chao, M. V. and Koff, A. (2001). p21cip1 is required for the differentiation of oligodendrocytes independently of cell cycle withdrawal. *EMBO Rep* **2**, 27-34.

Zhan, Q., Lord, K. A., Alamo, I., Jr., Hollander, M. C., Carrier, F., Ron, D., Kohn, K. W., Hoffman, B., Liebermann, D. A. and Fornace, A. J., Jr. (1994). The gadd and MyD genes define a novel set of mammalian genes encoding acidic proteins that synergistically suppress cell growth. *Mol Cell Biol* **14**, 2361-71.

Zhang, N., Norton, C. R. and Gridley, T. (2002). Segmentation defects of Notch pathway mutants and absence of a synergistic phenotype in lunatic fringe/radical fringe double mutant mice. *Genesis* **33**, 21-8.

Zhang, W., Bae, I., Krishnaraju, K., Azam, N., Fan, W., Smith, K., Hoffman, B. and Liebermann, D. A. (1999). CR6: A third member in the MyD118 and Gadd45 gene family which functions in negative growth control. *Oncogene* **18**, 4899-907.

Zhang, W., Hoffman, B. and Liebermann, D. A. (2001). Ectopic expression of MyD118/Gadd45/CR6 (Gadd45beta/alpha/gamma) sensitizes neoplastic cells to genotoxic stress-induced apoptosis. *Int J Oncol* **18**, 749-57.

Zhao, H., Jin, S., Antinore, M. J., Lung, F. D., Fan, F., Blanck, P., Roller, P., Fornace, A. J., Jr. and Zhan, Q. (2000). The central region of Gadd45 is required for its interaction with p21/WAF1. *Exp Cell Res* **258**, 92-100.

Zimmerman, K., Shih, J., Bars, J., Collazo, A. and Anderson, D. J. (1993). XASH-3, a novel Xenopus achaete-scute homolog, provides an early marker of planar neural induction and position along the mediolateral axis of the neural plate. *Development* **119**, 221-32.